

Phylogeny of araphid diatoms, inferred from morphological and molecular data

Dissertation

zur

Erlangung des Akademischen Grades
eines Doktors der Naturwissenschaften

-Dr. rer. nat.-

im Fachbereich 2 (Biologie/Chemie)
der Universität Bremen

vorgelegt von

Shinya Sato

Bremerhaven, Mai 2008

Erster Gutachter: Prof. Dr. Victor Smetacek
Zweiter Gutachter: Prof. Dr. Ulrich Bathmann

Tag und Ort des öffentlichen Kolloquiums: 3 Juli 2008, Universität Bremen

Hiermit erkläre ich, dass ich die vorliegende Dissertation selbständig verfasst und keine anderen als die angegebenen Quellen und Hilfsmittel verwendet habe. Die entnommenen Stellen aus benutzten Werken wurden wörtlich oder inhaltlich als solche kenntlich gemacht.

Shinya Sato

CONTENTS

1. GENERAL INTRODUCTION	1
1.1. HISTORICAL OVERVIEW OF THE SYSTEMATICS OF DIATOMS	1
1.2. MOLECULAR PHYLOGENY – THE PROBLEMATIC ‘ARAPHID’ DIATOMS	2
1.3. LIFE HISTORY AND AUXOSPORES	3
1.4. AIM OF THE THESIS	4
1.5. OUTLINE OF THE THESIS	5
2. PUBLICATION	6
2.1. LIST OF PUBLICATIONS WITH THE STATEMENT OF THE CANDIDATE’S CONTRIBUTION.	6
2.2. PUBLICATION I:	8
2.3. PUBLICATION II:	15
2.4. PUBLICATION III:	22
2.5. PUBLICATION IV:	50
2.6. PUBLICATION V:	65
2.7. PUBLICATION VI:	81
2.8. PUBLICATION VII:	118
2.9. PUBLICATION VIII:	136
2.10. PUBLICATION IX:	161
2.11. PUBLICATION X:	200
3. SYNTHESIS	231
3.1. LIFE CYCLE AND AUXOSPORE STRUCTURE - THE EVOLUTIONARY SIGNIFICANCE	231
3.2. UNVEILED NATURE OF ARAPHID DIVERSITY AND PHYLOGENY	231
3.3. PERSPECTIVES FOR FUTURE RESEARCH	233
4. REFERENCES	235
5. SUMMARY	238
6. ZUSAMMENFASSUNG	239
7. SUMMARY (IN JAPANESE)	240
8. ACKNOWLEDGEMENT	241
9. APPENDIX	242
9.1. PUBLICATION XI:	242
9.2. PUBLICATION XII:	256
9.3. CURRICULUM VITAE:	269

Phylogeny of araphid diatoms, inferred from morphological and molecular data

1. GENERAL INTRODUCTION

1.1. Historical overview of the systematics of diatoms

The diatoms are the most species-rich group of the eukaryotic algae, containing more than 10,000 described species and potentially many more cryptic species (Mann 1999). They are widespread ecologically, have a global significance in the carbon and silicon cycles and are increasingly used in ecological monitoring, paleoecological reconstructions, and stratigraphic correlations. Fig. 1 (A-D) shows the special cell wall of diatoms, which is comprised of two overlapping halves (thecae), each of which consists of two larger elements at opposite ends of the cell (valves) and strips (girdle bands) or scales covering the region in between (Round et al. 1990).

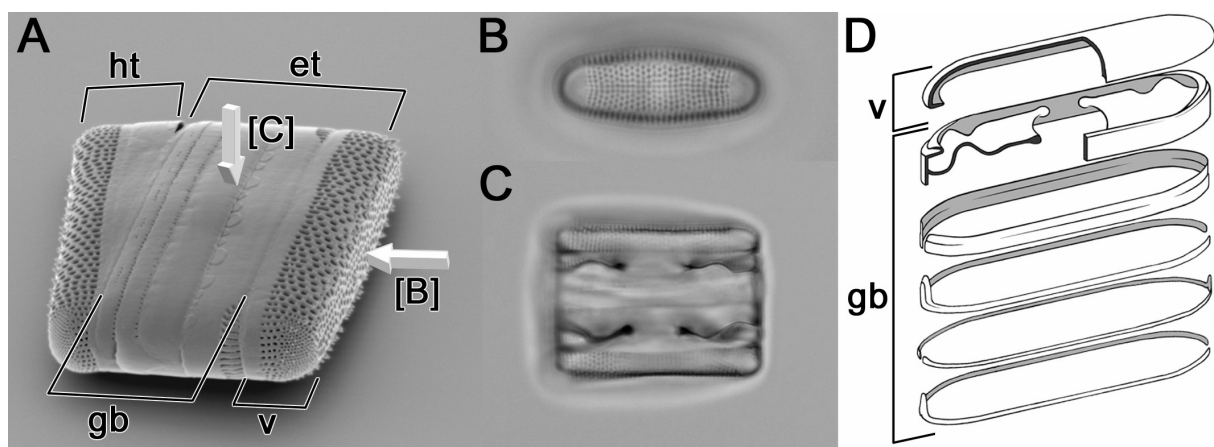


Fig. 1. Cell wall structure of diatom. (A) Slightly disrupted frustule of *Grammatophora* under SEM, showing the overlap between the epitheca (et) and hypotheca (ht), each of which consists of a valve (v) and a set of girdle bands (gb) attached to it. Valve view (B) is obtained when frustule is observed from direction of arrow [B] under LM as indicated in (A), whereas girdle view (C) from arrow [C]. (D) Schematic drawing of theca.

Historically they have been assumed to contain two major groups: the centrics and the pennates, which can be distinguished by their pattern centres or valve symmetry, mode of sexual reproduction, and plastid number and structure (Round et al. 1990). The oogamous centrics, with radially symmetric ornamentation of their valves and with numerous discoid plastids, are distinct from the isogamous pennate with bilaterally symmetrical pattern centres and generally fewer, plate-like plastids. Morphologically, pennates can further be subdivided into two groups by the presence or absence of a slit (raphe) in the valve for movement, i.e., motile pennates possessing raphes are ‘raphid’ diatom, whereas immotile pennates lacking raphes are ‘araphid’ diatoms.

Since 1878, when Kirchner divided the diatoms into two groups, centrics and pennates, this system had been well-accepted by taxonomists (e.g., Simonsen 1979). For example, Simonsen (1979) established the system that adopted the bipartition system (Fig. 2A), placing diatoms at the rank of class, viz., Bacillariophyceae. It should be noted that he recognized centrics as paraphyletic as seen in his phylogenetic tree (*ibid.*, fig. 3), although this idea was not reflected in his classification system. Some researchers (e.g., Patrick and Reimer 1966) rejected this bipartition because the border between the two groups was indistinct.

The first classification system of diatoms taking SEM-based information into account was proposed by Round et al. (1990), who recognized three classes: Coscinodiscophyceae (centric diatoms), Fragilariophyceae (araphid diatoms) and Bacillariophyceae (raphid dia-

toms), giving equal ranking to the araphid and raphid diatoms (Fig. 2B). The diatoms were then placed at the rank of the division, viz., Bacillariophyta.

The most recent classification system, in which diatoms consisted of three classes, was established by Medlin and Kaczmarska (2004) mainly based on rDNA phylogenies but which also took into account reproductive and cytological features. This system (Fig. 2C) separates the division Bacillariophyta into two groups at the rank of subdivision: Coscinodiscophytina comprising the radial centrics, and Bacillariophytina comprising the rest of the diatoms that exhibit polarity in the shape of their valves, except where this has been lost secondarily. The latter subdivision is further divided into two classes: Mediophyceae and Bacillariophyceae. The class Mediophyceae comprises the bi/multi polar centric diatoms and the radial Thalassiosirales. The entire group of pennates, including araphid and raphid diatoms, are now treated as one class, the Bacillariophyceae. Therefore, the traditional morphology-based recognition of diatoms into two groups is not valid except for the pennates. Nevertheless, we can use the terms *araphid*, *raphid* and *centric*, because they refer to key morphological features or their absence. In this thesis, the term *araphid pennate diatom* follows the traditional definition, i.e., a diatom that has an elongate valve with a central or slightly lateral sternum, apical pore fields and often also apical labiate process, but that lacks a raphe slit. We do not imply that this corresponds to a mono- (holo-) phyletic group, or that it should be accorded any taxonomic status.

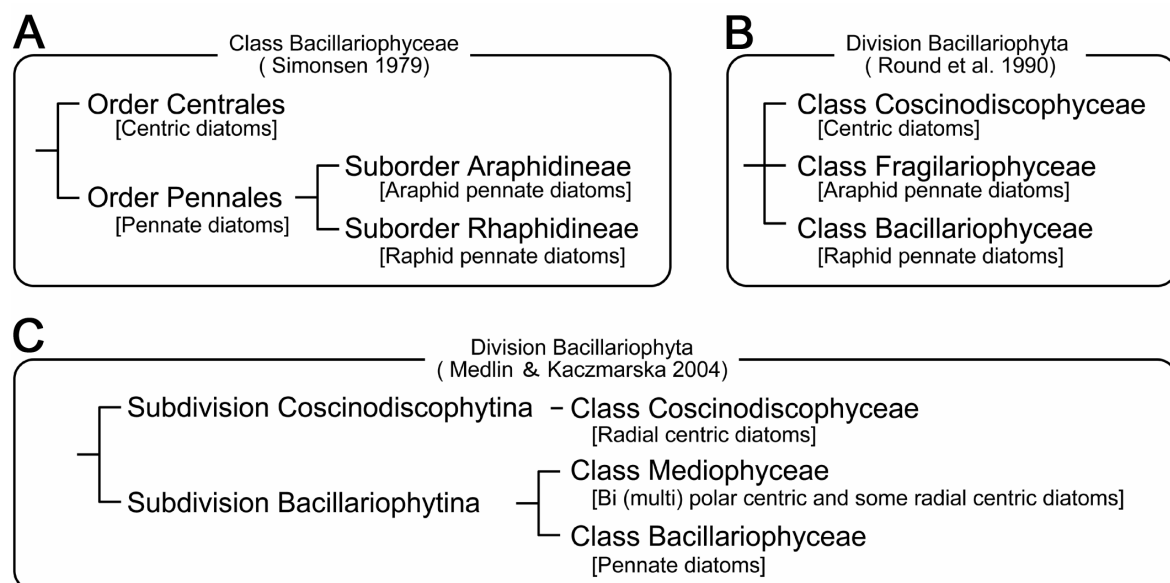


Fig. 2. Previous and current systems of diatoms. (A) Example of bipartition system presented by Simonsen (1979). (B) Tripartition system proposed by Round et al. (1990). Note araphid and raphid diatoms are equally treated to centrics. (C) Phylogeny based system recently revised by Medlin and Kaczmarska (2004). Note centrics are not natural group, and araphid and raphid diatoms lost their own status.

1.2. Molecular phylogeny – The problematic ‘araphid’ diatoms

Molecular phylogenetic approaches were introduced into diatom systematics by Medlin et al. (1988, 1991). They used the nuclear-coded small subunit (SSU) of ribosomal DNA (a.k.a. 18S rDNA) as a phylogenetic marker. There are some reasons why the SSU rDNA is still being used in the field of eukaryotic phylogeny, such as: 1) it is universally distributed in all eukaryotes; 2) its multi-copy nature facilitates PCR amplification; and 3) it contains slowly and

highly variable regions, making it possible to study both distantly and closely related group of organisms, respectively.

The diatoms undoubtedly belong to heterokont algae, which are characterized by chlorophylls *a* and *c*, and two heterodynamic flagella. The apically inserted flagellum bears tripartite mastigonemes (Andersen 2004). Although the internal phylogenetic relationships of heterokonts remains unresolved, it is clear that the bolidophytes are the closest relatives of the diatoms (Guillou et al. 1999).

Phylogenetic studies of diatoms using molecular markers have revealed that the centrics were paraphyletic, whereas the pennates were monophyletic (see review in Mann and Evans 2007), except highly elongated diatom *Toxarium*, which belongs to mediophycean lineage and acquired its elongated valve independently from pennate lineage (Kooistra et al. 2003). The validity of the class Mediophyceae has been argued (e.g., Alverson and Theriot 2005; Sorhannus 2004, 2007; Williams and Kociolek 2007) because the group sometimes appears paraphyletic in molecular phylogenies; however, this intensive debate has only used the nuclear-coded small subunit ribosomal DNA analyses because of the paucity of data from other gene markers. The class Bacillariophyceae is, in contrast to the problematic Mediophyceae, recovered as well-supported monophyly in all SSU rDNA phylogenies published in the past (Mann and Evans 2007). Most of the molecular phylogenetic studies of diatoms showed araphid diatoms to be paraphyletic (e.g., Medlin and Kaczmarska 2004; Alverson et al. 2006; Sorhannus 2007). Indeed, although there are some common morphological characters, i.e., an elongate valve with a central or slightly lateral sternum, apical pore fields and often with apical labiate processes, these are not strictly seen in all araphid diatoms and there are many exceptions. Thus, araphid diatoms are, like the invertebrates and the cryptogams in animal and plant systematics, respectively, a dump for all pennates lacking a raphe.

Taxonomically, araphid diatoms have long been neglected, perhaps because of their morphological simplicity; according to Round et al. (1990), 'in many ways the classification of the araphid group is the most difficult, because unlike the centric series their valve structure is rather simple, and unlike the raphid series the plastids and their arrangements have few distinguishing features'. Thus, in spite of their high abundance, the defining features of the main groups of araphid diatoms are not fully established. Araphid diatoms are also important components of coastal assemblages, particularly among communities attached to macrophytes and macroalgae, animals, rocks and sand-grains (Round et al. 1990). Along the coasts of Japan, for instance, epiphytic araphid diatoms are often dominant on the thalli of *Porphyra* spp. that are cultivated e.g., for nori production. Such attached diatoms consume nutrients around the *Porphyra* and also change the colour and taste of nori so that its value is reduced (Ohgai et al. 1988); they are therefore regarded as nuisance algae. An understanding of the nature of araphid diatoms may therefore be valuable for industry, as well as having biological interest.

1.3. Life history and auxospores

In most diatoms, a progressive diminution of cell size occurs with vegetative divisions because daughter cells are formed inside the mother cell (Round et al. 1990). The typical life cycle of a diatom is shown in Fig. 3. When a certain size is reached and if environmental conditions are suitable, gametogenesis is triggered; the successful fusion of gametes results in a zygote, termed the auxospore, which then expands in volume. In turn, the expanded auxospore gives rise to an initial cell, which is the largest cell of the life cycle, thus restoring the cell size to a maximum characteristic of the species or population (Edlund and Stoermer 1997; Round et al. 1990).

In the past 40 years, information about auxospore structure has greatly increased particularly with the advent of SEM (e.g., Crawford 1974; von Stosch 1982; Mann 1982; Cohn et al. 1989; Mann 1989; Kaczmarska et al. 2000, 2001; Schmid and Crawford 2001; Nagumo 2003; Amato et al. 2005; Tiffany 2005; Toyoda et al. 2005, 2006; Pouličková and Mann 2006; Pouličková et al. 2007). Although it has become clear that some aspects of the fine structure of auxospores have phylogenetic significance at higher taxonomic levels (e.g., Medlin and Kaczmarska 2004); there is still insufficient information to reveal how the structure and development of auxospores have evolved in the major diatom groups. In fact, of the 33 diatoms listed in their paper (Table 2 in Medlin and Kaczmarska 2004), only one araphid diatom was included (*Rhabdonema*) and this was based on LM observations, making it impossible to discuss on the evolutionary relationship of auxospores among araphid diatoms.

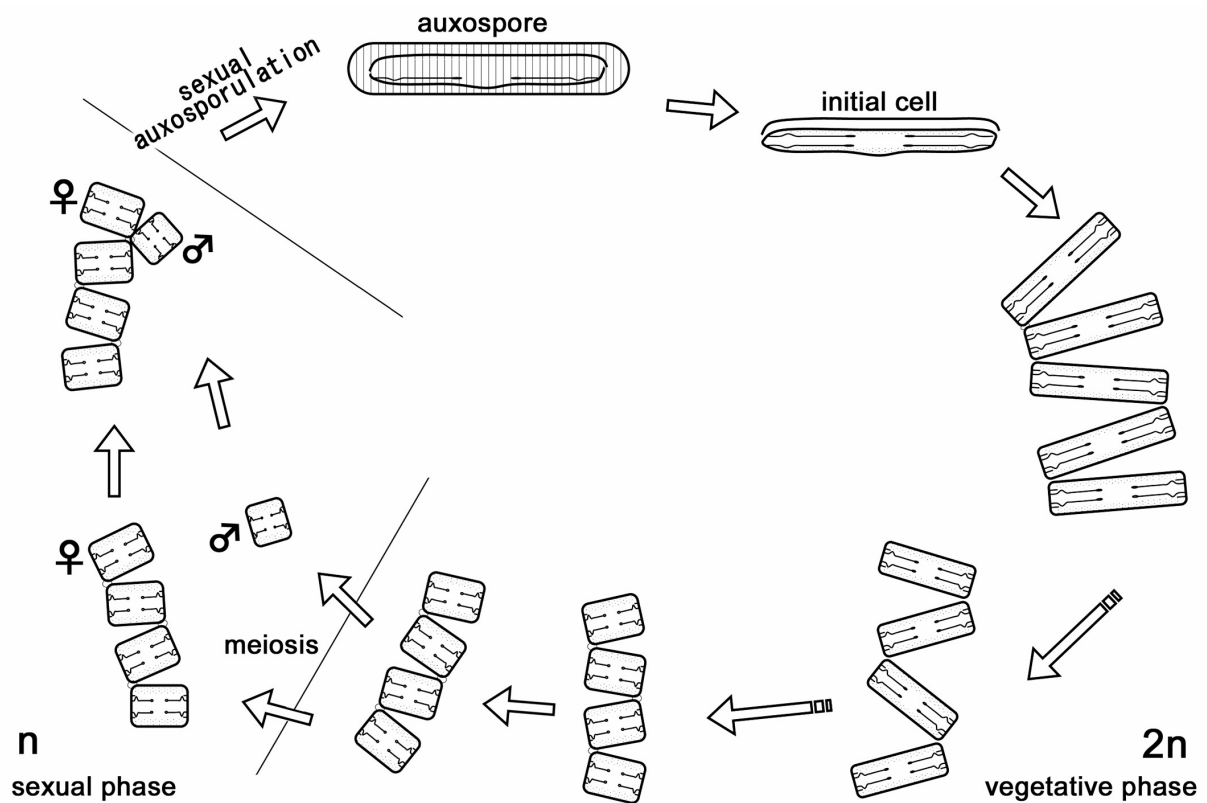


Fig. 3. Life cycle of diatoms. (see also p. 49, fig. 51 in Publication III)

1.4. Aim of the thesis

The topic of this thesis is an investigation into the evolution of ‘araphid’ diatoms. The aim was to obtain a more complete picture of the natural history of this problematic group of diatoms using molecular phylogeny and comparative morphology, particularly using details of auxospore structure. Morphological comparison was undertaken on carefully manipulated specimens, which made it possible to observe rare events (e.g., auxospore formation) under SEM. Furthermore, I also focused on the observation of living cells, which had largely been neglected in diatom studies presumably because of the difficulty of keeping strains in culture over a long time (Chepurnov et al. 2004). For the molecular work, LSU rDNA, *rbcL* and *psbA* genes were newly explored to establish the diatom phylogeny in addition to the SSU rDNA which is widely used in the phylogenetic research of diatoms as a standard marker. Finally, the divergence time of pennates was estimated using both sequence and fossil information.

1.5. Outline of the thesis

Living specimens of *Licmophora hyalina* were observed in **Publication I**, in which an unexpected motility of this araphid diatom was reported, implying the involvement of its labiate process in a gliding movement. In **Publication II**, five species of the marine epiphytic genus *Grammatophora* were observed with SEM to reveal the fine-structural details of each species. The comparative morphological examinations had never been undertaken in the genus so far. Of five species observed in the paper, I then selected one cosmopolitan species, *Grammatophora marina*, to study life cycle of the species based on culture strains as well as natural specimens (**Publication III**). In this paper, unexpected complexity of the life cycle was reported in the species and the fine-structure of auxospore was also reported. The auxospores of other araphid diatoms were examined in detail with SEM in *Gephyria media* (**Publication IV**), *Tabularia parva* (**Publication V**) and *Pseudostriatella oceanica* (**Publication VI**). The latter genus, *Pseudostriatella*, was described in the paper based on morphological features as well as SSU rDNA phylogeny, which placed it as the sister genus to *Striatella*. In **Publication VII**, a new araphid genus, *Plagiostriata*, was described based on the combination of morphology and SSU rDNA phylogeny. The family Plagiogrammaceae was then re-examined in **Publications VIII** and **IX**. Detailed SEM observations of the four Plagiogrammacean diatoms were undertaken in **Publication VIII**, and a new genus *Psammogramma* was described. The establishment of this genus was also supported by the phylogenetic analyses of the partial LSU rDNA sequences. An additional new plagiogrammacean genus, *Psammoneis*, was described in **Publication IX**, which used both SSU and the partial LSU rDNA sequences as molecular markers. In this paper, three distinct genotypes were detected in LSU rDNA and subsequent morphometric analyses supported this separation. Thus, three species were described in the new genus *Psammoneis*. In **Publication X**, first I summarized previous SSU rDNA based phylogenies using the supertree method showing that araphid diatoms were certainly paraphyletic and could be divided into several subclades, which were supported by morphological and/or ecological features. Then multi-gene markers (SSU and LSU rDNA from the nuclear, *rbcL* and *psbA* from the plastid genome) were used to reconstruct the phylogeny of diatoms, suggesting the taxonomical revision of pennates into three subgroups, basal and core araphid, and raphid diatoms. Finally, the divergence time of pennates was estimated by the Bayesian method with multiple age calibration with fossil records. This revealed that the early radiation of pennates into three major subclades took place over a short time; although no geographical event possibly driving in the diversification could be determined.

The other publications, **Publications XI** and **XII**, can be found at the end of this thesis, in the section Appendix. **Publication XI** proved that the highly elongated mediophycean diatoms (*Ardissonea*, *Climacosphenia* and *Toxarium*) acquired their shape independently from pennates based on SSU rDNA phylogeny. I reviewed the recent phylogenetic study of diatoms in **Publication XII**, which was printed in a non-peer-reviewed Japanese journal.

2. PUBLICATION

2.1. List of publications with the statement of the candidate's contribution.

- I. Sato S, Medlin LK (2006) Note: Motility of non-araphid diatoms. *Diatom Research* 21: 473-477.

The concept was developed and the work was carried out by the candidate. The manuscript was written by the candidate in discussion with the co-author.

- II. Sato S, Nagumo T, Tanaka J (2004) Morphology and taxonomy of marine attached diatoms in genus *Grammatophora* Ehrenberg (Bacillariophyceae) in Japan. *The Japanese Journal of Phycology* 52: 183-187.

The concept was developed and the work was carried out by the candidate. T. Nagumo provided help concerning taxonomic background. The manuscript was written by the candidate in discussion with the co-authors.

- III. Sato S, Mann DG, Nagumo T, Tanaka J, Tadano T, Medlin LK (2008) Auxospore fine structure and variation in modes of cell size changes in *Grammatophora marina* (Bacillariophyta). *Phycologia* 47: 12-27.

The concept was developed and the work was carried out by the candidate. T. Tadano provided the Japanese specimen. The manuscript was written by the candidate in discussion with the co-authors.

- IV. Sato S, Nagumo T, Tanaka J (2004) Auxospore formation and initial cell in the marine araphid diatom *Gephyria media* (Bacillariophyceae). *Journal of Phycology* 40: 684-691.

The concept was developed and the work was carried out by the candidate. The manuscript was written by the candidate in discussion with the co-authors.

- V. Sato S, Kuriyama K, Tadano T, Medlin KL (2008) Auxospore fine structure in a marine araphid diatom *Tabularia parva*. *Diatom Research* (in press)

The concept was developed and the work was carried out by the candidate. T. Tadano provided the Japanese specimen. K. Kuriyama provided help concerning taxonomic background. The manuscript was written by the candidate in discussion with the co-authors.

- VI. Sato S, Mann DG, Matsumoto S, Medlin LK (2008) *Pseudostriatella pacifica* gen. et sp. nov. (Bacillariophyta); a new araphid diatom genus and its fine-structure, auxospore and phylogeny. *Phycologia* 47: 371-391.

The concept was developed and the work was carried out by the candidate. S. Matsumoto provided the Japanese specimen. The manuscript was written by the candidate in discussion with the co-authors.

- VII. Sato S, Matsumoto S, Medlin LK (2008) Fine structure and SSU rDNA phylogeny of a marine araphid pennate diatom *Plagiostriata goreensis* gen. et sp. nov. (Bacillariophyta). Phycological Research (in press)

The concept was developed and the work was carried out by the candidate. S. Matsumoto provided the Senegalese specimen. The manuscript was written by the candidate in discussion with the co-authors.

- VIII. Sato S, Watanabe T, Crawford RM, Kooistra WHCF, Medlin LK (2008) Morphology of four plagiogrammeacean diatoms; *Dimeregramma minor* var. *nana*, *Neofragilaria nicobarica*, *Plagiogramma atomus* and *Psammogramma vigoensis* gen. et sp. nov., and their phylogenetic relationship inferred from partial LSU rDNA. Phycological Research (in press)

The concept was developed and the work was carried out by the candidate. T. Watanabe provided the Japanese specimen. W.H.C.F. Kooistra provided a partial LSU rDNA sequence of Talaroneis posidoniae. The manuscript was written by the candidate in discussion with the co-authors.

- IX. Sato S, Kooistra WHCF, Watanabe T, Matsumoto S, Medlin LK (2008) A new araphid diatom genus *Psammoneis* gen. nov. (Plagiogrammeaceae, Bacillariophyta) with three new species based on SSU and LSU rDNA sequence data and morphology. Phycologia (in press)

The concept was developed and the work was carried out by the candidate. T. Watanabe and S. Matsumoto provided the Japanese and Senegalese specimen, respectively. The manuscript was written by the candidate in discussion with the co-authors.

- X. Sato S, Kooistra WHCF, Mayama S, Medlin LK (submitted) Phylogeny and divergence time of diatoms with special reference to the evolution of araphid diatoms inferred from multi-gene analyses. Molecular Phylogenetics and Evolution

The concept was developed and the work was carried out by the candidate. S. Mayama and W.H.C.F. Kooistra provided the DNA of Pseudohimantidium pacificum and Ardissonaea baculus, respectively. The manuscript was written by the candidate in discussion with the co-authors.

[In Appendix]

- XI. Medlin LK, Sato S, Mann DG, Kooistra WHCF (2008) Molecular evidence confirms sister relationship of *Ardissonaea*, *Climacosphenia* and *Toxarium* within the bipolar centric diatoms (Bacillariophyta, Mediophyceae) and cladistic analyses confirms that extremely elongated shape has arisen twice in the diatoms. Journal of Phycology (in press)

Sampling, sequencing and the part of phylogenetic calculation were carried out by the candidate. The part of manuscript was written by the candidate.

- XII. Sato S, Medlin LK (2006) Molecular phylogeny and evolution of the diatoms. Aquabiology 166: 477-483. (in Japanese with English abstract)

The concept was developed and the work was carried out by the candidate. The manuscript was written by the candidate in discussion with the co-author.

2.2. Publication I:

NOTE: MOTILITY OF NON-RAPHID DIATOMS

SHINYA SATO & LINDA K. MEDLIN

*Alfred Wegener Institute for Polar and Marine Research, Am Handelshafen 12, D-27570
Bremerhaven, Germany*

Abstract

Motility of the araphid diatom *Licmophora hyalina* was observed in cultured material. Gliding movement was nearly straight and only towards the broader pole, and the colonies rotated before settling. Although mucilage secretion was not observed with the light microscopy, the links between motility and the labiate process and/or the multiscissura are suggested. Other motile members in non-raphid (centric and araphid) diatoms are briefly reviewed. Several non-raphid species exhibit motility, suggesting that there might be more motile araphid diatoms.

Movements generated by the raphe are well known in raphid pennate diatoms. Hasle (1974) proposed that the raphe evolved from the labiate process based on ultrastructural observation under SEM. If the labiate process is precursor of the raphe, motility associated with labiate processes is very likely. Here we briefly refer some observations on non-raphid diatoms exhibiting motility.

The first report of motility in a centric diatom was in *Actinocyclus subtilis* (Gregory) Ralfs (Medlin *et al.* 1986). This diatom exhibited a forward movement as the cell rotated in the plane of the valve. Forward and rotational movements were not seen to reverse, although cells did stop and start again. Based on histochemistry and TEM, it was concluded that the motility was achieved by the secretion of mucopolysaccharides through the labiate processes. *Odontella sinensis* (Greville) exhibited continuous shuffling, rocking, and twitching movements without translocation and remained relatively fixed in position (Pickett-Heaps *et al.* 1986). From ultrastructural examination under TEM, Pickett-Heaps *et al.* (1986) concluded that the movements were an indirect result of active mucilage secretion through the labiate process. They also observed that mucilage secretion in *Ditylum brightwellii* (West) Grunow was similar to that in *O. sinensis*. A large aggregation of mucilage vesicles was found at the base of the labiate process; however, they did not detect any cellular movement in *D. brightwellii*.

There are several reports of motility in araphid diatoms. Motility was firstly observed in *Tabularia tabulata* (Agardh) Snoeijs (as *Synedra tabulata*) by Hopkins [We were unable to obtain Hopkins' Ph.D. thesis (1969), but the result was cited by Harper (1977)]. Pickett-Heaps *et al.* (1991) observed a gliding movement in *Ardissonaea crystallina* (Agardh) Kützing. This movement was reversible but basically straight forward, and it was associated with mucilage secretion from one end of the cell. The most distinct characteristic of this movement was the persistent bilinear trails visible on the slide after the cell passed. Kooistra *et al.* (2003) reported straight, bent and curved path movement by the pennate-like centric diatom *Toxarium undularum* Bailey. The long axis of the cell was not necessarily parallel to the direction of movement because only one tip of the cell was in contact with the substratum. The mucilage secreted at the valve mantle or girdle at the poles presumably confer motility in this species. In this report *Toxarium* was confirmed to be centric diatom with the support of both the 18S rDNA sequence and the morphological features, and the possibility that the motile genus *Ardissonaea* (mentioned above) also belongs to the centric lineage was suspected because *Toxarium* and *Ardissonaea* share the lack of some morphological characteristics, i.e. labiate processes, obvious apical pore fields and median sterna. At this moment any molecular sequence data of *Ardissonaea* is unavailable.

In the present study, a straight forward movement of solitary cells (Fig. 1) and a rotation of ball-like colonies (Figs 2-3) were observed in *Licmophora hyalina* (Kützing) Grunow. This highly polarized diatom exhibited gliding movement only towards the head (broader)

pole, suggesting that the movement might be associated with the mucilage secreted at the multiscissura [apical slit field at basal pole; see Honeywill (1998) for terminology] and/or labiate process at the basal pole of the valve. Movement was generated either in valve view or in girdle view. Mean gliding speed $1.7 \mu\text{m}\cdot\text{s}^{-1}$ in this species was almost the same as that of *Ardissonea* and *Toxarium* (Table 1). Movement was frequently modulated and maximum speed $3.8 \mu\text{m}\cdot\text{s}^{-1}$ was recorded for less than 10s. No trail was observed after movement with light microscopy (Fig. 1). Solitary cells were attached to the bottom of a culture dish by a mucilage pad, and when they were harvested and placed onto a slide, movement then began. Sometimes many cells were attached to each other at the basal pole making the ball-like colony in the culture dish (Figs 2-3). The ball-like colonies, which reminded us of the spirally arranged scales which form in the *Synura* Ehrenberg (Chrysophyta), also exhibited motility, in the form of continuous rotation, with a reeling forward movement. The forward movement of this colony was somewhat unsteady and its speed was therefore not recordable. It is possible that colony movement was an artifact caused by fluid movement in the culture dish but even though some of our other culture strains (e.g., species of *Licmophora*, *Synedra* Ehrenberg, *Tabularia* Williams et Round) also formed ball-like colonies, rotation of the colonies was exclusive to this species. It was impossible to verify the movement because of the difficulty of maintaining a culture strain as noted by Mann & Chepurnov (2004), mainly due to the specific mode of their cell division, thus our strain of *L. hyalina* had already died off and therefore inaccessible.

In normal gliding movement of raphid diatoms, the raphe acts as the motility apparatus with a putative actin/myosin motor (Poulsen *et al.* 1999). Recently, Higgins *et al.* (2003) observed the mucilage tethers secreted from the raphe, and proposed that they had a major role in initial cell adhesion and reorientation. This may support the idea that the raphe and the labiate process are evolutionarily homologous, because the secretion from the labiate process to attach the species to the substratum was also reported in some centric species, e.g. *Melosira* Agardh (Crawford 1975) and *Aulacodiscus* Ehrenberg (Sims & Holmes 1983). In *Coscinodiscus wailesii* Gran et Angst, intimate and regular contacts between the plasma membrane and labiate processes and the inner face of the frustule was observed (Kühn & Medlin 2004, Schmid 1984). This contact suggests that, at least in this species, the labiate process plays an important role in their metabolism by connecting to the exterior environment through the cell wall.

Motility associated with mucilage secretion is widely seen in the other unicellular organisms, e.g. spores of Rhodophyta (Pickett-Heaps *et al.* 2001), Cyanophyta (Bold & Wynne 1978) and some desmids, e.g. *Closterium* Nitzsch, *Micrasterias* C Agardh (Bourrelly 1972), implying that mobility confers obvious advantages to their life. Once again we strongly recommend that diatomists study living cells before boiling with acid or extraction of DNA. There are still many more interesting observations to be made on living diatoms.

REFERENCES

- Bold, H. C. and Wynne, M. J. (1978). *Introduction to the Algae*. 706 pp. Prentice-Hall, Inc., Englewood Cliffs, New Jersey.
- Bourrelly, P. (1972). *Les Algues d'eau douce. Initiation à la Systématique, I. Les Algues Vertes*. 572 pp. N. Boubée & Cie, Paris.
- Crawford, R. M. (1975). The frustule of the initial cells of some species of the diatom genus *Melosira* C. Agardh. *Nova Hedwigia, Beiheft*, **53**, 37-50.
- Harper, M. A. (1977). Movements. In *The Biology of Diatoms*, (D. Werner, ed.), 224-249. Blackwell Scientific Publications, Oxford.

- Hasle, G. R. (1974). The mucilage pore of pennate diatoms. *Nova Hedwigia*, **45**, 167-186.
- Higgins, M. J., Molino, P., Mulvaney, P. & Wetherbee, R. 2003. The structure and nanomechanical properties of the adhesive mucilage that mediates diatom-substratum adhesion and motility. *Journal of Phycology*, **39**, 1181-1193.
- Honeywill, C. (1998). A study of British *Licmophora* species and a discussion of its morphological features. *Diatom research*, **13**, 221-271.
- Hopkins, J. T. (1969). Diatom motility: its mechanism, and diatom behaviour patterns in estuarine mud. Ph.D. Thesis University of London, pp.1-251.
- Kooistra, W. H. C. F., De Stefano, M., Mann, D. G., Salma, N. & Medlin, L. K. (2003). Phylogenetic position of *Toxarium*. A pennate-like lineage within centric diatoms (Bacillatiophyceae). *Journal of Phycology*, **39**, 185-197.
- Kühn, S. & Medlin, L. K. (2004). Diatom plasma membranes: Internalisation and recycling in living cells. 18th International Diatom Symposium, Międzyzdroje, Abstract, p.126.
- Mann, D. G. & Chepurnov, V. 2004. What have the Romans ever done for us? The past and future contribution of culture studies to diatom systematics. *Nova Hedwigia*, **79**, 237-291.
- Medlin, L. K., Crawford, R. M. & Andersen, R. A. (1986). Histochemical and ultrastructural evidence for the function of the labiate process in the movement of centric diatoms. *British Phycological Journal*, **21**, 297-301.
- Pickett-Heaps, J. D., Hill, D. R. A. & Wetherbee, R. (1986). Cellular movement in the centric diatom *Odontella sinensis*. *Journal of Phycology*, **22**, 334-339.
- Pickett-Heaps, J. D., Hill, D. R. A. & Blaze, K. L. (1991). Active gliding motility in an araphid marine diatom, *Ardissonea* (formerly *Synedra*) *crystallina*. *Journal of Phycology*, **27**, 718-725.
- Pickett-Heaps, J. D., West, J. A., Wilson, S. M. and McBride, D. L. 2001. Time-lapse video-microscopy of cell (spore) movement in red algae. *European Journal of Phycology*, **36**, 9-22.
- Poulsen, N. C., Spector, I., Spurck, T. P., Schultz, T. F. & Wetherbee, R. 1999. Diatom gliding is the result of an actin-mosin motility system. *Cell Motility and the Cytoskeleton*, **44**, 23-33.
- Schmid, A.-M. M. (1984). Wall morphogenesis in *Thalassiosira eccentrica*: comparison of auxospore formation and the effects of MT-inhibitors. In: *Proceedings of the 7th International Diatom Symposium, Philadelphia 1982* (D.G. Mann, ed.), pp. 47-70. Otto Koeltz, Koenigstein.
- Sims, P. A. & Holmes, R. W. (1983). Studies on the "kittonii" group of *Aulacodiscus* species. *Bacillaria*, **6**, 267-292.

Table 1. Comparison of movement speed ($\mu\text{m}\cdot\text{s}^{-1}$) in non-raphid diatoms.

Species	Mean	Max	References
<i>Tabularia tabulata</i> ^a	0.1 - 1	-	Hopkins (1969)
<i>Actinocyclus subtilis</i>	ca 1	-	Medlin et al. (1986)
<i>Ardissonaea crystallina</i>	1 - 2	2.6	Pickett-Heaps et al. (1991)
<i>Toxarium undulatum</i>	0.5 - 2	ca 6 ^b	Kooistra et al. (2003)
<i>Licmophora hyalina</i>	1.7	3.8	This study

^aAs *Synedra tabulata*

^bMaximum average for 1 min was $3.5 \mu\text{m}\cdot\text{s}^{-1}$

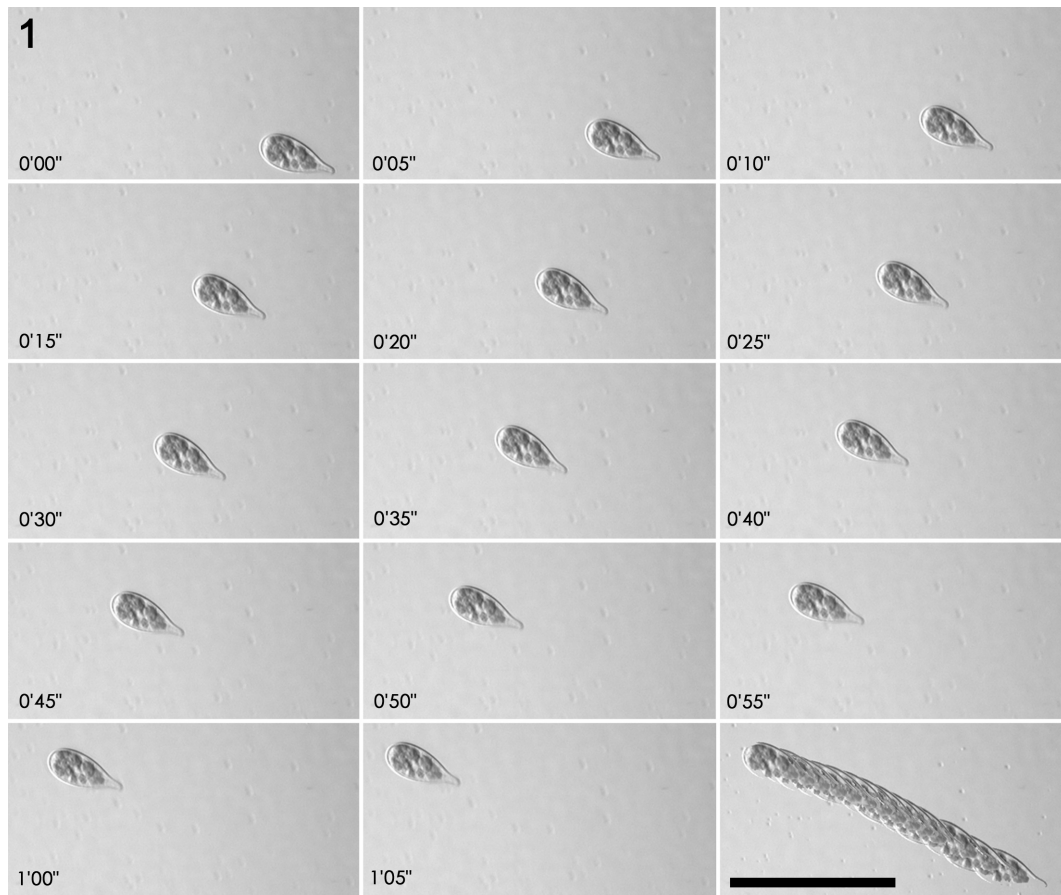
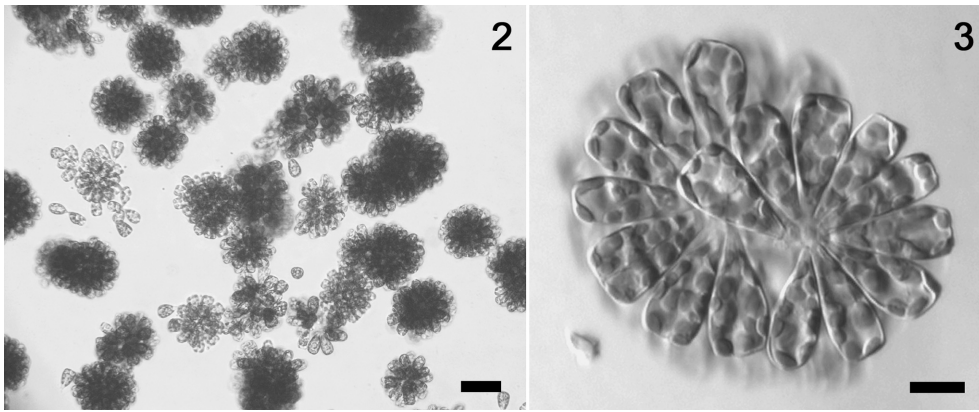


Fig. 1. Time-lapse sequence for a movement of *Licmophora hyalina* during a total of 1 min 05 sec. Overlain images (right bottom) showing nearly straight line, and the movement in the time period between 0'00" and 0'15" was faster than afterwards. Note no trail is seen after the cell passed. Scale = 100 μ m.



Figs 2-3. Light micrographs of *Licmophora hyalina* **Fig. 2.** Ball-like colonies and attached cells in culture vessel. Scale = 50 μ m. **Fig. 3.** Enlargement of a ball-like colony showing cells attached to each other at the basal pole. Scale = 10 μ m.

2.3. Publication II:

Morphology and taxonomy of five marine attached diatoms in the genus *Grammatophora* Ehrenberg (Bacillariophyceae) in Japan

SHINYA SATO,¹ TAMOTSU NAGUMO² & JIRO TANAKA¹

¹*Tokyo University of Fisheries, Konan 4-5-7, Minato-ku, 108-8477 Tokyo, Japan*

²*The Nippon Dental University, Fujimi 1-9-20, Chiyoda-ku, 102-8159 Tokyo, Japan*

Abstract

Five marine attached diatoms in the genus *Grammatophora*, *G. angulosa* Ehrenberg, *G. hamulifera* Kützing, *G. marina* (Lyngbye) Kützing, *G. oceanica* Ehrenberg and *G. subtilissima* Ralfs were collected from littoral regions in Japan. They were observed using light and scanning electron microscopy with the bleaching method. The common characteristics among them were 1) septum of valvocopula, 2) plaques on the abvalvar edge of the valvocopula, 3) open copulae except valvocopula, 4) prominent areas of areolae around both apices of the valvocopula, 5) rimoportulae arranged on the apical axis. Differences among species were found in spines on the apical pore field, areolae on the copula, the shape of areolae on the apices of the valvocopula.

KEY WORDS: diatom, fine structure, *Grammatophora*, *G. angulosa*, *G. hamulifera*, *G. marina*, *G. oceanica*, *G. subtilissima*, morphology, taxonomy.

INTRODUCTION

The genus *Grammatophora* was established by Ehrenberg (1839) and composed of 47 species (VanLandingham 1971), and it is characterized by the conspicuous septum. Species of the genus secrete mucilaginous substances from apical pore fields at both ends of valve and their cells are joined with each other to make a zig-zag colony. The taxonomic characteristics used at the rank of species have been the shape of septum and valve, and the density of striae. However, distinction of each species is difficult by light microscopy (LM). Therefore, five species of *Grammatophora* spp. were observed mainly by scanning electron microscopy (SEM).

MATERIALS AND METHOD

The populations of *Grammatophora* obtained on seaweeds collected from the littoral regions in Japan at the following localities:

***Grammatophora angulosa* Ehrenberg**

Kiritappu, Hamanaka Town, Hokkaido Pref., 31. vii. 2001. Epiphytic on *Neoptilota asplenoides* (Esper) Kylin (Ceramiaceae, Rhodophyceae) collected by A. Kobayashi (sample no. ss-0023).

***G. hamulifera* Kützing**

Shirahama, Shimoda City, Shizuoka Pref., 19. iii. 2002. On an artificial substratum collected by S. Sato (ss-0016).

***G. marina* (Lyngbye) Kützing**

Nojima-kouen, Yokohama City, Kanagawa Pref., 27. xi. 2000. Epiphytic on *Polysiphonia urceolata* (Lightfoot) Greville (Rhodomelaceae, Rhodophyceae) collected by A. Kobayashi (ss-0003).

***G. oceanica* Ehrenberg**

Toyama Prefectural Fisheries Research Institute, 25. iii. 2002. In a tank filled with deep sea water, collected by T. Nagumo (ss-0027).

***G. subtilissima* Ralfs**

Douno-ura, Naruto City, Tokushima Pref., 15. xi. 2001. Epiphytic on *Caulerpa okamurai* W. v. Bosse (Caulerpaceae, Ulvophyceae) collected by S. Sato (ss-0007).

All materials were cleaned using the bleaching method (Nagumo 1995). For LM, mounting media as MGK-S (MATSUNAMI) or Mountmedia (WAKOH) was used. For SEM, cleaned material was dried on glass cover slips and coated with platinum-palladium. Specimens were observed using a HITACHI S-4000 SEM.

RESULTS AND DISCUSSION

The common characteristics among five species of *Grammatophora* were follows; 1) each valvocopula has two septa (Figs 21, 23, 25, 27, 29), 2) plaques are present on the abvalvar edge of the valvocopula (Figs 11, 13, 15, 17, 19), 3) copulae are open bands, while valvocopula is closed one (Figs 11, 13, 15, 17, 19), 4) prominent areas of areolae are present around apices of the valvocopula (Figs 12, 14, 16, 18, 20), 5) rimoportulae are arranged on the apical axis (Figs 22, 24, 26, 28, 30).

***Grammatophora angulosa* Ehrenberg 1839 (Figs 1a, b, 2, 11, 12, 21, 22)**

Valves narrow elliptic to lanceolate, 8.0-73.5 μm long, 4.0- 7.5 μm wide. Striae parallel, 12-15 in 10 μm . A cingulum is composed of three to five copulae. The valvocopula bears undulated and hook-shaped septa at the end. The areola of the valvocopula is circular, the copulae are plain.

***G. hamulifera* Kützing 1844 (Figs 3a, b, 4, 13, 14, 23, 24)**

Valves narrow elliptic to lanceolate, 15.0-42.5 μm long, 7.0- 7.5 μm wide. Striae parallel, 17-18 in 10 μm . Striae parallel. A cingulum is composed of three to four copulae. The valvocopula bears hook-shaped septa at the both ends. The areola of the valvocopula is circular. The copulae are plain.

***G. marina* (Lyngbye) Kützing 1844 (Figs 5a, b, 15, 16, 25, 26)**

Valves linear with capitate apices to lanceolate, 9.5-82.5 μm long, 4.0-7.0 μm wide. Striae quincunx, 23-25 in 10 μm . Cingulum is composed of three to five copulae. The valvocopula bears flat septa curved near the valve ends. The areola of the valvocopula is elongated. The copulae have rows of areolae. Sometimes spines are present on the apical pore field.

***G. oceanica* Ehrenberg 1839 (Figs 7a, b, 8, 17, 18, 27, 28)**

Valves linear with capitate apices to lanceolate, 18.0-71.0 μm long, 4.5-6.0 μm wide. Striae quincunx, 25-28 in 10 μm . Cingulum is composed of three to four copulae. The valvocopula bears flat septa curved near the valve ends. The areola of the valvocopula is circular to elongated. The copulae have rows of areolae. Sometimes spines are present on the apical pore field (not shown).

***G. subtilissima* Ralfs 1861 (Figs 9a, b, 10, 19, 20, 29, 30)**

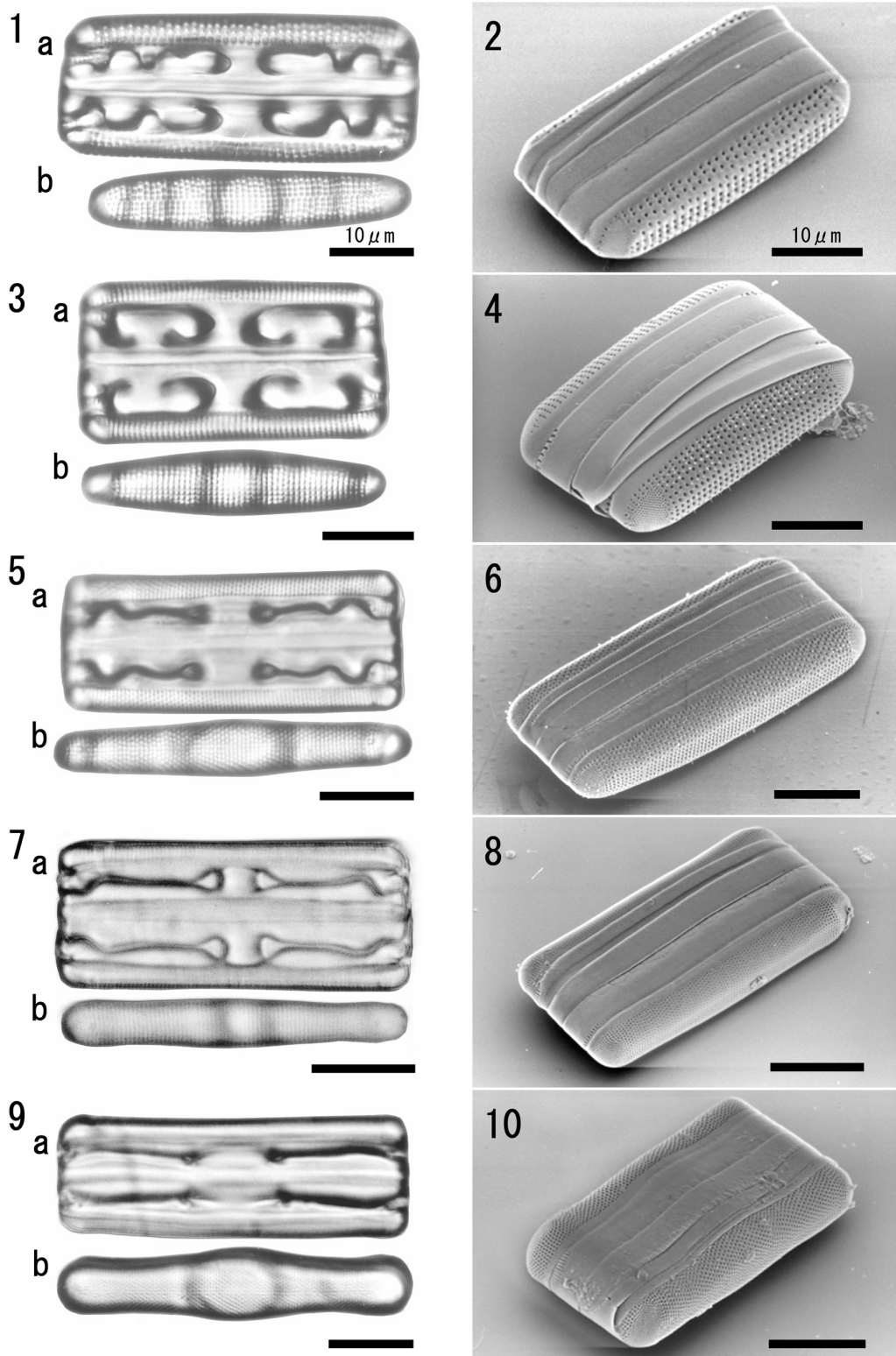
Valves narrow elliptic with capitate apices, 18.5-83.0 μm long, 7.5-9.0 μm wide. Striae quincunx, 32-33 in 10 μm . Cingulum is composed of three to five copulae. The valvocopula bears mostly flat septa. The areola of the valvocopula is elongated. The copulae have rows of areolae. Sometimes spines are present on the apical pore field.

Although the densities of striae are slightly different between *G. angulosa* and *G. hamulifera*, it is sometimes difficult to distinguish two species especially in small cells. No ultrastructural differences between *G. angulosa* and *G. hamulifera* were detected in this study. Further studies are necessary to clarify the species definition of these species, especially for the type species of the genus, *G. angulosa*.

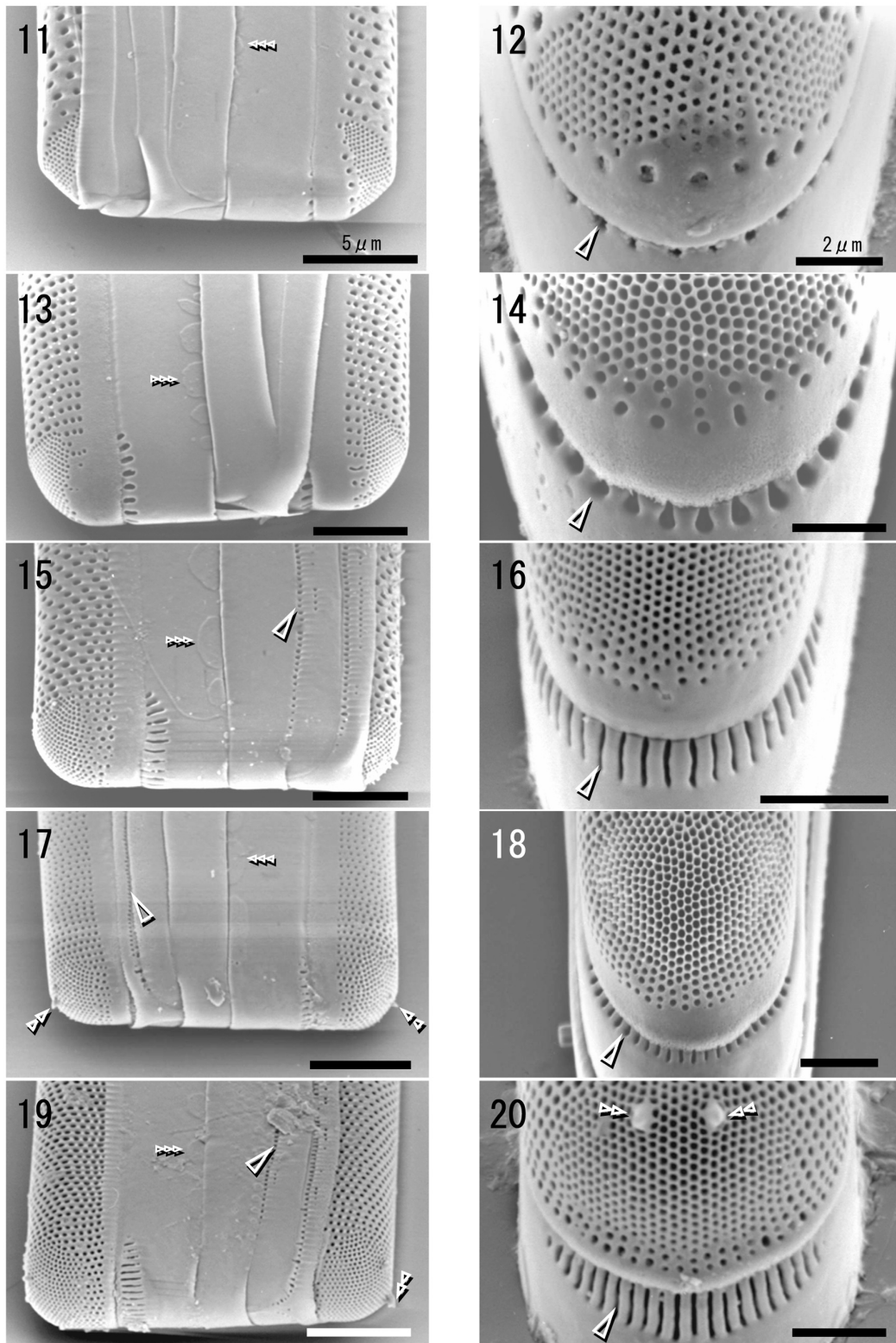
This is the first comparative study based on the fine structure of the genus *Grammatophora*. A few characteristics (i.e. spines on the apical pore field, areolae on the copula, the shape of areolae on the apices of the valvocopula) are useful as criteria at the rank of species.

REFERENCES

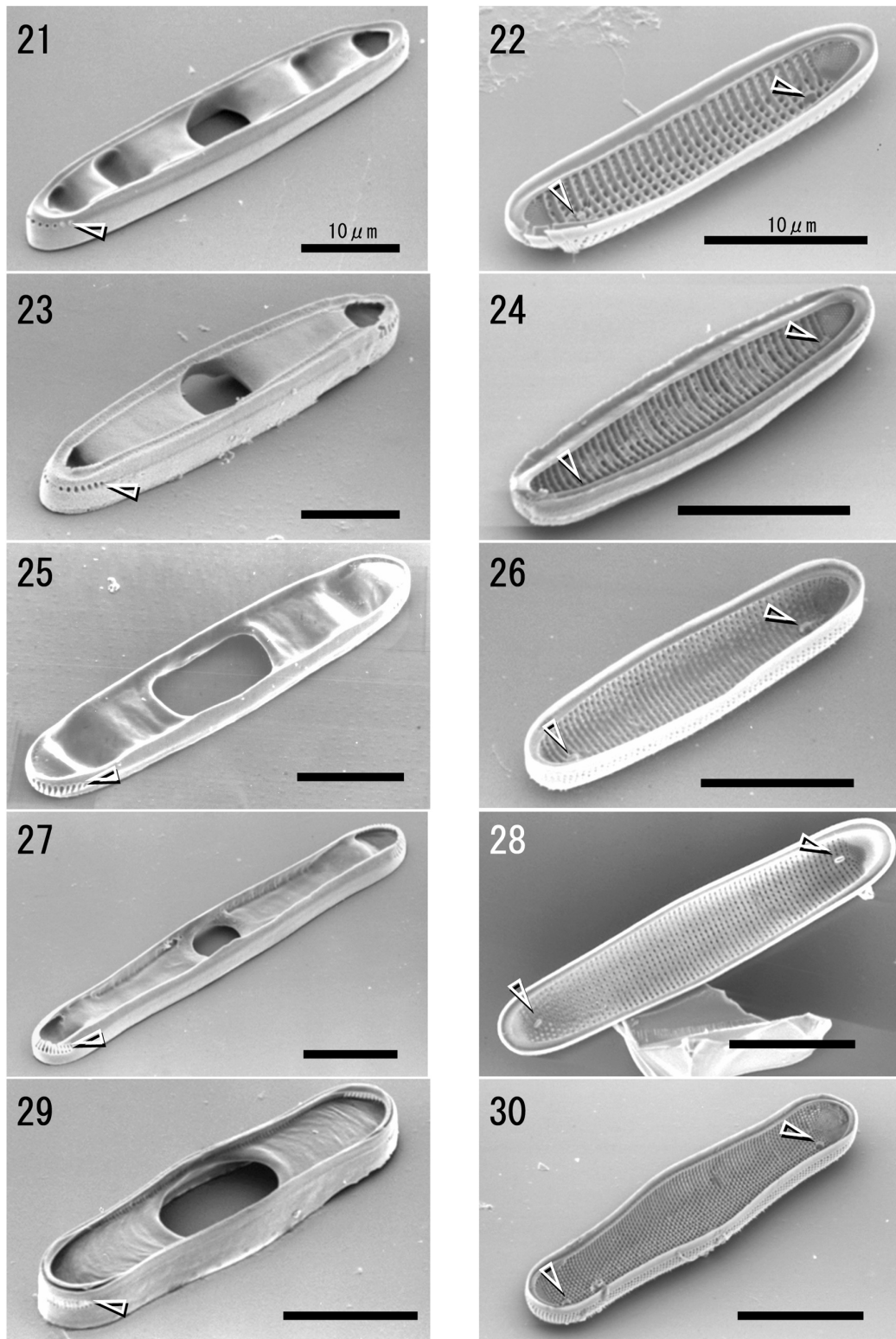
- Ehrenberg, C. G. 1839. *Über nach jetzt zahlreich lebende Thierarten der Kreidebildung und den Organismis der Polythalamien*. Abh. k. Akad. Wiss. Berlin, pp. 126-54.
- Kützing, F. T. 1844. *Die Kieselschaligen Bacillarien oder Diatomeen*. Nordhausen. pp. 128-9.
- Nagumo, T. 1995. Simple and safe cleaning methods for diatom samples. *Diatom* **10** : 88.
- Ralfs, J. 1861. The family diatomeae or diatomaceae. In A. Pritchard. (Eds) *A history of infusoria*. Whittaker and Co. London, pp. 807-809.
- VanLandingham, S. L. 1971. *Catalogue of the fossil and recent genera and species of diatoms and their synonyms. Part. IV. Fragilaria through Naunema*. Cramer Lehre, Germany, pp. 1966-90.



Figs 1-10. *Grammatophora* spp. 1-2. *G. angulosa*. 3-4. *G. hamulifera*. 5-6. *G. marina*. 7-8. *G. oceanica*. 9-10. *G. subtilissima*. 1a, 3a, 5a, 7a, 9a. Girdle view of a frustule, LM. 1b, 3b, 5b, 7b, 9b. Valve view of a frustule, LM. 2, 4, 6, 8, 10. Oblique view of a frustule, SEM.



Figs 11-20. Scanning micrographs of *Grammatophora* spp. 11-12. *G. angulosa*. 13-14. *G. hamulifera*. 15-16. *G. marina*. 17-18. *G. oceanica*. 19-20. *G. subtilissima*. 11, 13, 15, 17, 19. Girdle view of frustule showing rows of areolae on copulae (arrowheads), spines on the apical pore field (double arrowheads) and plaques on valvocopula (triple arrowheads). 12, 14, 16, 18, 20. Polar view of the valvocopula showing prominent area of the areolae (arrowheads) and spines on apical pore field (double arrowheads).



Figs 21-30. Scanning micrographs of *Grammatophora* spp. 21-22. *G. angulosa*. 23-24. *G. hamulifera*. 25-26. *G. marina*. 27-28. *G. oceanica*. 29-30. *G. subtilissima*. 21, 23, 25, 27, 29. Internal view of each valvocopula showing septa and areolae (arrowheads). 22, 24, 26, 28, 30. Internal view of each valve showing the rimoportulae (arrowheads).

2.4. Publication III:

Auxospore fine structure and variation in modes of cell size changes in *Grammatophora marina* (Bacillariophyta)

SHINYA SATO^{1*}, DAVID G. MANN², TAMOTSU NAGUMO³, JIRO TANAKA⁴, TOMOYA TADANO⁵ &
LINDA K. MEDLIN¹

¹*Alfred Wegener Institute for Polar and Marine Research, Am Handelshafen 12, D-27570
Bremerhaven, Germany*

²*Royal Botanic Garden, Edinburgh EH3 5LR, Scotland, UK*

³*The Nippon Dental University, 1-9-20 Fujimi, Chiyoda-ku, 102-8159 Tokyo, Japan*

⁴*Tokyo University of Marine Science and Technology, 4-5-7 Konan, Minato-ku, 108-8477
Tokyo, Japan*

⁵*Doris Japan co. ltd., 2-34-24 Izumihoncho, Komae-City, Tokyo, Japan*

Abstract

Examination of *Grammatophora marina* from rough and clonal cultures showed that cell size changes were more flexible than is generally reported for diatoms. Allogamous sexual auxosporulation took place through copulation between small male cells and larger female cells, but only in mixed rough culture and never in clonal cultures. Auxospores were also formed without copulation in clonal cultures ('uniparental auxosporulation') and these, like sexual auxospores, developed through formation of a perizonium, which consisted of a series of transverse bands. All of these bands, including the primary band, were open. Circular scales were present in the auxospore wall before initiation of perizonium formation and irregular, elongate structures lined the suture of the transverse perizonium. Perizonium and scales resembled those of another araphid pennate diatom, *Gephyria media*. Initial cells were formed within the perizonium and consisted of an initial epivalve with a simplified structure, an initial hypovalve (formed beneath the perizonium suture) and a third, normally-structured valve formed beneath the epivalve; the epivalve was then sloughed off. Initial cells of similar configuration but often aberrant morphology could also be formed through expansion from vegetative cells, without involvement of a perizonium. Vegetative cells were also capable of limited enlargement through simple expansion without formation of an initial cell, and abrupt size reduction. Cell size ranges in populations from different regions suggest that *G. marina* may contain pseudocryptic species.

KEY WORDS: Abrupt cell size reduction, Auxospore, Diatoms, Fine structure, *Grammatophora marina*, Life cycle, Perizonium, Scales, Vegetative cell enlargement

INTRODUCTION

In most diatoms, a progressive diminution of cells in size occurs with vegetative divisions. When a certain size is reached and if environmental conditions are suitable, gametogenesis is triggered; the successful fusion of gametes results in a zygote, termed the auxospore, which then expands in volume. In turn, the expanded auxospore gives rise to an initial cell, which is the largest cell of the life cycle, thus restoring cell size to a maximum characteristic of the species or population (Edlund & Stoermer 1997; Round *et al.* 1990). This diatom-specific mode of life cycle is well known (e.g. Bold & Wynne 1985; South & Whittick 1987), but there are exceptions: 1) several diatoms are known to be able to increase cell size without auxosporulation, and 2) abrupt cell size reduction can occur (Chepurnov *et al.* 2004). Geitler (1932) proposed that there are cardinal points in the life history of a diatom, characterized by particular cell sizes and marked by physiological and/or cytological changes in the cells (see also Chepurnov *et al.* 2004). In this study, an araphid diatom, *Grammatophora marina* (Lyngbye) Kützing, was examined in culture to investigate its life-cycle.

Grammatophora Ehrenberg is a genus of marine araphid diatoms, whose cells attach to each other by mucilage pads to form zig-zag colonies (Sato *et al.* 2004a; Round *et al.* 1990). *G. marina* is a cosmopolitan species in coastal areas, and is often abundant (Witkowski *et al.* 2000). Along the coasts of Japan, for instance, this species is sometimes dominant on the thalli of *Porphyra* spp. that are cultivated e.g. for nori production. Such attached diatoms consume nutrients around the *Porphyra* and also change the colour and taste of nori so that its value is reduced (Ohgai *et al.* 1988); they are therefore regarded as nuisance algae. An understanding of the life cycle of *G. marina* may therefore be valuable for industry, as well as having biological interest.

According to von Stosch & Drebes (1964, p. 211) sexual reproduction of *G. marina* occurs dioeciously and some features of auxosporulation have been described from natural populations by Karsten (1926), Lebour (1930) and Magne-Simon (1960, 1962). These authors showed that: (1) sexualized small cells become attached to a chain of large cells; (2) the small cells and the larger cells to which they are attached differentiate into gametangia; (3) each gametangium produces one gamete; (4) the smaller gametangia produce active 'male' cells, whereas the gametes produced by the large cells are passive ('female'); (5) fertilization occurs inside the female theca; (6) the auxospore expands by adding many transverse perizonial bands; and (7) the initial cells are formed inside the auxospores. These observations were made by light microscopy (LM). Magne-Simon (1962) studied Feulgen-stained material of natural populations and was able to demonstrate stages in meiosis, the expulsion of one nucleus into a small residual cell at meiosis I, and the degeneration of one daughter nucleus at meiosis II to leave a single functional nucleus in each mature gametangium. Fusion of the male and female nuclei took place soon after plasmogamy, before the auxospore expanded.

In the past 40 years, information about auxospore structure has greatly increased (e.g. Crawford 1974; von Stosch 1982; Mann 1982a; Cohn *et al.* 1989; Mann 1989; Kaczmarska *et al.* 2000, 2001; Schmid & Crawford 2001; Nagumo 2003; Sato *et al.* 2004b; Amato *et al.* 2005; Tiffany 2005; Toyoda *et al.* 2005, 2006; Pouličková & Mann 2006). However, although it has become clear that some aspects of the fine structure of auxospores have phylogenetic significance at higher taxonomic levels (e.g. Medlin & Kaczmarska 2004), there is still insufficient information to reveal how the structure and development of auxospores have evolved in the major diatom groups, especially among the lineages of araphid pennate diatoms. Indeed, the only detailed information available concerning araphid pennates is the account of *Rhabdonema arcuatum* Kützing by von Stosch (1962, 1982) and the SEM study of *Gephyria media* Arnott by Sato *et al.* (2004b). In the present study, we report details of auxospore formation in *Grammatophora marina*, using LM and SEM.

MATERIALS AND METHODS

Vegetative cells of *Grammatophora marina* were collected in Japan, North America and Europe (Table 1). Initially, periphytic diatoms were removed from their seaweed hosts or substrata and inoculated into Petri dishes to establish rough cultures. Within a week, single cells or short cell chains were isolated into clonal culture. Each sample was maintained in IMR medium (Eppley *et al.* 1967) at 15°C under cool-white fluorescent light on a 14:10 (L: D) photoperiod, at a photon flux density of 30–40 $\mu\text{mol photons m}^{-2}\text{s}^{-1}$. Two other media were used to induce vegetative initial cell formation and vegetative cell enlargement, respectively: silica-enriched (45 mg l^{-1} $\text{Na}_2\text{SiO}_3 \cdot 9\text{H}_2\text{O}$) KW21 medium (Daiichi Seimo, Kumamoto, Japan, available at <http://www.seimo.co.jp/KW21-English.htm>), and double-strength IMR with soil extract. Strains were reinoculated approximately once per month, except strain s0050/01, which was kept ca. 3 months without transfer.

LM observations were made using Zeiss Axioplan (Zeiss, Oberkochen, Germany) or Olympus BH-2 (Tokyo, Japan) microscopes with bright field or differential interference contrast (DIC) optics; preparations were made as described in Nagumo (2003) unless stated otherwise. To photograph live specimens (Figs 5–8), we used an inverted microscope (ID02, Zeiss) equipped with a Panasonic DMC-FX5 digital camera (Matsushita Electric Industrial, Osaka, Japan). For the observation of vegetative initial cell formation (Figs 30, 31), we used an Olympus CK2 inverted microscope with integral digital camera (Camedia C-3020, Olympus). For scanning electron microscopy (SEM), specimens were treated by three different methods. After rinsing with distilled water, intact cells were either (1) air-dried onto the cover glass or (2) cleaned by the bleaching method introduced by Nagumo & Kobayasi (1990); al-

ternatively, (3) cells were freeze-dried to keep auxospore structure intact. For this, cells were fixed with 10 % glutaraldehyde for 2 hours at 4 °C, rinsed with distilled water several times to remove glutaraldehyde, and dehydrated using increasing amounts of t-butyl alcohol; then they were freeze-dried using an ID-2 instrument (Eiko Engineering, Ibaraki, Japan). After mounting specimens onto glass cover-slips, extra cells and dust particles were removed with a glass needle under LM. Cover slips were fixed onto SEM stubs with carbon tape and specimens were coated with Pt–Pd using an E-1030 ion sputter coater (Hitachi, Tokyo, Japan), or with gold using SC 500 (Emscope, Ashford, England). S-4000 (Hitachi, Tokyo, Japan) and QUANTA 200F (FEI Company, Eindhoven, The Netherlands) SEMs were used at accelerating voltages of 3, 5 or 10 kV, and c. 10 mm working distance. All captured images were adjusted with Adobe Photoshop. Digitally saved LM and SEM images were used for measurements of valve length using Scion Image (<http://www.scioncorp.com>). Voucher specimens of cleaned material of the clonal cultures were mounted as permanent slides and have been deposited in the Hustedt Collection, Alfred Wegener Institute, Bremerhaven, Germany (Voucher no. Zu6/22-26, Table 1).

Terminology follows Anonymous (1975) and (particularly for auxospore structures) Round *et al.* (1990). Molecular phylogenetic studies of diatoms have revealed that historical diatom classifications do not reflect a natural system and araphid pennate diatoms are paraphyletic in most gene phylogenies, e.g. using nuclear 18S rDNA and plastid 16S rDNA (Medlin & Kaczmarska 2004). Nevertheless, we use the terms *araphid* and *centric* here, because they refer to key morphological features or their absence. In this paper, the term *araphid pennate diatom* follows the traditional definition, i.e., a diatom that has an elongate valve with a central or slightly lateral sternum, apical pore fields and often also apical rimoportulae, but that lacks a raphe slit. We do not imply that this corresponds to a mono-(holo-) phyletic group, nor that it should be accorded any taxonomic status.

RESULTS

Vegetative cells

In culture, cells formed zig-zag colonies (Figs 1–3), as in nature. Both valves secreted mucilage from apical pore fields, either from the same end of the cell or from opposite ends (Figs 2, 3). Rimoportulae were located at the both ends of the valve (not shown; see Sato *et al.* 2004a). The most advalvar girdle band (valvocopula) was a complete hoop, from which septa extended inwards from both poles (Figs 3, 4). In larger cells, the septa formed undulating siliceous plates, each pierced by a hole at the centre, opposite the nucleus (Figs 3, 4). The septa became less strongly undulate with cell size reduction and finally became planar (Fig. 4). The valvocopula bore several slits at each pole (Fig. 2) but the function of the slits was unclear, because no mucilage was secreted from them (Fig. 2, see also Figs 26, 42, 50). No other perforations were present in the valvocopula. As many as five additional bands (copulae) were present in the epicingulum and each had one or two rows of round areolae (Fig. 2). The nucleus was located in the centre of the cell (Fig. 3). Elongate or lobed chloroplasts were present throughout the cell, although their distribution was constrained by the presence of the septa.

Auxosporulation

Auxospores were formed in both rough cultures and clonal cultures. Auxosporulation as a result of gametic fusion was observed in a rough culture during a few weeks after inoculation

into the medium. As described by previous authors, copulation took place between small male cells and larger female cells. Each male cell was solitary and became attached to the mucilage pad connecting the female cell to an adjacent large cell (Figs 6, 7), or apparently to the adjacent cell itself (Fig. 5). The mechanism by which sexualized male and female cells became juxtaposed was unclear. Only a single auxospore was produced by each pair of copulating cells and it was always formed above the larger gametangium (Figs 5–8), confirming that the single male gamete is active and the single female is essentially passive. Empty male thecae remained attached to the female chain after plasmogamy (Figs 5–8). Female gametangia became elongate in perivalvar direction through the addition of extra girdle bands to the hypotheca (Fig. 6): ca. 10 were present (Fig. 15), compared to 3–5 in vegetative cells (Fig. 2). Addition of extra bands was not observed in male gametangia.

Nuclear behaviour was not observed in this study and the earliest stage directly observed was the freeing of the zygote from the female gametangium (Fig. 5). Extracellular material apparently containing degenerating chloroplasts was visible near the zygote (Fig. 5) and a residual body of cytoplasm was present within one of the thecae of the female gametangium, adhering to one of the septa (Fig. 5). The young auxospore was connected to the female gametangium by a mucilage envelope (Fig. 6). The auxospore expanded at right-angles to the perivalvar axis of the gametangium and parallel to its longitudinal axis (Figs 6–8). No caps were observed on the ends of the auxospores at any stage during expansion. Mature auxospores possessed a delicate perizonium (see below) and were cylindrical and often slightly arcuate, with a convex dorsal side (Fig. 8).

No sexual auxosporulation was observed in clonal cultures, but single auxospores were nevertheless produced (Figs 9–13). These auxospores were never accompanied by smaller cells, nor by empty male thecae. We refer to this phenomenon as *uniparental auxosporulation*. We were unable to establish whether this represented autogamic reproduction (fusion of haploid nuclei within an undivided protoplast after meiosis) or apomixis (absence of meiosis and parthenogenetic development of an unfertilized egg cell). The subsequent expansion and development of the auxospores were identical to allogamous sexual auxosporulation. However, there was a significant difference in initial cell size between the two methods of auxosporulation, those produced sexually being smaller (Table 2).

Scales

Scales of various sizes and shapes were observed on both sexually produced and uniparental auxospores. Auxospores that had emerged from their mother cells but had not yet begun to expand were covered with circular scales (Figs 14–16). Expanding auxospores possessed transverse perizonial bands, but these were overlain by scales (Fig. 17). Scales could still be found in the final stages of expansion and development, even after the initial epivalves had been formed, although there appeared to be fewer of them and they no longer formed a complete covering (Fig. 27). Each scale had an annulus, which bore irregularly branching fimbriae. Within the annulus, the scale was often weakly or only irregularly and partly silicified (Fig. 18).

Fine structure of the perizonium

The transverse perizonium developed as the auxospore expanded; young auxospores (Figs 17, 19) therefore had many fewer bands than mature ones (Fig. 26). The primary (central) band (Figs 19–21, 23, 25) was wider than the secondary bands that flanked it on either side and it was also symmetrical, having a central axis and equal fringes of fimbriae. All of the trans-

verse perizonial bands (including the primary band) were open and aligned, forming a distinct, wide suture parallel to the long axis of the auxospore (Figs 19, 20, 22, 23). We will refer to the side occupied by the suture as “ventral” and this side always lay closest to the female gametangial cell wall from which the auxospore emerged.

All of the transverse perizonial bands consisted of two parts: (1) a rib along the long axis of the band, and (2) two rows of irregularly branching fimbriae (Figs 19–25). The bands were tightly associated and the distal fringe of fimbriae overlapped the proximal fringe of the next band (Figs 19–20, 22–24); the proximal and distal fringes are therefore analogous to the pars interior and pars exterior, respectively, of diatom girdle bands. The fimbriae of the pars interior were slightly shorter than those of the pars exterior (Fig. 24, pi and pe). On the ventral side, the open ends of the primary transverse perizonial bands were centripetally curved, whereas on the dorsal side the bands were strictly parallel (Fig. 29; see also Figs 19, 23). The primary transverse perizonial band had double-length fringes and a somewhat broader rib (Figs 19, 20, 23), although the latter was also somewhat shorter because of the size of the fimbriae. The primary band rib often had pores along its centre (Fig. 21) and in a few specimens it had a hoop-like end resembling an annulus (Fig. 25).

During intermediate stages of auxospore development, irregular, elongate silicified structures were observed along the suture on the ventral side of auxospore (Fig. 20). Although these structures were also found on mature auxospores encasing the initial cell, there were considerably fewer than during earlier stages of development. No longitudinal perizonial band as seen in *Rhabdonema arcuatum* (von Stosch 1982) was observed in any stage of auxospore development.

Initial cells and ‘cardinal points’

The initial cells produced by sexual or uniparental auxosporulation were nearly identical in morphology; they were straight or slightly curved and usually \pm symmetrical about the apical and median transapical planes. However, we also observed some initial cells that appeared to have been formed without auxosporulation and were not associated either with mating cells or with empty male thecae around the mother cell, indicating they had been formed without prior inter- or intracloonal mating. This phenomenon – which we will refer to as *vegetative initial cell formation* – was only observed in a rough culture. Whereas the initial cells formed through both sexual and uniparental auxosporulation were covered with scales and perizonium, the initial cell formed by vegetative initial cell formation had no trace of these coverings (Figs 30–38), despite use of preparation methods identical to those used for Figs 14–17. Abnormal cell outlines (e.g. Figs 37, 38) were much more frequent in these initial cells than in those formed through sexual or uniparental auxosporulation.

Vegetative initial cell formation differed from vegetative cell enlargement (below) in that initial epivalves were not produced after vegetative cell enlargement (Fig. 51). Initial epivalves differed from normal vegetative valves in having (1) no distinct valve mantle; (2) a wider valve margin (the plain strip of silica around the edge of the valve); and (3) small apical pore fields or none (Figs 27–29, 32–36). The valvocopulae associated with the initial epivalves also differed from those of vegetative cells, because they (1) lacked septa, (2) were narrower and more fragile, (3) lacked slits at the apices, and (4) possessed instead a single (or partly double) row of round or elliptical poroids (Figs 27–29).

The initial epitheca was produced on the dorsal side of the auxospore and the initial hypotheca was formed opposite, beneath the perizonial suture (Fig. 39). The initial hypovalve resembled a normal valve in shape and structure (Figs 27–29), except that its central portion was sometimes slightly swollen (Fig. 26), corresponding to a slight bulge in the auxospore

where it abutted onto the gametangium (Figs 7, 13). The valvocopula of the initial hypotheca was also normal, possessing septa. The second valve had a valvocopula with septa (Figs 8, 39). Beneath the initial epivalve, a third valve with a septum-bearing valvocopula was formed to complete a frustule of \pm normal appearance (Figs 30, 39), whereupon the initial epivalve was sloughed off. Any abnormalities of shape in the initial cells were gradually lost during subsequent vegetative divisions (e.g. Fig. 30). Unlike vegetative cells and chains, the uniparentally produced initial cells often floated in the culture vessel.

The first cardinal point of diatom sexual reproduction concerns the size of the initial cells. The size range of initial cells produced by the three modes differed (Table 2). Initial cells produced by allogamous sexual auxosporulation were the smallest, being 52.3–70.4 μm (mean 63 μm), as opposed to 68.8–96.3 μm (mean 84.3 μm) with uniparental auxosporulation. This was surprising because (1) the sizes of the asexual mother cells (uniparental auxosporulation) and female gametangia (allogamous sexual auxosporulation) were comparable (indeed, the gametangia were larger on average), and (2) sexual auxospores also received a contribution of cytoplasm and organelles from the male gametangium. Vegetative initial cells were slightly larger than sexual initial cells (Table 2).

The second cardinal point is the upper size threshold for sexualisation and auxosporulation. The maximum size for a female cell in this study was 24.7 μm .

The third cardinal point is the critical minimal size for size restitution via auxospores, below which a clone will survive only through mitotic division and (in some cases) vegetative cell enlargement. The smallest cell observed to be capable of uniparental auxosporulation was 14.7 μm . The smallest female sexual gametangium was 19.4 μm and the smallest male was 13.6 μm . Because most of the male cells were attached to the females at an angle (e.g. Fig. 7), only three specimens were measurable, the largest (15.9 μm) being smaller than any of the females measured.

Abnormal cells

Abnormal cells were detected in many of the culture strains of *G. marina*, with substantial differences in valve length between epi- and hypovalve (Figs 40–50). These appear to reflect not only abrupt reductions in size but also abrupt increases.

With abrupt cell size reduction, the apical dimension of the hypotheca was suddenly and drastically reduced (Figs 43–46, and presumably Fig. 40) by up to 50% relative to the epitheca. Reduction occurred spontaneously in old cultures (a few months after inoculation) and resulted from unequal division of parent cells; faulty division was presumably responsible too for producing cells with a constriction at one side of the frustule (Fig. 42), which were also frequent in old cultures.

In some cases, cells had larger hypothecae than epithecae (Figs 47–50), implying expansion before or during cell division. The alternative explanation – slippage and reconfiguration of the girdle bands during specimen preparation – seems unlikely and so *G. marina* appears to be able to perform vegetative cell enlargement, which can produce 25–100% increase, relative to the epitheca. This mode of enlargement could sometimes be induced by inoculation into double strength IMR medium with soil extract.

DISCUSSION

Auxospore coverings

The first study of auxospore coverings using electron microscopy was a brief report of scales in the auxospore wall of *Melosira varians* Agardh with TEM (Reimann 1960). Since then, our knowledge of auxospore fine structure has gradually increased, revealing a diversity of structures, including scales of various shapes and sizes, and different kinds of properizonia (in bi- and multipolar centric diatoms) and perizonia (von Stosch 1982; Round *et al.* 1990). ‘Perizonium’ was apparently used by Reimann (1960) to refer to the all kinds of auxospore wall, but the term is now restricted to the system of hoops and split bands (longitudinal and transverse) found in pennate diatoms (Round *et al.* 1990; Kaczmarska *et al.* 2001). The perizonium is accompanied by \pm circular scales in some but not all pennate diatoms. These include four araphid diatoms; *Rhabdonema arcuatum* (von Stosch 1982), *Gephyria media* (Sato *et al.* 2004b) and *Grammatophora marina* (this study), and also the raphid diatoms *Pseudo-nitzschia multiseriis* (Hasle) Hasle (Kaczmarska *et al.* 2000, but not in *P. delicatissima* (Cleve) Heiden: Amato *et al.* 2005) and *Diploneis papula* (Schmidt) Cleve (M. Idei, in Kaczmarska *et al.* 2001). Recently, the auxospores of *Nitzschia fonticola* (Grunow) Grunow and *Pinnularia* cf. *gibba* have been shown to possess systems of fine transverse strips, lying outside the perizonium and formed before it (Trobajo *et al.* 2006; Pouličková *et al.*, in press). At least in *Pinnularia* cf. *gibba*, these strips are silicified and they may be homologous with the circular scales of the araphid pennates, *Pseudo-nitzschia* spp. and *Diploneis papula*. Trobajo *et al.* (2006) have suggested that the parts of the auxospore wall that surround the perizonium and that are formed before it should be referred to as ‘incunabula’. In *G. marina* and *Gephyria media*, the incunabula would comprise the organic wall and circular scales of the auxospore, but not the elongate scales along the perizonial suture in *G. marina* (this study) or the ‘elongate sprawling structure’ in an equivalent position in *Gephyria media* (Sato *et al.* 2004b).

The difference of the degree of silicification and the shape of the scales are different between those produced by sexual and uniparental auxosporulation (Figs 16 and 18, respectively). However, it is likely that these differences are not because of the mode of auxosporulation (i.e. sexual or uniparental), because a great diversity of the scale shape has also been reported on a single auxospore in centric diatoms, e.g. *Arachnoidiscus ornatus* Ehrenberg (Kobayashi *et al.* 2001) and *Ellerbeckia arenaria* (Moore) Crawford (Schmid & Crawford 2001).

The primary (central) transverse perizonial band of *G. marina* is open on one side, as in *Rhabdonema arcuatum* (von Stosch 1962) and *Gephyria media* (Sato *et al.* 2004b). This is probably a primitive characteristic for pennate diatoms because the properizonium, which is presumably homologous to the perizonium but occurs in mediophycean centric diatoms (Medlin & Kaczmarska 2004), also has an open central band (e.g. in *Chaetoceros didymum* Ehrenberg and *Lithodesmium undulatum* Ehrenberg: von Stosch 1982). On the other hand, in most raphid pennate diatoms, the primary transverse perizonial band is generally a complete hoop, e.g. in *Amphora copulata* (Kützing) Schoeman & R.E.M. Archibald (Nagumo 2003), *Caloneis* cf. *silicula* (Mann 1989), *Craticula cuspidata* (Kützing) Mann (Cohn *et al.* 1989), *Navicula cryptocephala* Kützing (Pouličková & Mann 2006), *Neidium affine* (Ehrenberg) Pfitzer (Mann 1984a), *Pinnularia* cf. *gibba* (Pouličková *et al.*, in press) and *Rhoicosphenia curvata* (Kützing) Grunow (Mann 1982a). However, open primary bands have been reported in *Pseudo-nitzschia multiseriis* (Kaczmarska *et al.* 2000) and *Nitzschia fonticola* (Trobajo *et al.* 2006) and it is unclear whether this reflects retention of a primitive character inherited from araphid pennates or homoplasy.

The end of the rib in the primary transverse perizonial band of *G. marina* was sometimes not solid, but perforate (Fig. 21) or hoop-like (Fig. 25), thus resembling an annulus (compare Fig. 25 with Fig. 18). Given that the primary band also bears fimbriae, it would be reasonable to suggest that it and the scales are homologous.

The irregular siliceous structures on the ventral side of the auxospore of *G. marina* (Fig. 20) are similar in morphology and position to the ‘elongate sprawling structure’ in *Gephyria media* (Sato *et al.* 2004b). These structures extend longitudinally along the suture and may help reinforce the auxospore wall in what would otherwise be a weak point. Longitudinal perizonial bands are formed by various pennate diatoms, including both raphids, e.g. *Rhoicosphenia curvata* (Mann 1982a) and *Amphora copulata* (Nagumo 2003), and the araphid *Rhabdonema arcuatum* (von Stosch 1962, 1982). We did not detect any such bands at any stage of auxosporulation in *G. marina* and there is no hint of any from previous studies (Karsten 1926; Lebour 1930; Magne-Simon 1960, 1962). A regular system of pores, resembling the striae of normal valves and initial valves, was sometimes seen beneath the perizonium (Figs 19–21) in auxospores of intermediate length (ca. 35 μm in Fig. 19), but we interpret these as an abnormally small initial valve (initial cells are usually at least 52.3 μm : Table 2).

Initial cell formation

The initial cells of pennate diatom are generally formed within (and moulded at least in part by) a perizonium consisting of transverse perizonial bands and sometimes also longitudinal perizonial bands (von Stosch 1982). Sexual and ‘uniparental’ initial cells of *Grammatophora marina* conform to this rule, but some other *Grammatophora* initial cells seem to be formed without production of a perizonium and here there was a higher frequency of deformities, supporting the idea that the perizonium helps to form the correct shape of the initial cell. Several diatoms form auxospores without a transverse perizonium, e.g. *Achnanthes brevipes* C. Agardh var. *intermedia* (Kützing) Cleve (Idei 1993), *A. cf. subsessilis* Kützing (Sabbe *et al.* 2004), *A. yaquinensis* McIntire & Reimer (Toyoda *et al.* 2005), *A. crenulata* Grunow (Toyoda *et al.* 2006), *Fragilariforma virescens* (Ralfs) Williams & Round (Williams 2001), *Licmophora communis* (Heiberg) Grunow (Chepurnov & Mann 2004), *L. gracilis* var. *anglica* (Kützing) Peragallo (Mann 1982b) and *Nitzschia recta* Hantzsch (Mann 1986), although *Achnanthes* species have a well-developed system of longitudinal perizonial bands. Williams (2001) proposed that the plethora of peculiar shapes that emerge in the immediate post auxospore valves in *F. virescens*, and presumably in *Diatoma moniliformis* Kützing (Potapova & Snoeijs 1997), were because of the absence of transverse perizonial bands; this could also be why irregularly shaped and triradiate auxospores (reported by Chepurnov & Roshchin 1995; Hendey 1951; Schmid in Pickett-Heaps *et al.* 1990) are common in *Achnanthes* spp. (Sabbe *et al.* 2004).

The initial epitheca of *G. marina* is structurally differentiated from subsequent thecae (reduced or no apical pore fields, no septum and no slits on the valvocopula) and is sloughed off after the formation of a third valve immediately beneath it. Given that we detected no separate longitudinal perizonial bands in *G. marina*, in contrast to *Rhabdonema arcuatum* (von Stosch 1962, 1982), it might be argued that we have misinterpreted the longitudinal perizonium as a valve and girdle bands. We reject this because the initial epitheca is formed on the dorsal side of the auxospore, not beneath the suture (contrast the longitudinal perizonia of e.g. *Rhabdonema arcuatum*, *Rhoicosphenia curvata* and *Amphora copulata*: von Stosch 1962, 1982; Mann 1982a; Nagumo 2003), and because of the presence of a normal stria system. Furthermore, the formation of each valve in diatoms, but not the formation of perizonial bands or girdle bands, is preceded by a mitosis (Geitler 1963; a rare exception during manipulation in culture is discussed by Pollock & Pickett-Heaps 2006) and Magne-Simon (1962, p. 84) stated that he detected a mitosis before formation of the initial epivalve ‘dans de nombreux cas’ in *G. marina*. We regard the acytokinetic mitosis that Magne-Simon (1962, figs 20,

21 and 25) detected *after* formation of the initial epivalve as that associated with the formation of the initial hypovalve.

The formation of the third valve and loss of the initial epitheca likewise follows a mitosis but, unlike the initial epivalve and hypovalve, formation of the third valve is accompanied by an unequal cell division (Magne-Simon 1962, figs 22, 23), the small cell formed under the initial epivalve gaining a nucleus but no or few chloroplasts and little cytoplasm. The small cell occasionally also produced a reduced valve in Magne-Simon's specimens (*ibid.*, fig. 27) but we did not detect any in our material.

Life cycle, cardinal points and species status of *Grammatophora marina*

In culture, the life cycle of *Grammatophora marina* from the U.S.A., Japan and W Europe exhibits several interesting and unusual features, including two different modes of auxosporulation (sexual and uniparental), vegetative initial cell formation, vegetative cell enlargement and abrupt cell size reduction. Some of the phenomena observed, such as vegetative cell enlargement, abrupt cell size reduction and vegetative formation of initial cells may perhaps not occur in nature, although Roshchin (1987, 1994) found that monoclonal cultures of *G. marina* from the Black Sea could also enlarge their cells. The greater size of clonal auxospores, relative to sexual auxospores, makes it highly unlikely that these and the healthy vegetative cells that they produce are haploids as seen in *Licmophora* species (Chepurnov et al. 2004). Vegetative cell size changes have also been recorded in other diatoms (e.g. von Stosch 1965; Drebes 1966; Mann *et al.* 2003; Chepurnov *et al.* 2004). In this study, changing the medium sometimes induced vegetative initial cell formation and vegetative cell enlargement; however, it is unclear which factor(s) triggered these phenomena directly. Long-term culture has often been observed to cause deformities in diatom cell walls (Jaworski *et al.* 1988; Round 1993; Estes & Dute 1994), but in our study long periods were not necessary to induce unusual behaviour: sexual, vegetative initial cell formation and vegetative cell enlargement took place within a month after culture establishment, and uniparental auxosporulation and abrupt cell size reductions took place 7 and 9-12 months after inoculation, respectively (Table 1).

The absence of sexual reproduction in any of our clones is consistent with previous statements (von Stosch & Drebes 1964, p. 211; von Stosch in Rozumek 1968, p. 382; Roshchin 1987, 1994) that *G. marina* is dioecious (heterothallic, i.e. it has separate male and female clones).

The size differences between our material and the *G. marina* population studied by Magne-Simon (1962) seem to be significant. The initial cells reported by Magne-Simon (1962) had a mean length more than double that in our material (Table 2), and the female and male gametangia were also much larger (30–70 vs. 19–25 μm , and 20–50 vs. c. 15 μm , respectively). It is quite likely, therefore, that the two sets of *G. marina* populations represent different races, or even different species. Cryptic or almost cryptic (pseudocryptic) species have been found in *Pseudo-nitzschia* (Amato *et al.* 2007), *Skeletonema* (Medlin *et al.* 1991; Zingone *et al.* 2005; Sarno *et al.* 2005, 2007) and *Sellaphora* (Evans *et al.*, in press), and also occur in other marine microalgae (e.g. Sáez *et al.* 2003). Further detailed morphological comparisons (e.g. with morphometric approaches like those conducted by Mann *et al.* 2004 or Beszteri *et al.* 2005), together with crossing experiments and molecular genetic studies, will be necessary to determine whether cryptic speciation has occurred in *G. marina*. Once this has been done, Lyngbye's type material will have to be examined to see whether it is possible to determine which segregate species should bear the name '*marina*'.

Ecological implications

In terms of evolutionary costs and benefits, a long period of cheap asexuality followed by a short period of expensive sexual recombination may be a successful strategy for unicellular organisms, especially if the sexual phase is timed to occur when growth is slow (Lewis 1983, 1984). Vegetative initial cell formation and vegetative cell enlargement may be retained, despite the production of aberrant cell morphology, because they enable sexually competent clones to persist when sexual reproduction is prevented by environmental conditions or availability of compatible mates. Alternatively, vegetative enlargement mechanisms may occur because they provide a less costly means of restoring size than allogamous sexual auxosporulation (although there is still a 'penalty' because cells cannot divide while they are expanding and forming new cell walls), the balance between sexual and non-sexual expansion being determined by the strength of selection for the unique feature of allogamous sexual auxosporulation, viz. meiosis and sexual recombination. Abrupt cell size reduction, if it occurs naturally, will shorten the life cycle (the factor controlling whether cells can be sexualized is cell size, not the age of the cell or lineage: von Stosch 1965; Chepurnov *et al.* 2004). Given that the unperturbed size reduction cycle may last several years in natural populations of diatoms (Mann 1988), a mechanism by which cells could by-pass this time restriction might be beneficial in some circumstances.

A feature of the initial epivalve of *Grammatophora marina* is its smaller or less differentiated apical pore fields (e.g. Figs 28, 29), compared to those of the initial hypovalve and vegetative cells (Sato *et al.* 2004a, Round *et al.* 1990). It is through the apical pore field that mucilage is secreted for attachment in *Grammatophora* and many araphid diatoms (Figs 1–3; for a review, see Hasle 1974) and so the initial epivalve is probably unable to attach to a substratum. Even if it could attach, the formation of the third valve close beneath the initial epivalve (Fig. 39) would first disconnect the cytoplasm from the apical region and then lead to detachment when the epivalve is sloughed off (Fig. 31). Furthermore, initial cells produced by uniparental auxosporulation often floated in the culture vessel, whereas most vegetative cells and colonies became attached to the bottom (data not shown). It is possible, therefore, that reduction of the apical pore fields is part of a dispersal mechanism, allowing the initial cells to become temporarily planktonic. The apical pore fields are also reduced in the initial cells of two raphid diatoms, *Rhoicosphenia curvata* and *Gomphonema constrictum* Ehrenberg (Mann 1984b). *Diatoma moniliformis*, another zig-zag colonial araphid diatom, is often found in the plankton of the Baltic Sea (Snoeijs 1993), which prompted Potapova & Snoeijs (1997) to suggest that large cells of the species might switch to pelagic life until they reach a certain minimum size, after which they would return to the benthos. Chepurnov & Mann (1999, p. 10) noted a tendency of inbred *Achnanthes longipes* Agardh to become positively buoyant in culture and suggested that this might be an 'escape' mechanism in nature, enhancing the chances of outbreeding. Species of *Grammatophora* are sometimes reported from the plankton (Abdul Azis *et al.* 2001; Chiang *et al.* 1997; Eashwar *et al.* 2001; Karsten 1905; Koenig *et al.* 2003; Lebour 1930; Meunier 1915; Ricard 1987) and this may perhaps be adaptive, rather than accidental suspension of cells by wave action or macrofaunal activity.

ACKNOWLEDGEMENTS

We would like to thank Klaus Valentin and William Wardle for providing us the living samples from France and Texas, respectively, used in this study; Friedel Hinz for support with SEM; Victor Chepurnov for helpful comments and information concerning A.M. Roshchin's

work; and Richard Crawford for correction of the manuscript and discussion. This study was supported by DAAD for doctoral research fellowship to Shinya Sato.

REFERENCES

- ABDUL AZIS P.K.A., AL-TISAN I. & SASIKUMAR N. 2001. Biofouling potential and environmental factors of seawater at a desalination plant intake. *Desalination* 135: 69–82.
- AMATO A., ORSINI L., D'ALELIO D. & MONTRESOR M. 2005. Life cycle, size reduction patterns, and ultrastructure of the pennate planktonic diatom *Pseudo-nitzschia delicatissima* (Bacillariophyta). *Journal of Phycology* 41: 542–556.
- AMATO A., KOOISTRA W.H.C.F., LEVIALDI GHIRON J.H., MANN D.G., PRÖSCHOLD T. & MONTRESOR M. 2007. Reproductive isolation among sympatric cryptic species in marine diatoms. *Protist* 158: 193–207.
- ANONYMOUS 1975. Proposals for a standardization of diatom terminology and diagnoses. *Nova Hedwigia, Beiheft* 53: 323–354.
- BEHNKE A., FRIEDL T., CHEPURNOV V.A. & MANN D.G. 2004. Reproductive compatibility and rDNA sequence analyses in the *Sellaphora pupula* species complex (Bacillariophyta). *Journal of Phycology* 40: 193–208.
- BESZTERI B., ÁCS É. & MEDLIN L.K. 2005. Conventional and geometric morphometric studies of valve ultrastructural variation in two closely related *Cyclotella* species (Bacillariophyta). *European Journal of Phycology* 40: 89–103.
- BOLD H.C. & WYNNE J.M. 1985. *Introduction to the algae*, Ed. 2. Prentice–Hall, Englewood Cliffs, New Jersey. 720 pp.
- CHEPURNOV V.A. & MANN D.G. 1999. Variation in the sexual behaviour of *Achnanthes longipes* (Bacillariophyta). II. Inbred monoecious lineages. *European Journal of Phycology* 34: 1–11.
- CHEPURNOV V.A. & MANN D.G. 2004. Auxosporulation of *Licmophora communis* (Bacillariophyta) and a review of mating systems and sexual reproduction in araphid pennate diatoms. *Phycological Research* 52: 1–12.
- CHEPURNOV V.A. & ROSHCHIN A.M. 1995. Inbreeding influence on sexual reproduction of *Achnanthes longipes* Ag. (Bacillariophyta). *Diatom Research* 10: 21–29.
- CHEPURNOV V.A., MANN D.G., SABBE K. & VYVERMAN W. 2004. Experimental studies on sexual reproduction in diatoms. *International Review of Cytology* 237: 91–154.
- CHEPURNOV V.A., MANN D.G., SABBE K., VANNERUM K., CASTELEYN G., VERLEYEN E., PEPPERZAK L. & VYVERMAN W. 2005. Sexual reproduction, mating system, chloroplast dynamics and abrupt cell size reduction in *Pseudo-nitzschia pungens* from the North Sea (Bacillariophyta). *European Journal of Phycology* 40: 379–395.
- CHIANG K.P., SHIAH F.K. & GONG G.C. 1997. Distribution of summer diatom assemblages in and around a local upwelling in the East China Sea northeast of Taiwan. *Botanical Bulletin of Academia Sinica* 38: 121–129.
- COHN S.A., SPURCK T.P., PICKETT-HEAPS J.D. & EDGAR L.A. 1989. Perizonium and initial valve formation in the diatom *Navicula cuspidata* (Bacillariophyceae). *Journal of Phycology* 25: 15–26.
- CRAWFORD R.M. 1974. The auxospore wall of the marine diatom *Melosira nummuloides* (Dillw.) C. Ag. and related species. *British Phycological Journal* 9: 9–20.
- DREBES G. 1966. On the life history of the marine plankton diatom *Stephanopyxis palmeriana*.

- Helgoländer wissenschaftlicher Meeresuntersuchungen* 13: 101–114.
- EASHWAR M., KUBERARAJ K., NALLATHAMBI T. & GOVINDARAJAN G. 2001. A note on the plankton from Barren Island region, Andamas. *Scientific Correspondence* 81: 651–654.
- EDLUND M.B. & STOERMER E.F. 1997. Ecological, evolutionary, and systematic significance of diatom life histories. *Journal of Phycology* 33: 897–918.
- EPPLEY R.W., HOLMES R.W. & STRICKLAND J.D.H. 1967. Sinking rates of the marine phytoplankton measured with a fluorochromometer. *Journal of Experimental Marine Biology and Ecology* 1: 191–208.
- ESTES L. & DUTE R.R. 1994 Valve abnormalities in diatom clones maintained in long-term culture. *Diatom Research* 9: 249–258.
- EVANS K.M., WORTLEY A.H. & MANN D.G. 2007. An assessment of potential diatom “barcode” genes (*cox1*, *rbcL*, 18S and ITS rDNA) and their effectiveness in determining relationships in *Sellaphora* (Bacillariophyta). *Protist* 158: 349–364.
- GEITLER L. 1932. Der Formwechsel der pennaten Diatomeen. *Archiv für Protistenkunde* 78: 1–226.
- GEITLER L. 1963. Alle Schalenbildungen der Diatomeen treten also Folge von Zell- oder Kernteilungen auf. *Berichte der Deutschen Botanischen Gesellschaft* 75: 393–396.
- HASLE G.R. 1974. The “mucilage pore” of pennate diatoms. *Nova Hedwigia, Beiheft* 45: 167–194.
- HENDEY N.I. 1951. Littoral diatoms of Chichester Harbour with special reference to fouling. *Journal of the Royal Microscopical Society* 71: 1–86.
- IDEI M. 1993. [*Achnanthes brevipes* C. Agardh var. *intermedia* (Kützing) Cleve.] In: *An Illustrated Atlas of the Life History of Algae, Vol. 3. Unicellular and Flagellated Algae* (Ed. by T. Hori). pp. 260–261. Uchida Rokakuho, Tokyo. (In Japanese).
- JAWORSKI G.H.M., WISEMAN S.W. & REYNOLDS C.S. 1988. Variability in sinking rate of the freshwater diatom *Asterionella formosa*: the influence of colony morphology. *British Phycological Journal* 23: 167–176.
- KACZMARSKA I., BATES S.S., EHRMAN J.M. & LÉGER C. 2000. Fine structure of the gamete, auxospore and initial cell in the pennate diatom *Pseudo-nitzschia multiseriata* (Bacillariophyta). *Nova Hedwigia* 71: 337–357.
- KACZMARSKA I., EHRMAN J.M. & BATES S.S. 2001. A review of auxospore structure, ontogeny and diatom phylogeny. In *Proceedings of the 16th International Diatom Symposium* (Ed. by A. Economou-Amilli), pp. 153–168. University of Athens, Greece.
- KARSTEN G. 1905. Das Phytoplankton des Antarktischen Meeres nach dem Material der Deutschen Tiefsee-Expedition 1898-1899. *Wissenschaftliche Ergebnisse der Deutschen Tiefsee-Expedition auf dem Dampfer Valdivia 1898-1899* 2: 1–136.
- KARSTEN G. 1926. Die Tabellarien und ihre Auxosporenbildung. *Leopoldina* 1: 65–68.
- KOENING M.L., LEÇA E.E., NEUMANN-LEITÃO S. & DE MACÊDO S.J. 2003. Impacts of the construction of the port of Suape on phytoplankton in the Ipojuca River estuary (Pernambuco-Brazil). *Brazilian Archives of Biology and Technology* 46: 73–81.
- KOBAYASHI A., OSADA K., NAGUMO T. & TANAKA J. 2001. An auxospore of *Arachnoidiscus ornatus* Ehrenberg. In: *Proceedings of the 16th International Diatom Symposium* (Ed. by A. Economou - Amilli), pp. 197–204. University of Athens, Greece.
- LEBOUR M. 1930. *The plankton diatoms of northern seas*. Ray Society. London. 244 pp.
- LEWIS W.M. JR. 1983. Interruption of synthesis as a cost of sex in small organisms. *American Naturalist* 121: 825–833.

- LEWIS W.M. JR. 1984. The diatom sex clock and its evolutionary importance. *American Naturalist* 123: 73–80.
- MAGNE-SIMON M.-F. 1960. Note sur le processus de l'auxosporulation chez une Diatomée marine, *Grammatophora marina* (Lyngbye) Kützing. *Comptes rendus de l'Académie des Sciences* (Paris) 251: 3040–3042.
- MAGNE-SIMON M.-F. 1962. L'auxosporulation chez une Tabellariacée marine, *Grammatophora marina* (Lyngbye) Kützing. *Cahiers de Biologie Marine* 3: 79–89.
- MANN D.G. 1982a. Structure, life history and systematics of *Rhoicosphenia* (Bacillariophyta). II. Auxospore formation and perizonium structure of *Rh. curvata*. *Journal of Phycology* 18: 264–274.
- MANN D.G. 1982b. Auxospore formation in *Licmophora* (Bacillariophyta). *Plant Systematics and Evolution* 139: 289–294.
- MANN D.G. 1984a. Auxospore formation and development in *Neidium* (Bacillariophyta). *British Phycological Journal* 19: 319–331.
- MANN D.G. 1984b. Structure, life history and systematics of *Rhoicosphenia* (Bacillariophyta) V. Initial cell and size reduction in *Rh. curvata*, and the description of the Rhoicospheniaceae, fam. nov. *Journal of Phycology* 20: 544–555.
- MANN D.G. 1986. Methods of sexual reproduction in *Nitzschia*: systematic and evolutionary implications (Notes for a monograph of the Bacillariaceae 3). *Diatom Research* 1: 193–203.
- MANN D.G. 1988. Why didn't Lund see sex in *Asterionella*? A discussion of the diatom life cycle in nature. In *Algae and the Aquatic Environment* (ed. by F.E. Round), pp. 383–412. Biopress, Bristol.
- MANN D.G. 1989. On auxospore formation in *Caloneis* and the nature of *Amphiraphia* (Bacillariophyta). *Plant Systematics and Evolution* 163: 43–52.
- MANN D.G., CHEPURNOV V.A. & IDEI M. 2003. Mating system, sexual reproduction and auxosporulation in the anomalous raphid diatom *Eunotia* (Bacillariophyta). *Journal of Phycology* 39: 1067–1084.
- MANN D.G., McDONALD S.M., BAYER M.M., DROOP S.J.M., CHEPURNOV V.A., LOKE R.E., CIOBANU A. & DU BUF J.M.H. 2004. Morphometric analysis, ultrastructure and mating data provide evidence for five new species of *Sellaphora* (Bacillariophyceae). *Phycologia* 43: 459–482.
- MEDLIN L.K. & KACZMARSKA I. 2004. Evolution of the diatoms: V. Morphological and cytological support for the major clades and a taxonomic revision. *Phycologia* 43: 245–270.
- MEDLIN L.K., ELWOOD H.J., STICKEL S. & SOGIN M.L. 1991. Morphological and genetic variation within the diatom *Skeletonema costatum* (Bacillariophyta): evidence for a new species, *Skeletonema pseudocostatum*. *Journal of Phycology* 27: 514–524.
- MEUNIER A. 1915. Microplancton de la Mer Flamande. Part 2. Les Diatomacées. *Mémoires du Musée Royal d'Histoire Naturelle de Belgique* 7: 1–118.
- NAGUMO T. 2003. Taxonomic studies of the subgenus *Amphora* Cleve of the genus *Amphora* (Bacillariophyceae) in Japan. *Bibliotheca Diatomologica* 49: 1–265.
- NAGUMO T. & KOBAYASI H. 1990. The bleaching method for gently loosening and cleaning a single diatom frustule. *Diatom* 5: 45–50.
- OHGAI M., TSUCHIDA H., SYAZUKI T., NAKASHIMA K., UEDA K. & SAKUMA M. 1988. Effects of the environmental factors on the propagation of epiphytic diatom *Grammatophora marina* (Lyngb.) Kütz. *Nippon Suisan Gakkaishi* 54: 795–799. (In Japanese with Eng-

- lish abstract.)
- PICKETT-HEAPS J.D., SCHMID A.-M.M. & EDGAR L.A. 1990. The cell biology of diatom valve formation. *Progress in Phycological Research* 7: 1–168.
- POLLOCK F.M. & PICKETT-HEAPS J.D. 2006. Valve formation without mitosis in the diatom *Ditylum* recovering from plasmolysis. *Nova Hedwigia, Beiheft* 130: 119–126.
- POTAPOVA M. & SNOEIJIS P. 1997. The natural life cycle in wild populations of *Diatoma moniliformis* (Bacillariophyceae) and its disruption in an aberrant environment. *Journal of Phycology* 33: 924–937.
- POULÍČKOVÁ A. & MANN D.G. 2006. Sexual reproduction in *Navicula cryptocephala* (Bacillariophyceae). *Journal of Phycology* 42: 872–886.
- POULÍČKOVÁ A., MAYAMA S., CHEPURNOV V.A. & MANN D.G. (in press). Heterothallic auxosporulation, incunabula and perizonium in *Pinnularia* (Bacillariophyceae). *European Journal of Phycology*
- REIMANN B. 1960. Bildung, Bau und Zusammenhang der Bacillariophyceenschalen. (Elektronenmikroskopische Untersuchungen). *Nova Hedwigia* 2: 349–373.
- RICARD M. 1987. *Atlas du phytoplancton marin. Volume II: Diatomophycées*. Éditions du CNRS, Paris. 297 pp.
- ROSHCHIN A.M. 1987. Odnodomnoe vosproizvedenie diatomovoj vodorosli *Grammatophora marina*. *Biologicheskie Nauki* (Moscow) 6: 65–69.
- ROSHCHIN A.M. 1994. *Zhiznennye tsikly diatomovykh vodoroslej*. Naukova Dumka, Kiev. 170 pp.
- ROUND F.E. 1993. A *Synedra* (Bacillariophyta) clone after several years in culture. *Nova Hedwigia, Beiheft* 106: 353–359.
- ROUND F.E., CRAWFORD R.M. & MANN D.G. 1990. *The diatoms. Biology and morphology of the genera*. Cambridge University Press, Cambridge. 747 pp.
- ROZUMEK K.-E. 1968. Der Einfluss der Umweltfaktoren Licht und Temperatur auf die Ausbildung der Sexualstadien bei der pennaten Diatomee *Rhabdonema adriaticum* Kütz. *Beiträge zur Biologie der Pflanzen* 44: 365–388.
- SABBE K., CHEPURNOV V.A., VYVERMAN W. & MANN D.G. 2004. Apomixis in *Achnanthes* (Bacillariophyceae); development of a model system for diatom reproductive biology. *European Journal of Phycology* 39: 327–341.
- SÁEZ A.G., PROBERT I., GEISEN M., QUINN P., YOUNG J.R. & MEDLIN L.K. 2003 Pseudocryptic speciation in coccolithophores. *Proceedings of the National Academy of Sciences of the United States of America* 100: 7163–7168.
- SARNO D., KOOISTRA W.C.H.F., MEDLIN L.K., PERCOPO I. & ZINGONE A. 2005. Diversity in the genus *Skeletonema* (Bacillariophyceae). II. An assessment of the taxonomy *S. costatum*-like species, with the description of four new species. *Journal of Phycology* 41: 151–176.
- SARNO D., KOOISTRA W.C.H.F., BALZANO S., HARGRAVES P.E. & ZINGONE A. 2007. Diversity in the genus *Skeletonema* (Bacillariophyceae): III. Phylogenetic position and morphological variability of *Skeletonema costatum* and *Skeletonema grevillei*, with the description of *Skeletonema ardens* sp. nov. *Journal of Phycology* 43: 156–170.
- SATO S., NAGUMO T. & TANAKA J. 2004a. Morphology and taxonomy of marine attached diatoms in genus *Grammatophora* Ehrenberg (Bacillariophyceae) in Japan. *The Japanese Journal of Phycology* 52 (supplement): 183–187.
- SATO S., NAGUMO T. & TANAKA J. 2004b. Auxospore formation and the morphology of the initial cell of the marine araphid diatom *Gephyria media* (Bacillariophyceae). *Journal*

- of Phycology* 40: 684–691.
- SCHMID A.-M.M. & CRAWFORD R.M. 2001. *Ellerbeckia arenaria* (Bacillariophyceae): formation of auxospores and initial cells. *European Journal of Phycology* 36: 307–320.
- SNOEIJIS P. (Ed.) 1993. *Intercalibration and distribution of diatom species in the Baltic Sea*, vol. 1. Opulus Press, Uppsala. 129 pp.
- SOUTH G.R. & WHITTICK A. 1987. *Introduction to phycology*. Blackwell Science, Oxford. 341 pp.
- STOSCH H.A. VON 1962. Über das Perizonium der Diatomeen. *Vorträge aus dem Gesamtgebiet der Botanik* 1: 43–52.
- STOSCH H.A. VON 1965. Manipulierung der Zellgrösse von Diatomeen in Experiment. *Phycologia* 5: 21–44.
- STOSCH H.A. VON 1982. On auxospore envelopes in diatoms. *Bacillaria* 5: 127–156.
- STOSCH H.A. VON & DREBES G. 1964. Entwicklungsgeschichtliche Untersuchungen an zentrischen Diatomeen IV. Die Planktondiatomee *Stephanopyxis turris* – ihre Behandlung und Entwicklungsgeschichte. *Helgoländer wissenschaftliche Meeresuntersuchungen* 11: 209–257.
- TIFFANY M.A. 2005. Diatom auxospore scales and early stages in diatom frustule morphogenesis: their potential for use in nanotechnology. *Journal of Nanoscience and Nanotechnology* 5: 131–139.
- TOYODA K., IDEI M., NAGUMO T. & TANAKA J. 2005. Fine-structure of the vegetative frustule, perizonium and initial valve of *Achnanthes yaquinensis* (Bacillariophyta). *European Journal of Phycology* 40: 269–279.
- TOYODA K., WILLIAMS D.M., TANAKA J. & NAGUMO T. 2006. Morphological investigations of the frustule, perizonium and initial valves of the freshwater diatom *Achnanthes crenulata* (Bacillariophyceae). *Phycological Research* 54: 173–182.
- TROBAJO R., MANN D.G., CHEPURNOV V.A., CLAVERO E. & COX E.J. 2006. Auxosporulation and size reduction pattern in *Nitzschia fonticola* (Bacillariophyta). *Journal of Phycology* 42: 1353–1372.
- WILLIAMS D.M. 2001. Comments on the structure of ‘postauxospore’ valves of *Fragilariforma virescens*. In: *Lange–Bertalot Festschrift, Studies on diatoms* (Ed. by R. Jahn, J.P. Kociolek, A. Witkowski & P. Compère), pp. 103–117. A.R.G. Gantner, Ruggell, Liechtenstein.
- WITKOWSKI A., LANGE-BERTALOT H. & METZELTIN D. 2000. Diatom flora of marine coasts I. *Iconographia Diatomologica* 7: 1–925.
- ZINGONE A., PERCOPO I., SIMS P.A. & SARNO D. 2005. Diversity in the genus *Skeletonema* (Bacillariophyceae). I. A reexamination of the type material of *S. costatum* with the description of *S. grevillei* sp. nov. *Journal of Phycology* 41: 140–150.

Table 1. Strains of *Grammatophora marina* examined in this study.^aSample no., because observation was done under a rough culture. Voucher slide was not deposited.

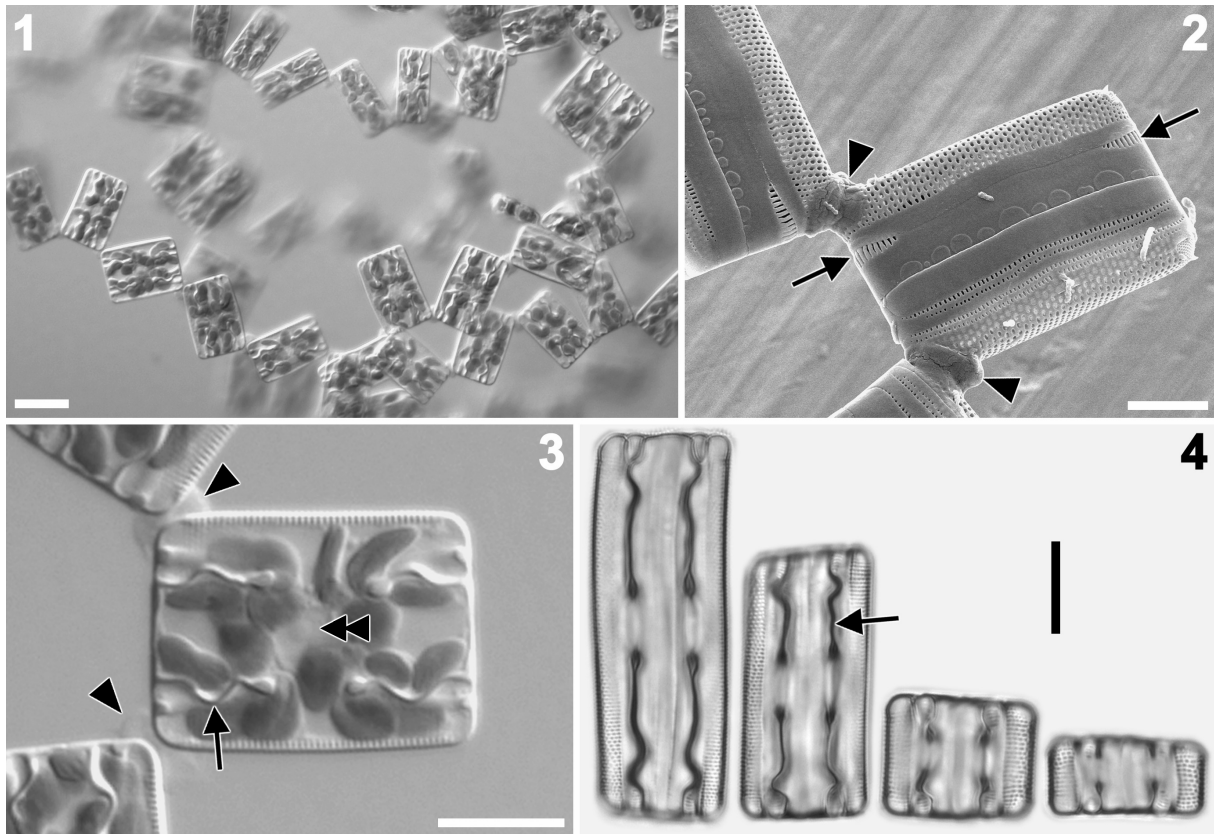
Strain no. (Voucher no.)	Observed phenomena	Collecting date	Observation date	Locality	Collector
AA1 ^a	Allogamous sexual auxosporulation	Apr. 2004	14. May 2004	Galveston Bay, Texas, USA	W. Wardle
SKR5-1 ^a	Vegetative initial cell formation	03. Apr. 2003	14. Apr. 2003	Rinnkou Park, Kanagawa Pref., Japan	S. Sato
s0050 (Zu6/22)	Uniparental auxosporulation	05. Apr. 2004	08. Nov. 2004	English Channel, Roscoff, France	K. Valentin
s0050/01 ^b (Zu6/23)	Abrupt cell size reduction	24. Jul. 2005 ^c	16. Oct. 2005	-	-
s0074 (Zu6/24)	Vegetative cell enlargement	Apr. 2004	06. Oct. 2005	Galveston Bay, Texas, USA	W. Wardle
s0130 (Zu6/25)	Abrupt cell size reduction	24. Feb. 2004	21. Feb. 2005	Port Park, Chiba Pref., Japan	T. Tadano
s0136 (Zu6/26)	Vegetative cell enlargement	24. Feb. 2004	21. Feb. 2005	Port Park, Chiba Pref., Japan	T. Tadano

^bF1 generation of s0050.^cRe-isolation date from s0050 strain.

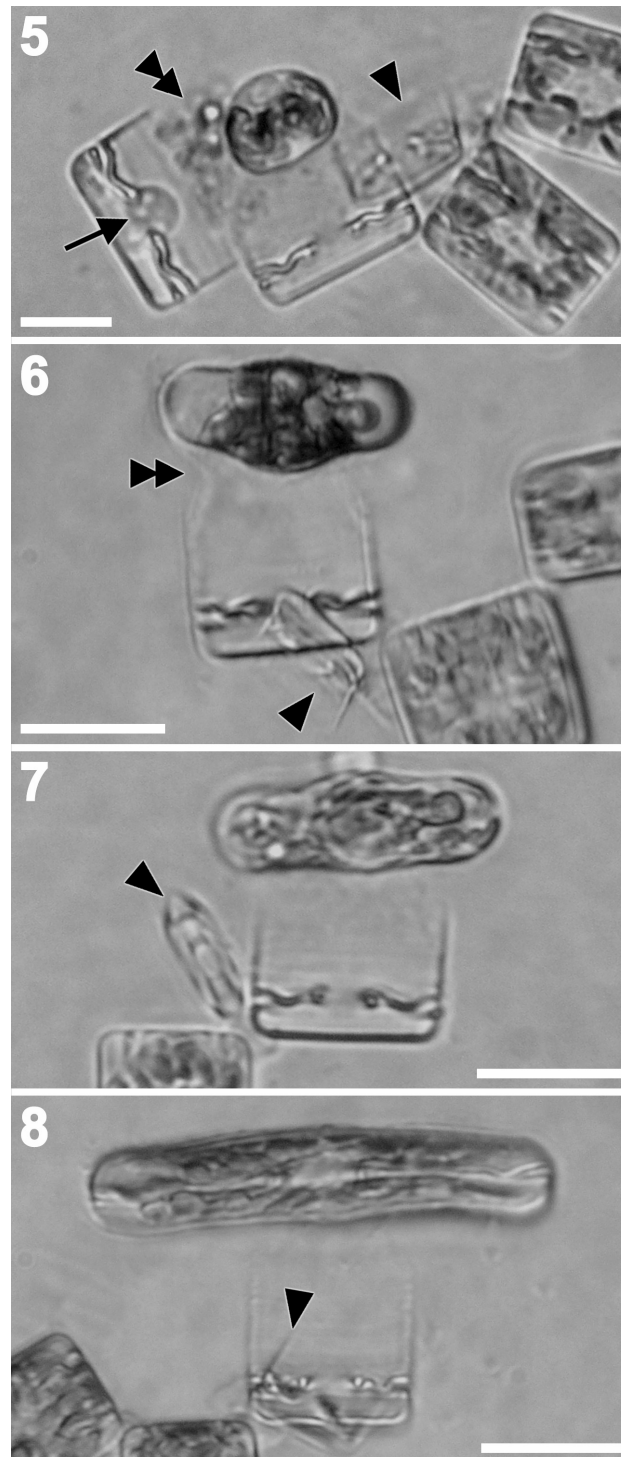
Table 2. Parental and initial cell lengths^a of this study and from literature.^aValues are range (means \pm SD): number of cells measured

Mode of reproduction	Mother cell ^b (μm)	Male cell (μm)	Initial cell (μm)
Allogamous sexual auxosporulation	19.4-24.7 (21.8 \pm 1.4) :17	13.6-15.9 (14.8 \pm 1.2) :3	52.3-70.4 (63 \pm 5.8) :9
Allogamous sexual auxosporulation ^c	30-70	20-50	122.9-158.3 (137.2 \pm 11.53) :8 ^d
Uniparental auxosporulation	14.7-20.3 (16.8 \pm 1.7) :7	-	68.8-96.3 (84.3 \pm 8.5) :9
Vegetative initial cell formation	16-20 (17.9 \pm 1.9) :5	-	66-73.5 (69.3 \pm 2.7) :6

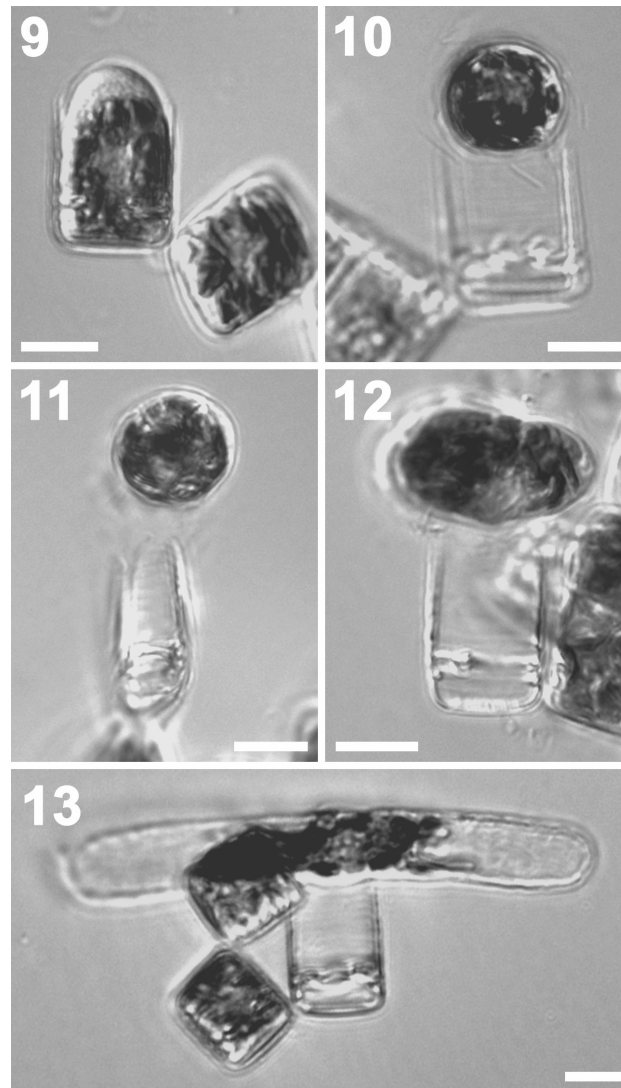
^bFor uniparental auxosporulation and vegetative initial cell formation, 'mother cell' indicates the cells that produced auxospore and initial cell, respectively.^cAccording to Magne-Simon (1962)^dMeasurement was done on figs 20-27 of Magne-Simon (1962)



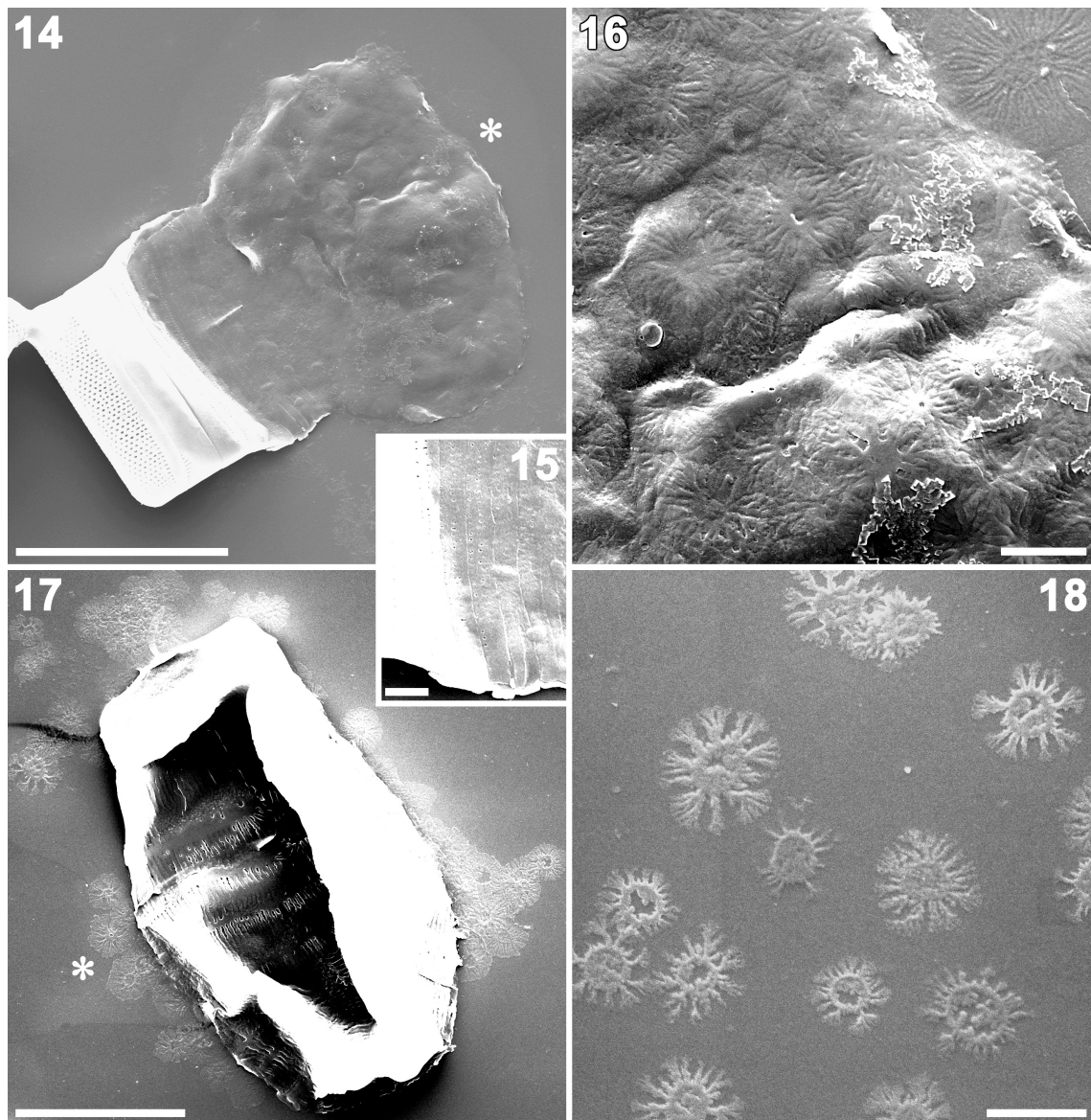
Figs 1–4. Vegetative phase of *Grammatophora marina* (natural material). Light microscopy (Figs 1, 3 and 4) and SEM (Fig. 2). Scale bars = 20 μm (Fig. 1), 5 μm (Fig. 2) and 10 μm (Figs 3, 4). **Fig. 1.** Zig-zag chains of living cells. **Fig. 2.** Attachment of a cell to its neighbour via mucilage (arrowheads) secreted from apical pore fields (cf. Fig. 27). Areas of slits on both ends of the valvocopula secrete no mucilage (arrows). **Fig. 3.** Living colony in girdle view, showing mucilage pads linking the cells (arrowheads). The central nucleus (double arrowhead) is surrounded by elongate chloroplasts, which extend around the septa (arrow). **Fig. 4.** Cleaned and mounted cells in girdle view. Gradual cell size reduction is accompanied by changes in perivalvar depth and in the shape of the septa (e.g. arrow).



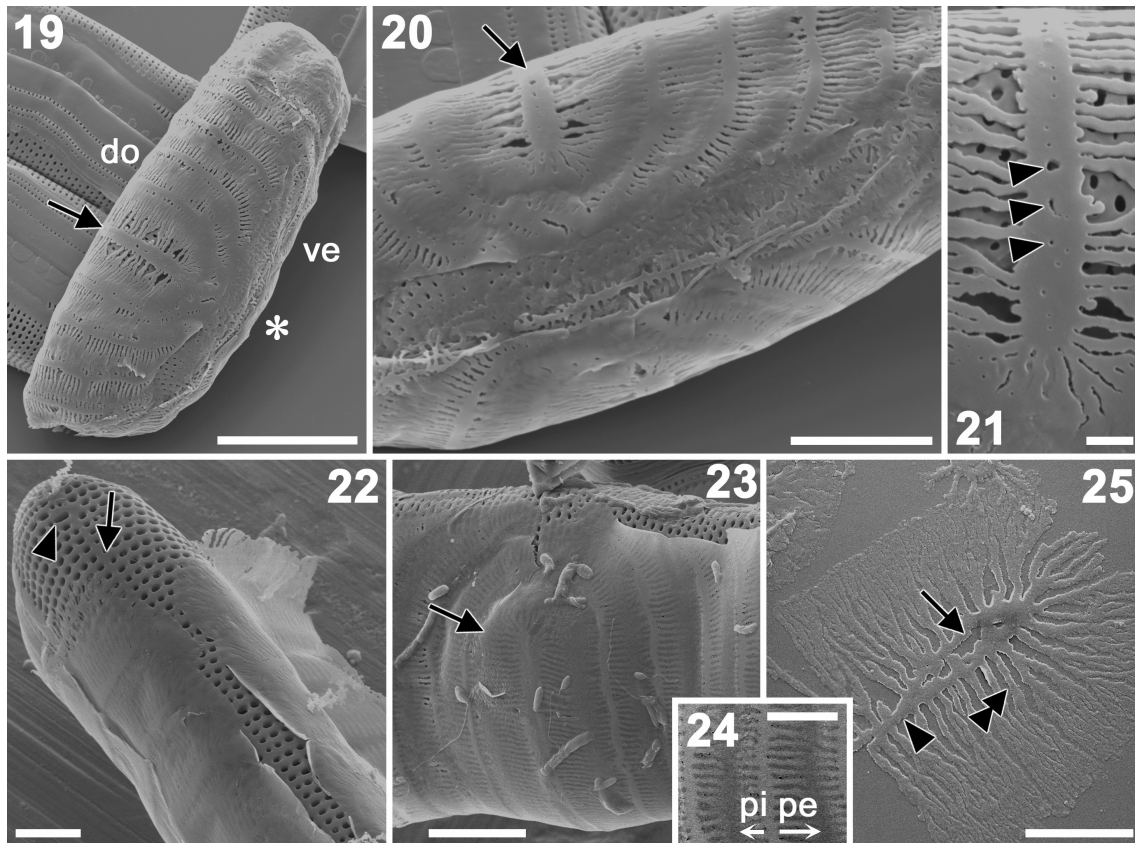
Figs 5–8. Allogamous sexual auxosporulation of *Grammatophora marina*. Rough culture of sample AA1, light microscopy. Empty male gametangia are indicated by arrowheads. Scale bars = 20 μm . **Fig. 5.** Early stage of auxospore development. The fertilized zygote has just vacated the female gametangium, leaving a small residual body (arrow). A degenerate chloroplast is also present (double arrowhead). **Figs 6, 7.** Expanding auxospores. Mucilage (double arrowhead) connects the auxospore to the female gametangium. **Fig. 8.** Mature auxospore containing initial cell. In this example, the male cell is almost completely out-of-focus (line at arrowhead).



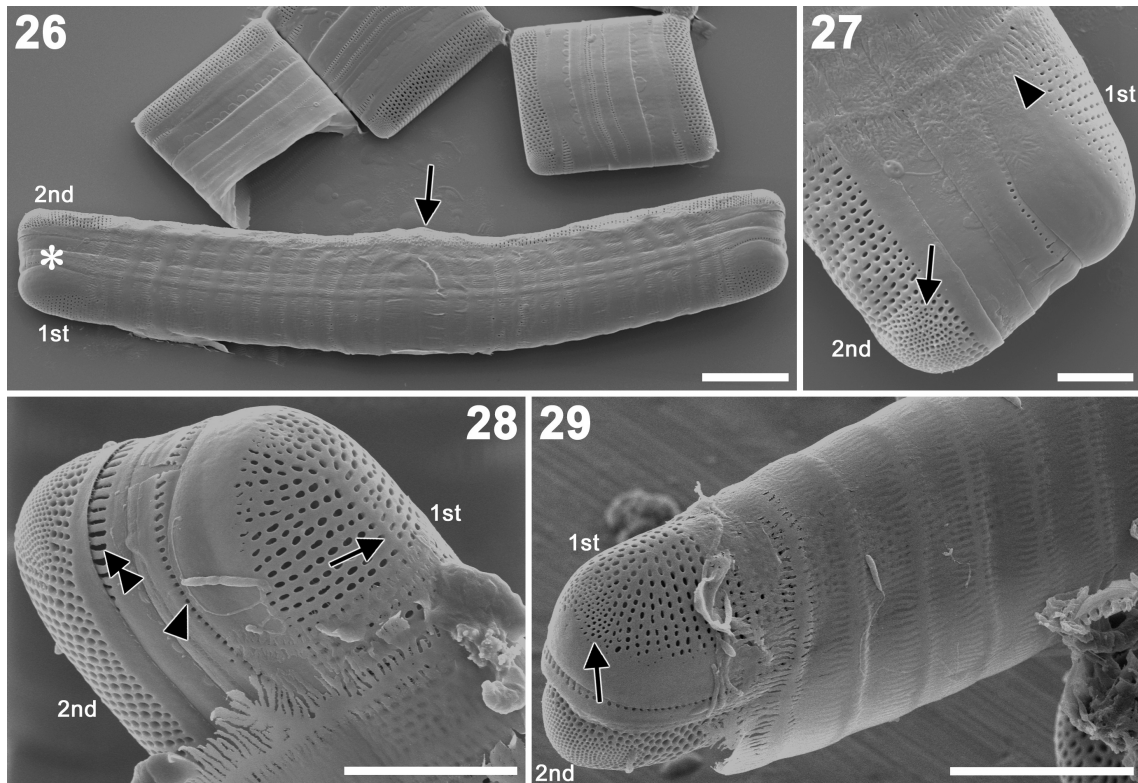
Figs 9–13. Uniparental auxosporulation of *Grammatophora marina*. Clone s0050, light microscopy. Scale bars = 10 μm . **Fig. 9.** Pre-auxospore stage: the free surface of the protoplast has rounded off following loss of the upper theca. **Figs 10, 11.** Young spherical auxospore near the mother-cell theca. **Figs 12.** Expanding auxospore. **Fig. 13.** Mature auxospore (as yet without initial valves).



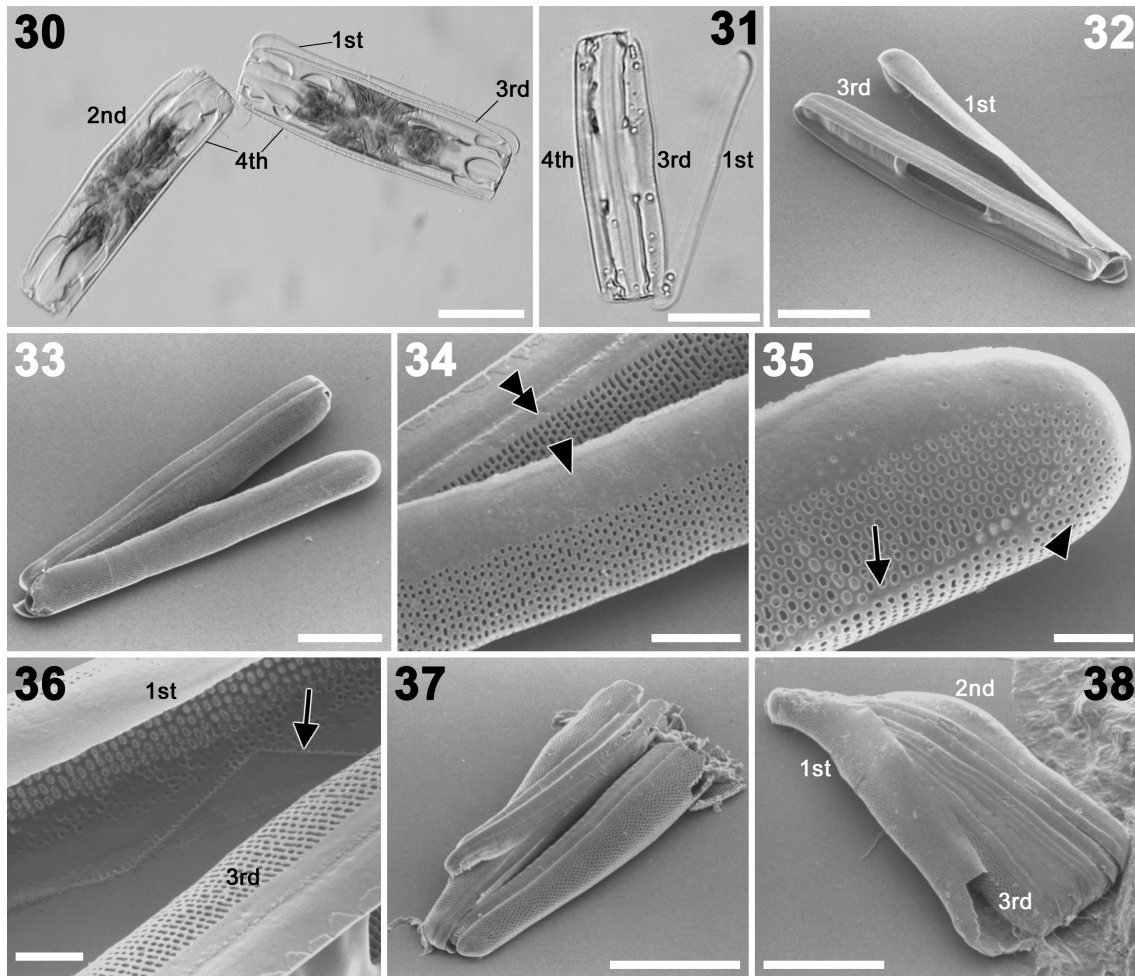
Figs 14-18. Auxospore scales of *Grammatophora marina*, SEM. Rough culture AA1 (Figs 14-16) and clone s0050 (Figs 17, 18). Scale bars = 10 μm (Figs 14, 17) and 2 μm (Figs 16, 18). **Fig. 14.** Young auxospore recently emerged from the mother-cell, before perizonium formation. **Fig. 15.** Detail of mother-cell girdle, showing numerous copulae. **Fig. 16.** Enlargement of Fig. 14 (at asterisk) showing circular scales on the surface of the auxospore. **Fig. 17.** Partly expanded auxospore with transverse perizonial bands, in high contrast to show the scales that have dropped around the auxospore. **Fig. 18.** Scales with annuli surrounded by fimbriae.



Figs 19–25. Perizonium of *Grammatophora marina*, SEM. Clone s0050. Scale bars = 10 μm (Fig. 19), 5 μm (Figs 20, 23), 1 μm (Fig. 21) and 2 μm (Figs 22, 24 and 25). **Fig. 19.** Small auxospore covered with transverse perizonial bands. Note the wider, symmetrical primary transverse band (arrow). The dorsal (do) and ventral (ve) sides are marked. **Fig. 20.** Detail of the part marked with asterisk in Fig. 19, showing the suture, where irregular siliceous structures are located. The end of the primary transverse band (arrow) is visible. **Fig. 21.** Primary transverse band, with pores along the central rib (arrows). **Fig. 22.** Ventral side of a mature auxospore, showing the suture and underlying initial hypovalve. None of the irregular longitudinal structures remain. The exterior opening of a rimoportula is visible (arrowhead) in the hypovalve, which has a normal striation extending out from the sternum (arrow). **Fig. 23.** Central part of mature auxospore showing the transverse perizonium bands, which are all asymmetrical apart from the primary band (arrow). **Fig. 24.** Detail of the secondary transverse perizonial bands: in each, the distal fimbriae (the pars exterior: pe) are longer than the proximal fimbriae (forming the pars interior: pi). **Fig. 25.** Tip of an isolated primary transverse band, showing an annulus-like development (arrow) of the primary rib (arrowhead). The primary rib bears secondary ribs (double arrowhead) on each side, which then split up into finer ribs, forming a fringe of fimbriae.



Figs 26–29. Initial cells of *Grammatophora marina*, SEM. Clone s0050. Valves are numbered in order of formation. Scale bars = 10 μm (Fig. 26), 3 μm (Fig. 27) and 5 μm (Figs 28, 29). **Fig. 26.** Initial cell within the perizonium. The second (hypo-) valve has a slightly convex centre (arrow). **Fig. 27** Enlargement of the part marked with asterisk in Fig. 26. Note the difference in striation between the 1st and 2nd valves. A few scales (arrowhead) are still present. **Fig. 28.** End of initial cell. Note the prominent sternum (arrow) and the absence of an apical pore field in the 1st (epi-) valve, and the difference in striation between the valvocopulae of the initial epitheca (arrowhead) and the initial hypotheca (double arrowhead). **Fig. 29.** Initial cell in which the initial epivalve has a much reduced apical pore field (arrow).



Figs 30–38. Initial cells of *Grammatophora marina* produced vegetatively. Light microscopy (Figs 30, 31) and SEM (Figs 32–38). Rough culture of SKR5-1 sample. Scale bars = 20 μm (Figs 30–33), 5 μm (Fig. 34), 3 μm (Figs 35, 36) and 10 μm (Figs 37, 38). **Figs 30–33.** A recently divided initial cell, with valves numbered in order of formation. The daughter cells are shown (alive) in Fig. 30: the initial epivalve (1st) is now superfluous, being replaced by a normally-structured valve (3rd). Following treatment by the bleaching method, the daughter cell possessing the initial epivalve was studied in LM (Fig. 31) and SEM (Figs 32, 33). **Figs 34, 35.** Enlargements of the centre (Fig. 34) and pole (Fig. 35) of the daughter cell of Figs 31–33. Note the broader valve margin of the initial epivalve (Fig. 34, arrowhead), relative to the vegetative valve beneath (double arrowhead). The initial epivalve has a prominent sternum (Fig. 35, arrow) and radially arranged pores at the apex (Fig. 35, arrowhead; contrast Figs 27–29). **Fig. 36.** Interior of the initial epivalve of Figs 30–33. Note valvocopula of initial valve (arrow). **Figs 37, 38.** Strongly deformed initial cell, in which one end has failed to develop properly.

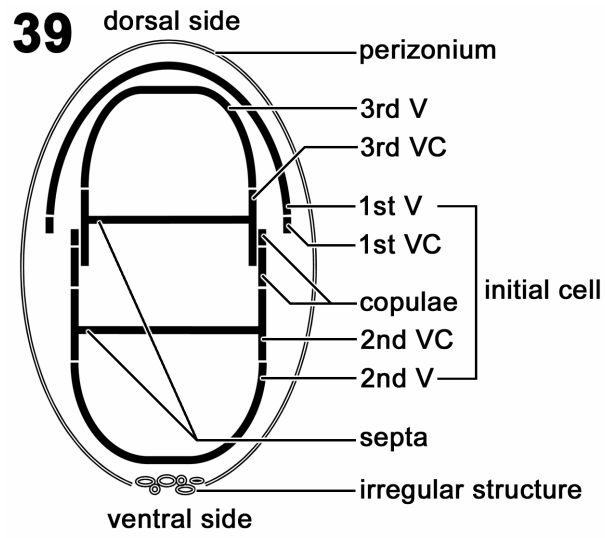
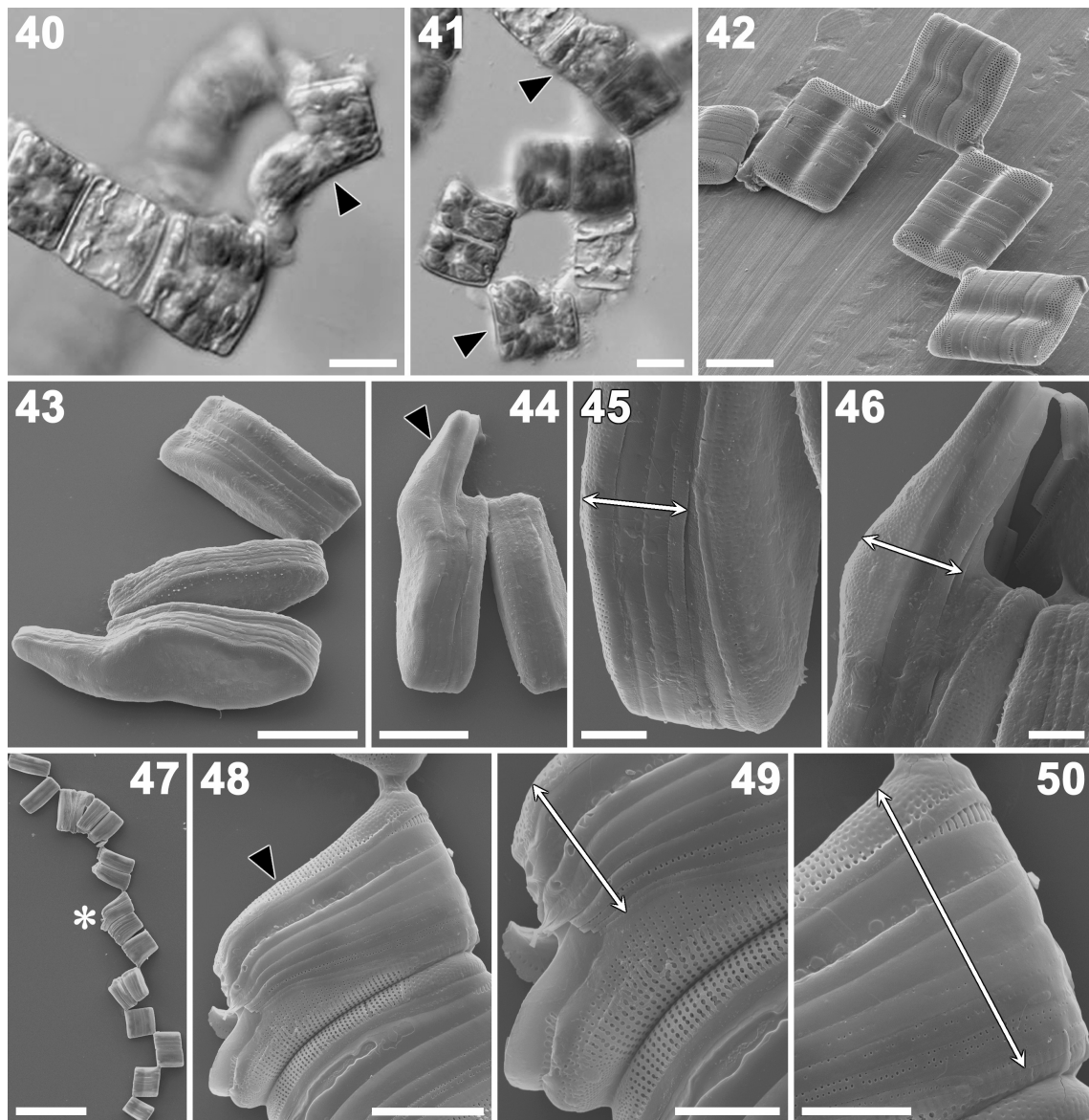


Fig. 39. Schematic section of the auxospore and initial cell. V = valve, VC = valvocopula.



Figs 40-50. Abrupt cell size reduction and vegetative enlargement in *Grammatophora marina*. Light microscopy (Figs 40, 41) and SEM (Figs 42-50). Clone s0130 (Fig. 40), s0136 (Fig. 41), s0050/01 (Figs 42-46), s0074 (Figs 47-50). Scale bars = 10 μm (Figs 40, 41, 43 and 48), 20 μm (Fig. 42), 5 μm (Figs 45, 46, 49 and 50) and 50 μm (Fig. 47). **Fig. 40.** Abrupt cell size reduction. Arrowhead indicates cell with large epitheca and considerably smaller hypotheca. **Fig. 41.** Vegetative cell enlargement. Arrowheads indicate the cell with small epitheca and larger hypotheca that gave rise to the chain of larger cells. **Fig. 42.** Zig-zag colony in which abrupt cell size reduction has taken place. Note that one side of each cell has a constriction. **Figs 43-46.** Abrupt cell size reduction. Arrowhead and arrows indicate the epitheca in the overall view (Fig. 44) and details (Figs 45, 46) of the cell in which size reduction occurred. **Figs 47-50.** Vegetative cell enlargement in the cell indicated by an asterisk in Fig. 47. The arrowhead and arrows indicate the position and extent of the epitheca.

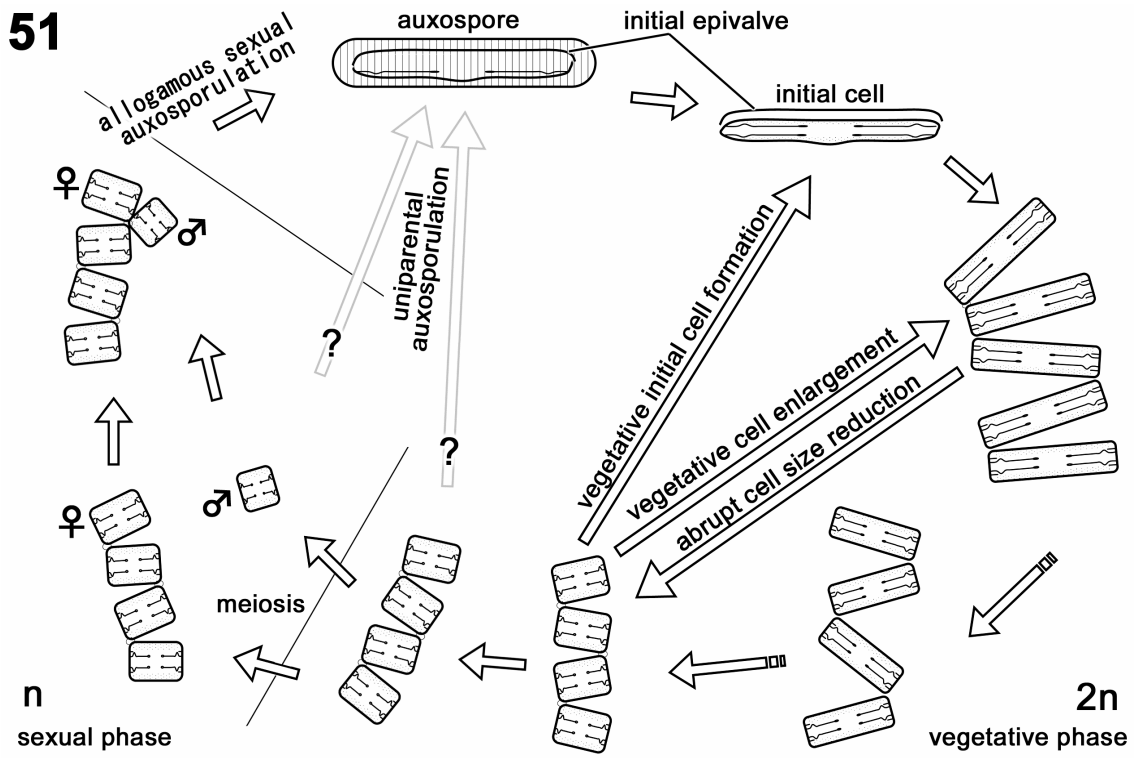


Fig. 51. The life cycle of *Grammatophora marina*.

2.5. Publication IV:

**AUXOSPORE FORMATION AND THE MORPHOLOGY OF THE
INITIAL CELL OF THE MARINE ARAPHID DIATOM *GEPHYRIA
MEDIA* (BACILLARIOPHYCEAE)**

SHINYA SATO^{1*} TAMOTSU NAGUMO² & JIRO TANAKA¹

¹*Tokyo University of Marine Science and Technology, Konan 4-5-7, Minato-ku, 108-8477
Tokyo, Japan*

²*The Nippon Dental University, Fujimi 1-9-20, Chiyoda-ku, 102-8159 Tokyo, Japan*

Abstract

Recent studies have led to a rapid increase in knowledge of auxospore formation in diatoms. However, these studies have been limited to centric and raphid pennate diatoms, and there is still very little information for the araphid pennate diatoms. Using LM and SEM, we studied the development of the auxospore and the initial cell of the marine epiphytic diatom *Gephyria media* Arnott. Auxospores were bipolar and curved in side view, as in many other pennate diatoms. SEM revealed many transverse perizonial bands, all of which were incomplete rings. There was an elongate, sprawling, silicified structure beneath the ventral suture of the transverse perizonial bands. This structure is presumably equivalent to the longitudinal perizonial band in other pennate diatoms, although we could not determine the homologous relationship between the two features. Scales were found both in the inner wall of the perizonium and around the primary perizonial bands. The presence or absence of scales may be of phylogenetic significance in diatoms, only during the final stages of auxospore formation because scales are found in early spherical stages. The distinctive finger-like structures observed throughout all stage of *G. media* have not been observed before in the other diatom taxa.

KEY WORDS: araphid diatom; auxospore; elongate sprawling structure; finger-like structure; “freeze method”; *Gephyria media*; initial cell; morphology; perizonium; scale

INTRODUCTION

Gephyria Arnott is an araphid pennate diatom genus whose members grow in marine coastal regions. The genus is characterized by flexed cells that attach to the substratum by mucilaginous pads, which are secreted from the apical pore fields at the poles of the concave valve. Because of its flexure and the presence of apical pore fields on the concave valve only, *Gephyria* is heterovalvate. The arcuate valves have a two-layered construction containing many chambers (Round et al. 1990). The morphological features of *G. media* were described by John (1984). Valve morphogenesis was studied by Tiffany (2002) using LM and SEM. Most diatoms may undergo sexual reproduction when their cell sizes are sufficiently small, after a series of mitotic cell divisions. After sexual reproduction, the zygote (auxospore) expands and an initial cell is formed within it. The evolutionary significance of auxospore structure in all major groups of diatoms is well accepted (Round and Crawford 1981, von Stosch 1982) and recently reconfirmed by Kaczmarek et al. (2000, 2001). For example, the auxospores of most centric diatoms, for example, *Ellerbeckia arenaria* f. *arenaria* (Moore ex Ralfs) R. M. Crawford, are covered with large numbers of scales (Schmid and Crawford 2001). However, the auxospores of many species of pennate diatoms, for example, *Rhoicosphenia curvata* (Kützing) Grunow, are enclosed by a perizonium (Mann 1982b), which is composed of many bands, often in two series, transverse and longitudinal. In *Pseudonitzschia multiseries* (Hasle) Hasle, scales have been observed on the surface of the gametes and the primary auxospore wall (Kaczmarek et al. 2000). Kaczmarek et al. (2000) speculated that scales may prove to be more common when more species are examined.

Knowledge of auxospore formation in diatoms is rapidly increasing (Mann 1982b, Cohn et al. 1989, Mann and Stickle 1989, Mayama 1992, Passy-Tolar and Lowe 1995, Kaczmarek et al. 2000, Kobayashi et al. 2001, Schmid and Crawford 2001, Nagumo 2003). However, this information is limited to studies on centric diatoms and raphid pennate diatoms, and there is still very little information for the araphid diatoms. Auxospore formation has been reported in several araphid diatoms: *Grammatophora marina* (Lyngbye) Kützing

(Magne-Simon 1960, 1962), *Rhabdonema adriaticum* Kützing (Karsten 1899, von Stosch 1958, 1962), *R. arcuatum* Kützing (Karsten 1899, von Stosch 1962, 1982), *R. minutum* Kützing (von Stosch 1958), *Diatoma Bory*, *Meridion* Agardh and *Synedra* (Geitler 1973), *Striatella unipunctata* (Lyngbye) Agardh, *Licmophora abbreviata* Agardh (Roshchin 1994), and *L. ehrenbergii* (Kützing) Grunow (Roshchin 1994, Roshchin and Chepurnov 1999), *L. gracilis* (Ehrenberg) Grunow var. *anglica* (Kützing) Peragallo (Mann 1982a). However, none of these studies included EM. In our study, several stages in the development of the auxospore and initial cell of *Gephyria media* were observed using SEM.

MATERIALS AND METHODS

Vegetative cells and auxospores of *G. media* attached to *Plocamium telfairiae* Harvey (Rhodophyceae, Plocamiaceae) were collected by S. Sato from Tenjin-jima, Kanagawa Prefecture, Japan on January 2003. All organic matter, outside and inside the cells, was removed by the bleaching method (Nagumo and Kobayasi 1990) to reveal the silicified valves and associated structures. To observe the initial cell without perizonial bands, “bleached” specimens were cleaned by boiling with concentrated sulfuric acid and potassium nitrate for about 10 min and then washed several times in distilled water (Patrick and Reimer 1966).

Samples were observed in LM with bright field or differential interference contrast optics. To keep auxospores intact for SEM observation, samples were prepared using a novel method, which we call the “freeze method.” Samples were fixed with 10% glutaraldehyde, rinsed with distilled water until all the glutaraldehyde was removed, frozen in a -20°C freezer, and placed in a vacuum (temperature maintained below freezing point) to allow the sample to sublime until ice was no longer visible. This method reduces labor time and does not require the use of many chemicals.

For SEM observations, dried specimens were placed on a cover glass, which was then fixed to a metal stub with carbon tape and paste. An S-4000 scanning electron microscope (Hitachi, Tokyo, Japan) was used at an accelerating voltage of 3 or 5 kV. The morphological terms in this article were taken from Anonymous (1975), Cox and Ross (1981), and, particularly with respect to the auxospores, from Round et al. (1990).

RESULTS

Auxospore formation

Vegetative cells usually exhibited three copulae per theca (Figs. 1, A–D, and 2A). Before auxospore formation, the number of copulae in the mother cell increased and numerous discoid chloroplasts were visible (Fig. 2B). After expansion of the girdle, the protoplasm contracted toward the center of the cell (Fig. 2, C–E), and the cell comprised one attached valve (concave) and about 20 copulae. By this time, the other convex valve had often been lost (Fig. 2, D and E). After the protoplasm had contracted, the early stage of the auxospore gradually grew away from the mother cell (Fig. 2, F–J), and the auxospore became covered with a mucilage envelope. The swelling of the auxospore ruptured some copulae (Fig. 2H), which were subsequently lost (Figs. 2, I and J, and 4, C and D). As the auxospore emerged from the mother cell, perizonial bands began to form at the center of the auxospore (Fig. 2J, arrowhead).

Meanwhile, many of the chloroplasts contracted toward the ventral side (Fig. 2, H–J). The number of the perizonial bands then increased, although perizonial caps were still at-

tached at both ends of the auxospore (Figs. 3, A and C, and 4D, double arrowhead). At this stage of auxospore formation, there were about 20 perizonial bands, and no special structure was observed on the ventral side (Fig. 3A). This central part of the ventral side formed a suture. The suture resulted from the fact that all the transverse perizonial bands were incomplete hoops, their open ends lying on the ventral side of auxospore. Subsequently, an elongate sprawling structure was formed beneath the suture (Fig. 3, B and C) on the ventral side, expanding until the auxospore had matured. When the auxospore reached its maximum size, it had a large number (approximately 60) of perizonial bands (Figs. 3C and 4). Formation of the initial epivalve commenced as soon as the auxospore reached its maximum size (Fig. 4B). After the initial epivalve had been completed, the initial hypovalve started to form (Fig. 4C, arrow). The mature auxospore, enclosing the complete initial cell, remained associated with the mother cell by mucilaginous substances (Fig. 4, C and D, between two arrowheads). By this stage, the perizonial caps had sometimes been lost but otherwise adhered to the ends of the auxospore (Fig. 4D, double arrowhead). We did not observe any evidence of male gametangia, fertilization, or autogamy in the present study.

Fine structure of the auxospore. SEM observation of the auxospore mother cell confirmed that it had numerous copulae (Fig. 5A), each of which was perforated by a row of areolae (Fig. 5B). The copulae were of the open type, with open and closed ends alternating at each pole (Fig. 5C). The perizonium consisted of a large number of perizonial bands (Fig. 5D), which were all open (Fig. 5E), including the primary band (not shown). The bands were closely associated with each other (Fig. 5F), and their fimbriate margins were slightly longer at the pars interior than the pars exterior (Fig. 5G). In external view, the center of suture was covered with a fragment similar to a perizonial band (Fig. 5H, arrow). In internal view, an elongate sprawling structure was observed on the ventral side of the auxospore. The structure extended in a longitudinal direction but was simpler in form than the perizonial band (Fig. 5, I and J). As the auxospore became longer, the elongate sprawling structure expanded transversely along the suture (Fig. 3, B and C).

Simple circular to elliptic scales, 5–15 μm in diameter, were observed against the inner wall of the auxospore (Fig. 6). The scales possessed a central boss without areolae surrounded by a fimbriate margin (Fig. 6, A, B, D, and E). The distribution of the scales differed from that in previously studied diatoms, because they were scattered throughout the perizonium (Fig. 6B) as well as over the inner and outer surfaces of the primary perizonial band (Fig. 6, C–E).

Initial cell

The length of the initial cell was about twice that of the mother cell (Fig. 4, C and D). Valves usually had an abnormal outline (Fig. 7, A and B), and the striae on the initial hypovalve were sometimes irregularly arranged (Fig. 7C). There were two rows of pores between each pair of virgae (biseriate striae) at the margin of the initial valve (Fig. 7D), whereas, according to John (1984), Round et al. (1990), and Tiffany (2002), vegetative valves have triseriate striae at their margins. Notably, the density of striae was different between the initial convex valve (13–14 in 10 μm) and the initial concave valve (12–13 in 10 μm) and from the vegetative convex valve (14–15 in 10 μm) and the vegetative concave valve (11 in 10 μm) (measured at the center of valve with SEM).

In the internal view of valve, many elliptic openings were seen (Fig. 7E, arrowheads). A rimoportula was observed at the apex of the initial epivalve (Fig. 7E, arrow). The position of the rimoportula on the vegetative valve was beneath the apical pore field; on the other hand, that of initial convex valve was located much further (ca. 10 μm) the valve apex (John 1984,

Tiffany 2002). Finger-like structures were found on the initial epi- and hypovalve (Fig. 7, F–H) of *G. media*. These structures could be seen through external areola opening (Fig. 7F), and the internal view showed that they wound themselves around the vimines (Fig. 7, G and H). Tiffany (2002, Figs. 13 and 14) concluded that these structures were fine rotae. However, rotae occlude the pores in two dimensions (e.g. *Triceratium shadboltianum* Greville) rather than in three dimensions as seen in *G. media*. The finger-like structures observed throughout all stage of *G. media* are distinctive and have never been observed in the other diatom taxa.

DISCUSSION

Auxospore formation and perizonium morphology

The production of additional copulae by the auxospore mother cell has been observed in a few other diatoms, both centric (e.g. *Arachnoidiscus ornatus* Ehrenberg; Kobayashi et al. 2001) and pennate (e.g. *Rhabdonema adriaticum*; Karsten 1899). There are also some parallels with *Arachnoidiscus* even though the convex valve of the mother cell is lost in *Gephyria* and the nonattached valve of *Arachnoidiscus* remains on its auxospore. Both taxa are haterovalvate, epiphytic, and relatively large cells. They were often observed together on the same substratum, for example, *Gelidium elegans* Kützing (Rhodophyceae, Gelidiales) and *Plocamium telfairiae* in our material. Further information is required, however, to determine the phylogenetic relationships between these two taxa.

Perizonial caps derived from the zygote wall of *G. media* differed in thickness from those of some raphid diatoms, for example, *Frustulia rhomboides* (Ehrenberg) De Toni var. *saxonica* (Rabenhorst) De Toni (Pfitzer 1871), *Neidium affine* (Ehrenberg) Pfitzer (Mann 1984), and *Seminavis* cf. *robusta* Danielidis and D. G. Mann (Chepurnov et al. 2002). When auxospore expansion is completed, most of the perizonial caps of *G. media* turn inside out (Figs. 3C, arrowhead, double arrowhead, and 4D, double arrowhead) and then are lost. The perizonium caps of *N. affine* contain a high proportion of silica and regulate the size of transverse perizonial bands formation (Mann 1984). The perizonial caps of *G. media* are presumably made by organic matter judging by its softness (easily turn inside out) and surface texture under SEM (not shown), which was rough, unlike that of *N. affine*. Therefore, we regard the perizonium caps of *G. media* as remnants on the auxospore without any active role.

The primary band of *G. media* could only be distinguished by its position. This is different from raphid pennate diatoms, in which the primary perizonial band often differs from the other bands and may be a closed hoop, for example, *Amphora copulata* (Kützing) Schoeman and Archbald (Nagumo 2003), *Craticula cuspidata* Kützing (Cohn et al. 1989), *Navicula oblonga* (Kützing) Kützing (Mann and Stickle 1989), *N. affine* (Mann 1984), and *R. curvata* (Mann 1982b). The secondary and the tertiary bands are distinguishable in width. The secondary bands are narrower than the tertiary bands (Fig. 5D), which is similar to that observed in *Gomphoneis mesta* Passy-Tolar and Lowe (Passy-Tolar and Lowe 1995) and *R. curvata* (Mann 1982b).

In general, diatoms construct their siliceous structures exquisitely and precisely, as exemplified by the regularity of scales, perizonia, and the valve striae. On the other hand, the elongate sprawling structure beneath the ventral suture in *Gephyria* is formed quickly and is relatively simple and irregular in shape. The elongate sprawling structure shows obvious similarities to the longitudinal perizonial band of *R. arcuatum* (von Stosch 1982, their Figs. 1 and 4c). Both structures are narrow in width and lie beneath the suture. Although the longitudinal perizonial band in *R. arcuatum* is a single structure, the elongate sprawling structure of *G. media* consists of multiple silicated fragments (Fig. 5, I and J). Furthermore, they are distin-

guished from each other by the presence or absence of apparent axial sternum. There are also clear differences in shape between the longitudinal perizonial band of many raphid diatoms and the elongate sprawling structure. The longitudinal perizonial band is often broader in width (e.g. *Navicula ulvacea* [Berkeley ex Kützing] Cleve; Mann 1994, Fig. 47A) and highly silicated (e.g. *Achnanthes yaquinensis* McIntire and Reimer [Toyoda et al. 2003], *A. copulata* [Nagumo 2003], *Diploneis papula* [Schmidt] Cleve [Idei 1993], and *R. curvata* [Mann 1982b]). Both the elongate sprawling structure and longitudinal perizonial band may play an important role in strengthening the auxospore wall in the longitudinal direction and reinforcement of the part of the suture. However, although these structures appear to play similar roles, we cannot assume that they are homologous.

Scale

Scales were found around the primary band and on the inner wall of the perizonium. We speculate that the early stages of the auxospore wall may be covered with scales for protection, like the postulated scale-bearing ancestor of the diatoms (Round and Crawford 1981, Round et al. 1990). Our interpretation of scale distribution on the perizonium wall of *G. media* is as follows: 1) early stages of the auxospore bear the scales, 2) the auxospore becomes larger and forms many perizonial bands, and 3) the scales are conveyed to both ends as the auxospore expands, although some scales remain at its equator. However, we cannot yet explain why scales were found at the inside of the perizonium.

It is likely that discoid scales are adequate for covering a spherical body, for example, on the gametes and primary auxospore wall in the pennate diatom *Pseudonitzschia multiseries* (Kaczmarek et al. 2000). However, band-like structures, rather than scales, may be required to cover a tubular structure. Therefore, when and where scales form depends on the morphological features of the auxospore. Further detailed study may reveal that the auxospores of other pennate diatoms bear scales, particularly during the spherical phase and/or on rounded surfaces of the cylindrical body.

ACKNOWLEDGEMENT

This work was supported in part by Grant-in-Aid no. 15570087 from the Ministry of Education, Science, Sports and Culture, Japan. We thank Akiyoshi Takahashi and Jin Bo (Physiological Laboratory at Tokyo University of Marine Science and Technology, Tokyo, Japan) for their assistance with the collection of samples at the Tenjin-jima. We thank Adrian Stotto (Laboratory of Fish Culture at Tokyo University of Marine Science and Technology, Tokyo, Japan) for improving the English. We are grateful to David G. Mann (Royal Botanic Garden, Edinburgh, U. K.) for discussion and comments on the manuscript.

REFERENCES

- Anonymous. 1975. Proposals for a standardization of diatom terminology and diagnoses. *Nova Hedw. Beih.* 53:323–54.
- Chepurnov, V. A., Mann, D. G., Vyverman, W., Sabbe, K. & Danielidis, D. B. 2002. Sexual reproduction, mating system, and protoplast dynamics of *Seminavis* (Bacillariophyceae). *J. Phycol.* 38:1004–19.

- Cohn, S. A., Spurck, T. P., Pickett-Heaps, J. D. & Edger, L. A. 1989. Perizonium and initial valve formation in the diatom *Navicula cuspidata* (Bacillariophyceae). *J. Phycol.* 25:15–26.
- Cox, E. J. & Ross, R. 1981. The striae of pinnate diatoms. In Ross, R. [Ed.] *Proceedings of the 6th International Diatom Symposium on Recent and Fossil Diatoms*. O. Koeltz, Koenigstein, pp. 267–78.
- Geitler, L. 1973. Auxosporenbildung und Systematik bei pennaten Diatomeen und die Cytologie von Cocconeis-Sippen. *Österreich. Botan. Zeitschr.* 122:299–321.
- Idei, M. 1993. *Diploneis papula* (A. Schmidt) Cleve. In Hori, T. [Ed.] *An Illustrated Atlas of the Life History of Algae. Vol. 3. Unicellular and Flagellated Algae*. Utida Rokakuho Publishing, Tokyo, pp. 284–5. (in Japanese).
- John, J. 1984. Observation on the ultrastructure of *Gephyria media* W. Arnott. In Richard M. [Ed.] *Proceedings of the 8th International Diatom Symposium*. Koeltz Scientific Books, Koenigstein, pp. 155–162.
- Kaczmarska, I., Bates, S. S., Ehrman, J. M. & Léger, C. 2000. Fine structure of the gamete, auxospore and initial cell in the pennate diatom *Pseudo-nitzschia multiseriata* (Bacillariophyta). *Nova Hedw.* 71:337–57.
- Kaczmarska, I., Ehrman, J. M. & Bates, S. S. 2001. A review of auxospore structure, ontogeny and diatom phylogeny. In Economou-Amilli, A. [Ed.] *Proceedings of the 16th International Diatom Symposium*. University of Athens, Greece, pp. 153–68. Karsten, G. 1899. Die Diatomeen der Kieler Bucht. *Wiss. Meeresunters.* 4:17–205.
- Kobayashi, A., Osada, K., Nagumo, T. & Tanaka, J. 2001. An auxospore of *Arachnoidiscus ornatus* Ehrenberg. In Economou-Amilli, A. [Ed.] *Proceedings of the 16th International Diatom Symposium*. University of Athens, Greece, pp. 197–204.
- Magne-Simon, M. F. 1960. Note sur le processus de l'auxosporulation chez une diatomée marine, *Grammatophora marina* (Lyngb.) Kütz. *C. R. Acad. Sci., Paris.* 251:3040–2.
- Magne-Simon, M. F. 1962. L'auxosporulation chez Tabellariacée marine, *Grammatophora marina* (Lyngb.) Kütz. (Diatomacée). *Cahiers Biol. Mar.* 3:79–89.
- Mann, D. G. 1982a. Auxospore formation in Licmophora (Bacillariophyta). *Plant Syst. Evol.* 139:289–94.
- Mann, D. G. 1982b. Structure, life history and systematics of *Rhoicosphenia* (Bacillariophyta). II. Auxospore formation and perizonium structure of *Rh. curvata*. *J. Phycol.* 18:264–74.
- Mann, D. G. 1984. Auxospore formation and development in *Neidium* (Bacillariophyta). *Br. Phycol. J.* 19:319–31.
- Mann, D. G. 1994. Auxospore formation, reproductive plasticity and cell structure in *Navicula ulvacea* and the resurrection of the genus *Dickieia* (Bacillariophyta). *Eur. J. Phycol.* 29: 141–57.
- Mann, D. G. & Stickle, A. J. 1989. Meiosis, nuclear cyclosis, and auxospore formation in *Navicula sensu stricto* (Bacillariophyta). *Br. Phycol. J.* 24:167–81.
- Mayama, S. 1992. Morphology of *Eunotia multiplastidica* sp. nov. (Bacillariophyceae) examined throughout the life cycle. *Korean J. Phycol.* 7:45–54.
- Nagumo, T. 2003. Taxonomic studies of the subgenus *Amphora* Cleve of the genus *Amphora* (Bacillariophyceae) in Japan. *Biblioth. Diatomol.* 49:1–265.
- Nagumo, T. & Kobayasi, H. 1990. The bleaching method for gently loosening and cleaning a single diatom frustule. *Diatom* 5:45–50.

- Passy-Tolar, S. I. & Lowe, R. L. 1995. *Gomphoneis mesta* (Bacillariophyta). II. Morphology of the initial frustules and perizonium ultrastructure with some inferences about diatom evolution. *J. Phycol.* 31:447–56.
- Patrick, R. & Reimer, C. W. 1966. *The Diatoms of the United States*. Vol. 1. Monogr. Acad. Nat. Sci., Philadelphia, 13: 1–688.
- Pfitzer, E. 1871. Untersuchungen über Bau und Entwicklung der Bacillriaceen. Botanische Abhandlungen aus dem Gebiet der Morphologie und Physiologie. Heft 2, Bonn, 183 pp.
- Roshchin, A. M. 1994. *Zhiznennyye tsikly diatomovykh vodoroslej*. Naukova Dumka, Kiev, 170 pp.
- Roshchin, A. M. & Chepurnov, V. A. 1999. Dioecy and monoecy in the pennate diatoms (with reference to the centric taxa). In Mayama, S. Idei, M. & Koizumi, I. [Eds.] *Proceedings of the 14th International Diatom Symposium*. Koeltz Scientific Books, Koenigstein, pp. 197–204.
- Round, E. F. & Crawford, R. M. 1981. The lines of evolution of the Bacillariophyta. I. Origin. *Proc. R. Soc. Lond. B* 211:237–60.
- Round, F. E., Crawford, R. M. & Mann, D. G. 1990. *The Diatoms: Biology and Morphology of the Genera*. Cambridge University Press, Cambridge, 747 pp.
- Schmid, A. M. & Crawford, R. M. 2001. *Ellerbeckia arenaria* (Bacillariophyceae): formation of auxospores and initial cells. *Eur. J. Phycol.* 36:307–20.
- Tiffany, M. A. 2002. Valve morphogenesis in the marine araphid diatom *Gephyria media* (Bacillariophyceae). *Diat. Res.* 17:391–400.
- Toyoda, K., Tanaka, J. & Nagumo, T. 2003. *Morphological Features of Vegetative and Initial Cells of Achnanthes yaquinensis McIntire and Reimer (Bacillariophyceae)*. Third European Phycological Congress, Belfast, Abstract, p. 94.
- von Stosch, H. A. 1958. Kann die oogame Araphidee *Rhabdonema adriaticum* als Bindeglied zwischen den beiden grossen Diatomeengruppen angesehen werden? *Ber. dt. Bot. Ges.* 71:241–9.
- von Stosch, H. A. 1962. Über das Perizonium der Diatomeen. *Vortr. Gesamt. Botan.* 1:43–52.
- von Stosch, H. A. 1982. On auxospore envelopes in diatoms. *Bacillaria* 5:127–56.

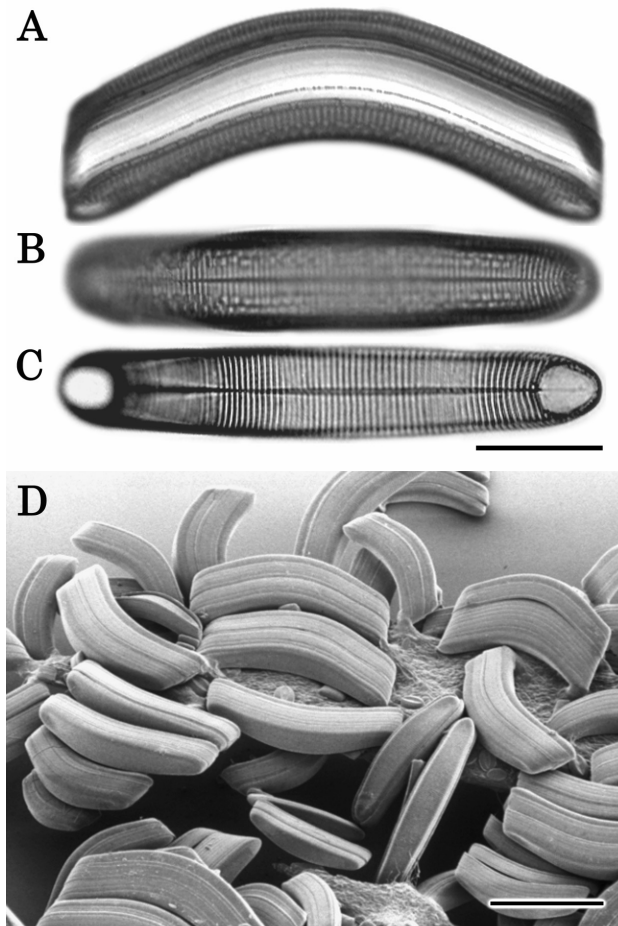


Fig. 1. Vegetative cells of *Gephyria media* with LM (A–C) and SEM (D). Scale bars: 30 μm (A–C) or 10 μm (D). (A) Girdle view of a cleaned frustule. (B) Valve view of the convex valve. (C) Valve view of the concave valve. (D) Colony on *Plocamium telfairiae* Harvey. Note that frustules are always attached by their concave valves to the host seaweed or another cell.

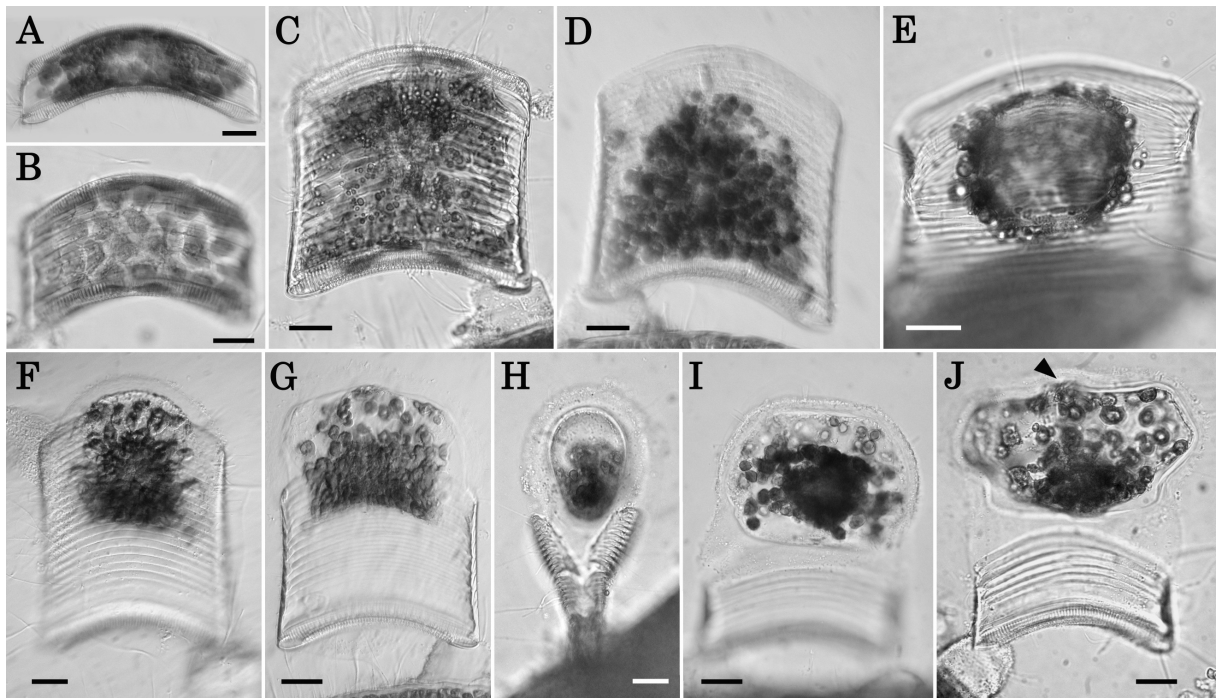


Fig. 2. Auxospore formation in *Gephyria media* under LM(A–G, I, J, girdle view; H, apical view). Scale bars, 10 μm . **(A)** Vegetative cell in girdle view. **(B)** Auxospore mother cell. Frustule girdle is deeper than in the vegetative cell and has an increased number of copulae. **(C)** Approximately twenty copulae in the wall. **(D)** Protoplasm starts to contract at the center of cell. Note that the nonattached (convex) theca is absent. **(E)** Protoplasm contraction complete. **(F)** Protoplast starts growing away from the mother cell. **(G)** Protoplast just emerging from the mother cell. **(H)** Copulae are broken by the auxospore as it swells. **(I)** Early stage of auxospore development. Note that the broken copulae have already disappeared. **(J)** Auxospore begins to increase the number of perizonial bands (arrowhead).

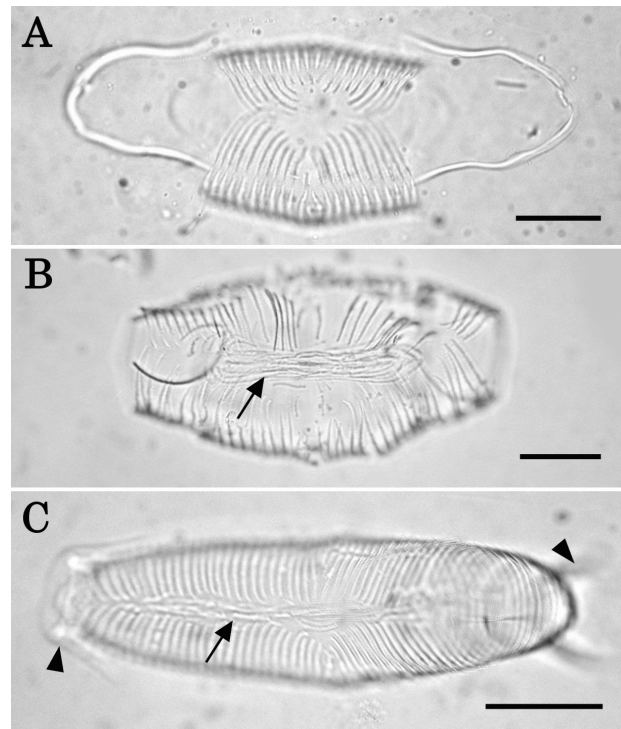


Fig. 3. Ventral view of three stages of auxospore development in *Gephyria media* under LM. Scale bars: 20 μm (A and B) or 50 μm (C). **(A)** Perizonium caps at both ends; no structure is observed under the suture. **(B)** Elongate sprawling structures present at suture (arrow). **(C)** Elongate sprawling structures longitudinally extended at suture (arrow): inside out perizonium caps (left arrowhead) and inside out cap (right arrowhead).

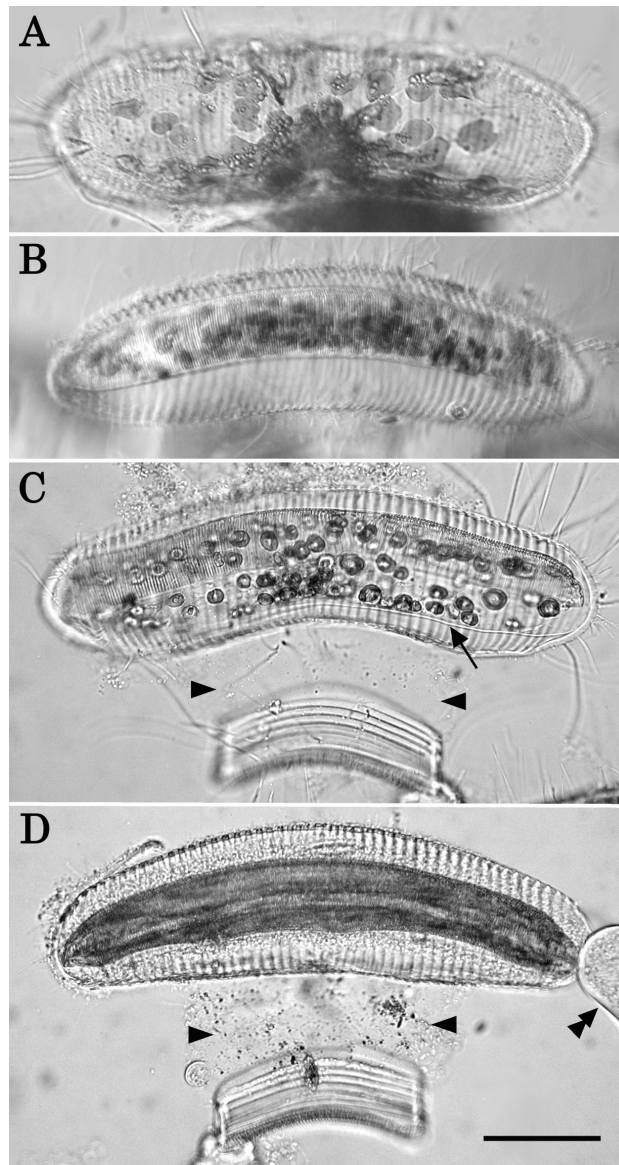


Fig. 4. Four stages of initial cell formation (girdle view) in the expanded auxospore under LM. Scale bars, 50 μm . **(A)** Most chloroplasts contracted close to the ventral side. **(B)** Initial epivalve in auxospore. Many chloroplasts inside the epivalve. **(C)** Initial hypovalve (arrow) forming in auxospore. Chloroplasts are now distributed throughout the initial cell. Arrowheads indicate mucilaginous material connecting the auxospore and its mother cell. **(D)** Complete initial cell in auxospore with perizonial cap (double arrowhead). Mucilaginous material present (between the arrowheads).

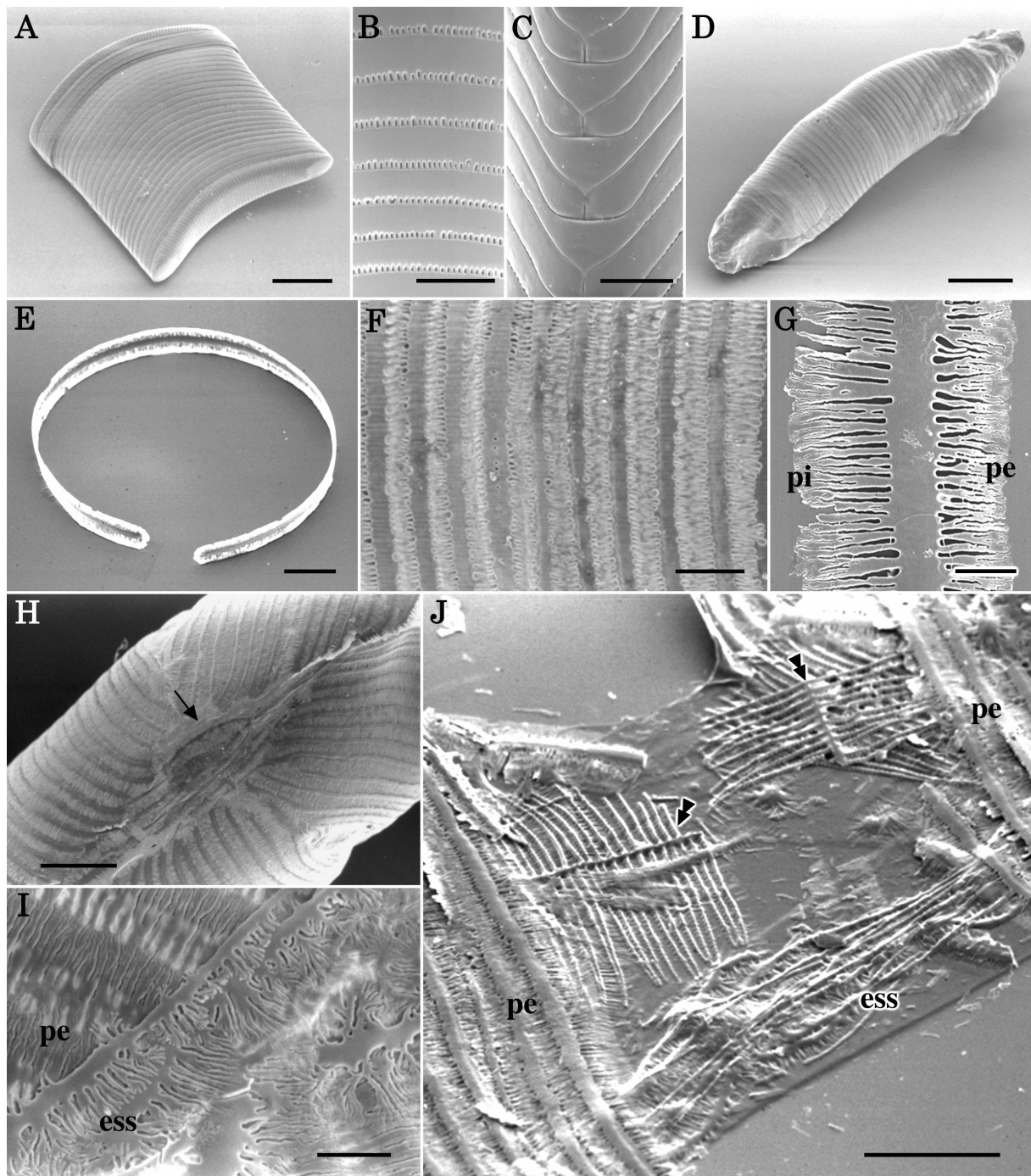


Fig. 5. Fine structure of auxospore mother cell and perizonium with SEM. Scale bars: 30 μm (A, J), 10 μm (B, C, E, F, H), 50 μm (D), or 5 μm (G). (A) Oblique view of auxospore mother cell with increase number of copulae. (B) Row of areolae on copulae of auxospore mother cell (external). (C) Apical view of the mother cell (external) showing overlapping copulae. (D) Oblique view of mature perizonium comprising numerous perizonial bands. (E) Split ring type of perizonial band. (F) Perizonial bands closely associated with each other. (G) Enlargement of perizonial band. Note the asymmetry of the fimbriate margins. Fimbriate margin of pars interior (pi) is longer than that of pars exterior (pe). (H) Elongate sprawling structures at the ventral suture. Arrow indicates a somewhat elliptic structure at the center. (I) Internal view of perizonium (pe) and the elongate sprawling structure (ess) at the ventral suture. (J) Separated perizonial components, showing the elongate sprawling structure (ess) in the perizonium (pe). Double arrowheads indicate fragments of the forming initial valve within the perizonium.

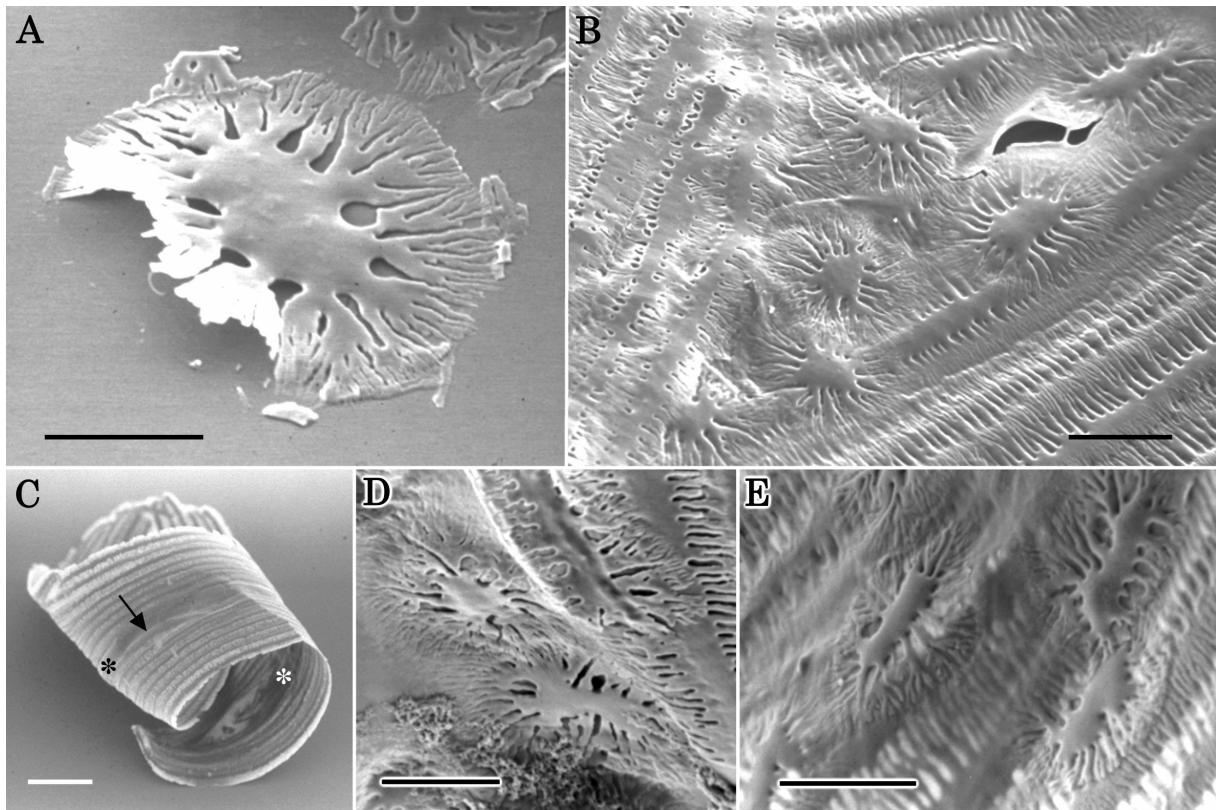


Fig. 6. Scales on perizonium under SEM. Scale bars: 3 μm (A), 5 μm (B, D, E), or 20 μm (C). (A) Oblique view of a scale. (B) Disrupted and deflated perizonium showing scales on inner wall. (C) Oblique view of portion of a disrupted perizonium. Arrow indicates primary perizonial band. (D) Enlargement of the part marked with a black asterisk in C. Scales on the outer surface of the primary perizonial band. (E) Enlargement of the part marked with a white asterisk in C. Scales on the inner surface of primary perizonial band.

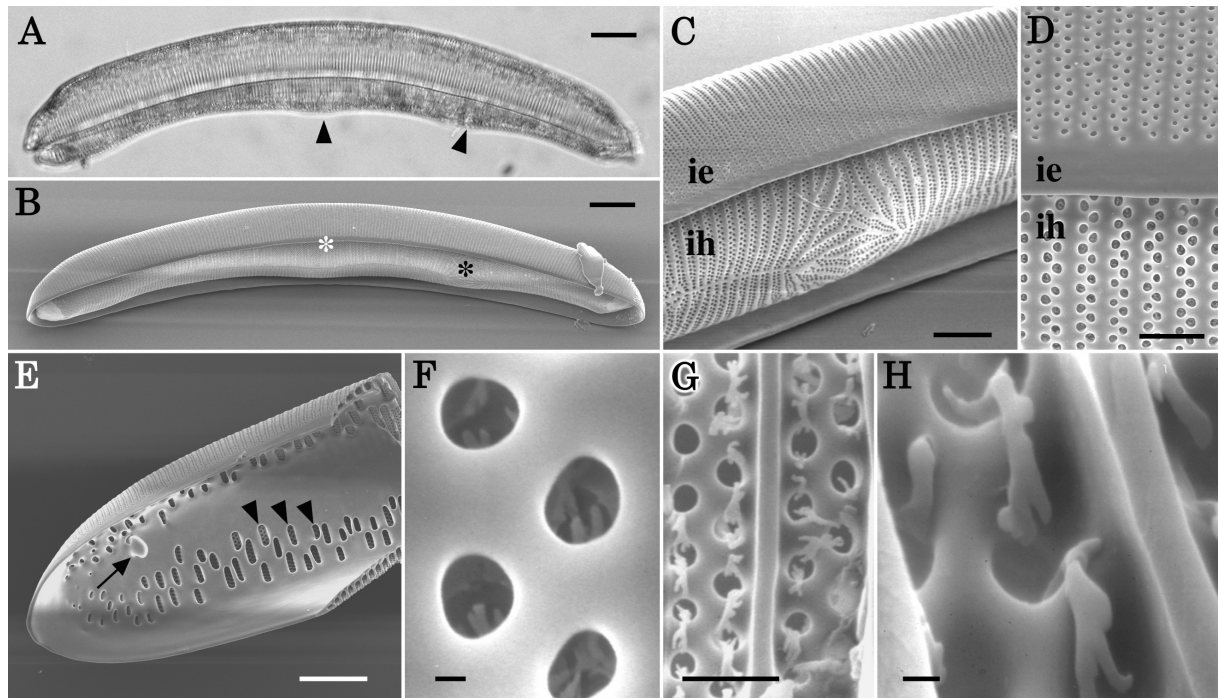


Fig. 7. Initial cells under LM (A) and SEM (B–H). Scale bars: 10 μm (A, B, E), 5 μm (C), 3 μm (D), 1mm (G), or 0.1 μm (F, H). (A) Initial cell removed from perizonium. Arrowheads indicate the abnormal shape of the initial hypovalve. (B) Oblique view of initial cell shown in A. (C) Enlargement of the part marked with a black asterisk in B showing initial epivalve (ie) and initial hypovalve (ih). Note the irregular arrangement of striae at initial hypovalve. (D) Enlargement of the part marked with a white asterisk in B. Note the stria density differs between the initial epi- (ie) and hypovalve (ih). (E) Internal view of initial epivalve. Arrow indicates the rimoportula near the valve apex. Arrowheads indicate chamber openings. (F) External view of initial epivalve. Note the finger-like structures are visible through the areola openings. (G) Internal view of initial epivalve. (H) Finger-like structures winding over the vimines.

2.6. Publication V:

Auxospore fine structure in a marine araphid diatom *Tabularia parva* (Bacillariophyta)

SHINYA SATO^{1*}, KANA KURIYAMA², TOMOYA TADANO³ & LINDA K. MEDLIN¹

¹*Alfred Wegener Institute for Polar and Marine Research, Am Handelshafen 12, D-27570
Bremerhaven, Germany*

²*Department of Ocean Sciences, Tokyo University of Marine Science and Technology, 4-5-7
Konan, Minato-ku, 108-8477 Tokyo, Japan*

³*Doris Japan co. ltd., 2-34-24 Izumihoncho, Komae-City, Tokyo, Japan*

Abstract

Recent studies have led to a rapid increase in knowledge of auxospore formation in diatoms. However, these studies have been limited to centric and raphid pennate diatoms, and there is still very little information for the araphid pennate diatoms. Using LM and SEM, we studied the fine structure of the auxospore of the marine epiphytic diatom *Tabularia parva*. Auxospores were bipolar, as in many other pennate diatoms. SEM revealed a series of transverse perizonial bands that might all be open hoops. Also, a series of longitudinal perizonial bands was observed beneath the transverse series. The well-developed structures of the longitudinal series observed in *T. parva* have not been reported before in the other araphid pennate diatom taxa. Scales were mainly found on the external surface of the perizonium, but curiously they also rarely existed on its inner surface, presumably because the scale formation is not strictly regulated during the latter stage of centrifugal perizonium development in the pennate diatoms.

INTRODUCTION

In the past 40 years, information concerning auxospore structure has greatly increased (e.g. Crawford 1974; von Stosch 1982; Mann 1982a; Cohn *et al.* 1989; Mann 1989; Kaczmarska *et al.* 2000, 2001; Schmid & Crawford 2001; Nagumo 2003; Sato *et al.* 2004b, in press; Amato *et al.* 2005; Tiffany 2005; Toyoda *et al.* 2005, 2006; Pouličková & Mann 2006; Trobajo *et al.* 2006). However, although it has become clear that some aspects of the fine structure of auxospores have phylogenetic significance at higher taxonomic levels (e.g. Medlin & Kaczmarska 2004), there is still insufficient information to reveal how the structure and development of auxospores have evolved in the major diatom groups, especially among the lineages of araphid pennate diatoms. Indeed, the only detailed information available concerning araphid pennates is the account of *Rhabdonema arcuatum* Kützing by von Stosch (1962, 1982) and the SEM study of *Gephyria media* Arnott by Sato *et al.* (2004a) and *Grammatophora marina* (Lyngbye) Kützing by Sato *et al.* (in press). In the present study, we compare the auxospore fine structure of *Tabularia parva* (Kützing) Williams & Round with those diatoms, and discuss the evolutionary relationships of the species.

As with most of the araphid diatoms the fine structure of auxospore of *T. parva* have never been observed although the vegetative cells of the species have been studied (e.g. Williams & Round 1986). The overall paucity of observations of auxospore structure may be due to the short duration of the sexual phase in diatoms' life cycle relative to that of vegetative phase (Mann 1988; Round *et al.* 1990) and the difficulty in seeing those stages in natural samples. However, when field specimens are inoculated into culture, the possibility of initiation of sexual reproduction in the 'seminatural' population will be increased in the few days followed inoculation (Chepurnov *et al.* 2004). In the present study, this strategy was adopted to induce auxosporulation.

MATERIALS AND METHODS

Collections and cultures

An Algal sample was collected from Port Park, Chiba Pref. Japan at 24. Feb. 2004 by TT. A colony of *Tabularia parva* attaching to *Cladophora* sp. was removed from the host by Pasteur

pipette and inoculated into culture medium. A semi-clonal culture was maintained at 15°C under cool white fluorescent light on a 14:10 (L:D) photoperiod at a photon flux density of 30-40 $\mu\text{mol photons m}^{-2}\text{s}^{-1}$ with IMR medium (Eppley et al. 1967). A 10 ml Petri dish was used for culture, and several coverslips were placed on the bottom to allow specimens to attach and form auxospores. Auxosporulations were found on at 2nd May 2004.

Microscopy

LM (Axioplan, Zeiss, Oberkochen, Germany) was used to observe living cells. To remove organic material from frustules, samples were treated as modified by Nagumo & Kobayashi (1990) as follows: (1) Centrifuge sample and discarded the supernatant to make pellet. (2) Suspend pellet with distilled water. Repeat (1) and (2) several times to complete demineralization. (3) Re-centrifuge, and then for dissolution of organic matter, add a similar volume of Drano Power-Gel (Johnson Wax GmbH, Haan, Germany), a strong domestic drain cleaner, to the pellet. (4) Vortex mixture and leave it at room temperature ca. 30 min. At the end, repeat (1) and (2) several times to complete demineralization. Cleaned frustules were then mounted on slide glass with Mountmedia (Wako, Osaka, Japan). For SEM examination, the cleaned material was dropped onto coverslips and air dried. A coverslip, on which auxosporulation took place, was fixed with 10 % glutaraldehyde for 2 hours at room temperature, and rinsed with distilled water several times to remove glutaraldehyde. Also auxospores produced in the Petri dish, but not on the coverslips, were picked up by Pasteur pipettes under LM and then washed as above followed by air drying on a coverslip. All coverslips were fixed to the SEM stubs with carbon tape, and coated with gold using SC 500 (Emscope, Ashford, England). QUANTA 200F scanning electron microscopy (FEI Company, Eindhoven, The Netherlands) was used at an accelerating voltage of 3 to 10 kV, and ca. 10 mm working distance. Captured images were adjusted with Adobe Photoshop.

RESULTS

In most cases, one end of a vegetative valve had a single oval rimoportula, whereas the other apex was plain (Figs 1-4). However, they were rare cases where variations in the distribution of rimoportulae were observed: either both ends had one rimoportula or one end had one rimoportula, the other two, thus three rimoportulae per valve. The presence of a rimoportula is recognizable externally as a slit-like opening (Fig. 2). Striae are biseriate (Figs 1-5), arranged 19-20 in 10 μm . Valve face and mantle are not separated by marginal rib (Fig. 5). Valve length ranges between 36.1 and 160.0 μm ; this range was recorded at the end of auxosporulation, i.e., a minimum length for auxospore mother cell (mean $52.8 \pm 7.8 \mu\text{m}$; $n = 15$) and maximum for the initial cell (mean $137.0 \pm 13.7 \mu\text{m}$; $n = 14$). Valve width measured at the mid-valve is 5.9 - 6.7 μm .

Auxospores were formed in the semi-clonal culture (Figs 6-8) although mating was never observed. A single auxospore was produced by a gametangial cell (Figs 6-8). The auxospore expands at right-angles to the perivalvar axis of the gametangium and parallel to its longitudinal axis (Figs 6-8). The initial cells often have an undulated outline (Fig. 9), but any abnormalities of shape in the initial cells are gradually lost during subsequent vegetative divisions.

Many scales were observed on the early stages of the auxospore (Figs 10-11). Scales are mainly composed of a central annulus with a surrounding fringe and are varied in shape and size (Fig. 11). At this stage, the auxospores are covered only with a mucilaginous envelope as well as with many scales (Fig. 11). Perizonial bands were never observed.

At a later stage, enlarged auxospores are covered with a series of transverse perizonial (TP) bands together with a mucilaginous envelope (Fig. 12). Beneath the TP bands, the formation of longitudinal perizonial (LP) band is progressing (Fig. 13). Immature LP bands consists of costae extending in a longitudinal direction; and subcostae extend transapically in parallel crossing at right angles with the costa (Fig. 14, arrow and arrowhead, respectively). The ends of auxospore have no TP bands yet but are covered only with a mucilaginous envelope. LP bands have already expanded throughout the inside of auxospore along the long axis in this stage (Fig. 14).

A well-developed series of TP bands was observed when an initial cell was formed inside an auxospore (Fig. 15). Like the LP bands, each TP band consists of a costa and subcostae (Figs 15-17). In the series of TP bands, the ends of subcostae become fringed, fusing neighbouring bands tightly (Figs 15-17). Scales are also included in this series of TP bands (Fig. 16, arrow). All TP bands are morphologically uniform so that the primary band, which is usually distinct in shape and located at the center of the auxospore among the series of TP bands in many pennate diatoms, was not detected. TP bands are open hoops (Figs 17, 25).

A series of LP bands are found around the initial cell (Fig. 18). Unlike the TP bands, the structure of mature LP bands is a simple strip, i.e. no differentiation into costa and subcostae is seen, whereas underdeveloped LP bands have costa/subcosta system as mentioned above (compare Fig. 19, with Fig. 14). A primary LP band is usually associated with subsequent bands at both sides, making a series of LP bands (Figs 18-21, 23, 25). The midrib of the primary LP band is slightly thickened (Fig. 19, arrow). The secondary bands are not closed hoops (Fig. 19), and tertiary bands, which are sometimes lost from the series, are probably open, too. All LP bands, primary, secondary and tertiary, are irregularly perforated (Figs 19-24). An exception in which regular arrangement of poroids in a row only along the one end of secondary band, overlapped with primary one is shown in Fig. 19, arrowhead. Because no LP bands have fringed subcosta, the mechanical association of bands like that found between TP bands is not possible. Although an interlocking mechanism has not been established, each band was linked firmly to the others so that the series was held in place even when the auxospore had collapsed (Figs 20, 22). Some remnants of TP bands were observed on the external surface of LP bands (Fig. 21).

The tertiary band is the narrowest among the series of LP bands, and is sparsely perforated (Fig. 23). The inside of the LPs is much more densely perforated than the external, indicating that not all poroids perforate the LP bands (Fig. 24). Scales are rarely found on the internal surfaces of LP bands (Fig. 24, arrow). A perizonial cap was never observed during auxosporulation in this species.

DISCUSSIONS

Preliminary results of this study were presented earlier by Sato et al. (2004b), but at that time, the species was identified as *Tabularia investiens* (W. Smith) Williams & Round. Further observations have revealed that the valve morphology of the species observed in that study agreed better with *T. parva*, which was described by Williams & Round (1986) as a new combination, although an incongruence was rarely observed in the number and shape of the rimoportula between our specimens and original description, as well as Kuylenstierna's report [we were unable to obtain his Ph.D. thesis (1989-1990), but the result was cited by Snoeijs (1991)]. The range of valve length obtained in this study was 36.1 - 160.0 μm and that of Williams & Round (1986) was 20-35 μm and Kuylenstierna (1989-1990) was 22 - 127. Therefore, the consensus range of valve length of the species is 20.0 - 160.0 μm .

The detailed developmental sequence of auxospore coverings as revealed in this study is summarized as follows; 1) an early auxospore is covered with scales, 2) an auxospore expands bi-polarly, TP bands are added toward both ends, 3) LP bands are formed beneath the series of TP bands, 4) an initial cell is formed inside of perizonium that is composed of series of TP and LP bands (Fig. 25).

The presence of scales on the auxospore of the araphid diatom *T. parva* is not surprising because reports of scales on araphid auxospore are increasing (e.g., Sato et al. 2004a, in press and unpublished observations). In the early stage of auxospore development, this result agrees with the idea that scales are common in spherical auxospore stages of pennate diatoms (Sato et al. 2004a). It is difficult to interpret the fact that scales were observed on the internal surface of LP bands even if they were few (Fig. 24). Scales are formed at the beginning of auxospore development, and the LP bands are formed beneath the series of TP bands at the final stage (Fig. 25). Therefore, scales may be located only on the external surface of LP bands. The scale formation of Coscinodiscophycean centric diatoms may have been under strong selective pressure because their entire auxospore is covered only with the scales (Round et al. 1990), on the other hand, the auxospore of pennate diatoms are protected by the scales for a short period just until the formation of TP and/or LP bands. Thus, it is likely that the scale formation in the pennate diatoms might be loosely regulated than that of Coscinodiscophycean diatoms, especially in the later stage of auxosporulation. The scales found at the internal surface of LP bands might have been, therefore, accidentally formed after the formation of LP band. This assumption can also explain the curious fact that the several scales were observed on the internal surface of TP bands in the araphid diatom *Gephyria media* Arnott (fig. 6E, Sato et al. 2004a).

A series of TP bands has been observed on most pennate diatoms where auxospore structure has been studied, although exceptions are also known in the araphids: no TP bands were found in *Diatoma moniliformis* Kützing (Potapova & Snoeijs 1997), *Fragilariforma virescens* (Ralfs) D. M. Williams & Round (Williams 2001) and *Licmophora* spp. (Mann 1982b; Chepurnov & Mann 2004). Given the morphological similarities and its function, it is reasonable that the series of TP bands are homologous with the properizonium of Mediophycean diatoms, e.g. *Lampriscus* spp. (Idei & Nagumo 2002), *Chaetoceros didymum* Ehrenberg, *Lithodesmium undulatum* Ehrenberg and *Bellerochea malleus* (Brightwell) Van Heurck (von Stosch 1982), that is, both series consist of siliceous bands for protecting the auxospores. Unlike the properizonial bands of Mediophycean diatoms, the TP bands in *T. parva* are open hoops. This state might be an adapted form to cover a highly elongated initial cell of pennate diatoms. A primary TP band was not recognized, presumably because it was simply overlooked or, more likely, there was no differentiation in shape between the primary band and others.

The early developmental stage of LP bands in *T. parva* consisted of costae and subcostae as seen in the LP bands of a raphid diatom *Achnanthes yaquinensis* McIntire & Reimer (Toyoda et al. 2005). However, the mature LP bands of *T. parva* are heavily silicified and the framework of costa/subcosta structure was fully masked leaving small amounts of scattered poroids; the same structure can be seen in a raphid diatom *Rhoicosphenia curvata* (Kützing) Grunow (Mann et al. 1982a). Among the araphid diatoms, *Gephyria media* and *Grammatophora marina* formed longitudinally expanded structures along the suture (Sato et al. 2004a and submitted a, respectively), and *Rhabdonema arcuatum* formed single LP bands (von Stosch 1982). A series of LP bands was only observed in *Pseudostriatella pacifica* S.Sato & Medlin among araphids but the structure seems to be more primitive (Sato et al. in prep), whereas the structure of LP bands in *T. parva* is heavily silicified and more sophisticated in shape. This descendant state of LP band agrees with the derived position of *Tabularia* among araphid lineage in 18S rDNA trees (e.g. Medlin & Kaczmarska; Sims et al. 2006).

ACKNOWLEDGEMENT

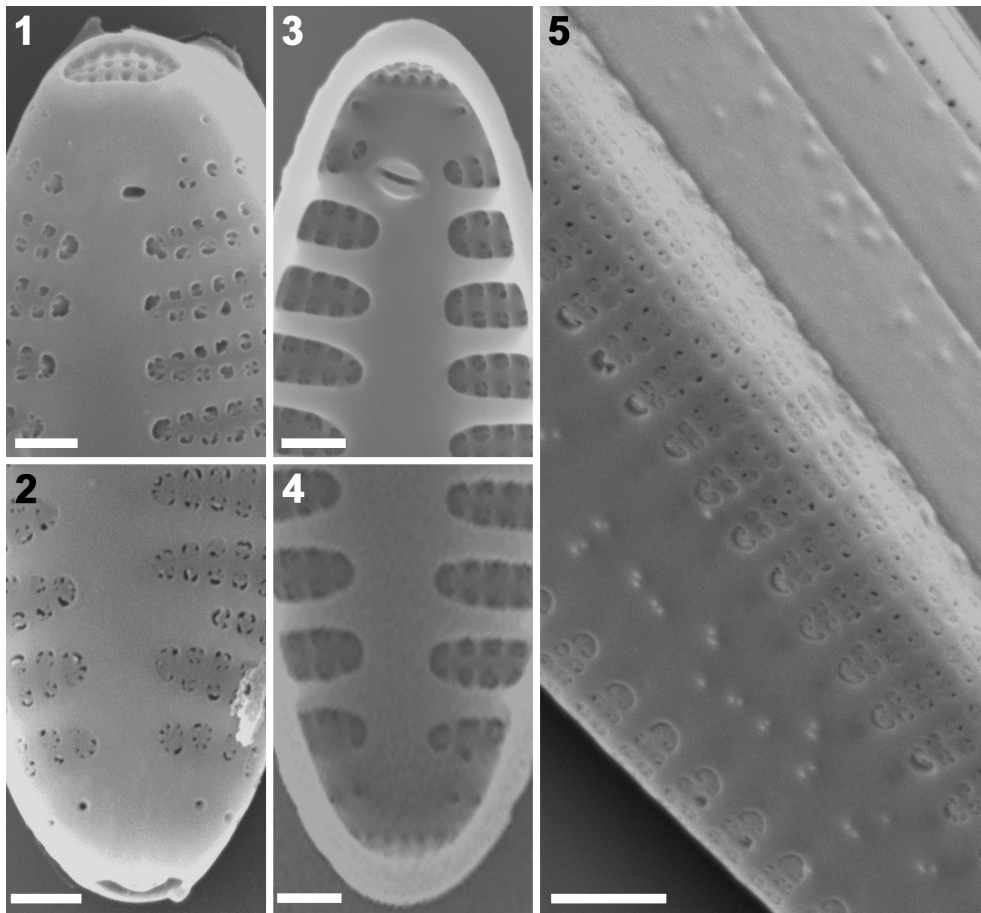
We would like to thank Richard Crawford for correction of the manuscript and discussion; Friedel Hinz for support with SEM; Mary Ann Tiffany for helpful comment on the identification of *T. parva*. This study was supported by a DAAD fellowship for doctoral research to Shinya Sato.

REFERENCES

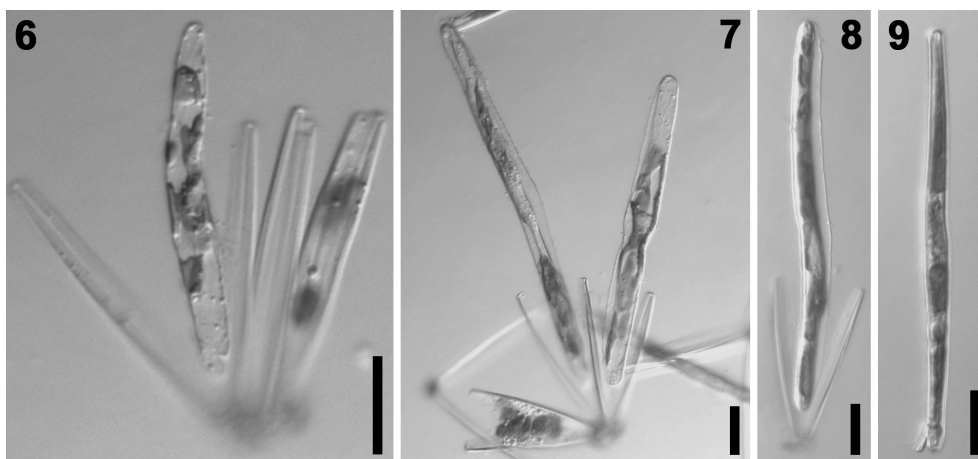
- AMATO, A., ORSINI, L., D'ALELIO, D. & MONTRESOR, M. (2005). Life cycle, size reduction patterns, and ultrastructure of the pennate planktonic diatom *Pseudo-nitzschia delicatissima* (Bacillariophyta). *Journal of Phycology* **41**, 542–556.
- CHEPURNOV, V. A. & MANN, D. G. (2004). Auxosporulation of *Licmophora communis* (Bacillariophyta) and a review of mating systems and sexual reproduction in araphid pennate diatoms. *Phycological Research* **52**, 1–12.
- CHEPURNOV, V. A., MANN, D. G., SABBE, K. & VYVERMAN, W. (2004). Experimental studies on sexual reproduction in diatoms. *International Review of Cytology* **237**, 91–154.
- COHN, S. A., SPURCK, T. P., PICKETT-HEAPS, J. D. & EDGAR, L. A. (1989). Perizonium and initial valve formation in the diatom *Navicula cuspidata* (Bacillariophyceae). *Journal of Phycology* **25**, 15–26.
- CRAWFORD, R. M. (1974). The auxospore wall of the marine diatom *Melosira nummuloides* (Dillw.) C. Ag. and related species. *British Phycological Journal* **9**, 9–20.
- EPPLEY, R. W., HOLMES, R. W. & STRICKLAND, J. D. H. (1967). Sinking rates of the marine phytoplankton measured with a fluorochromometer. *Journal of Experimental Marine Biology and Ecology* **1**, 191–208.
- IDEI, M. & NAGUMO, T. (2002). Auxospore structure of the marine diatom genus *Lampriscus* with triangular/quadrangular forms. In: *Abstract 17th International Diatom Symposium*, p. 166.
- KACZMARSKA, I., BATES, S. S., EHRMAN, J. M. & LÉGER, C. (2000). Fine structure of the gamete, auxospore and initial cell in the pennate diatom *Pseudo-nitzschia multiseries* (Bacillariophyta). *Nova Hedwigia* **71**, 337–357.
- KACZMARSKA, I., EHRMAN, J. M. & BATES, S. S. (2001). A review of auxospore structure, ontogeny and diatom phylogeny. In *Proceedings of the 16th International Diatom Symposium* (Ed. by A. Economou-Amilli), pp. 153–168. University of Athens, Greece.
- KOBAYASHI, A., OSADA, K., NAGUMO, T. & TANAKA, J. (2001). An auxospore of *Arachnoidiscus ornatus* Ehrenberg. In: *Proceedings of the 16th International Diatom Symposium* (Ed. by A. Economou - Amilli). pp. 197–204. University of Athens, Greece.
- KUYLENSTIERNA, M. (1989–1990). *Benthic algal vegetation in the Nordre Älv Estuary (Swedish west coast)*. Doctoral thesis, Department of Marine Botany, University of Göteborg. Vol 1 (Text, 1990) 244 pp, Vol. 2 (Plates, 1989) 76 Pl.
- MANN, D. G. (1982a). Structure, life history and systematics of *Rhoicosphenia* (Bacillariophyta). II. Auxospore formation and perizonium structure of *Rh. curvata*. *Journal of Phycology* **18**, 264–274.

- MANN, D. G. (1982b). Auxospore formation in *Licmophora* (Bacillariophyta). *Plant Systematics and Evolution* **139**, 289–294.
- MANN, D. G. (1988). Why didn't Lund see sex in *Asterionella*? A discussion of the diatom life cycle in nature. In *Algae and the Aquatic Environment* (ed. by F.E. Round). pp. 383–412. Biopress, Bristol.
- MANN, D. G. (1989). On auxospore formation in *Caloneis* and the nature of *Amphiraphia* (Bacillariophyta). *Plant Systematics and Evolution* **163**, 43–52.
- MEDLIN, L. K. & KACZMARSKA, I. (2004). Evolution of the diatoms: V. Morphological and cytological support for the major clades and a taxonomic revision. *Phycologia* **43**, 245–270.
- NAGUMO, T. (2003). Taxonomic studies of the subgenus *Amphora* Cleve of the genus *Amphora* (Bacillariophyceae) in Japan. *Bibliotheca Diatomologica* **49**, 1–265.
- NAGUMO, T & KOBAYASHI, H. (1990). The bleaching method for gently loosening and cleaning a single diatom frustule. *Diatom* **5**, 45-50
- POTAPOVA, M. & SNOEIJIS, P. (1997). The natural life cycle in wild populations of *Diatoma moniliformis* (Bacillariophyceae) and its disruption in an aberrant environment. *Journal of Phycology* **33**, 924–937.
- POULÍČKOVÁ, A. & MANN, D. G. (2006). Sexual reproduction in *Navicula cryptocephala* (Bacillariophyceae). *Journal of Phycology* **42**, 872–886.
- POULÍČKOVÁ, A., MAYAMA, S., CHEPURNOV, V. A. & MANN, D. G. (2007). Heterothallic auxosporulation, incunabula and perizonium in *Pinnularia* (Bacillariophyceae). *European Journal of Phycology* (in press).
- ROUND, F. E., CRAWFORD, R. M. & MANN, D. G. (1990). *The diatoms. Biology and morphology of the genera*. Cambridge University Press, Cambridge. 747 pp.
- SATO, S., NAGUMO, T. & TANAKA, J. (2004a). Auxospore formation and the morphology of the initial cell of the marine araphid diatom *Gephyria media* (Bacillariophyceae). *Journal of Phycology* **40**, 684–691.
- SATO, S., MEDLIN, L. K., NAGUMO, T. & TANAKA, J. (2004b). Are the scales on the auxospore any longer the patent for the centric diatoms? In *18th International Diatom Symposium*, Abstracts Book. p. 131. (Abstract.)
- SATO, S., MANN, D. G., NAGUMO, T., TANAKA, J., TADANO, T. & MEDLIN, L. K. (2008). inpress. Auxospore fine structure and variation in modes of cell size changes in *Grammatophora marina* (Bacillariophyta). *Phycologia*
- SATO, S., MATSUMOTO, S. & MEDLIN, L. K. (in prep.). *Pseudostriatella pacifica* gen. et sp. nov. (Bacillariophyta); a new araphid pennate diatom and its fine-structure, auxospore and phylogeny.
- SCHMID, A.-M. M. & CRAWFORD, R. M. (2001). *Ellerbeckia arenaria* (Bacillariophyceae): formation of auxospores and initial cells. *European Journal of Phycology* **36**, 307–320.
- SIMS, P. A., MANN, D. G. & MEDLIN, L. K. (2006). Evolution of the diatoms: insights from fossil, biological and molecular data. *Phycologia* **45**, 361-402.
- SNOEIJIS, P. & KUYLENSTIERNA, M. (1991). Two new diatom species in the genus *Tabularia* from the Swedish coast. *Diatom Research* **6**, 351–365.
- STOSCH H., A, VON (1982). On auxospore envelopes in diatoms. *Bacillaria* **5**, 127–156.
- TIFFANY, M. A. (2005). Diatom auxospore scales and early stages in diatom frustule morphogenesis: their potential for use in nanotechnology. *Journal of Nanoscience and Nanotechnology* **5**, 131–139.

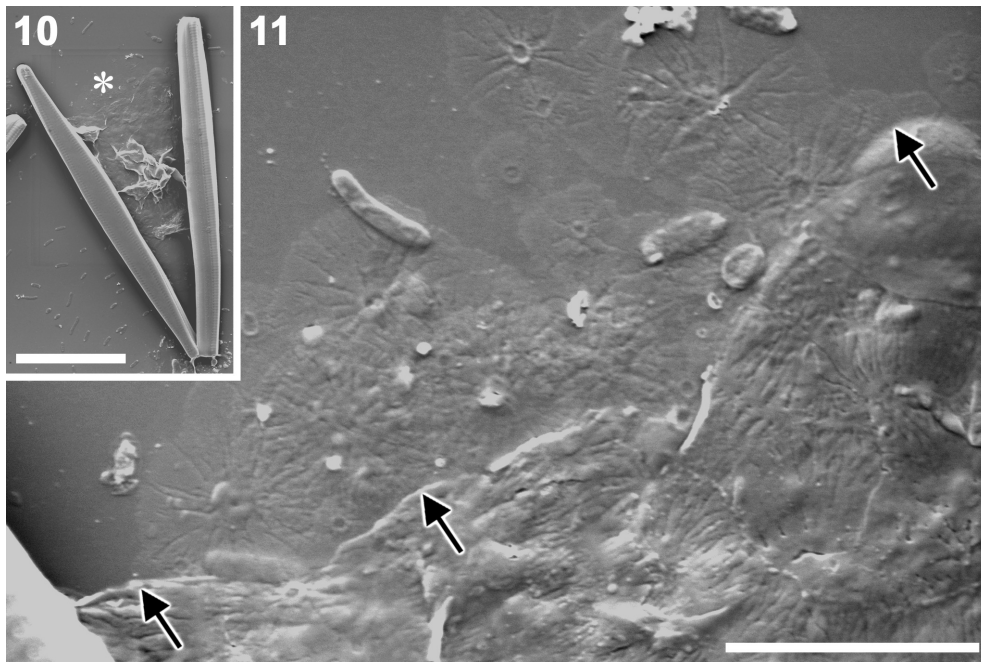
- TOYODA, K., IDEI, M., NAGUMO, T. AND TANAKA, J. (2005). Fine-structure of frustule, perizonium and initial valve of *Achnanthes yaquinensis* McIntire and Reimer (Bacillariophyceae). *European Journal of Phycology* **40**, 269–279.
- TOYODA, K., WILLIAMS, D. M., TANAKA, J. & NAGUMO, T. (2006). Morphological investigations of the frustule, perizonium and initial valves of the freshwater diatom *Achnanthes crenulata* Grunow (Bacillariophyceae). *Phycological Research* **54**, 173–182.
- TROBAJO, R., MANN, D. G., CHEPURNOV, V. A., CLAVERO, E. & COX, E. J. (2006). Auxosporulation and size reduction pattern in *Nitzschia fonticola* (Bacillariophyta). *Journal of Phycology* **42**, 1353–1372.
- WILLIAMS, D. M. (2001). Comments on the structure of ‘postauxospore’ valve of *Fragilari-forma virescens*. In Jahn, R., Kociolek, J. P., Witkowski, A. & Compe`re, P. [Eds.] Lange-Bertalot- Festschrift. Gantner, Ruggell, Liechtenstein, pp. 103–117.
- WILLIAMS, D. M. & ROUND F. E. (1986). Revision of the genus *Synedra* Ehrenb. *Diatom Research* **1**, 313–339.



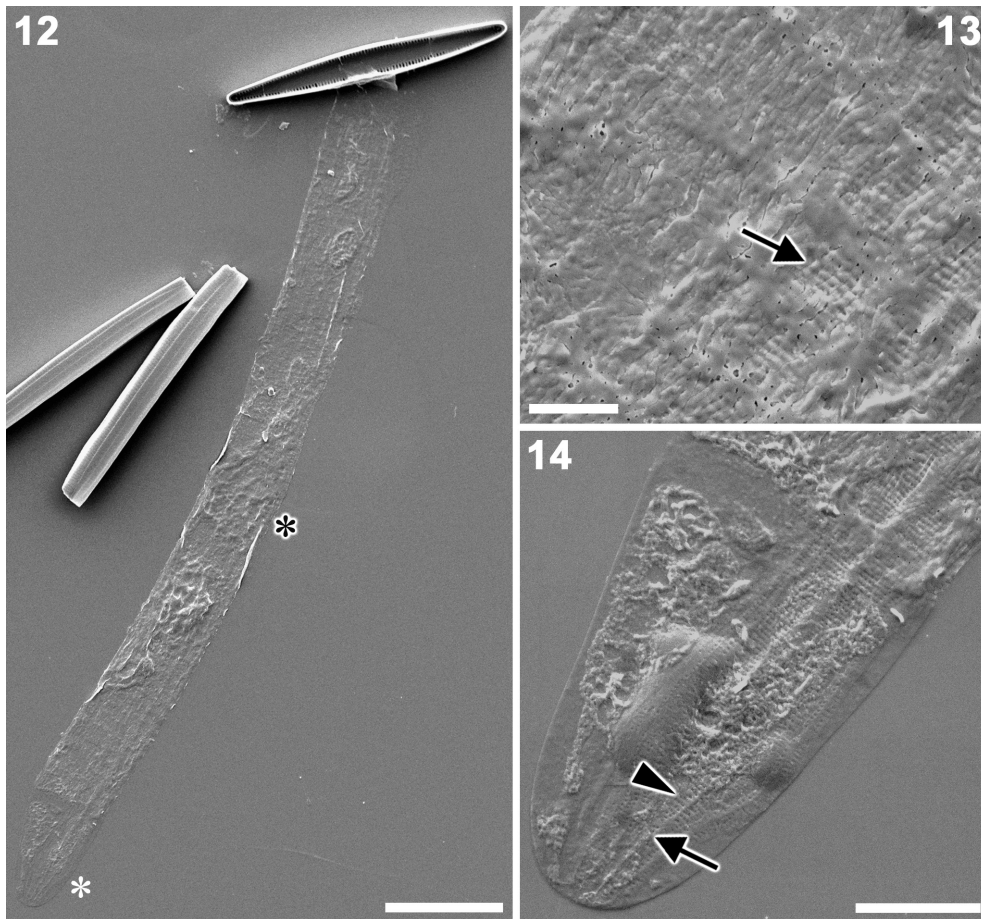
Figs 1-5. Vegetative cell. SEM. **Fig. 1.** External apex of valve. **Fig. 2.** External apex of valve with opening of rimoportula. **Fig. 3.** Internal view of valve. **Fig. 4.** Internal apex of valve with rimoportula **Fig. 5.** Rounded valve mantle without marginal rib. Scale bars = 0.5 μm (Figs 1-4), 1 μm (Fig. 5).



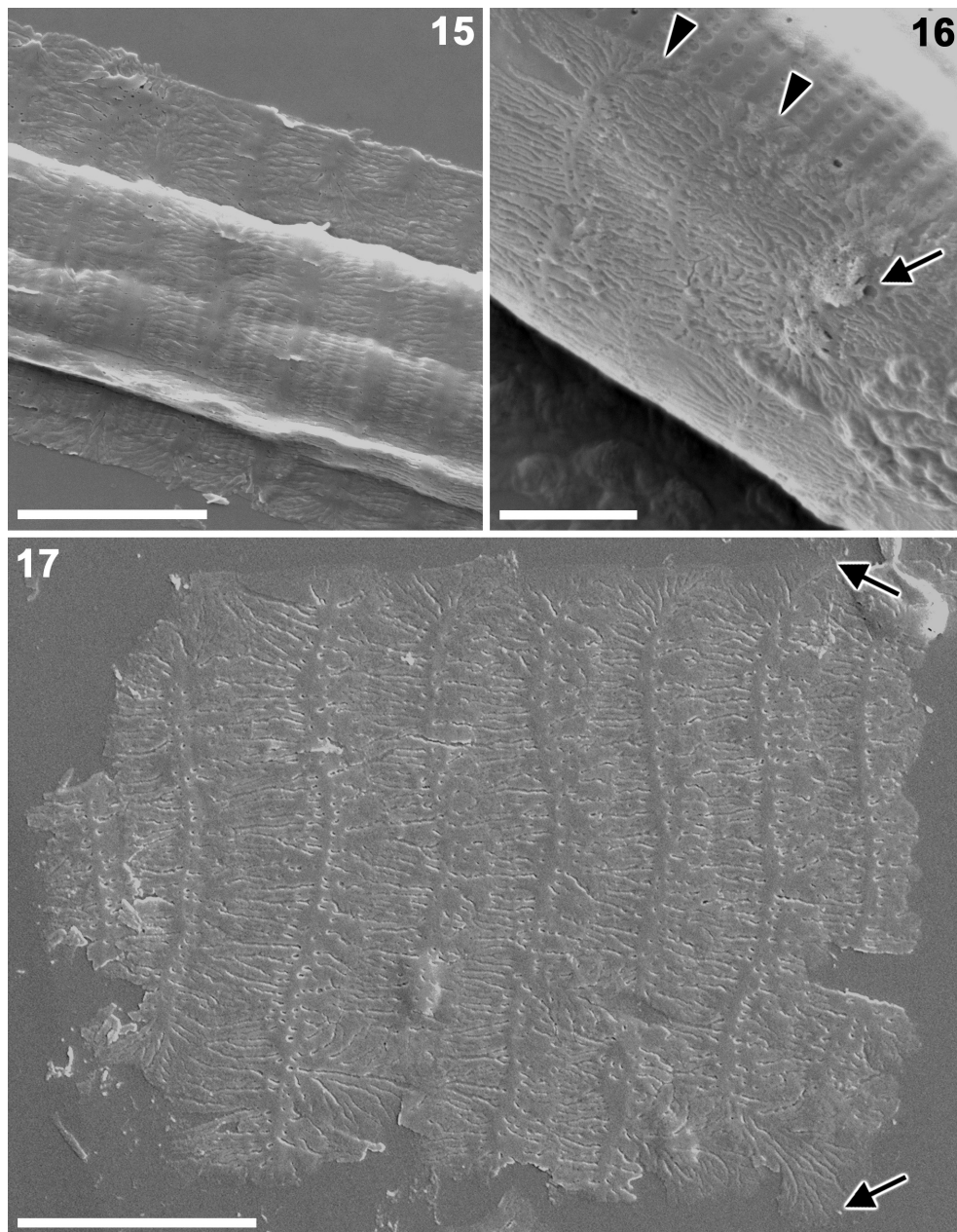
Figs 6-9. Auxosporulation. LM. **Fig. 6.** Expanding auxospore. **Figs 7-8.** Expanded auxospores. **Fig. 9.** Initial cell. Scale bars = 20 μm .



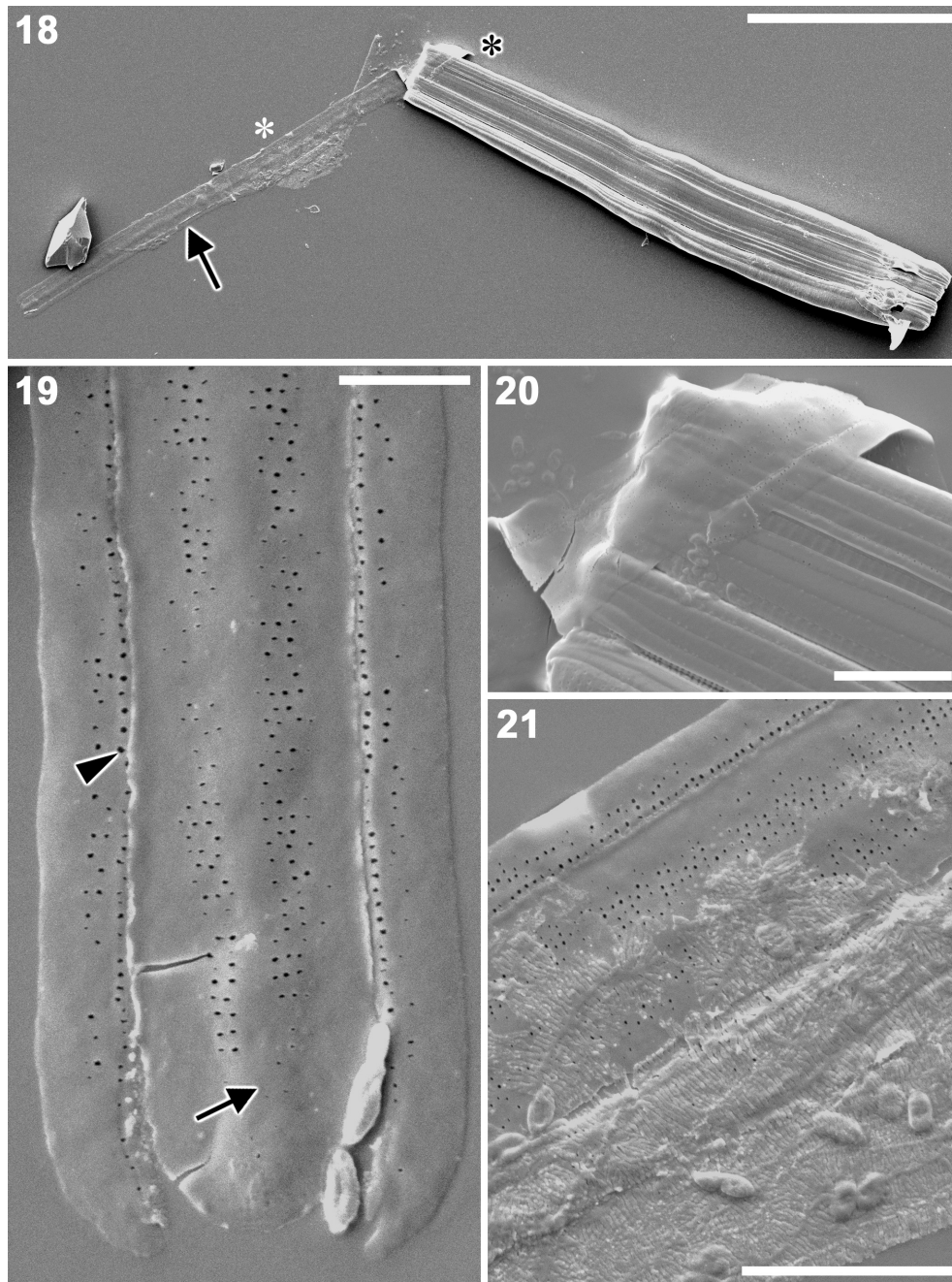
Figs 10-11. Scales. SEM. **Fig. 10.** Early stage auxosporulation. **Fig. 11.** Enlarged view of area marked by asterisk in Fig. 10. Arrows indicate border of mucilaginous envelope. Scale bars = 20 μm (Fig. 10), 5 μm (Fig. 11).



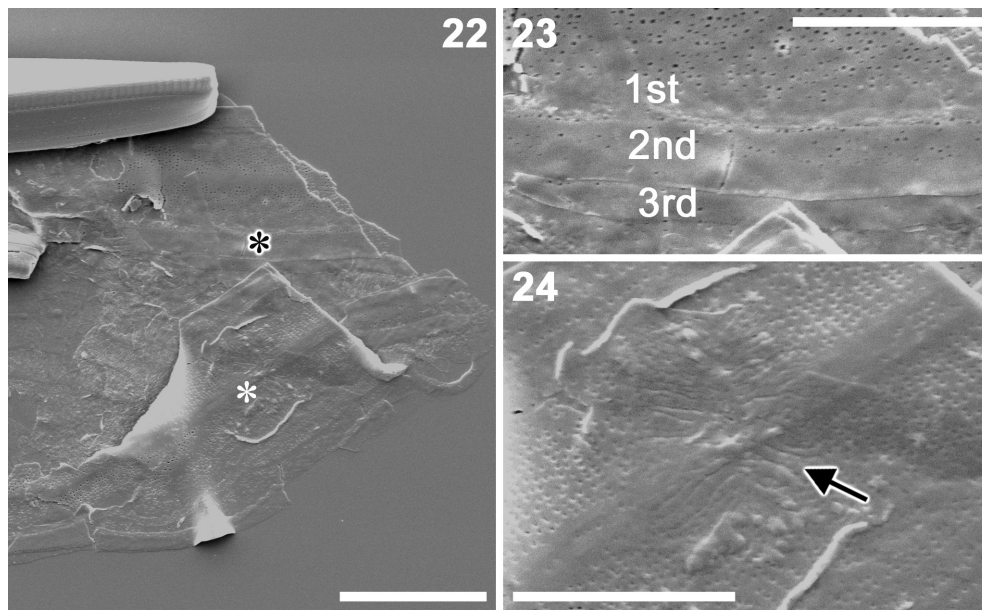
Figs 12-14. Expanded auxospore. SEM. **Fig. 12.** Expanded auxospore covered with mucilaginous envelope and series of TP bands. **Fig. 13.** Enlarged view of area marked by black asterisk in Fig. 12. Arrow indicates developing LP band. **Fig. 14.** Enlarged view of area marked by white asterisk in Fig. 12. Arrow indicates costa, arrowhead indicates subcosta of LP band. Note no TP band exists at end of auxospore. Scale bars = 20 μm (Fig. 12), 2 μm (Fig. 13), 5 μm (Fig. 14)



Figs 15-17. Series of TP bands. SEM. **Fig. 15.** Initial cell formed within series of TP bands. **Fig. 16.** Series of TP bands containing scale (arrow). Arrowheads indicate open end of bands. **Fig. 17.** Firmly linked series. Arrows indicate end of open band. Scale bars = 5 μm (Figs 15, 17), 2 μm (Fig. 16)



Figs 18-21. Series of LP bands. SEM. **Fig. 18.** Initial cell with LP bands (arrow). **Fig. 19.** Enlarged view of end of LP bands. Arrow indicates thickened midrib of primary band. Arrowhead indicates row of areolae along edge of secondary band. **Fig. 20.** Enlarged view of area marked by black asterisk in Fig. 18. Note firmly linked series of LP bands is. **Fig. 21.** Enlarged view of area marked by white asterisk in Fig. 18. Fragments of TP bands attach to external LP bands. Scale bars = 50 μm (Fig. 18), 2 μm (Fig. 19), 5 μm (Figs 20-21).



Figs 22-24. Disrupted LP bands. SEM. **Fig. 22.** Disrupted LP bands **Fig. 23.** Enlarged view of area marked by black asterisk in Fig. 22 showing series of LP bands up to tertiary one. **Fig. 24.** Enlarged view of area marked by white asterisk in Fig. 22. Arrow indicates scale at internal surface of LP bands. Note somewhat regular and frequent perforation on LP bands, internally. Scale bars = 10 μm (Fig. 22), 5 μm (Figs 23-24)

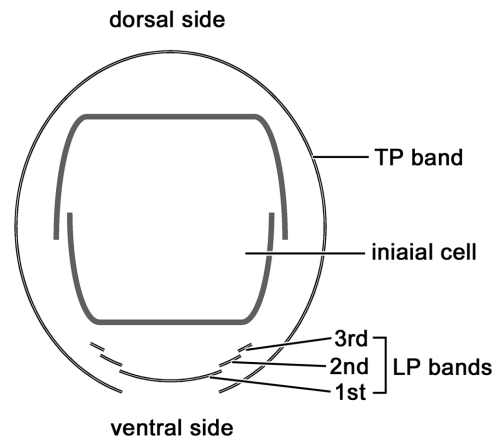


Fig. 25. Schematic section of the auxospore and initial cell.

2.7. Publication VI:

***Pseudostriatella* (Bacillariophyta); a description of a new araphid diatom genus based on observations of frustule and auxospore structure and 18S rDNA phylogeny**

SHINYA SATO^{1*}, DAVID G. MANN², SATOKO MATSUMOTO³ & LINDA K MEDLIN¹

¹*Alfred Wegener Institute for Polar and Marine Research, Am Handelshafen 12, D-27570 Bremerhaven, Germany*

²*Royal Botanic Garden, Edinburgh EH3 5LR, Scotland, United Kingdom*

³*Choshi Fisheries High School, 1-1-12 Nagatsuka Cho, Choshi City, Chiba, Japan*

Abstract

Pseudostriatella oceanica gen et. sp. nov. is a marine benthic diatom that resembles *Striatella unipunctata* in gross morphology, attachment to the substratum by a mucilaginous stalk, and possession of septate girdle bands. In LM, *P. oceanica* can be distinguished from *S. unipunctata* by plastid shape, absence of truncation of the corners of the frustule, indiscernible striation, and absence of polar rimoportulae. With SEM, *P. oceanica* can be distinguished by a prominent but unthickened longitudinal hyaline area, pegged areolae, multiple marginal rimoportulae, and perforated septum. The hyaline area differs from the sterna of most pennate diatoms in being porous towards its expanded ends; in this respect, it resembles the elongate annuli of some centric diatoms, e.g. *Attheya* and *Odontella*. 18S rDNA phylogeny places *P. oceanica* among the pennate diatoms and supports a close relationship between *P. oceanica* and *S. unipunctata*, but the genetic distance between them, coupled with the morphological differences, justifies separation at genus level. However, the affinity of the *P. oceanica* – *S. unipunctata* clade remains unresolved both in molecular and morphological study. Both genera are only distantly related to *Hyalosira* and *Grammatophora*, despite similarities in frustule structure and growth habit, arguing against their inclusion in the same family. The auxospore is covered with series of transverse and longitudinal bands but the structure and arrangement of these bands appear to be more similar to the properizonia of some centric diatoms than to the classic type of perizonium seen in other pennate diatoms; a few scales are also present. The differences between properizonia and perizonia are discussed.

KEY WORDS: 18S rDNA, Araphid diatom, Auxospore, Evolution, Fine structure, Morphology, Perizonium, Phylogeny, *Pseudostriatella oceanica*, *Striatella*, Taxonomy.

INTRODUCTION

Benthic diatoms are ubiquitous in shallow coastal environments and are one of the most taxonomically diverse groups of organisms in estuarine ecosystems (Sullivan & Currin 2000). Because of their high primary production rates, benthic diatoms play an important role in the functioning of benthic trophic webs in intertidal mudflats and shallow water ecosystems of temperate to tropical regions (Cahoon 1999; Underwood & Kromkamp 1999). Araphid pennate diatoms (diatoms with a sternum but lacking a raphe system, see Material and Methods: Terminology) are important components of these coastal assemblages, particularly among communities attached to macrophytes and macroalgae, animals, rocks and sand-grains (Round *et al.* 1990). Taxonomically, araphid diatoms have long been neglected, perhaps because of their morphological simplicity; according to Round *et al.* (1990), ‘in many ways the classification of the araphid group is the most difficult, because unlike the centric series their valve structure is rather simple, and unlike the raphid series the plastids and their arrangements have few distinguishing features’. Thus, in spite of their high abundance, the defining features of the main groups of araphid diatoms are not fully established.

To obtain a more complete picture of the natural history of araphid diatoms, we have been collecting samples worldwide from coastal regions. Recently we encountered a new diatom that superficially resembled *Striatella unipunctata* (Lyngbye) Agardh. Scanning electron microscopy (SEM) revealed, however, that this diatom differed from *S. unipunctata* in several features that are generally used as taxonomic characters among araphid diatoms, including characteristics of the sternum, striae, areolae, apical pore field, rimoportula and septum. Given

these observations, together with information on the plastids and 18S rDNA sequences, we conclude that the diatom should be described as a new genus, *Pseudostriatella*.

We have also been able to make detailed observations on the fine structure of auxospores produced spontaneously in monoclonal cultures. With the advent of electron microscopy, particularly SEM, information about auxospore structure has greatly increased (e.g. Crawford 1974; von Stosch 1982; Mann 1982b; Cohn *et al.* 1989; Kaczmarska *et al.* 2000, 2001; Kobayashi *et al.* 2001; Schmid & Crawford 2001; Nagumo 2003; Sato *et al.* 2004, 2008a, b; Amato *et al.* 2005; Tiffany 2005; Toyoda *et al.* 2005, 2006; Trobajo *et al.* 2006; Pouličková & Mann 2006; Pouličková *et al.* 2007). However, although it has become clear that some aspects of the fine structure of auxospores have phylogenetic significance (e.g. Medlin & Kaczmarska 2004), there is still insufficient information to reveal how the structure and development of auxospores have evolved in the major diatom groups, especially among the lineages of araphid pennate diatoms. Indeed, the only detailed information available concerning araphid pennates is the account of *Rhabdonema* Kützing by von Stosch (1962, 1982) and the SEM studies of *Gephyria media* Arnott (Sato *et al.* 2004), *Grammatophora marina* (Lyngbye) Kützing (Sato *et al.* 2008a) and *Tabularia parva* (Kützing) Williams & Round (Sato *et al.* 2008b). In the present study, we compare the auxospore fine structure in these diatoms with that of *Pseudostriatella oceanica* and discuss the evolutionary relationships of *Pseudostriatella*.

MATERIAL AND METHODS

Collections and cultures

Both natural specimens and clonal cultures were examined in this study. Vegetative cells of the *Pseudostriatella oceanica* examined here were collected by S. Matsumoto at Yumigahama Beach, Minamiizu, Shizuoka Pref., Japan on 20. May 2005, attached to *Cladophora* sp., and by B.K. Petkus at Horseneck State Beach, Westport, Massachusetts, USA, on Aug. 2006, from bottom sand. For morphological comparison, *Striatella unipunctata*, the generitype of the genus *Striatella*, was collected by L.K. Medlin from Banyuls sur Mer, France, on 13 February 2005. Single cells were isolated from the American and French samples to obtain clonal cultures. Cultures were maintained in IMR medium (Eppley *et al.* 1967) at 15°C under cool-white fluorescent light on a 14:10 (L:D) photoperiod at a photon flux density of 30–40 $\mu\text{mol photons m}^{-2} \text{s}^{-1}$. A cover-slip was placed on the bottom of the culture vessel to be colonized with cells producing auxospores. Both strains examined in this study, *Pseudostriatella oceanica* s0384 and *Striatella unipunctata* s0208, are currently available upon request to the first author, but may not survive long-term in culture (cf. Chepurnov *et al.* 2004).

Microscopy

An Axioplan (Zeiss, Oberkochen, Germany) light microscope (LM) with bright field (BF), differential interference contrast (DIC) or phase contrast (PC) optics was used to observe living cells and cleaned frustules. To photograph live specimens attached to the bottom of the culture vessel, a Zeiss Axiovert 35 inverted microscope was used, equipped with an AxioCam MRc digital camera. To remove organic material from the frustule, samples were treated as follows (modified from Nagumo & Kobayashi 1990): (1) the sample was centrifuged to make a pellet and the supernatant discarded; (2) the pellet was re-suspended in distilled water; stages (1) and (2) were then repeated several times to remove salts; (3) to remove organic

matter, the pellet was suspended (using a vortex mixer) in an equal volume of Drano Power-Gel (Johnson Wax GmbH, Haan, Germany), a strong domestic drain cleaner; (4) the suspension was left at room temperature for *c.* 30 min; (5) steps (1) and (2) were repeated several times to remove decomposition products. Cleaned frustules were then mounted in Mountmedia (refractive index $n_{20/D}=1.50$; Wako, Osaka, Japan).

For SEM examination, cleaned material was air-dried onto cover slips. To observe auxospores, cover slips to which the auxospore mother-cells had already become attached were immersed in 10% glutaraldehyde for 1 hour at room temperature, then washed with distilled water, air-dried, and fixed to SEM stubs with carbon tape. For observations of cells still attached to the substratum by mucilaginous stalks, host plants were fixed with 10% glutaraldehyde for 2 h at 4°C, rinsed with distilled water several times to remove the glutaraldehyde, dehydrated using increasing concentrations of *t*-butyl alcohol, and freeze-dried using a JFD-310 instrument (JEOL, Tokyo, Japan). Freeze dried specimens were attached to the stub directly with carbon tape. All SEM specimens were coated with gold using an SC 500 sputter coater (Emscope, Ashford, England). A QUANTA 200F (FEI, Eindhoven, The Netherlands) was used for SEM observation at an accelerating voltage of 3–10 kV, and *c.* 10 mm working distance. All of the images included in this paper are from cultured strains, except for those from freeze-dried material (Figs 9–13). Captured images were adjusted with Adobe Photoshop.

DNA methods

Samples of *c.* 500 mL of culture were filtered through 3 µm pore-diameter membrane filters (Millipore SA, Molsheim, France). Filters were immersed in 500 µL DNA extraction buffer containing 2% (w/v) CTAB, 1.4 M NaCl, 20 mM EDTA, 100 mM Tris-HCl, pH 8, 0.2% (w/v) PVP, 0.01% (w/v) SDS, and 0.2% β-mercaptoethanol. Immersed filters were incubated at 65°C for 5 min, vortexed for a few seconds, and then discarded. Subsequently, the buffer was cooled briefly on ice. DNA was extracted with an equal volume of chloroform–isoamyl alcohol (24:1 [v/v]) and centrifuged in a table-top Eppendorf microfuge (Eppendorf AG, Hamburg, Germany) at maximum speed (14,000 rpm) for 10 min. The aqueous phase was collected, re-extracted with chloroform–isoamyl alcohol and centrifuged as above. Next, the aqueous phase was mixed thoroughly with 0.8 volumes ice-cold 100% isopropanol, left on ice for 5 min, and subsequently centrifuged in a precooled Eppendorf microfuge at maximum speed for 15 min. DNA pellets were washed in 500 µL 70% (v/v) ethanol, centrifuged for 6 min, and then allowed to air-dry after decanting off the ethanol. DNA pellets were dissolved overnight in 100 µL water. The quantity and quality of DNA were examined by agarose gel electrophoresis against known standards.

The targeted marker sequence comprised the 18S rDNA within the nuclear rDNA cistron. The marker was PCR-amplified in 25 µL volumes containing 10 ng DNA, 1 mM dNTPs, 0.5 µM of forward primer, 0.5 µM of reverse primer, 1 x Roche diagnostics PCR reaction buffer (Roche Diagnostics, GmbH, Mannheim, Germany), and 1 unit *Taq* DNA polymerase (Roche). The PCR cycling comprised an initial 4-min heating step at 94°C, followed by 35 cycles of 94°C for 2 min, 56°C for 4 min, and 72°C for 2 min, and a final extension at 72°C for 10 min. PCR products were generated using the forward primer A and a reverse primer B (Medlin *et al.* 1988) without the polylinkers. The quantity and length of products were examined by agarose gel electrophoresis against known standards. Excess primers and dNTPs were removed from PCR product using the QIAQuick purification kit (QIAGEN, Germany), following the manufacturer's instructions. The cleaned PCR products were then electrophoresed on an ABI 3100 Avant sequencer (Applied Biosystems, CA, USA) using Big Dye Terminator

v3.1 sequencing chemistry (Applied Biosystems, CA, USA) with the sequencing primers specified by Elwood *et al.* (1985).

Data analyses

The obtained 18S rDNA sequences were aligned with publicly available sequences retrieved from GenBank (Table 1) first using ClustalX (Thompson *et al.* 1997), and then refined by referring to the secondary structure model of the 18S rRNA at the database of the structure of rRNA (Van de Peer *et al.* 1998). There is extreme length variation in some rRNAs (e.g. Gillespie *et al.* 2005) and replication slippage often leads to convergence on similar primary and secondary structures (Hancock & Vogler 2000; Shull *et al.* 2001). Homology assessment in such regions was difficult or impossible, so that the highly variable regions (most peripheral regions of the 18S rRNA secondary structure) were removed from the alignment using BioEdit 7.0.2 (Hall 1999), by referring to the variability map of *Saccharomyces cerevisiae* (Van de Peer *et al.* 1993), resulting 1713 nucleotides in the dataset.

The dataset consisted of 181 OTUs including the closest relatives of the diatom *Bolidomonas mediterranea* Guillou & Chrétiennot-Dinet and *B. pacifica* Guillou & Chrétiennot-Dinet (Guillou *et al.* 1999) as outgroups. The alignment examined in this study is available at TreeBASE (SN3793).

To determine which model of sequence evolution best fits the data, hierarchical likelihood ratio tests (hLRTs) and Akaike Information Criterion (AIC) were performed using Modeltest 3.7 (Posada & Crandall 1998), and both tests selected the GTR + I + G model. This model had following parameters: base frequencies = A: 0.2685, C: 0.1643, G: 0.2539 and T: 0.3133; substitution rates were: A-C = 1.2232, A-G = 3.1535, A-T = 1.2675, C-G = 1.4955, C-T = 5.5072 and G-T = 1.0000; the proportion of invariant sites was 0.2825, among-site rate heterogeneity was described by a gamma distribution with a shape parameter of 0.6058. Phylogenies were reconstructed with PAUP* version 4.0b10 (Swofford 2002) using neighbour joining (NJ) of likewise constrained pair-wise ML distances. Nodal support was estimated using NJ bootstrap analyses using the same settings (1,000 replicates).

Maximum parsimony (MP) tree searches were done with the “new technology” search algorithm implemented in the Willi Hennig Society edition of TNT 1.1 (<http://www.zmuc.dk/public/phylogeny/TNT>). One hundred random addition sequence replicates were performed with default values. Nonparametric bootstrap analyses were done 1,000 times with the “traditional” search algorithm in TNT.

Maximum likelihood (ML) analyses were performed by RAxML-VI-HPC, v2.2.3 (Stamatakis *et al.* 2005) with GTRMIX model. The analyses were performed 100 times to find the best topology receiving the best likelihood using different random starting MP trees (one round of taxon addition) and the rapid hill-climbing algorithm (i.e. option -f d in RAxML). Bootstrap values were obtained by 100 replications with GTRCAT model.

The Message Passing Interface (MPI) version of MrBayes 3.1.2 (Huelsenbeck & Ronquist 2001; Ronquist & Huelsenbeck 2003; Altekar 2004) was used for Bayesian analyses with the GTR + I + G model to estimate the posterior probability distribution using Metropolis-Coupled Markov Chain Monte Carlo (MCMCMC) (Ronquist & Huelsenbeck 2003). MCMCMC from a random starting tree was used in this analysis with two independent runs and 1 cold and 3 heated chains. The Bayesian analyses were run for 20 million generations each with trees sampled every 100th generation. To increase the probability of chain convergence, we sampled trees after the standard deviation values of the two runs dipped below 0.01 to calculate the posterior probabilities (i.e., after 8,300,000 generations). The remaining phylogenies were discarded as burn-in.

Terminology

Terminology follows Anonymous (1975) and (particularly for auxospore structures) Round *et al.* (1990). Molecular phylogenetic studies of diatoms have revealed that historical diatom classifications do not reflect a natural system and araphid pennate diatoms are paraphyletic in most gene phylogenies, e.g. using nuclear 18S ribosomal DNA (rDNA) and plastid 16S rDNA (Medlin & Kaczmarska 2004). Nevertheless, we use the terms *araphid* and *centric* here, because they refer to key morphological features or their absence. In this paper, the term *araphid pennate diatom* follows the traditional definition, i.e. a diatom that has an elongate valve with a central or slightly lateral sternum, apical pore fields and often also apical rimoportulae, but that lacks a raphe slit. We do not imply that this corresponds to a mono- (holo-) phyletic group, or that it should be accorded any taxonomic status.

RESULTS

Pseudostriatella S. Sato, Mann & Medlin *gen. nov.*

Figs 1–53

Cellulae rectangulares in aspectu cincturae angulis rotundatis, angulo unico per stipitem mucii ad substratum adhaerentes. Chloroplasti c. 10 dispersi et cellulam complentes. Taeniae cincturae numerosae apertae septo conspicuo poros aliquot praebenti. Valvae lanceolatae, oculo ad utrumque polum, fronte in sectione transversali arcuata, sine limbo distincto. Striae irregulares in LM non manifestae. Sternum typicum nullum sed area hyalina secus axem longam adest. Areolae per clavulas oclusae, igitur aperturis dendriticis instructae. Rimoportulae multae dispersae, forma interna variabili.

Cells attached to the substratum by a mucilage stalk at one corner of the frustule, rectangular in girdle view, with rounded corners. Plastids c. 10 per cell, scattered and filling the cell. Copulae numerous open hoops, each with a conspicuous septum containing several pores. Valve lanceolate, with an apical pore field (ocellus) at each pole. Valve face arched, without a distinct mantle. Striae irregular, unresolved with LM. Sternum apparently absent, but a hyaline area is present along the long axis. Areolae occluded by peg-like structures and therefore with dendritic apertures. Many rimoportulae present, of variable form internally.

Type species: *P. oceanica* S. Sato, Mann & Medlin *sp. nov.*

Descriptio speciei eadem est ac descriptio generis; valvae 16.0–47.8 μm longae, 4.4–5.3 μm latae.

HOLOTYPE: BRM Zu6/38

ISOTYPE: TNS-AL-53995

TYPE LOCALITY; Horseneck State Beach, Westport, Massachusetts, U.S.A.

DISTRIBUTION: Known only from the type locality and Yumigahama Beach, Minamiizu, Shizuoka Pref., Japan

Morphology of vegetative cells

In the culture vessel, cells of *Pseudostriatella oceanica* attached to the bottom, usually by means of a mucilaginous stalk secreted from one corner, which reached a maximum length of ca. 20 μm (Fig. 1). Cells occasionally attached to each other to make zigzag chains (not shown), but this was only seen in culture and chains of over five cells were never found. About 10 lobed plastids were scattered through the cell (Fig. 2). A prominent body, likely a pyrenoid, was often visible at the centre of a plastid (Fig. 2, arrow). In girdle view, when the focus was on the surface of the cell, longitudinal rib-like thickenings were visible on some of the girdle bands (Fig. 3). Spots could sometimes be seen on the valve mantle (e.g. at arrow, Fig. 3) and tiny projections were sometimes visible extending inwards from the valve face (e.g. at the centre of the valve in Fig. 4); these features probably represent rimoportulae (see below).

The valves were lanceolate with acute ends (Figs 4, 5). No striae could be resolved in LM with bright field (Fig. 5), DIC (Fig. 6) or phase contrast optics (not shown). The valve length was 16.0–47.8 μm . Auxospore mother cells measured $16.9 \pm 0.6 \mu\text{m}$ (mean $\pm s$, $n = 8$) and initial cells were $41.1 \pm 3.1 \mu\text{m}$ ($n = 12$). The valve width was 4.4–5.3 μm . Apical pore fields were recognisable in LM as hyaline areas at both ends of a valve (Figs 5, 6).

The frustule had numerous girdle bands (ca. 10 per theca: Figs 8, 10), each being an incomplete hoop, open at one end (Fig. 7). The closed end of each band bore a septum, which extended inwards by one-sixth to one-eighth of the valve length (Figs 4, 7). The alternation of the septa (Figs 8, 12, 32) gave a *Striatella*-like appearance to the cell in girdle view (Fig. 3).

Observations of freeze-dried specimens from field material revealed that the surface of the host plant was covered with bacteria (Figs 9, 10, 13). The long mucilaginous stalk (Fig. 9) was secreted from one of the apical pore fields (Fig. 11) but no secretion occurred from other (Fig. 12). The thickness of the stalk was ca. 1 μm (Figs 9, 10, 13). The surface of the mucilaginous stalk was not uniform, but comprised many fine strings and thus appeared fibrous (Fig. 13).

The valve face was smoothly rounded (Fig. 14), lacking an abrupt change between it and the mantle. The areolae were irregularly scattered over some parts of the valve, especially towards the poles, but formed parallel striae towards the centre and radiating striae elsewhere (Fig. 14). A clearly-defined sternum was absent, but there was an irregular hyaline area along the long axis of the valve (Fig. 14). This hyaline area (1) did not occupy the whole but at most only about one-half of the long axis of the valve (Fig. 14), (2) was wider at both ends than in the centre (Fig. 14), and (3) was perforated by small pores in the two wide end-sections (Fig. 15). Apical pore fields were present at both ends of the valve. They had slightly thickened rims and contained small round pores in a strict hexagonal array (Fig. 16). This structure conforms to the definition of an ocellus (Ross *et al.* 1979). The areolae were \pm isodiametric and each was occluded by two to several pegs leaving a dendritic aperture (Figs 17, 18).

On the inner surface of the valve, the hyaline area was less obvious than on the exterior, but still recognizable (Fig. 19). The peg-like occlusions of the areolae were slightly sunk below the surface internally (Fig. 22), suggesting that these structures were external developments (contrast Figs 17, 18). A few of the pores within the widened ends of the hyaline area penetrated the valve (Fig. 20). The ocelli were not rimmed internally (Fig. 21), in contrast to the external appearance (Fig. 16). Approximately 15–30 rimoportulae were found scattered around the edge of each valve (Figs 19, 23, 24), all of them having a similar size but varying

in shape (Figs 25–28). The most common form was ‘C-shaped’, the lips of the process being continuous on one side. This type of process could be either circular (Fig. 25) or elliptical (Fig. 26). Processes with two entire labiate slits (Fig. 27) were also commonly seen. This bilabiate process is not the same as the bilabiate process in the *Lithodesmiales*. Rarely, fused processes were observed (Fig. 28). The basal part of each rimoportula always overlapped part of an areola (Figs 25–28). Externally, the openings of the rimoportulae were undetectable (Figs 14–18).

The closed end of each girdle band bore a septum (Fig. 29), which was irregularly perforated by many scattered pores of variable size (Figs 29–31). The pars exterior was perforated by simple slit-like areolae arranged in short striae (Fig. 32); its margins were plain (Fig. 32, arrow and arrowhead, respectively). The closed end of the band was widened in the peralvar direction to form a ligula (pointing towards the valve) and a smaller antiligula (pointing away from the valve), which were also perforated (Fig. 33). Towards the open ends of the band, the septum became shallower, finally becoming a simple interstria (Fig. 33). The girdle band areolae were slightly sunken internally (Figs 33, 34).

Auxospore structure

Auxosporulation occurred spontaneously in the clonal culture. Nuclear behaviour was not observed in this study and the earliest stages directly observed were the dehiscence of the auxospore mother-cell, the liberation of the protoplast from its frustule, and its bodily movement to a position beyond the open end of one vacated theca (Figs 35–37). The auxospore maintained this position subsequently (Figs 37–38) and must have been physically connected to the empty mother-cell wall, presumably by mucilage, but the exact nature of the connection could not be established. The young auxospore was \pm spherical (Fig. 37). It then expanded at right-angles to the peralvar axis of the gametangium and parallel to its longitudinal axis (Fig. 38). No perizonial caps were observed at any stage of auxosporulation. All mother-cells observed in this study were associated with only a single auxospore (Figs 35–38).

In the earliest stage observed by SEM (Fig. 39), the organic spherical auxospore did not seem to be covered with a mucilage layer, nor with any siliceous structures. Slightly expanded auxospores (Fig. 40), however, were bordered by a plain fringe of material, which probably represented a delicate mucilaginous envelope (Fig. 41). In auxospores that had already expanded significantly (Figs 42, 43), a striated siliceous structure (Fig. 43) could be seen within the mucilaginous layer (Fig. 43), and this can probably be regarded as a longitudinal perizonial (LP) band (cf. Fig. 54). No transverse perizonial (TP) bands were seen in this stage. The LP band comprised a longitudinal rib and a series of closely spaced ribs extending out from it at right angles (Fig. 43). At this stage, the body of cell appeared lumpy, which may represent chloroplasts within the auxospore or a partial covering of silica scales (see below).

When the expansion was complete, an initial valve was produced within the auxospore (Fig. 44). By then, the auxospore could be seen to possess not only longitudinal but also transverse bands (Figs 45, 46). The TP bands were very weakly silicified (Figs 45–47) but could be seen to be finely and irregularly porous (Figs 46, 47, 49). Like the first LP band seen earlier in expansion, the TP bands also often consisted of a longitudinal rib bearing transverse ribs (Fig. 47, arrow and arrowhead, respectively), though these were very feebly developed. The ends of the transverse elements of the TP bands sometimes bore a fringe (Fig. 47).

The series of TP bands and LP bands covered the auxospore (Figs 48, 54). We will refer to the side closest to the theca of the auxospore mother-cell as ‘ventral’ and it was on this side that the LP bands lay. There were several TP bands (Fig. 49), all closed hoops except for the primary band, which was a simple strap passing from one side of the auxospore to the other (Fig. 54). The closed hoops, which we will refer to as secondary bands, did not girdle

the auxospore fully. Instead, each was divided into two broader segments on the dorsal side of the auxospore, connected by a narrower strip along the ventral side (Figs 49, 54).

The primary band and the adjacent secondary TP band (Fig. 49: '1st' and '2nd', respectively) were so delicate and closely associated that the boundary between them was indistinct and they may even have been fused together. The more distal TP bands ('3rd' and '4th', in Figs 49, 54) appeared to be slightly more robust than the first two band and bore distinct longitudinal ribs. The fringed margins of the bands never interlocked with each other (except perhaps between the primary band and its neighbour) but overlapped from the centre outwards, the presumably older bands being external to the younger ones (Fig. 49). Rimoportulae were detected on the initial epivalve (Fig. 49). In fully expanded auxospores, scales were found on the ventral side (Fig. 50). They were thin and delicate and difficult to detect under SEM, unless a strongly contrasted image was produced. They varied in shape but in the most frequent type there was a central pore field ringed by a prominent annulus bearing a delicate fringe of fine radiating fimbriae (Fig. 50, arrow). Much simpler scales were also found (Fig. 50, arrowhead), lacking the prominent annulus and fringe; they were sometimes fused to each other.

When initial cell formation was complete, the series of TP bands was released from the initial cell (Fig. 51, arrow). There were at least three LP bands. The widest lay furthest towards the ventral side (Fig. 52) and was always flanked in our images by two narrower bands (Figs 52-53, see also Fig. 54). The transverse ribs of the LP bands were not straight, plain straps but sinuous or branched or even fused (Fig. 53).

Phylogeny

Highly variable regions were excluded from the 18S rDNA alignment. The analysis used 1713 aligned positions and for this, *Pseudostriatella oceanica* differed from its closest relative, *Striatella unipunctata*, in 104 substitutions and 28 indels.

A Bayesian tree inferred from 18S rDNA sequences of 174 diatoms and 7 Bolidophyceae (Table 1) confirmed paraphyly for the araphid diatoms within a robust clade of pennate diatoms (Fig. 55). The same result was also obtained with NJ, MP and ML analyses (topologies not shown). Within the pennates, the *Asterionellopsis* Round–*Asteroplanus* Gardner & Crawford–*Talaroneis* Kooistra & De Stefano clade and *Rhaphoneis belgica* emerged first, and then a clade containing all other sequenced araphid pennates and a clade of raphid diatoms diverged (Fig. 55: the outgroup centric diatoms and bolidomonads have been omitted for clarity). *P. oceanica* formed a robust monophyly with *S. unipunctata*, this in turn emerging from within raphid diatoms, being sister to the genus *Achnanthes* Bory (MP) or *Eunotia* Ehrenberg (NJ, ML and BI; only the Bayesian tree is shown in Fig. 55).

DISCUSSION

Taxonomic comment on the order Striatellales and the family Striatellaceae

Round *et al.* (1990) proposed that the genus *Striatella* Agardh should be regarded as a monospecific genus because the other (rarely reported) species assigned to it (Van Landingham 1978) differ from the type species *Striatella unipunctata*. We have only encountered and isolated *S. unipunctata* during this study, and the plastids and fine structure of the other species are unknown. Two of the 12 species considered to be valid by VanLandingham (1978) have been transferred to *Hyalosira* Kützing by Navarro & Williams (1991). There are thus 10 species currently in the genus *Striatella*.

Striatella is the nominate genus of the order Striatellales, which was established by Round *et al.* (1990) and contains the single family Striatellaceae (Kützing 1844). In turn, Round considered the Striatellaceae as comprising three marine benthic genera: *Striatella*, *Hyalosira* and *Grammatophora* Ehrenberg. Judging by the description given by Round *et al.* (1990, p. 655) for the Striatellales, these three genera were linked because they have a narrow or indistinct sternum, well-differentiated apical pore fields (in which the pores are in a strict hexagonal array), and porous septate girdle bands. They also have a rimoportula at each apex. Molecular phylogenies show, however, that although *Hyalosira* and *Grammatophora* form a clade, this does not contain *Striatella*, nor is it a close relative of *Striatella* (Fig. 55, see also Sims *et al.* 2006, fig. 2). These results suggest that the family Striatellaceae and the order Striatellales should contain only the nominate genus *Striatella* and *Pseudostriatella*; the monophyly of this group is strongly supported by 18S rDNA data and a wider taxonomic revision is currently in preparation using multiple gene markers. With the benefit of hindsight, it is noticeable that *Striatella* differs from *Hyalosira* and *Grammatophora* in the arrangement of the sternum and rimoportula. The rimoportula is adjacent or lateral to the sternum in *Hyalosira* and *Grammatophora* (Round *et al.* 1990; our unpublished observations), but in *Striatella* they are not associated with each other. Instead, the sternum ends some distance short of the apical pore field and the rimoportula lies within a small area of apically orientated striae. The rimoportulae lie within the striae in *Pseudostriatella* also, but are not restricted to the cell apex.

Comparison of *Pseudostriatella* and *Striatella*

There are many morphological and ecological similarities between *Pseudostriatella oceanica* and *Striatella unipunctata*, such as the numerous copulae and their areolation and prominent septa; the attachment of cells to substrata in the marine littoral and sublittoral by a long mucilaginous stalk; and the production of this stalk via a rimmed apical pore field (ocellus). Because of the morphological similarities of *P. oceanica* and *S. unipunctata*, especially with LM, it is quite possible that the species has been misidentified as *S. unipunctata* in the past. On the other hand, there are also many differences, which we regard as sufficient to differentiate these taxa at the rank of genus. The most striking features are the unusual striation, prominent hyaline area, pegged areolae, multiple marginal rimoportulae, and perforated septum. Furthermore, if living specimens are obtainable, it is easy to identify them because the plastids of *S. unipunctata* are unmistakable, because of their rod-shape and radial arrangement (Fig. 56). With care, cleaned material of the genera can also be separated in LM. Thus, in *S. unipunctata*, each corner of the frustule is sharply truncated (Fig. 56) because of the sunken apical pore fields (see Round *et al.* 1990, p. 432 figs d, e), whereas rounded corners occur in *P. oceanica* (Figs 2–4). Again, in valve views of *S. unipunctata* the sternum is prominent and runs almost the whole length of the valve, the striae are regularly arranged (with staggered areolae giving a pattern of transversely orientated diamonds), can be observed (Fig. 57), and the apical rimoportulae are clearly visible; none of these features exist in *P. oceanica* (Figs 5, 6).

Pseudostriatella oceanica is smaller than *S. unipunctata*. The range observed for *P. oceanica* (16.0–47.8 μm) is probably close to the maximum for the species, because we observed both auxospore mother-cells and initial cells. It is possible that smaller cells may be formed on occasion, because cells of other species sometimes continue to divide after the minimum threshold for sexual reproduction has been passed (Geitler 1932). Furthermore, the sizes of the initial cells can sometimes depend on the sizes of the gametangia or auxospore mother-cells (Davidovich 2001) and this seems to be true in *S. unipunctata* (Chepurnov in Roshchin 1994, table 12). However, *S. unipunctata* can attain lengths of more than double the maximum seen in *P. oceanica*. Because *S. unipunctata* is widespread in tropical, subtropical

and temperate climate zones (Witkowski *et al.* 2000), there are many records and measurements of this species (e.g. Van Landingham 1978). The widest range, 35–125 μm , is given by Hustedt (1931). Chepurnov in Roshchin (1994) observed sexual auxosporulation of *S. unipunctata* in culture and found that gametangia of 32–42 μm gave rise to initial cells of 107–126 μm ; in his illustrations the largest auxospore is 154 μm long (measured on his plate 29). In monoclonal cultures (which cannot auxosporulate because *S. unipunctata* is dioecious), some cells continued to divide until they were 22 μm long before dying. Overall, therefore, although the size ranges of *P. oceanica* and *S. unipunctata* do overlap, they differ enough that valve length can help to distinguish the species in LM.

Rimoportula function

In araphid diatoms, there is some variation in the distribution of the rimoportulae, although they are most often located along the long axis, mostly near one or both ends of the sternum. Normally too each rimoportula has its own special opening externally, which is separate and different from the external openings of the areolae. The consistency of these features suggests that they are maintained by selection, but their significance is unknown because the function of the rimoportula is unclear. In some cases, it has been shown that diatoms secrete mucilage through the rimoportula for movement, e.g. in *Actinocyclus* Ehrenberg (Medlin *et al.* 1986) and *Odontella* Agardh (Pickett-Heaps *et al.* 1986), or adhesion, e.g. in *Melosira* Agardh (Crawford 1975) and *Aulacodiscus* Ehrenberg (Sims & Holmes 1983, p. 270). Schmid (1994) has suggested that the internal part of the rimoportula is used as a cytological anchor for the nucleus during interphase and new valve formation recently, Kühn & Brownlee (2005) have provided evidence that the rimoportula is a site for endocytosis and therefore involved in membrane recycling. It is quite possible that rimoportulae serve multiple roles in diatoms (Medlin *et al.* 1986). In *P. oceanica*, the rimoportulae have no external openings of their own and connect to the outside instead through part of an areola (Figs 25–28). This, together with their scattered distribution on the valve, makes it unlikely that the rimoportulae function in movement in *P. oceanica* or in the production of robust structured mucilage for adhesion. Altogether, the characteristics of the rimoportulae in *P. oceanica* suggest relaxed functional constraints, relative to other araphid pennates.

On the other hand, the rimoportulae have not been lost altogether in *P. oceanica*, in contrast to members of the Plagiogrammaceae (including *Talaroneis*, *Dimeregramma* Ralfs, *Plagiogramma* Paddock) and other genera, such as *Staurosira* (Ehrenberg) Williams & Round, *Nanofrustulum* Round, Hallsteinsen & Paasche, *Opephora* Petit, *Punctastriata* Williams & Round, *Staurosirella* Mereschkowsky, *Pseudostaurosiropsis* Morales and *Pseudostaurosira* Williams & Round (Round *et al.* 1990, 1999; Morales 2001, 2005; Kooistra *et al.* 2004). Among these rimoportula-lacking diatoms, few seem to be able to grow as epiphytes – possibly only *Talaroneis* (Kooistra *et al.* 2004); the rest grow attached to rocks or sand-grains or live planktonically. Possession of rimoportulae may therefore be important in araphid pennates for attachment to plants.

Phylogeny

The 18S rDNA phylogeny gave strong support not only to the monophyly of the *Pseudostriatella oceanica*–*Striatella unipunctata* clade (Bootstrap supports in NJ and ML analyses = 100; Bayesian posterior probability = 1.0), but also to the establishment of a new genus for *P. oceanica* because of the long branches connecting both species. The high divergence between these taxa (104 substitutions and 28 indels) contrasts, for example, with the shorter branch

lengths within *Grammatophora* Ehrenberg and *Eunotia* (see Fig. 55). We accept, of course, that there is no absolute standard for the amount of sequence difference that justifies generic status. Although *P. oceanica* and *S. unipunctata* lie at the ends of long branches, the possibility that the tree has been distorted by long-branch artifacts can probably be excluded, because the two taxa also share a very long node with high statistical support. Preliminary analyses using several gene markers also show that monophyly of the clade containing the two genera is robust (Sato, unpublished data).

Many phylogenetic studies of diatoms made using 18S rDNA have revealed that the araphid pennate diatoms are paraphyletic. They divide into two groups: (1) a relatively small clade of marine diatoms containing the Rhabdonemataceae, Plagiogrammaceae, *Asterionellopsis* and *Asteroplanus*, and (2) a larger, 'core' group (grade) containing the rest of the araphid diatoms that is the sister group to the raphid diatoms (e.g. Medlin & Kaczmarska 2004; Alverson *et al.* 2006; Sims *et al.* 2006). This relationship was recovered in the present analysis. Some features of our tree, such as the sister relationship between the *P. oceanica*–*S. unipunctata* clade and the raphid genus *Eunotia*, have high support but are frankly implausible, because of morphological and reproductive evidence. For example, the pattern of auxosporulation in *Striatella* (*cis* anisogamy coupled with expansion of the auxospore at the mouth of the female gametangium and at right angles to it: Chepurnov in Roshchin 1994) is not shared by *Eunotia* (Mann *et al.* 2003) nor with any other raphid diatoms (Round *et al.* 1990), but does agree well, though not perfectly, with auxosporulation in *Rhabdonema* Kützing and *Grammatophora* (von Stosch 1962, Sato *et al.* 2008a). There are also no vestiges of a raphe in *Pseudostriatella* (contrast *Cocconeis* Ehrenberg 'pseudoraphe' valves, *Semiorbis* R. Patrick, and some *Asterionella*-like diatoms: Mann 1982a; Round *et al.* 1990; Kociolek & Rhode 1998). The poorly supported relationship to the raphid diatoms probably results from well-known analytical artifacts, such as taxon sampling or substitution bias: the long branches seen in *P. oceanica*–*S. unipunctata* clade suggest an accelerated rate of base substitution, which may make it difficult to reconstruct the phylogeny correctly.

Indeed, 18S rDNA analyses undertaken so far have placed *S. unipunctata* in various phylogenetic positions. Some put the genus at the root of the raphid diatoms (Kooistra *et al.* 2003a, b, 2004). Given the hypothesis of Hasle (1974) that the rimoportula might be the predecessor of the raphe, Kooistra *et al.* (2003a) implied that the slightly elongated external opening of the rimoportula in *Striatella* illustrates how the raphe could have arisen, by elongation towards the centre of the valve, creating two slits splitting the sternum. By contrast, in Medlin & Kaczmarska's (2004) analyses, the sister to *Striatella* is *Staurosira construens* Ehrenberg, which has no morphological features in common with *Striatella* and *Pseudostriatella* beyond its elongate shape (Round *et al.* 1990). In an 18S rDNA tree using almost the same dataset of Medlin & Kaczmarska (2004) but constructed by direct optimization (DO), an heuristic maximum parsimony algorithm, *Striatella* is sister to the marine araphid genus *Licmophora* Agardh (Sorhannus 2004). Finally, the genus has appeared within the raphid diatoms, as sister to an *Anomoeoneis* Pfitzer–*Cymbella* Agardh clade (Medlin *et al.* 2000). None of these relationships are robust (i.e. they receive low bootstrap support or Bayesian posterior probabilities; statistical support data are not available in Sorhannus 2004).

One recent result from a Bayesian 18S rDNA analysis, using a doublet model that takes base substitutions in rRNA secondary structure into account, constructed a robust *Striatella*–*Rhabdonema* clade as one of a radiated group of pennate diatoms (Alverson *et al.* 2006 fig. 5). However, the consensus most-parsimonious tree disconnected *Striatella* from *Rhabdonema* and put the taxa into polytomy (fig. 6, Alverson *et al.* 2006). Sims *et al.* (2006) used a huge dataset that placed *Striatella* at the root of the 'core' araphid+raphid clade with high support. In the ML tree presented by Sorhannus (2007), *Striatella* also diverges at the root of the core araphid clade, but with low bootstrap support.

We conclude, therefore, that it is probably impossible at this time to obtain a fully resolved phylogeny resolving the correct phylogenetic placement of the *P. oceanica*–*S. unipunctata* clade, and it may remain impossible while 18S rDNA sequences are used in a single gene phylogeny. It is particularly important to establish the position of the clade because of the unusual structure of the auxospore (see below) and pattern centre in *P. oceanica*. The pennate diatoms are usually monophyletic in trees based on a variety of genes (molecular studies of diatoms are listed by Mann & Evans 2007), supporting the idea that the ‘pennate’ Bauplan is a synapomorphy, i.e., the possession of a single longitudinal rib-like element (sternum) at the centre of the pattern and deposited first during valve formation, which subtends sets of transverse ribs on either side (e.g. Round *et al.* 1990, p. 31). Some diatoms previously regarded as ‘pennates’, such as *Toxarium*, *Ardissona* and *Climacosphenia*, which have a different kind of pattern centre (Mann 1984), have been shown to belong outside the pennate clade (Kooistra *et al.* 2003b; Alverson *et al.* 2006). However, the pattern-centre in *P. oceanica* is unlike anything found previously in pennate diatoms partly because it is a wide unthickened hyaline area, but more importantly because its wider terminal sections contain pores. In fact, the hyaline area resembles a highly elongate annulus – a more extreme version of the elongate annuli seen in some *Odontella* (e.g. Pickett-Heaps *et al.* 1990, fig. 40e) and *Attheya* species (Crawford *et al.* 1994). Until a robust phylogeny is available, it will be unclear whether the resemblance between the *Pseudostriatella* pattern-centre and an annulus is a symplesiomorphy (i.e. *Pseudostriatella* does not have and has never had a true sternum) or the result of convergent evolution.

Auxosporulation and auxospore fine structure

We were not able to establish how the auxospores arise in monoclonal cultures of *P. oceanica*, because the earliest stages were not seen. It is very unlikely that the auxospores developed through allogamous sexual reproduction, because we are confident that we would have observed the empty frustules of any ‘male’ cells close to the expanding auxospores (Roshchin 1994; Chepurnov *et al.* 2004). Therefore, we have referred to the auxosporulating cells as ‘auxospore mother-cells’ rather than as gametangia. Further work is needed to determine whether auxosporulation involves meiosis and automictic fusion, or whether it is apomictic. Non-allogamous formation of auxospores and vegetative cell enlargement has been recorded in other araphid pennates, including *Grammatophora* (Sato *et al.* 2008a) and *Licmophora* (Kumar 1978).

The structure of the auxospore in *P. oceanica* is unlike anything described so far and prompts re-examination of the nature of ‘perizonia’ and ‘properizonia’. In its overall lay-out, the auxospore casing of *P. oceanica* resembles the envelopes of *Rhabdonema* (von Stosch 1962, 1982), *Gephyria* (Sato *et al.* 2004) and *Grammatophora* (Sato *et al.* 2008a), in that it possesses small \pm isodiametric or slightly elongate scales and also separate series of longitudinal and transverse bands. However, there are also significant differences, notably in the structure of the transverse bands and the spatio-temporal organization of auxospore development.

There are very few scales in *Pseudostriatella oceanica*, compared to other araphid diatoms (Sato *et al.* 2004, 2008a, b) and we found them only on the mature auxospore (although we cannot wholly exclude that they were present). As in other diatoms (e.g. von Stosch 1962, 1982; Crawford 1974; Kobayashi *et al.* 2001; Schmid & Crawford 2001), the scales varied in shape within a single auxospore. Some scales had an annulus and were morphologically similar to that of centric diatoms (Round *et al.* 1990). In *P. oceanica*, the auxospores never had a complete covering of scales. The few scales present were restricted to the ventral side in nearly mature or mature examples. A ventral distribution is also present in fully developed

auxospores of the mediophycean centric diatom *Chaetoceros didymum* Ehrenberg (von Stosch 1982, fig 2), although here the scales can also be detected from the earliest stages (von Stosch *et al.* 1973; von Stosch 1982).

Some details of perizonial structure were obscured by collapse of the auxospore during air drying. However, the widest LP band was always located at the most ventral end (Fig. 52) and it was associated with two additional bands. We therefore infer that the widest band is the primary band and that the additional bands flanking it are a secondary and a tertiary LP band (Fig. 54). We believe, however, that some of the LP bands were hidden by folding of the auxospore, which seems likely because all of the longitudinal perizonia reported so far in pennate diatoms are structurally symmetrical (e.g. von Stosch 1962, 1982; Mann 1982b; Toyoda *et al.* 2005), even in *Amphora* (Nagumo 2003). There would therefore be five longitudinal bands in *P. oceanica* (Fig. 59) and a similar arrangement has been found in *Tabularia parva* (Sato *et al.* 2008b). Interestingly, even though the valves of *P. oceanica* have a poorly expressed and irregular sternum–stria system, the LP bands have strictly parallel patterning, resembling the striation of normal araphid diatom valves.

The usual structure of the transverse perizonium in pennate diatoms – both araphid and raphid – is that there is a central primary band with a separate series of secondary bands on each side (von Stosch 1982; Mann 1982b). The primary band is either a short cylinder wholly encircling the centre of the auxospore (i.e., it is ‘closed’: e.g. Poulíčková & Mann 2006), or it is a split ring (an ‘open’ band) with its ends almost touching (e.g. Sato *et al.* 2004). The secondary bands are usually open, again with their ends closely associated. The TP bands combine to form a cigar-shaped perizonium with a narrow ventral suture, beneath which there is often a set of LP bands, again differentiated into a central primary band and two short flanking series of secondary bands (e.g. Mann 1982b; Mann & Stickle 1993; Nagumo 2003; Sato *et al.* 2004; Toyoda *et al.* 2005). The function of the perizonium appears to be to support and constrain anisometric expansion of the auxospore (Mann 1994).

Many centric diatoms also exhibit anisometric expansion and again this is apparently controlled through the formation of band-shaped stiffening elements, which together constitute a structure called the ‘properizonium’ (von Stosch 1982). The key difference between properizonia and perizonia identified by von Stosch (von Stosch & Kowallik 1969; von Stosch *et al.* 1973; von Stosch 1982) is that perizonia are independent from the original zygote wall both structurally and developmentally (the perizonium is “eine von der ursprünglichen Zygotenhülle unabhängige Struktur”: von Stosch & Kowallik 1969, p. 469). In contrast, properizonia are supposed to be structurally and developmentally continuous with the scale-containing layers that precede them (the otherwise helpful review by Kaczmarška *et al.* 2001 may be misleading in this respect). Thus, von Stosch (1982, p. 146) considered that, for the evolutionary transition from properizonial casings to perizonial diatoms like *Rhabdonema*, “the first item necessary would be a developmental and spatial hiatus between scale layers and properizonial band systems”. No other features have been identified that are diagnostic for the perizonium vs. the properizonium, but it is generally considered (von Stosch 1982; Round *et al.* 1990; Kaczmarška *et al.* 2001; Medlin & Kaczmarška 2004) that perizonia are characteristic of pennate diatoms, whereas properizonia are restricted to some lineages of multipolar centric diatoms. Our observations of *P. oceanica* revealed no clear developmental separation between a primary scale-bearing wall and the ‘perizonium’. Scales were rare and produced apparently only towards the end of auxospore expansion, and it appears too that longitudinal perizonial elements are produced before the transverse perizonium. In retrospect, we believe that a similar continuity of development may occur also in *Gephyria*, where we (Sato *et al.* 2004) detected scales on the inside of the primary TP band.

Another curious, ‘transitional’ feature of *P. oceanica* auxospores concerns the nature of the secondary TP bands. As noted above, the secondary bands on either side of the primary

TP band are separate entities in the perizonia of all raphid and araphid pennates studied until now, as they are also in a few properizonia (those of *Odontella* and *Biddulphia*: von Stosch 1982). *Pseudostriatella* is quite different, because the secondary TP elements are continuous from one end of the auxospore to the other around the ventral side (Fig. 54). Each is therefore a complex hoop, shaped like the margin of a saddle. Thus, although the expansion of the auxospore is bipolar in *P. oceanica*, the development of the TP itself is unipolar, beginning from the strap-like primary band and extending out both laterally (towards the poles) and ventrally. Exactly the same unipolar pattern of development occurs in the properizonia of *Chaetoceros*, *Bacteriastrum*, *Attheya*, *Lithodesmium* (here the topology is more complex, because most auxospores are triradiate) and *Bellerochea* (von Stosch 1982), and also in *Lampriscus* (Idei & Nagumo 2002). Thus, it would be as reasonable to regard the auxospore casing of *P. oceanica* as a properizonium, as it is to describe it as a true perizonium, despite the fact that this species clearly belongs phylogenetically to the pennate lineage. The presence of longitudinal elements in the *Pseudostriatella* casing is not conclusive support for interpretation as a perizonium, because (1) longitudinal elements are present beneath the ‘transverse’ bands in the triradiate centric *Lithodesmium* (von Stosch 1982; see also Round *et al.* 1990) and (2) the longitudinal bands of *P. oceanica* seem to be formed before the transverse bands, whereas during perizonium formation in raphid diatoms the converse is true.

A simple conclusion can be drawn: there is simply too little information from too few taxa to allow detailed analysis of the evolution of auxospore structure and that the distinction between properizonia and perizonia needs to be re-evaluated. All that can be said at the moment is that classification into scaly, properizonial and perizonial auxospores (cf. the ‘isometric’, ‘anisometric’ and ‘bilateral’ auxospores of Kaczmarek *et al.* 2001) is perhaps too simple, but that the development of shape *is* generally associated with stiffening of the auxospore wall during expansion by silica bands and hoops.

ACKNOWLEDGEMENT

The authors are grateful to Beth K. Petkus for collection of living specimen, and brought us it from U.S.A. to Germany with her; Richard M. Crawford for correction of the manuscript and discussion; Stephan Frickenhaus for establishing parallel processing for Bayesian analyses; Paul A. Fryxell for helping to translate the Latin diagnosis; Friedel Hinz for technical help for LM and SEM; Masahiko Idei for allowing us to access his poster for the 17th International Diatom Symposium. We also thank two anonymous reviewers for their valuable comments and suggestions. This study was supported by DAAD for doctoral research fellowship to Shinya Sato.

REFERENCES

- ALTEKAR G., DWARKADAS S., HUELSENBECK J. P. & RONQUIST F. 2004. Parallel Metropolis-coupled Markov chain Monte Carlo for Bayesian phylogenetic inference. *Bioinformatics* 20: 407–415.
- ANONYMOUS 1975. Proposals for a standardization of diatom terminology and diagnoses. *Nova Hedwigia, Beiheft* 53: 323–354.
- AMATO A., ORSINI L., D’ALELIO D. & MONTRESOR M. 2005. Life cycle, size reduction patterns, and ultrastructure of the pennate planktonic diatom *Pseudo-nitzschia delicatissima* (Bacillariophyta). *Journal of Phycology* 41: 542–556.

- ALVERSON A.J., CANNONE J.J., GUTELL R.R. & THERIOT E.C. 2006. The evolution of elongate shape in diatoms. *Journal of Phycology* 42: 655–668.
- CAHOON L.B. 1999. The role of benthic microalgae in neritic ecosystems. *Oceanography and Marine Biology. An Annual Review* 37: 47–86
- CHEPURNOV V.A., MANN D.G., SABBE K. & VYVERMAN W. 2004. Experimental studies on sexual reproduction in diatoms. *International Review of Cytology* 237: 91–154.
- COHN S.A., SPURCK T.P., PICKETT-HEAPS J.D. & EDGAR L.A. 1989. Perizonium and initial valve formation in the diatom *Navicula cuspidata* (Bacillariophyceae). *Journal of Phycology* 25: 15–26.
- CRAWFORD R.M. 1974. The auxospore wall of the marine diatom *Melosira nummuloides* (Dillw.) C. Ag. and related species. *British Phycological Journal* 9: 9–20.
- CRAWFORD R.M. 1975. The frustule of the initial cells of some species of the diatom genus *Melosira* C. Agardh. *Nova Hedwigia, Beiheft* 53: 37–50.
- CRAWFORD R.M., GARDNER C. & MEDLIN L.K. 1994. The genus *Attheya*. I. A description of four new taxa, and the transfer of *Gonioceros septentrionalis* and *G. armatus*. *Diatom Research* 9: 27–51.
- DAVIDOVICH N.A. 2001. Species-specific sizes and size range of sexual reproduction in diatoms. In *Proceedings of the 16th International Diatom Symposium* (Ed. by A. Economou-Amilli), pp. 191–196. University of Athens, Greece.
- ELWOOD H.J., OLSEN G.J. & SOGIN M.L. 1985. The small subunit ribosomal DNA gene sequences from the hypotrichous ciliates *Oxytricha nova* and *Stylonichia pustulata*. *Molecular Biology and Evolution* 2: 399–410.
- EPPLEY R.W., HOLMES R.W. & STRICKLAND J.D.H. 1967. Sinking rates of the marine phytoplankton measured with a fluorochromometer. *Journal of Experimental Marine Biology and Ecology* 1: 191–208.
- GEITLER L. 1932. Der Formwechsel der pennaten Diatomeen. *Archiv für Protistenkunde* 78: 1–226.
- GILLESPIE J.J., MCKENNA C.H., YODER M.J., GUTELL R.R., JOHNSTON J.S., KATHIRITHAMBY J., COGNATO A.I. 2005. Assessing the odd secondary structural properties of nuclear small subunit ribosomal RNA sequences (SSU) of the twisted-wing parasites (Insecta: Strepsiptera). *Insect Molecular Biology* 14: 625–643.
- GUILLOU L., CHRETIENNOT-DINET M.-J., MEDLIN L.K., CLAUSTRE H., LOISEAUX-DE GOËR S. & VAULOT D. 1999. *Bolidomonas*: a new genus with two species belonging to a new algal class, the Bolidophyceae class. nov. (Heterokonta). *Journal of Phycology* 35: 368–381.
- HALL T.A. 1999. BioEdit: a user-friendly biological sequence alignment editor and analysis program for Windows 95/98/NT. *Nucleic Acids Symposium Series* 41: 95–98.
- HANCOCK J.M. & VOGLER A.P. 2000. How slippage-derived sequences are incorporated into rRNA variable-region secondary structure: implications for phylogeny reconstruction. *Molecular Phylogenetics and Evolution* 14: 366–374.
- HASLE G.R. 1974. The ‘mucilage pore’ of pennate diatoms. *Nova Hedwigia, Beiheft* 45: 167–194.
- HUELSENBECK J.P. & RONQUIST F. 2001. MRBAYES: Bayesian inference of phylogeny. *Bioinformatics* 17: 754–755.
- HUSTEDT F. 1931. Die Kieselalgen Deutschlands, Österreichs und der Schweiz. In: *Dr L Rabenhorsts Kryptogamenflora von Deutschland, Österreich und der Schweiz*, vol. 7(2:1), pp. 1–176. Akademische Verlagsgesellschaft, Leipzig.

- IDEI M. & NAGUMO T. 2002. Auxospore structure of the marine diatom genus *Lampriscus* with triangular/quadrangular forms. In: *Abstracts, 17th International Diatom Symposium* (Ed. by M. Poulin), p. 166. Ottawa, Canada.
- KACZMARSKA I., BATES S.S., EHRMAN J.M. & LÉGER C. 2000. Fine structure of the gamete, auxospore and initial cell in the pennate diatom *Pseudo-nitzschia multiseriata* (Bacillariophyta). *Nova Hedwigia* 71: 337–357.
- KACZMARSKA I., EHRMAN J.M. & BATES S.S. 2001. A review of auxospore structure, ontogeny and diatom phylogeny. In: *Proceedings of the 16th International Diatom Symposium* (Ed. by A. Economou-Amilli), pp. 153–168. University of Athens, Greece.
- KOBAYASHI A., OSADA K., NAGUMO T. & TANAKA J. 2001. An auxospore of *Arachnoidiscus ornatus* Ehrenberg. In: *Proceedings of the 16th International Diatom Symposium* (Ed. by A. Economou-Amilli), pp. 197–204. University of Athens, Greece.
- KOCIOLEK J.P. & RHODE K. 1998. Raphe vestiges in *Asterionella* species from Madagascar: evidence for a polyphyletic origin of the araphid diatoms? *Cryptogamie: Algologie* 19: 57–74.
- KOOISTRA W.H.C.F., DE STEFANO M., MANN D.G. & MEDLIN L.K. 2003a. The phylogeny of the diatoms. *Progress in Molecular and Subcellular Biology* 33: 59–97.
- KOOISTRA W., DE STEFANO M., MANN D.G., SALMA N. & MEDLIN L.K. 2003b. Phylogenetic position of *Toxarium*, a pennate-like lineage within centric diatoms (Bacillariophyceae). *Journal of Phycology* 39: 185–197.
- KOOISTRA W.H.C.F., FORLANI G., STERRENBURG F.A.S. & DE STEFANO M. 2004. Molecular phylogeny and morphology of the marine diatom *Talaroneis posidoniae* gen. et sp. nov. (Bacillariophyta) advocate the return of the Plagiogrammaceae to the pennate diatoms. *Phycologia* 43: 58–67.
- KÜHN S.F. & BROWNLEE C. 2005. Membrane organisation and dynamics in the marine diatom *Coscinodiscus wailesii* (Bacillariophyceae). *Botanica Marina* 48: 297–305.
- KUMAR R. 1978. Auxospore formation in species of the marine diatom *Licmophora* Agardh. *Veröffentlichungen des Instituts für Meeresforschungen in Bremerhaven* 17:15–20.
- KÜTZING F.T. 1844. *Die kieselschaligen Bacillarien oder Diatomeen*. Nordhausen. 152 pp.
- MANN D.G. 1982a. Structure, life history and systematics of *Rhoicosphenia* (Bacillariophyta) I. The vegetative cell of *Rh. curvata*. *Journal of Phycology* 18: 162–176.
- MANN D.G. 1982b. Structure, life history and systematics of *Rhoicosphenia* (Bacillariophyta) II. Auxospore formation and perizonium structure of *Rh. curvata*. *Journal of Phycology* 18: 264–274.
- MANN D.G. 1984. An ontogenetic approach to diatom systematics. In: *Proceedings of the 7th International Diatom Symposium* (Ed. by D.G. Mann), pp. 113–144. O. Koeltz, Koenigstein.
- MANN, D.G. 1994. The origins of shape and form in diatoms: the interplay between morphogenetic studies and systematics. In: *Shape and form in plants and fungi* (Ed. by D.S. Ingram & A.J. Hudson), pp. 17–38. Academic Press, London.
- MANN, D. G. & EVANS, K. M. (2007). Molecular genetics and the neglected art of diatomics. In: *Unravelling the algae – the past, present and future of algal molecular systematics* (Ed. by J. Brodie & J.M. Lewis), pp. 232–266. CRC Press, Boca Raton, Florida.
- MANN D.G. & STICKLE A.J. 1993. Life history and systematics of *Lyrella*. *Nova Hedwigia, Beiheft* 106: 43–70.

- MANN D.G., CHEPURNOV V.A. & IDEI M. 2003. Mating system, sexual reproduction and auxosporulation in the anomalous raphid diatom *Eunotia* (Bacillariophyta). *Journal of Phycology* 39: 1067–1084.
- MEDLIN L.K. & KACZMARSKA I. 2004. Evolution of the diatoms: V. Morphological and cytological support for the major clades and a taxonomic revision. *Phycologia* 43: 245–270.
- MEDLIN L.K., CRAWFORD R.M. & ANDERSEN R.A. 1986. Histochemical and ultrastructural evidence for the function of the labiate process in the movement of centric diatoms. *British Phycological Journal* 21: 297–301.
- MEDLIN L., ELWOOD H.J., STICKEL S. & SOGIN M.L. 1988. The characterization of enzymatically amplified eukaryotic 16S-like rRNA coding regions. *Gene* 71: 491–499.
- MEDLIN L.K., KOOISTRA W.H.C.F. & SCHMID A.M.-M. 2000. A review of the evolution of the diatoms – a total approach using molecules, morphology and geology. In: *The origin and early evolution of the diatoms: fossil, molecular and biogeographical approaches* (Ed. by A. Witkowski & J. Sieminska), pp. 13–35. Szafer Institute of Botany, Polish Academy of Science, Cracow, Poland.
- MEDLIN L.K., JUNG I., BAHULIKAR R., MENDGEN K., KROTH P. & KOOISTRA W.H.C.F. 2008. Evolution of the diatoms. VI. Assessment of the new genera in the araphids using molecular data. *Nova Hedwigia* 133: 81–100.
- MORALES E. 2001. Morphological studies in selected fragilarioid diatoms (Bacillariophyceae) from Connecticut waters (U.S.A.). *Proceedings of the Academy of Natural Sciences of Philadelphia* 151: 39–54.
- MORALES E. 2005. Observations of the morphology of some known and new fragilarioid diatoms (Bacillariophyceae) from rivers in the USA. *Phycological Research* 53: 113–133.
- NAGUMO T. 2003. Taxonomic studies of the subgenus *Amphora* Cleve of the genus *Amphora* (Bacillariophyceae) in Japan. *Bibliotheca Diatomologica* 49: 1–265.
- NAGUMO T & KOBAYASHI H. 1990. The bleaching method for gently loosening and cleaning a single diatom frustule. *Diatom* 5: 45–50
- NAVARRO N.J. & WILLIAMS D.M. 1991. Description of *Hyalosira tropicalis* sp. nov. (Bacillariophyta) with notes on the status of *Hyalosira* Kützing and *Microtabella* Round. *Diatom Research* 6: 327–336.
- PICKETT-HEAPS J.D., HILL D.R.A. & WETHERBEE R. 1986. Cellular movement in the centric diatom *Odontella sinensis*. *Journal of Phycology* 22: 334–339.
- PICKETT-HEAPS J.D., SCHMID, A.-M.M. & EDGAR L.A. 1990. The cell biology of diatom valve formation. *Progress in Phycological Research* 7: 1–168.
- POSADA D. & CRANDALL K.A. 1998. Modeltest: testing the model of DNA substitution. *Bioinformatics* 14: 817–818.
- POULÍČKOVÁ A. & MANN D.G. 2006. Sexual reproduction in *Navicula cryptocephala* (Bacillariophyceae). *Journal of Phycology* 42: 872–886.
- POULÍČKOVÁ A., MAYAMA S., CHEPURNOV V.A. & MANN D.G. (2007). Heterothallic auxosporulation, incunabula and perizonium in *Pinnularia* (Bacillariophyceae). *European Journal of Phycology* 42: 367–390.
- RONQUIST F. & HUELSENBECK J.P. 2003. MrBayes 3: Bayesian phylogenetic inference under mixed models. *Bioinformatics* 19: 1572–1574.
- ROSHCHIN A.M. 1994. *Zhiznennyye tsikly diatomovykh vodoroslej*. Naukova Dumka, Kiev, 170 pp.

- ROSS R., COX E.J., KARAYEVA N.I., MANN D.G., PADDOCK T.B.B., SIMONSEN R. & SIMS P.A. 1979. An amended terminology for the siliceous components of the diatom cell. *Nova Hedwigia, Beiheft* 64: 513–533.
- ROUND F.E., CRAWFORD R.M. & MANN D.G. 1990. *The diatoms. Biology and morphology of the genera*. Cambridge University Press, Cambridge. 747 pp.
- ROUND F.E., HALLSTEINSEN H. & PAASCHE E. 1999. On a previously controversial “fragilarioid” diatom now placed in a new genus *Nanofrustulum*. *Diatom Research* 14: 343–356.
- SATO S., NAGUMO T. & TANAKA J. 2004. Auxospore formation and the morphology of the initial cell of the marine araphid diatom *Gephyria media* (Bacillariophyceae). *Journal of Phycology* 40: 684–691.
- SATO S, MANN D.G., NAGUMO T., TANAKA J. & MEDLIN L.K. 2008a. Life cycle of *Grammatophora marina* (Bacillariophyta) with special reference to its auxospore fine structure. *Phycologia* 47:12-27.
- SATO S, KURIYAMA K, TADANO T & MEDLIN K.L. 2008b. Auxospore fine structure in a marine araphid diatom *Tabularia parva* (Bacillariophyta). *Diatom Research* in press.
- SCHMID A.-M.M. 1994. Aspects of morphogenesis and function of diatom cell walls with implications for taxonomy. *Protoplasma* 181: 43–60.
- SCHMID A.-M.M. & CRAWFORD R.M. 2001. *Ellerbeckia arenaria* (Bacillariophyceae): formation of auxospores and initial cells. *European Journal of Phycology* 36: 307–320.
- SHULL V.L., VOGLER A.P., BAKER M.D., MADDISON D.R. & HAMMOND P.M. 2001. Sequence alignment of 18S ribosomal RNA and the basal relationships of adephagan beetles: evidence for monophyly of aquatic families and the placement of Trachypachidae. *Systematic Biology* 50: 945–969.
- SIMS P.A. & HOLMES R.W. 1983. Studies on the “kittonii” group of *Aulacodiscus* species. *Bacillaria* 6: 267–292.
- SIMS P.A., MANN D.G. & MEDLIN L.K. 2006. Evolution of the diatoms: insights from fossil, biological and molecular data. *Phycologia* 45: 361–402.
- SORHANNUS U. 2004. Diatom phylogenetics inferred based on direct optimization nuclear-encoded SSU rRNA sequences. *Cladistics* 20: 487–497.
- SORHANNUS U. 2007. A nuclear-encoded small-subunit ribosomal RNA timescale for diatom evolution. *Marine Micropaleontology* 65: 1-12.
- STAMATAKIS A, LUDWIG T, MEIER H. 2005. RAxML-III: A fast program for maximum likelihood-based inference of large phylogenetic trees. *Bioinformatics* 21: 456–463.
- STOSCH H.A. VON 1962. Über das Perizonium der Diatomeen. *Vorträge aus dem Gesamtgebiet der Botanik* 1: 43–52.
- STOSCH H.A. VON 1982. On auxospore envelopes in diatoms. *Bacillaria* 5: 127–156.
- STOSCH H.A. VON. & KOWALLIK K.V. 1969. Der von Geitler aufgestellte Satz über die Notwendigkeit einer Mitose für jede Schalenbildung von Diatomeen. Beobachtung über die Reichweite und Überlegungen zu seiner zellmechanischen Bedeutung. *Österreichische botanische Zeitschrift* 116: 454–474.
- STOSCH H.A. VON, THEIL G. & KOWALLIK K.V. 1973. Entwicklungsgeschichtliche Untersuchungen an zentrischen Diatomeen. V. Bau und Lebenszyklus von *Chaetoceros didymum*, mit Beobachtungen über einige andere Arten der Gattung. *Helgoländer wissenschaftliche Meeresuntersuchungen* 25: 384–445.
- SULLIVAN M.J. & CURRIN C.A. 2000. Community structure and functional dynamics of benthic microalgae in salt marshes. In: *Concepts and controversies in tidal marsh*

- ecology* (Ed. by M.P. Weinstein & D.A. Kreeger), pp. 81–106. Kluwer Academic Publishers, Dordrecht Germany.
- SWOFFORD D. L. 2002. *PAUP**. *Phylogenetic Analysis Using Parsimony (* and other methods)*. Version 4.0b10. Sinauer Associates, Sunderland, MA.
- TIFFANY M.A. 2005. Diatom auxospore scales and early stages in diatom frustule morphogenesis: their potential for use in nanotechnology. *Journal of Nanoscience and Nanotechnology* 5: 131–139.
- THOMPSON J.D., GIBSON T.J., PLEWNIAK F., JEANMOUGIN F. & HIGGINS D.G. 1997. The ClustalX windows interface: flexible strategies for multiple sequence alignment aided by quality analysis tools. *Nucleic Acids Research* 24: 4876–4882.
- TOYODA K., IDEI M., NAGUMO T. AND TANAKA J. 2005. Fine-structure of frustule, perizonium and initial valve of *Achnanthes yaquinensis* McIntire and Reimer (Bacillariophyceae). *European Journal of Phycology* 40: 269–79.
- TOYODA K, WILLIAMS D.M., TANAKA J. & NAGUMO T. 2006. Morphological investigations of the frustule, perizonium and initial valves of the freshwater diatom *Achnanthes crenulata* Grunow (Bacillariophyceae). *Phycological Research* 54: 173–182.
- TROBAJO R., MANN D.G., CHEPURNOV V.A., CLAVERO E. & COX E.J. 2006. Auxosporulation and size reduction pattern in *Nitzschia fonticola* (Bacillariophyta). *Journal of Phycology* 42: 1353–1372.
- UNDERWOOD G.J.C. & KROMKAMP J. 1999. Primary production by phytoplankton and microphytobenthos in estuaries. *Advances in Ecological Research* 29: 93–153
- VAN DE PEER Y., CAERS A., DE RIJK P. & DE WACHTER R. 1998. Database on the structure of small ribosomal subunit RNA. *Nucleic Acids Research* 26: 179–182
- VAN DE PEER Y., NEEFS J.-M, DE RIJK P. & DE WACHTER R. 1993. Reconstructing evolution from eukaryotic small-ribosomal-subunit RNA sequences: calibration of the molecular clock. *Journal of Molecular Evolution*. 37: 221–232.
- VANLANDINGHAM S.L. 1978. *Catalogue of the fossil and recent genera and species of diatoms and their synonyms. Part VII. Rhoicosphenia through Zygodon*. J. Cramer, Vaduz.
- WITKOWSKI A., LANGE-BERTALOT H. & METZELTIN D. 2000. Diatom flora of marine coasts I. *Iconographia Diatomologica* 7: 1–925.

Table 1. List of taxon and GenBank accessions for 18S rDNA sequences used in this study.

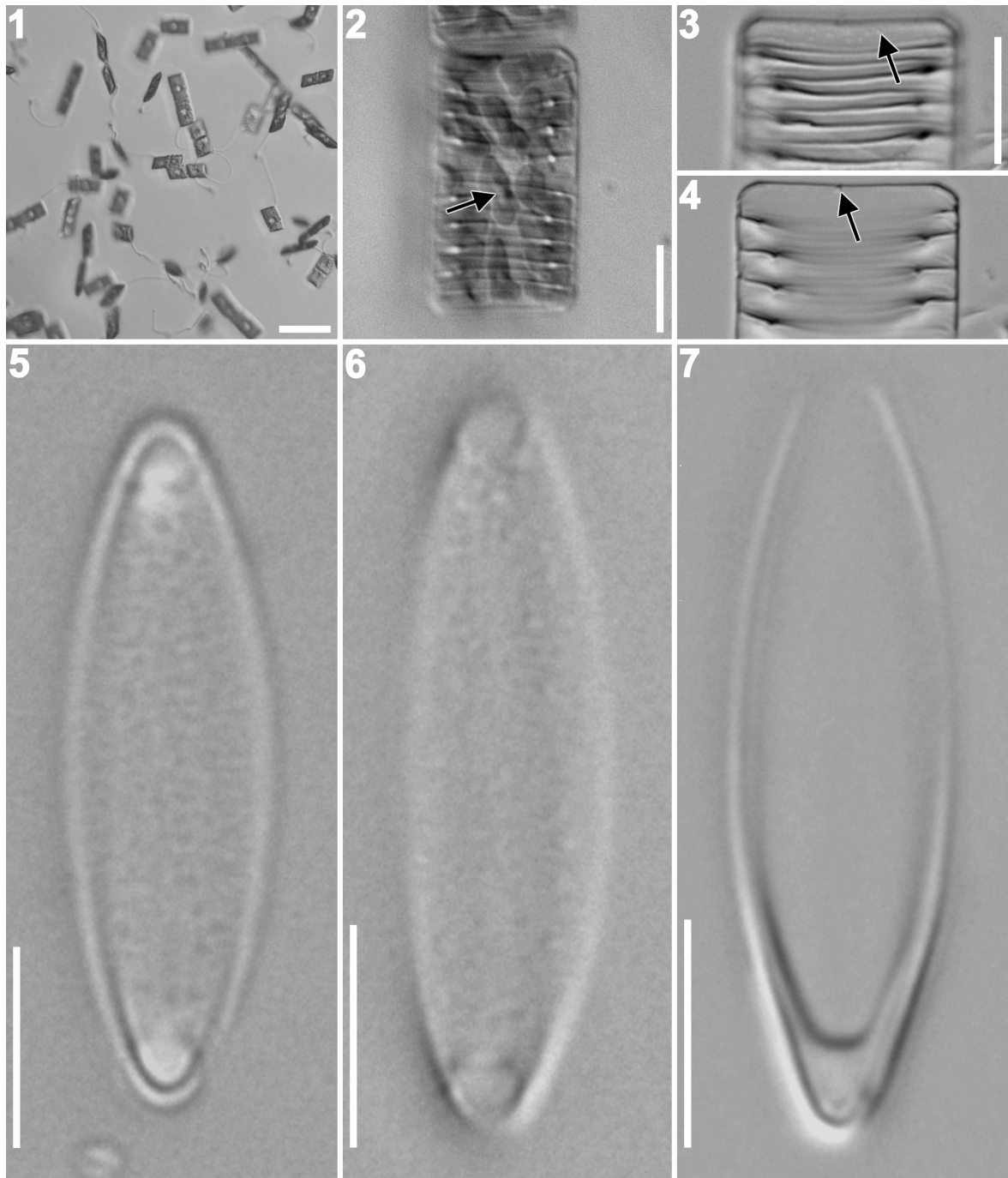
Taxon	accession
<i>Aulacoseira ambigua</i> (Grunow) Simonsen	X85404
<i>Aulacoseira baicalensis</i> (Meyer) Simonsen	AJ535185
<i>Aulacoseira baicalensis</i> (Meyer) Simonsen	AJ535186
<i>Aulacoseira baicalensis</i> (Meyer) Simonsen	AY121821
<i>Aulacoseira distans</i> (Ehrenberg) Simonsen	X85403
<i>Aulacoseira islandica</i> (Müller) Simonsen	AJ535183
<i>Aulacoseira islandica</i> (Müller) Simonsen	AY121820
<i>Aulacoseira nyassensis</i> (Müller) Simonsen	AJ535187
<i>Aulacoseira nyassensis</i> (Müller) Simonsen	AY121819
<i>Aulacoseira skvortzowii</i> Edlund, Stoermer et Taylor	AJ535184
<i>Aulacoseira subarctica</i> (Müller) Haworth	AY121818
<i>Actinocyclus curvatus</i> Janisch	X85401
<i>Actinoptychus seniarius</i> (Ehrenberg) Héribaud	AJ535182
<i>Bellerochea malleus</i> (Brightwell) Van Heurck	AF525671
<i>Biddulphiopsis titiana</i> (Grunow) von Stosch et Simonsen	AF525669
<i>Chaetoceros curvisetus</i> Cleve	AY229895
<i>Chaetoceros debilis</i> Cleve	AY229896
<i>Chaetoceros didymus</i> Ehrenberg	X85392
<i>Chaetoceros gracilis</i> Schütt	AY229897
<i>Chaetoceros rostratus</i> Lauder	X85391
<i>Chaetoceros</i> sp.	AF145226
<i>Chaetoceros</i> sp.	AJ535167
<i>Chaetoceros</i> sp.	X85390
<i>Corethron criophilum</i> Castracane	X85400
<i>Corethron inerme</i> Karsten	AJ535180
<i>Corethron hystrix</i> Hensen	AJ535179
<i>Coscinodiscus radiatus</i> Ehrenberg	X77705
<i>Cyclotella meneghiniana</i> Kützing	AJ535172
<i>Cyclotella meneghiniana</i> Kützing	AY496206
<i>Cyclotella meneghiniana</i> Kützing	AY496207
<i>Cyclotella meneghiniana</i> Kützing	AY496210
<i>Cyclotella meneghiniana</i> Kützing	AY496212
<i>Cyclotella</i> cf. <i>scaldensis</i>	AY496208
<i>Cymatosira belgica</i> Grunow	X85387
<i>Detonula confervacea</i> (Cleve) Gran	AF525672
<i>Ditylum brightwellii</i> (West) Grunow in Van Heurck	AY188181
<i>Ditylum brightwellii</i> (West) Grunow in Van Heurck	AY188182
<i>Ditylum brightwellii</i> (West) Grunow in Van Heurck	X85386
<i>Eucampia antarctica</i> (Castracane) Mangin	X85389
<i>Guinardia delicatula</i> (Cleve) Hasle	AJ535192
<i>Guinardia flaccida</i> (Castracane) H. Peragallo	AJ535191
<i>Helicotheca tamesis</i> (Schrubsole) Ricard	X85385
<i>Lampriscus kittonii</i> Schmidt	AF525667
<i>Lauderia borealis</i> Cleve	X85399
<i>Leptocylindrus danicus</i> Cleve	AJ535175
<i>Leptocylindrus minimus</i> Gran	AJ535176
<i>Lithodesmium undulatum</i> Ehrenberg	Y10569
<i>Melosira varians</i> Agardh	AJ243065
<i>Melosira varians</i> Agardh	X85402

<i>Odontella sinensis</i> (Greville) Grunow	Y10570
<i>Papiliocellulus elegans</i> Hasle, von Stosch et Syvertsen	X85388
<i>Paralia sol</i> (Ehrenberg) Crawford	AJ535174
<i>Planktoniella sol</i> (Wallich) Schütt	AJ535173
<i>Pleurosira laevis</i> (Ehrenberg) Compère	AF525670
<i>Porosira pseudodenticulata</i> (Hustedt) Jousé	X85398
<i>Proboscia alata</i> (Brightwell) Sundström	AJ535181
<i>Rhizosolenia imbricate</i> Brightwell	AJ535178
<i>Rhizosolenia similoides</i> Cleve-Euler	J535177
<i>Rhizosolenia setigera</i> Brightwell	M87329
<i>Skeletonema costatum</i> (Greville) Cleve	X52006
<i>Skeletonema costatum</i> (Greville) Cleve	X85395
<i>Skeletonema menzelii</i> Guillard, Carpenter et Reimer	AJ535168
<i>Skeletonema menzelii</i> Guillard, Carpenter et Reimer	AJ536450
<i>Skeletonema pseudocostatum</i> Medlin	AF462060
<i>Skeletonema pseudocostatum</i> Medlin	X85393
<i>Skeletonema subsalsum</i> (Cleve-Euler) Bethge	AJ535166
<i>Skeletonema</i> sp.	AJ535165
<i>Stephanopyxis</i> cf. <i>broschii</i>	M87330
<i>Thalassiosira eccentrica</i> (Ehrenberg) Cleve	X85396
<i>Thalassiosira guillardii</i> Hasle	AF374478
<i>Thalassiosira oceanica</i> Hasle	AF374479
<i>Thalassiosira pseudonana</i> Hasle et Heimdal	AJ535169
<i>Thalassiosira pseudonana</i> Hasle et Heimdal	AF374481
<i>Thalassiosira rotula</i> Meunier	AF374480
<i>Thalassiosira rotula</i> Meunier	AF462058
<i>Thalassiosira rotula</i> Meunier	AF462059
<i>Thalassiosira rotula</i> Meunier	X85397
<i>Thalassiosira weissflogii</i> (Grunow) Fryxell et Hasle	AF374477
<i>Thalassiosira weissflogii</i> (Grunow) Fryxell et Hasle	AJ535170
<i>Thalassiosira</i> sp.	AJ535171
<i>Toxarium undulatum</i> Bailey	AF525668
<i>Asterionella formosa</i> Hassall	AF525657
<i>Asterionellopsis glacialis</i> (Castracane) Round	X77701
<i>Asterionellopsis glacialis</i> (Castracane) Round	AY216904
<i>Asteroplanus karianus</i> ¹ (Grunow in Cleve et Grunow) Gardner et Crawford	Y10568
<i>Cyclophora tenuis</i> Castracane	AJ535142
<i>Diatoma hyemalis</i> (Roth) Heiberg	AB085829
<i>Diatoma tenue</i> Agardh	AJ535143
<i>Fragilaria crotonensis</i> Kitton	AF525662
<i>Fragilariforma virescens</i> (Ralfs) Williams et Round	AJ535137
<i>Grammatophora gibberula</i> Kützing	AF525656
<i>Grammatophora oceanica</i> Ehrenberg	AF525655
<i>Grammatophora marina</i> (Lyngbye) Kützing	AY216906
<i>Grammonema striatula</i> Agardh ¹	X77704
<i>Grammonema</i> cf. <i>islandica</i> ¹	AJ535190
<i>Grammonema</i> sp. ¹	AJ535141
<i>Hyalosira delicatula</i> Kützing	AF525654
<i>Licmophora juergensii</i> Agardh	AF525661
<i>Nanofrustulum shiloi</i> (Lee, Reimer et McEnery) Round, Hallsteinsen et	AF525658

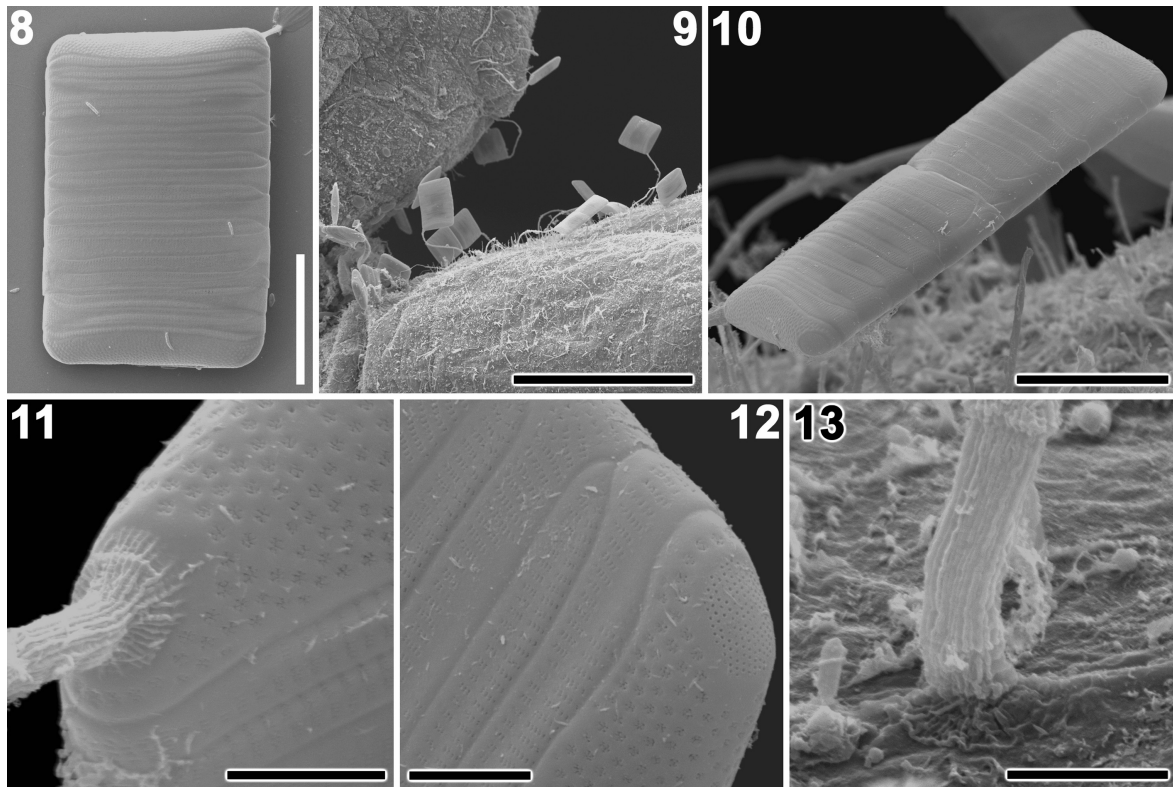
Paasche	
<i>Pseudostriatella oceanica</i> S. Sato, Mann et Medlin	AB379680
<i>Rhabdonema arcuatum</i> (Agardh) Kützing	AF525660
<i>Rhaphoneis belgica</i> (Grunow in Van Heurck) Grunow in Van Heurck	X77703
<i>Staurosira construens</i> Ehrenberg	AF525659
<i>Striatella unipunctata</i> (Lyngbye) Agardh	AF525666
<i>Synedra</i> sp. ³	AJ535138
<i>Tabularia tabulata</i> (Agardh) Williams et Round	AY216907
<i>Talaroneis posidoniae</i> Kooistra et De Stefano	AY216905
<i>Thalassionema nitzschioides</i> (Grunow) Hustedt	X77702
<i>Thalassionema</i> sp.	AJ535140
<i>Synedra ulna</i> Nitzsch	AJ535139
<i>Achnanthes bongrainii</i> (M. Peragallo) A. Mann	AJ535150
<i>Achnanthes</i> sp.	AJ535151
<i>Amphora montana</i> Krasske	AJ243061
<i>Amphora</i> cf. <i>capitellata</i>	AJ535158
<i>Amphora</i> cf. <i>proteus</i>	AJ535147
<i>Anomoeoneis sphaerophora</i> (Ehrenberg) Pfitzer	AJ535153
<i>Bacillaria paxillifer</i> (Müller) Hendey	M87325
<i>Campylodiscus ralfsii</i> Gregory	AJ535162
<i>Cocconeis</i> cf. <i>molesta</i>	AJ535148
<i>Cylindrotheca closterium</i> (Ehrenberg) Reimann et Lewin	M87326
<i>Cymbella cymbiformis</i> Agardh	AJ535156
<i>Encyonema triangulatum</i> Kützing	AJ535157
<i>Entomoneis</i> cf. <i>alata</i>	AJ535160
<i>Eolimna minima</i> (Grunow) Lange-Bertalot	AJ243063
<i>Eolimna subminuscula</i> (Manguin) Moser, Lange-Bertalot et Metzeltin	AJ243064
<i>Eunotia formica</i> var. <i>sumatrana</i> Hustedt	AB085830
<i>Eunotia monodon</i> var. <i>asiatica</i> Skvortzow	AB085831
<i>Eunotia pectinalis</i> (Dillwyn) Rabenhorst	AB085832
<i>Eunotia</i> cf. <i>pectinalis</i> f. <i>minor</i>	AJ535146
<i>Eunotia</i> sp.	AJ535145
<i>Fragilariopsis sublineata</i> Hasle	AF525665
<i>Gomphonema parvulum</i> Kützing	AJ243062
<i>Gomphonema pseudoaugur</i> Lange-Bertalot	AB085833
<i>Lyrella atlantica</i> (Schmidt) D. G. Mann	AJ544659
<i>Navicula cryptocephala</i> var. <i>veneta</i> (Kützing) Grunow	AJ297724
<i>Navicula diserta</i> Hustedt	AJ535159
<i>Navicula pelliculosa</i> (Brébisson ex Kützing) Hilse	AJ544657
<i>Nitzschia apiculata</i> (Gregory) Grunow	M87334
<i>Nitzschia frustulum</i> (Kützing) Grunow	AJ535164
<i>Pinnularia</i> cf. <i>interrupta</i>	AJ544658
<i>Pinnularia</i> sp.	AJ535154
<i>Phaeodactylum tricornutum</i> Bohlin	AJ269501
<i>Planothidium lanceolatum</i> (Brébisson ex Kützing) Round et Bukhtiyarova	AJ535189
<i>Pleurosigma</i> sp.	AF525664
<i>Pseudogomphonema</i> sp.	AF525663
<i>Pseudogomphonema</i> sp.	AJ535152
<i>Pseudo-nitzschia multiseriis</i> (Hasle) Hasle	U18241
<i>Pseudo-nitzschia pungens</i> (Grunow ex Cleve) Hasle	U18240
<i>Rossia</i> sp.	AJ535144

<i>Sellaphora capitata</i> Mann et McDonald	AJ535155
<i>Sellaphora pupula</i> (Kützing) Mereschkowsky	AJ544645
<i>Sellaphora pupula</i> (Kützing) Mereschkowsky	AJ544651
<i>Sellaphora pupula</i> (Kützing) Mereschkowsky	AJ544647
<i>Sellaphora pupula</i> (Kützing) Mereschkowsky	AJ544648
<i>Sellaphora pupula</i> (Kützing) Mereschkowsky	AJ544649
<i>Sellaphora pupula</i> (Kützing) Mereschkowsky	AJ544650
<i>Sellaphora pupula</i> (Kützing) Mereschkowsky	AJ544652
<i>Sellaphora pupula</i> (Kützing) Mereschkowsky	AJ544653
<i>Sellaphora pupula</i> (Kützing) Mereschkowsky	AJ544654
<i>Sellaphora laevissima</i> (Kützing) D. G. Mann	AJ544655
<i>Sellaphora laevissima</i> (Kützing) D. G. Mann	AJ544656
<i>Surirella fastuosa</i> var. <i>cuneata</i> (Schmidt) H. Peragallo et M. Peragallo	AJ535161
<i>Thalassiosira antarctica</i> Comber	AF374482
<i>Undatella</i> sp.	AJ535163
<i>Bolidomonas mediterranea</i> Guillou et Chrétiennot-Dinet	AF123596
<i>Bolidomonas pacifica</i> Guillou et Chrétiennot-Dinet	AF123595
<i>Bolidomonas pacifica</i> Guillou et Chrétiennot-Dinet	AF167153
<i>Bolidomonas pacifica</i> Guillou et Chrétiennot-Dinet	AF167154
<i>Bolidomonas pacifica</i> Guillou et Chrétiennot-Dinet	AF167155
<i>Bolidomonas pacifica</i> Guillou et Chrétiennot-Dinet	AF167156
<i>Bolidomonas pacifica</i> Guillou et Chrétiennot-Dinet	AF167157
<i>Convoluta convoluta</i> diatom endosymbiont	AY345013
<i>Peridinium foliaceum</i> endosymbiont	Y10567
<i>Peridinium balticum</i> endosymbiont	Y10566
Uncultured diatom	AY180014
Uncultured diatom	AY180015
Uncultured diatom	AY180016
Uncultured diatom	AY180020
Uncultured eukaryote	AY082977
Uncultured eukaryote	AY082992
Uncultured marine diatom	AF290085

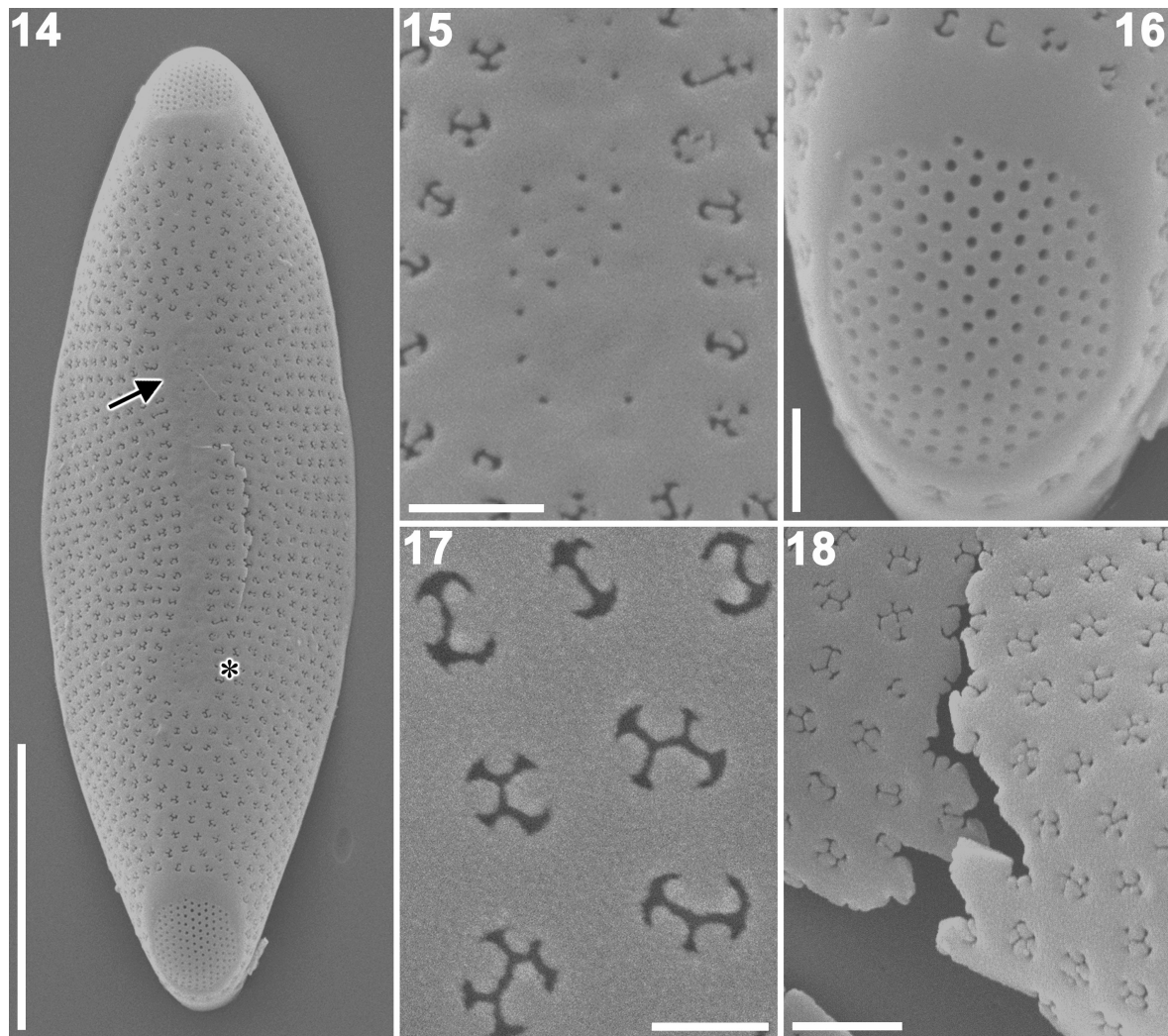
¹name change since deposit; ² likely a new genus collected from a marine habitat (Medlin et al. 2008)



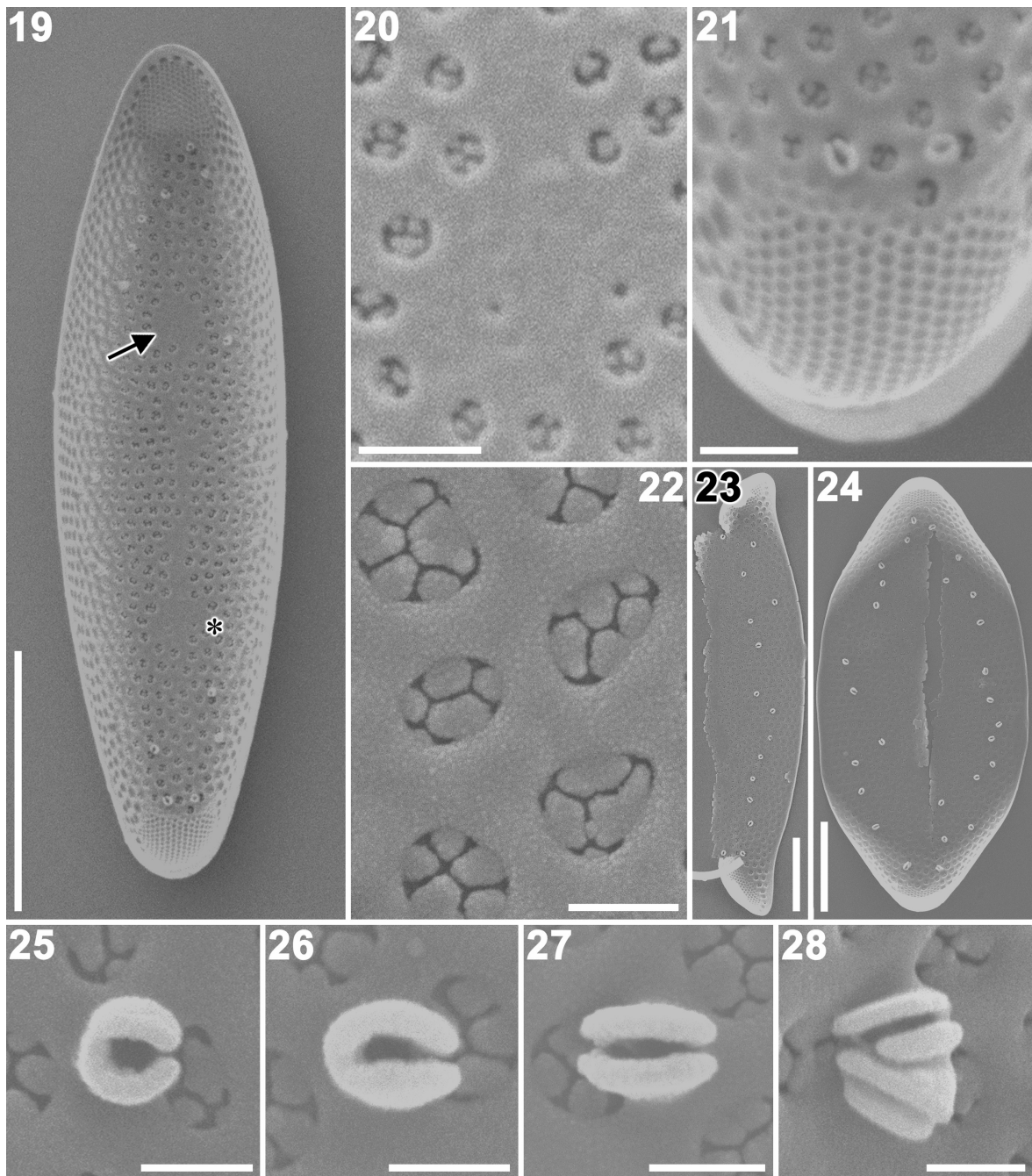
Figs 1–7. *Pseudostriatella oceanica*: living and cleaned cells (LM). Scale bars = 100 μm (Fig. 1), 10 μm (Figs 2, 3) or 5 μm (Figs 5–7). **Fig. 1.** Living cells growing in culture vessel. **Fig. 2.** Living cell showing multiple-plastids. Arrow indicates presumable pyrenoid. **Fig. 3.** Cleaned frustule, focused on surface to show prominent ribs along the girdle bands, continuous with the septa. The arrow indicates a white spot on the valve that is probably a rimoportula. **Fig. 4.** Median focus of the frustule in Fig. 3, showing septate girdle bands; arrow indicates probable rimoportula. **Fig. 5.** Cleaned valve. (BF). **Fig. 6.** Cleaned valve. (DIC). **Fig. 7.** Single girdle band with septum at closed end.



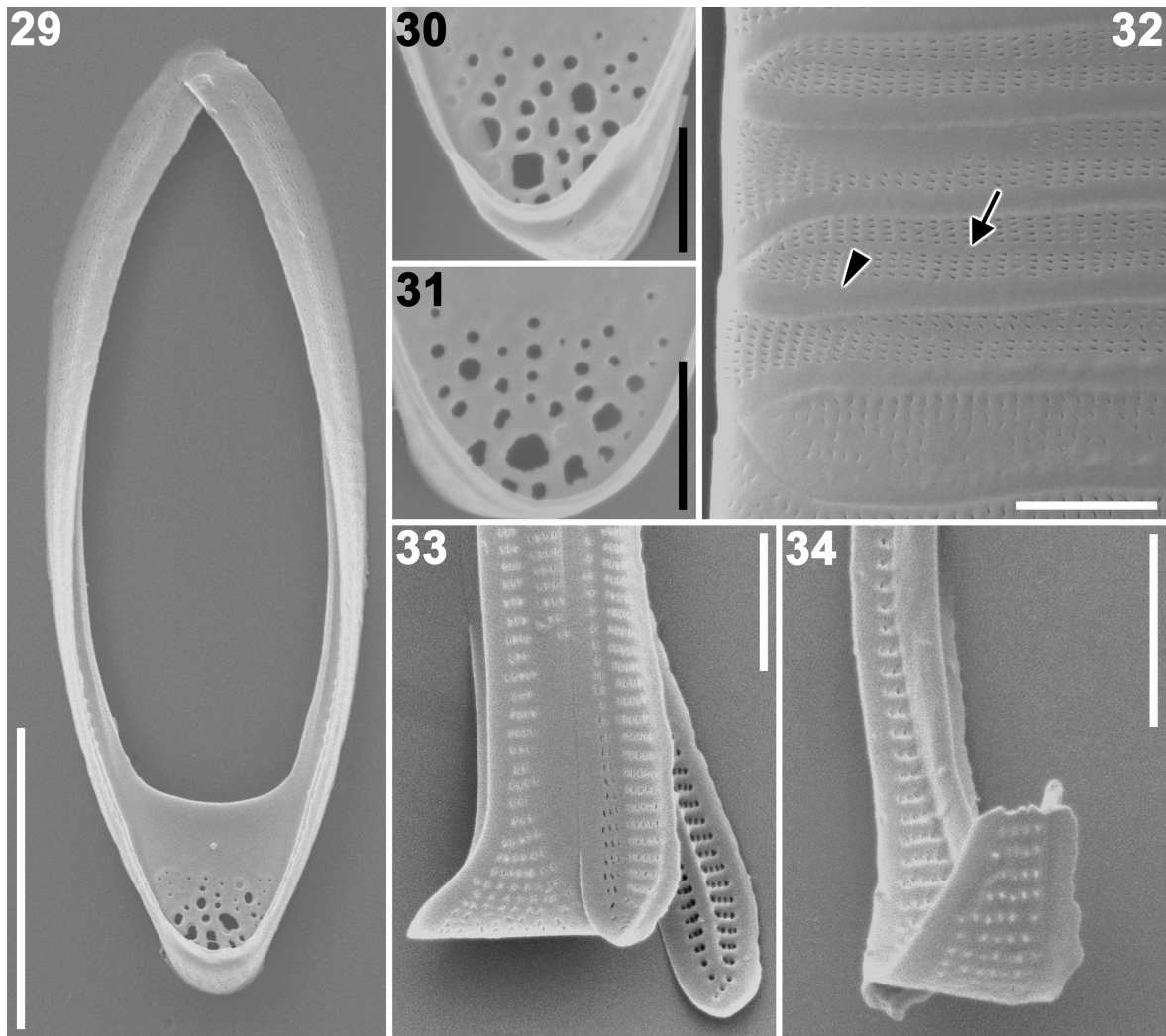
Figs 8–13. *Pseudostriatella oceanica*; intact cells, SEM. Scale bars = 10 μm (Figs 8, 10). 100 μm (Fig. 9) or 2 μm (Figs 11–13). **Fig. 8.** Frustule with mucilage stalk secreted at upper right corner. **Fig. 9.** Colonies on *Cladophora* sp. Note the cells raised above bacterial community on algal surface by long mucilage stalks. **Fig. 10.** Side view of frustules just after cell division. **Fig. 11.** Mucilage stalk secreted from apical pore field. **Fig. 12.** Free end of valve showing apical pore field secreting no mucilage. **Fig. 13.** Mucilage stalk attachment to substratum. Note stalk is composed of fine mucilaginous strings.



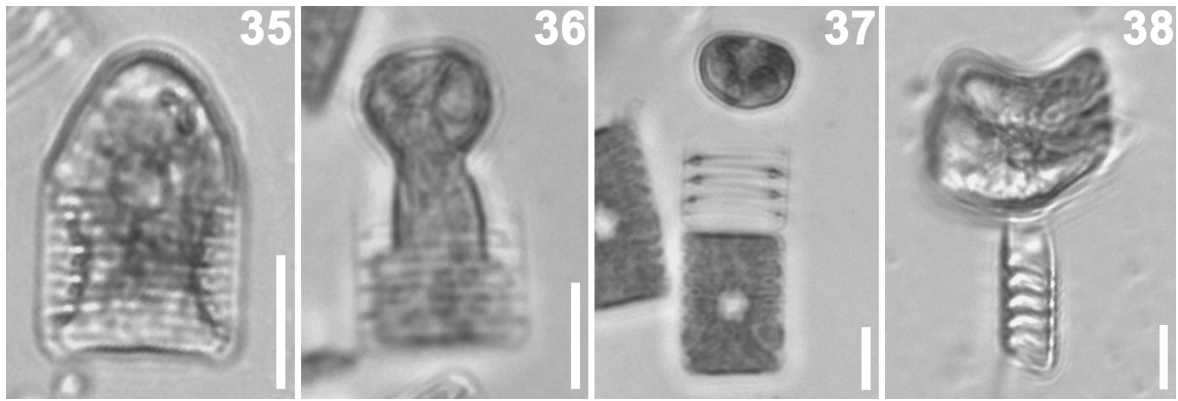
Figs 14–18. *Pseudostriatella oceanica* valves: external views (SEM). Scale bars = 5 μm (Fig. 14), 0.5 μm (Figs 15, 16, 18) or 0.2 μm (Fig. 17). **Fig. 14.** Whole showing central hyaline area (arrow) and irregular striation. **Fig. 15.** Enlarged view of part marked by asterisk in Fig. 14 showing small simple pores within the end of the hyaline area. **Fig. 16.** Detail of apical pore field surrounded by plain rim. **Fig. 17.** Areolae occluded by pegs that vary in shape and number. **Fig. 18.** Broken valve showing simple non-chambered valve structure.



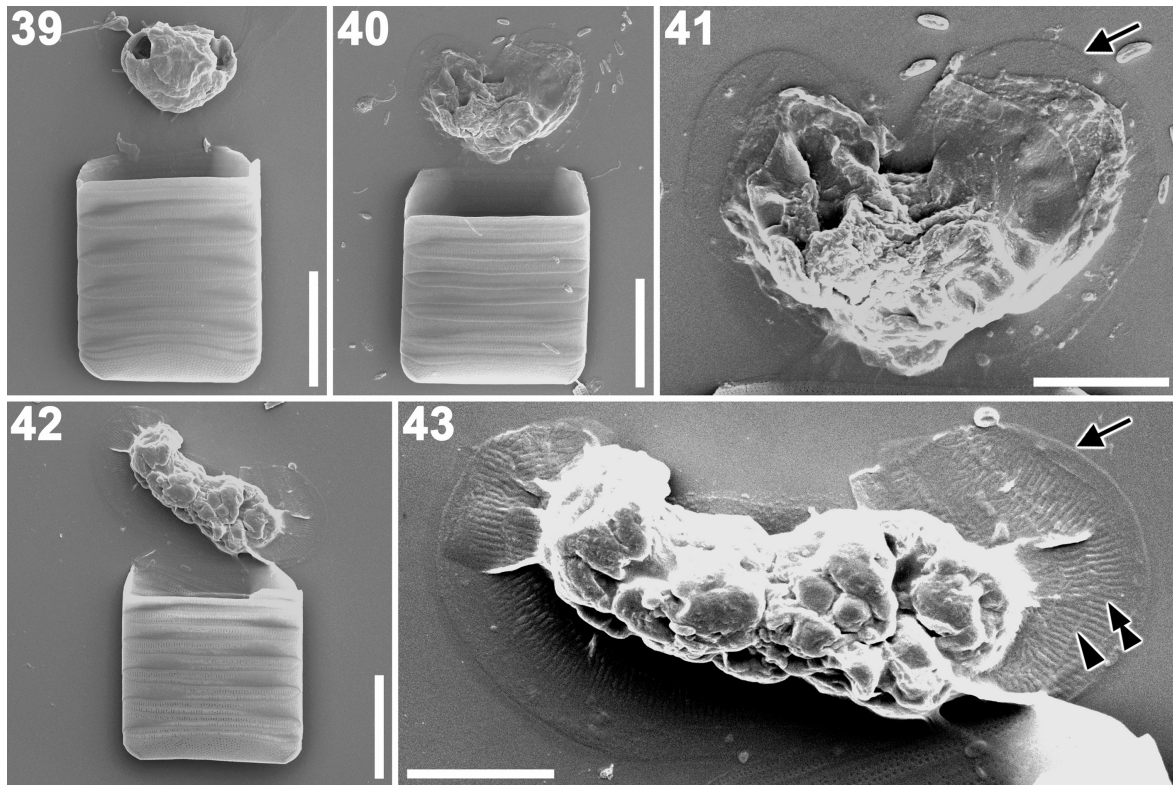
Figs 19–28. *Pseudostriatella oceanica* valves: internal views (SEM). Scale bars = 5 μm (Fig. 19), 0.5 μm (Figs 20, 21), 0.2 μm (Figs 22, 25–28) or 0.3 μm (Figs 23, 24). **Fig. 19.** Whole interior. The arrow indicates the hyaline area. Note the many irregularly scattered rimoportulae. **Fig. 20.** Enlarged view of part marked by asterisk in Fig. 19 showing a few small, simple pores within the hyaline area. **Fig. 21.** Detail of apical pore field. **Fig. 22.** Areolae occluded by pegs, which are slightly recessed below the internal valve surface. **Figs 23, 24.** Broken valve showing irregularly distributed rimoportulae around the valve margin. **Figs 25, 26.** Circular and elliptical C-shaped rimoportulae. **Fig. 27.** Normal ‘labiate’ rimoportula. **Fig. 28.** Compound rimoportula.



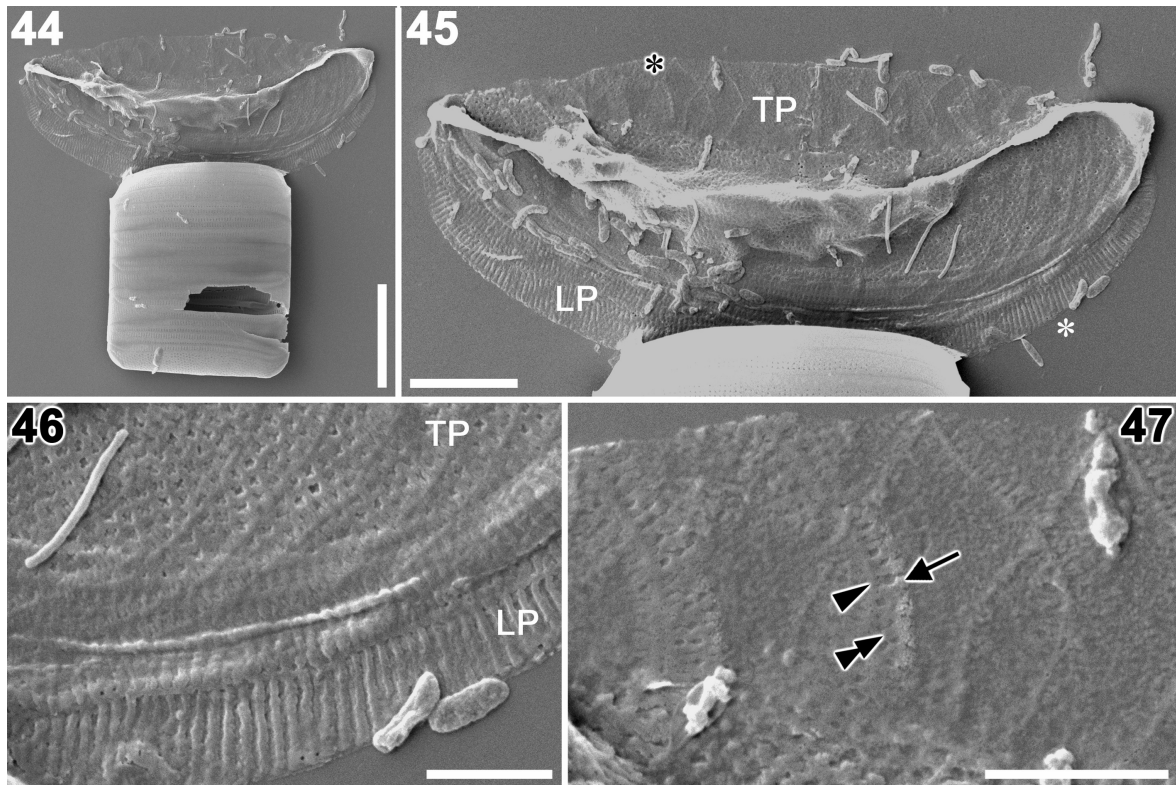
Figs 29–34. *Pseudostriatella oceanica* girdle (SEM). Scale bars = 5 μm (Fig. 29), 1 μm (Figs 30, 31) or 2 μm (Figs 32–34). **Fig. 29.** Single band with a perforated septum. **Figs 30, 31.** Variation of perforation pattern in septa. **Fig. 32.** Complete girdle showing interlocking bands. Note the regular striation, except for a hyaline area along the long axis (arrow) and advalvar edge (arrowhead). **Fig. 33.** Disrupted cingulum showing the outside and inside of an open end (right) and the outside of a closed end. The plain longitudinal strip is thickened and rib-like. Note that the interstriae region are also rib-like. **Fig. 34.** Broken copula showing the inside of a closed end. Note that the longitudinal rib becomes more prominent and widens into the septum.



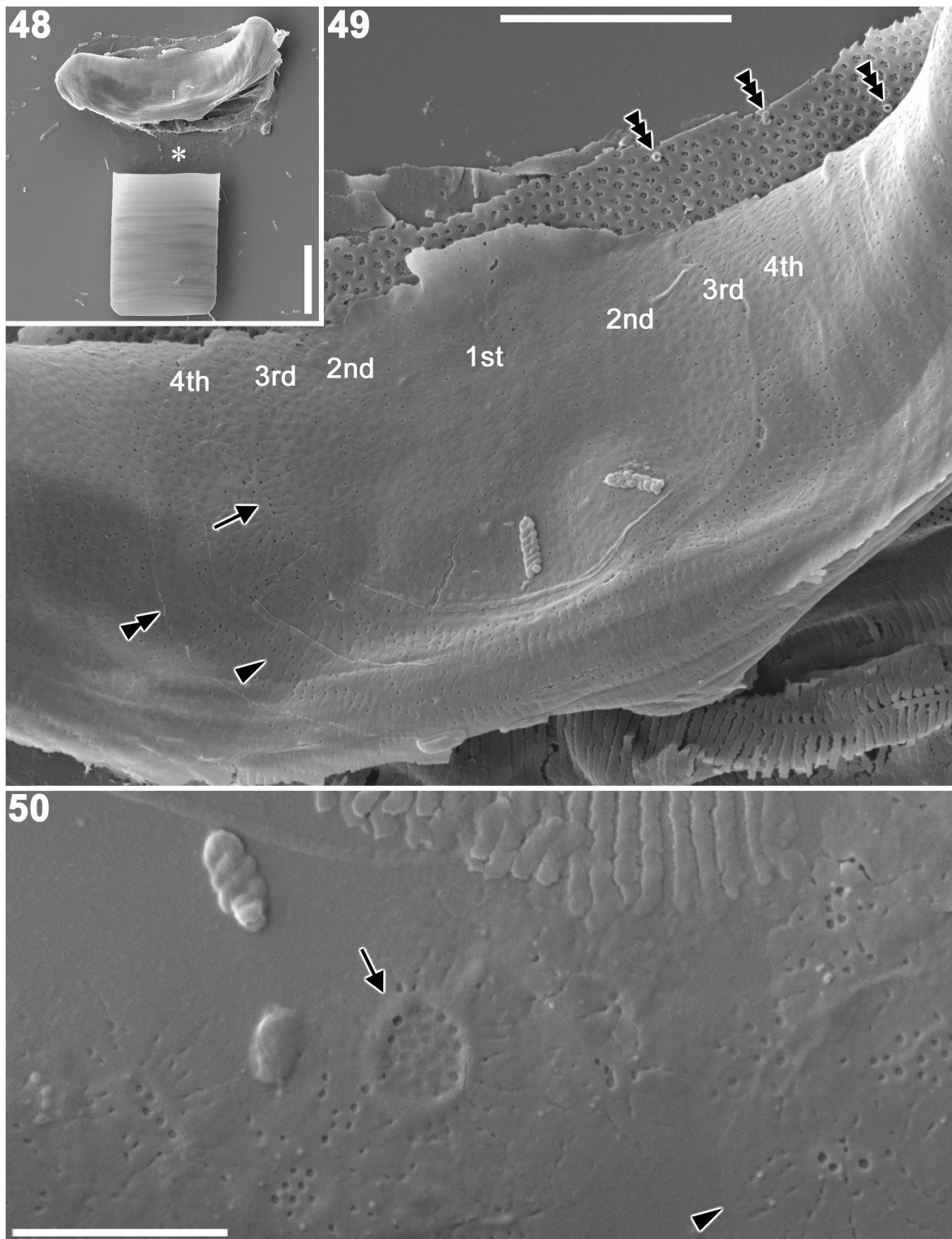
Figs 35–38. *Pseudostriatella oceanica*: clonal auxosporulation (LM). Scale bars = 10 μm . **Figs 35, 36.** Young auxospores being liberated from their mother-cells. **Fig. 37.** Contracted \pm spherical auxospore. **Fig. 38.** Mature auxospore containing initial cell, lying slightly oblique to the object plane.



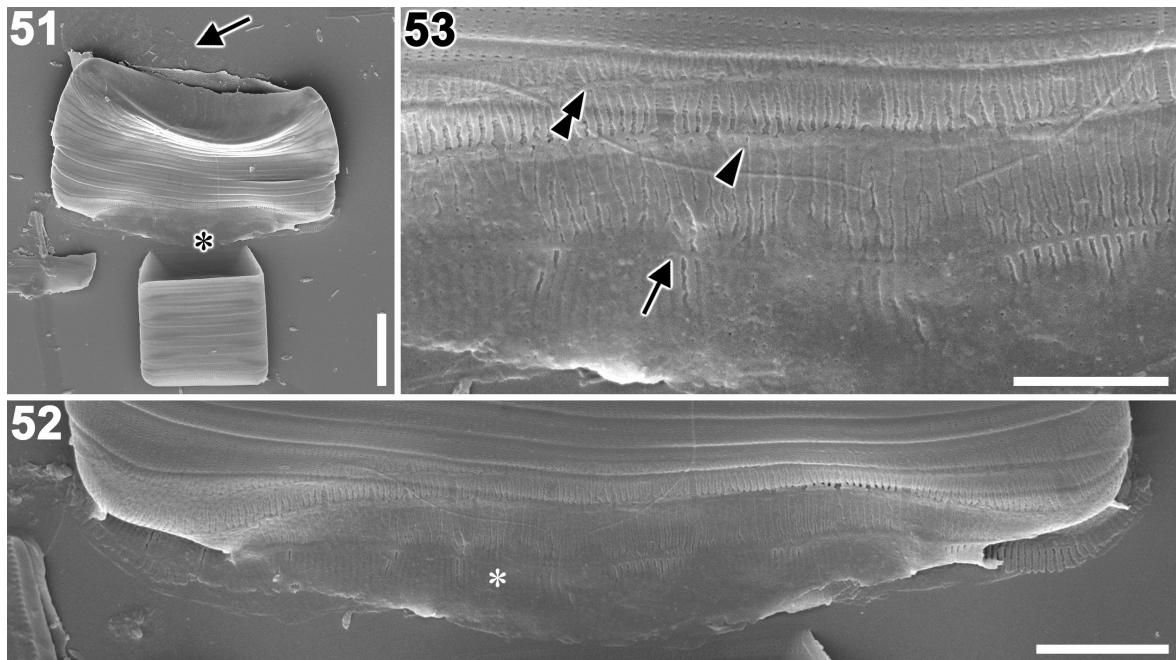
Figs 39–43. *Pseudostriatella oceanica*: early stages of auxosporulation (SEM). Scale bars = 10 μm (Figs 39, 40, 42) or 5 μm (Figs 41, 43). **Fig. 39.** Spherical auxospore. No covering is visible. **Fig. 40.** Slightly expanded auxospore. **Fig. 41.** Enlarged view of auxospore of Fig. 40. Arrow indicates mucilaginous layer covering auxospore. **Fig. 42.** Expanding auxospore. **Fig. 43.** Enlarged view of auxospore of Fig. 42. Arrow indicates mucilaginous layer. Arrowhead and double arrowhead indicate longitudinal and transverse ribs of a LP band, which has probably been bent during specimen preparation (cf. Fig. 59). Note that a transverse perizonium is absent.



Figs 44–47. *Pseudostriatella oceanica*: fully expanded auxospore containing an immature initial epivalve (SEM). Scale bars = 10 μm (Fig. 44), 5 μm (Fig. 45) or 2 μm (Figs 46, 47). **Fig. 44.** Whole auxospore still associated with auxospore mother-cell. **Fig. 45.** Enlarged view of auxospore: the initial valve is detectable via its larger, coarser areolae, visible along the midline of the collapsed cell. The auxospore is covered by transverse perizonial bands (TP) dorsally and longitudinal perizonial bands (LP) ventrally. **Fig. 46.** Enlargement (at black asterisk in Fig. 45), showing the structural differences between the transverse (TP) and longitudinal perizonial bands (LP). **Fig. 47.** Enlargement (at white asterisk in Fig. 45), showing the delicate TP bands. No regular striae exist. The arrowhead and double arrowhead indicate the longitudinal and transverse ribs of a TP band, respectively; the arrow indicates a fringe.



Figs 48–50. *Pseudostriatella oceanica*: final stage of auxosporulation (SEM). Scale bars = 10 μm (Fig. 48) and 5 μm (Fig. 49) and 2 μm (Fig. 50). **Fig. 48.** Auxospore containing a mature initial epivalve. **Fig. 49.** Enlarged view of middle of auxospore of Fig. 48, showing that the initial valve is covered by TP and LP (bottom right) bands. TP bands are numbered from primary (1st) to fourth (4th). Note fuzzy border of 1st and 2nd bands. Bands 1 and 2 do not have rib thickenings, whereas bands 3 and 4 bands do (arrow and double arrowhead, respectively). The edge of band 4 overlap onto band 5 (double arrowhead). Triple arrowheads indicate rimoportulae at internal initial valve. **Fig. 50.** Enlargement of area marked by asterisk in Fig. 48, showing scales on the ventral side of the auxospore. Two types are present, with (arrow) and without (arrowhead) an annulus.



Figs 51–53. *Pseudostriatella oceanica*: initial cell still within auxospore envelope (SEM). Scale bars = 10 μm (Fig. 51), 5 μm (Fig. 52) or 3 μm (Fig. 53). **Fig. 51.** Whole initial cell, with auxospore mother-cell still attached. The series of TP bands (arrow) appears to be detaching from the initial cell. **Fig. 52.** Enlarged view of area marked by black asterisk in Fig. 51, showing the series of LP bands. **Fig. 53.** Enlarged view of area marked by white asterisk in Fig. 52. The LP appears to consist of three bands – primary (arrow), secondary (arrowhead) and tertiary (double arrowhead) – but collapse of the auxospore may have hidden two other bands (cf. Fig. 54).

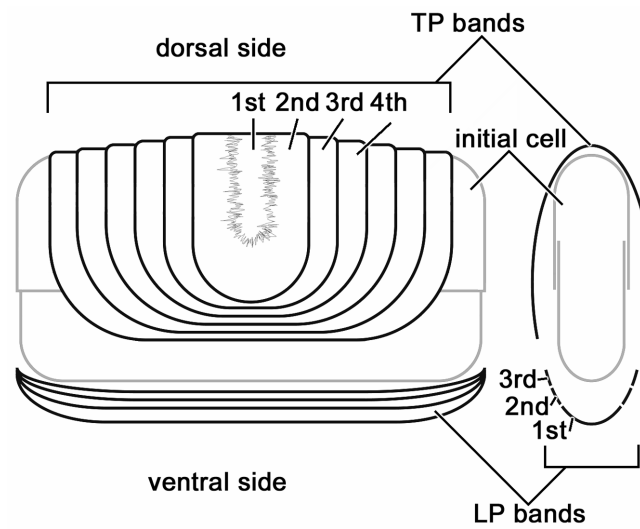


Fig. 54. *Pseudostriatella oceanica*: plan diagram and section (right) of 'perizonium' and initial cell.

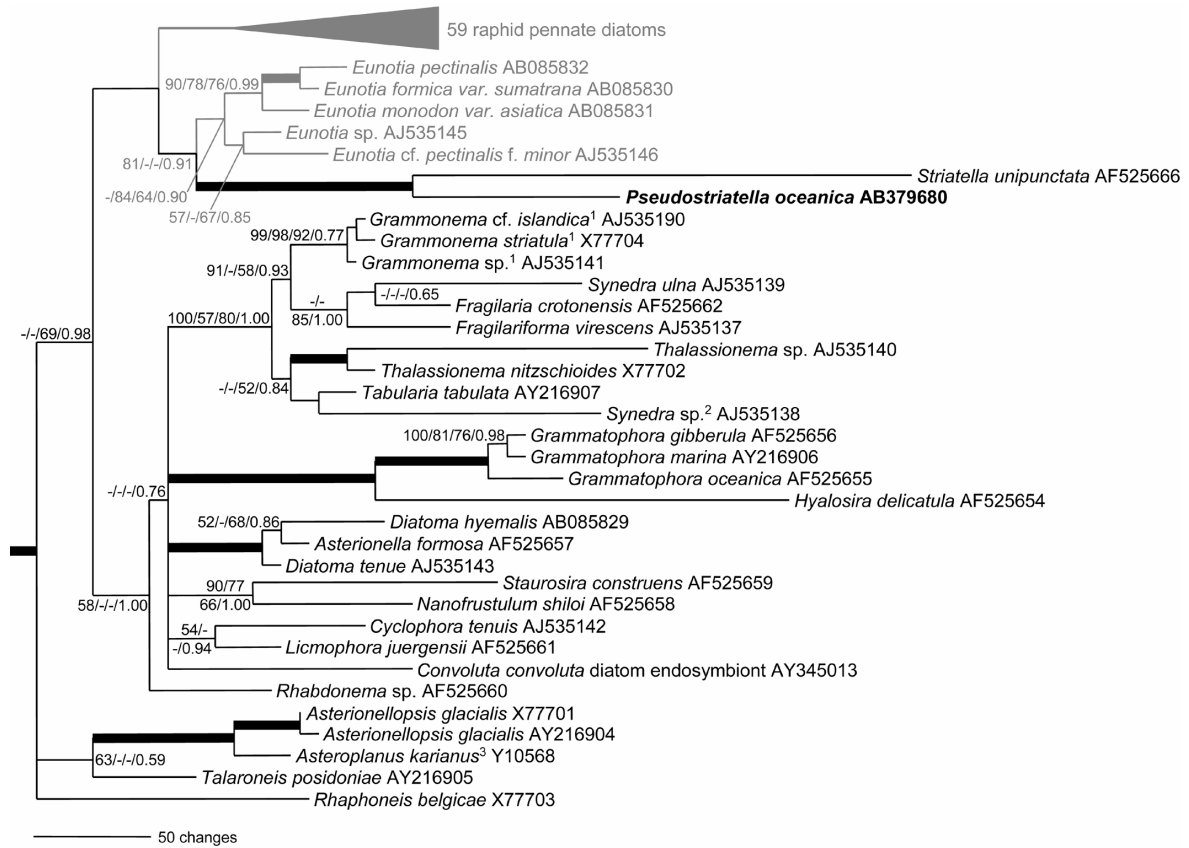
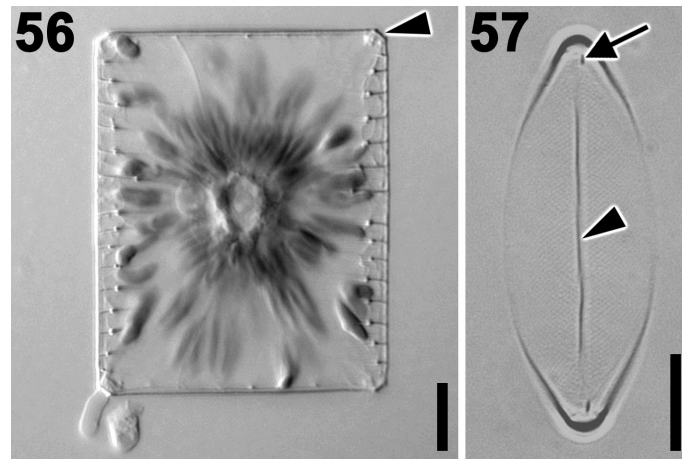


Fig. 55. Molecular phylogeny of araphid pennate diatoms inferred from 18S rDNA sequence using 1713 aligned positions. The tree shown resulted from Bayesian inference using a GTR + I + G model. Outgroup bolidomonads and centric diatoms were excluded and a clade comprises raphid diatoms is collapsed into triangle for clarity. Nodal support values greater than 50 (NJ, MP and ML) and 0.50 (BI) are shown. Nodes with strong supports (Bootstrap support > 90 in NJ, MP and ML, and posterior probability > 0.95 in BI) are shown as thick lines. ¹Name change since deposit; ²likely a new genus collected from a marine habitat (Medlin et al. 2008); ³annotated as *Asterionellopsis kariana* in Genebank.



Figs 56, 57. *Striatella unipunctata* (LM). Scale bars = 10 μm . **Fig. 56.** Living cell showing distinctive plastids. Arrowhead indicates truncated corner of cell. **Fig. 57.** Cleaned valve taken with PC optics. Arrow indicates rimoportula, arrowhead indicates sternum.

2.8. Publication VII:

Fine structure and 18S rDNA phylogeny of a marine araphid pennate diatom *Plagiostriata goreensis* gen. et sp. nov. (Bacillariophyta)

SHINYA SATO^{1*}, SATOKO MATSUMOTO² & LINDA K MEDLIN¹

¹*Alfred Wegener Institute for Polar and Marine Research, Am Handelshafen 12, D-27570 Bremerhaven, Germany*

²*Choshi Fisheries High School, 1-1-12 Nagatsuka Cho, Choshi City, Chiba, Japan*

2008. *Phycological Research* (in press)

Abstract

A marine araphid pennate diatom *Plagiosiriata goreensis* is described from the sand grains of Goree Island, Dakar, The Republic of Senegal, based on observations of fine structures of the frustule. The most striking feature of the species is its striation, which is angled *c.* 60° across the robust sternum. The other defining features of the species are its highly reduced rimoportula and apical pores located at the both ends of the valve margin. In the 18S rDNA phylogeny, the species appears as a member of a 'small-celled clade' of araphid pennate diatoms that consist of *Nanofrustulum*, *Opephora* and *Staurosira*. The results of the phylogenetic analyses suggest that the distinct characters of the diatom, i.e., oblique striae and apical pores, may have been acquired independently. However, it remains unclear whether the rimoportula of *P. goreensis* is a reduced state or *P. goreensis* acquired its morphologically curious rimoportula independently after the loss of an ancient rimoportula at the root of the small-celled clade.

KEY WORDS: 18S rDNA phylogeny, araphid pennate diatom, evolution, morphology, *Plagiosiriata goreensis*

INTRODUCTION

Benthic diatoms are ubiquitous in shallow coastal environments and are one of the most taxonomically diverse groups of organisms in estuarine ecosystems (Sullivan & Currin, 2000). Because of their high primary productivity rates, benthic diatoms play an important role in the functioning of benthic trophic webs in intertidal mudflats and shallow water ecosystems of temperate to tropical regions (Cahoon 1999; Underwood & Kromkamp 1999). In these coastal assemblages, araphid pennate diatoms, which lack a raphe slit on their valves, appear largely as epiphytic/epizoic/epipsammic taxa (Round *et al.* 1990). Taxonomically, araphid pennate diatoms have long been neglected, perhaps because of their morphological simplicity. As stated by Round *et al.* (1990); 'in many ways, the classification of the araphid group is the most difficult, because unlike the centric series, their valve structure is rather simple, and unlike the raphid series, the plastids and their arrangements have few distinguishing features'. Thus, in spite of their high abundance, taxonomic relationships of marine araphid pennate diatoms are not yet fully established.

To understand and describe a more complete picture of the natural history of araphid pennate diatoms, particularly marine species, we have been collecting samples from global coastal regions. Recently, we encountered a hitherto undescribed diatom from the coastal region of The Republic of Senegal. In this study, we describe the genus *Plagiosiriata*, with its type species, *P. goreensis*, based on the fine structural features of the frustule. 18S rDNA phylogenetic analysis was also undertaken to reveal the phylogenetic position of this diatom.

MATERIAL AND METHODS

Collections and cultures

Vegetative cells of the *Plagiosiriata goreensis* examined here were collected by S. Matsumoto at the inside of the main port of Goree Island, Dakar, The Republic of Senegal on Sep. 8, 2006 from bottom sands. Because the sample contained only few cells of the species, cultured

material was used for the microscopic examination in this study. Single cells were collected from the sample to obtain clonal cultures. Cultures were left at room temperature, *c.* 20°C with IMR medium (Eppley et al. 1967) plus soil extract. A clonal culture of *Opephora guenter-grassii* (Witkowski et Lange-Bertalot) Sabbe et Vyverman, which was collected by SS at the Doppelschleuse, Weser River, Bremerhaven, Germany on 14th May 2004, was also used for the phylogenetic analysis because the species had morphological similarities to *P. goreensis*.

Microscopy

LM (Axioplan, Zeiss, Oberkochen, Germany) with bright field (BF), differential interference contrast (DIC) or phase contrast (PC) optics were used to observe living cells and cleaned frustules. To remove organic material from the frustule, samples were treated as Sato et al. (2008). SEM specimens were coated with gold using SC 500 (Emscope, Ashford, England). QUANTA 200F SEM (FEI Company, Eindhoven, Netherlands) was used for SEM observation at an accelerating voltage of 3 to 10 kV, 45° tilt (if applicable) and *c.* 10 mm working distance. Captured images were adjusted with Adobe Photoshop.

Terminology

Morphological terms were taken from Anonymous (1975), Cox & Ross (1981) and Round *et al.* (1990). In this paper we use the terms *centric* and *pennate*, which is subdivided into *araphid* and *raphid* by the absence/presence of raphe slit because they refer to key morphological features or their absence, although the classical system does not reflect diatom phylogeny as has been pointed out by morphological (e.g. Simonsen 1972, 1979) and molecular phylogenetic (e.g. Medlin & Kaczmarska 2004) points of view (for review see Sims et al. 2006, p. 366). In this paper, the term *araphid pennate diatom* follows a traditional definition, i.e., a diatom that has an elongate valve with a central or slightly lateral sternum, apical pore fields and often apical rimoportulae, but the valves lack a raphe slit. We do not imply that this corresponds to a mono- (holo-) phyletic group, nor that it should be accorded any taxonomic status.

DNA methods and phylogenetic analysis

Samples of *c.* 500 mL of medium containing growing cells were filtered through 3 µm pore diameter membrane filters (Millipore SA, Molsheim, France). Filters were immersed in 500 µL DNA extraction buffer containing 2% (w/v) CTAB, 1.4 M NaCl, 20 mM EDTA, 100 mM Tris-HCl, pH 8, 0.2% (w/v) PVP, 0.01% (w/v) SDS, and 0.2% β-mercaptoethanol. Immersed filters were incubated at 65°C for 5 min, vortexed for a few seconds, and then discarded. Subsequently, the buffer was cooled briefly on ice. DNA was extracted with an equal volume of chloroform–isoamyl alcohol (24:1 [v/v]) and centrifuged in a table-top Eppendorf microfuge (Eppendorf AG, Hamburg, Germany) at maximum speed (14,000 rpm) for 10 min. The aqueous phase was collected and back extracted with chloroform–isoamyl alcohol and centrifuged as above. Next, the aqueous phase was mixed thoroughly with 0.8 volumes ice cold 100% isopropanol, then left on ice for 5 min, and subsequently centrifuged in a precooled Eppendorf microfuge at maximum speed for 15 min. DNA pellets were washed in 500 µL 70% (v/v) ethanol, centrifuged 6 min, and, after decanting the ethanol, allowed to air dry. DNA pellets

were dissolved overnight in 100 μ L water. Quantity and quality of DNA were examined by agarose gel electrophoresis against known standards.

The targeted marker sequence comprises the SSU rDNA within the nuclear rDNA cistron. The marker was PCR amplified in 25 μ L volumes containing 10 ng DNA, 1 mM dNTPs, 0.5 μ M of forward primer, 0.5 μ M of reverse primer, 1 x Roche diagnostics PCR reaction buffer (Roche Diagnostics, GmbH, Mannheim, Germany), and 1 unit *Taq* DNA Polymerase (Roche). The PCR cycling comprised an initial 4-min heating step at 94°C, followed by 35 cycles of 94°C for 2 min, 56°C for 4 min, and 72°C for 2 min, and a final extension at 72°C for 10 min. PCR products were generated using the forward primer A and a reverse primer B (Medlin et al. 1988). Quantity and length of products were examined by agarose gel electrophoresis against known standards. Excess primers and dNTPs were removed from PCR products by the QIAQuick PCR Product Purification Kit (QIAGEN, Germany) following manufacturer's instructions. Sequencing reactions took place in a PCR cycler using Big Dye Terminator v3.1 sequencing chemistry (Applied Biosystems, CA, USA) with sequencing primers described in Elwood et al. (1985). The sequencing products were then electrophoresed on an ABI 3100 Avant sequencer (Applied Biosystems, CA, USA)

The obtained 18S rDNA sequence of *Plagiostriata goreensis* and *Opephora guentergrassii* were aligned with 188 sequences retrieved from GenBank (Table 1) first using ClustalX (Thompson et al. 1997), and then refined by referring to the secondary structure model of the 18S rRNA at the database of the structure of rRNA (Van de Peer et al. 1998). Finally, ambiguously aligned positions were excluded using BioEdit 7.0.2 (Hall 1999), resulting in 1704 nucleotides in the dataset. The dataset consisted of 190 operational taxonomic units (OTUs) including the closest relatives of the diatom *Bolidomonas mediterranea* Guillou & Chrétiennot-Dinet and *B. pacifica* Guillou & Chrétiennot-Dinet (Guillou et al. 1999) as outgroups. The alignment examined in this study is available upon request to SS. To determine which model of sequence evolution best fits the data, hierarchical likelihood ratio tests (hLRTs) and Akaike Information Criterion (AIC) were performed using Modeltest 3.7 (Posada & Crandall 1998), and both tests selected the GTR + I + G model. This model had following parameters: base frequencies = A: 0.2705, C: 0.1655, G: 0.2549 and T: 0.3091; substitution rates were: A-C = 1.1756, A-G = 3.0078, A-T = 1.2623, C-G = 1.4965, C-T = 5.4711 and G-T = 1.0000; the proportion of invariant sites was 0.2767, among-site rate heterogeneity was described by a gamma distribution with a shape parameter of 0.6066. Phylogenies were reconstructed with PAUP* version 4.0b10 (Swofford 2002) using neighbour joining (NJ) of likewise constrained pair-wise ML distances. Nodal support was estimated using NJ bootstrap analyses using the same settings (1000 replicates).

Maximum likelihood (ML) analyses was performed by RAxML-VI-HPC, v2.2.3 (Stamatakis et al. 2005) with GTRMIX model, which approximates the tree under the GTR model (GTRCAT) and evaluates the final tree under the GTR+G model (GTRGAMMA). The analyses were performed 100 times to find the best topology receiving the best likelihood using distinct random starting MP tree (one round of taxon addition) and the rapid hill-climbing algorithm (i.e., option -f d in RAxML). Bootstrap values were obtained by 100 replications.

The MPI version MrBayes 3.1.2 (Huelsenbeck & Ronquist 2001, Ronquist & Huelsenbeck 2003; Altekar 2004) was used for Bayesian inference (BI) to estimate the posterior probability distribution using Metropolis-Coupled Markov Chain Monte Carlo (MCMCMC) (Ronquist & Huelsenbeck 2003). We used the default priors from MrBayes with the GTR + I + G model. Each run used four chains, one cold and three heated, with temperature set to 0.2. We performed two independent run, 20,000,000 generations in each run with trees sampled every 100th generation. To increase the probability of chain convergence, we sampled trees after the standard deviation values of the two runs dropped below 0.01 to calculate the posterior probabilities (i.e., after 7,000,000 generations). The remaining phylogenies were dis-

carded as burn-in. A 50 % majority-rule consensus tree was calculated with 130,000 post-burn-in trees.

RESULTS

Plagiostriata gen. nov. S. Sato et Medlin

Cellulae solitariae, chloroplastis uno vel duobus in quoque cellula, in aspectu cingulari rectangularibus faciebus plus minusve convexis. Valvae lanceolatae. Superficies valvae in limbo leniter devexa et projecturae ullae carentibus. Striae trans costam sub angulo 60° positae, non manifeste in LM. Rimoportula reducta solitaria circa centrum costi. Pori apicales dilatati, 1-2 in quoque extremo valvarae.

Cells solitary. 1-2 plastids per cell. Frustule rectangular in girdle view with slightly convex valve faces. Valves lanceolate. Sternum distinct. Valve face gently slopes into mantle and lacks any projection. Striae angled *c.* 60° across the sternum and are unresolvable with LM. Single reduced rimoportula per valve located approximately midway along the sternum. Apical pores, consisting of one to two dilated pores at the both ends of the valve.

Type species: *P. goreensis* sp. nov. S. Sato et Medlin

Plagiostriata goreensis sp. nov. S. Sato et Medlin

Morphological features are those of the genus description. Valve length 5.9-7.0, width 2.5-2.9. Striae 5-6 per 1 µm

HOLOTYPE SLIDE: Zu6/60 (Alfred Wegener Institute, Bremerhaven, Germany). Cleaned material, from which the holotype slide was prepared, is available under the accession number R938 at the same institution.

ISOTYPE SLIDE: TNS-AL-53999 (National Museum of Nature and Science, Tsukuba, Japan).

TYPE LOCALITY: Inside of the main port of Goree Island, Dakar, The Republic of Senegal (14°40'N, 17°25'W).

ETYMOLOGY: The genus name was given for the oblique striation on the valve. The species name after the type locality.

Morphology

LM

Solitary cells of *Plagiostriata goreensis* grew attached to the bottom of the culture vessel; no obvious mucilaginous pad/stalk was seen either in the culture or the field material. Frustules are rectangular in girdle view with a slight convexity of both valve faces (Figs 1-3). 1-2 plate

like plastids per cell (Figs 1-3). In valve view, the lanceolate valve has a robust sternum, but striae are unresolvable with LM even with BF, DIC or PC optics (Figs 4, 5 and 6, respectively). Valves ranged from 5.9-7.0 μm in length and 2.5-2.9 μm in width. A rimoportula was recognizable, especially with PC optics (Fig. 6), as a prominent hyaline area along one side of the sternum. A slight degree of deviation in the position of the rimoportula was detected, but mostly it was located at the valve centre (Figs 4-6).

SEM

The valve face is smoothly rounded (Figs 7-8), giving a gradual change between mantle and valve. Valve edge is plain and narrow (Fig. 8). Striae are 5-6 per 1 μm . Striae are parallel but angled in their orientation at *c.* 60° across the robust sternum (Figs 7-8, 11-17). Viminis, the crossbars between the interstriae, also arranged in parallel between striae at *c.* 60° against the striae (Figs 11, 14). The external slit-like opening of a rimoportula, which was elongated in parallel with striae, was observed along the sternum around the centre of the valve (Fig. 7, arrow). Valves lacking this opening (thus, rimoportula) were rarely (less than 10 %) observed (Fig. 8). The sternum narrowed in thickness towards the valve apex (Fig. 8). The end of valve has no apical pore field, which is the field comprising small pores in a hexagonal array as seen in the most of araphid pennate diatoms; instead 1-2 dilated pore(s) are located within a slightly widened valve edge (Figs 9-10).

The rimoportula situated along the sternum can easily be recognized internally (Figs 12-13). The rimoportula is conspicuous because the area around the slit-like opening is heavily silicified (Figs 14-15). This thickness can be sometimes easily observed in a collapsed valve, in which the thickened area of rimoportula remains intact even when the neighboring structure is disrupted (Figs 11, 17). Internally, both longer sides of the rim of the opening have grooves along the slit (Figs 14-15). The narrowed part of the sternum at the valve apex is also recognizable internally (Fig. 16). Both valve apices were elevated in a pervalvar direction (Figs 13, 16).

The striae on both valves are arranged antithetically between epi- and hypovalve (Fig. 17). The frustule shown in Fig. 17 had only a single rimoportula per cell, but such heterovalvy is not a predominant feature (less than 10 %); this was also supported by the fact that rimoportula-lacking valves were rare in the cleaned material (above). Epi- and hypocingulum comprise *c.* 5 bands. All bands are plain and open (Figs 17-19), alternating with each another (Figs 18-19). No distinct ligula was detected on the bands.

Phylogeny

Within the pennates clade, an araphid pennate clade of *Striatella unipunctata* (Lyngby) Agardh and *Pseudostriatella oceanica* S. Sato, Mann et Medlin was sister to *Eunotia* Ehrenberg and was included within the raphid pennate diatoms. This curious phylogenetic position of *Striatella* and *Pseudostriatella* made both araphid and raphid pennate diatoms paraphyletic. Other species of *Striatella* should be targeted for sequencing to obtain better support for the position of these araphid diatoms. For clarity, we only show the topology of pennate diatoms in Fig. 20, excluding the outgroup taxa: bolidomonads and centric diatoms. The original trees containing all analyzed OTUs are available upon request to the first author.

Asterionellopsis Round/*Asteroplanus* (Grunow in Cleve et Grunow) Gardner et Crawford/*Rhaphoneis* Ehrenberg/*Talaroneis* Kooistra et De Stefano clade emerged basal in the araphid pennate clade, and then a clade containing all other sequenced araphid pennates di-

verged. After the divergence of *Rhabdonema* Kützing at the basal position, the internal relationship of this clade was not well resolved making polytomy. It should be noted that these major radiation of the araphid pennates recovered in BI were only supported low bootstrap values (<50 in NJ and ML). In all analyses, *Plagiotriata goreensis* fell into a clade, which comprised *Opephora guenter-grassii*, *Nanofrustulum shiloi* Round, Hallsteinsen et Paasche, *Staurosira construens* (Ehrenberg) Williams et Round and an uncultured stramenopile, although the bootstrap supports were low in NJ and ML. Within the clade containing *P. goreensis*, *S. construens* emerged at the base and then *P. goreensis* and the other members diverged in BI and ML trees. In the NJ analysis, however, *P. goreensis* diverged at the base of the clade and then the diversification subsequently took place (not shown).

DISCUSSION

We have termed the clade, in which *P. goreensis* is included, as a ‘small-celled clade’ because its members are characterized by relatively small cell sizes ($c. < 20 \mu\text{m}$), as well as having plain bands and being benthic (e.g. Williams & Round 1987, Witkowski & Lange-Bertalot 1993, Sabbe & Vyverman 1995, Round et al. 1999, Sar & Sunesen 2003, Medlin et al. 2008).

The oblique striation seen in *Plagiotriata goreensis* has not been reported in any diatom lineage. The other prominent morphological feature of *P. goreensis* is the apical pore at both valve apices. Although the function of these pores remains unclear, the most probable explanation is that the area acts as a site for mucilage secretion because a morphologically similar structure, the apical pore field, does so in most araphid pennate diatoms (e.g., Hasle 1974). Generally apical pore fields are located at each valve apex and secrete mucilaginous substances from there to attach to a substratum. The apical pores of *P. goreensis* are located at the valve margin. *Licmophora* spp. also have an apical slit area, the ‘multiscissura’ *sensu* Honeywill (1998), located at the basal pole of the valve, which acts as a mucilage secretion point (Honeywill 1998). The apical pore of *P. goreensis* resembles *Licmophora*’s multiscissura in position and shape, but the number of the pores differs in the two genera. Because of the low support for the branching of the araphid pennate diatoms, it is still uncertain that whether these pores of *Licmophora* and *Plagiotriata* are homologous. It should be noted that the valve heterogeneity observed in *Plagiotriata*, i.e. the presence or absence of rimoportula in a valve, has also been known in *Licmophora* (Honeywill 1998).

In general, the rimoportula of araphid pennate diatoms possess internal labiate-shaped processes, although the shape of the labiate part itself vary greatly among the araphid genera. The rimoportula observed in *P. goreensis* is unique in morphology and distribution and lacks the typical labiate morphology making it difficult to establish the homologous relationship with the others. The other members of the small-celled clade lack a rimoportula, i.e., *Nanofrustulum shiloi* (Round et al. 1999), *Opephora guenter-grassii* (Witkowski & Lange-Bertalot 1993) and *Staurosira construens* (Williams & Round 1987), and the review for this clade by Medlin et al. (2008). In our BI and ML analyses, *S. construens* diverged at the root of the small-celled clade suggesting that the rimoportula of *P. goreensis* has been acquired independently after the loss of the structure at the root of the clade, as the sister members of the unresolved clade all possess rimoportulae. Thus, if this is the case, the rimoportula of *P. goreensis* is not homologous with the rimoportula of the other araphid pennates or it has retained the ancestral character. However, the NJ tree places *P. goreensis* at the root of the small-celled clade, and our preliminary phylogenetic analysis using 4 gene markers (18S and partial 28S rDNA, *rbcL* and *psbA*) also support this placement (Sato unpublished). If the basal position of *P. goreensis* in the small-celled clade is the correct position for this taxon, the rimoportula has been lost somewhere after the divergence of *P. goreensis* at the small-

celled clade, and thus the rimoportula of *P. goreensis* is a reduced state. Further investigations are needed to elucidate this issue.

Because of its small cell size, *P. goreensis* might have been overlooked in other floristic surveys, or possibly misidentified as a raphid naviculoid diatom because the rimoportula and its surrounding thickened area appear as a light spot with LM, especially with PC optics, giving a false impression of a central nodule of raphe structure.

ACKNOWLEDGEMENTS

The authors are grateful to Richard M. Crawford for correction of the manuscript and for discussion; Paul A. Fryxell for translation of Latin diagnosis; Friedel Hinz for technical help for LM and SEM. We also thank two anonymous reviewers for their valuable comments and suggestions. This study was supported by a DAAD fellowship for doctoral research to Shinya Sato.

REFERENCES

- Altekar, G., Dwarkadas, S., Huelsenbeck, J. P. & Ronquist F. 2004. Parallel Metropolis-coupled Markov chain Monte Carlo for Bayesian phylogenetic inference. *Bioinformatics* **20**: 407–15.
- Anonymous 1975. Proposals for a standardization of diatom terminology and diagnoses. *Nova Hedwigia Beih.* **53**: 323–54.
- Cahoon, L. B. 1999. The role of benthic microalgae in neritic ecosystems. *Oceanogr. Mar. Biol., Annu. Rev.* **37**: 47–86
- Cox, E. J. & Ross, R. 1981. The striae of pinnate diatoms. In: Ross, R. (Ed.): *Proceedings of the 6th International Diatom Symposium on Recent and Fossil Diatoms*. O. Koeltz, Koenigstein, pp. 267–78.
- Elwood, H. J., Olsen, G. J. & Sogin, M. L. 1985. The small subunit ribosomal DNA gene sequences from the hypotrichous ciliates *Oxytricha nova* and *Stylonichia pustulata*. *Mol. Biol. Evol.* **2**: 399–410.
- Eppley, R. W., Holmes, R. W. & Strickland, J. D. H. 1967. Sinking rates of the marine phytoplankton measured with a fluorochromometer. *J. Exp. Mar. Biol. Ecol.* **1**: 191–208.
- Guillou, L., Chrétiennot-Dinet, M. -J., Medlin, L. K., Claustre, H., Loiseaux-de Goër, S. & Vaulot, D. 1999. *Bolidomonas*: a new genus with two species belonging to a new algal class, the Bolidophyceae class. nov. (Heterokonta). *J. Phycol.* **35**: 368–81.
- Hall, T. A. 1999. BioEdit: a user-friendly biological sequence alignment editor and analysis program for Windows 95/98/NT. *Nucl. Acids. Symp. Ser.* **41**: 95–8.
- Hasle, G. R. 1974. The mucilage pore of pennate diatoms. *Nova Hedwigia*, **45**: 167–86.
- Honeywill, C. 1998. A study of British *Licmophora* species and a discussion of its morphological features. *Diatom Res.* **13**: 221–71.
- Huelsenbeck, J. P. & Ronquist, F. 2001. MRBAYES: Bayesian inference of phylogeny. *Bioinformatics* **17**: 754–5.
- Medlin, L. K. & Kaczmarska, I. 2004. Evolution of the diatoms: V. Morphological and cytological support for the major clades and a taxonomic revision. *Phycologia* **43**: 245–70.
- Medlin, L., Elwood, H. J., Stickel, S. & Sogin, M. L. 1988. The characterization of enzymatically amplified eukaryotic 16S-like rRNA coding regions. *Gene* **71**: 491–9.

- Medlin, L. K., Jung, I., Bahulikar, R., Mendgen, K., Kroth, P. & Kooistra, W. H. C. F. 2008. Evolution of the Diatoms. VI. Assessment of the new genera in the araphids using molecular data. *Nova Hedwigia* **133**: 81-100.
- Posada, D. & Crandall, K. 1998. Modeltest: testing the model of dna substitution. *Bioinformatics* **14**: 817-8.
- Ronquist, F. & Huelsenbeck, J. P. 2003. MrBayes 3: Bayesian phylogenetic inference under mixed models. *Bioinformatics* **19**: 1572-4.
- Round, F. E., Crawford, R. M. & Mann, D. G. 1990. The diatoms. Biology and morphology of the genera. Cambridge University Press, Cambridge.
- Round, F. E., Hallsteinsen, H. & Paasche, E. 1999. On a previously controversial 'fragilarioid' diatom now placed in a new genus *Nanofrustulum*. *Diatom Res.* **14**: 343-56.
- Sabbe, K. & Vyverman, W. 1995. Taxonomy, morphology and ecology of some widespread representatives of the diatom genus *Opephora*. *Eur. J. Phycol.* **30**: 235-49.
- Sar, E. A. & Sunesen, I. 2003. *Nanofrustulum shiloi* (Bacillariophyceae) from the Gulf of San Matías (Argentina): Morphology, distribution and comments about nomenclature. *Nova Hedwigia* **77**: 399-406.
- Sato, S., Mann, D. G., Nagumo, T., Tanaka, J., Tadano, T. & Medlin, L. K. 2008. Auxospore fine structure and variation in modes of cell size changes in *Grammatophora marina* (Bacillariophyta). *Phycologia* **47**: 12-27.
- Simonsen, R. 1972. Ideas for a more natural system of the centric diatoms. *Nova Hedwigia Beih.* **39**: 37-54.
- Simonsen, R. 1979. The diatom system: ideas on phylogeny. *Bacillaria* **2**: 9-71.
- Sims, P. A., Mann, D. G. & Medlin, L. K. 2006. Evolution of the diatoms: insights from fossil, biological and molecular data. *Phycologia* **45**: 361-402.
- Stamatakis, A., Ludwig, T. & Meier, H. 2005. RAxML-III: A fast program for maximum likelihood-based inference of large phylogenetic trees. *Bioinformatics* **21**: 456-63.
- Sullivan, M. J. & Currin, C. A. 2000. Community structure and functional dynamics of benthic microalgae in salt marshes. In Weinstein, M.P. & Kreeger, D.A. (eds): *Concepts and Controversies in Tidal Marsh Ecology*. Kluwer Academic Publishers, Dordrecht, pp. 81-106.
- Swofford, D. L. 2002. *PAUP*. Phylogenetic Analysis Using Parsimony (* and other methods)*. Version 4.0b10. Sinauer Associates, Sunderland, MA.
- Thompson, J. D, Gibson, T. J., Plewniak, F., Jeanmougin, F. & Higgins, D. G. 1997. The CLUSTAL_X windows interface: flexible strategies for multiple sequence alignment aided by quality analysis tools. *Nucleic Acids Res.* **25**: 4876-82.
- Underwood, G. J. C. & Kromkamp, J. 1999. Primary production by phytoplankton and microphytobenthos in estuaries. *Adv. Ecol. Res.* **29**: 93-153
- Van de Peer, Y., Caers, A., De Rijk, P. & De Wachter, R. 1998. Database on the structure of small ribosomal subunit RNA. *Nucleic Acids Res.* **26**: 179-82
- Williams, D. M. & Round, F. E. 1987. Revision of the genus *Fragilaria*. *Diatom Res.* **2**: 267-88.
- Witkowski, A. & Lange-Bertalot, H. 1993. Established and new diatom taxa related to *Fragilaria schulzii* Brockmann. *Limnologica* **23**: 59-70.

Table 1. List of taxon and GenBank accessions for 18S rDNA sequences used in this study.

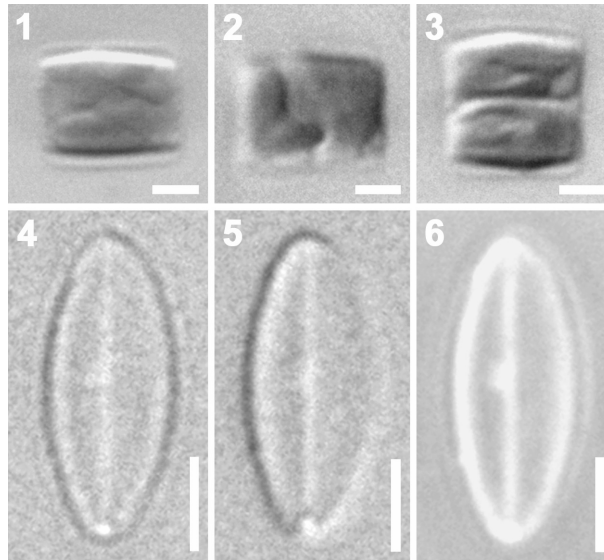
Taxon	Accession
<i>Aulacoseira ambigua</i> (Grunow) Simonsen	X85404
<i>Aulacoseira baicalensis</i> (Meyer) Simonsen	AJ535185
<i>Aulacoseira baicalensis</i> (Meyer) Simonsen	AJ535186
<i>Aulacoseira baicalensis</i> (Meyer) Simonsen	AY121821
<i>Aulacoseira distans</i> (Ehrenberg) Simonsen	X85403
<i>Aulacoseira islandica</i> (Müller) Simonsen	AJ535183
<i>Aulacoseira islandica</i> (Müller) Simonsen	AY121820
<i>Aulacoseira nyassensis</i> (Müller) Simonsen	AJ535187
<i>Aulacoseira nyassensis</i> (Müller) Simonsen	AY121819
<i>Aulacoseira skvortzowii</i> Edlund, Stoermer et Taylor	AJ535184
<i>Aulacoseira subarctica</i> (Müller) Haworth	AY121818
<i>Actinocyclus curvatulus</i> Janisch	X85401
<i>Actinoptychus seniarius</i> (Ehrenberg) Héribaud	AJ535182
<i>Bellerochea malleus</i> (Brightwell) Van Heurck	AF525671
<i>Biddulphiopsis titiana</i> (Grunow) von Stosch et Simonsen	AF525669
<i>Chaetoceros curvisetus</i> Cleve	AY229895
<i>Chaetoceros debilis</i> Cleve	AY229896
<i>Chaetoceros didymus</i> Ehrenberg	X85392
<i>Chaetoceros gracilis</i> Schütt	AY229897
<i>Chaetoceros rostratus</i> Lauder	X85391
<i>Chaetoceros</i> sp.	AF145226
<i>Chaetoceros</i> sp.	AJ535167
<i>Chaetoceros</i> sp.	X85390
<i>Corethron criophilum</i> Castracane	X85400
<i>Corethron inerme</i> Karsten	AJ535180
<i>Corethron hystrix</i> Hensen	AJ535179
<i>Coscinodiscus radiatus</i> Ehrenberg	X77705
<i>Cyclotella meneghiniana</i> Kützing	AJ535172
<i>Cyclotella meneghiniana</i> Kützing	AY496206
<i>Cyclotella meneghiniana</i> Kützing	AY496207
<i>Cyclotella meneghiniana</i> Kützing	AY496210
<i>Cyclotella meneghiniana</i> Kützing	AY496211
<i>Cyclotella meneghiniana</i> Kützing	AY496212
<i>Cyclotella</i> cf. <i>scaldensis</i>	AY496208
<i>Cymatosira belgica</i> Grunow	X85387
<i>Detonula confervacea</i> (Cleve) Gran	AF525672
<i>Ditylum brightwellii</i> (West) Grunow in Van Heurck	AY188181
<i>Ditylum brightwellii</i> (West) Grunow in Van Heurck	AY188182
<i>Ditylum brightwellii</i> (West) Grunow in Van Heurck	X85386
<i>Eucampia antarctica</i> (Castracane) Mangin	X85389
<i>Guinardia delicatula</i> (Cleve) Hasle	AJ535192
<i>Guinardia flaccida</i> (Castracane) H. Peragallo	AJ535191
<i>Helicotheca tamesis</i> (Schrubsole) Ricard	X85385
<i>Lampriscus kittonii</i> Schmidt	AF525667
<i>Lauderia borealis</i> Cleve	X85399
<i>Leptocylindrus danicus</i> Cleve	AJ535175
<i>Leptocylindrus minimus</i> Gran	AJ535176
<i>Lithodesmium undulatum</i> Ehrenberg	Y10569
<i>Melosira varians</i> Agardh	AJ243065

<i>Melosira varians</i> Agardh	X85402
<i>Odontella sinensis</i> (Greville) Grunow	Y10570
<i>Papiliocellulus elegans</i> Hasle, von Stosch et Syvertsen	X85388
<i>Paralia sol</i> (Ehrenberg) Crawford	AJ535174
<i>Planktoniella sol</i> (Wallich) Schütt	AJ535173
<i>Pleurosira laevis</i> (Ehrenberg) Compère	AF525670
<i>Pleurosira</i> cf. <i>laevis</i>	AJ535188
<i>Porosira pseudodenticulata</i> (Hustedt) Jousé	X85398
<i>Proboscia alata</i> (Brightwell) Sundström	AJ535181
<i>Rhizosolenia imbricate</i> Brightwell	AJ535178
<i>Rhizosolenia similoides</i> Cleve-Euler	AJ535177
<i>Rhizosolenia setigera</i> Brightwell	M87329
<i>Skeletonema costatum</i> (Greville) Cleve	X52006
<i>Skeletonema costatum</i> (Greville) Cleve	X85395
<i>Skeletonema menzelii</i> Guillard, Carpenter et Reimer	AJ535168
<i>Skeletonema menzelii</i> Guillard, Carpenter et Reimer	AJ536450
<i>Skeletonema pseudocostatum</i> Medlin	AF462060
<i>Skeletonema pseudocostatum</i> Medlin	X85393
<i>Skeletonema subsalsum</i> (Cleve-Euler) Bethge	AJ535166
<i>Skeletonema</i> sp.	AJ535165
<i>Stephanopyxis</i> cf. <i>broschii</i>	M87330
<i>Thalassiosira eccentrica</i> (Ehrenberg) Cleve	X85396
<i>Thalassiosira guillardii</i> Hasle	AF374478
<i>Thalassiosira oceanica</i> Hasle	AF374479
<i>Thalassiosira pseudonana</i> Hasle et Heimdal	AJ535169
<i>Thalassiosira pseudonana</i> Hasle et Heimdal	AF374481
<i>Thalassiosira rotula</i> Meunier	AF374480
<i>Thalassiosira rotula</i> Meunier	AF462058
<i>Thalassiosira rotula</i> Meunier	AF462059
<i>Thalassiosira rotula</i> Meunier	X85397
<i>Thalassiosira weissflogii</i> (Grunow) Fryxell et Hasle	AF374477
<i>Thalassiosira weissflogii</i> (Grunow) Fryxell et Hasle	AJ535170
<i>Thalassiosira</i> sp.	AJ535171
<i>Toxarium undulatum</i> Bailey	AF525668
<i>Asterionella formosa</i> Hassall	AF525657
<i>Asterionellopsis glacialis</i> (Castracane) Round	AY216904
<i>Asterionellopsis glacialis</i> (Castracane) Round	X77701
<i>Asteroplanus karianus</i> (Grunow in Cleve et Grunow) Gardner et Crawford ¹	Y10568
<i>Cyclophora tenuis</i> Castracane	AJ535142
<i>Diatoma hyemalis</i> (Roth) Heiberg	AB085829
<i>Diatoma tenue</i> Agardh	AJ535143
<i>Fragilaria crotonensis</i> Kitton	AF525662
<i>Fragilariforma virescens</i> (Ralfs) Williams et Round	AJ535137
<i>Grammatophora gibberula</i> Kützing	AF525656
<i>Grammatophora oceanica</i> Ehrenberg	AF525655
<i>Grammatophora marina</i> (Lyngbye) Kützing	AY216906
<i>Grammonema striatula</i> Agardh ¹	X77704
<i>Grammonema</i> cf. <i>islandica</i> ¹	AJ535190
<i>Grammonema</i> sp. ¹	AJ535141
<i>Hyalosira delicatula</i> Kützing	AF525654

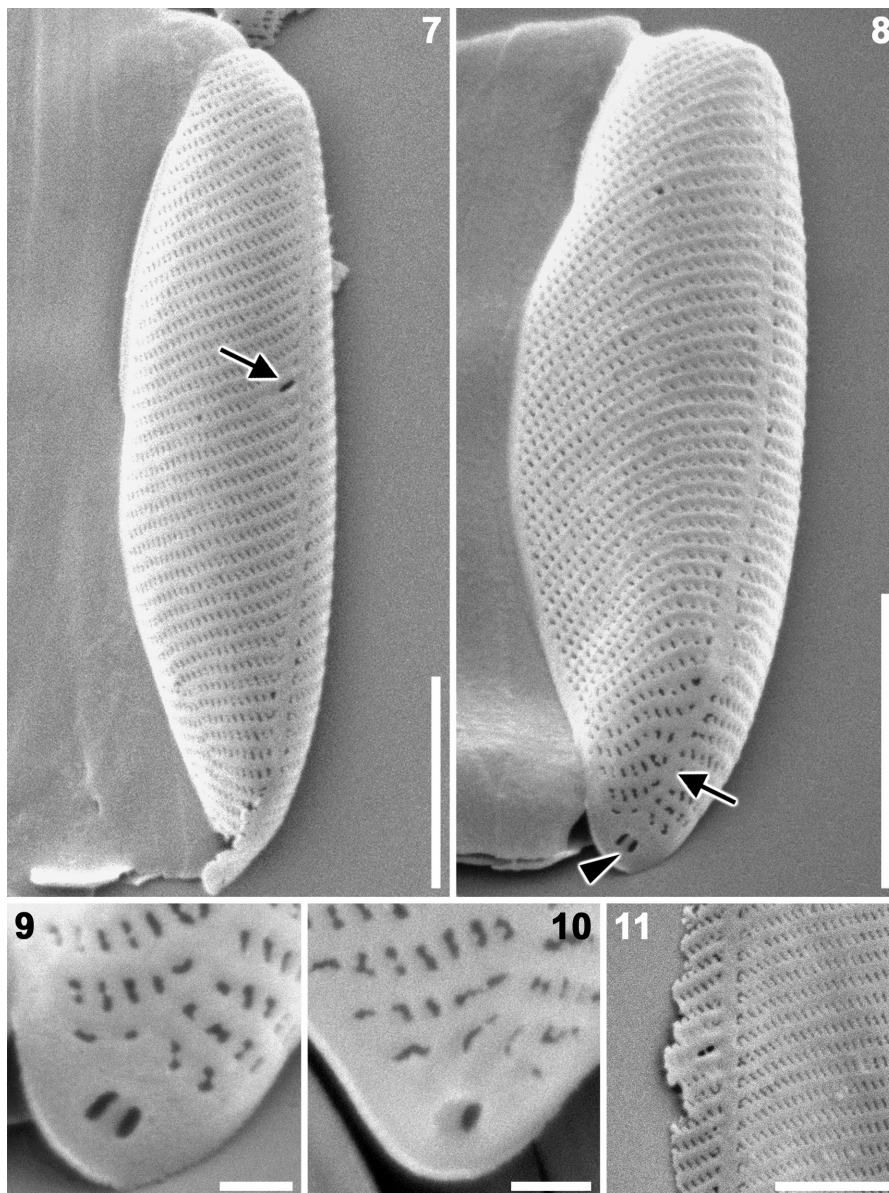
<i>Licmophora juergensii</i> Agardh	AF525661
<i>Nanofrustulum shiloi</i> (Lee, Reimer et McEney) Round, Hallsteinsen et Paasche	AF525658
<i>Nanofrustulum shiloi</i> (Lee, Reimer et McEney) Round, Hallsteinsen et Paasche	AY485505
<i>Nanofrustulum shiloi</i> (Lee, Reimer et McEney) Round, Hallsteinsen et Paasche	EF491891
<i>Opephora guenter-grassii</i> (Witkowski et Lange-Bertalot) Sabbe et Vyverman	AB436781
<i>Plagiostriata goreensis</i> S. Sato et Medlin	AB430605
<i>Pseudostriatella oceanica</i> S. Sato et Medlin	AB379680
<i>Rhabdonema arcuatum</i> (Agardh) Kützing	AF525660
<i>Rhaphoneis</i> cf. <i>belgica</i>	X77703
<i>Staurosira construens</i> Ehrenberg	AF525659
<i>Striatella unipunctata</i> (Lyngbye) Agardh	AF525666
<i>Synedra</i> sp. ²	AJ535138
<i>Tabularia tabulata</i> (Agardh) Williams et Round	AY216907
<i>Talaroneis posidoniae</i> Kooistra et De Stefano	AY216905
<i>Thalassionema nitzschioides</i> (Grunow) Hustedt	X77702
<i>Thalassionema</i> sp.	AJ535140
<i>Ulnaria ulna</i> (Nitzsch) Compère	AJ535139
<i>Achnanthes bongrainii</i> (M. Peragallo) A. Mann	AJ535150
<i>Achnanthes</i> sp.	AJ535151
<i>Amphora montana</i> Krasske	AJ243061
<i>Amphora</i> cf. <i>capitellata</i>	AJ535158
<i>Amphora</i> cf. <i>proteus</i>	AJ535147
<i>Anomooneis sphaerophora</i> (Ehrenberg) Pfitzer	AJ535153
<i>Bacillaria paxillifer</i> (Müller) Hendey	M87325
<i>Campylodiscus ralfsii</i> Gregory	AJ535162
<i>Cocconeis</i> cf. <i>molesta</i>	AJ535148
<i>Cylindrotheca closterium</i> (Ehrenberg) Reimann et Lewin	M87326
<i>Cymbella cymbiformis</i> Agardh	AJ535156
<i>Encyonema triangulatum</i> Kützing	AJ535157
<i>Entomoneis</i> cf. <i>alata</i>	AJ535160
<i>Eolimna minima</i> (Grunow) Lange-Bertalot	AJ243063
<i>Eolimna subminuscula</i> (Manguin) Moser, Lange-Bertalot et Metzeltin	AJ243064
<i>Eunotia formica</i> var. <i>sumatrana</i> Hustedt	AB085830
<i>Eunotia monodon</i> var. <i>asiatica</i> Skvortzow	AB085831
<i>Eunotia pectinalis</i> (Dillwyn) Rabenhorst	AB085832
<i>Eunotia</i> cf. <i>pectinalis</i> f. <i>minor</i>	AJ535146
<i>Eunotia</i> sp.	AJ535145
<i>Fragilariopsis sublineata</i> Hasle	AF525665
<i>Gomphonema parvulum</i> Kützing	AJ243062
<i>Gomphonema pseudoaugur</i> Lange-Bertalot	AB085833
<i>Lyrella atlantica</i> (Schmidt) D. G. Mann	AJ544659
<i>Lyrella</i> sp.	AJ535149
<i>Navicula cryptocephala</i> var. <i>veneta</i> (Kützing) Grunow	AJ297724
<i>Navicula diserta</i> Hustedt	AJ535159
<i>Navicula pelliculosa</i> (Brébisson ex Kützing) Hilse	AJ544657
<i>Nitzschia apiculata</i> (Gregory) Grunow	M87334
<i>Nitzschia frustulum</i> (Kützing) Grunow	AJ535164

<i>Pinnularia</i> cf. <i>interrupta</i>	AJ544658
<i>Pinnularia</i> sp.	AJ535154
<i>Phaeodactylum tricornutum</i> Bohlin	AJ269501
<i>Planothidium lanceolatum</i> (Brébisson ex Kützing) Round et Bukhtiyarova	AJ535189
<i>Pleurosigma</i> sp.	AF525664
<i>Pseudogomphonema</i> sp.	AF525663
<i>Pseudogomphonema</i> sp.	AJ535152
<i>Pseudo-nitzschia multiseriis</i> (Hasle) Hasle	U18241
<i>Pseudo-nitzschia pungens</i> (Grunow ex Cleve) Hasle	U18240
<i>Rossia</i> sp.	AJ535144
<i>Sellaphora pupula</i> (Kützing) Mereschkowsky	AJ544645
<i>Sellaphora pupula</i> (Kützing) Mereschkowsky	AJ544651
<i>Sellaphora pupula</i> (Kützing) Mereschkowsky	AJ544646
<i>Sellaphora pupula</i> (Kützing) Mereschkowsky	AJ544647
<i>Sellaphora pupula</i> (Kützing) Mereschkowsky	AJ544648
<i>Sellaphora pupula</i> (Kützing) Mereschkowsky	AJ544649
<i>Sellaphora pupula</i> (Kützing) Mereschkowsky	AJ544650
<i>Sellaphora pupula</i> (Kützing) Mereschkowsky	AJ544652
<i>Sellaphora pupula</i> (Kützing) Mereschkowsky	AJ544653
<i>Sellaphora pupula</i> (Kützing) Mereschkowsky	AJ544654
<i>Sellaphora pupula</i> f. <i>capitata</i> (Skvortsov et Meyer) Poulin in Poulin, Hamilton et Proulx	AJ535155
<i>Sellaphora laevisissima</i> (Kützing) D. G. Mann	AJ544655
<i>Sellaphora laevisissima</i> (Kützing) D. G. Mann	AJ544656
<i>Surirella fastuosa</i> var. <i>cuneata</i> (Schmidt) H. Peragallo et M. Peragallo	AJ535161
<i>Thalassiosira antarctica</i> Comber	AF374482
<i>Undatella</i> sp.	AJ535163
<i>Bolidomonas mediterranea</i> Guillou et Chrétiennot-Dinet	AF123596
<i>Bolidomonas pacifica</i> Guillou et Chrétiennot-Dinet	AF123595
<i>Bolidomonas pacifica</i> Guillou et Chrétiennot-Dinet	AF167153
<i>Bolidomonas pacifica</i> Guillou et Chrétiennot-Dinet	AF167154
<i>Bolidomonas pacifica</i> Guillou et Chrétiennot-Dinet	AF167155
<i>Bolidomonas pacifica</i> Guillou et Chrétiennot-Dinet	AF167156
<i>Bolidomonas pacifica</i> Guillou et Chrétiennot-Dinet	AF167157
<i>Convoluta convoluta</i> diatom endosymbiont	AY345013
<i>Peridinium foliaceum</i> endosymbiont	Y10567
<i>Peridinium balticum</i> endosymbiont	Y10566
Uncultured diatom	AY180014
Uncultured diatom	AY180015
Uncultured diatom	AY180016
Uncultured diatom	AY180020
Uncultured eukaryote	AY082977
Uncultured eukaryote	AY082992
Uncultured marine diatom	AF290085
Uncultured stramenopile	AY179997

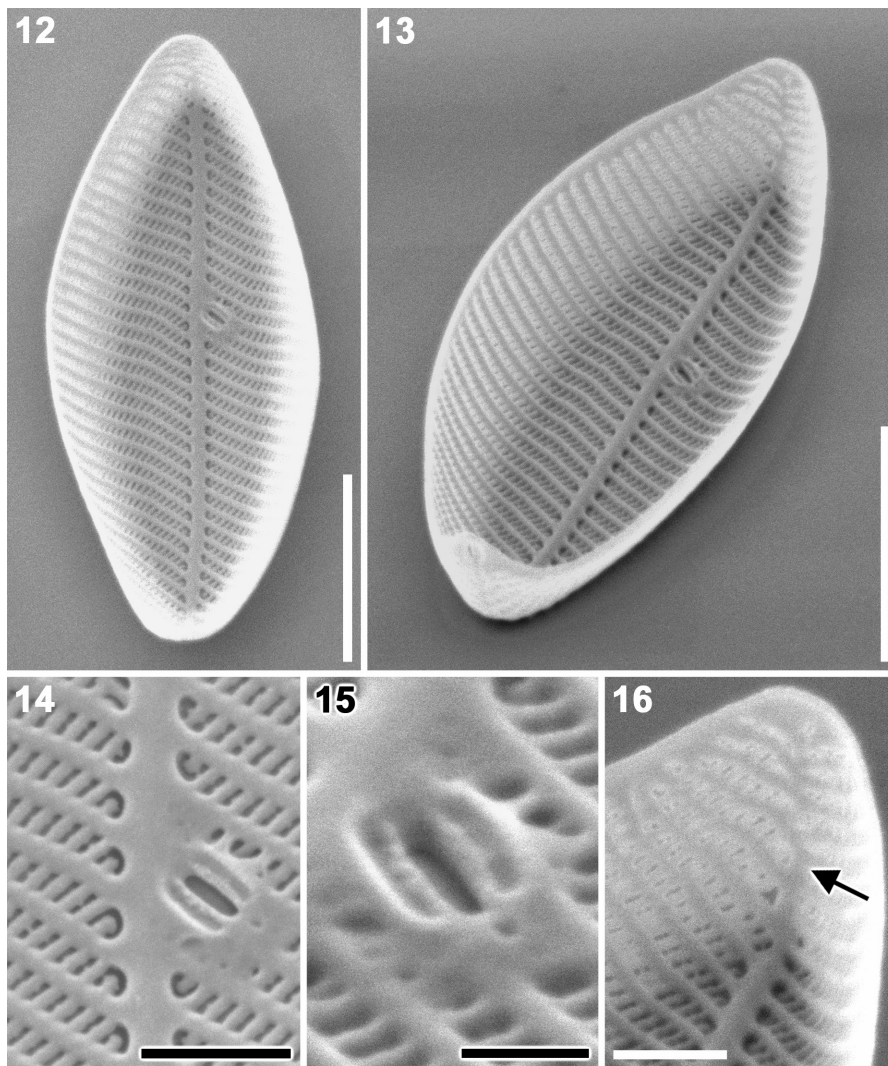
Nomenclatural notes: ¹ name change since deposit, ² likely a new genus collected from a marine habitat (Medlin et al. 2008).



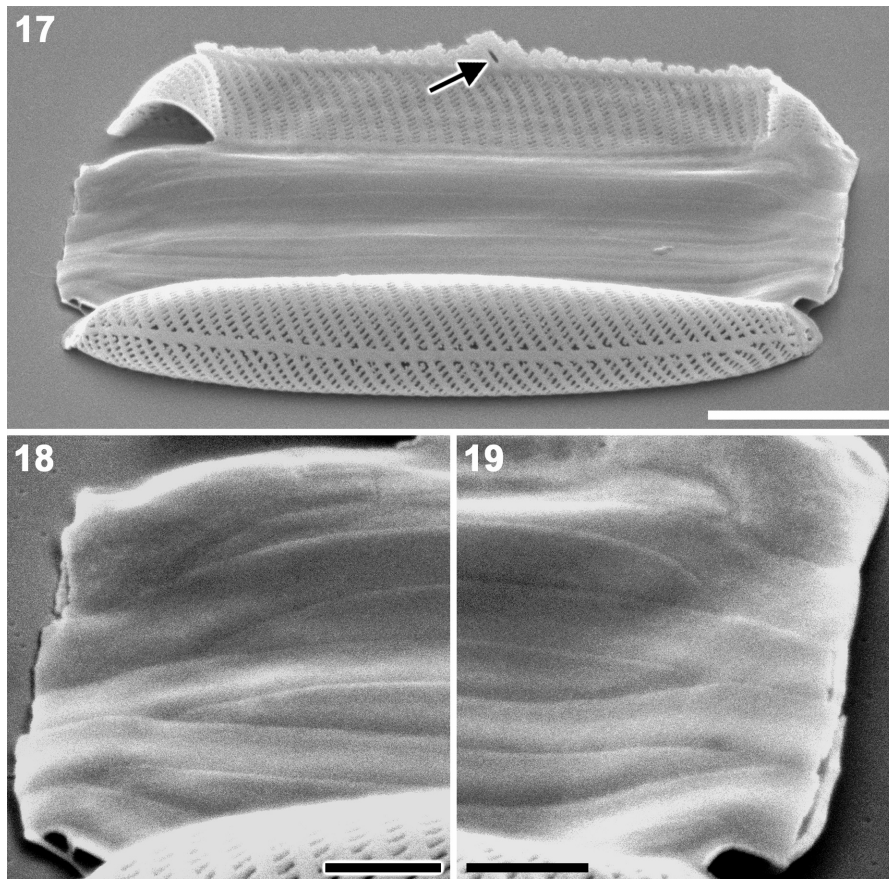
Figs 1-6. Living cell and cleaned cell (LM). Scale bars 2 μm . **Figs 1-3.** Living cells showing plastids. **Figs 4-6.** Cleaned valves. Fig. 4 (BF), Fig. 5 (DIC optic), Fig. 6 (PC).



Figs 7-11. External view of valve (SEM). Scale bars =2 μm (Figs 7-8), 0.2 μm (Figs 9-10), 1 μm (Fig. 11). **Fig. 7.** Valve with slit shaped opening of rimoportula (arrow). **Fig. 8.** Valve with two apical pores (arrow). **Fig. 9.** Enlargement view of apical pores in Fig. 8. **Fig. 10.** Valve apex of other valve with one apical pore. **Fig. 11.** Broken valve showing sternum and rimoportula opening (arrow).



Figs 12-16. Internal view of valve (SEM). Scale bars =2 μm (Figs 12-13), 0.5 μm (Figs 14, 16), 0.2 μm (Fig. 15). **Fig. 12.** Internal valve showing rimoportula along sternum (arrow). **Fig. 13.** Tilted specimen of Fig.12. Note sternum and vimines are thickened. **Fig. 14.** Enlarged view of rimoportula in Fig. 12. **Fig. 15.** Tilted specimen of Fig. 14. **Fig. 16.** Enlarged view of valve apex in Fig. 13. Arrow indicates narrowed sternum.



Figs 17-19. Collapsed frustule (SEM). Scale bars 2 μm (Fig. 17), 0.5 μm (Figs 18-19). **Fig. 17.** Frustule showing plain copulae. Arrow indicates rimoportula. Note antithetically arranged striae on opposite valves. **Figs 18, 19.** Enlarged view of both end of frustule in Fig. 17, showing interlaced copulae.

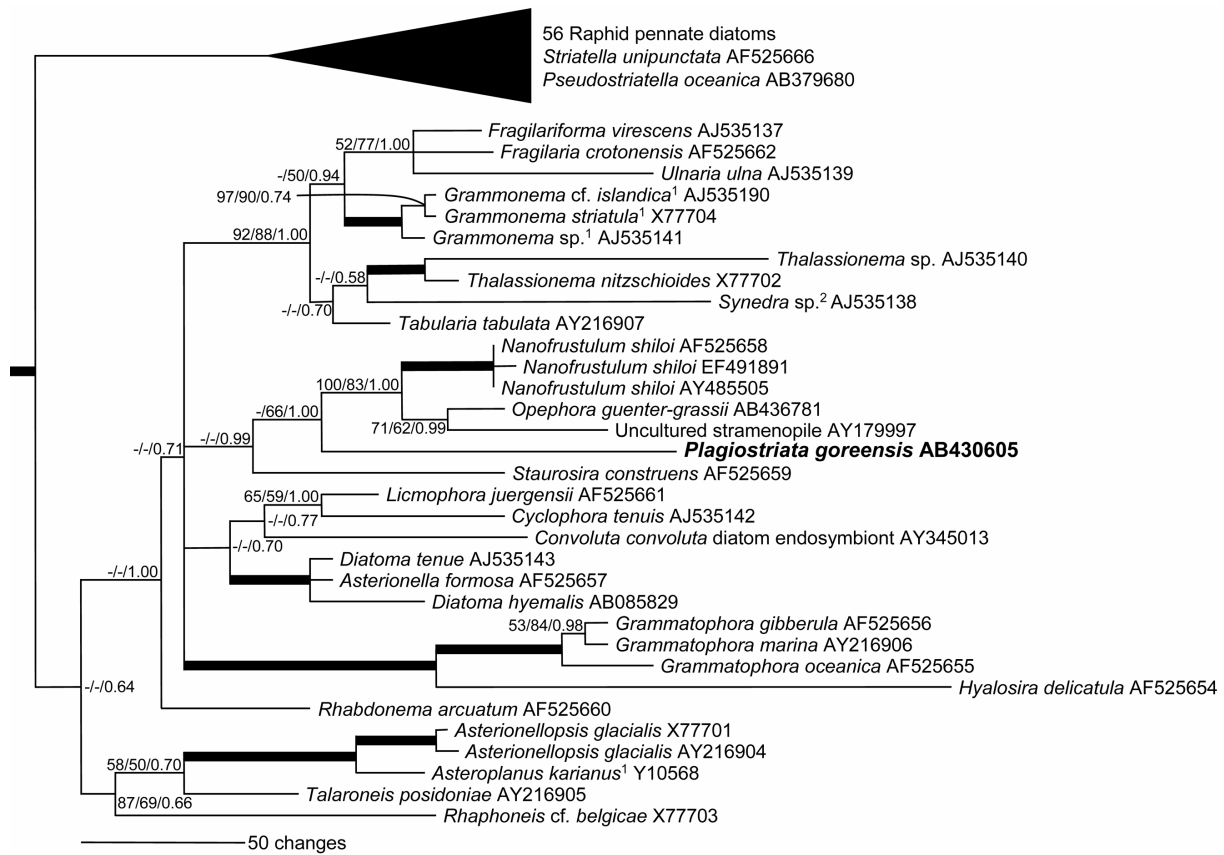


Fig. 20. Molecular phylogeny of diatoms inferred from 18S rDNA sequence using 1704 aligned positions. The tree shown resulted from Bayesian inference using a GTR + I + G model. For clarity, we only show the topology of pennate diatoms. Also, a clade comprises raphid diatoms and two araphid pennate diatoms *Striatella unipunctata*/*Pseudostriatella oceanica* are collapsed into triangle. Nodal support values greater than 50 (NJ and ML) and 0.50 (BI) are shown. Nodes with strong supports (Bootstrap support > 90 in NJ and ML, and posterior probability > 0.95 in BI) are shown as thick lines. Nomenclatural notes: ¹ annotated as *Synedra ulna*. ² annotated as *Fragilaria* in Genbank. ³ possible misidentification because this diatom was collected from marine. ⁴ annotated as *Asterionellopsis kariana*.

2.9. Publication VIII:

Morphology of four plagiogrammacean diatoms; *Dimeregramma minor* var. *nana*, *Neofragilaria nicobarica*, *Plagiogramma atomus* and *Psammogramma vigoensis* gen. et sp. nov., and their phylogenetic relationship inferred from partial LSU rDNA

SHINYA SATO^{1*}, TSUYOSHI WATANABE², RICHARD M. CRAWFORD¹, WIEBE H C F KOOISTRA³
& LINDA K MEDLIN¹

¹*Alfred Wegener Institute for Polar and Marine Research, Am Handelshafen 12, D-27570 Bremerhaven, Germany*

²*Tokyo University of Marine Science and Technology, 4-5-7 Konan, Minato-ku, 108-8477 Tokyo, Japan*

³*Stazione Zoologica 'Anton Dohrn', Villa Comunale, 80121 Naples, Italy*

Abstract

A marine araphid pennate diatom obtained from sand grains sampled at two sites at Vigo, Spain is described as *Psammogramma vigoensis* S. Sato *et* Medlin, a member of the family Plagiogrammaceae, based on observations of frustule fine structure. The species possesses elongated valves with apical pore fields and parallel rows of striae oriented perpendicular to the apical axis. Valve poroids are occluded by perforated rotae. There is a weak sternum along the apical axis and rimoportulae are absent. Detailed observations of *Dimeregramma minor* var. *nana* (Gregory) Ralfs, *Neofragilaria nicobarica* Desikachary, Prasad *et* Prema and *Plagiogramma atomus* Greville, were also undertaken. Based on morphological features, the transfer of *Neofragilaria nicobarica* from the Fragilariaceae to the Plagiogrammaceae is proposed. Partial LSU rDNA phylogeny also supported inclusion of both *Psammogramma* and *Neofragilaria* in Plagiogrammaceae.

KEY WORDS: araphid pennate diatom, *Dimeregramma minor* var. *nana*, evolution, morphology, *Neofragilaria nicobarica*, partial LSU rDNA phylogeny, *Plagiogramma atomus*, Plagiogrammaceae, *Psammogramma vigoensis*, *Talaroneis posidoniae*

INTRODUCTION

The family Plagiogrammaceae (De Toni 1890) currently includes 4 genera, *Plagiogramma* Greville, *Dimeregramma* Ralfs in Pritchard, *Glyphodesmis* Greville and *Talaroneis* Kooistra *et* De Stefano. The genus *Talaroneis*, characterized by the presence of two silica wings flanking a furrow near each apical pore field, was recently proposed because of the invalidity of the former genus *Dimeregrammopsis* Ricard (Kooistra *et al.* 2004). The family had long been placed in the araphid diatoms (e.g. De Toni 1890; Hustedt 1959; Simonsen 1979; Ricard 1987; Round and Crawford 1990), but it was later transferred to the centric diatoms and included in the Triceratales based on valve morphology (Round *et al.* 1990). Recently, using a SSU rDNA phylogenetic study together with a re-evaluation of morphological characters, Plagiogrammaceae was returned to the araphid pennate diatoms by Kooistra *et al.* (2004).

The problematic taxonomic history of Plagiogrammaceae may have arisen from their morphological features; i.e., they lack some of the features of araphid diatoms, viz. parallel striae, apical rimoportulae and a prominent sternum. Kooistra *et al.* (2004) suggested that “such problematic taxa are often in critical positions in phylogenetic appraisals”. In spite of their phylogenetic significance, the living cells and fine structure of the Plagiogrammaceae have rarely been examined, except for the recently described genus *Talaroneis*.

To obtain a more complete picture of Plagiogrammacean diversity, we collected samples of sand grains from shallow coastal regions of Japan and Spain because most plagiogrammacean species reported have been collected in such habitats. The Japanese sample contained three rarely reported taxa, *Dimeregramma minor* var. *nana* (Gregory) Ralfs and *Plagiogramma atomus* Greville in the Plagiogrammaceae, and *Neofragilaria nicobarica* Desikachary, Prasad *et* Prema from the Fragilariaceae. Also, a new diatom species was found at two sites on the Spanish coast, which we described here as *Psammogramma vigoensis* S. Sato *et* Medlin and which we place within the Plagiogrammaceae. Based on the morphological features of *Neofragilaria nicobarica*, we propose the transfer of this species from Fragilariaceae to Plagiogrammaceae. A phylogenetic study was performed using partial LSU rDNA se-

quences to assess the inclusion of both *Psammogramma* and *Neofragilaria* in the Plagiogrammaceae.

MATERIALS AND METHODS

Collections and cultures

Living cells of *Psammogramma vigoensis* were collected by M. Taketa at Samil Beach, Vigo, Pontevedra, Spain on 22 Oct. 2006 (strain s0391), and by R. Sousa at La Fuente (42°14'N, 8°43'W), Vigo, Pontevedra, Spain on 23 Dec. 2006 (SC1). *Dimeregramma minor* var. *nana* and *Neofragilaria nicobarica* were collected by T. Watanabe at Iriomote Island (24°21'N, 123°43'E), Okinawa Pref., southern part of Japan on 16th. Oct. 2005 (strain s0355 and s0371, respectively), and *Plagiogramma atomus* was collected by T. Watanabe at the same place on 17 Oct. 2005 (strain s0330). All samples were taken from sand. Previous phylogenetic studies on diatoms using SSU rDNA identified *Asterionellopsis* Round / *Asteroplanus* Gardner *et* Crawford and/or *Rhaphoneis* Ehrenberg / *Delphineis* Andrews as nearest sisters of the Plagiogrammaceae (Kooistra *et al.* 2004; Alverson *et al.* 2006; Sorhannus 2007). Thus, the outgroups chosen for the phylogenetic analyses were: *Asterionellopsis gracialis* (Castracane) Round and *Asteroplanus karianus* (Grunow) Gardner *et* Crawford collected by L. K. Medlin at Bristol, U.K. on Dec. 1984 (strain p119 and p132, respectively) and *Rhaphoneis amphiceros* Ehrenberg, collected by S. Sato at Grimershörn Bucht, Cuxhaven, Germany on 21 Aug. 2005 (strain s0296). Clonal cultures were established through isolation of a single cell and maintained at room temperature (ca. 20°C) in IMR medium (Eppley *et al.* 1967) in front of a North-facing window. Natural material was studied in sample SC1.

Microscopy

An Axioplan light microscope (Zeiss, Oberkochen, Germany) with bright field (BF), differential interference contrast (DIC) or phase contrast (PC) optics were used to observe living cells and cleaned frustules. To remove organic material from frustules, samples were treated as modified by Nagumo and Kobayasi (1990) as follows: (1) Sample centrifuged and the supernatant discarded to make pellet. (2) Pellet suspend with distilled water. (1) and (2) repeated several times to complete demineralization. (3) Re-centrifuged, and then for dissolution of organic matter, a similar volume of Drano Power-Gel (Johnson Wax GmbH, Haan, Germany), a strong domestic drain cleaner, added to the pellet. (4) Mixture vortexed and left at room temperature ca. 30 min. At the end, (1) and (2) repeated several times to complete demineralization. Cleaned frustules were then mounted onto glass slides with Mountmedia (Wako, Osaka, Japan). For SEM examination, the cleaned material was dropped onto cover slips, air dried, and coated with gold using an SC 500 (Emscope, Ashford, England). A QUANTA 200F scanning electron microscope (FEI Company, Eindhoven, Netherlands) was used for SEM observation at an accelerating voltage of 3 to 10 kV, and ca. 10 mm working distance. Captured images were adjusted with Adobe Photoshop. Valve length were determined from digital images using Scion Image (<http://www.scioncorp.com>).

Terminology

Morphological terms were taken from Anonymous (1975), Cox and Ross (1981) and Round *et al.* (1990). Molecular phylogenetic studies of diatoms have revealed that historical diatom

classifications do not reflect a natural system and araphid pennate diatoms are paraphyletic in most of the gene phylogenies, e.g., in nuclear and plastid SSU rDNA phylogenies (Medlin and Kaczmarska 2004). Nevertheless, we use the terms *araphid* and *centric* here descriptively because they refer to key morphological features or their absence. In this paper, the term *araphid diatom* follows a traditional definition, viz., a diatom with an elongated valve with a central or slightly lateral sternum, apical pore fields and often apical rimoportulae, but lacking a raphe slit. We do not imply that this corresponds to a mono- (holo-) phyletic group, nor that it should be accorded any taxonomic status.

DNA extractions and PCR

Strains were harvested by filtration. Extraction, PCR and sequencing of partial LSU rDNA, the D1/D2 region of the nuclear 28S rDNA (~ 607 bp), were as described by Beszteri *et al.* (2005). DNA of *Talaroneis posidoniae* Kooistra et De Stefano extracted by Kooistra *et al.* (2004) was also used. Because the amplification of *Psammogramma vigoensis* SSU rDNA was not successful despite a considerable effort of PCR, we only used partial LSU rDNA as a marker, although SSU rDNA is also appropriate maker in order to establish the relationship of Plagiogrammacean genera.

Saturation analysis

Substitutional noises of a gene marker make it difficult to retrieve phylogenetic signal, especially when the gene evolves in fast rate, such as the D1/D2 region of the nuclear 28S rDNA. The saturation is caused by multiple substitutions at the same site. In order to examine the substitutional saturation in our dataset, the observed number of substitutions were plotted against corrected distances estimated from ML using GTR + I + G model with parameters estimated in PAUP as below.

Phylogenetic analyses

GenBank accessions of sequences used in this study have been listed in Table 1. Sequences were first aligned manually with BioEdit 7.0.2 (Hall 1999), and then refined referring to the secondary structure model (Sato unpubl.). Ambiguously alignable positions were excluded from phylogenetic analyses, resulted in 585 bp in the dataset. The final dataset consisted of 8 OTUs including *Asterionellopsis gracialis*, *Asteroplanus karianus* and *Rhaphoneis amphiceros* as outgroups. The alignment is available from the first author upon request. Base frequency was calculated using BioEdit to assess the heterogeneity of the dataset.

Phylogenies were reconstructed with PAUP* version 4.0b10 (Swofford 2002). For maximum likelihood (ML) and distance-based tree calculations, likelihood scores of different nucleotide substitution models were compared on a neighbor joining (NJ) tree using Modeltest 3.7 (Posada and Crandall 1998). The best-fit model according to the Akaike Information Criterion (AIC) was GTR + I + G, and this was used for phylogenetic analyses using ML and NJ tree inference with ML distances. The chosen model had the following parameters; base frequencies were: A: 0.2464, C: 0.2075, G: 0.3090 and T: 0.2371; substitution rates were: A-C = 0.4311, A-G = 1.1942, A-T = 0.8526, C-G = 0.3558, C-T = 3.7215 and G-T = 1.0000; the proportion of invariant sites was 0.5068, among-site rate heterogeneity was described by a gamma distribution with a shape parameter of 0.5931. Maximum parsimony (MP) and ML trees were obtained by exhaustive search. For bootstrapping of MP and ML

analyses, branch-and-bound search was used. All bootstrap analyses were performed with 1,000 replicates. For Bayesian analysis, MrBayes 3.1.2 (Huelsenbeck and Ronquist 2001, Ronquist and Huelsenbeck 2003) was used to estimate the posterior probability distribution using Metropolis-Coupled Markov Chain Monte Carlo (MCMCMC) (Ronquist and Huelsenbeck 2003) with the GTR + I + G model. We used the default priors from MrBayes. Each run used four chains, one cold and three heated, with temperature set to 0.2. We performed two independent runs, during 5,000,000 generations, and saving every 100th tree. The first 10,000 trees were discarded as burn-in; the remaining 40,000 post-burn-in trees were used to construct a 50 % majority-rule consensus tree.

RESULTS

Psammogramma S. Sato *et* Medlin gen. nov.

Cellulae inter se affixis in coloniis cateniformibus rectis, in aspectu cingulari rectangulares, chloroplastis ca. 4 in quaque cellula. Taeniae ca. 5-10 omnibus apertis sine poris, inter se implexae. Valvae ellipticae. Superficies valvae rotundata sine limbo abrupto. Sternum obscurum. Striae uniseriatae ad sternum interdum alternantes. Areae apicales pororum extus ornatae intus inornatae. Rimoportula carens.

Cells remain attached to form straight chain colonies. Cells rectangular in girdle view. Plastids 4 per cell. Bands ca. 5-10, all of them are plain and open. All bands interlace with one another. Valve elliptical. Valve face rounded without an abrupt mantle. Sternum indistinct. Striae uniseriate, and sometimes arrange alternately on the each side of sternum. The apical pore field is ornamented externally but not internally. Rimoportula absent.

Type species: *P. vigoensis* S. Sato *et* Medlin gen. *et* sp. nov. (Figs 1-19)

Propriis generis, valvis 6.3-14.0 μm longis, 2.2-2.6 μm latis, striis 20-22 in 10 μm

Morphological features as in the genus. Valve length 6.3 - 14.0, width 2.2 - 2.6. Striae 20-22 per 10 μm

HOLOTYPE: Zu6/39 (Alfred Wegener Institute, Bremerhaven, Germany).

ISOTYPE: TNS-AL-53999 (National Museum of Nature and Science, Tsukuba, Japan)

TYPE LOCALITY: Samil Beach, Vigo, Pontevedra, Spain

ETYMOLOGY: The genus name was given for the epipsammic habitat. The specific name derives from the type locality

Cells are attached to each other by their valve faces, making straight chains (Fig. 1). Each frustule is rectangular in girdle view (Figs 1-2) and appears to contain four plastids, which surround the central nucleus (Fig. 1). The valves are linear-elliptical to elliptical (Figs 3-5),

6.3 - 14.0 μm in long, 2.2 - 2.6 μm in wide, with 20 - 22 striae in 10 μm (the maximum and the minimum valve length were recorded from SEM observations of sample SC1). Hyaline areas are visible at the both ends of valve (Figs 3-5), representing the apical pore fields (see below). The sternum is usually barely recognizable, but sometimes becomes distinct when the focus is on the transverse striae, which are arranged alternately on each side of sternum (Fig. 5).

The frustules have many bands, ca. 5-10 per theca (Figs 6-9), all being open and unperforated (Figs 6-9). At the both poles the bands curved in the advalvar direction (Fig. 8). All band interlace with one another (Fig. 9). The perivalvar edge of copula of the epitheca often has a comb-like fine fringe (Figs 9-11).

The sternum is distinct externally, but barely distinguishable internally (Figs 12, 16). The valve surface has no projections except at the valve face-mantle junction, where sometimes granules (Fig. 12) or spinules (Fig. 13) are formed. Externally an apical pore field has ornaments that are irregularly scattered and often obscure the arrangement of pore system, whereas internally the apical pore field is not ornamented, as on the outer surface such a regular pore system is thus visible (Figs 14, 17). Areolae are occluded by rotae, which are recessed into the internal valve surface (Figs 15, 19). Valves have no rimoportula (Figs 16, 17). The valve is a simple, single-layered structure (Fig. 18).

***Dimeregramma minor* var. *nana* (Gregory) Ralfs (Figs 20-37)**

SYN.: *Denticula nana* Gregory, *Dimerogramma nanum* Ralfs

LITERATURE: Hustedt 1931-1959, p. 119, fig. 641

Cells attach to each other by their valve faces, making a straight chain (Figs 20, 21). Each frustule is rectangular in girdle view, with 1 or 2 plastids surrounding the central nucleus (Fig. 22). The valves are linear elliptical (Figs 23, 24) to elliptical, 9.3 - 11.0 μm long, 3.5 - 4.5 μm wide, with 12 - 14 striae in 10 μm . The sternum and apical pore fields are recognizable as hyaline areas (Figs 23, 24). The valve face is not flat in girdle view in larger cells, but the central boss and apical pore fields are somewhat elevated (Fig. 25), whereas nearly flat in smaller cell (not shown).

The valve face-mantle junction bears complex branched spines externally but not internally. (Figs 26, 29). The external surface of the middle of the valve has central boss, which is unrecognizable internally and bears many tiny granules (Figs 27, 29, 30). The apical pore fields have granules externally, but internally scarcely have any ornament (Figs 28, 31). The granules on the external surface of the apical pore fields are irregularly arranged, making it difficult to see the arrangement of pores underneath (Fig. 28). Rimoportulae are absent (Fig. 29). The areolae are occluded by complex rotae (Fig. 30).

Each theca contains several bands (Figs 32-34). All are open and interlaced with one another (Fig. 33). The width of the bands narrows at both ends of the cell (Figs 32, 33, 35). The valvocopula is plain but all other bands are perforated by one row of areolae (Figs, 32, 35) and sometimes they are fragmented (Fig. 34). The abvalvar end of the most abvalvar band in epitheca is sawtooth-shaped (Fig. 34). Cells attach to each other mainly by mucilage secreted from apical pore fields rather than mechanically by the spines (Figs 35, 36). The central boss is not attached to that of the opposite valve (Fig. 36), but possibly has an organic connection *in vivo*. The valve is a single layer, and rotae are located close to the external surface of areola (Fig. 37).

***Neofragilaria nicobarica* Desikachary, Prasad *et* Prema in Desikachary *et* Prema (Figs 38-55)**

LITERATURE: Desikachary and Prema 1987 p. 8, fig. 306: 9,10, 12-14, fig. 400A: 1, 2; Foged 1975, fig. VIII: 19-20 (as *Rhaphoneis bilineata*); Witkowski *et al.* 2000, p.487, pl. 22, figs 17, 24, 25

Cells are attached to each other by the corners of the cells, making zig-zag (Fig. 38) or stellate (Fig. 39) colonies. Frustules are rectangular in girdle view, with 1 or 2 plastids (Figs 38-40). Valves are 4.5 - 26.8 μm in length, 9.3 - 10.3 μm in width, with 4 - 6 striae per 10 μm . Valves are lanceolate to rhomboid in valve view (Figs 41, 42). The sternum appears slightly zig-zag in shape (Figs 41, 42) because the striae are so wide. The apical pore fields are visible in LM as hyaline areas (Fig. 42). The valve face is nearly flat in girdle view, bearing spines at the valve face-mantle junction (Fig. 43).

The valve face-mantle junction is ornamented with spines, whose tips are bifurcate (Figs 44, 54, 55). The external surface of the sternum bears many tiny granules, whereas it is plain internally (Figs 45, 47, 48). The ends of valve have several slits that form the apical pore fields (Fig. 46). The margin of the apical slits are ornamented externally, but internally lack any ornamentation (Figs 46, 49). The external apical slits are bordered by numerous irregularly located granules, obscuring the arrangement of slits (Fig. 46). A simple conical spine is sometimes observed between the apical pore field and the end of the sternum (Fig. 46). Rimoportulae are absent (Figs 47, 49). Areolae are occluded by a broad, plate-like cribrum (Fig. 48). Each mature theca contains three bands (Figs 50, 51), all of which are open, unperforated and interlaced with one another; they narrow at both ends of cell (Figs 50, 51). They bear numerous granules (Fig. 51). The valve is a single layer, and cribra are located close to the internal areolar surface (Fig. 52). Cells are attached to each other mainly by mucilage secreted from apical pore fields but the spines also contribute to chain formation (Figs 39-40, 53-55). The bifurcated part of each spines fits against a cribrum on the opposite valve (Figs 54-55).

***Plagiogramma atomus* Greville (Figs 56-73)**

LITERATURE: Greville 1863, p. 536, fig. 9; Williams 1988, p. 42, fig. 49: 4,5; Witkowski *et al.* 2000, p.449, pl. 3, figs 8,9

Cells are attached to each other by their corners, making zig-zag colonies (Fig. 56). Each frustule is rectangular in girdle view, containing one or two plastids (Figs 56, 57) and lipid droplets, which float away when the cells are broken (Fig. 58). Valves are 23.5 - 26.2 μm long with rostrate ends and strongly constricted centre (Fig. 57). The valve width at the widest part is 10.6 - 11.7 μm , but at the center only 4.8 - 5.9 μm ; there are 10 - 12 striae in 10 μm . At the central constriction, the valve face is hyaline (Fig. 59). A sternum is unresolvable, and apical pore fields are recognizable as hyaline areas (Fig. 59). Prominent spines are often observed at the corners of the cell (Fig. 60). A deep valve mantle is seen in girdle view (Fig. 61). A weak, narrow sternum is visible externally as well as internally (Figs 62, 65, 66). The central hyaline area is plain (Fig. 62), apart from some small granules externally (Fig. 63). A single conical spine is sometimes present between the apical pore field and the end of sternum (Fig. 64). The ends of valve have several rows of pores that make an apical pore field (Fig. 64). The external surface of the apical pores has ornamentation along the vertical edge of the pores, which is somewhat irregularly developed, making it difficult to see the regular arrangement of pores

(Fig. 64). On the other hand, the internal surface of the apical pore field is plain (Fig. 67). Regularly arranged external ornamentation of the apical pore field gives a different impression of arranged pores when the same structure is observed internally (Fig. 67). A central constricted part is surrounded by heavily silicified walls traversing the cell and the edge of the valve is also heavily thickened inwardly, forming a septum around the valve margin and connecting to the central transverse walls (Figs 65, 66). Rimoportulae are absent (Figs 65-67). Each mature theca contains three bands, and all are plain (Figs 68-70), open and interlaced with one another; they narrow at the both ends of the cell (Figs 68-70). The areolae are occluded by complex rotae (Fig. 71). The valve is composed of a single layer (Figs 72-73), and the rotae are located close to the internal openings of the areolae (Fig. 73).

Phylogeny

Saturation analysis of our dataset showed a linear proportional distribution of plots indicating no evidence of a potential negative effect of multiple substitutions (Fig. 74). Comparison of their base frequencies revealed there were no substantial bias, although *P. atomus* was slightly GC rich (Table 1).

In all analyses, *Dimeregramma minor* var. *nana*, *Neofragilaria nicobarica*, and *Plagiogramma atomus* formed a clade with the latter two as nearest neighbors (*D*, (*N*, *P*)), although with low bootstrap support (Fig. 75). In the trees inferred from the NJ analyses *Talaroneis* and *Psammogramma* (*T*, *P*) formed a clade as sister to the (*D*, (*N*, *P*)) clade (Fig. 75), whereas a ladder-like pattern of relationships (*T*, (*P*, (*D*, (*N*, *P*)))) was recovered in the MP-tree. Relationships were not fully resolved in BI making a trichotomy (*T*, *P*, (*D*, (*N*, *P*))) at the root of the plagiogrammacean clade. Plagiogrammacean clade was firstly connected to the robust Fragilariacean clade (*Asterionellopsis gracialis* and *Asteroplanus karianus*), and subsequently connected to *Rhaphoneis amphiceros* by a very long branch.

DISCUSSION

The family Plagiogrammaceae

We propose *Psammogramma* as a new member of the family Plagiogrammaceae given the results of our morphological and molecular studies. The valve morphology of *Psammogramma vigoensis* is congruent with the circumscription of the family Plagiogrammaceae (Kooistra *et al.* 2004) as follows: elongate valve with apical pore fields and parallel rows of striae, oriented perpendicular to the apical axis; valve poroids occluded by volae or perforated rotae; most genera with a sternum along the apical axis; absence of rimoportula. Results of molecular phylogenetic analyses also support the inclusion of *P. vigoensis* within Plagiogrammaceae, although the phylogenetic position has not perfectly resolved yet by solely using partial LSU rDNA.

Neofragilaria was described as a member of the Fragilariaceae (Desikachary and Prema 1987) probably because of the prominent marginal spines that implied linking spines of *Fragilaria* Lyngbye although the spines of *Neofragilaria* do not link the cells into chains, such as in *Fragilaria* (Figs 53-55). We propose that the genus *Neofragilaria* should be included in the family Plagiogrammaceae based on the criteria that it possesses the following characters: 1) presence of ornamented apical pore fields, 2) absence of rimoportulae and 3) areolae occluded areola by rotae. None of these characters define *Fragilaria*, the nominate genus of the family Fragilariaceae.

Although the distinctive morphological characters of *N. nicobarica* by Desikachary and Prema (1987) fit well to our specimen, subtle qualitative difference can be seen in striation, i.e. our specimen is striated more coarsely (4-6 in 10 μm) than the original one (6-7 in 10 μm). The sternum of our specimen seems to be broader than in the original. *Rhaphoneis bilineata* Grunow *et* Cleve is morphologically similar to *N. nicobarica*, but is more finely striated (7 in 10 μm ; Cleve 1888 as *R.? bilineata*; 7-8 in 10 μm by Foged 1975). Some valves illustrated in Witkowski *et al.* (2000) also show finely striated *Neofragilaria* (figs 15-16, 19 as *N. nicobarica* and fig. 26 as *Neofragilaria* sp.). If results of further SEM and molecular studies indicate that *R. bilineata* and *N. nicobarica* are single species, they should be described as a new combination *Neofragilaria bilineata* because Grunow *et* Cleve's name bears nomenclatural priority.

In the partial LSU rDNA tree, the very long branches of *P. atomus* and *R. amphiceros* are not negligible. The existence of these long branches suggest that the substitution rate of each species has been accelerated, making it difficult to reconstruct their phylogeny properly. In fact, the sequence of *P. atomus* is slightly biased in favor of GC base compositions. Nevertheless, although local difference exists, basically the same tree topology was recovered using completely different strategies, i.e., distance-, character based- and model based methods; the last is known as a relatively powerful method against heterogeneous dataset. Our molecular phylogenetic trees placed *N. nicobarica* as sister to *Plagiogramma atomus* with substantially high bootstrap/Bayesian posterior probability, supporting the transference of the genus to the family Plagiogrammaceae.

In many molecular phylogenetic analyses performed so far, the plagiogrammacean diatom *Talaroneis posidoniae* formed a robust clade with *Asterionellopsis* / *Asteroplanus* and the family Rhaphoneidaceae, which includes *Rhaphoneis* and *Delphineis* (e.g. Kooistra *et al.* 2004; Alverson *et al.* 2006; Sorhannus 2007). This basal clade of araphid diatoms emerges at the root of pennate diatoms, after which the raphid diatoms diverge from the rest of the araphid diatoms (Kooistra *et al.* 2004; Medlin & Kaczmarska 2004; Alverson *et al.* 2006; Sorhannus 2007). The basal clade of araphid diatoms, which is shown to be an ancestral lineage at least in SSU rDNA phylogenies, is characterized by having areola occlusions. Four plagiogrammacean genera observed in this study were collected from sand along subtropical shallow coasts. Rhaphoneidaceae are known as sand dwelling diatoms (Andrews 1975; Round *et al.* 1990), being abundant in subtropical areas (Takano 1964). Exceptions are *Asterionellopsis*/*Asteroplanus*; which are planktonic. Apparently, the planktonic state of *Asterionellopsis* and *Asteroplanus* is derived and the sand dwelling state of plagiogrammacean and rhaphoneidacean taxa is ancestral. Kooistra *et al.* (2007) have suggested that most of the planktonic pennates have been seeded from the benthos, being tychopelagic.

Morphological implications

At the centre of valves of *Plagiogramma atomus* and other species of the genus (Montgomery 1978), there is a distinctive cavity, which appears externally as a plain transverse area termed a fascia by Round *et al.* (1990, p. 238). Although we have no evidence to suggest any function of the cavity, mechanical reinforcement of valve structure might be an explanation. It is also possible that this part plays a role involving some cellular activity, because the cavity is only open toward the cell interior and lacks any perforations to the outside. There are some other pennate diatoms possessing a similar cavity, e.g., the araphid diatom *Cyclophora tenuis* Castracane (Navarro, 1982), some species (*lanceolate* type) of the monoraphid genus *Planothidium* Round *et* Bukhtiyarova (1996) and species of *Hustedtiella* Simonsen (Crawford *et al.* 1993) indicating that the structure has been acquired several times independently. Speculation on the function of these structures is not justified yet. We need to know if any element of the

protoplast is consistently found within these cavities in these diatoms. If none are, then it is likely that the structure has some structural significance.

Most members of the (*D*, (*N*, *P*)) clade (see phylogenetic results and Fig. 75) possess prominent marginal spines. *Plagiogramma atomus* does not possess marginal spines but other *Plagiogramma* species do (Round *et al.* 1990, pp. 238-239). These spines do not link the cells tightly through formation of interlocking ends. The spines of one valve fit imperfectly over the adjacent valve in the chain when it is relaxed (i.e., not bent by means of externally applied force), so there is possibility for some bending in the chain. Because the spines of one valve do not touch the adjacent valve in the relaxed chain, the spines might serve as buffers preventing the chains from bending over too far or from twisting. Alternatively, they might obstruct access of parasites to the cribra, the structurally thinnest and therefore potentially the structurally weakest parts of the silica frustule.

Another interesting feature observed in *N. nicobarica* is that the spines of one valve touch the cribra of its sister valve. Recently, however, Hamm *et al.* (2003) revealed an unexpected elasticity of the silica structure of diatoms. A girdle band of *Thalassiosira punctigera* (Castracane) Hasle was bent heavily by a glass microneedle under the light microscope but the structure was too elastic to be broken (Hamm *et al.* 2003, fig. 3), probably because of a unique component, i.e., inorganic particles associated with an organic matrix (Kröger *et al.* 1999; Fortin and Vargas 2000). Therefore, the combination of bifurcated spine and cribrum might act as a cushion minimizing damage under pressure and avoiding direct contact of valve faces. The ends of spines of *Dimeregramma* as observed by Round *et al.* (1990, p. 242-243, figs d-e, g-h) are intricately branched, and contact of each end of opposite spines could perhaps cushion the wall against impact or stress during bending of the colony or external shock. In several genera of the Cymatosiraceae spines in a similar location may serve as linking spines but no such function can be envisaged here (see Crawford 1979; Hasle *et al.* 1983). Habitat amongst sand grains would likely entail greater impact to the cells as sand grains are lifted and redeposited.

ACKNOWLEDGEMENTS

We would like to thank Rafael Sousa Hervés and Maki Taketa for the Spanish samples; Andrzej Witkowski and Lourenço Ribeiro for valuable comments on the taxonomy of *Psammogramma*; Friedel Hinz for support with SEM. We also thank two anonymous reviewers for their helpful comments that improved the manuscript. This study was supported by DAAD for doctoral research fellowship to Shinya Sato.

REFERENCES

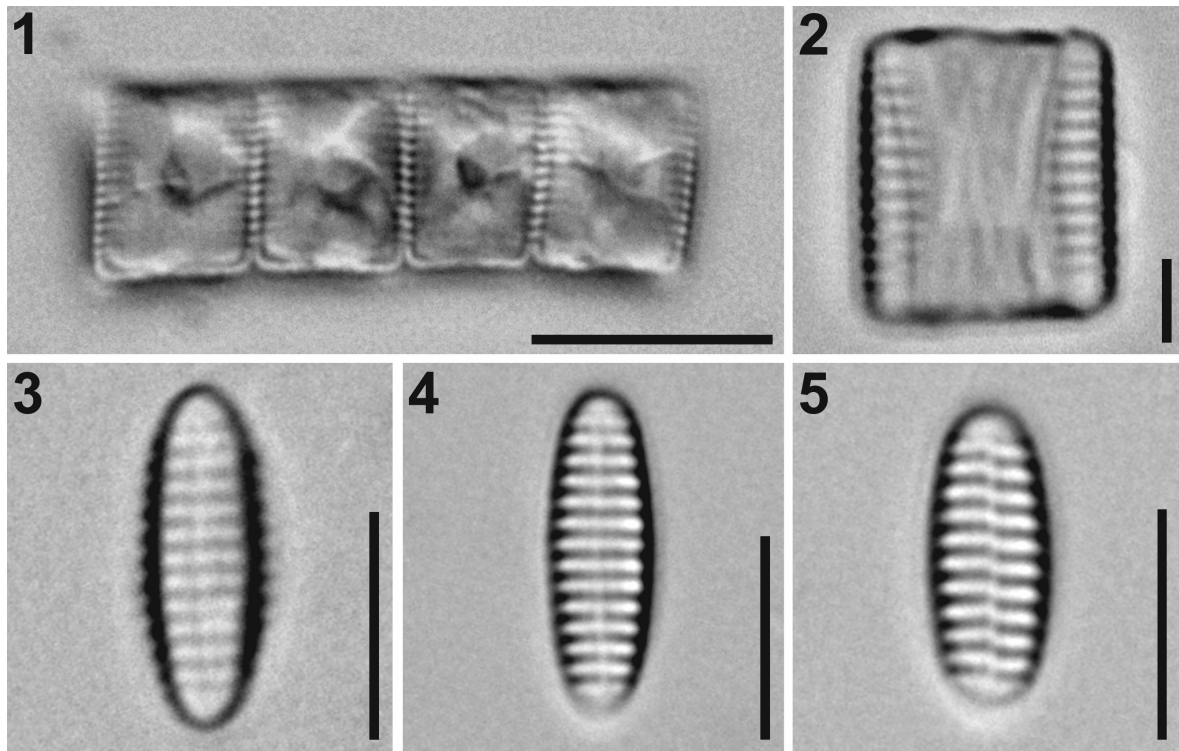
- Alverson, A. J., Cannone, J. J., Gutell, R. R. and Theriot, E. C. 2006. The evolution of elongate shape in diatoms. *J. Phycol.* **42**: 655-668.
- Andrews, G. W. 1975. Taxonomy and stratigraphic occurrence of the marine diatom genus *Rhaphoneis*. *Nova Hedwigia Beih.* **53**: 193-227.
- Anonymous 1975. Proposals for a standardization of diatom terminology and diagnoses. *Nova Hedwigia Beih.* **53**: 323-354.
- Beszteri, B., Ács, É. and Medlin, L. K. 2005. Ribosomal DNA sequence variation among sympatric strains of the *Cyclotella meneghiniana* complex (Bacillariophyceae) reveals cryptic diversity. *Protist* **156**: 317-333.

- Cleve, P. T. 1883. Diatoms, collected during the expedition of the Vega. *Vega-Expeditionens Vetenskapliga Iakttagelser* **3**: 455-517.
- Cox, E. J. and Ross, R. 1981. The striae of pennate diatoms. In Ross, R. (Ed.) *Proceedings of the 6th International Diatom Symposium on Recent and Fossil Diatoms*. O. Koeltz, Koenigstein, pp. 267–278.
- Crawford, R. M. 1979. Filament formation in the diatom genera *Melosira* C.A. Agardh and *Paralia* Heiberg. *Nova Hedwigia* **64**: 121–133.
- Crawford, R. M., Simonsen, R., Hinz, F. and Gardner, C. 1993: The diatoms *Hustedtiella baltica* and *H. sinuata* sp. nov. and the systematic position of the genus. *Nova Hedwigia Beih.* **106**: 151-160.
- De Toni, G. B. 1890. Sulla *Navicula* aponina Kuetz. e sui due generi *Brachysira* Kuetz. e *Libellus* Cleve. *Atti Reale Ist. Veneto. Sci. Lett. Arti.* **1890**: 967-971.
- Desikachary, T. V. and Prema, P. 1987. Diatoms from the Bay of Bengal. In Desikachary, T.V. (ed.) *Atlas of diatoms*, vol. 3: Madras Science Foundation, Madras.
- Eppley, R. W., Holmes, R. W. and Strickland, J. D. H. 1967. Sinking rates of the marine phytoplankton measured with a fluorochromometer. *J. Exp. Mar. Biol. Ecol.* **1**: 191–208.
- Foged, N. 1975. Some littoral diatoms from the coast of Tanzania. *Biblioth. Phycol.* **6**: 1-127.
- Fortin, D. and Vargas, M. A. 2000. The spectrum of composites: new techniques and materials. *J. Am. Dental. Assoc.* **131**: 26–30.
- Greville, R. 1863. Descriptions of new genera and species of diatoms from the South Pacific. *Trans. Bot. Soc. Edinb.* **7**: 534-543
- Hall, T. A. 1999. BioEdit: a user-friendly biological sequence alignment editor and analysis program for Windows 95/98/NT. *Nucl. Acids. Symp. Ser.* **41**: 95-98.
- Hamm, C. E., Merkel, R., Springer, O., Jurkojc, P., Maier, C., Prechtel, K. and Smetacek, V. 2003. Architecture and material properties of diatom shells provide effective mechanical protection. *Nature* **421**: 841–843.
- Hasle, G. R., von Stosch, H. A. and Syvertsen, E. E. 1983. Cymatosiraceae, a new diatom family. *Bacillaria* **6**: 9–156
- Huelsenbeck, J. P. and Ronquist, F. 2001. MRBAYES: Bayesian inference of phylogeny. - *Bioinformatics* **17**: 754-755.
- Hustedt, F. 1959. Die Kieselalgen Deutschlands, Österreichs und der Schweiz. In: Rabenhorst, L. (ed.) *Kryptogamen-Flora von Deutschland, Osterreich und der Schweiz, Band VII, Teil 2*, Koenigstein, Germany: Otto Koeltz Science Publishers, 845 pp.
- Kooistra, W. H. C. F., Gersonde, R., Medlin, L. K. and Mann, D. G. 2007. The origin and evolution of the diatoms: their adaptation to a planktonic existence. In: Falkowski, P.G. and Knoll, A.H. (Eds.). *Evolution of primary producers in the sea*. pp. 207-249.
- Kooistra, W. H. C. F., Forlani, G., Sterrenburg F. A. S. and De Stefano, M. 2004. Molecular phylogeny and morphology of the marine diatom *Talaroneis posidoniae* gen. et sp. nov. (Bacillariophyta) advocate the return of the Plagiogrammaceae to the pennate diatoms. *Phycologia* **43**: 58–67.
- Kröger, N., Deutzmann, R. and Sumper, M. 1999. Polycationic peptides from diatom biosilica that direct silica nanosphere formation. *Science* **286**: 1129–1132.
- Medlin, L. K. and Kaczmarek, I. 2004. Evolution of the diatoms: V. Morphological and cytological support for the major clades and a taxonomic revision. *Phycologia* **43**: 245–270.

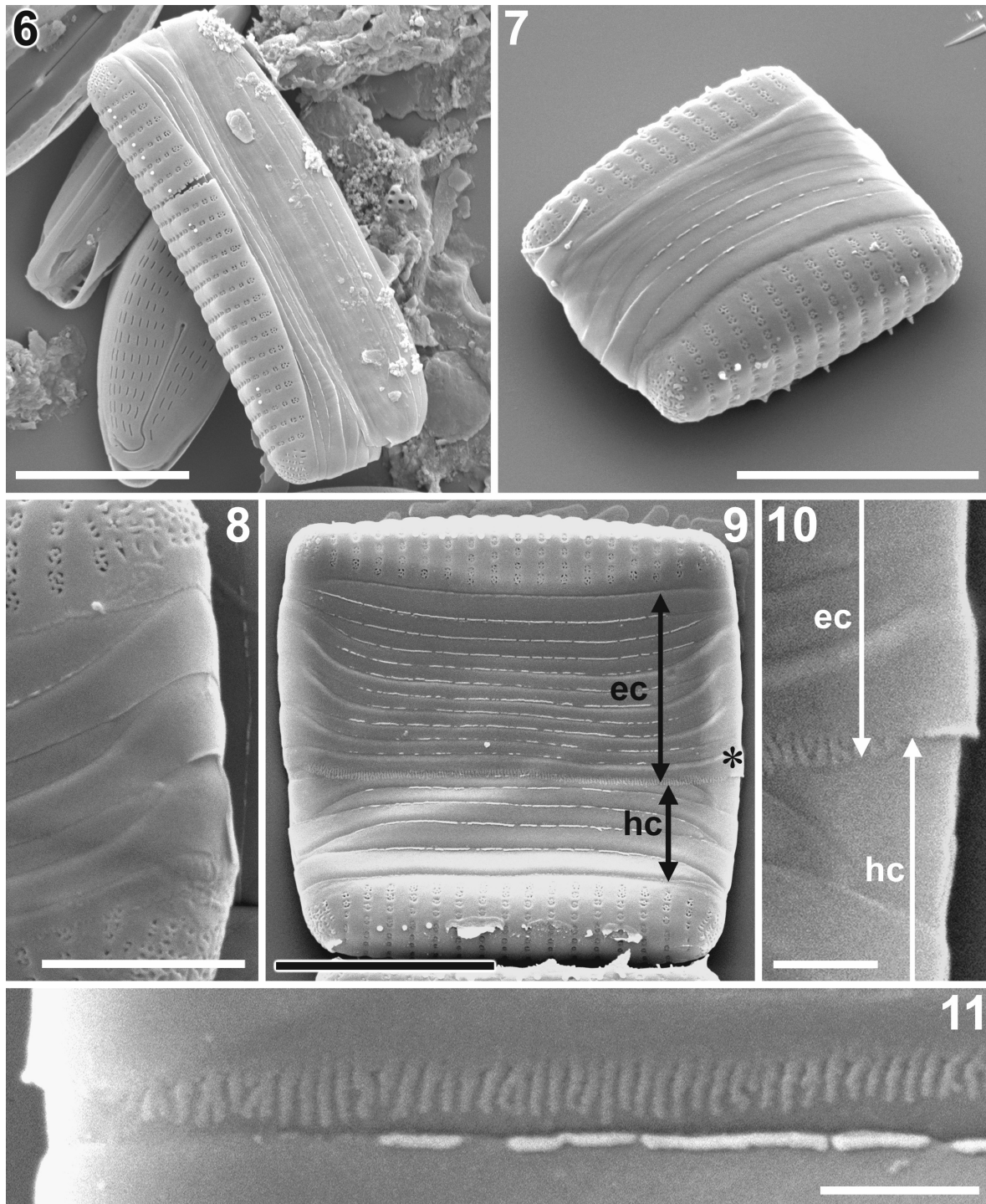
- Montgomery, R. T. 1978. *Environmental and ecological studies of the diatom communities associated with the coral reefs of the Florida Keys*. Ph.D. Dissertation. Florida State University.
- Nagumo, T and Kobayashi, H. 1990. The bleaching method for gently loosening and cleaning a single diatom frustule. *Diatom* **5**: 45-50.
- Navarro, J. N. 1982. A survey of the marine diatoms of Puerto Rico. IV. Suborder Araphidinea: Families Diatomaceae and Protoraphidaceae. *Botanica Marina* **25**: 247-263.
- Posada, D. and Crandall, K. A. 1998. Modeltest: testing the model of DNA substitution. *Bioinformatics* **14**: 817-818.
- Ricard, M. 1987. Diatomophycées. In: *Atlas du phytoplancton marin* (Ed. By A. Sournia), vol. 2. Editions de CNRS, Paris, France, 297 pp.
- Ronquist, F and Huelsenbeck, J. P. 2003. MRBAYES 3: Bayesian phylogenetic inference under mixed models. *Bioinformatics* **19**: 1572-1574.
- Round, F. E. and Bukhtiyarova, L. 1996. Four new genera based on *Achnanthes* (*Achnanthidium*) together with a re-definition of *Achnanthidium*. *Diatom Res.* **11**: 345-361.
- Round, F. E. and Crawford, R. M. 1990. Phylum Bacillariophyta. In Margulis, L., Corliss, J. O., Melkonian, M. and Chapman, D. J. (Eds.) *Handbook of Protoctista*. Jones and Bartlett, Boston, pp. 574-596.
- Round, F. E., Crawford, R. M. and Mann, D. G. 1990. *The diatoms. Biology and morphology of the genera*. Cambridge University Press, Cambridge, 747 pp.
- Simonsen, R. 1979. The diatom system: ideas on phylogeny. *Bacillaria* **2**: 9-71.
- Sorhannus, U. 2007. A Nuclear-Encoded Small-Subunit Ribosomal RNA timescale For Diatom Evolution. *Mar. Micropaleontol.* **65**: 1-12.
- Swofford, D. L. 2002. "PAUP*. *Phylogenetic Analysis Using Parsimony (* and other methods)*. Version 4.0b10," Sinauer Associates, Sunderland, MA.
- Takano, H. 1964. Notes on marine littoral diatoms from Japan-II. *Bull. Tokai Reg. Fish. Res. Lab.* **39**: 13-23.
- Williams, M. D. 1988. An illustrated catalogue of the type specimens in the Greville diatom herbarium. *Bull. Br. Mus. (Nat. Hist.) Bot.* **18**: 1-148.
- Witkowski, A., Lange-Bertalot, H. and Metzeltin, D. 2000. *Diatom Flora of Marine Coasts I. Iconographia Diatomologica Vol. 7*. A.R.G. Gantner Verlag K.G., Ruggell, Liechtenstein, 925 pp.

Table 1. List of taxa used in this study.

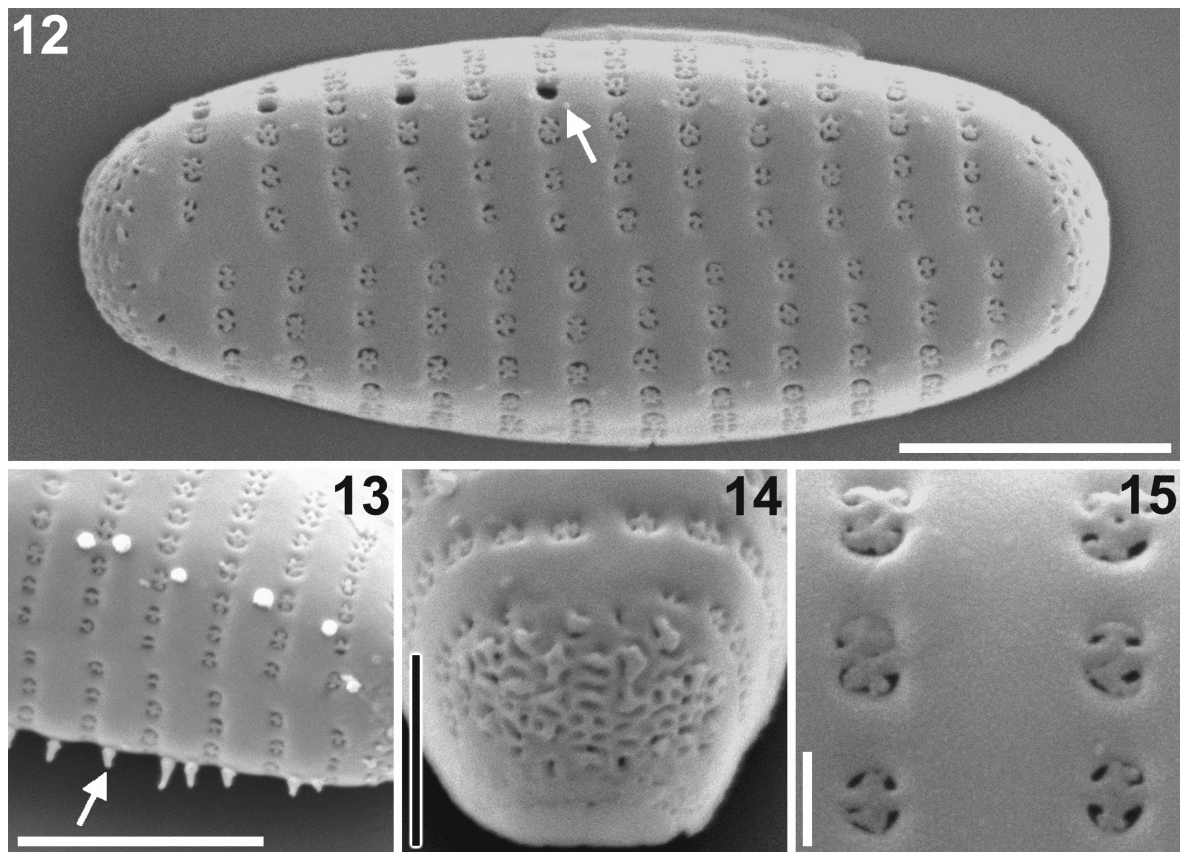
Taxa	Strain	accession	GC (%)
<i>Asterionellopsis gracialis</i> (Castracane) Round	p119	AB425080	46.67
<i>Asteroplanus karianus</i> (Grunow) Gardner <i>et</i> Crawford	p132	AB425081	46.84
<i>Dimeregramma minor</i> var. <i>nana</i> (Gregory) Ralfs	s0355	AB425083	49.40
<i>Neofragilaria nicobarica</i> Desikachary, Prasad <i>et</i> Prema	s0371	AB425084	47.35
<i>Plagiogramma atomus</i> Greville	s0330	AB425082	51.62
<i>Psammogramma vigoensis</i> S.Sato <i>et</i> Medlin	s0391	AB425085	47.01
<i>Rhaphoneis amphiceros</i> Ehrenberg	s0296	AB425087	46.50
<i>Talaroneis posidoniae</i> Kooistra <i>et</i> De Stefano	WK59	AB425086	48.72



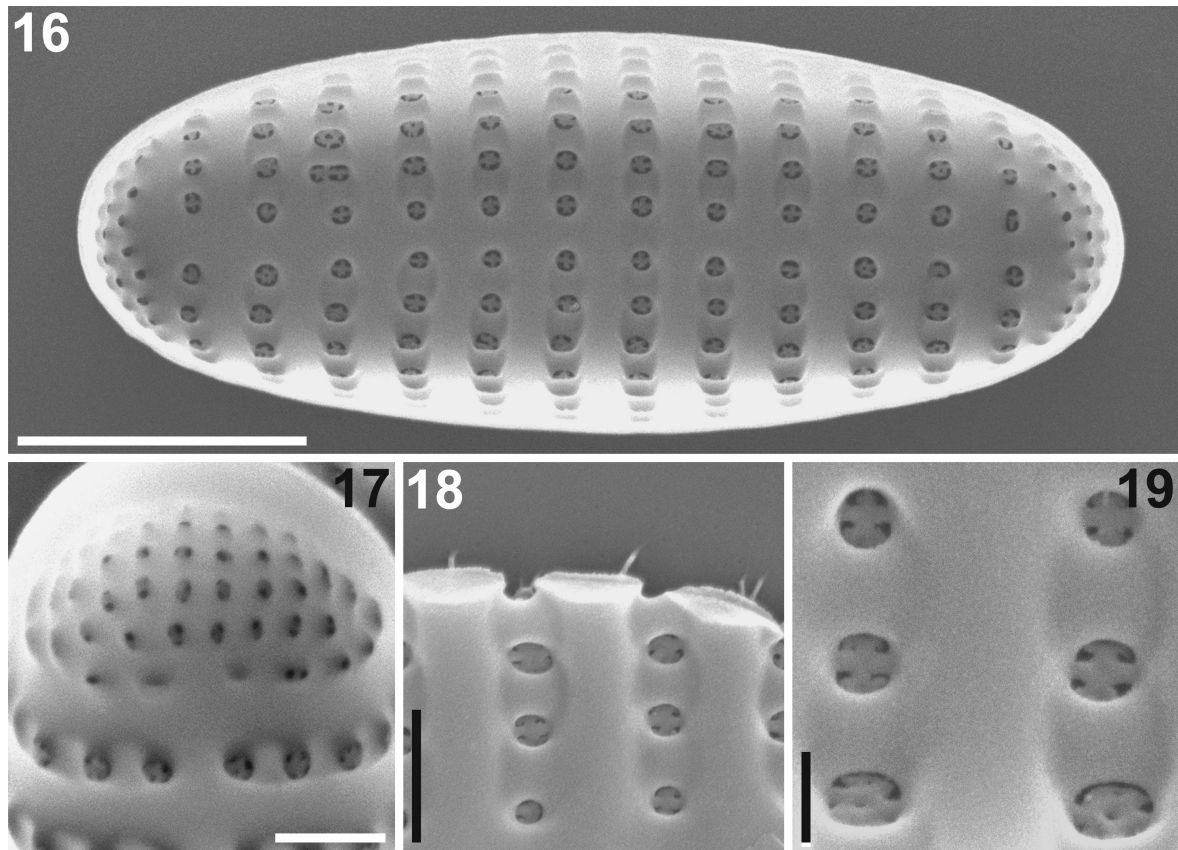
Figs 1-5. *Psammogramma vigoensis*. Strain s0391. LM. **Fig. 1.** Living cells forming a chain colony. **Fig. 2.** Cleaned frustule in girdle view. **Figs 3-5.** Cleaned valve in valve view. Scale bars = 10 μm (Fig. 1) and 2 μm (Figs 2-5).



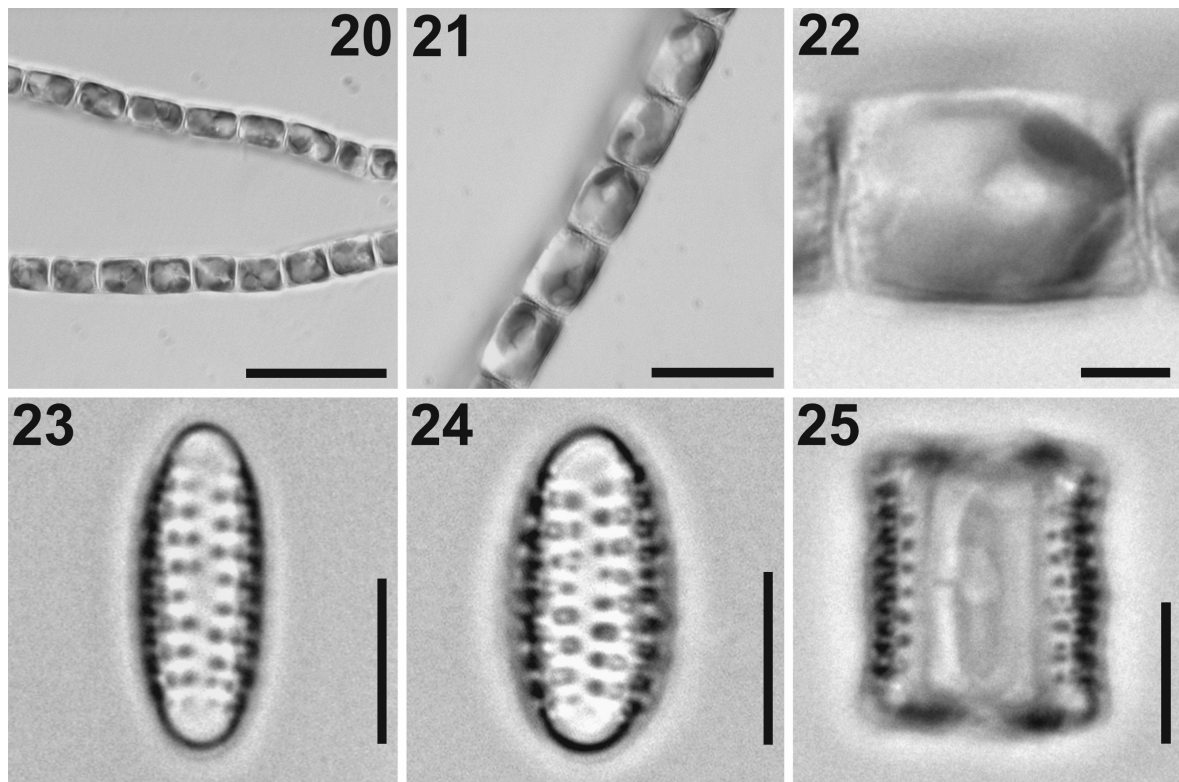
Figs 6-11. *Psammogramma vigoensis*. Field sample SC1 (Fig. 6) and strain s0391 (Figs 7-11). Frustule. SEM. **Fig. 6.** Large frustule. **Fig. 7.** Frustule. Note all bands are plain. **Fig. 8.** Tilted view of frustule end showing curved copulae. **Fig. 9.** Frustule showing epicingulum (ec) overlapping hypocingulum (hc). **Fig. 10.** Enlarged view of area marked by asterisk in Fig. 9. Perivalvar end of hypocingulum often has fringed copula. **Fig. 11.** Fringed end of copula. Scale bars = 5 μm (Figs 6, 7), 1 μm (Fig. 8), 2 μm (Fig. 9) and 0.5 μm (Figs 10, 11).



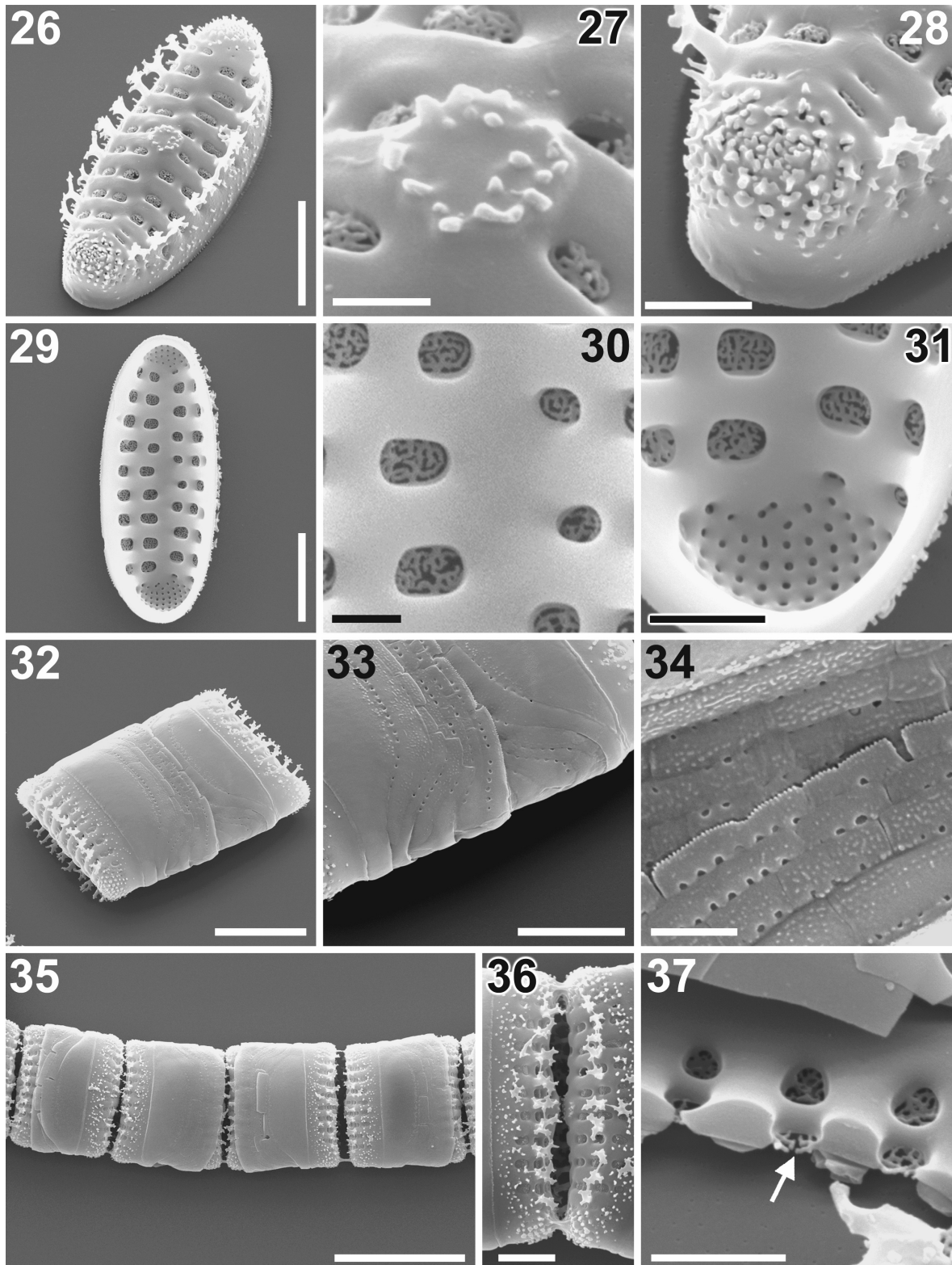
Figs 12-15. *Psammogramma vigoensis*. Strain s0391. External view of valve. SEM. **Fig. 12.** Whole valve. Arrow indicates granule on valve face-mantle junction. **Fig. 13.** Enlargement of tilted valve. Arrow indicates spinule on valve face-mantle junction. **Fig. 14.** Apical pore field. Note regular pore system is obscured by fine ornament. **Fig. 15.** Fine rotulae occluding areolae. Scale bars = 2 μm (Figs 12-13) and 1 μm (Fig. 14) and 0.2 μm (Fig. 15).



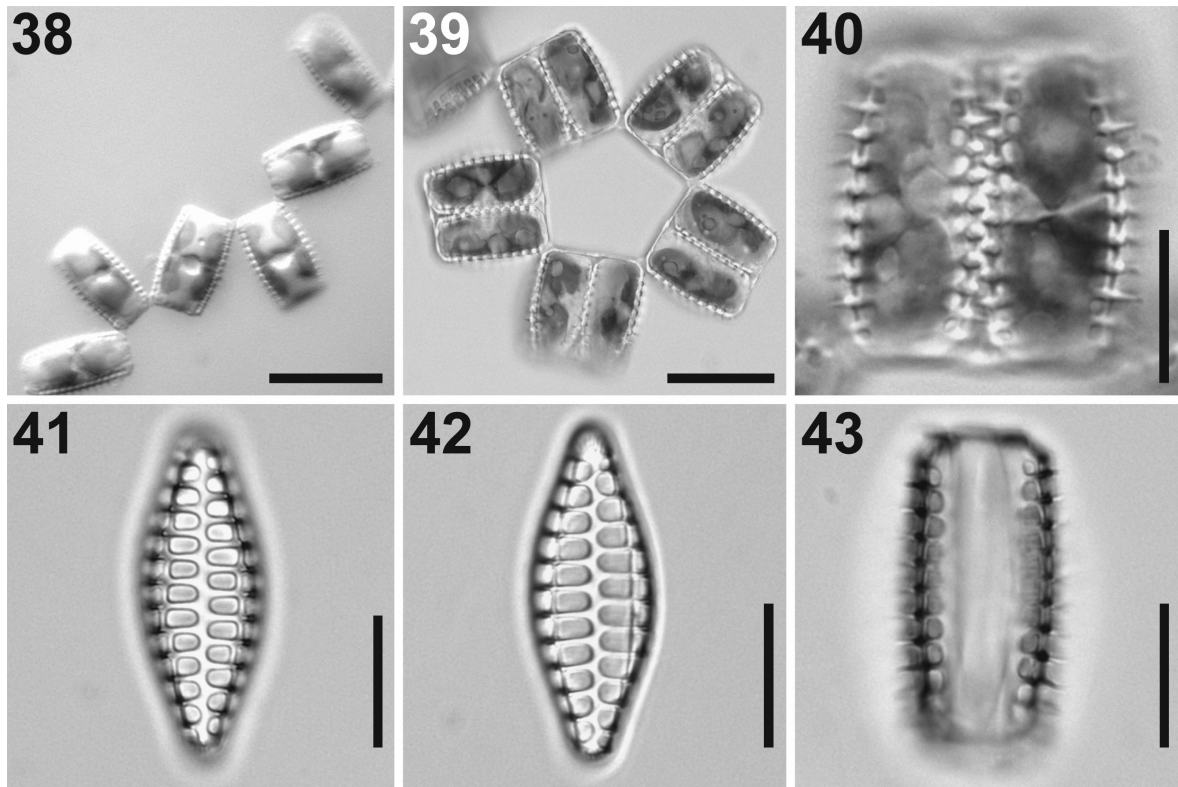
Figs 16-19. *Psammogramma vigoensis*. Strain s0391. Internal view of valve. SEM. **Fig. 16.** Whole valve. **Fig. 17.** Enlargement of apical pore field. Note fine regular arrangement of pores. **Fig. 18.** Broken valve showing single layered valve. Spines are seen at external side. **Fig. 19.** Fine rotae occluding areolae. Scale bars =2 μm (Fig. 16), 0.5 μm (Figs 17-18) and 0.2 μm (Fig. 19).



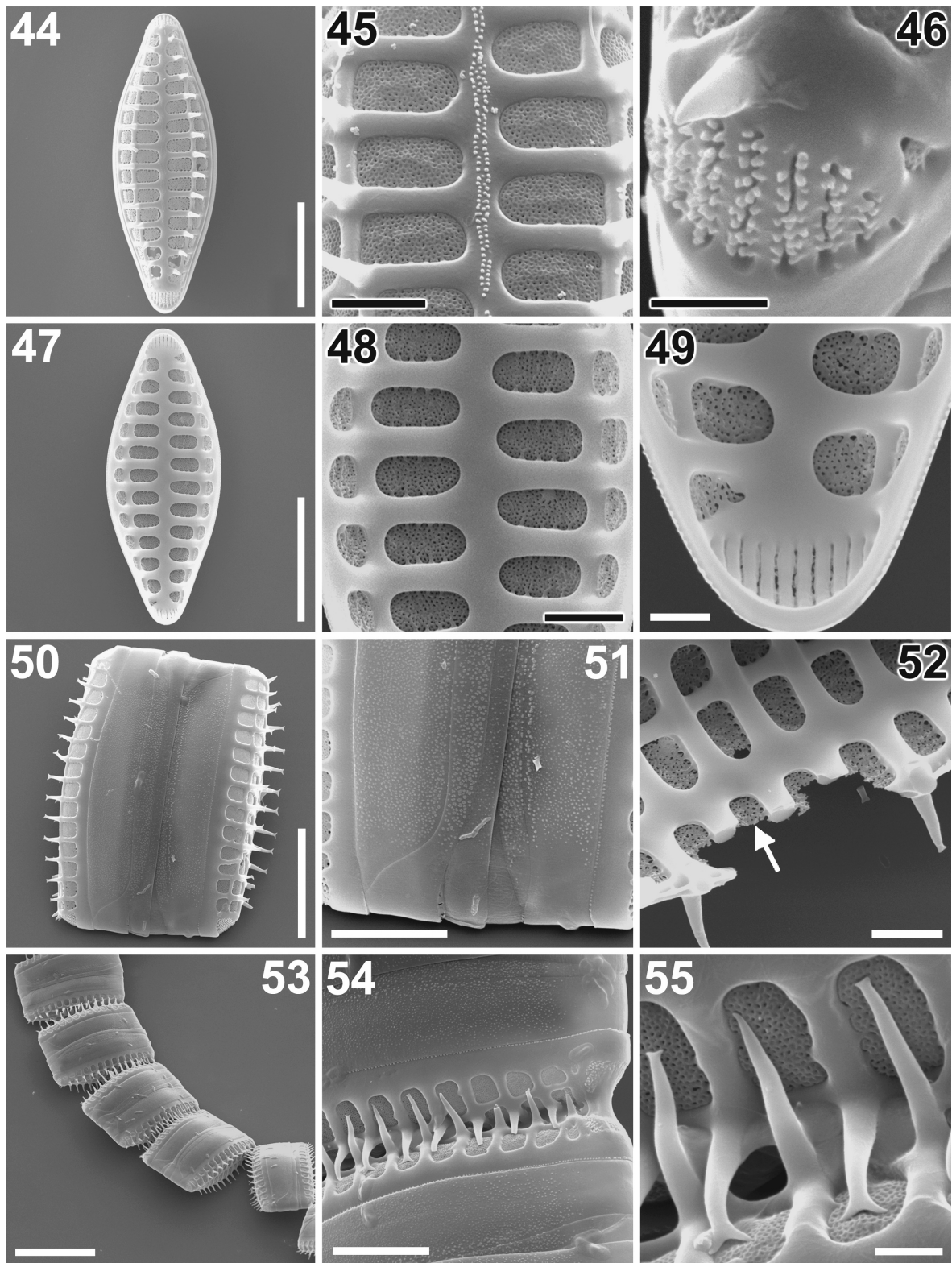
Figs 20-25. *Dimeregramma minor* var. *nana*. Strain s0355. LM. **Figs 20-21.** Chain colony. **Fig. 22.** Enlarged living cell showing plastids surrounding nucleus. **Figs 23-24.** Cleaned valve. **Fig. 25.** Cleaned frustule in girdle view. Scale bars = 20 μm (Figs 20-21); 5 μm (Figs 22-25).



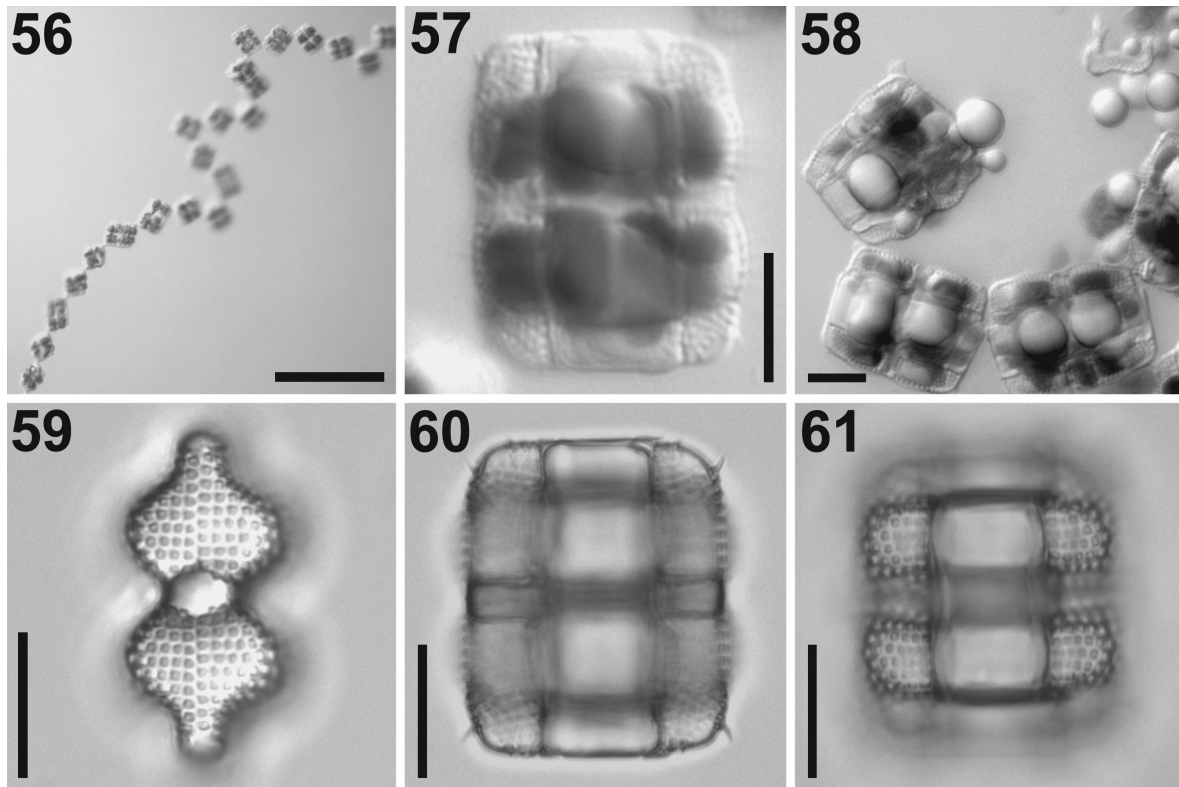
Figs 26-37. *Dimeregramma minor* var. *nana*. Strain s0355. SEM. **Fig. 26.** External valve view. **Fig. 27.** Enlarged view of Fig. 26 showing central boss at middle of valve. **Fig. 28.** Apical pore field covered with ornaments. **Fig. 29.** Internal valve view. **Fig. 30.** Enlarged view of Fig. 29 showing valve middle. Note central boss is unrecognizable internally. **Fig. 31.** Internal apical pore field. **Fig. 32.** Frustule. **Fig. 33.** Enlarged view of Fig. 32 showing one end of frustule. **Fig. 34.** Areolate copulae. Note some copulae are fragmented. **Fig. 35.** Chain colony. **Fig. 36.** Enlarged view of Fig. 35 showing connected part of cells. Note spines and central boss are not involved with colony formation. **Fig. 37.** Broken valve showing single layered valve. Arrow indicates rota located close to external surface. Scale bars = 3 μm (Figs 26, 29, 33), 0.5 μm (Figs 27, 30), 1 μm (Figs 28, 31, 34, 37), 5 μm (Fig. 32), 10 μm (Fig. 35) and 2 μm (Fig. 36).



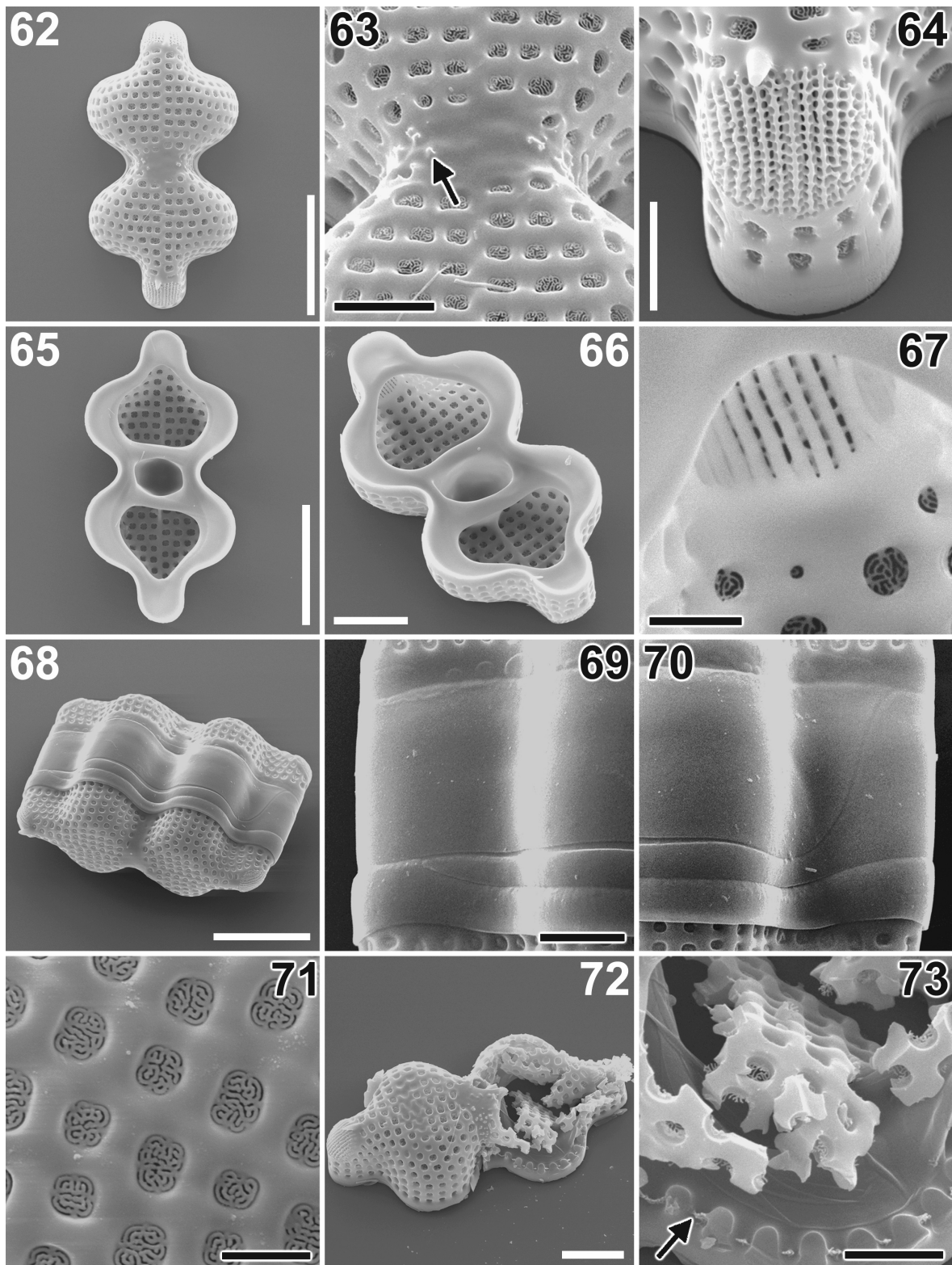
Figs 38-43. *Neofragilaria nicobarica*. Strain s0371. LM. **Fig. 38.** Zig-zag colony. **Fig. 39.** Stellate colony. **Fig. 40.** Living cell showing chloroplast structure. **Figs 41, 42.** Cleaned valves. **Fig. 43.** Cleaned frustule in girder view. Scale bars = 20 μm (Figs 38, 39) and 10 μm (Figs 40-43).



Figs 44-55. *Neofragilaria nicobarica*. Strain s0371. SEM. **Fig. 44.** External valve view. **Fig. 45.** Enlarged view of Fig. 44 showing granuled sternum. **Fig. 46.** Spine and apical slit area ornamented with granules. **Fig. 47.** Internal valve view. **Fig. 48.** Enlarged view of Fig. 47 showing valve middle. Note sternum is plain internally. **Fig. 49.** Internal apical slit area. **Fig. 50.** Frustule. **Fig. 51.** Enlarged view of Fig. 50 showing one end of frustule. **Fig. 52.** Broken valve showing single layered valve. Arrow indicates cribrum located close to internal surface. **Fig. 53.** Chain colony. **Fig. 54.** Connecting part of colony. Note spines do not contribute to linking. **Fig. 55.** Enlarged view of Fig. 54 showing bifurcate end of spine fitted to cribrum of sibling valve. Scale bars = 10 μm (Figs 44, 47, 50), 2 μm (Figs 45, 48, 52), 1 μm (Figs 47, 49, 55), 5 μm (Figs 51, 54) and 20 μm (Fig. 53).



Figs 56-61. *Plagiogramma atomus*. Strain s0330. LM. **Fig. 56.** Zig-zag colony. **Fig. 57.** Living cell showing chloroplast structure. **Fig. 58.** Broken cells. Note lipid escaped from cells. **Fig. 59.** Cleaned valves. **Figs 60, 61.** Cleaned frustule in girdle view, different focus. Scale bars = 100 μm (Fig. 56); 10 μm (Figs 57-61).



Figs 62-73. *Plagiogramma atomus*. Strain s0330. SEM. **Fig. 62.** External valve view. **Fig. 63.** Enlarged view of Fig. 62 showing central hyaline area. Arrow indicates granules. **Fig. 64.** Spine and apical slit area ornamented with ornament on interslit. **Fig. 65.** Internal valve view. **Fig. 66.** Tilted view of Fig. 65. **Fig. 67.** Enlarged view of Fig. 66 showing internal apical pore field. **Fig. 68.** Frustule. **Figs 69-70.** Enlarged view of Fig. 68 showing each end of frustule. **Fig. 71.** External view of rota. **Fig. 72.** Broken valve showing single layered valve. **Fig. 73.** Enlarged view of Fig. 72. Arrow indicates fragment of rota locates close to external surface. Scale bars = 10 μm (Figs 62, 65, 68), 1 μm (Figs 63, 64, 71), 2 μm (Figs 67, 69, 73) and 5 μm (Figs 66, 72)

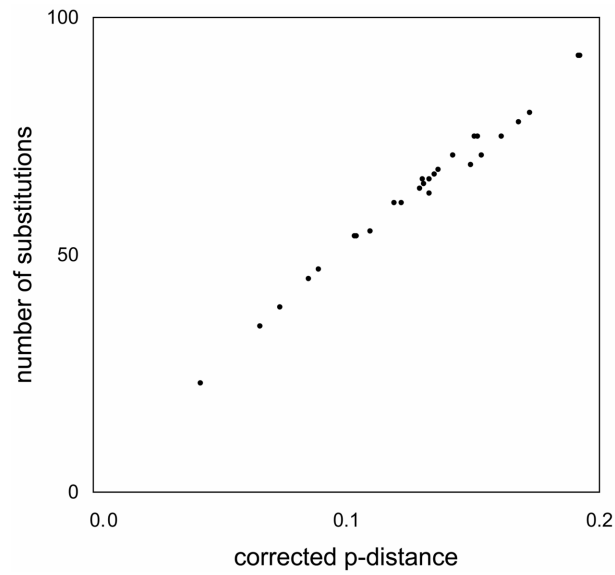


Fig. 74. Saturation plot of partial LSU rDNA. Corrected p -distances versus observed substitutions. Linear proportional distribution of plots indicating no evidence of a potential negative effect of multiple substitutions in the phylogenetic analyses. Corrected p -distances are calculated using a GTR + I + G model with parameters estimated in PAUP.

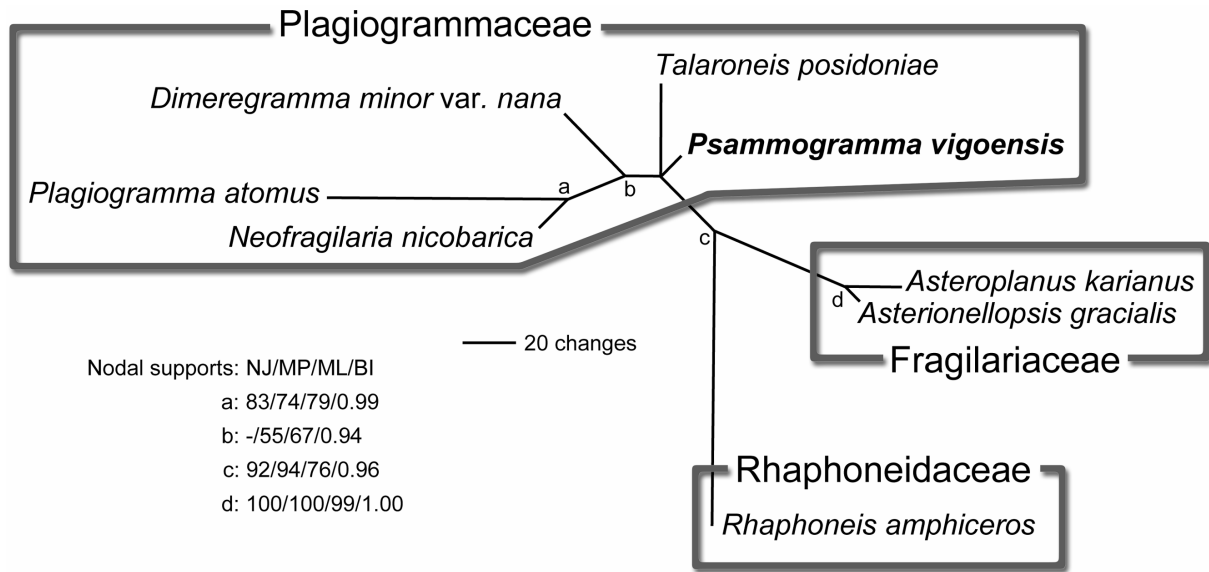


Fig. 75. Phylogenetic tree of Plagiogrammaceae inferred from maximum likelihood (ML) analysis of partial LSU rDNA. Scale bar represents 20 substitutions.

2.10. Publication IX:

**A new araphid diatom genus *Psammoneis* gen. nov. (Plagiogram-
maceae, Bacillariophyta) with three new species based on SSU and
LSU rDNA sequence data and morphology**

SHINYA SATO^{1*}, WIEBE H. C. F. KOOISTRA², TSUYOSHI WATANABE³, SATOKO MATSUMOTO⁴ &
LINDA K. MEDLIN¹

¹*Alfred Wegener Institute for Polar and Marine Research, Am Handelshafen 12, D-27570
Bremerhaven, Germany*

²*Stazione Zoologica 'Anton Dohrn', Villa Comunale, 80121 Naples, Italy*

³*Tokyo University of Marine Science and Technology, 4-5-7 Konan, Minato-ku, 108-8477
Tokyo, Japan*

⁴*Choshi Fisheries High School, 1-1-12 Nagatsuka Cho, Choshi City, Chiba, Japan*

Abstract

Five strains of a hitherto undescribed diatom genus, *Psammoneis*, were established from Japanese and Senegalese marine benthic samples. The strains were analysed using nuclear-encoded sequence markers and morphometric parameters of their silica frustules. Valves of all strains show a sternum with striae perpendicular thereupon, typical for pennate diatoms. They possess apical pore fields and lack a raphe, typical for araphids, but also rimoportulae. Areolar occlusions are not prominent and often appear to be totally absent. Sequence comparison of both the SSU rDNA and the D1/D2 region of the LSU rDNA revealed that the strains group into three markedly distinct genotypes. The strains from different genotypes were also distinguishable by a principal component analysis using four morphometric variables measured on the external valve surface. They are described as three new species in a new genus *Psammoneis*: *P. japonica*, *P. pseudojaponica* and *P. senegalensis*. Molecular phylogenies support placement of the genus *Psammoneis* as a member of the Plagiogrammaceae. The recent observation of frustule fine-structures and the addition of *Psammoneis* to the family alter the circumscription of the family Plagiogrammaceae. Therefore, we provide an emended description of the family.

KEY WORDS: araphid diatom; phylogeny; morphometry; partial LSU rDNA; *Psammoneis*; *P. japonica*; Plagiogrammaceae; *P. pseudojaponica*; *P. senegalensis*; secondary structure; SSU rDNA

INTRODUCTION

Benthic diatoms are ubiquitous in shallow coastal environments and are one of the taxonomically most diverse groups of organisms in estuarine ecosystems (Sullivan & Currin 2000). Because of their high primary production rates, benthic diatoms play an important role in the functioning of benthic trophic webs in intertidal mudflats and shallow water ecosystems of temperate to tropical regions (Cahoon 1999; Underwood & Kromkamp 1999). The large majority of the benthic diatoms in such unstable substrata consists of raphid pennates. These diatoms possess a slit, called a raphe, in their valves and with this organelle they can actively move. Araphid pennate diatoms, which lack a raphe slit in their valves, are largely epiphytic, epizoic, or epipsammic (Round *et al.* 1990). Araphid pennates constitute a paraphyletic assemblage within the monophyletic pennates (e.g. Alverson *et al.* 2006; Kooistra *et al.* 2007; Sims *et al.* 2007; Sinninghe-Damsté *et al.* 2003). In most phylogenetic appraisals, the araphid pennates have a basal separation in two lineages. One consists of a clade containing *Rhaphoneis* Ehrenberg and *Delphineis* Andrews and the planktonic taxa *Asterionellopsis* Round and *Asteroplanus* Gardner et Crawford. The other lineage is vastly more diverse, it contains all other araphid pennate genera and also is sister to a clade to which all of the raphid pennate diatoms belong (Sims *et al.* 2006).

The family Plagiogrammaceae is generally placed in the araphid diatoms (e.g. De Toni 1890; Hustedt 1959; Simonsen 1979). Although the valve outline of plagiogrammacean diatoms is a typical araphid one, they lack some of the distinctive characteristics that can be seen in most of the araphid diatoms, e.g. rimoportulae and a prominent sternum. For these reasons, Round *et al.* (1990) placed the Plagiogrammaceae in the centric diatoms. Kooistra *et al.* (2004) wrote “such problematic taxa are often in critical positions in phylogenetic appraisals.” Results of a SSU rDNA phylogenetic study together with a re-evaluation of morphological characteristics by Kooistra *et al.* (2004) revealed that *Talaroneis* Kooistra et De Stefano be-

longs to the Plagiogrammaceae and is a member of the basal araphid pennate clade that contains *Rhaphoneis*, *Asterionellopsis* and their relatives. Sato *et al.* (2008a) tested this hypothesis by examining additional plagiogrammacean diatoms using morphological and phylogenetic approaches, and described an additional genus *Psammogramma* S. Sato et Medlin, being sister to *Talaroneis posidoniae*. They also transferred the genus *Neofragilaria* Desikachary, Prasad et Prema from Fragilariaceae to the Plagiogrammaceae. As a result, the Plagiogrammaceae currently includes 6 genera: *Dimeregramma* Ralfs, *Glyphodesmis* Greville, *Neofragilaria*, *Plagiogramma* Paddock, *Psammogramma* and *Talaroneis*.

To further address the taxonomy and phylogeny of the Plagiogrammaceae, we have collected additional samples from coastal regions of Japan and Senegal. From the samples, another new genus, *Psammoneis*, is described as a member of the Plagiogrammaceae. We assessed sequence diversity among the specimens using nuclear SSU and partial LSU rDNA and inferred phylogenetic relationships from these sequences. In addition, we examined gross morphological features of living cells and cleaned valves in light microscopy (LM), and recorded frustule ultrastructural details utilising scanning electron microscopy (SEM). We then assessed if specimens could be grouped based on morphometric features gleaned from the SEM pictures and if the groups obtained supported clades inferred from the sequence data. Based on the information obtained, we describe three new species in *Psammoneis*: *P. japonica*, *P. pseudojaponica* and *P. senegalensis*.

MATERIALS AND METHODS

Both natural specimens and clonal cultures were observed in this study. The details of samples examined in this study are summarized in Table 1. All vegetative cells of *Psammoneis* spp. were taken from sands. Single cells were collected to obtain clonal cultures, which were left at ca. 20°C with IMR medium (Eppley *et al.* 1967) in front of a North facing window. Strains were reinoculated approximately once a month. Abnormally small cells sometimes produced by a strain s0354a were reisolated to establish a small-celled culture termed strain s0354b. Culture strains are available upon request to the first author, but may not survive long-term in culture (cf. Chepurnov *et al.* 2004). Voucher specimens of cleaned material of the strains were mounted as permanent slides and have been deposited in the Hustedt Collection, Alfred Wegener Institute, Bremerhaven, Germany (Table 1).

LM (Axioplan, Zeiss, Oberkochen, Germany) with bright field (BF), differential interference contrast (DIC) optics or phase contrast (PC) were used to observe living cells and the cleaned frustules mentioned. To photograph live specimens attaching to the bottom of the culture vessel, an inverted microscope (Axiovert 35, Zeiss) equipped with a digital camera (AxioCam MRc, Zeiss) was used. Fixation was done with 10 % glutaraldehyde for 2 hours at room temperature after which the sample was rinsed several times with distilled water to remove glutaraldehyde. To remove organic material from frustules, samples were treated as modified by Nagumo & Kobayashi (1990) as follows: (1) Centrifuge sample and discard the supernatant to make pellet. (2) Suspend pellet with distilled water. Repeat (1) and (2) several times to complete demineralisation. (3) Re-centrifuge, and then for dissolution of organic matter, add a similar volume of Drano Power-Gel (Johnson Wax GmbH, Haan, Germany), a strong domestic drain cleaner, to the pellet. (4) Vortex mixture and leave it at room temperature for *c.* 30 min. At the end, repeat (1) and (2) several times to complete demineralization.

Cleaned frustules were then mounted on glass slides with Mountmedia (Wako, Osaka, Japan). For SEM examination, the cleaned material was dropped onto cover slips and air dried. Cover slips were fixed onto the SEM stubs by carbon tape, and then coated with gold using SC 500 (Emscope, Ashford, England). A QUANTA 200F (FEI Company, Eindhoven, The

Netherlands) was used for SEM observation at an accelerating voltage of 3 to 25 kV, and 10 - 15 mm working distance. Captured images were adjusted with Adobe Photoshop. Digitally saved LM images were used for measurements of valve length using Scion Image (<http://www.scioncorp.com>).

For morphometric analyses, all scanning electron micrographs were taken under identical conditions to exclude potential mechanical errors being involved in SEM: an accelerating voltage = 10 kV, working distance = 10 mm, magnification = 80,000 and spot size = 3 and no tilt. Exterior views of five valves, which were perpendicular to the electron beam, were taken from the each strain. The measured parts as variables were: V_1) width of virgae, which are silica strips between the striae demarking the punctate areolae, V_2) length of vimines (= length of areola), V_3) width of vimines, which are cross connections of virgae forming areolae, V_4) width of the punctate areolae (Fig. 41). On each valve, measurements were done five times on different points, which were selected randomly from the middle of the valve. As the areola of the interior end of the areolae row, thus alongside the sternum, often had an abnormal shape (see Fig. 41), a second areola from the sternum was measured. The measurements were made on five valves of each strain under SEM.

A principal component analysis (PCA) was calculated from the correlation matrix of the variables. The analysis was carried out with R 2.5.1 (<http://www.R-project.org>). All SEM photographs and data sheets are available from the first author upon request.

Morphological terms were taken from Anonymous (1975), Cox & Ross (1981) and Round *et al.* (1990). In this paper, we use the terms *centric* and *pennate*; the latter is subdivided into *araphid* and *raphid* by the absence/presence of raphe slit because they refer to key morphological features or their absence. These terms do not reflect diatom phylogeny as has been pointed out by morphological (e.g. Simonsen 1972, 1979) and molecular phylogenetic (e.g. Medlin & Kaczmarska 2004) points of view (for review see Sims *et al.* 2006, p. 366) but they do confer an image of a diatom valve. Hereafter the term *araphid pennate diatom* follows a traditional definition, i.e., a diatom that has an elongate valve with a central or slightly lateral sternum, apical pore fields and often apical rimoportulae, but the valves lack a raphe slit. We do not imply that this corresponds to a mono- (holo-) phyletic group, nor that it should be accorded any taxonomic status.

For DNA extraction, samples of *c.* 500 mL of culture were filtered through 3 μ m pore-diameter membrane filters (Millipore SA, Molsheim, France). Filters were immersed in 500 μ L DNA extraction buffer containing 2% (w/v) CTAB, 1.4 M NaCl, 20 mM EDTA, 100 mM Tris-HCl, pH 8, 0.2% (w/v) PVP, 0.01% (w/v) SDS, and 0.2% β -mercaptoethanol. Immersed filters were incubated at 65°C for 5 min, vortexed for a few seconds, and then discarded. Subsequently, the buffer was cooled briefly on ice. DNA was extracted with an equal volume of chloroform-isoamyl alcohol (24:1 [v/v]) and centrifuged in a table-top Eppendorf microfuge (Eppendorf AG, Hamburg, Germany) at maximum speed (14,000 rpm) for 10 min. The aqueous phase was collected, re-extracted with chloroform-isoamyl alcohol and centrifuged as above. Next, the aqueous phase was mixed thoroughly with 0.8 volumes ice-cold 100% isopropanol, left on ice for 5 min, and subsequently centrifuged in a precooled Eppendorf microfuge at maximum speed for 15 min. DNA pellets were washed in 500 μ L 70% (v/v) ethanol, centrifuged for 6 min, and then allowed to air-dry after decanting off the ethanol. DNA pellets were dissolved overnight in 100 μ L water. The quantity and quality of DNA were examined by agarose gel electrophoresis against known standards.

The targeted marker sequence comprised the SSU rDNA within the nuclear rDNA cistron. The marker was PCR-amplified in 25 μ L volumes containing 10 ng DNA, 1 mM dNTPs, 0.5 μ M of forward primer, 0.5 μ M of reverse primer, 1 x Roche diagnostics PCR reaction buffer (Roche Diagnostics, GmbH, Mannheim, Germany), and 1 unit *Taq* DNA polymerase (Roche). The PCR cycling comprised an initial 4-min heating step at 94°C, followed by 35

cycles of 94°C for 2 min, 56°C for 4 min, and 72°C for 2 min, and a final extension at 72°C for 10 min. PCR products were generated using the forward primer A and a reverse primer B (Medlin *et al.* 1988) without the polylinkers. The quantity and length of the PCR products were examined by agarose gel electrophoresis against known standards. Excess primers and dNTPs were removed from the PCR product using the QIAQuick purification kit (QIAGEN, Germany), following the manufacturer's instructions. The cleaned PCR products were then electrophoresed on an ABI 3100 Avant sequencer (Applied Biosystems, CA, USA) using Big Dye Terminator v3.1 sequencing chemistry (Applied Biosystems, CA, USA) with the sequencing primers specified by Elwood *et al.* (1985).

Besides the *Psammoneis* spp. sequences, sequences of *Talaroneis posidoniae* (Kooistra *et al.* 2004) and four other members of the Plagiogrammaceae (Sato *et al.* 2008a), *Dimeregramma minor* var. *nana*, *Neofragilaria nicobarica*, *Plagiogramma atomus* and *Psammogramma vigoensis* (only LSU), were included in this study.

The obtained 18S rDNA sequences were aligned with publicly available sequences retrieved from GenBank (Table 2) first using ClustalX (Thompson *et al.* 1997), and then refined by referring to the secondary structure model of the 18S rRNA at the database of the structure of rRNA (Van de Peer *et al.* 1998). Finally, ambiguously aligned positions were excluded using BioEdit 7.0.2 (Hall 1999), resulting 1686 positions in the dataset. The dataset consisted of 188 operational taxonomic units (OTUs) including *Bolidomonas* as outgroup (Guillou *et al.* 1999). The alignment examined in this study is available on TreeBASE (SN3864).

PCR and sequencing of LSU, the D1/D2 regions of the nuclear 28S rDNA, was done following Beszteri *et al.* (2005). The obtained partial LSU rDNA sequences were appended to the alignment of Sato *et al.* (2008a), and refined by eye referring to its secondary and tertiary structural information (below). Then, ambiguously aligned positions were excluded, resulting in 10 OTUs and 576 positions in the alignment.

In both SSU and partial LSU rDNA, the sequences of s0305 were identical to s0328 belonging to *P. japonica* and s0354 were identical to s0356 belonging to *P. pseudojaponica*, so s0328 and s0356 were excluded from subsequent phylogenetic analyses.

The secondary structure of the D1-D2 region of LSU rDNA sequenced from *Psammoneis japonica* s0305 was predicted from the secondary structural model of the bryophyte *Funaria hygrometrica* Hedwig (X74114) (Capesius & Van de Peer 1997) as a guideline to aid in the alignment as well as to check the position of mutations in this molecule within the species. The thermodynamical folding prediction was performed by RNA structure 4.5 (Mathews *et al.* 2004) with default parameters. The positional numbering of the SSU rRNA sequence is according to *Bacillaria paxillifer* (M87325) from The European Ribosomal RNA databank (Van de Peer *et al.* 1998; <http://rrna.uia.ac.be>). The terminology of the secondary structure of the SSU rRNA followed Van de Peer *et al.* (1998) and that of the LSU rRNA followed Capesius & Van de Peer (1997).

To determine which model of sequence evolution best fits the data, Akaike Information Criterion (AIC) was performed using Modeltest 3.7 (Posada & Crandall 1998), and the test selected the TIM + I + G model for the SSU and GTR + I + G for the partial LSU rDNA. These models had the following parameter settings: **SSU**, A: 0. 2718, C: 0. 1775, G: 0. 2527 and T: 0. 2980; substitution rates were: A-C = 1.0000, A-G = 2.5768, A-T = 1.0000, C-G = 1.0000, C-T = 4.5111 and G-T = 1.0000; the proportion of invariant sites was 0. 2626, among-site rate heterogeneity was described by a gamma distribution with a shape parameter of 0.5581; **partial LSU**, A: 0. 2464, C: 0. 2075, G: 0. 3090 and T: 0. 2371; substitution rates were: A-C = 0.4311, A-G = 1. 1942, A-T = 0. 8526, C-G = 0. 3558, C-T = 3.7215 and G-T = 1.0000; the proportion of invariant sites was 0. 5068, among-site rate heterogeneity was described by a gamma distribution with a shape parameter of 0.5931.

Phylogenies were estimated using neighbour joining (NJ) , maximum parsimony (MP) , maximum likelihood (ML) and Bayesian inference (BI).

NJ: For the SSU and the partial LSU rDNA, NJ trees were inferred with PAUP* 4.0b10 (Swofford 2002) using NJ of likewise constrained pair-wise ML distances using the model specified by Modeltest 3.7 (above). Nodal support was estimated using NJ bootstrap analyses using the same settings (1,000 replicates).

MP: Only the partial LSU rDNA dataset was analysed with MP analysis. The MP topology was obtained with an exhaustive search in PAUP* 4.0b10. Branch-and-bound search with simple addition sequence option was used for 1,000 bootstrap replications.

ML: Because of large dataset of SSU rDNA, ML analysis was performed using the relatively fast program RAxML-VI-HPC, v2.2.3 (Stamatakis *et al.* 2005) with the GTRMIX model. The analyses were performed 100 times to find the topology receiving the best likelihood using a distinct random starting MP tree and the rapid hill-climbing algorithm. Bootstrap values were obtained by 100 replications with GTRCAT model. For partial LSU rDNA, an exhaustive search was performed using PAUP* 4.0b10 with the model selected by Modeltest 3.7 (above). Branch-and-bound search was used for 1,000 bootstrap replications.

BI: For SSU and partial LSU rDNA, the Message Passing Interface (MPI) version of MrBayes 3.1.2 (Huelsenbeck & Ronquist 2001; Ronquist & Huelsenbeck 2003; Altekar 2004) was used for BI with the GTR + I + G model to estimate the posterior probability distribution using Metropolis-Coupled Markov Chain Monte Carlo (MCMCMC) (Ronquist & Huelsenbeck 2003). MCMCMC from a random starting tree was used in these analyses with two independent runs and 1 cold and 3 heated chains. The Bayesian analyses were run for 20 million and 10 million generations for SSU and LSU dataset, respectively with trees sampled every 100th generation. To increase the probability of chain convergence, we sampled trees after the standard deviation values (ASDSF) of the two runs were below 0.01 to calculate the posterior probabilities (i.e., after 10,200,000 and 2,000,000 generations, for SSU and partial LSU rDNA, respectively). The remaining phylogenies were discarded as burn-in.

RESULTS

Psammoneis gen. nov. S. Sato, Kooistra et Medlin

Cellulae inter se affixis in coloniis cateniformibus rectis vel fractiflexis, in aspectu cingulari rectangularibus, chloroplastis duobus in quoque cellula. Taeniae numerosae sine poris atque circularia apertae, inter se implexae. Valvae lanceolatae vel ellipticae. Superficies valvae plana, limbo non profundo. Costa centralis distincta. Striae uniseriatae et interdum in quoque latere costae alternatim dispositae. Areolae longitudinaliter elongatae. Areae pororum apicalium in extremis ambobus dispositae. Rimoportula carens.

Cells attach to form zig-zag or straight chain colonies. Cells rectangular in girdle view. Two plastids per cell. Bands numerous, all are plain and open hoops. Bands interlaced one another. Valves lanceolate to elliptic. Valve face flat with shallow mantle. Sternum distinct. Striae uniseriate, and sometimes arranged alternately on the each side of sternum. Areolae longitudinally elongated. Apical pore fields at both ends of valve. Rimoportula absent.

This genus can be distinguished from the other Plagiogrammacean genera by the longitudinally elongated areolae as well as their placement in a molecular phylogeny. The absence of rimoportulae are also seen in the other araphid lineage, which is designated clade 2 *sensu* Medlin *et al.* (2008a) and which includes *Staurosira* Mereschkowsky and its relatives. However, *Psammoneis* differs from these Clade 2 genera in having a straight, prominent sternum, to which parallel striae are arranged perpendicularly. Furthermore, the valve margin of the *Psammoneis* lacks any linking structure that can usually be observed in the members of the clade 2 genera (Medlin *et al.* 2008a).

TYPE SPECIES: *P. japonica* sp. nov. S. Sato, Kooistra et Medlin

***Psammoneis japonica* sp. nov. S. Sato, Kooistra et Medlin**

Figs 1-2, 6-9, 15-17, 22-26, 29-33

Valvae lanceolatae vel ellipticae, 5.5-12.3 μm longae, 2.6-4.3 μm latae, striis 30-31 per 10 μm, areolis 31.15 (± 4.51) nm latae. Ordines in atomis genericis dictis 18S et 28S rDNA propriis/ae. Descriptio sequentiae geneticae 18S rDNA AB433336 et 28S rDNA AB433342.

Valves lanceolate to elliptical. Valve length 5.5-12.3 μm, width 2.6-4.3 μm. Striae 30-31 per 10 μm. Width of areola 31.15 nm (± 4.51). Nucleotide sequences of 18S (AB433336) and 28S rDNA (AB433342) distinctive.

HOLOTYPE: Zu6/44

ISOTYPE: TNS-AL-53996

TYPE STRAIN: s0305

TYPE LOCALITY: Iriomote Island, Okinawa Pref., Japan.

***Psammoneis pseudojaponica* sp. nov. S. Sato, Kooistra et Medlin**

Figs 3-4, 18-20, 27, 34

Valvae ellipticae 2.0-4.8 μm longae 2.3-2.8 μm latae, striis 29-32 per 10 μm, areolis 13.89 (± 0.87) nm latae. Cellulae interdum in formis fragilis (leniter siliceae). Ordines in atomis genericis dictis 18S et 28S rDNA propriis/ae. Descriptio sequentiae geneticae 18S rDNA AB433339 et 28S rDNA AB433343.

Valves elliptical. Valve length 2.0-4.8 μm, width 2.3-2.8 μm. Striae 29-32 per 10 μm. Width of areola 13.89 nm (± 0.87). Cells can produce weakly silicified morphs. Nucleotide sequences of 18S (AB433339) and 28S rDNA (AB433343) distinctive.

Holotype: Zu6/46

Isotype: TNS-AL-53997

Type strain: s0354

Type locality: Iriomote Island, Okinawa Pref., Japan.

***Psammoneis senegalensis* sp. nov. S. Sato, Kooistra et Medlin**

Figs 5, 10-11, 12-14, 21, 28, 35

Valvae ellipticae 4.3-14.0 μm longae 2.7-3.6 μm latae, striis 26 per 10 μm, areolis 26.33 (± 3.42) nm latae. Ordines in atomis genericis dictis 18S et 28S rDNA propriis/ae. Descriptio sequentiae geneticae 18S rDNA AB433341 et 28S rDNA AB433344.

Valves elliptical. Valve length 4.3-14.0 μm, width 2.7-3.6 μm. Striae 26 per 10 μm. Width of areola 26.33 nm (± 3.42). Nucleotide sequences of 18S (AB433341) and 28S rDNA (AB433344) distinctive.

Holotype: Zu6/49

Isotype: TNS-AL-53998

Type strain: s0387

Type locality: Goree Island, Dakar, Senegal.

Morphological data

Observations of the living material of *Psammoneis japonica* showed sequential movement of the plastids during the cell cycle, although not all of the stages have been recorded (Fig. 1). Each cell of *Psammoneis* spp. contained two plastids (Figs 1-5). Rectangular cells were attached to each other usually at both or one end of the valve making straight or zig-zag chains (Figs 1-5, 13-14).

No significant difference in gross morphology among the species was observed in LM except for valve outline, which was generally a consequence of cell size difference in diatoms. Valves were lanceolate in *P. japonica* (Figs 6-7), whereas elliptical valves were found in *P. pseudojaponica* and *P. senegalensis* (Figs 9-11). Parallel striae were arranged perpendicular to the sternum (Figs 6-11). Valve dimensions measured on each strain are summarized in Table 3. The largest cells of *P. senegalensis* were observed in the natural sample, and were measured only with SEM (in Fig. 14).

Cells of *P. senegalensis* formed a chain and were attached to the substratum by secreting mucilaginous substances from the apical pore fields in their valve apex (Figs 12-14). Cells belonging to two distinct size classes were found (Fig. 14). The largest cells bore no remnants of auxosporulation, e.g. a fragment of the perizonial bands. All copulae were plain and open (Fig. 15). Frustules of *Psammoneis* spp. had numerous (*c.* 10) copulae (Figs 16-21). Weakly silicified frustules were observed in *P. pseudojaponica* strain s0356 and s0354b, which was sub-sampled from s0354a (compare Fig. 18 and 19).

Valves of *Psammoneis* spp. had a distinct sternum (Figs 22-23, 26-28). At times, a slit-like external opening was observed at one end of the sternum in *P. japonica* (Fig. 22). The valve surface of *Psammoneis* spp. was flat, gently curving into a shallow valve mantle (Fig. 23, 26-28). Apical pore fields were located at the both ends of valve (Fig. 24). Areolae were simple, slit-like perforations elongating longitudinally (Fig. 25). Oclusions were difficult to discern. The valve edge was plain (Fig. 25). Valve shape was similar across all species (Figs

26-28), except for the weakly silicified strains of *P. pseudojaponica* (Figs 19-20). In *P. pseudojaponica* strain s0328, the middle of the striae sometimes had short bars extending transapically across the areolae around the valve mantle (Fig. 26). This valve also showed a possible remnant of areolar occlusions, e.g. 3 rd and 5 th striae from bottom left near the sternum and in the 5 th stria from top right in the first two areolae next to sternum.

Internally, rimoportulae were absent in all species (Figs 29-35). Valves lacked any layered structure (Fig. 32). No significant difference was detected in the qualitative morphology among the species (Figs 29, 33-35). Fig. 34 showed a remnant of an areolar occlusion near the sternum.

Molecular data

SEQUENCE COMPARISONS: Three species of *Psammoneis*, *P. japonica* (strains s0305 and s0328), *P. pseudojaponica* (strains s0354 and s0356) and *P. senegalensis* (strain s0387), were separated by both SSU and partial LSU rDNA sequences. Strains s0305 and s0328 of *P. japonica* shared identical SSU sequences as did strains s0354 and s0356 of *P. pseudojaponica*, whereas the three SSU and LSU genotypes obtained were markedly distinct and corresponded to the three species (Table 4). Most substitutions in the SSU rDNA, including insertions/deletions (indels) and compensating base pair changes (CBCs) in stem regions, were concentrated on helices 17 and 49 (Fig. 36). Most changes did not alter secondary structure; the same pattern was also observed in the partial LSU rRNA (Table 4), in which the D1 segment (helices numbers indicated by B in Fig. 37) was more conserved than the D2 segment (helices numbers indicated by C in Fig. 37). All substitutions in the D1 region were in loops, whereas one CBC and many Hemi-CBCs (changes on one side only, *sensu* Marin *et al.* 2003, Coleman 2000, 2003) were observed in the D2 region. Among the species, 5 multisite gaps, covering in total 15 positions, were observed among the species *P. senegalensis*-*P. japonica* and *P. senegalensis*-*P. pseudojaponica*.

The three new species can easily be distinguished by their secondary structural features in SSU rRNA (Fig. 36). *Psammoneis japonica* has a C-G base pair in position 470-489 in helix 17 and U-G in position 1678-1705 in helix 49. For *P. pseudojaponica*, there is a C-G base pair in position 470-489 in helix 17, and G-U in position 1678-1705 in helix 49. For *P. senegalensis*, the base pair in position 470-489 in helix 17 is A-U, and in position 1678-1765 in helix 49 it is G-U.

PHYLOGENIES: A Bayesian tree inferred from SSU rDNA sequences of 181 diatoms and 7 Bolidophyceae (Table 2) confirmed paraphyly of the araphid diatoms within a robust clade of pennate diatoms (Fig. 38). At the root of the pennate diatoms, the raphoneidacean genera, *Raphoneis* and *Delphineis*, diverged followed by the divergence of a clade with *Asterionellopsis*/*Asteroplanus* and the family Plagiogrammaceae (Fig. 38). The latter clade was sister to a clade consisting in its turn of a polytomy composed of a series of araphid pennate clades and a clade with the araphid diatom *Striatella unipunctata* (Lyngby) Agardh and all raphid pennate diatoms. It should be noted that the clade holding the clade of *Asterionellopsis*/*Asteroplanus*/Plagiogrammaceae and the clade with the remainder of pennates had no support.

Within the Plagiogrammacean clade, *Talaroneis posidoniae* diverged first followed by a clade with *Neofragilaria nicobarica* and *Plagiogramma atomus*, and then by *Dimeregramma minor* var. *nana*. The latter was sister to a clade with the three species of *Psammoneis* obtained in this study. Of the latter three, *P. senegalensis* was the first to diverge (Fig. 38). The topology within the family was resolved with significantly high Bayesian posterior probabilities (BPPs) but not with high bootstrap supports (BSs).

Phylogenetic analyses of partial LSU rDNA sequences resulted in a topology among the Plagiogrammaceae different from that obtained with SSU rDNA sequences. Also, topologies constructed by neighbour joining (NJ), maximum parsimony (MP), (maximum likelihood) ML analyses and Bayesian inference (BI) were incongruent (Fig. 39). The results obtained by ML and BI analyses were substantially similar, despite the fact that the BI tree was not fully resolved. Results of all analyses recovered the same relationships among the three species of *Psammoneis* as well as the sister relationship between *Neofragilaria nicobarica* and *Plagiogramma atomus* (Fig. 39).

Morphometric data

MORPHOMETRIC COMPARISONS: It should be noted that no morphological differences were detected between cleaned (e.g. Fig. 25) and non-cleaned (e.g. Fig. 16) specimens even in high magnification ($\sim \times 100,000$) under SEM, suggesting that the influence of cleaning procedure is negligible. The measured parts as variables are illustrated in Figs 40, 41 and values are presented in Table 5. Because of the weak silicification of *P. pseudojaponica* strain s0354b and s0356, V_3 (width of vimines) and V_4 (width of areolae) could not be measured. We assume that this species is genetically predisposed to weak silicification. The width of areolae, V_4 in Fig. 41, appears the only distinguishing character of each species. Features of striae were examined and summarised in Table 3. Despite the high degree of diversity seen in the width of the virgae and the length of the vimines (V_1 and V_2 in Fig. 41, respectively), the sum of $V_1 + V_2$, indicating a striae density, was not markedly different (Table 3). To see a variability pattern of the striae density in each strain, the width of the virgae (V_1) was plotted against the length of vimines (V_2) (Fig. 42). This showed that the distribution of plots of each strain were partly overlapping, making the feature of the striae density unsuitable as a marker for distinguishing strains/species. The overall plots were distributed on the linear approximation ($R^2 = 0.7728$, Fig. 42), suggesting that stria density is conserved in this group of diatoms.

PRINCIPAL COMPONENTS ANALYSIS: To summarise the variation in four recorded variables (width of virgae, striae, vimines and areolae; see more details in Methods), a principal components analysis of their correlation matrix was performed. The first and second principal components (PCs) accounted for 61.9 and 25.2 % of the total (standardised) variance, respectively (87.1 % of the total variance, Table 6). The third and fourth PCs accounted for 12.9 % of the variance. Inclusion of PCs beyond the second did not contribute substantially to resolve the different strains. Therefore, only the first two PCs were included in further analyses.

Component loadings and variance explained for the PCs are shown in Table 6. V_1 describing the width of virgae (Fig. 41) revealed the heaviest loading on the first PC. The length and width of vimines (V_2 and V_3 , respectively) were also heavily loaded on the first PC. Thus, PC1 reflects the overall dimension of the imperforated area in our sample. V_4 , the width of areolae, had the heaviest loading on the second PC. A plot of these first two PCs for all strains of the species is shown in Fig. 43. Whereas the plots of two strains of *P. japonica* were partly mixed, each species was distinguished in the PCA plot with no overlap (Fig. 43). Because the cultures were always harvested when they were rapidly growing, it is unlikely that silicification differences played a role in these species differences.

DISCUSSION

Three species of *Psammoneis* were described in the present study based on morphological and SSU and LSU rDNA. These species are indistinguishable under LM, but molecular and morphometric analysis of ultrastructural features can separate the taxa. The considerable rDNA

sequence differences among the three species encountered amongst the strains of *Psammoneis* (7-13 in SSU and 19-21 in partial LSU) are surprising given the subtle morphometric differences among the genus. These differences bear comparison with those reported in previous studies on intraspecific and even interspecific differences in diatoms (see Table 7) supporting the species-level differentiation in this genus.

Strain-specific characters were only detected in the strain s0328, which had bars on the middle of the striae around the valve mantle, which extended transapically (indicated by an arrow in Fig. 26). This structure was not found in s0305, belonging to the same species, *P. Japonica*, and likely represents a strain-specific difference. Weakly silicified frustules were only found in *P. pseudojaponica*. Notably, both normal and weakly silicified morphs, observed in s0354a and b strains, respectively, were derived from a single cell of *P. pseudojaponica* (see Methods). Phenotypic plasticity was not tested for both morphs. Long-term culture has often been observed to cause deformities in diatom cell walls (Jaworski *et al.* 1988; Round 1993; Estes & Dute 1994). Although the weakly silicified morph was produced after slightly longer cultivation comparing to the other strains in this study (Table 1), it might not be the primary factor for induction because there is no substantial difference in the cultivated period as follows: normal morph; s0305, s0328, s0354a and s0387 for *c.* 3, 6, 7 and 3 months, respectively after the establishment of the culture, whereas weakly silicified morph; s0354b and s0356 for 8 months. Further study is required to elucidate the biological and ecological role of the weakly silicified morph.

The strains of the different species of *Psammoneis* were indistinguishable in LM and no qualitative feature showed clear differences in SEM. They can only be distinguished clearly by the quantitative and mostly continuous characters using morphometric analyses. Although the difference is very subtle, principal components analysis supported the division of the strains. The three species could thus be considered pseudocryptic *sensu* Mann & Evans (2007). *P. senegalensis* strain s0387 is particularly distinct from others in CBCs in helix 17 of SSU rRNA and insertion/deletions in partial LSU rRNA as well as morphometric valve features. Two relatively closely related Japanese species can also be distinguished using the CBC in helix 49 and other substitutions in both rRNA regions (see Table 4), together with the principal component 2, which was mostly loaded by the width of areolae (V_4 , see Table 6 and Fig. 43), despite being derived from almost sympatric samples. It should be noted that we only examined one or two clones in this study and the morphological plasticity of the characters was not tested. Also, we cannot exclude the possible that the morphological features observed/measured in this study were affected by the age of the cultures; however we harvested only rapidly growing cultures for SEM examination as soon as possible after strain establishment. Thus, the described species are hypotheses that need to be examined with more specimens. Furthermore, detailed crossing experiments with a larger dataset to determine the sexual isolation of each species is also encouraged to assess the biological species limits of *Psammoneis* spp.

Historically, stria density -generally number of striae per 10 μm - has been used as a taxonomic character at the rank of species with the assumption that the stria density is stable in any one species. However, stria densities can vary with environmental conditions (Stoermer 1967; McBride & Edgar 1998; Lundholm *et al.* 1997). This study demonstrated that, at least in *Psammoneis*, the stria density is weakly but certainly conserved even in the strain whose morphology is dramatically deformed as seen in our strains (s0354a and s0354b).

THE FAMILY PLAGIOGRAMMACEAE: Given these morphological and molecular results, we propose that the newly described genus *Psammoneis* is a member of the family Plagiogrammaceae. Other Plagiogrammacean diatoms have prominent, large areolae, which can easily be viewed in LM (Round *et al.* 1990; Sato *et al.* 2008a). SEM highlights this feature clearly, i.e.

the areolae of all members of the family are occluded by a velum (rotae, cribrum or volae). On the other hand, such prominent structures were not observed in *Psammoneis*, although the existence of a delicate occlusion was suggested by the possible siliceous remnants (Figs 26, 34). It is likely that the areolar occlusions of *Psammoneis* are so delicate or organic such that most of them are lost during the cleaning process. The areolar structure and its possible weakly structured occlusions observed in *Psammoneis* is morphologically atypical in the family Plagiogrammaceae. However, morphological variability of areolar occlusions have been reported in other closely related diatoms in pennates, for example, in *Staurosira* and *Punctastriata* (Williams & Round 1986; Medlin *et al.* 2008a), and even within single genera *Licmophora* Agardh (Honeywill 1998), *Opephora* (Sabbe & Vyverman 1995) and *Tabularia* (Kützing) Williams et Round (Williams & Round 1986; Snoeijs & Kuylenstierna 1991; Snoeijs 1992). Medlin *et al.* (2008a), in demonstrating the paraphyly of *Staurosira*, *Staurosirella*, *Punctastriata*, *Pseudostaurosira*, suggested that a loss of external valve occlusions would result in the latter two genera, whereas the loss of internal valve occlusions formed the former two genera. They documented fossil taxa containing both the external valve occlusions of *Staurosira* and *Staurosirella* and the internal valve occlusions of *Punctastriata* (Medlin *et al.* 2008a).

The absence of a rimoportula is also typical for this family. This organelle was probably secondarily lost because the Rhaphoneidaceae, *Asterionellopsis*, *Asteroplanus* and the clade with the remainder of the araphid pennates almost all possess rimoportulae. In araphid diatoms, the absence of rimoportulae can also be seen in a clade that comprises *Nanofrustulum* Round, Hallsteinsen & Paasche, *Opephora* Petit, *Pseudostaurosira* Williams et Round, *Pseudostaurosira* Morales, *Punctastriata* Williams et Round, *Staurosira* and *Staurosirella* Williams et Round (Medlin *et al.* 2008a); however, this clade is only distantly related to *Psammoneis* in the 18S rDNA phylogeny (Fig. 38).

The recent observations of frustule fine-structures (Kooistra *et al.* 2004; Sato *et al.* 2008a; and this study) and the addition of *Psammoneis* to the family alter the circumscription of the family Plagiogrammaceae as follows;

Family Plagiogrammaceae De Toni, emend. S. Sato, Kooistra et Medlin

Elongated valves possess apical pore fields and parallel rows of striae, oriented perpendicular to the apical axis; most genera possess a sternum along the apical axis; areolae occluded; absence of rimoportula; Marine habitat.

GENERA GROUPING INTO THIS FAMILY ARE: *Dimeregramma*, *Glyphodesmis*, *Neofragilaria*, *Plagiogramma*, *Psammogramma*, *Psammoneis*

GENERAL PHYLOGENETIC FINDINGS ON SSU rDNA TOPOLOGY OF DIATOMS: As previous phylogenetic studies using SSU rDNA have already shown, the current taxonomic system of the araphid diatoms does not represent their phylogenetic history (e.g. Medlin *et al.* 2000, 2008a, b; Medlin & Kaczmarska 2004; Kooistra *et al.* 2003, 2004; Alverson *et al.* 2006; Sims *et al.* 2006; Sorhannus 2007). For example, the planktonic fragilariacean diatoms *Asterionellopsis*/*Asteroplanus* are distantly related to the nominate genus *Fragilaria* Lyngbye. The clade of *Asterionellopsis*/*Asteroplanus* formed a “basal araphid” clade of pennate diatoms with the Rhaphoneidaceae (only *Rhaphoneis* and *Delphineis* had been used in the past as representatives of the family) and one Plagiogrammaceae (*Talaroneis* had been used), and the rest of “core araphid” pennate diatoms and the raphid diatoms separated after the divergence of the basal araphid diatoms (e.g., Kooistra *et al.* 2004).

In the present study, however, inclusion of additional sequences into the basal araphid diatoms has changed the topology, particularly around the root of pennate diatoms. Now there are three araphid clades. The first one is that of the Rhaphoneidaceae (*Rhaphoneis* and *Delphineis*), which are the first divergence at the base of the pennate diatoms, although the low support of the clade (BPP 0.73 and BSs <50) following the divergence of rhaphoneidacean clade might indicate instability of this relationship. The Plagiogrammaceae and *Asterionellopsis/Asteroplanus* then diverged from the remaining clade of the core araphids sister to the raphid diatoms.

SEXUALITY: In the field material of *P. senegalensis*, cells belonging to two distinct size ranges were found. The absence of cells belonging to the intermediate range might indicate that auxosporulation occurred, although no remnants of the auxospore perizonial band were found. Therefore, it is also possible that the larger cells were not formed after sexual reproduction but through vegetative initial cell formation or vegetative cell size enlargement, as reported in an araphid diatom *Grammatophora marina* (Lyngbye) Kützing (Sato *et al.* 2008b). Sexual reproduction of members in the basal araphid diatoms, including the Plagiogrammaceae, has never been reported. An initial cell was observed in *Plagiogramma staurophorum* (Gregory) Heiberg by Hasle *et al.* (1983, fig. 99) but they mentioned no detail of sexuality in the species. Chepurinov & Mann (2004) reported that they have grown *Rhaphoneis amphiceros* (Ehrenberg) Ehrenberg in culture but have never succeeded in inducing sexual reproduction, either in monoclonal or mixed cultures, even in small-celled clones.

ACKNOWLEDGEMENTS

The authors are grateful to Richard M. Crawford for correction of the manuscript and discussion; Stephan Frickenhaus for establishing parallel processing for Bayesian analyses; Paul A. Fryxell for providing the Latin diagnoses; Friedel Hinz for technical help for LM and SEM; Alberto Amato for kindly providing us the alignment of LSU rDNA of *Pseudo-nitzschia*. We also thank two anonymous reviewers and the associate editor Koen Sabbe for their valuable comments and suggestions. This study was supported by DAAD for doctoral research fellowship to Shinya Sato.

REFERENCES

- ALTEKAR G., DWARKADAS S., HUELSENBECK J. P. & RONQUIST F. 2004. Parallel Metropolis-coupled Markov chain Monte Carlo for Bayesian phylogenetic inference. *Bioinformatics* 20: 407–415.
- ALVERSON A.J., CANNONE J.J., GUTELL R.R. & THERIOT E.C. 2006. The evolution of elongate shape in diatoms. *Journal of Phycology* 42: 655–668.
- ALVERSON A.J. & KOLNICK L. 2005. Intragenomic nucleotide polymorphism among small subunit (18S) rDNA paralogs in the diatom genus *Skeletonema* (Bacillariophyta). *Journal of Phycology* 41:1248–1257.
- AMATO A., KOOISTRA W.H.C.F., LEVIALDI GHIRON J.H., MANN D.G., PRÖSCHOLD T. & MONTRESOR M. 2007 Reproductive isolation among sympatric cryptic species in marine diatoms. *Protist* 158: 193–207.
- ANONYMOUS 1975. Proposals for a standardization of diatom terminology and diagnoses. *Nova Hedwigia, Beiheft* 53: 323–354.
- AKTAN Y. & AYKULU G. 2005. Colonisation of Epipellic Diatoms on the Littoral Sediments of Üzmit Bay. *Turkish Journal of Botany* 29: 83–94

- BEHNKE A., FRIEDL T., CHEPURNOV V.A. & MANN D.G. 2004. Reproductive compatibility and rDNA sequence analyses in the *Sellaphora pupula* species complex (Bacillariophyta). *Journal of Phycology* 40: 193–208.
- BESZTERI B., ÁCS É. & MEDLIN L.K. 2005a. Ribosomal DNA sequence variation among sympatric strains of the *Cyclotella meneghiniana* complex (Bacillariophyceae) reveals cryptic diversity. *Protist* 156: 317–333
- BESZTERI B., ÁCS É. & MEDLIN L.K. 2005b. Conventional and geometric morphometric studies of valve ultrastructural variation in two closely related *Cyclotella* species (Bacillariophyta). *European Journal of Phycology* 40: 89–103.
- BESZTERI B., JOHN U. & MEDLIN L.K. 2007. An assessment of cryptic genetic diversity within the *Cyclotella meneghiniana* species complex (Bacillariophyta) based on nuclear and plastid genes, and amplified fragment length polymorphisms. *European Journal of Phycology* 42: 47–60
- CAHOON L.B. 1999. The role of benthic microalgae in neritic ecosystems. *Oceanography and Marine Biology. An Annual Review* 37: 47–86
- CAPESIUS I. & VAN DE PEER Y. 1997. Secondary structure of the large ribosomal subunit RNA of the moss *Funaria hygrometrica*. *Journal of Plant Physiology* 151: 239–241
- CHEPURNOV V.A. & MANN D.G. 2004. Auxosporulation of *Licmophora communis* (Bacillariophyta) and a review of mating systems and sexual reproduction in araphid pennate diatoms. *Phycological Research* 52: 1–12
- COLEMAN A.W. 2000. The significance of a coincidence between evolutionary landmarks found in mating affinity and a DNA sequence. *Protist* 151: 1–9
- COLEMAN A.W. 2003. ITS2 is a double-edged tool for eukaryote evolutionary comparisons. *TRENDS in Genetics* 19: 370–375
- COX E.J. & ROSS R. 1981. The striae of pinnate diatoms. In: *Proceedings of the 6th International Diatom Symposium on Recent and Fossil Diatoms* (Ed. by R. Ross), pp. 267–278. O. Koeltz, Koenigstein.
- DE TONI G.B. 1890. Sulla *Navicula aponina* Kuetz. e sui due generi *Brachysira* Kuetz. e *Libellus* Cleve. *Atti del Rale Istituto Veneto di Scienze, Lettere ed Arti* 1890: 967–971
- ELWOOD H.J., OLSEN G.J. & SOGIN M.L. 1985. The small subunit ribosomal DNA gene sequences from the hypotrichous ciliates *Oxytricha nova* and *Stylonichia pustulata*. *Molecular Biology and Evolution* 2: 399–410.
- EPPLEY R.W., HOLMES R.W. & STRICKLAND J.D.H. 1967. Sinking rates of the marine phytoplankton measured with a fluorochromometer. *Journal of Experimental Marine Biology and Ecology* 1: 191–208.
- ESTES L. & DUTE R.R. 1994 Valve abnormalities in diatom clones maintained in long-term culture. *Diatom Research* 9: 249–258.
- EVANS K.M., WORTLEY A.H. & MANN D.G. 2007. An assessment of potential diatom “barcode” genes (*cox1*, *rbcL*, 18S and ITS rDNA) and their effectiveness in determining relationships in *Sellaphora* (Bacillariophyta). *Protist* 158: 349–364.
- GUILLOU L., CHRETIENNOT-DINET M.-J., MEDLIN L.K., CLAUSTRE H., LOISEAUX-DE GOËR S. & VAULOT D. 1999. *Bolidomonas*: a new genus with two species belonging to a new algal class, the Bolidophyceae class. nov. (Heterokonta). *Journal of Phycology* 35: 368–381.
- HALL T.A. 1999. BioEdit: a user-friendly biological sequence alignment editor and analysis program for Windows 95/98/NT. *Nucleic Acids Symposium Series* 41: 95–98.

- HASLE G.R., VON STOSCH H.A. & SYVERTSEN E.E. 1983. Cymatosiraceae, a new diatom family. *Bacillaria* 6: 9–156
- HONEYWILL C. 1998. A study of British *Licmophora* species and a discussion of its morphological features. *Diatom Research* 13: 221–271
- HUELSENBECK J.P. & RONQUIST F. 2001. MRBAYES: Bayesian inference of phylogeny. *Bioinformatics* 17: 754–755.
- HUSTEDT F. 1931. Die Kieselalgen Deutschlands, Österreichs und der Schweiz. In: *Dr L Rabenhorsts Kryptogamenflora von Deutschland, Österreich und der Schweiz*, vol. 7(2:1), pp. 1–176. Akademische Verlagsgesellschaft, Leipzig.
- JAWORSKI G.H.M., WISEMAN S.W. & REYNOLDS C.S. 1988. Variability in sinking rate of the freshwater diatom *Asterionella formosa*: the influence of colony morphology. *British Phycological Journal* 23: 167–176.
- KOOISTRA W., DE STEFANO M., MANN D.G., SALMA N. & MEDLIN L.K. 2003b. Phylogenetic position of *Toxarium*, a pennate-like lineage within centric diatoms (Bacillariophyceae). *Journal of Phycology* 39: 185–197.
- KOOISTRA W.H.C.F., FORLANI G., STERRENBURG F.A.S. & DE STEFANO M. 2004. Molecular phylogeny and morphology of the marine diatom *Talaroneis posidoniae* gen. et sp. nov. (Bacillariophyta) advocate the return of the Plagiogrammaceae to the pennate diatoms. *Phycologia* 43: 58–67.
- KOOISTRA W.H.C.F., GERSONDE R., MEDLIN L.K. & MANN D.G. 2007a. The origin and evolution of the diatoms: their adaptation to a planktonic existence. In: *Evolution of primary producers in the sea* (eds. by P.G. Falkowski & A.H. Knoll), pp. 207–249. Academic Press
- KOOISTRA W.H.C.F., SARNO D., BALZANO S., GU H., ANDERSEN R.A. & ZINGONE A. 2007b. Global Diversity and Biogeography of *Skeletonema* Species (Bacillariophyta). *Protist* (in press) doi:10.1016/j.protis.2007.09.004
- LUNDHOLM N., SKOV J., POCKLINGTON R. & MOESTRUP O. 1997. Studies on the marine planktonic diatom *Pseudo-nitzschia*. 2. Autoecology of *P. pseudodelicatissima* based on isolates from Danish coastal waters. *Phycologia* 36: 381–388
- MANN, D. G. & EVANS, K. M. 2007. Molecular genetics and the neglected art of diatomics. In: *Unravelling the algae – the past, present and future of algal molecular systematics* (Ed. by J. Brodie & J.M. Lewis), pp. 232–266. CRC Press, Boca Raton, Florida.
- MARIN B., PALM A., KLINGBERG M. & MELKONIAN M. 2003. Phylogeny and taxonomic revision of plastid-containing euglenophytes based on SSU rDNA sequence comparison and synapomorphic signatures in the SSU rRNA secondary structure. *Protist* 154: 99–145.
- MATHEWS D.H., DISNEY M.D., CHILDS J.L., SCHROEDER S.J., ZUKER M. & TURNER D.H. 2004. Incorporating chemical modification constraints into a dynamic programming algorithm for prediction of RNA secondary structure. *Proceedings of the National Academy of Sciences of the United States of America* 101: 7287–7292.
- MCBRIDE S.A. & EDGAR R.K. 1998. Janus cells unveiled: frustular morphometric variability in *Gomphonema angustatum*. *Diatom Research* 13: 293–310
- MEDLIN L.K. & KACZMARSKA I. 2004. Evolution of the diatoms: V. Morphological and cytological support for the major clades and a taxonomic revision. *Phycologia* 43: 245–270.
- MEDLIN L., ELWOOD H.J., STICKEL S. & SOGIN M.L. 1988. The characterization of enzymatically amplified eukaryotic 16S-like rRNA coding regions. *Gene* 71: 491–499.

- MEDLIN L.K., ELWOOD H.J., STICKEL S. & SOGIN M.L. 1991. Morphological and genetic variation within the diatom *Skeletonema costatum* (Bacillariophyta): evidence for a new species, *Skeletonema pseudocostatum*. *Journal of Phycology* 27: 514–524.
- MEDLIN L.K., KOOISTRA W.H.C.F. & SCHMID A.M.-M. 2000. A review of the evolution of the diatoms – a total approach using molecules, morphology and geology. In: *The origin and early evolution of the diatoms: fossil, molecular and biogeographical approaches* (Ed. by A. Witkowski & J. Sieminska), pp. 13–35. Szafer Institute of Botany, Polish Academy of Science, Cracow, Poland.
- MEDLIN L.K., JUNG I., BAHULIKAR R., MENDGEN K., KROTH P. & KOOISTRA W.H.C.F. 2008a. Evolution of the Diatoms. VI. Assessment of the new genera in the araphids using molecular data. *Nova Hedwigia* 133: 81–100.
- MEDLIN L.K., SATO S., MANN D.G. & KOOISTRA W.H.C.F. 2008b. Molecular evidence confirms sister relationship of *Ardissonea*, *Climacosphenia* and *Toxarium* within the bipolar centric diatoms. *Journal of Phycology* (in press)
- NAGUMO T & KOBAYASHI H. 1990. The bleaching method for gently loosening and cleaning a single diatom frustule. *Diatom* 5: 45–50
- POSADA D. & CRANDALL K.A. 1998. Modeltest: testing the model of DNA substitution. *Bioinformatics* 14: 817–818
- R DEVELOPMENT CORE TEAM. 2005. R: A language and environment for statistical computing. R Foundation for Statistical Computing, Vienna, Austria. (<http://www.R-project.org>)
- RICARD M. 1987. Diatomophycées. In: *Atlas du phytoplancton marin, vol. 2* (Ed. by A. Sournia), pp.1–297. Editions de CNRS, Paris, France.
- RONQUIST F. & HUELSENBECK J.P. 2003. MrBayes 3: Bayesian phylogenetic inference under mixed models. *Bioinformatics* 19: 1572–1574.
- ROUND F.E. 1993. A *Synedra* (Bacillariophyta) clone after several years in culture. *Nova Hedwigia, Beiheft* 106: 353–359.
- ROUND F.E., CRAWFORD R.M. & MANN D.G. 1990. *The diatoms. Biology and morphology of the genera*. Cambridge University Press, Cambridge. 747 pp.
- SABBE K. & VYVERMAN W. 1995. Taxonomy, morphology and ecology of some widespread representatives of the diatom genus *Opephora*. *European Journal of Phycology* 30: 235–249
- SARNO D., KOOISTRA W.C.H.F., MEDLIN L.K., PERCOPO I. & ZINGONE A. 2005. Diversity in the genus *Skeletonema* (Bacillariophyceae). II. An assessment of the taxonomy *S. costatum*-like species, with the description of four new species. *Journal of Phycology* 41: 151–176.
- SARNO D., KOOISTRA W.C.H.F., BALZANO S., HARGRAVES P.E. & ZINGONE A. 2007. Diversity in the genus *Skeletonema* (Bacillariophyceae): III. Phylogenetic position and morphological variability of *Skeletonema costatum* and *Skeletonema grevillei*, with the description of *Skeletonema ardens* sp. nov. *Journal of Phycology* 43: 156–170.
- SATO S, MANN D.G., NAGUMO T., TANAKA J., TADANO T., MEDLIN L.K. 2008. Auxospore fine structure and variation in modes of cell size changes in *Grammatophora marina* (Bacillariophyta). *Phycologia* 47: 12–27
- SATO S., WATANABE T., KOOISTRA W.H.C.F. & MEDLIN L.K. (submitted). Morphology of four plagiogrammecean diatoms; *Dimeregramma minor* var. *nana*, *Neofragilaria nicobarica*, *Plagiogramma atomus* and *Psammogramma vigoensis* gen. et sp. nov., and their phylogenetic relationship inferred from partial 28S rDNA. *Phycological Research*

- SIMONSEN R. 1979. The diatom system: ideas on phylogeny. *Bacillaria* 2: 9-71
- SIMS P.A., MANN D.G. & MEDLIN L.K. 2006. Evolution of the diatoms: insights from fossil, biological and molecular data. *Phycologia* 45: 361–402.
- SNOEIJIS P. 1992. Studies in the *Tabularia fasciculata* complex. *Diatom Research* 7: 313–344
- SNOEIJIS P. & KUYLENSTIERNA M. 1991. Two new diatom species in the genus *Tabularia* from the Swedish coast. *Diatom Research* 6: 351–365.
- SORHANNUS U. 2007. A nuclear-encoded small-subunit ribosomal RNA timescale for diatom evolution. *Marine Micropaleontology* 65: 1-12.
- STAMATAKIS A, LUDWIG T, & MEIER H. 2005. RAxML-III: A fast program for maximum likelihood-based inference of large phylogenetic trees. *Bioinformatics* 21: 456–463.
- STOERMER E.F. 1967. Polymorphism in *Mastogloia*. *Journal of Phycology* 3: 73-77
- SWOFFORD D. L. 2002. *PAUP**. *Phylogenetic Analysis Using Parsimony (* and other methods)*. Version 4.0b10. Sinauer Associates, Sunderland, MA.
- SULLIVAN M.J. & CURRIN C.A. 2000. Community structure and functional dynamics of benthic microalgae in salt marshes. In: *Concepts and controversies in tidal marsh ecology* (Ed. by M.P. Weinstein & D.A. Kreeger), pp. 81–106. Kluwer Academic Publishers, Dordrecht Germany.
- THOMPSON J.D., GIBSON T.J., PLEWNIAK F., JEANMOUGIN F. & HIGGINS D.G. 1997. The ClustalX windows interface: flexible strategies for multiple sequence alignment aided by quality analysis tools. *Nucleic Acids Research* 24: 4876-4882.
- UNDERWOOD G.J.C. & KROMKAMP J. 1999. Primary production by phytoplankton and micro-phytobenthos in estuaries. *Advances in Ecological Research* 29: 93–153
- VAN DE PEER Y., CAERS A., DE RIJK P. & DE WACHTER R. 1998. Database on the structure of small ribosomal subunit RNA. *Nucleic Acids Research* 26: 179–182
- WILLIAMS D.M. & ROUND F.E. 1986. Revision of the genus *Synedra* Ehrenb. *Diatom Research* 1: 313–339
- WUYTS J., RIJK P.D., VAN DE PEER, Y., PISON G., ROUSSEEUW P. & WACHTER R.D. 2000. Comparative analysis of more than 3000 sequences reveals the existence of two pseudoknots in area V4 of eukaryotic small subunit ribosomal RNA. *Nucleic Acids Research* 28: 4698-4708.

Table 1. Details of sample examined in this study.

Species	Strain	Voucher	Locality	Collection	Harvest ^a
<i>P. japonica</i>	s0305	Zu6/44	Iriomote Island, Okinawa, Japan	17.Oct.2005	24. Jan. 2006
<i>P. japonica</i>	s0328	Zu6/45	Iriomote Island, Okinawa, Japan	17.Oct.2005	21. Apr. 2006
<i>P. pseudojaponica</i>	s0354a	Zu6/46	Iriomote Island, Okinawa, Japan	16.Oct.2005	16. May 2006
<i>P. pseudojaponica</i>	s0354b	Zu6/47	Iriomote Island, Okinawa, Japan	16.Oct.2005	20. Jun. 2006
<i>P. pseudojaponica</i>	s0356	Zu6/48	Iriomote Island, Okinawa, Japan	16.Oct.2005	20. Jun. 2006
<i>P. senegalensis</i>	s0387	Zu6/49	Goree Island, Dakar, The Republic of Senegal	08.Sep.2006	4. Dec. 2006

^aDate of filtration of culture strains.

Table 2. List of taxon and GenBank accessions for SSU and LSU rDNA sequences used in this study.

Taxon	SSU	LSU
<i>Aulacoseira ambigua</i> (Grunow) Simonsen	X85404	
<i>Aulacoseira baicalensis</i> (Meyer) Simonsen	AJ535185	
<i>Aulacoseira baicalensis</i> (Meyer) Simonsen	AJ535186	
<i>Aulacoseira baicalensis</i> (Meyer) Simonsen	AY121821	
<i>Aulacoseira distans</i> (Ehrenberg) Simonsen	X85403	
<i>Aulacoseira islandica</i> (Müller) Simonsen	AJ535183	
<i>Aulacoseira islandica</i> (Müller) Simonsen	AY121820	
<i>Aulacoseira nyassensis</i> (Müller) Simonsen	AJ535187	
<i>Aulacoseira nyassensis</i> (Müller) Simonsen	AY121819	
<i>Aulacoseira skvortzowii</i> Edlund, Stoermer et Taylor	AJ535184	
<i>Aulacoseira subarctica</i> (Müller) Haworth	AY121818	
<i>Actinocyclus curvatulus</i> Janisch	X85401	
<i>Actinoptychus seniarius</i> (Ehrenberg) Héribaud	AJ535182	
<i>Bellerocha malleus</i> (Brightwell) Van Heurck	AF525671	
<i>Biddulphiopsis titiana</i> (Grunow) von Stosch et Simonsen	AF525669	
<i>Chaetoceros curvisetus</i> Cleve	AY229895	
<i>Chaetoceros debilis</i> Cleve	AY229896	
<i>Chaetoceros didymus</i> Ehrenberg	X85392	
<i>Chaetoceros gracilis</i> Schütt	AY229897	
<i>Chaetoceros rostratus</i> Lauder	X85391	
<i>Chaetoceros</i> sp.	AF145226	
<i>Chaetoceros</i> sp.	AJ535167	
<i>Chaetoceros</i> sp.	X85390	
<i>Corethron criophilum</i> Castracane	X85400	
<i>Corethron inerme</i> Karsten	AJ535180	
<i>Corethron hystrix</i> Hensen	AJ535179	
<i>Coscinodiscus radiatus</i> Ehrenberg	X77705	
<i>Cyclotella meneghiniana</i> Kützing	AJ535172	
<i>Cyclotella meneghiniana</i> Kützing	AY496206	
<i>Cyclotella meneghiniana</i> Kützing	AY496207	
<i>Cyclotella meneghiniana</i> Kützing	AY496210	
<i>Cyclotella meneghiniana</i> Kützing	AY496212	
<i>Cyclotella</i> cf. <i>scaldensis</i>	AY496208	
<i>Cymatosira belgica</i> Grunow	X85387	
<i>Detonula confervacea</i> (Cleve) Gran	AF525672	
<i>Ditylum brightwellii</i> (West) Grunow in Van Heurck	AY188181	
<i>Ditylum brightwellii</i> (West) Grunow in Van Heurck	AY188182	
<i>Ditylum brightwellii</i> (West) Grunow in Van Heurck	X85386	
<i>Eucampia antarctica</i> (Castracane) Mangin	X85389	
<i>Guinardia delicatula</i> (Cleve) Hasle	AJ535192	
<i>Guinardia flaccida</i> (Castracane) H. Peragallo	AJ535191	
<i>Helicotheca tamesis</i> (Schrubsole) Ricard	X85385	
<i>Lampriscus kittonii</i> Schmidt	AF525667	
<i>Lauderia borealis</i> Cleve	X85399	
<i>Leptocylindrus danicus</i> Cleve	AJ535175	
<i>Leptocylindrus minimus</i> Gran	AJ535176	
<i>Lithodesmium undulatum</i> Ehrenberg	Y10569	
<i>Melosira varians</i> Agardh	AJ243065	

<i>Melosira varians</i> Agardh	X85402	
<i>Odontella sinensis</i> (Greville) Grunow	Y10570	
<i>Papiliocellulus elegans</i> Hasle, von Stosch et Syvertsen	X85388	
<i>Paralia sol</i> (Ehrenberg) Crawford	AJ535174	
<i>Planktoniella sol</i> (Wallich) Schütt	AJ535173	
<i>Pleurosira laevis</i> (Ehrenberg) Compère	AF525670	
<i>Pleurosira</i> cf. <i>laevis</i>	AJ535188	
<i>Porosira pseudodenticulata</i> (Hustedt) Jousé	X85398	
<i>Proboscia alata</i> (Brightwell) Sundström	AJ535181	
<i>Rhizosolenia imbricate</i> Brightwell	AJ535178	
<i>Rhizosolenia similoides</i> Cleve-Euler	J535177	
<i>Rhizosolenia setigera</i> Brightwell	M87329	
<i>Skeletonema costatum</i> (Greville) Cleve	X52006	
<i>Skeletonema costatum</i> (Greville) Cleve	X85395	
<i>Skeletonema menzelii</i> Guillard, Carpenter et Reimer	AJ535168	
<i>Skeletonema menzelii</i> Guillard, Carpenter et Reimer	AJ536450	
<i>Skeletonema pseudocostatum</i> Medlin	AF462060	
<i>Skeletonema pseudocostatum</i> Medlin	X85393	
<i>Skeletonema subsalsum</i> (Cleve-Euler) Bethge	AJ535166	
<i>Skeletonema</i> sp.	AJ535165	
<i>Stephanopyxis</i> cf. <i>broschii</i>	M87330	
<i>Thalassiosira eccentrica</i> (Ehrenberg) Cleve	X85396	
<i>Thalassiosira guillardii</i> Hasle	AF374478	
<i>Thalassiosira oceanica</i> Hasle	AF374479	
<i>Thalassiosira pseudonana</i> Hasle et Heimdal	AJ535169	
<i>Thalassiosira pseudonana</i> Hasle et Heimdal	AF374481	
<i>Thalassiosira rotula</i> Meunier	AF374480	
<i>Thalassiosira rotula</i> Meunier	AF462058	
<i>Thalassiosira rotula</i> Meunier	AF462059	
<i>Thalassiosira rotula</i> Meunier	X85397	
<i>Thalassiosira weissflogii</i> (Grunow) Fryxell et Hasle	AF374477	
<i>Thalassiosira weissflogii</i> (Grunow) Fryxell et Hasle	AJ535170	
<i>Thalassiosira</i> sp.	AJ535171	
<i>Toxarium undulatum</i> Bailey	AF525668	
<i>Asterionella formosa</i> Hassall	AF525657	
<i>Asterionellopsis glacialis</i> (Castracane) Round	X77701	AB425080
<i>Asteroplanus karianus</i> ¹ (Grunow in Cleve et Grunow)	Y10568	AB425081
Gardner et Crawford		
<i>Cyclophora tenuis</i> Castracane	AJ535142	
<i>Delphineis</i> sp.	AY485465	
<i>Diatoma hyemalis</i> (Roth) Heiberg	AB085829	
<i>Diatoma tenue</i> Agardh	AJ535143	
<i>Dimeregramma minor</i> var. <i>nana</i> (Gregory) Ralfs	AB430598	AB425083
<i>Fragilaria crotonensis</i> Kitton	AF525662	
<i>Fragilariforma virescens</i> (Ralfs) Williams et Round	AJ535137	
<i>Grammatophora gibberula</i> Kützing	AF525656	
<i>Grammatophora oceanica</i> Ehrenberg	AF525655	
<i>Grammatophora marina</i> (Lyngbye) Kützing	AY216906	
<i>Grammonema striatula</i> Agardh ¹	X77704	
<i>Grammonema</i> cf. <i>islandica</i> ¹	AJ535190	
<i>Grammonema</i> sp. ¹	AJ535141	

<i>Hyalosira delicatula</i> Kützing	AF525654	
<i>Licmophora juergensii</i> Agardh	AF525661	
<i>Nanofrustulum shiloi</i> (Lee, Reimer et McEnery) Round, Hallsteinsen et Paasche	AF525658	
<i>Neofragilaria nicobarica</i> Desikachary, Prasad et Prema	AB433340	AB425084
<i>Plagiogramma atomus</i> Greville	AB433338	AB425082
<i>Psammogramma vigoensis</i> S. Sato et Medlin		AB425085
<i>Psammoneis japonica</i> S. Sato, Kooistra et Medlin	AB433336	AB433342
<i>Psammoneis pseudojaponica</i> S. Sato, Kooistra et Medlin	AB433339	AB433343
<i>Psammoneis senegalensis</i> S. Sato, Kooistra et Medlin	AB433341	AB433344
<i>Rhaphoneis amphiceros</i> Ehrenberg	AB433337	AB425087
<i>Rhabdonema arcuatum</i> (Agardh) Kützing	AF525660	
<i>Rhaphoneis</i> cf. <i>belgica</i>	X77703	
<i>Staurosira construens</i> Ehrenberg	AF525659	
<i>Striatella unipunctata</i> (Lyngbye) Agardh	AF525666	
<i>Synedra ulna</i> (Nitzsch) Compère	AJ535139	
<i>Synedra</i> sp. ²	AJ535138	
<i>Tabularia tabulata</i> (Agardh) Williams et Round	AY216907	
<i>Talaroneis posidoniae</i> Kooistra et De Stefano	AY216905	AB425086
<i>Thalassionema nitzschioides</i> (Grunow) Hustedt	X77702	
<i>Thalassionema</i> sp.	AJ535140	
<i>Achnanthes bongrainii</i> (M. Peragallo) A. Mann	AJ535150	
<i>Achnanthes</i> sp.	AJ535151	
<i>Amphora montana</i> Krasske	AJ243061	
<i>Amphora</i> cf. <i>capitellata</i>	AJ535158	
<i>Amphora</i> cf. <i>proteus</i>	AJ535147	
<i>Anomoeoneis sphaerophora</i> (Ehrenberg) Pfitzer	AJ535153	
<i>Bacillaria paxillifer</i> (Müller) Hendey	M87325	
<i>Campylodiscus ralfsii</i> Gregory	AJ535162	
<i>Cocconeis</i> cf. <i>molesta</i>	AJ535148	
<i>Cylindrotheca closterium</i> (Ehrenberg) Reimann et Lewin	M87326	
<i>Cymbella cymbiformis</i> Agardh	AJ535156	
<i>Encyonema triangulatum</i> Kützing	AJ535157	
<i>Entomoneis</i> cf. <i>alata</i>	AJ535160	
<i>Eolimna minima</i> (Grunow) Lange-Bertalot	AJ243063	
<i>Eolimna subminuscula</i> (Manguin) Moser, Lange-Bertalot et Metzeltin	AJ243064	
<i>Eunotia formica</i> var. <i>sumatrana</i> Hustedt	AB085830	
<i>Eunotia monodon</i> var. <i>asiatica</i> Skvortzow	AB085831	
<i>Eunotia pectinalis</i> (Dillwyn) Rabenhorst	AB085832	
<i>Eunotia</i> cf. <i>pectinalis</i> f. <i>minor</i>	AJ535146	
<i>Eunotia</i> sp.	AJ535145	
<i>Fragilariopsis sublineata</i> Hasle	AF525665	
<i>Gomphonema parvulum</i> Kützing	AJ243062	
<i>Gomphonema pseudoaugur</i> Lange-Bertalot	AB085833	
<i>Lyrella atlantica</i> (Schmidt) D. G. Mann	AJ544659	
<i>Navicula cryptocephala</i> var. <i>veneta</i> (Kützing) Grunow	AJ297724	
<i>Navicula diserta</i> Hustedt	AJ535159	
<i>Navicula pelliculosa</i> (Brébisson ex Kützing) Hilse	AJ544657	
<i>Nitzschia apiculata</i> (Gregory) Grunow	M87334	
<i>Nitzschia frustulum</i> (Kützing) Grunow	AJ535164	

<i>Pinnularia cf. interrupta</i>	AJ544658
<i>Pinnularia</i> sp.	AJ535154
<i>Phaeodactylum tricornerum</i> Bohlin	AJ269501
<i>Planothidium lanceolatum</i> (Brébisson ex Kützing) Round et Bukhtiyarova	AJ535189
<i>Pleurosigma</i> sp.	AF525664
<i>Pseudogomphonema</i> sp.	AF525663
<i>Pseudogomphonema</i> sp.	AJ535152
<i>Pseudo-nitzschia multiseriis</i> (Hasle) Hasle	U18241
<i>Pseudo-nitzschia pungens</i> (Grunow ex Cleve) Hasle	U18240
<i>Rossia</i> sp.	AJ535144
<i>Sellaphora capitata</i> Mann et McDonald	AJ535155
<i>Sellaphora pupula</i> (Kützing) Mereschkowsky	AJ544645
<i>Sellaphora pupula</i> (Kützing) Mereschkowsky	AJ544651
<i>Sellaphora pupula</i> (Kützing) Mereschkowsky	AJ544647
<i>Sellaphora pupula</i> (Kützing) Mereschkowsky	AJ544648
<i>Sellaphora pupula</i> (Kützing) Mereschkowsky	AJ544649
<i>Sellaphora pupula</i> (Kützing) Mereschkowsky	AJ544650
<i>Sellaphora pupula</i> (Kützing) Mereschkowsky	AJ544652
<i>Sellaphora pupula</i> (Kützing) Mereschkowsky	AJ544653
<i>Sellaphora pupula</i> (Kützing) Mereschkowsky	AJ544654
<i>Sellaphora laevissima</i> (Kützing) D. G. Mann	AJ544655
<i>Sellaphora laevissima</i> (Kützing) D. G. Mann	AJ544656
<i>Surirella fastuosa</i> var. <i>cuneata</i> (Schmidt) H. Peragallo et M. Peragallo	AJ535161
<i>Thalassiosira antarctica</i> Comber	AF374482
<i>Undatella</i> sp.	AJ535163
<i>Bolidomonas mediterranea</i> Guillou et Chrétiennot-Dinet	AF123596
<i>Bolidomonas pacifica</i> Guillou et Chrétiennot-Dinet	AF123595
<i>Bolidomonas pacifica</i> Guillou et Chrétiennot-Dinet	AF167153
<i>Bolidomonas pacifica</i> Guillou et Chrétiennot-Dinet	AF167154
<i>Bolidomonas pacifica</i> Guillou et Chrétiennot-Dinet	AF167155
<i>Bolidomonas pacifica</i> Guillou et Chrétiennot-Dinet	AF167156
<i>Bolidomonas pacifica</i> Guillou et Chrétiennot-Dinet	AF167157
<i>Convolvata convoluta</i> diatom endosymbiont	AY345013
<i>Peridinium foliaceum</i> endosymbiont	Y10567
<i>Peridinium balticum</i> endosymbiont	Y10566
Uncultured diatom	AY180014
Uncultured diatom	AY180015
Uncultured diatom	AY180016
Uncultured diatom	AY180020
Uncultured eukaryote	AY082977
Uncultured eukaryote	AY082992
Uncultured marine diatom	AF290085

Sequences obtained in this study were indicated in bold.

¹ Name change since deposit; ² likely a new genus collected from a marine habitat (Medlin *et al.* 2008a).

Table 3. Valve dimensions (with LM) and striae densities (with SEM). Ten valves were used for measurement in each strain. NA = not available.

species	strain	valve length (μm) ^a	valve width (μm)	V_1+V_2 ^a (nm)	Striae per 10 μm ^b
<i>P. japonica</i>	s0305	9.9 - 12.3 (11.05 \pm 0.83)	2.8 - 4.1 (3.29 \pm 0.36)	334.0 (\pm 13.09)	30.0 (\pm 1.15)
<i>P. japonica</i>	s0328	5.5 - 7.1 (6.31 \pm 0.55)	2.6 - 4.3 (3.68 \pm 0.71)	322.1 (\pm 13.03)	31.1 (\pm 1.21)
<i>P. pseudojaponica</i>	s0354a	3.2 - 4.7 (3.95 \pm 0.67)	2.3 - 2.8 (2.65 \pm 0.24)	326.2 (\pm 17.52)	30.7 (\pm 1.64)
<i>P. pseudojaponica</i>	s0354b ^c	2.9 - 4.8 (3.57 \pm 0.62)	NA	340.3 (\pm 16.28)	29.4 (\pm 1.37)
<i>P. pseudojaponica</i>	s0356	2.0 - 2.6 (2.40 \pm 0.25)	NA	307.6 (\pm 21.72)	32.7 (\pm 2.35)
<i>P. senegalensis</i>	s0387	4.3 - 14.0 (5.14 \pm 0.77)	2.7 - 3.6 (2.99 \pm 0.32)	375.2 (\pm 13.78)	26.7 (\pm 0.97)

^aSee Fig. 41 for variables. Values are average (\pm standard deviation).

^bCalculated as 10 μm divided by the average of the sum of the width of vimines and virgae (V_1+V_2).

^csubsampled from s0354a. See Methods for detail.

Table 4. Number of pairwise nucleotide differences among the species on SSU rDNA and partial LSU rDNA sequences. SSU rDNA for upper diagonal, partial LSU rDNA for lower diagonal. Bold number is sum of base changes. L: Loop region, H: Helix region, CBC: Compensatory base pair changes (1 CBC involves 2 substitutions), HCBC: Hemi-CBC, indel: insertion and deletion. Continuous indels were counted as a single event.

	<i>P. japonica</i>	<i>P. pseudojaponica</i>	<i>P. senegalensis</i>
<i>P. japonica</i>	-	7 L: 3 (indel=1) H: 4 (CBC=1)	13 L: 6 (indels=3, unfixed change=1) H: 7 (CBCs=2, HCBCs=2)
<i>P. pseudojaponica</i>	19 L: 8 H: 11 (CBC=1, HCBCs=7, unfixed change=1)	-	9 L: 4 (indels=2, unfixed change=1) H: 5 (CBC=1, HCBCs=2)
<i>P. senegalensis</i>	21 L: 12 (indels=4) H: 9 (CBC=1, HCBCs=4, indel=1)	20 L: 12 (indels=4) H: 8 (HCBCs=7, indel=1, unfixed change=1)	-

Table 5. Summary of measurements of variables (nm) in Fig. 41. Average (\pm standard deviation)¹. NA = not available.

species	Strain	V ₁	V ₂	V ₃	V ₄
<i>P. japonica</i>	s0305	220.08 (\pm 9.07)	113.95 (\pm 10.42)	64.64 (\pm 4.80)	31.46 (\pm 2.56)
<i>P. japonica</i>	s0328	169.49 (\pm 15.90)	191.79 (\pm 15.95)	65.26 (\pm 6.50)	30.84 (\pm 3.44)
<i>P. pseudojaponica</i>	s0354a	191.79 (\pm 16.50)	134.42 (\pm 17.10)	65.78 (\pm 2.79)	13.89 (\pm 0.87)
<i>P. pseudojaponica</i>	s0354b ²	134.26 (\pm 17.57)	206.05 (\pm 15.96)	NA	NA
<i>P. pseudojaponica</i>	s0356	206.05 (\pm 15.94)	154.27 (\pm 16.81)	NA	NA
<i>P. senegalensis</i>	s0387	290.57 (\pm 13.48)	84.62 (\pm 15.66)	83.74 (\pm 4.54)	26.33 (\pm 3.42)

¹n=25 for each strain.²subsampled from s0354a. See methods for detail.

Table 6. Results of principal components (PC) analysis on variables measured based on Fig. 41 for four strains, s0305, s0328, s0354a, s0387.

	PC1	PC2	PC3	PC4
	Component loadings			
V ₁	0.6097035	-0.08013043	0.2183755	-0.7577288
V ₂	-0.5861640	0.02557928	-0.5169237	-0.6233357
V ₃	0.5333162	0.09045965	-0.8209203	0.1829774
V ₄	-0.0157263	-0.99234161	-0.1057914	0.0617980
	Percent of total variance explained			
	61.9	25.2	10.6	2.3

Table 7. Summary of intraspecific/genotypic and interspecific/genotypic sequence differences of rDNA in diatom genera. Note that all sequences were obtained with cloning by Alverson & Kolnick (2005), whereas the others were sequenced directly.

genus	inter-specific/genotypic		intra-specific/genotypic	
	SSU	Partial LSU	SSU	Partial LSU
<i>Cyclotella</i>	1-11 ^a	8-45 ^{a, b}	0-1 ^a	1-13 ^b
<i>Psammoneis</i>	7-13	19-21	0	0
<i>Pseudo-nitzschia</i>	-	0-30 ^c	-	0-1 ^c
<i>Sellaphora</i>	3-8 ^d	-	0-2 ^e	-
<i>Skeletonema</i>	>5 ^f	2-65 ^g	1-2 ^f (10-32) ^h	0-25 ^g

^aBeszteri *et al.* 2005

^bBeszteri *et al.* 2007

^cAmato *et al.* 2007. The dataset used in the study was obtained from the author and the numbers of the sequence differences were counted only on the D1/D2 region, although the original dataset contains D1 to D3 regions.

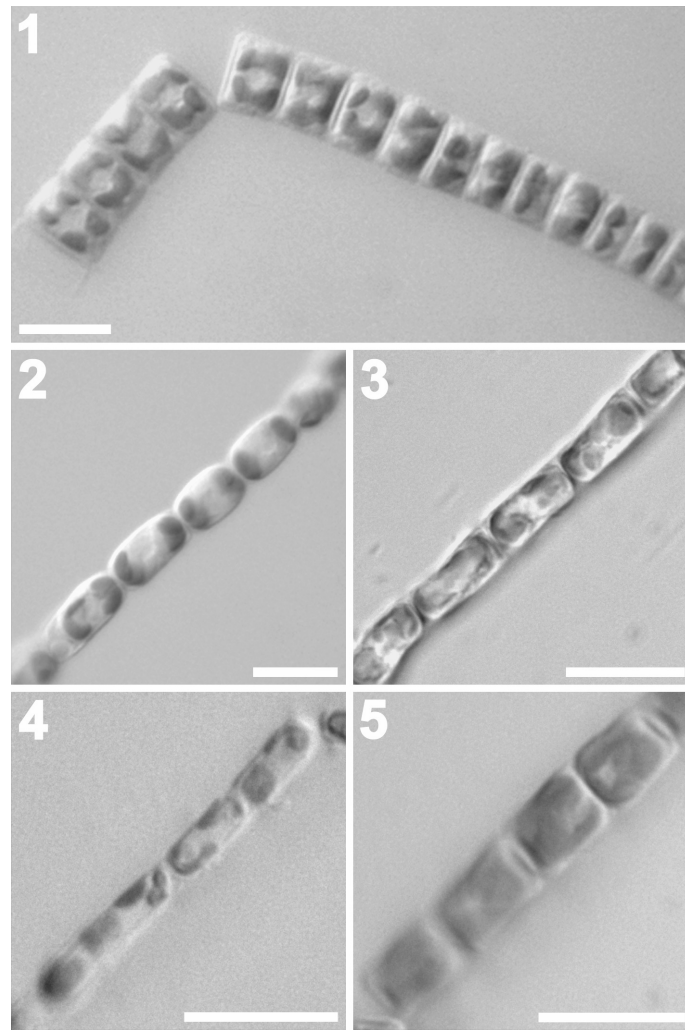
^dEvans *et al.* 2007

^eBehnke *et al.* 2004

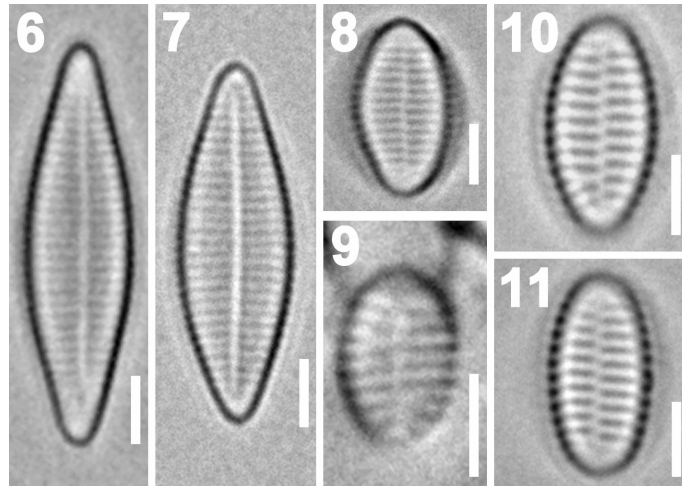
^fSarno *et al.* 2005

^gKooistra *et al.* 2008. The dataset used in the study was retrieved from Treebase and the numbers of the sequence differences were counted only on the D1/D2 region, although the original dataset contains D1 to D3 regions.

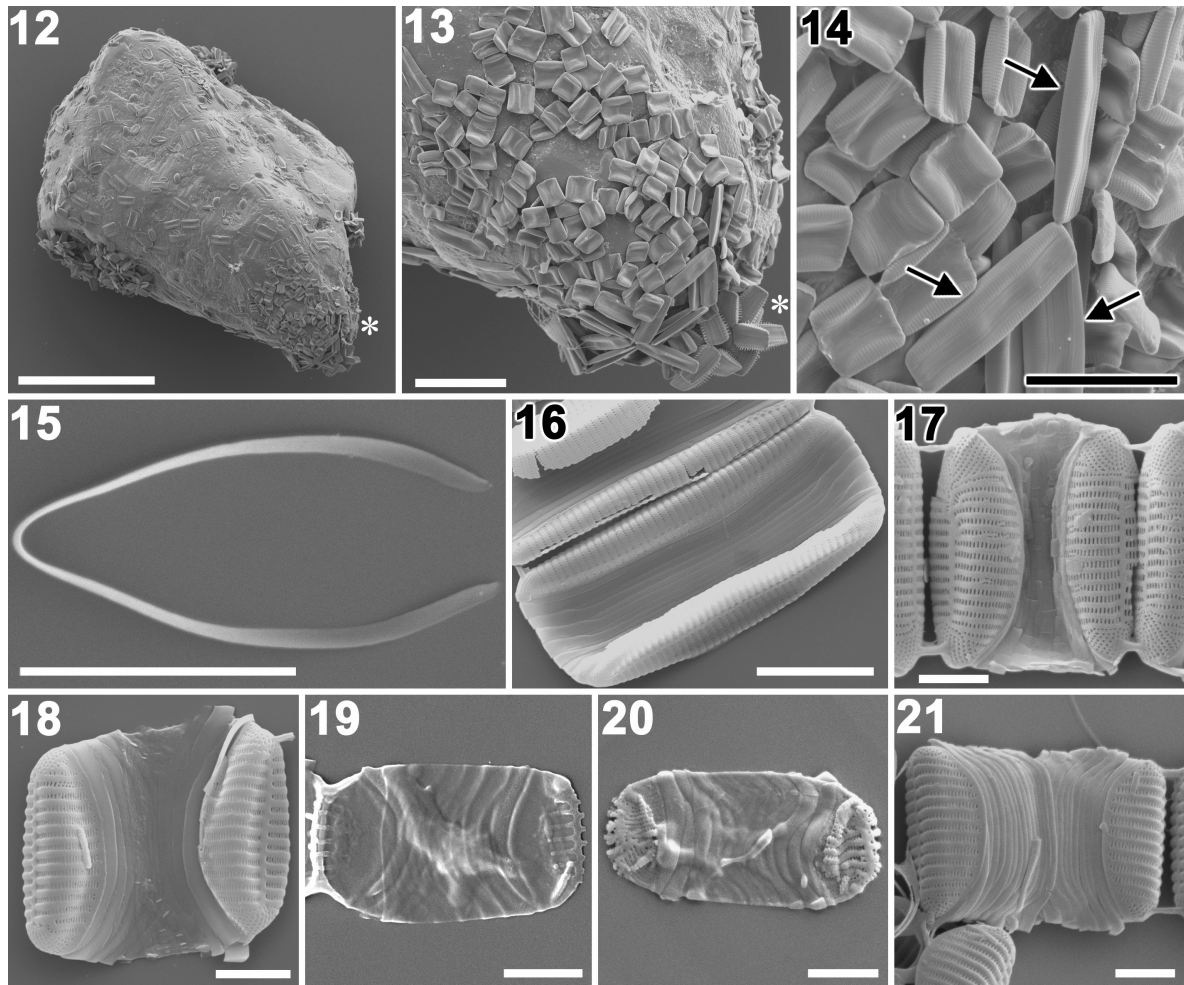
^hNumber of intragenomic polymorphisms by Alverson & Kolnick (2005).



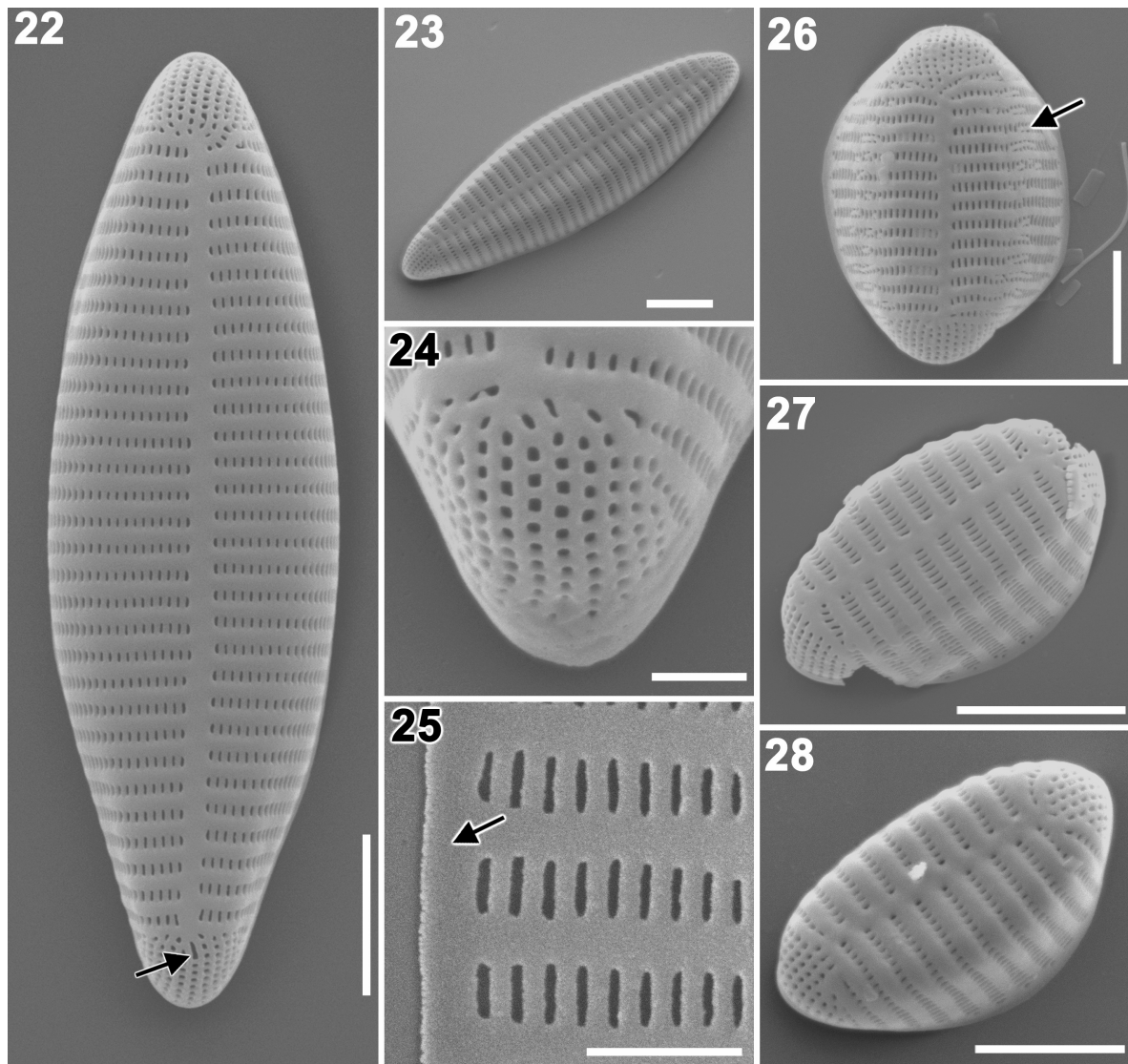
Figs 1-5. Living cells (LM). Scale bars = 10 μm . **Fig. 1.** *Psammoneis japonica*, strain s0305 showing sequential plastid division. **Fig. 2.** *P. japonica*, strain s0328. **Fig. 3.** *P. pseudojaponica*, strain s0354a. **Fig. 4.** *P. pseudojaponica*, strain s0356. **Fig. 5.** *P. senegalensis*, strain s0387.



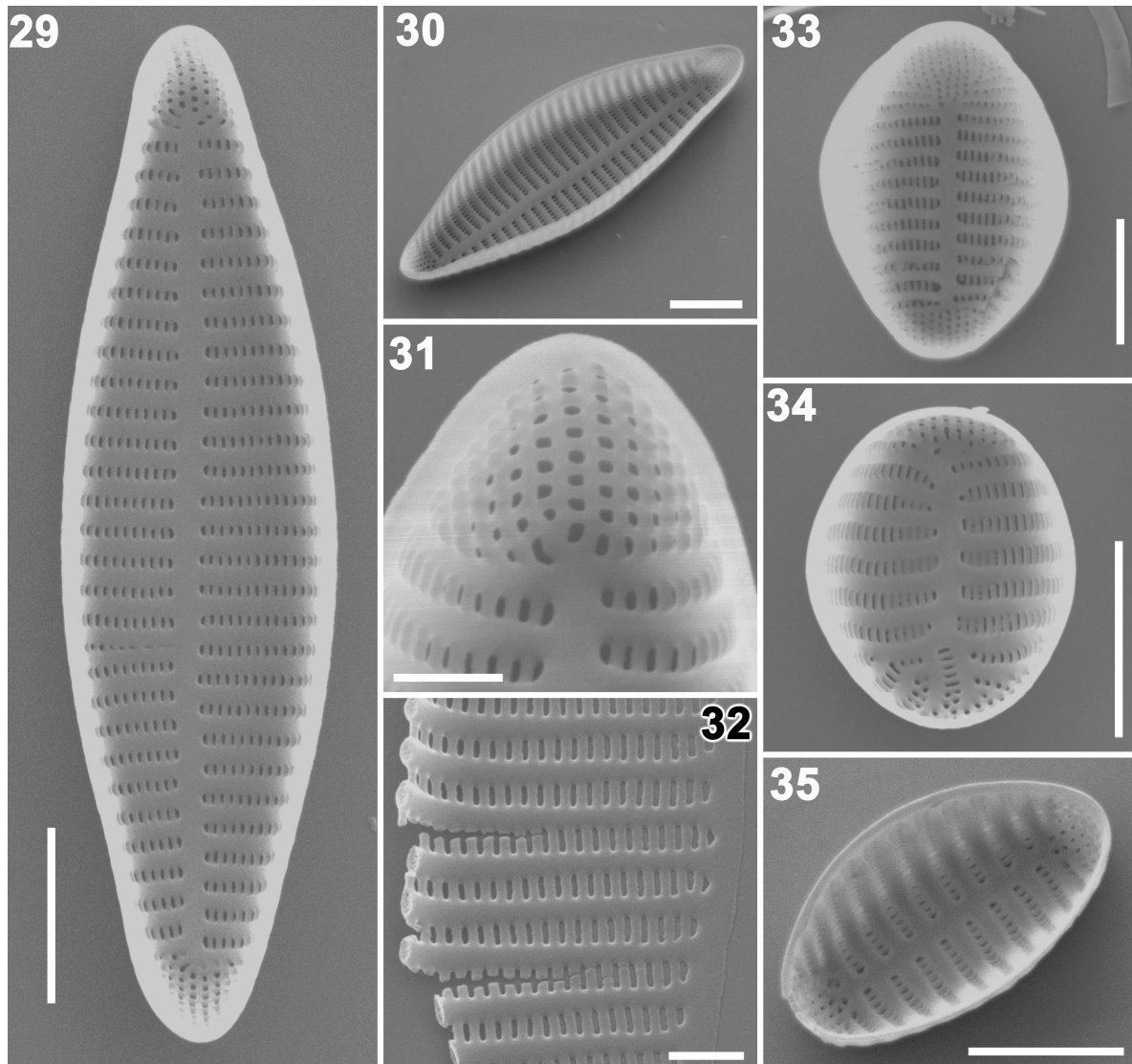
Figs 6-11. Cleaned valve (LM). Scale bars = 2 μm . **Figs 6-7.** *Psammoneis japonica*, strain s0305 (Zu6/44). **Fig. 8.** *P. japonica*, strain s0328 (Zu6/45). **Fig. 9.** *P. pseudojaponica*, strain s0354a (Zu6/46). **Figs 10-11.** *P. senegalensis*, strain s0387 (Zu6/49).



Figs 12-21. Frustules (SEM). Scale bars = 100 μm (Fig. 12), 20 μm (Fig. 13), 10 μm (Fig. 14), 5 μm (Figs 15-16) and 2 μm (Figs 17-21). **Fig. 12.** Sand grain covered with *Psammoneis senegalensis* together with *Amphora* spp., *Nitzschia* spp. and *Opephora* spp. Specimen was taken from Senegalese sample, from which s0387 was isolated. **Fig. 13.** Enlargement view of area marked by asterisk in Fig. 12 showing chain attaching to tip of sand grain. **Fig. 14.** Enlargement view of area marked by asterisk in Fig. 13. Note that existence of distinctly larger cells (arrows). **Fig. 15.** Plain and open band of *P. japonica*, strain s0305. **Fig. 16.** *P. japonica*, strain s0305. **Fig. 17.** *P. japonica*, strain s0328. **Fig. 18.** *P. pseudojaponica*, strain s0354a. **Fig. 19.** *P. pseudojaponica*, strain s0354b, subsampled from s0354a. **Fig. 20.** *P. pseudojaponica*, strain s0356. **Fig. 21.** *P. senegalensis*, strain s0387.



Figs 22-28. External view of valves (SEM). Scale bars = 2 μm (Figs 22-23, 26-28), 0.5 μm (Figs 24-25). **Fig. 22.** *Psammoneis japonica*, strain s0305. Arrow indicates slit-like opening. **Fig. 23.** *P. japonica*, strain s0305. Tilted view. **Fig. 24.** *P. japonica*, strain s0305. Enlarged view of valve apex showing apical pore field. **Fig. 25.** *P. japonica*, strain s0305. Enlarged view of valve edge (arrow). Note simple areolae lacking occlusions. **Fig. 26.** *P. japonica*, strain s0328. Arrow indicates bar on middle of striae extending transapical direction. Note remnant of areolar occlusion near sternum. **Fig. 27.** *P. pseudojaponica*, strain s0354a. Tilted view. **Fig. 28.** *P. senegalensis*, strain s0387. Tilted view.



Figs 29-35. Internal view of valves (SEM). Scale bars = 2 μm (Figs 29-30, 33-35), 0.5 μm (Figs 31-32). **Fig. 29.** *Psammoneis japonica*, strain s0305. Note absence of rimoportula. **Fig. 30.** *P. japonica*, strain s0305. Tilted view. **Fig. 31.** *P. japonica*, strain s0305. Enlarged view of valve apex showing apical pore field. **Fig. 32.** *P. japonica*, strain s0305. Enlarged view of valve edge. Note simple architecture of valve. **Fig. 33.** *P. japonica*, strain s0328. **Fig. 34.** *P. pseudojaponica*, strain s0354a. Note remnant of areolar occlusion near sternum. **Fig. 35.** *P. senegalensis*, strain s0387. Tilted view.

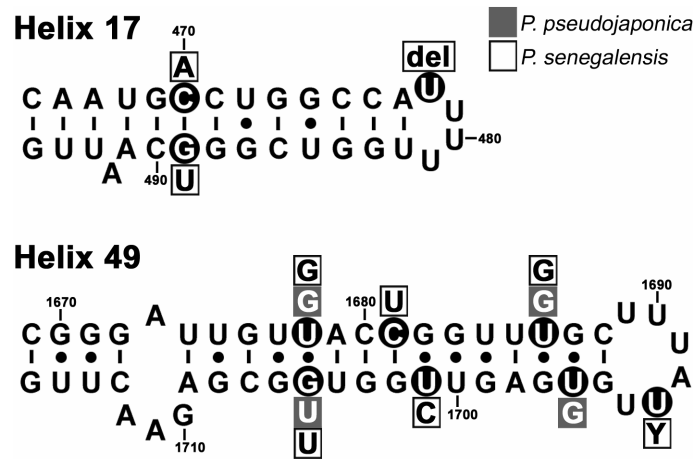


Fig. 36. Nuclear SSU rRNA secondary structure diagram of *Psammoneis japonica* showing helix 17 and 49. **Helix 17:** CBC took place at position 470 (A) - 489 (U) in *P. senegalensis*. **Helix 49:** CBC took place at position 1678 (G) - 1705 (U) in *P. senegalensis* and *P. pseudojaponica*. Sequence positions in which *P. japonica* differed from the other clones are indicated by a white letter on black background and the corresponding base of the sequences is shown next to the sequence position; open square = *P. senegalensis*, shaded square = *P. pseudojaponica*. Base pairing is indicated as follows: standard canonical pairs by circle (C-G, G-C, A-U, U-A); wobble G-U pairs by hyphen.

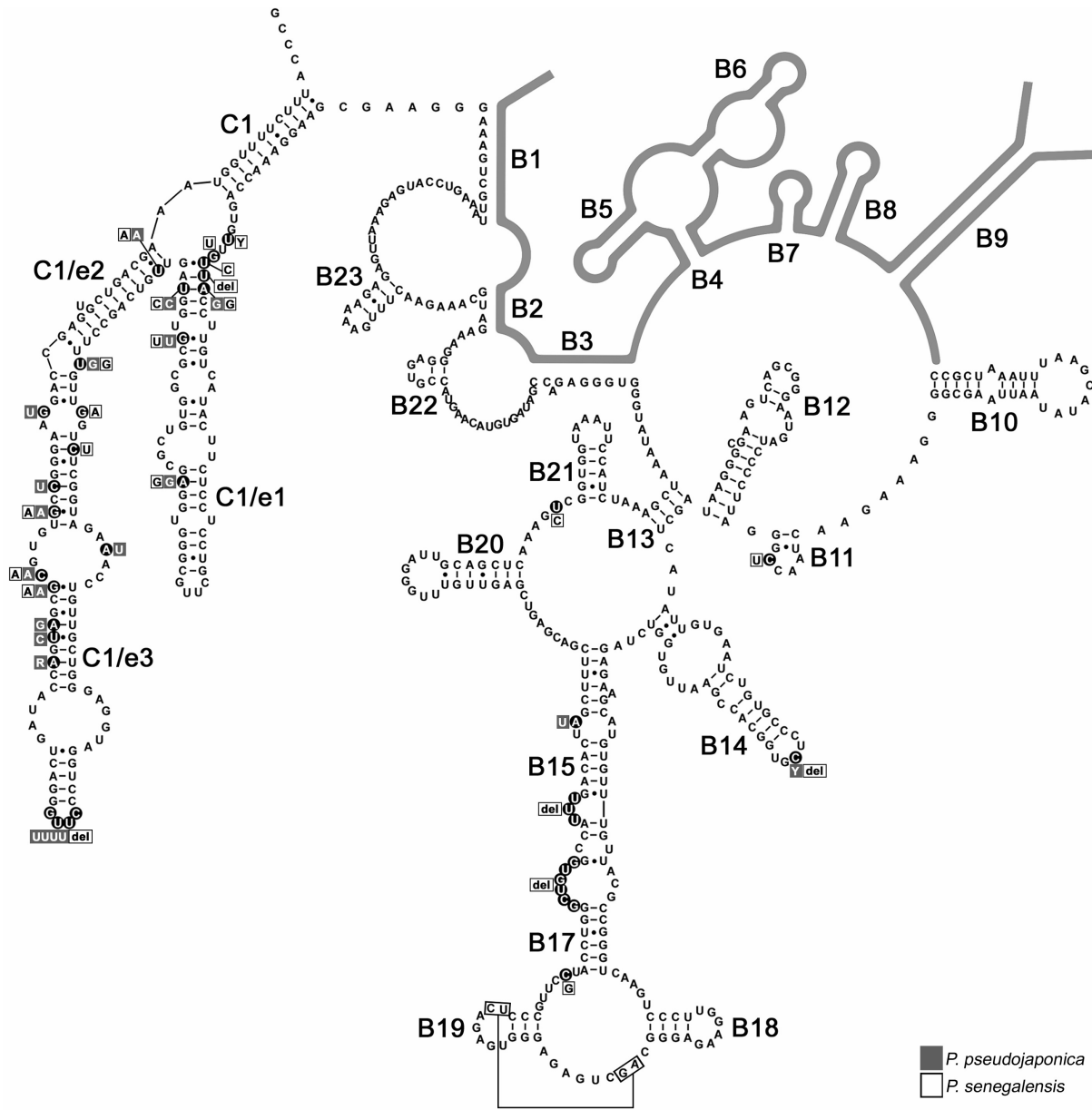


Fig. 37. D1/D2 region of nuclear LSU rRNA secondary structure diagram of *Psammoneis japonica*. Sequence positions in which *P. japonica* differed from the other clones are indicated by a white letter on black background and the corresponding base of the sequences is shown next to the sequence position; open square = *P. senegalensis*, shaded square = *P. pseudojaponica*. Base pairing is indicated as follows: standard canonical pairs by circle (C-G, G-C, A-U, U-A); wobble G-U pairs by hyphen. Tertiary interaction is connected by line.

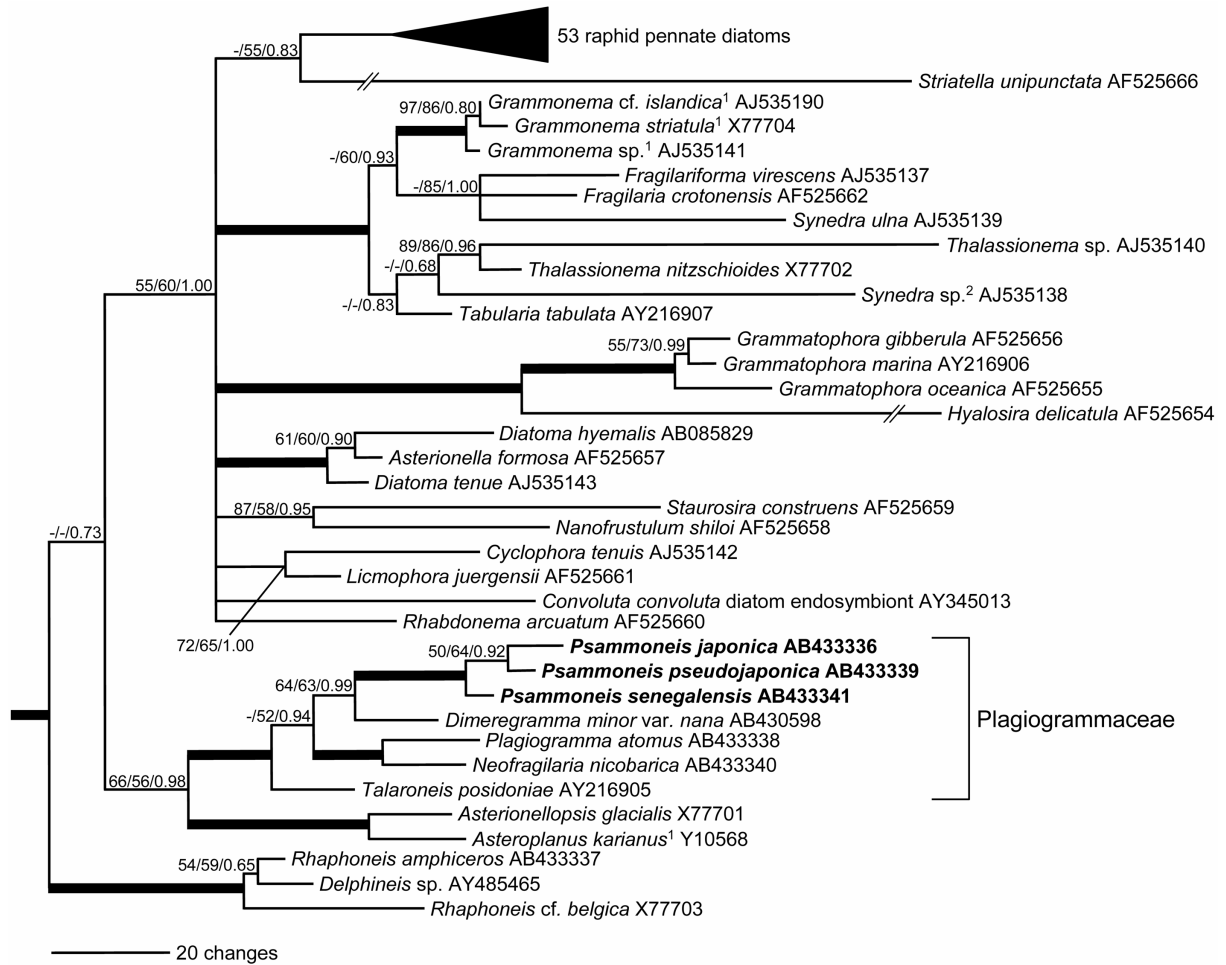


Fig. 38. Molecular phylogeny of araphid pennate diatoms inferred from 18S rDNA sequence using 1686 aligned positions. The tree shown resulted from Bayesian inference using a GTR + I + G model. Outgroup bolidomonads and centric diatoms were excluded and a clade comprising raphid diatoms is collapsed into triangle for clarity. Nodal support values greater than 50 (NJ and ML) and 0.50 (BI) are shown. Nodes with strong supports (Bootstrap support > 90 in NJ and ML, and posterior probability > 0.95 in BI) are shown as thick lines. ¹Name change since deposit; ² likely a new genus collected from a marine habitat (Medlin *et al.* 2008a).

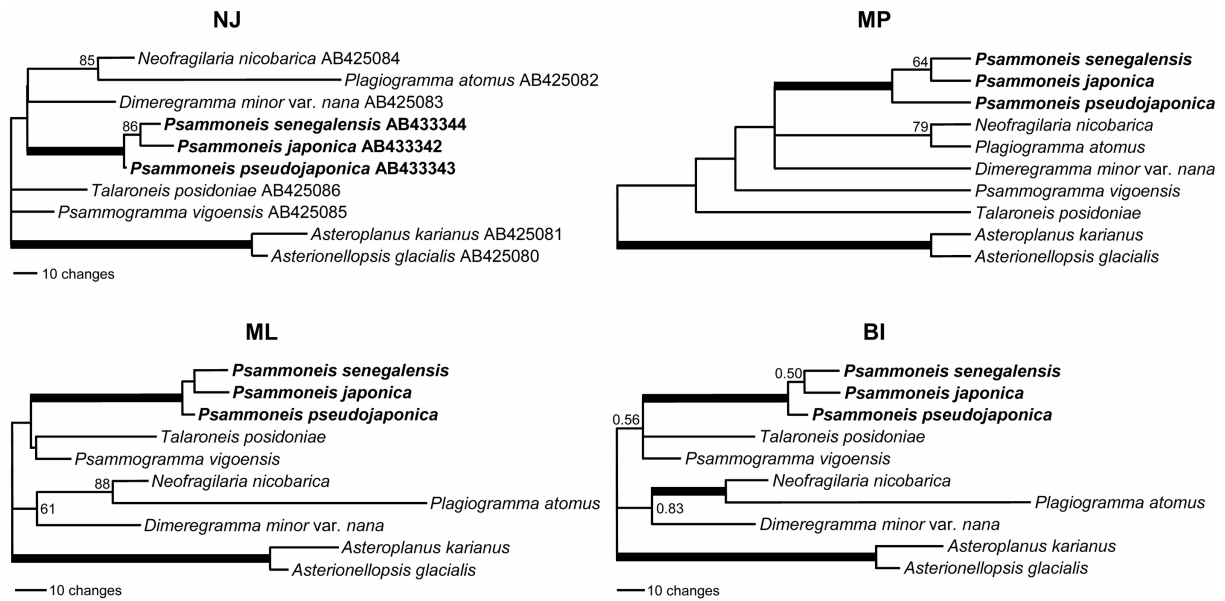
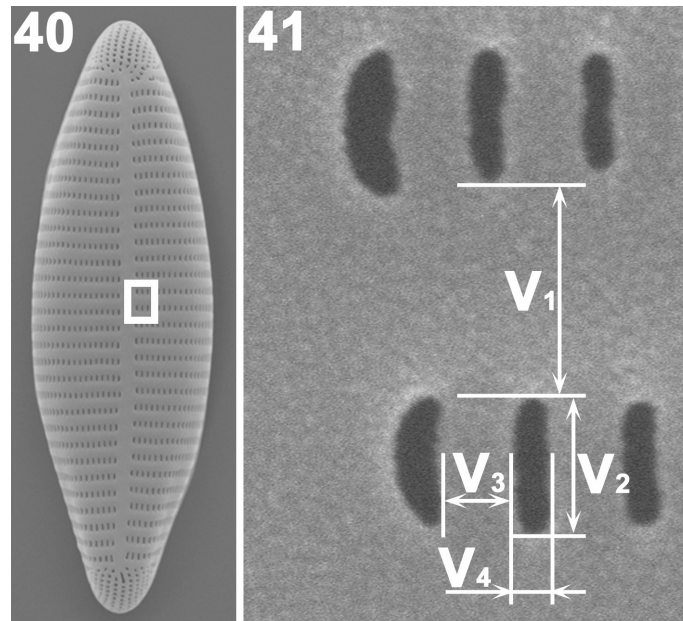


Fig. 39. Phylogenies of Plagiogrammaceae inferred from partial LSU rDNA sequences with 10 OTUs and 576 nucleotides. **NJ:** ML distance used. **MP:** Exhaustive search with un-weighted character. **ML:** Exhaustive search with GTR + G model. **BI:** GTR + G model. Nodal support values greater than 50 (NJ and ML) and 0.50 (BI) are shown. Thicker lines are nodes supported with 100 % bootstrap replications or high Bayesian posterior probabilities(> 0.99).



Figs 40-41. Variables used for the morphometric analyses. **Fig. 40.** External valve surface of s0305 showing measured part. **Fig. 41.** Enlargement view of part encircled by line in Fig. 40 at middle of valve. V_1 - width of virgae; V_2 - length of vimines (= width of striae); V_3 - width of vimines; V_4 - width of areolae. See methods for detail.

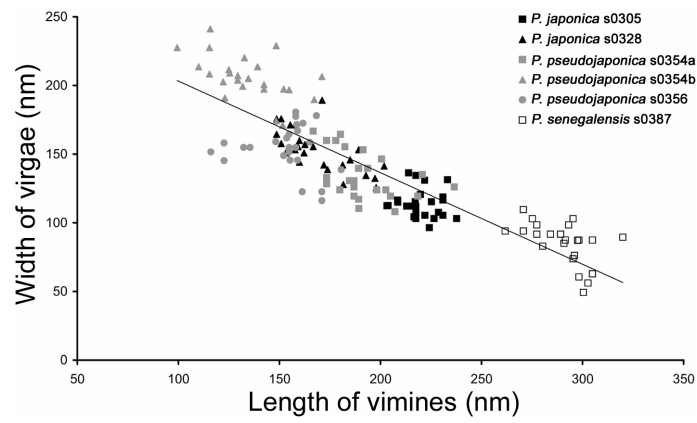


Fig. 42. Scatter plot of the width of virgae (V_1) against the length of vimines (V_2). Linear approximation was shown as line. $R^2 = 0.7728$.

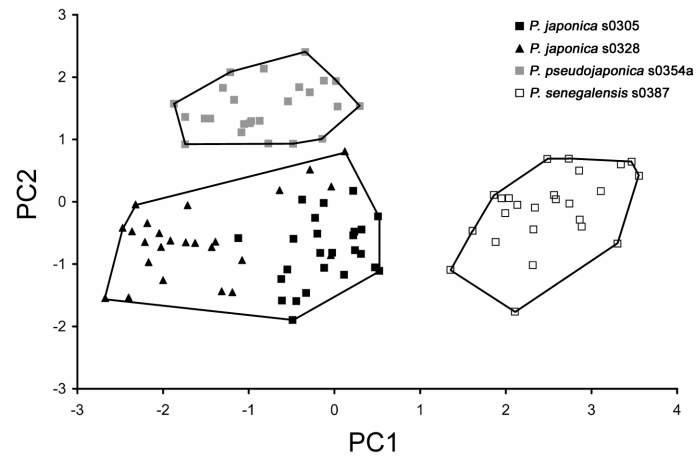


Fig. 43. Scatter plot on the first two principal component axis of the morphometric dataset. Genotype outliers are connected by lines.

2.11. Publication X:

Phylogeny and divergence time estimation of ‘araphid’ diatoms

SHINYA SATO^{1,*}, WIEBE H.C.F. KOOISTRA², SHIGEKI MAYAMA³ & LINDA K. MEDLIN¹

¹*Alfred-Wegener-Institute for Polar and Marine Research, Am Handelshafen 12, D-27570 Bremerhaven, Germany*

²*Stazione Zoologica Anton Dohrn, Villa Comunale, 80121 Naples, Italy*

³*Department of Biology, Tokyo Gakugei University, Koganei-shi, 184-0015 Tokyo, Japan*

Abstract

Phylogenetic relationships among the araphid pennate diatom lineage were estimated using multi-gene markers, SSU and LSU rDNA, *rbcL* and *psbA* (total 4352 bp), whereas previous studies have been made largely based on single gene phylogenies, e.g., SSU rDNA. The LSU rDNA and the third codon position of *rbcL* were recoded R (A+G) and Y (T+C) because of substitution saturation detected at these positions. Two strategies for tree rooting were explored, 1) one bolidomonad as the closest relative of the diatoms and, 2) one bolidomonad and more distantly related heterokontophyte outgroups. The tree topologies of pennates were nearly identical in all analyses. Pennates were clearly divided into three major subgroups: basal araphid, core araphid and raphid diatoms. The interclade relationship of core araphid diatoms, which was unresolved in previous SSU rDNA phylogenies, was resolved. We employed the Thorne/Kishino method of molecular dating, allowing for simultaneous constraints from the fossil record and varying rates of molecular evolution of different branches on the phylogenetic tree, to estimate the divergence time of pennates. Our estimation suggested that the radiation of pennates into three major subgroups took place in a short period of geological time before their first appearance in the fossil record.

KEYWORDS: araphid pennate, diatom, divergence time, phylogeny, Thorne/Kishino method

1. INTRODUCTION

The diatoms are the most species-rich group of eukaryotic algae, containing more than 10,000 described species and potentially many more cryptic species (Mann, 1999). The special type of the cell wall of diatoms comprises two overlapping halves (thecae), which consist of two dish- or vessel-shaped elements, called valves, at opposite ends of the cell and strips (girdle bands) or scales covering the region in between (Round et al., 1990). The diatoms have historically been divided into two groups: the centrics and the pennates, which can be distinguished by their pattern centres or symmetry of the valve, mode of sexual reproduction, and plastid number and structure (Round et al., 1990). The centrics are oogamous, show a radially symmetrical ornamentation of their valves and usually possess numerous discoid plastids. The pennates are isogamous, have bilaterally symmetrical pattern centres in their valves and generally possess fewer, plate-like plastids.

The current classification system, in which diatoms receives the rank of a division, has recently been revised by Medlin and Kaczmarska (2004) mainly based on rDNA phylogenies but also supported by reproductive and cytological features. This system (Fig. 1) separates the division Bacillariophyta into two groups at the rank of subdivision: Coscinodiscophytina comprising radial centrics, and Bacillariophytina comprising the rest of the diatoms that exhibit polarity in the shape of their valves, except where this has been lost secondarily. The pennates are now given a rank of the class Bacillariophyceae, which forms a well-supported monophyly in all the nuclear-encoded small subunit ribosomal DNA (SSU) phylogenies published in the past (e.g., Medlin and Kaczmarska, 2004; Shinninghe-Damste et al., 2003; Alverson et al., 2006; Sorhannus, 2007). These species all share a midrib or sternum, and rows of poroids, called striae, perpendicular thereupon.

Morphologically, pennates can further be subdivided into two groups by the presence or absence of a slit, called a raphe, in the valve. The “raphid” pennates, i.e., those that possess a raphe, are potentially actively motile. This group is also monophyletic. In contrast, the

“araphid” pennates, i.e, those lacking a raphe, do not move actively, or at times, move very slowly (Sato and Medlin, 2006). This group is paraphyletic in all studies to date (Medlin and Kaczmarska, 2004; Alverson et al., 2006; Sims et al., 2006; Kooistra et al., 2007; Sorhannus, 2007; Sato et al., 2008b) and there are no morphological features that are uniquely shared among all members of the group, except for the absence of a raphe. Most members have labiate processes and apical pore fields. The araphid and raphid diatoms have historically been recognized as independent taxonomic entities (e.g., Round et al., 1990), but are grouped together within a single class Bacillariophyceae by Medlin and Kaczmarska (2004). In the present study, we extensively sampled araphid diatoms to evaluate phylogenetic relationships of various groups. As markers we utilized multiple genes including the *SSU* and the D1/D2 region of the nuclear-encoded large subunit ribosomal DNA (*LSU*), as well as the plastid encoded ribulose-1,5-bisphosphate carboxylase/oxygenase gene (*rbcL*) and photosystem II reaction center D1 protein gene (*psbA*). Here we still use the terms *centric*, *araphid* and *raphid* in spite of the paraphyly of the first two in the current classification system, because they refer to key morphological features or their absence. We do not imply that this corresponds to a mono- (holo-) phyletic group, or that it should be accorded any taxonomic status.

Diatoms possess an excellent fossil record because their silicified cell wall preserved well (e.g., Forti and Schulz, 1932; Gersonde and Harwood, 1990; Harwood and Gersonde, 1990). Both the fossil record and molecular phylogenies indicate that the pennates evolved from the centrics as suggested by early workers (e.g., Fritsch, 1935; Simonsen, 1979). However, the fossil record of the diatoms is not entirely free of problems. Although most extant taxonomic groups have fossil representatives, there is no substantial fossil record of the key evolutionary transitions from centrics to pennates, and from araphid to raphid diatoms because of poor preservation during this time frame.

Molecular phylogenetic methods can address these issues by calibrating fossil dates with internodes in phylogenies inferred from sequence data, thus allowing the estimation of divergence times across the entire gene tree of a group. In the past this has been accomplished assuming a molecular clock, that is, constancy of evolutionary rates across lineages (Kooistra and Medlin, 1996). Under this assumption, the estimated branch lengths can be converted into absolute divergence times using fossil calibration. However, most datasets appear to violate the clock model (Graur and Martin, 2004), which can cause serious biases in divergence time estimation (e.g., Rambaut and Broham, 1998; Soltis et al., 2002). Consequently, a relaxed clock model has recently been introduced to overcome the inconstancy of the clock to study divergence time estimation of diatoms (Sorhannus, 2007; see also Berney and Pawlowski, 2006). Those studies utilised, as in most phylogenetic studies of diatoms, solely *SSU* sequence data. In the present study, the divergence time of the pennates was estimated using four genetic markers and Bayesian frameworks that account for rate variation of substitution when estimating divergence times and incorporate multiple genetic markers and multiple fossil calibration points (Thorne and Kishino, 2002).

2. METHODS

2.1. Taxon sampling

A supertree was constructed using Clann 3.0.0 (Creevey and McInerney, 2005) with default settings under the Matrix representation using Parsimony (MRP) method to summarize the results of previous *SSU* trees. Topologies used to construct the supertree were taken from Medlin et al. (2000), Medlin and Kaczmarska (2004), Kooistra et al. (2003a, b, 2004), Sinninghe-Damsté et al. (2004), Alverson et al. (2006, fig. 5), Sato et al. (2008a, b, c),

Sorhannus (2004, 2007). All topologies were coded into newick format manually and entered into the program. In this procedure, all centrics were simply coded into one OTU to root the supertree, and all raphid diatoms were also coded as one OTU 'raphid diatoms'. The araphid diatom *Striatella unipunctata* was pruned from the input trees when this species appeared in the clade of raphid diatoms (Medlin et al., 2000; Kooistra et al., 2003a, b, 2004; Sato et al., 2008a, b, c). The topology of the recent paper of Medlin et al. (2008) was not included in the analysis because the phylogenetic tree was rooted with an araphid diatom *Rhabdonema*, making it impossible to compare the phylogenetic relationship of araphid diatoms under the same standard with the other studies, which were rooted by centrics. Also, we plotted the other source of information (ecological/morphological features) onto the supertree (Fig. 2) referring to the original description of each species or some monographic works (e.g., Hustedt, 1959; Round et al., 1990; Witkowski et al., 2000; Kobayasi et al., 2006) to see whether any other features correlated with any clade. Then, a few araphid taxa were selected from each clade as representatives to be included in the further multi-gene analyses. Beside the araphid diatoms included in the *SSU* supertree, hitherto unanalyzed species were also added: *Hyalosira tropicalis*, *Pteroncola inane* and *Pseudohimantidium pacificum*.

As outgroup selection can alter the topology of the ingroup (Milinkovitch and Lyons-Weiler, 1998; Tarrío et al., 2000), two strategies were deployed to compare the effect of outgroup selection. The first dataset used *Bolidomonas pacifica* (Bolidophyceae, Guillou et al., 1999) as single closest outgroup taxon of the diatoms. The second dataset used multiple outgroups of heterokont algae, including *Bumilleriopsis filiformis* (Xanthophyceae), *Dictyota dichotoma* (Phaeophyceae) and *Heterosigma akashiwo* (Rhaphidophyceae) as well as *Bolidomonas*. This rooting strategy was used because Medlin & Kaczmarska (2004) suggested that inclusion/exclusion of distant outgroups affects the monophyly of three major classes: Coscinodiscophyceae, Mediophyceae and Bacillariophyceae. Hereafter, each dataset will be referred to as Bolido-In and Multiple-In, respectively.

Among the dataset, 5 are Coscinodiscophyceae, 9 are Mediophyceae and 28 are Bacillariophyceae, of which the latter included 6 raphid and 22 araphid diatoms. Culture strains used in this study (Table 1) are currently available upon request to the first author, but may not survive long-term in culture (cf. Chepurnov et al., 2004); instead voucher slides are available in the slide collection of Sato for examination of these isolates.

2.2. DNA extraction, PCR, and sequencing

Samples of *c.* 500 mL of culture were harvested by filtration and DNA was extracted using a modified CTAB protocol (Doyle and Doyle, 1990) or by the PAN Plant Kit (PAN Biotech, Aidenach, Germany). The quantity and quality of DNA were examined by agarose gel electrophoresis against known standards. Partial fragments of *SSU* (~1657 bp), *LSU* (~659 bp), *rbcL* (~1461 bp) and *psbA* (~933 bp) were amplified by PCR (see Table 2 for primers).

The markers were PCR-amplified in 25 μ L volumes containing 10 ng DNA, 1 mM dNTPs, 0.5 μ M of forward primer, 0.5 μ M of reverse primer, 1 x Roche diagnostics PCR reaction buffer (Roche Diagnostics, GmbH, Mannheim, Germany), and 1 unit *Taq* DNA polymerase (Roche). The PCR cycling of nuclear genes comprised an initial 4-min heating step at 94°C, followed by 35 cycles of 94°C for 2 min, 56°C for 4 min, and 72°C for 2 min, and a final extension at 72°C for 10 min; of plastid genes comprised an initial 5-min heating step at 94°C, followed by 35 cycles of 95°C for 1.5 min, 47°C for 2 min, and 72°C for 2 min, and a final extension at 72°C for 6 min. The quantity and length of products were examined by agarose gel electrophoresis against known standards. Excess primers and dNTPs were removed from PCR product using the QIAQuick purification kit (QIAGEN, Germany). The cleaned PCR

products were then electrophoresed on an ABI 3100 Avant sequencer (Applied Biosystems, CA, USA) using Big Dye Terminator v3.1 sequencing chemistry (Applied Biosystems, CA, USA).

The obtained rDNA sequences were aligned first using ClustalX (Thompson et al., 1997), and then refined by referring to the secondary structure model of the rRNA at the database of the structure of rRNA (Van de Peer et al., 1998 for *SSU*; Sato et al., 2008c for *LSU*). There is extreme length variation in some rRNAs (e.g. Gillespie et al., 2005) and replication slippage often leads to convergence on similar primary and secondary structures (Hancock and Vogler, 2000; Shull et al., 2001). Homology assessment in such regions was difficult or impossible, so that the highly variable regions (mostly peripheral regions of the rRNA secondary structure) were removed from the alignment using BioEdit 7.0.2 (Hall, 1999), by referring to the variability map of *Saccharomyces cerevisiae* (Van de Peer et al., 1993 for *SSU*; Ben Ali et al., 1999 for *LSU*). Sequences for the protein coding genes *psbA* and *rbcL* lacked indels and were aligned manually. Finally, the dataset comprised 4352 bp.

2.3. Sequence analysis

Substitutional noise in a gene marker makes it difficult to retrieve phylogenetic signal, especially when the gene is evolving fast. Saturation is caused by multiple substitutions at the same site. Because transitions occur more frequently than transversions (DeSalle, 2005), transitions can likely suffer from saturation especially in a fast-evolving region of a gene, i.e., D1/D2 region of the nuclear *LSU* and third codon position of the protein coding genes in our dataset. Therefore, saturation of both transitions and transversions were tested by DAMBE 4.5.56 (Xia and Xie, 2001). Because the saturation plot showed a serious saturation in *LSU* and the third codon of *rbcL* (Figs 3B and C), only transversions were used in subsequent phylogenetic analyses, by coding purine (G and A) into R, and pyrimidine (C and T) into Y.

2.4. Phylogenetic analyses

All phylogenetic analyses were performed on either dataset, Bolido-In and Distant-In.

For model based estimations, maximum likelihood (ML) and Bayesian inference (BI), each nuclear gene and each codon position of protein coding genes was treated as a separate partition (i.e., 8 partitions in the dataset) with independent model parameters, whereas a concatenated dataset was used for neighbour joining (NJ) and maximum parsimony (MP) analyses. RAxML-VI-HPC, v2.2.3 (Stamatakis et al., 2005) was used for ML analyses with the GTRMIX model. The Gamma correction value of each partition was obtained automatically by the program. The analyses were performed 1,000 times to find the best topology receiving the best likelihood using different random starting MP trees (one round of taxon addition) and the rapid hill-climbing algorithm (i.e., option `-f d` in RAxML). Bootstrap values were obtained by 1,000 replications with GTRCAT model.

The Message Passing Interface (MPI) version of MrBayes 3.1.2 (Huelsenbeck and Ronquist, 2001; Ronquist and Huelsenbeck, 2003; Altekar, 2004) was used for Bayesian analyses with the GTR + I + G model for each partition, as suggested by MrModeltest 2.2 (Nylander, 2004), to estimate the posterior probability distribution using Metropolis-Coupled Markov Chain Monte Carlo (MCMCMC) (Ronquist and Huelsenbeck, 2003). Gamma correction values and a proportion of invariable site of each partition were obtained automatically by the program. MCMCMC from a random starting tree were used in this analysis with two independent runs and 1 cold and 9 heated chains with temperature set 0.05. Bayesian analyses

were run for 20 million generations each with trees sampled every 100th generation. To increase the probability of chain convergence, we sampled trees after the standard deviation values of the two runs dipped below 0.01 to calculate the posterior probabilities (i.e., after 810,000 and 500,000 generations for Bolido- and Distant-In, respectively). The remaining phylogenies were discarded as burn-in.

For NJ analyses, PAUP* version 4.0b10 (Swofford, 2002) was used with JC distances. Nodal support was estimated using NJ bootstrap analyses using the same settings (1,000 replicates).

MP searches were done with the “new technology” search algorithm implemented in the Willi Hennig Society edition of TNT 1.1 (available at <http://www.zmuc.dk/public/phylogeny/TNT>). One hundred random addition sequence replicates were performed with default values. Nonparametric bootstrap analyses were done 1,000 times with the “traditional” search algorithm in TNT.

2.5. Testing alternative hypotheses

To compare some tree alternatives, we used the Shimodaira-Hasegawa-test as implemented in PAUP (Shimodaira and Hasegawa, 1999; test option FullOpt; 1,000 bootstrap replicates). We also generated the alternative topologies by introducing constraints, i.e., monophyly of centrics and araphid diatoms.

2.6. Divergence time estimation

With the dataset, divergence times of pennates were estimated following the Bayesian methods (Thorne et al., 1998; Kishino et al., 2001; Thorne and Kishino, 2002) using the program package of mulidistribute 9/25/03 (Thorne and Kishino, 2002) and PAML 3.15 (Yang, 1997). Original sequences were used in this process (i.e., all sequences were not RY re-coded), because the preliminary analyses using RY re-coded dataset showed that the likelihoods obtained from the baseml and estbranches analyses were very different, suggesting that one or both programs failed to optimize the likelihood. Analyses were performed either using BI and ML topologies. As we focused on dating the evolution of the pennates, there was no difference within pennate topology between the two datasets Bolido- and Distant-In. Therefore, the topologies of Bolido-In dataset were used in order to reduce calculation time. Although the entire topology was used for each analysis, we only present the result of pennate lineage because the divergence pattern of pennates is nearly identical using BI and ML analyses making the results comparable. Branch lengths were estimated with the estbranches 8/5/03 of mulidistribute in conjunction with the BI/ML topology. We used the F84 model incorporating among-site rate variation modeled by a gamma distribution (Yang, 1994) of sequence evolution (F84+G model). This is the most complex model implemented in this program. This model is less parameterized than the best-fit models selected by MrModeltest 2.2 (above); however, previous studies (Yang and Yoder, 2003; and references therein) have shown that it is actually the rate variation among sites parameter that has the greatest effect on divergence time estimation. All the parameters within the model as well as the branch lengths were estimated separately for every gene. Markov chain Monte Carlo (MCMC) approximations were obtained with a burnin period of 100,000 proposal cycles. Thereafter, samples of the Markov chain were taken every 100 cycles until a total of 1,000,000 generations were obtained. The uncertainty of divergence time estimates was accounted for by using the 95% credibility intervals of these 10,000 samples. To diagnose possible failure of the Markov chains to converge to their stationary distribution, we performed two replicate MCMC runs with different

initial starting points for each analysis. Application of the multidivtime program requires a value for the mean of the prior distribution for the time separating the ingroup root from the present (rttm). We used a maximum (250 Ma) and minimum estimate (190 Ma) as rttm (see below about the calibration strategy), and the SD for the prior on the root rate (rttmsd) was set at half the prior on the root rate. The highest possible time between tips and root (bigtime) was also set at 250 and 190 Ma for each analysis. Other parameters for running multidivtime were set referring Rutschmann (2004) as follows: $rtrate = X/rttm$, where rtrate is the mean of prior distribution for the rate at the root node and X is the median amount of evolution from the ingroup root to the ingroup tips, which was obtained by TreeStat 1.1 (available at <http://tree.bio.ed.ac.uk/software/treestat/>); $rratesd = rtrate$, where rratesd is the standard deviation of rtrate; $rttm * brownmean = 1$, where brownmean is the mean of the prior distribution for the autocorrelation parameter (m); and $brownsd = brownmean$, where brownsd is the standard deviation of the prior distribution for m.

2.7. Reference fossils

The occurrences of a taxon in the fossil record was used as minimum age constraint. If sister taxa had a fossil record, the earlier age was taken as the minimum constraint.

Medlin et al. (1997) speculated that the pigmented heterokonts, to which the diatoms belong, diversified following the P/T boundary (c. 250 Ma) mainly based on molecular clock method. Therefore, we assumed the maximum age of the diatoms at 250 Ma. Although using the constraint which was obtained solely by molecular clock method as a calibration point might be risky, the age after P/T boundary was also supported by paleoecological discussions (Medlin et al., 1997), making the assumption reasonable. Tappan (1980) reported no diatoms from the well-preserved Palaeozoic cherts (659-c. 250 Ma), which contained radiolarians and sponges. The assumption of the minimum age of the origin is much more straightforward. We set 190 Ma for the minimum age of the origin. This assumption is based on the earliest generally accepted record of diatoms described by Rothpletz (1896, 1990), which has been found from the Toarcian stage of the Jurassic (c. 190 Ma by Sims et al., 2006). Thus, the time estimation was undertaken for four conditions using BI and ML topologies, assuming the the origin of the diatoms 250 and 190 Ma.

The other calibration points were selected from the recent review of the fossil diatoms by Sims et al. (2006), in which reliable fossils were introduced, allowing us to use them in this divergence time estimation. Calibrated ages and fossils used here are shown in Table 3. Although the fossil records of *Thalassiosira* and its potential affinities, e.g., *Praethalassiosiroopsis* and *Thalassiosiroopsis*, are abundant in fossil records, they were not used for the calibration by way of caution because the evolutionary relationship of these fossil and the modern taxa is not confidently established (see discussion for details). With the same reason, fossil records of resting spores ‘presumably’ formed by *Chaetoceros* were not used in the present study.

3. Results

3.1. SSU supertree of araphid diatoms

A supertree constructed by 12 SSU trees displayed eight clades. Fig. 2 shows only the pennate portion of the tree. Araphid diatoms were paraphyletic because monophyletic raphid pennates were recovered inside it. The ‘basal’ araphid clade (comprising marine clades 6, 7 and 8) was

the first to diverge followed by the clade of raphid pennates and a clade containing the remainder of 'core' araphid diatom comprising clades 1 to 5 and two undescribed species. *Rhabdonema* and *Striatella* appeared in a polytomy of the clade of core araphid diatoms. Most clades were consistent with morphological and/or ecological features. Clade 1 diatoms mostly consisted of highly elongated species (length/width ratio greater than 15:1 in their maximum valve size). The ocellulimbus at the end of valve is the structure, which is exclusively observed in this clade. All clade 2 diatoms were marine and had an apical slit area (a.k.a. multiscissura *sensu* Honeywill, 1998). Clade 3 could be characterized by the presence of septate girdle bands. Usually the members of this clade attached to seaweeds forming zig-zag chains. Clade 4 diatoms were relatively small in size and had no labiate process on their valve, though a highly reduced process had been seen in *Plagiostriata* (Sato et al., 2008a). Members of clade 5 inhabited non-marine environments (brackish/limnic), and their cells attached to each other to make zig-zag or stellate chains. All species of clade 6 appeared in marine coastal regions, being benthic. Their valves were small and lacked labiate processes. Clade 7 comprised planktonic members forming stellate chains, which were connected at the broader end of their polarized valve. Clade 8 species had complex occlusions on their pores of valve.

Unlike the other families of araphid diatoms, Plagiogrammaceae and Rhabdioneidae formed a clade as clade 6 and clade 8, respectively. Interclade relationships of core araphid diatoms, vis., clades 3, 4 and 5, were unresolvable in this SSU supertree.

3.2. Multi-gene phylogeny of the diatoms

Monophyly of the diatoms was recovered in the most analyses (Fig. 4); only one exception was found in MP Distant-In analysis in which a coscinodiscophycean diatom *Stephanopyxis turris* diverged before the divergence of *Bolidomonas* and all other diatoms (Topology not shown). The constrained topologies of the monophyly of the 'centrics' and 'araphid diatoms' were rejected significantly (Table 4).

The class Coscinodiscophyceae was monophyletic in all analyses, although the BS value of ML analyses were low. The internal topology of the clade was identical in all analyses, i.e., (*Rhizosolenia*, (*Stephanopyxis*, (*Hyalodiscus*, (*Melosira*, *Aulacoseira*))))). Class Mediophyceae was monophyletic only in the ML Distant-In analysis with BS support < 50, whereas the class was resolved as a grade in the tree resulting from the other analyses. In these trees, ML Bolido-In and both BI, a clade of *Eunotogramma* and Thalassiosirales (*Stephanodiscus*, (*Thalassiosira*, *Cyclotella*)) always diverged at the root of the subdivision Bacillariophytina. Also, the robust clade of *Lampriscus* and *Ardissona* diverged lastly among the Mediophycean diatoms in these three analyses, being at the root of pennates. The relationship of the rest of Mediophycean genera, *Chaetoceros*, *Cymatosira* and *Odontella*, remained unresolved.

The pennates formed a robust clade in all analyses, which displayed substantially the same topology (Fig. 4). Only a single incongruence was found in a polytomy from BI versus monophyly from ML of the marine epiphytic genera, *Grammatophora*, *Rhabdonema* and two species of *Hyalosira*. The only exception was the araphid diatom *Asteroplanus*, which appeared in the core araphid lineage in BI but at the root of the pennates in ML. Not all clades of the SSU supertree were recovered in the multi-gene phylogenies; corresponding clades if any, are marked in Fig. 5. The following divergence pattern of pennates was commonly observed in all analyses: A robust clade of marine araphid diatoms (*Rhabdioneis*, (*Dimeregramma*, (*Striatella*, *Pseudostriatella*))) diverged first from the remaining pennate lineage. Then, the raphid diatoms' clade (*Navicula*, ((*Nitzschia*, *Psammodictyon*), (*Phaeodactylum*,

(*Cocconeis*, *Campylodiscus*))) diverged from the rest of the core araphid diatoms. The first divergence of the core araphid diatoms was a clade comprising small-celled diatoms (*Plagiostriata*, (*Opephora*, (*Pseudostaurosira*, *Nanofrustulum*))), which is equivalent to clade 4 in the *SSU* supertree. Subsequently, a marine epiphytic clade in ML (*Hyalosira delicatula*, *Grammatophora*), (*Hyalosira tropicalis*, *Rhabdonema*) diverged, but the clade was unresolved in BI. This result strongly indicates the paraphyletic nature of the genus *Hyalosira*, whose generitype *H. delicatula* formed a clade with *Grammatophora*; whereas the other species *H. tropicalis*, which lacks septate girdle bands unlike other members of *Hyalosira*, formed a clade with *Rhabdonema*. A revised systematic treatment of *H. tropicalis* is now in preparation. Then, a clade of *Cyclophora* (epiphytic) and *Pseudohimantidium* (epizooic) diverged. The only shared character in this clade was their attached marine habitat and a slit structure located at the ends of their valve. Following the separation of a non-marine clade comprising *Diatoma* and *Asterionella*, *Licmophora* diverged from clade of elongated araphid diatoms, which included *Pteroncola* at the root (*Pteroncola*, (*Fragilaria*, (*Tabularia*, *Thalassiothrix*))). In this multi-gene analyses, *Licmophora* separated from the remaining araphid diatoms, being different from its position in the *SSU* supertree in which the genus was included in the clade of *Cyclophora* and *Pseudohimantidium* sharing both habitat and apical slit structure. Medlin et al. (2008) and Sims et al. (2006) found *Licmophora* separated into two clades depending on their means of attachment.

3.3. Divergence time estimation of pennate diatoms

The results indicate that the early divergence of the pennates into three major clades, basal araphid, core araphid and raphid diatoms, took place in a very short period (Fig. 5). All major clades of araphid diatoms (i.e., clade 1 to 8) appeared by the end of the Cretaceous in all analyses.

Although two topologies (BI and ML) of pennates used in the divergence time estimation were not identical as regarding the position of *Asteroplanus*, the timing of the divergence was very similar (Fig. 5, compare gray and black line, respectively). Estimated divergence times of the pennate and raphid diatoms are summarized in Table 5. Briefly, under the assumption of a diatom origin at 190 Ma, pennate emerged from 159.4 (BI) to 156.9 (ML) Ma and raphid diatoms emerged from 144.6 (BI) to 143.1 (ML) Ma. Whereas with the assumption of a 250 Ma origin, the emergence of the pennate was pushed back to 200.0 (BI) to 199.0 (ML) and the raphid origin from 180.2 (ML) to 179.9 (BI) Ma. Therefore, a consensus range of the divergence time of the pennate is from 200.0-156.9 Ma, and that of raphid diatoms is 180.2-143.1 Ma.

4. Discussion

4.1. Phylogeny of the diatoms

Ardissonea, a highly elongated diatom (Round et al., 1990), diverged last among Mediophyccean diatoms being always sister to *Lampriscus* at the root of the pennate lineage except in a ML Distant-In analysis.

Asteroplanus was the only pennate taxon that showed a totally different phylogenetic position in both BI and ML analyses. To elucidate the phylogenetic position of *Asteroplanus*, affinities of the genus should be included in the further analysis, such as *Asterionellopsis*,

known as its sister genus in *SSU* tree (see Fig. 2) and *Bleakeleya* Round, probable its sister genus judged by its morphology (p. 394-395, Round et al., 1990).

An early divergence of the clade of *Striatella* and *Pseudostriatella* among the pennates has never been shown by previous *SSU* studies because the position of *Striatella* has always been unstable and has even appeared within the raphid lineage (see Sato et al., 2008b) but has never appeared at the root of pennates as seen in our multi-gene analyses. Nevertheless, the placement of the clade can be well explained by the morphological feature of its auxospore, which is a special cell of diatoms generally produced only after sexual reproduction, and known to have evolutionary significance (Medlin and Kaczmarska, 2004). The transverse 'perizonium', covering structure of auxospore, of *Pseudostriatella* is similar to that of Mediophyceae, e.g., *Chaetoceros* (von Stosch, 1982) and *Lampriscus* (Idei and Nagumo, 2002) possessing saddle-shaped bands rather than cigar-shaped ones of core araphid/raphid diatoms, whereas the longitudinal perizonium is similar to core araphid/raphid diatoms and no centric bears this structure on their auxospores (Sato et al., 2008b). Therefore, *Pseudostriatella* possesses characters of both groups, implying that it has an intermediate state between Mediophyceae and the clade of core araphid/raphid diatoms. Unfortunately, perizonial structure of the family Rhaphoneidaceae and Plagiogrammaceae, closest relatives of *Striatella/Pseudostriatella*, still remains unknown preventing further speculation.

The interclade relationship of core araphid diatoms, which was largely a polytomy in our *SSU* supertree, was resolved in the multi-gene analyses. Although the clade of *Grammatophora/Hyalosira delicatula* and *Rhabdonema/Hyalosira tropicalis* diverged as a polytomy in BI, it is supported by reproductive, morphological and ecological characters, i.e., anisogamy in *Grammatophora* and *Rhabdonema*, mostly having septate girdle bands, and an epiphytic life form making zig-zag chains by means of mucilage secreted from the valve ends. *Licmophora* formed a clade with *Cyclophora/Protoraphis* in the *SSU* supertree but came to the root of clade of elongate diatoms in the multi-gene tree. The placement of *Pseudohimantidium/Protoraphis* within the core araphid clade rejected the idea that a raphe-like slit in these diatoms, called labiate groove, is a precursor of the raphe (Simonsen, 1970).

This study reconfirmed the paraphyly of araphid diatoms. The three subclades recovered within the pennate (= Class Bacillariophyceae) are 1) basal araphid, 2) core araphid sister to 3) raphid diatoms. They deserve to have equal rank preferably at the rank of Subclass in order to conserve current Order level systematics. Nevertheless, this cannot be done yet because current dataset is insufficient to establish the precise nature of pennate phylogeny and lacking some morphologically interesting members whose affinities are yet unknown, such as *Diprora* (Main, 2003), *Florella* (Navarro, 1982), *Gephyria* (Sato et al., 2004), *Nephronopsis* (Amspoker, 1989), *Podocystis* (Round et al., 1990, p. 396-397) and *Porannulus* (Hamilton et al., 1997).

4.2. Radiation of the pennate diatoms

None of pennate diatom has been discovered in well-preserved Early Cretaceous diatom floras reported in the past (Harwood et al., 2007), i.e., Early Albian flora from near the Antarctic margin (Gersonde and Harwood, 1990; Harwood and Gersonde, 1990), Australia (Dun et al., 1901; Harper 1977; Haig and Barnbaum 1978; Nikolaev et al., 2001) and Germany (Forti and Schulz, 1932). Although these floras have been intensively examined, none of these deposits are situated in a benthic environment, which is known as the main habitat for the most of the extant members of pennates. Moreover, the late Cretaceous is known for its abundance of pyritized diatoms (Sims et al., 2006). Thus, it is still possible that the earliest pennate has simply not been discovered. In fact, our estimation showed that the origin of the pennates between

200.0 and 156.9 Ma, greatly predating their first occurrence of fossils from the deposit of the Campanian (Sims et al., 2006). The origin of the raphid diatoms was also estimated 180.2 and 143.1 Ma predating their fossils from the deposit of the Maastrichtian (Singh et al., 2007). Furthermore, one of the earliest fossils of the raphid diatoms is now classified in the genus *Lyrella*, which is not a basal lineage within the raphid diatoms, either in 18S rDNA or *rbcL* analyses (Behnke et al., 2004; Jones et al., 2005). Therefore, if the molecular data are correct, the fossil record must significantly underestimate the age of the pennates, pushing back the origin of the entire pennate group (Sims et al., 2006).

However, it should be also noted that we cannot exclude any possibility that the results were suffered from an analytical artefact. One possibility is that the estimation was influenced by the unequal taxon sampling in the present study, i.e., known as node-density artefact (Fitch and Bruschi, 1987; Fitch and Beintema, 1990). As our primary emphasis in the present study was to reveal the phylogeny of the 'araphid diatoms', nearly half (22 out of 46 OTUs) was covered with this grade of diatoms. It might be suspected the densely sampled area of a tree can cause overestimated branch lengths, pushing the node back in time using a divergence time estimation. Although a statistical method (the delta test) that detects the node-density artifact in trees (Webster et al., 2003; available at <http://www.evolution.reading.ac.uk/pe/index.htm>) detected no evidence for punctuated evolution or the node density artefact in our ML topologies (BI topologies were not subjected to the test because the program rejects trees containing polytomies), the influence of the unequal taxon sampling in this estimation could not completely rejected.

Because a perfect coverage of fossil deposits of Mesozoic, and probably even Cenozoic age, will never be achieved, the time estimation using the fossils for calibration always involve some potential errors. Nevertheless, present study strongly suggested that the first major radiation of pennates into three clades, basal araphid, core araphid and raphid diatoms, took place in a very early stage of pennates evolution in a short period before their first appearance in the fossil record. Because of large confidence intervals of these estimations (Table 5), it remains unknown whether any geological event drove this pennate radiation.

ACKNOWLEDGEMENTS

The authors are grateful to Rainer Gersonde for invaluable comments and discussion about fossil records of diatoms; Satoko Matsumoto, Tamotsu Nagumo, Beth Petkus, Zhongmin Sun, Klaus Valentin, William Wardle and Tsuyoshi Watanabe, who provided us the living specimen, from which clonal cultures were established; Shuji Ohtani for providing a *Pseudohimantidium pacificum* clone; Andrzej Witkowski for help sampling in Poland; Stephan Frickenhaus for establishing parallel processing for Bayesian analyses; Friedel Hinz for technical help with LM and SEM. This study was supported by DAAD for doctoral research fellowship to Shinya Sato.

REFERENCES

- Altekar, G., Dwarkadas, S., Huelsenbeck, J.P., Ronquist, F., 2004. Parallel Metropolis-coupled Markov chain Monte Carlo for Bayesian phylogenetic inference. *Bioinformatics* 20, 407–415.
- Alverson, A.J., Theriot, E. C., 2005. Comments on recent progress toward reconstructing the diatom phylogeny. *J. Nanosci. Nanotechnol.* 5, 57–62.

- Alverson, A.J., Cannone, J.J., Gutell, R.R., Theriot, E.C., 2006. The evolution of elongate shape in diatoms. *J. Phycol.* 42, 655–668.
- Amspoker, M.C., 1989. *Nephronais macintirei*, gen. et sp. nov., A marine araphid diatom from California, U.S.A. *Diat. Res.* 4, 171-177.
- Andrews, G.W., 1975. Taxonomy and stratigraphic occurrence of the marine diatom genus *Rhaphoneis*. *Nova Hedwigia, Beih.* 53, 193– 227.
- Behnke, A., Friedl, T., Chepurnov, V.A., Mann, D.G., 2004. Reproductive compatibility and rDNA sequence analyses in the *Sellaphora pupula* species complex (Bacillariophyta). *J. Phycol.* 40, 193–208.
- Ben Ali, A., Wuyts, J., De Wachter, R., Meyer, A. and Van de Peer, Y., 1999. Construction of a variability map for eukaryotic large subunit ribosomal RNA. *Nucleic Acids Res.* 27, 2825–2831.
- Berney, C., Pawlowski, J., A., 2006. A molecular time-scale for eukaryote evolution recalibrated with the continuous microfossil record. *Proc. Biol. Sci.* 273, 1867–1872.
- Bradbury, J.P., Krebs, W.N., 1995. Fossil continental diatoms: paleolimnology, evolution and biochronology. In: Babcock, L.E., Ausich, W.I. (Eds.), *Siliceous microfossils (Short Courses in Paleontology, no. 8)*, The Paleontological Society, Knoxville, Tennessee, pp. 119–138.
- Chepurnov, V.A., Mann, D.G., Sabbe K., Vyverman, W., 2004. Experimental studies on sexual reproduction in diatoms. *Int. Rev. Cytol.* 237, 91–154.
- Crawford, R.M., Sims, P.A., 2006. The diatoms *Radialiplicata sol* (Ehrenb.) Gleser and *R. clavigera* (Grun.) Gleser and their transfer to *Ellerbeckia*, thus a genus with freshwater and marine representatives. *Nova Hedwig. Beih.* 130, 137-162.
- Creevey, C.J., McInerney, J.O., 2005. Clann: investigating phylogenetic information through supertree analyses. *Bioinformatics* 21, 390-392.
- Daugbjerg, N., Andersen, R.A., 1997. A molecular phylogeny of the heterokont algae based on analyses of chloroplast encoded *rbcl* sequence data. *J. Phycol.* 33, 1031–1041.
- DeSalle, R., 2005. What's in a character? *J. Biomed. Inform.* 39, 6-17
- Desikachary, T.V., Sreelatha, P.M., 1989. Oamaru diatoms. *Bibliotheca Diatomologica* 19, 1–330.
- Doyle, J.J., Doyle, J.L., 1990. Isolation of plant DNA from fresh tissue. *Focus* 12, 13–15.
- Edwards, A.R., 1991. The Oamaru diatomite. *New Zeal. Geol. Surv. Paleontol. Bull.* 64, 1–260.
- Elwood, H.J., Olsen G.J., Sogin M.L., 1985. The small subunit ribosomal DNA gene sequences from the hypotrichous ciliates *Oxytricha nova* and *Stylonichia pustulata*. *Mol. Biol. Evol.* 2, 399–410.
- Fenner, J.M., 1991. Taxonomy, stratigraphy and paleoceanographic implications of Paleocene diatoms. *Proc. Ocean Drill. Program Sci. Results.* 114, 123–154.
- Fenner, J.M., 1994. Diatoms of the Fur Formation, their taxonomy and biostratigraphic interpretation – results from the Harre borehole, Denmark. *Aarhus Geoscience* 1, 99–163.
- Fitch, W.M., Beintema, J.J., 1990. Correcting parsimonious trees for unseen nucleotide substitutions: the effect of dense branching as exemplified by ribonuclease. *Mol. Biol. Evol.* 7 (), pp. 438–443.
- Fitch, W.M., Bruschi, M., 1987. The evolution of prokaryotic ferredoxins - with a general method correcting for unobserved substitutions in less branched lineages. *Mol. Biol. Evol.* 4, 381–394.

- Fritsch, E., 1935. Structure and reproduction of the algae, vol.1. Cambridge University Press, Cambridge.
- Forti, A., Schulz, P., 1932. Erste Mitteilungen über Diatomeen aus dem Hannoverschen Gault. Beih. Bot. Zentralbl. 50, 241–246.
- Gersonde, R., Harwood, D.M., 1990. Lower Cretaceous diatoms from ODP Leg 113 site 693 (Weddell Sea) Part 1: vegetative cells. Proc. Ocean Drill. Program Sci. Results. 113, 365–402.
- Gillespie, J.J., McKenna, C.H., Yoder M.J., Gutell R.R., Johnston J.S., Kathirithamby J., Cognato, A.I., 2005. Assessing the odd secondary structural properties of nuclear small subunit ribosomal RNA sequences (SSU) of the twisted-wing parasites (Insecta: Strepsiptera). Insect Mol. Biol. 14, 625–643.
- Gradstein, F.M., Ogg, J.G., 2004. Geological Time Scale 2004 – Why, how, and where next! *Lethaia* 37, 175–181.
- Graur, D., Martin, W., 2004. Reading the entrails of chickens: molecular timescales of evolution and the illusion of precision. *Trends Genet.* 20, 80–86.
- Guillou, L., Chrétiennot-Dinet, M.-J., Medlin, L.K., Claustre, H., Loiseaux-de Goër, S., Vaultot, D., 1999. *Bolidomonas*: a new genus with two species belonging to a new algal class, the Bolidophyceae class. nov. (Heterokonta). *J. Phycol.* 35, 368–381.
- Hajós, M., 1968. Die Diatomeen der Miozänen Ablagerungen des Matravorlandes. *Geol. Hung., Ser. palaeontol.* 37, 1–40.
- Hajós, M., 1986. Stratigraphy of Hungary's Miocene diatomaceous earth deposits. *Geol. Hung., Ser. palaeontol.* 49, 1–339.
- Hajós, M., Strander, H., 1975. Late Cretaceous Archaeomonadaceae, Diatomaceae and Silicoflagellatae from the South Pacific Ocean. Deep Sea Drilling Project Leg 29, site 275. *Init. Repts. DSDP.* 29, 913–1109.
- Hall, T.A., 1999. BioEdit: a user-friendly biological sequence alignment editor and analysis program for Windows 95/98/NT. *Nucleic Acids Symp. Ser.* 41, 95–98.
- Hamilton, P.B., Poulin, M., Yang, J.-R., Klöser, H., 1997. A new diatom genus, *Porannulus* (Bacillariophyta), associated with marine sponges around King George Island, South Shetland Islands, Antarctica. *Diat. Res.* 12, 229–242.
- Hancock, J.M., Vogler, A.P., 2000. How slippage-derived sequences are incorporated into rRNA variable-region secondary structure: implications for phylogeny reconstruction. *Mol. Phylogenet. Evol.* 14, 366–374.
- Harwood, D.M., 1988. Upper Cretaceous and lower Paleocene diatom and silicoflagellate biostratigraphy of Seymour Island, eastern Antarctic Peninsula. *Geol. Soc. Am. Mem.* 169, 55–129.
- Harwood, D.M., Gersonde, R., 1990. Lower Cretaceous diatoms from ODP Leg 113 Site 693 (Weddell Sea). Part 2: resting spores, chrysophycean cysts, an endoskeletal dinoflagellate and notes on the origin of diatoms. Proc. Ocean Drill. Program Sci. Results 113, 403–425.
- Harwood, D.M., Nikolaev, V.A., 1995. Cretaceous diatoms: morphology, taxonomy, biostratigraphy. In: Babcock, L.E., Ausich, W.I. (Eds.), *Siliceous microfossils (Short Courses in Paleontology, no. 8)*, The Paleontological Society, Knoxville, Tennessee, pp. 81–106.
- Homann, M., 1991. Die Diatomeen der Fur-Formation (Alttertiär, Limfjord/ Dänemark). *Geol. Jb. ser. A* 123, 1–285.

- Honeywill, C., 1998. A study of British *Licmophora* species and a discussion of its morphological features. *Diatom Res.* 13, 221-271.
- Huelsenbeck, J.P., Ronquist, F., 2001. MRBAYES: Bayesian inference of phylogeny. *Bioinformatics* 17, 754-755.
- Hustedt, F., 1959. Die Kieselalgen Deutschlands, Österreichs und der Schweiz. In: Rabenhorst, L. (Ed.), *Kryptogamen-Flora von Deutschland, Österreich und der Schweiz*, Band VII, Teil 2, Otto Koeltz Science Publishers Koenigstein, Germany.
- Idei, M., Nagumo, T., 2002. Auxospore structure of the marine diatom genus *Lampriscus* with triangular/quadrangular forms. In: Poulin, M. (Ed.), *Abstracts book of 17th International Diatom Symposium*, Ottawa, Canada, p. 166.
- Jones, H.M., Simpson, G.E., Stickle A.J., Mann, D.G., 2005. Life history and systematics of *Petronis* (Bacillariophyta), with special reference to British waters. *Eur. J. Phycol.* 40, 43-71.
- Kaczmarska, I., Beanton, M., Bertoit, A.C., Medlin, L.K., 2006. Molecular phylogeny of selected members of the order Thalassiosirales (Bacillariophyta) and evolution of the fulstoportula. *J. Phycol.* 42, 121-138.
- Kishino, H., Hasegawa, M., 1989. Evaluation of the maximum likelihood estimate of the evolutionary tree topologies from DNA sequences, and the branching order of Hominoidea. *J. Mol. Evol.* 29, 170-179.
- Kooistra, W.H.C.F., Gersonde, R., Medlin, L.K., Mann, D.G., 2007. The origin and evolution of the diatoms: their adaptation to a planktonic existence. In: Falkowski, P.G. and Knoll, A.H. (Eds.). *Evolution of primary producers in the sea*, pp. 207-249.
- Kooistra, W.H.C.F., Medlin, L.K., 1996. Evolution of the diatoms (Bacillariophyta). IV. A reconstruction of their age from small subunit rRNA coding regions and the fossil record. *Mol. Phylogenet. Evol.* 6, 391-407.
- Kooistra, W.H.C.F., De Stefano, M., Mann, D.G., Salma, N., Medlin, L.K., 2003b. Phylogenetic position of *Toxarium*, a pennate-like lineage within centric diatoms (Bacillariophyceae). *J. Phycol.* 39, 185-197.
- Kooistra, W.H.C.F., De Stefano, M., Mann, D.G., Medlin, L.K., 2003a. The phylogeny of the diatoms. *Progr. Mol. Subcell. Biol.* 33, 59-97.
- Kooistra, W.H.C.F., Forlani, G., Sterrenburg, F.A.S., De Stefano, M., 2004. Molecular phylogeny and morphology of the marine diatom *Talaroneis posidoniae* gen. et sp. nov. (Bacillariophyta) advocate the return of the Plagiogrammaceae to the pennate diatoms. *Phycologia* 43, 58-67.
- Kuehn and Medlin 2006
- Lohman, K.E., Andrews, G.W., 1968. Late Eocene nonmarine diatoms from the Beaver Divide area, Fremont County, Wyoming. *Contributions to Paleontology. US Geological Survey Professional Paper 593-E*, 1-26.
- Lupkina, Y.G., Dolmatova, L.M., 1975. The Paleogene lagoonal diatom flora of Kamchatka. *Paleontological Journal* 1, 120-128.
- Main, S.P., 2003. *Diprora haenaensis* gen. et sp. nov., a filamentous, pseudoaerial, araphid diatom from Kaua'i (Hawaiian Islands). *Diat. Res.* 18, 259-272.
- Mann, D. G., 1999. The species concept in diatoms. *Phycologia* 38, 437-495.
- Mann, D.G., Evans, K.M., 2007. Molecular genetics and the neglected art of diatomics. In Brodie, J., Lewis, J. (Eds.) *Unravelling the Algae – The Past, Present and Future of Algal Systematics*, CRC Press, Boca Raton, Florida, pp. 231-265.
- Medlin, L.K., Kaczmarska, I., 2004. Evolution of the diatoms: V. Morphological and cyto-

- logical support for the major clades and a taxonomic revision. *Phycologia* 43, 245–270.
- Medlin, L.K., Kooistra, W.H.C.F., Gersonde, R., Sims, P.A., Wellbrock, U., 1997. Is the origin of the diatoms related to the end - Permian mass extinction? *Nova Hedwigia* 65, 1–11.
- Medlin, L.K., Kooistra, W.H.C.F., Schmid, A.-M., 2000. A review of the evolution of the diatoms - a total approach using molecules, morphology and geology. In: Witkowski, A., Sieminska, J. (Eds.), *The Origin and Early Evolution of the Diatoms: Fossil, Molecular and Biogeographical Approaches*. Szafer Institute of Botany, Polish Academy of Sciences, Cracow, pp. 13–35.
- Medlin, L.K., Jung, I., Bahulikar, R., Mendgen, K., Kroth, P., Kooistra, W.H.C.F., 2008. Evolution of the diatoms. VI. Assessment of the new genera in the araphids using molecular data. *Nova Hedwigia* 133, 81–100.
- Medlin, L., Elwood, H.J., Stickel, S., Sogin, M.L., 1988. The characterization of enzymatically amplified eukaryotic 16S-like rRNA coding regions. *Gene* 71, 491–499.
- Medlin, L.K., Sato, S., Kooistra W.H.C.F., Mann, D.G, 2008. Molecular evidence confirms sister relationship of *Ardissonea*, *Climacosphenia* and *Toxarium* within the bipolar centric diatoms and cladistic analyses confirm that extremely elongated shape has arisen twice in the diatoms (Bacillariophyta, Mediophyceae). *J. Phycol.*, in press.
- Milinkovitch, M.C., Lyons-Weiler, J., 1998. Finding optimal ingroup topologies and convexities when the choice of outgroups is not obvious. *Mol. Phylogenet. Evol.* 9, 348–357.
- Navarro, N.J., 1982. A survey of the marine diatoms of Puerto Rico IV. Suborder Araphidinea: Families Diatomaceae and Protoraphidaceae. *Bot. Mar.* 25, 247–263.
- Nylander, J.A.A., 2004. MrModeltest. Program distributed by the author. Evolutionary Biology Centre, Uppsala University.
- Pantocsek, J., 1889. Beiträge zur Kenntniss der fossilen Bacillarien Ungarns. II Brackwasser Bacillarien. Julius Platzko, Nagy-Tapolcsány, Hungary.
- Round, F.E., Crawford, R.M., Mann, D.G., 1990. *The Diatoms: Biology and Morphology of the Genera*. Cambridge University Press, Cambridge.
- Rambaut, A., Broham, L., 1998. Estimating divergence data from molecular sequences. *Mol. Biol. Evol.* 15, 442–448.
- Reháková, Z., 1980. Süßwasserdiatomeenflora des oberen Miozäns in der Tschechlowakei. *Sbornik Geologickýck ved Praha (Journal of Geological Sciences) paleontologie* 23, 83–184.
- Reinhold, T., 1937. Fossil diatoms of the Neogene of Java and their zonal distribution. Overgedrukt uit de Verhandelingen van het Geologisch- Mijnbouwkundig Genootschap voor Nederland en Kolonien. *Geologische Serie* 12, 43–132.
- Ronquist, F., Huelsenbeck, J.P., 2003. MrBayes 3: Bayesian phylogenetic inference under mixed models. *Bioinformatics* 19, 1572–1574.
- Rothpletz, A., 1896. Über die Flysch-Fucoiden und einige andere fossile Algen, sowie uberliasische diatomeen führende Hornschwamme. *Z. Dtsch. Geol. Ges.* 48, 854–915.
- Rothpletz, A., 1900. Über einen neuen jurassischen Hornschwamme und die darin eingeschlossenen Diatomeen. *Z. Dtsch. Geol. Ges.* 52, 154–160.
- Rutschmann, F., 2004. Bayesian molecular dating using PAML/multidivtime. A step-by-step manual. University of Zurich, Switzerland. <http://www.plant.ch>.
- Sato, S., Nagumo, T., Tanaka, J., 2004. Auxospore formation and the morphology of the initial cell of the marine araphid diatom *Gephyria media* (Bacillariophyceae). *J. Phycol.* 40, 684–691.

- Sato, S., Kooistra, W.H.C.F., Watanabe, T., Matsumoto, S., Medlin, L.K., 2008a. Phylogenetics and morphometrics reveal pseudocryptic diversity in a new araphid diatom genus *Psammoneis* (Plagiogrammaceae, Bacillariophyta) gen. nov.. *Phycologia*, accepted.
- Sato, S., Matsumoto, S., Medlin, L.K., 2008b. *Pseudostriatella pacifica* gen. et sp. nov. (Bacillariophyta); a new araphid diatom genus and its fine-structure, auxospore and phylogeny. *Phycologia*, in press
- Sato, S., Matsumoto, S., Medlin, L.K., 2008c. Fine structure and 18S rDNA phylogeny of a marine araphid pennate diatom *Plagiostriata goreensis* gen. et sp. nov. (Bacillariophyta). *Phycol. Res.* accepted.
- Scholin, M.A., Villac, M.C., Buck, K.R., Powers, J.M., Fryxell, G.A., Chavez, F.P., 1994. Ribosomal DNA sequences discriminate among toxic and non-toxic *Pseudonitzschia* species. *Natural Toxins* 2, 152–165.
- Schrader, H.-J., Fenner, J., 1976. Norwegian Sea Cenozoic diatom biostratigraphy and taxonomy. Part 1. *Init. Repts. DSDP.* 38, 921–1099.
- Schrader, H.-J., Gersonde, R., 1978. The Late Messinian Mediterranean brackish to freshwater environment, diatom floral evidence. *Init. Repts. DSDP.* 42, 761–775.
- Shull, V.L., Vogler, A.P., Baker, M.D., Maddison, D.R., Hammond, P.M., 2001. Sequence alignment of 18S ribosomal RNA and the basal relationships of adephagan beetles: evidence for monophyly of aquatic families and the placement of Trachypachidae. *Syst. Biol.* 50, 945–969.
- Sims, P.A., Mann, D.G., Medlin, L.K., 2006. Evolution of the diatoms: insights from fossil, biological and molecular data. *Phycologia* 45, 361–402.
- Shimodaira, H., Hasegawa, M., 1999. Multiple comparisons of log-likelihoods with applications to phylogenetic inference. *Mol. Biol. Evol.* 16, 1114–1116.
- Simonsen, R., 1979. The diatom system: ideas on phylogeny. *Bacillaria* 2, 9–71.
- Sinninghe-Damsté, J.S., Muyzer, G., Abbas, B., Rampen, S.W., Masse, G., Allard, W.G., Belt, S.T., Robert, J.-M., Rowland, S.J., Moldowan, J.M., Barbanti, S.M., Fago, F.J., Denisovich, P., Dahl, J., Trindade, L.A.F., and Schouten, S., 2004. The rise of the rhizosolenid diatoms. *Science* 304, 584–587.
- Sorhannus, U., 2004. Diatom phylogenetics inferred based on direct optimization of nuclear-encoded SSU rRNA sequences. *Cladistics* 20, 487–497.
- Sorhannus, U., 2007. A nuclear-encoded small-subunit ribosomal RNA timescale for diatom evolution. *Mar. Micropaleontol.* 65, 1–12.
- Soltis, P.S., Soltis, D.E., Savolainen, V., Crane, P.R., Barraclough, T.G., 2002. Rate heterogeneity among lineages of tracheophytes: integration of molecular and fossil data and evidence for molecular living fossils. *Proc. Natl. Acad. Sci. USA* 99, 4430–4435.
- Stamatakis, A., Ludwig, T., Meier, H., 2005. RAxML-III: A fast program for maximum likelihood-based inference of large phylogenetic trees. *Bioinformatics* 21, 456–463.
- Stosch, H.A. von, 1982. On auxospore envelopes in diatoms. *Bacillaria* 5, 127–156.
- Swofford, D. L., 2002. PAUP*. Phylogenetic Analysis Using Parsimony (* and other methods). Version 4.0b10. Sinauer Associates, Sunderland, MA.
- Syvertsen, E.E., Hasle, G.R., 1982. The marine planktonic diatom *Lauderia annulata* Cleve, with particular reference to the processes. *Bacillaria* 5, 243–256.
- Tapia, P.M., 1996. Campanian diatom biostratigraphy and paleoecology of Arctic Canada. M.Sc. Thesis. University of Nebraska.

- Tapia, P.M., Harwood, M., 2002. Upper Cretaceous diatom biostratigraphy of the Arctic Archipelago and northern continental margin, Canada. *Micropaleontology* 48, 303–342.
- Tarrio, R., Rodriguez-Trelles, F., Ayala, F.J., 2000. Tree rooting with outgroups when they differ in their nucleotide composition from the ingroup: the *Drosophila saltans* and *willistonig* groups, a case study. *Mol. Phylogenet. Evol.* 16, 344–349
- Tappan, H., 1980. The paleobiology of plantprotists. W.H.Freeman and Company, San Francisco.
- Thompson, J.D., Gibson, T.J., Plewniak, F., Jeanmougin, F., Higgins, D.G., 1997. The ClustalX windows interface: flexible strategies for multiple sequence alignment aided by quality analysis tools. *Nucleic Acids Res.* 24, 4876–4882.
- Thorne, J.L., Kishino, H., Painter, I.S., 1998. Estimating the rate of evolution of the rate of molecular evolution. *Mol. Biol. Evol.* 15, 1647–1657.
- Thorne, B.L., Grimaldi, D.A., Krishna, K., 2000. Early fossil history of termites. In: Abe, T., Bignell, D.E., Higashi, M. (Eds.), *Termites: Evolution, Sociality, Symbioses, Ecology*. Kluwer Academic Publishers., Dordrecht, pp. 77–93.
- Thorne, J.L., Kishino, H., 2002. Divergence time and evolutionary rate estimation with multi-locus data. *Syst. Biol.* 51, 689–702.
- Van de Peer, Y., Neefs, J.-M., De Rijk, P., De Wachter, R., 1993. Reconstructing evolution from eukaryotic small-ribosomal-subunit RNA sequences: calibration of the molecular clock. *J. Mol. Evol.* 37, 221–232.
- Van de Peer, Y., Caers, A., De Rijk, P., De Wachter, R., 1998. Database on the structure of small ribosomal subunit RNA. *Nucleic Acids Res.* 26, 179–182
- VanLandingham, S.L., 1967. Paleocology and microfloristics of Miocene diatomites from the Otis Basin – Juntura Region of Harney and Malheur Counties, Oregon. *Nova Hedwigia, Beih.* 26, 1–77.
- VanLandingham, S.L., 1985. Potential Neogene diagnostic diatoms from the western Snake River basin, Idaho and Oregon. *Micropaleontology* 31, 167–174.
- Webster, A.J., Payne, R.J.H., Pagel, M., 2003. Molecular phylogenies link rates of evolution and speciation, *Science* 301, 478.
- Williams, D.M., Kociolek, P.J., 2007. Pursuit of a natural classification of diatoms: History, monophyly and the rejection of paraphyletic taxa. *Eur. J. Phycol.* 42, 313–319.
- Witkowski, A., Lange-Bertalot, H., Metzeltin, D., 2000. *Diatom Flora of Marine Coasts I. Iconographia Diatomologica Vol. 7*. A.R.G. Gantner Verlag K.G., Ruggell, Liechtenstein.
- Witt, O.N., 1886. Ueber den Polierschiefer von Archangelsk-Kurojedowo im Gouv. Simbirsk. *Verhandlungen der Russisch-Kaiserlichen Mineralogischen Gesellschaft zu St Petersburg, series 2*, 22, 137–177.
- Wolfe, A.P., Edlund, M.B., 2005. Taxonomy, phylogeny and paleoecology of *Eoseira wilsonii* gen. et sp. nov, a Middle Eocene diatom (Bacillariophyceae: Aulcoseiraceae) from lake sediments at Horse Fly, British Columbia, Canada. *Can. J. Earth Sci.* 42, 243–257.
- Xia, X., Xie, Z., 2001 DAMBE: Data analysis in molecular biology and evolution. *J. Hered.* 92, 371–373.
- Yang, Z., 1997. PAML: A program package for phylogenetic analysis by maximum likelihood. *Comput. Appl. Biosci.* 13, 555–556.

-
- Yang, Z., Yoder, A.D., 2003. Comparison of likelihood and Bayesian methods for estimating divergence times using multiple gene loci and calibration points, with application to a radiation of cute-looking mouse Lemur species. *Syst. Biol.* 52, 705–716.
- Yoon, H.S., Hackett, J.D., Bhattacharya, D., 2002. A single origin of the peridinin- and fucoxanthin-containing plastids in dinoflagellates through tertiary endosymbiosis. *Proc. Natl. Acad. Sci. USA* 99, 11724–11729.

Table 1. List of species used in this analysis.

Taxa	Strain	SSU	LSU	<i>rbcL</i>	<i>psbA</i>
Coccosinodiscophyceae [centrics]					
<i>Aulacoseira granulata</i> (Ehrenberg) Simmons	p778	AB430586	AB430619	AB430659	AB430699
<i>Hyalodiscus scoticus</i> (Kützing) Grunow	s0284	AB430587	AB430620	AB430660	AB430700
<i>Melosira dubia</i> Kützing	s0076	AB430588	AB430621	AB430661	AB430701
<i>Rhizosolenia setigera</i> Brightwell	p1692	AB430589	AB430622	AB430662	AB430702
<i>Stephanopyxis turris</i> (Greville et Amott) Ralfs	p121	AB430590	AB430623	AB430663	AB430703
Mediophyceae [centrics]					
<i>Ardissonaea baculus</i> (Gregory) Grunow	wk76	AF525668	AB430624	AB430664	AB430704
<i>Cyclotella meneghiniana</i> Germain	p567	AB430591	AB430625	AB430665	AB430705
<i>Chaetoceros radicans</i> Schütt	CCMP197	AB430592	AB430626	AB430666	AB430706
<i>Cymatosira belgica</i> Grunow	p189	X85387	AB430627	AB430667	AB430707
<i>Eumotogramma laevis</i> Grunow in Van Heurck	s0382	AB430593	AB430628	AB430668	AB430708
<i>Lampriscus kittonii</i> Schmidt	p535	AF525667	AB430629	AB430669	AB430709
<i>Odontella sinensis</i> (Greville) Grunow	CCMP1815	Y10570	AB430630	Z67753	
<i>Thalassiosira pseudonana</i> Hasle et Heimdal	CCMP1335	EF208793		EF067921	
<i>Stephanodiscus</i> sp.	p404	AB430594	AB430631	AB430670	AB430710
Bacillariophyceae [Pennate]					
Araphid diatoms					
<i>Asterionella formosa</i> Hassall	s0339	AB430595	AB430632	AB430671	AB430711
<i>Asteroplanus karianus</i> (Grunow) Gardner et Crawford	s0381	AB430596	AB430633	AB430672	AB430712
<i>Cyclophora tenuis</i> Castracane	p438	AJ535142	AB430634	AB430673	AB430713
<i>Diatoma moniliforme</i> Kützing	s0383	AB430597	AB430635	AB430674	AB430714
<i>Dimerogramma minor</i> var. <i>nana</i> (Gregory) Ralfs	s0355	AB430598	AB425083	AB430675	AB430715
<i>Fragilaria bidens</i> Heiberg	s0327	AB430599	AB430636	AB430676	AB430716
<i>Grammatophora marina</i> (Lyngbye). Kützing	s0190	AB430600	AB430637	AB430677	AB430717
<i>Hyalosira delicatula</i> Kützing	p439	AF525654	AB430638	AB430678	AB430718
<i>Licmophora paradoxa</i> (Lyngbye) Agardh	s0213	AB430601	AB430639	AB430679	AB430719
<i>Nanofrustulum shiloi</i> (Lee, Reimer et McEney) Round, Hallsteinsen et Paasche	p194	AM746971	AB430640	AB430680	AB430720
<i>Rhaphoneis</i> sp.	s0366	AB430602	AB430641	AB430681	AB430721

<i>Rhabdonema minutum</i> Kützing	s0351	AB430603	AB430642	AB430682	AB430722
<i>Opephora</i> sp.	s0357	AB430604	AB430643	AB430683	AB430723
<i>Plagiosiriata goreensis</i> S. Sato et Medlin	s0388	AB430605	AB430644	AB430684	AB430724
<i>Pseudohimantidium pacificum</i> Hustedt et Krasske	mhk033	AB430606	AB430645	AB430685	AB430725
<i>Pseudostriatella pacifica</i> S. Sato et Medlin	s0384	AB379680	AB430646	AB430686	AB430726
<i>Pteroncola inane</i> (Giffen) Round	s0247	AB430607	AB430647	AB430687	AB430727
<i>Pseudostaurosira brevisiriata</i> (Grunow in Van Heurck) Williams et Round	s0398	AB430608	AB430648	AB430688	AB430728
<i>Siriatella unipunctata</i> Agardh	s0208	AB430609	AB430649	AB430689	AB430729
<i>Tabularia laevis</i> Kützing	s0021	AB430610	AB430650	AB430690	AB430730
<i>Thalassiothrix longissima</i> Cleve et Grunow	p441	AB430611	AB430651	AB430691	AB430731
<i>Hyalosira tropicalis</i> Navarro	s0252	AB430612	AB430652	AB430692	AB430732
Raphid diatoms					
<i>Campylodiscus thuretii</i> Brébisson	s0223	AB430613	AB430653	AB430693	AB430733
<i>Cocconeis stauroneiformis</i> (Rabenhorst) Okuno	s0230	AB430614	AB430654	AB430694	AB430734
<i>Navicula</i> sp.	s0020	AB430615	AB430655	AB430695	AB430735
<i>Nitzschia dubiiformis</i> Hustedt	s0311	AB430616	AB430656	AB430696	
<i>Phaeodactylum tricornatum</i> Bohlin	CCAP1055/1	EF553458		EF067920	
<i>Psammodyctyon constrictum</i> (Gregory) Mann	s0309	AB430617	AB430657	AB430697	AB430737
Outgroup					
<i>Bolidomonas pacifica</i> Guillou et Chréteinnot-Dinet [Bolidophyceae]	p380	AB430618	AB430658	AB430698	AB430738
<i>Bumilleriopsis filiformis</i> Vischer [Xanthophyceae]	NA ^a	AF083398	NA ^a	X79223	
<i>Dictyota dichotoma</i> (Hudson) Lamouroux [Phaeophyceae]	NA ^a	AF350227	AF331152	AY748321	
<i>Heterosigma akashiwo</i> (Hara) Hara [Rhaphidophyceae]	NA ^a	DQ470662		AY119759	

^aNot available.

Table 2. Primers used in this study

Marker	name	reference
<i>SSU</i>	A ^a	Medlin et al. (1988) ^c
	528F	Elwood (1985)
	1055F	Elwood (1985)
	536R	Elwood (1985)
	1055R	Elwood (1985)
	B ^b	Medlin et al. (1988) ^c
LSU	D1RF ^a	Scholin et al. (1994)
	D2CR ^b	Scholin et al. (1994)
<i>rbcL</i>	DPrbcL1 ^a	Daugbjerg and Andersen (1997)
	AraphidF ^a	This study ^d
	16F	Jones et al. (2005)
	14R	Jones et al. (2005)
	DPrbcL7 ^b	Daugbjerg and Andersen (1997)
<i>psbA</i>	psbA-F ^a	Yoon et al. (2002)
	psbA500F	Yoon et al. (2002)
	psbA-R2 ^b	Yoon et al. (2002)
	psbA600R	Yoon et al. (2002)

^aForward PCR amplification primer.

^bReverse PCR amplification primer.

^cWithout polylinkers.

^d5'-GTCTCAATCTGTATCAGAAC-3'

Table 3. Geographic records (in Ma) of diatoms introduced in Sims et al. (2006) and Singh et al. (2007) used as minimum age constraints in divergence time estimation.

Genus/Clade	Appearance age ^a	Calibration ^b	Literature cited in Sims et al. (2006) (except Singh et al., 2007)
<i>Asterionellopsis</i> ^c	Messinian (6.5-5.3)	5.3	Schrader and Gersonde (1978)
<i>Aulacoseira</i>	Uppermost Upper Cretaceous	65.5 ^d	Wolfe et al. (2006); Lohman and Andrews (1968)
<i>Chaetoceros</i>	Palaocene (c. 65-55)	55	Fenner (1991)
Coscinodiscophyceae	Aptian-Albian (115-110)	110	Gersonde and Harwood (1990); Harwood and Gersonde (1990)
<i>Cyclotella</i>	Early Eocene (24)	24	Bradbury and Krebs (1995)
<i>Cymatosira</i>	Early Eocene (c. 50-55)	50	Homann (1991); Fenner (1994)
<i>Diatoma</i>	Late Eocene to Oligocene	33.9	Lupkina and Dolmatova (1975)
<i>Dimerogramma</i>	Miocene	5.33	Schrader and Fenner 1976; Reháková (1980)
<i>Eunotogramma</i>	Upper Cretaceous	65.5	- (p. 377, Sims et al., 2006)
<i>Fragilaria</i>	Late Eocene (c. 45-40)	40	Lohman and Andrews (1968)
<i>Grammatophora</i>	Late Eocene (c. 45-40)	40	Desikachary and Sreelatha (1989); Edwards (1991)
<i>Hyalodiscus</i>	Albian-Campanian	70.6	Tapia (1996); Tapia and Harwood (2002)
Mediophyceae	Aptian-Albian (115-110)	110	Gersonde and Harwood (1990); Harwood and Gersonde (1990)
<i>Odonitella</i>	Upper Cretaceous	65.5	Hajòs and Stradner (1975); Harwood (1988)
<i>Opephora</i>	Early late Miocene	7.25	VanLandingham (1985)
Pennate	Campanian (75)	75	- (p. 381, Sims et al., 2006)
<i>Rhabdonema</i>	Late Eocene (c. 45-40)	40	Desikachary and Sreelatha (1989); Edwards (1991)
<i>Rhaphoneis</i>	Late Eocene (c. 45-40)	40	Andrews (1975)
Raphid diatom	Maastrichtian	65.5	Singh et al., 2007
<i>Rhizosolenia</i> ^e	Upper Turonian (91.5±1.5)	90	Shinninghe-Damste et al. (2004)
<i>Staurosira</i> ^f	Miocene	5.33	Hajòs (1968)
<i>Stephanodiscus</i>	Miocene	5.33	VanLandingham (1967)
<i>Stephanopyxis</i>	Late Cenomanian-Santonian (95-80)	80 ^g	Tapia (1996)
Surirellaceae	Middle Miocene	16.61	Reinhold (1937); Hajòs (1968), (1986)
<i>Thalassiothrix</i>	Early Oligocene	28.4	- (p. 388, Sims et al., 2006)

^aAges in parentheses are given in Sims et al. (2006).

^bMinimum ages were taken if range is shown in Sims et al. (2006). Otherwise dates are obtained by assigning them to top of reported chronostratigraphic unit in the Geologic Time Scale of Gradstein and Ogg (2004).

^cUsed for the constraint of *Asteroplanus*, being regarded as a first appearance of the clade 7 in the SSU supertree.

^dLower Cretaceous marine genus *Archeptyrgus* can be ancestor of *Aulacoseira* (Gersonde and Harwood, 1990; Harwood and Nikolaev, 1995; Sims et al., 2006); however, the first appearance of *Archeptyrgus* at 110 Ma was not used for a calibration point of *Aulacoseira* in this analysis because this assumption violates the maximum node constraint of *Rhizosolenia* at 93 Ma, which diverged earlier than *Aulacoseira* in our cladogram (see discussion).

^eNot fossil but abrupt increase of C₂₅ HBI alkene.

^fUsed for the constraint of *Pseudostaurosira*, being regarded as a first appearance of Staurosioide form.

^gAlthough Sims et al. (2006) found *Stephanopyxis* in the slide of Lower Cretaceous sediments of ODP Site 693, this could be a contamination of Oligocene specimens (Harwood et al., 2007, p. 35).

Table 4. Tests of Bayesian topologies versus alternative topologies derived from other optimization methods (maximum likelihood, parsimony and neighbor joining trees) as well as maximum likelihood searches with constraint, assuming the Bayesian topology as best tree.

Topology	-ln L	Difference	KH-test	SH-test
Bayesian tree ^a (Figs 4A, C)	36823.34274			
Maximum likelihood tree				
Bolido-In (Fig. 4B)	36832.10415	8.76141	0.685	0.892
Distant-In (Fig. 4D)	36835.36331	12.02057	0.599	0.824
Maximum parsimony tree				
Bolido-In	37039.32655	215.98381	<0.001 ^b	0.140
Distant-In	36848.35294	25.01019	0.353	0.733
Neighbor joining tree				
Bolido-In	36940.31975	116.97701	<0.001 ^b	0.329
Distant-In	36981.26151	157.91876	<0.001 ^b	0.233
Constrained trees				
Centrics as monophyly	39693.97789	2870.63515	<0.001 ^b	<0.001 ^b
Araphid diatoms as monophyly	39967.73758	3144.39483	<0.001 ^b	<0.001 ^b

The presented analyses test *a posteriori* hypotheses, a situation in which the Kishino-Hasegawa-test (KH-test; Kishino and Hasegawa, 1989) is not appropriate. Therefore, we also used the Shimodaira-Hasegawa-test (SH-test; one-tailed error probability; Shimodaira and Hasegawa, 1999). Nevertheless, for comparative seasons, we give the two-tailed error probabilities for the KH-test.

^aBayesian topologies were identical with either outgroup selection; a single (*Bolidomonas pacifica*) or multiple (*Heterosigma akashiwo*, *Dicyota dichotoma*, *Bumilleriopsis filiformis* and *Bolidomonas pacifica*) outgroup.

^bHypotheses that were rejected at $P = 0.05$.

Table 5. Divergence time of pennates and its credibility intervals for the nodes (in Ma). With the assumption of root at 250 - 190 Ma. 95% credibility range in square bracket.

	origin of araphid diatoms (=origin of pennates)	origin of raphid diatoms
This study		
BI topology	200.0 [226.6-163.0] - 159.4 [174.6-138.9]	179.9 [205.8-146.2] - 144.6 [159.7-125.8]
ML topology	199.0 [224.5-166.3] - 156.9 [171.4-138.6]	180.2 [203.1-150.0] - 143.1 [157.6-125.7]
Previous studies		
Kooistra and Medlin (1996)	86 [159] ^c	-
Berney and Pawlovski (2006)	98 [110-77]	-
Sorhannus (2007)	125	93.8

^aMaximum constraint of pennates at 110 Ma: based on the fact that no hint of pennates has been discovered from the well-preserved flora (Harwood et al., 2007).

^bAge and credibility intervals are identical in both assumption of root at 250 and 190 Ma.

^cAge in square bracket is 95% confidence limit of the earliest time.

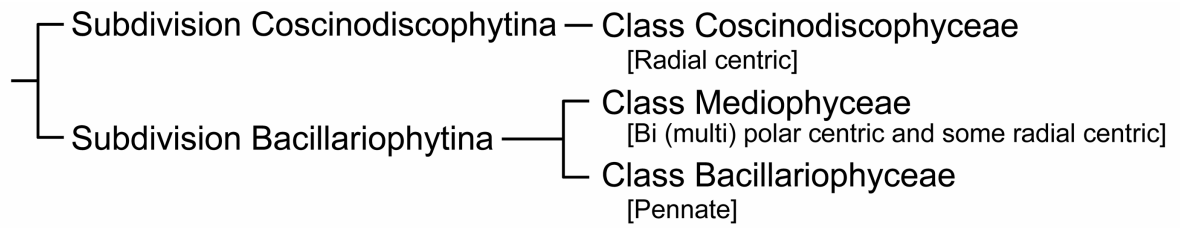


Fig. 1. Schematic representations of current diatom classification system from Medlin and Kaczmarska (2004) showing the relationship between the major lineages within the diatoms (Division Bacillariophyta).

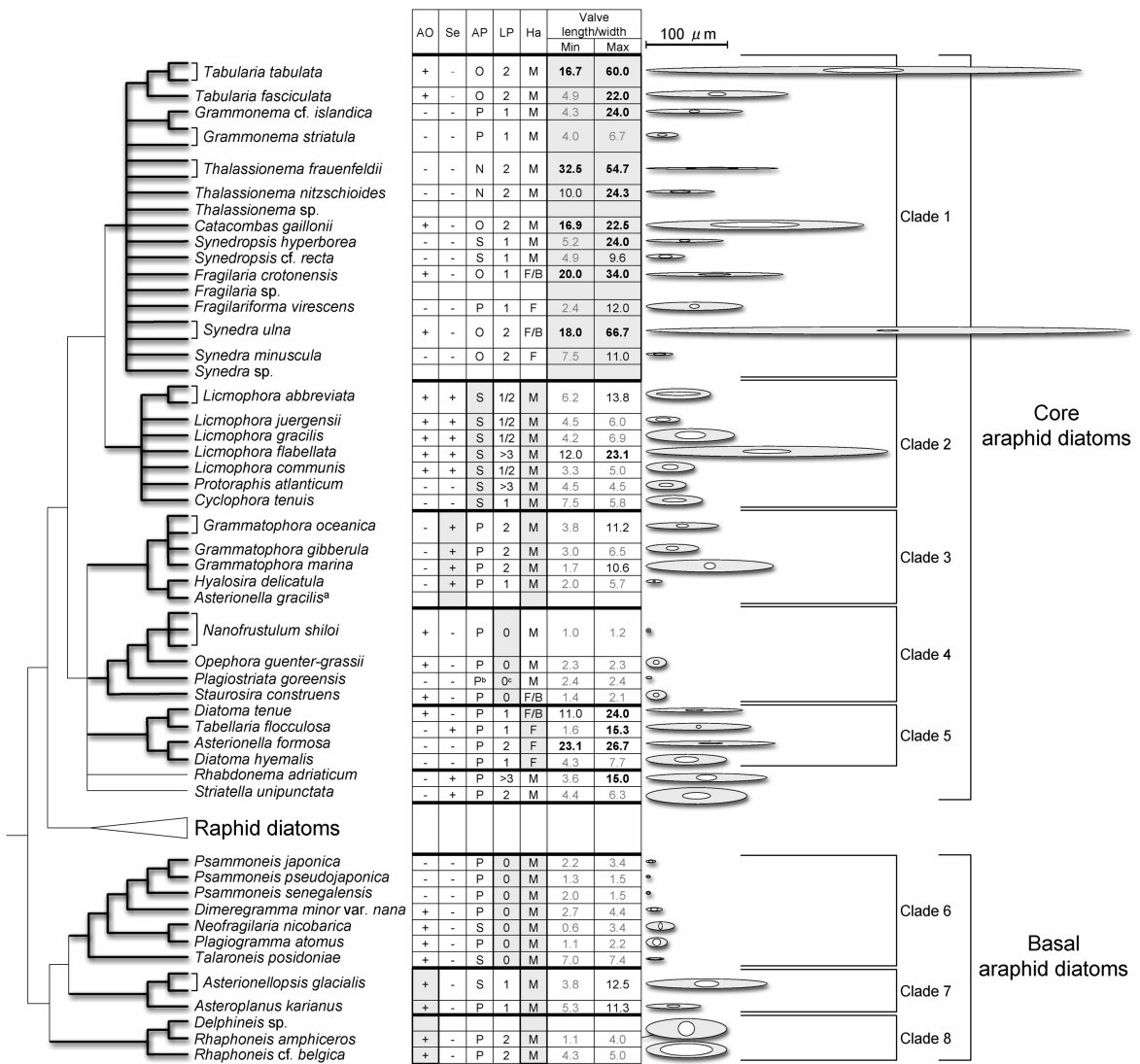


Fig. 2. Supertree of pennates (but only araphid diatoms are emphasized) constructed from various *SSU* trees published so far (see Materials and methods for source topologies). Each clade was highlighted with bold line in the tree. Explanations of characters plotted here are as follows: Areolar Occlusion (AO) is a membrane-like structure occluding the pore of the valve; presence or absence is plotted. Septum (Se) is formed inside of girdle band extending toward inside of cell; presence or absence is plotted. Apical Pore area (AP) locates at the end(s) of valve, usually possessing discrete area for mucilage secretion, such like Ocellulimbus (O)- depressed below the surface of the valve; apical pore field (P)- aggregated small pores; apical slit area (S)- one row of slits arranged in parallel; or no such area (N). Labiate process (LP) is a structure situated inside of the valve; the number of LP is plotted. Habitat (Ha) is ranged from marine (M), brackish (B) to fresh water (F). The degree of valve elongation is shown as the length/width ratio, which is classified into three categories sensu Medlin et al., (2008), i.e., l/w ratio greater than 15:1 (in bold black), 8:1 to 15:1 (black) and less than 8:1 (gray). The ratio was measured on maximum and minimum valve size of each species. Also, maximum and minimum size ranges of valve are illustrated. It should be noted that the inner/outer circle does not correspond to the valve outline of each species, but only displays the size range. Shaded boxes are discriminative characters of each clade. Presences of characters are only emphasized by shadow, except for the secondary loss of LP. All environmental and endosymbiont sequences were removed from the analyses. Kooistra et al. (2003) misidentified *Protoraphis atlanticum* as *Pseudohiman-*

tidium pacificum. Also, clade comprising three OTUs of *Microtabella* sp. in their paper was coded as *Hyalosira delicatula*. *Grammatophora* in Medlin et al. (2000) was coded as *Grammatophora oceanica*; *Diatoma* was coded as *Diatoma tenuis*; *Microtabella* was coded as *Hyalosira delicatula*. ^aAnnotated as *Asterionella gracilis* (AY485447) in Shinninge-Damste et al. (2003) and Sorhannus (2007) might be *Hyalosira* species, judging from its phylogenetic position. ^bThe AP of *Plagiostriata* is can be regarded as slit-type but unique in shape (Sato et al., 2008a). ^cThe LP of *Plagiostriata* is present but highly reduced.

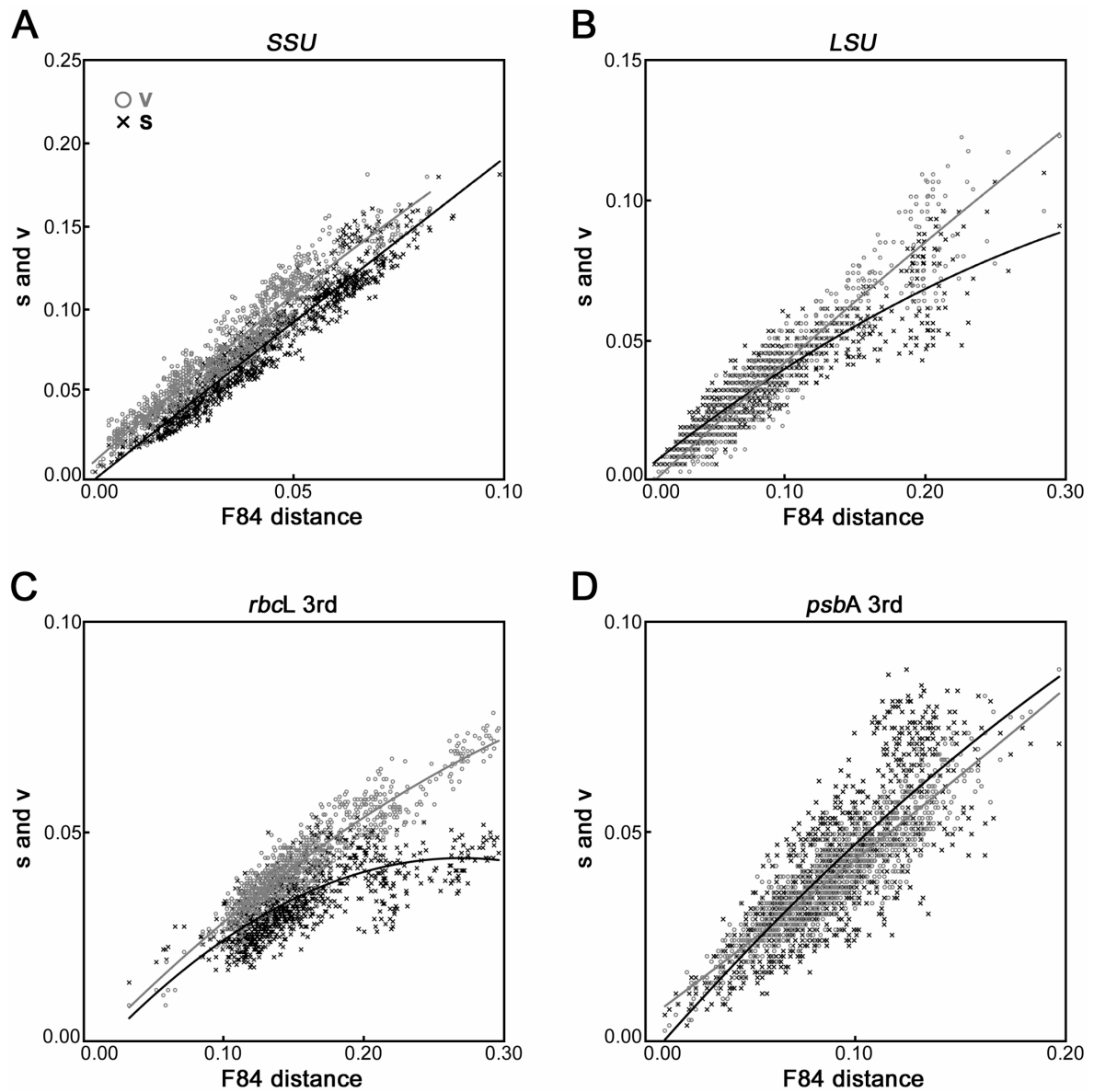


Fig. 3. Transitions (s) and transversions (v) of *SSU* (A), *LSU* (B), third codon position of *rbcL* (C) and *psbA* (D) sequences plotted versus F84 genetic distance. Saturation can be seen in B and C, but not A and D. Each black cross or gray circle in the fields represent a transition or transversion, respectively.

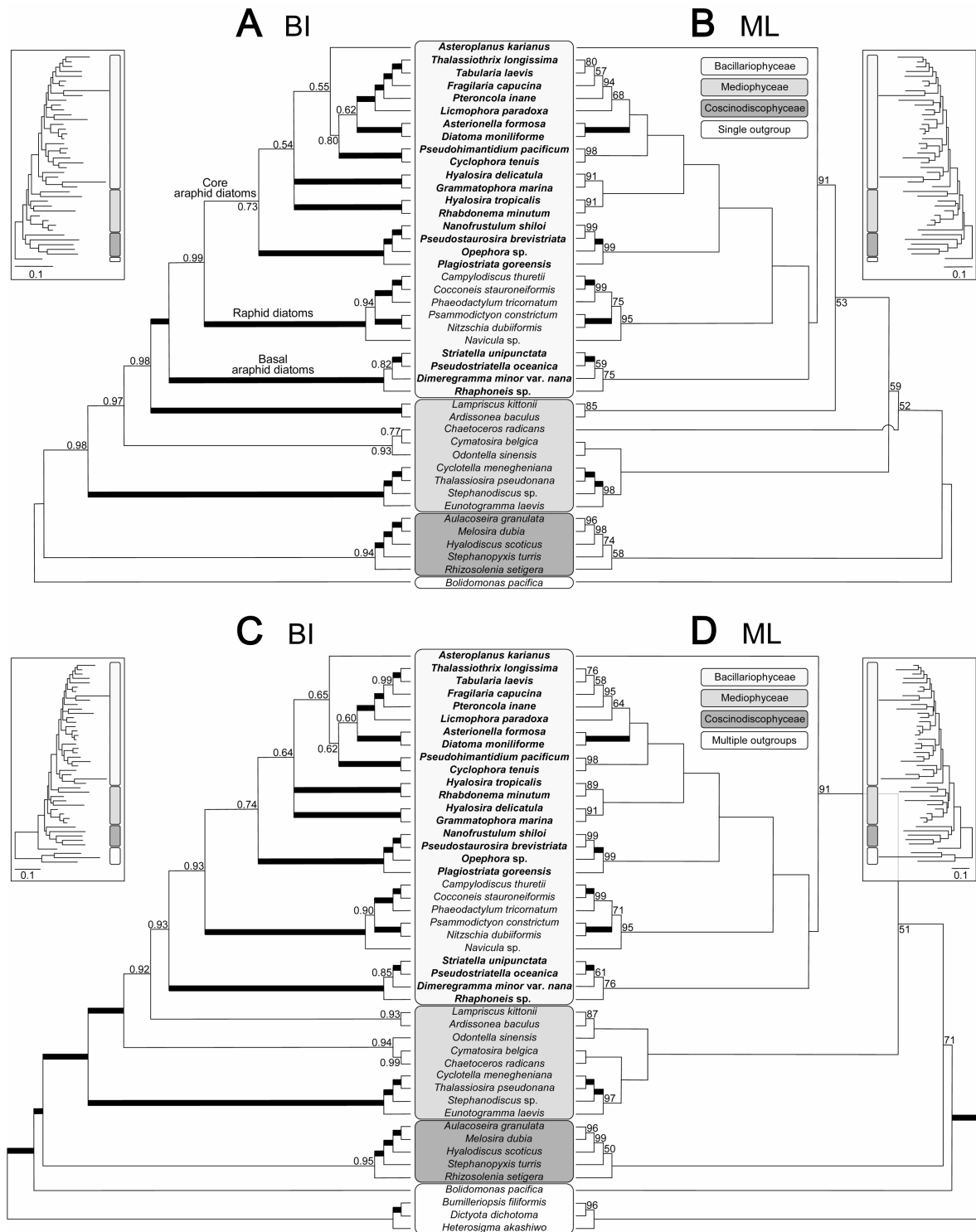


Fig. 4. Evolutionary relationships of diatoms inferred from DNA sequences of *SSU* and *LSU*, *rbcL* and *psbA*. Note *LSU* and third codon position of *rbcL* were re-coded into RY to ignore saturated transitions. Phylogenies inferred from Bayesian inferences (A, C) and Maximum Likelihood analyses (B, D). Trees are rooted with single outgroup *Bolidomonas* (A, B) or multiple outgroups of Heterokonta (C, D). Branch length of each topology is shown inside upper rectangles. Each class in the current systematics is indicated by colored enclosure. Three major subgroups of pennates, e.g., basal araphid, core araphid and raphid diatoms, are shown in A, although they are invalid in the current system. Taxon name in Bold cases are araphid diatoms. The thick nodes represent 1.00 Bayesian posterior probability (A, C) or 100 % bootstrap value in ML analyses (B, D).

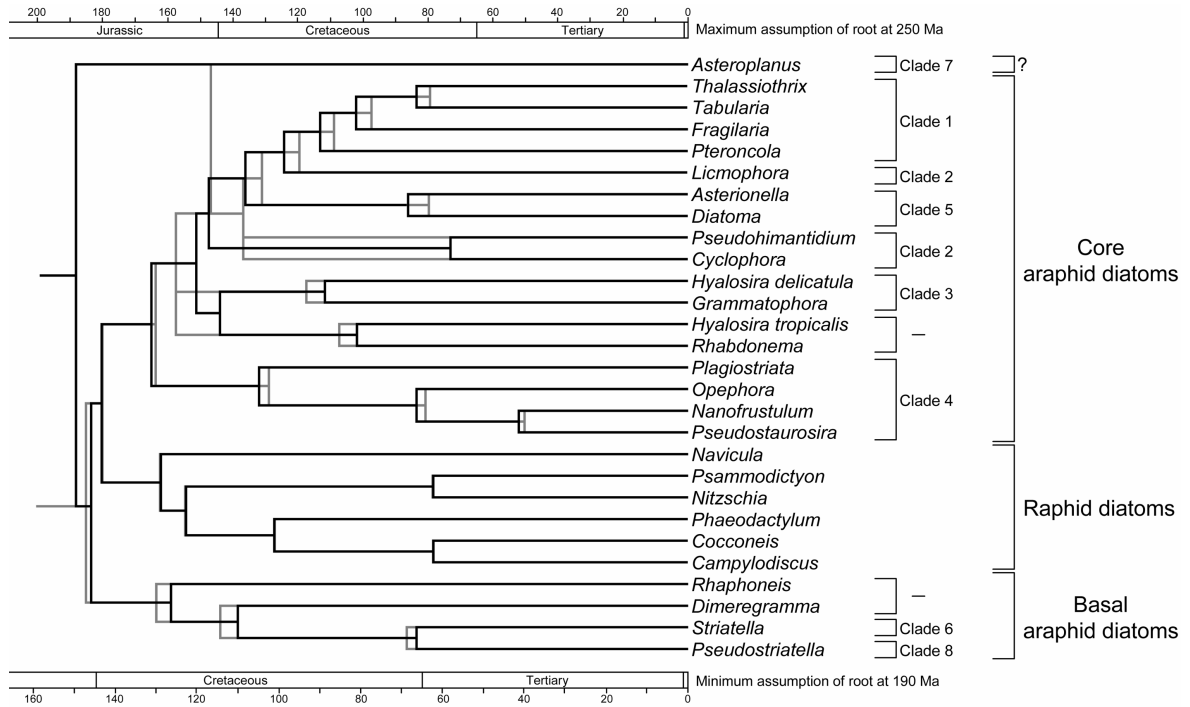


Fig. 5. Molecular timescale for pennates of BI (gray) and ML (black) tree based on Bolido-In dataset in Fig. 4A and B, respectively. Prior of 250 and 190 Ma for the root of diatoms and respective time scales are indicated above and below topology. Clade in *SSU* supertree in Fig. 2 is indicated. Basal and core araphid diatoms are also marked. Note the unresolved araphid *Asteroplanus* which belongs to basal araphid with BI but core araphid with ML.

3. SYNTHESIS

3.1. Life cycle and auxospore structure - the evolutionary significance

In **Publication III**, examination of *Grammatophora marina* from rough and clonal cultures showed that cell size changes were more flexible than generally reported for diatoms. Alogamous sexual auxosporulation took place through copulation between small male cells and larger female cells, but only in mixed rough cultures and never in clonal cultures. Auxospores were also formed without copulation in clonal cultures ('uniparental auxosporulation') and these, like sexual auxospores, developed through formation of a perizonium, which consisted of a series of transverse bands. All of these bands, including the primary band, were open. Circular scales were present in the auxospore wall before the initiation of perizonium formation and irregular, elongate structures lined the suture of the transverse perizonium. Perizonium and scales resembled those of another araphid pennate diatom, *Gephyria media* (**Publication IV**), but were simpler than those of *Pseudostriatella oceanica* (**Publication VI**) and *Tabularia parva* (**Publication V**) in their longitudinal perizonial structure. In these two diatoms, five well-developed longitudinal perizonial bands formed a series, situated at the ventral suture of the auxospore. The series of transverse bands of *P. oceanica* appears to be more similar to the properizonia of some bipolar centric diatoms than to the classic type of perizonium seen in other pennate diatoms. This similarity corresponds to the phylogenetic position of *P. oceanica* in that the species was placed in basal araphid diatoms situated between bipolar mediophycean centrics and core araphid diatoms in four genes phylogeny (**Publication X**). Scales were mainly found on the external surface of the perizonium, but curiously they were rarely found on its inner surface (**Publications IV and V**), presumably because scale formation is not strictly regulated during the latter stage of centrifugal perizonium development in the araphid diatoms. In all araphid diatoms observed in this study (**Publications III-VI**), initial cells were formed within the perizonium and consisted of an initial epivalve with a simplified structure, an initial hypovalve (formed beneath the perizonium suture) and a third, normally-structured valve formed beneath the epivalve; the epivalve was then sloughed off. In **Publication III**, Initial cells of similar configuration but often aberrant morphology could also be formed through expansion of vegetative cells, without the involvement of a perizonium. Vegetative cells were also capable of a limited enlargement through simple expansion without formation of an initial cell, and abrupt size reduction. Cell size ranges in populations from different regions suggest that *G. marina* may contain pseudocryptic species.

In summary, the observations of the auxospores have shown that longitudinal perizonial structure might be a synapomorphy of all pennates. All araphid diatoms observed in this study possessed scales on their auxospore, suggesting that scales are not a structure restricted to the auxospores of centrics, but can also be widely seen in pennates. The properizonium of mediophycean diatoms evolved into the series of transverse perizonium bands to facilitate covering the elongated cell of pennates. The perizonial structure seen in *Pseudostriatella* can be regarded as the intermediate state in the transition of a properizonium to a transverse perizonium.

3.2. Unveiled nature of araphid diversity and phylogeny

Pseudostriatella oceanica gen. et sp. nov., (**Publication VI**) was a marine benthic diatom that resembles *Striatella unipunctata* in gross morphology, attachment to the substratum by a mu-

ciliginous stalk, and possession of septate girdle bands. In LM, *P. oceanica* can be distinguished from *S. unipunctata* by plastid shape, absence of truncation of the corners of the frustule, indiscernible striation, and absence of polar labiate process. With SEM, *P. oceanica* can be distinguished by a prominent but unthickened longitudinal hyaline area, pegged areolae, multiple marginal rimoportulae, and perforated septum. The hyaline area differs from the sternum of most pennate diatoms in being porous towards its expanded ends; in this respect, it resembles the elongate annuli of some bipolar centric diatoms, e.g., *Attheya* and *Odontella*. SSU rDNA phylogeny places *P. oceanica* among the pennate diatoms and supports a close relationship between *P. oceanica* and *S. unipunctata*, but the genetic distance between them, coupled with the morphological differences, justifies separation at generic level. The affinity of the *P. oceanica* – *S. unipunctata* clade was not clear with SSU rDNA phylogeny and morphological study, but only resolvable with a combined four gene phylogeny. Both genera are only distantly related to *Hyalosira* and *Grammatophora*, despite similarities in frustule structure and growth habit, arguing against their inclusion in the same family.

Plagiosiriata goreensis gen. et sp. nov. (**Publication VII**) was described from the sand grains based on observations of frustule fine structure. The most striking feature of the species was its striation, which was angled c. 60° across the robust sternum. The other defining feature of the species was its highly reduced rimoportula and apical pores located at the both end of the valve margin. In the SSU rDNA phylogeny, the species appeared as a member of a ‘small-celled clade’ of araphid pennate diatoms that consisted of *Nanofrustulum*, *Opephora* and *Staurosira*. The results of the phylogenetic analyses suggested that the distinct characters of the diatom, i.e., its oblique striae and apical pores, may have been acquired independently. It is likely that the ancestral diatom of this lineage retained rimoportulae, but they were lost secondarily during the evolution of this clade, retaining them in a highly reduced state in *P. goreensis*, which is at the base of this lineage in four gene phylogeny.

Psammogramma vigoensis gen. et sp. nov. (**Publication VIII**) was a member of the family Plagiogrammaceae, described based on observations of frustule fine structure. The species possesses elongated valves with apical pore fields and parallel rows of striae oriented perpendicular to the apical axis. Valve poroids were occluded by perforated rotae. There is a weak sternum along the apical axis and rimoportulae were absent. Detailed observations of *Dimeregramma minor* var. *nana*, *Neofragilaria nicobarica* and *Plagiogramma atomus* supported the transfer of *Neofragilaria nicobarica* from the Fragilariaceae to the Plagiogrammaceae. Partial LSU rDNA phylogeny also supported inclusion of both *Psammogramma* and *Neofragilaria* in Plagiogrammaceae.

A new genus, *Psammoneis*. (**Publication IX**) was described based on five strains of marine benthic samples. Strains were analysed using nuclear-encoded sequence markers and morphometric parameters of their silica frustules. Valves of all strains show a sternum with striae perpendicular thereupon, typical for pennate diatoms. They possess apical pore fields and lack a raphe, rimoportulae and areolar occlusions. Sequence comparison of both the SSU rDNA and the D1/D2 region of the LSU rDNA revealed that the strains group into three markedly distinct genotypes. The strains with different genotypes are distinguishable also by a principal component analysis using four morphometric variables measured on the external valve surface, thus they are pseudocryptic species *sensu* Mann and Evans (2007). They were described as three species in *Psammoneis* as: *P. japonica* sp. nov., *P. pseudojaponica* sp. nov. and *P. senegalensis* sp. nov. Molecular phylogenies support placement of *Psammoneis* as a member of the Plagiogrammaceae. However, this placement renders this family morphologically more heterogeneous, especially with regards to areolar structure. Therefore, we provided an emended description of the family.

In **Publication X**, phylogenetic relationships among the araphid pennate diatom lineage were estimated using multi-gene markers, whereas previous studies have been made

largely based on SSU rDNA phylogenies. Phylogenies were reconstructed using SSU and LSU rDNA, *rbcL* and *psbA* (total 4352 bp) based on optimal criteria of Bayesian, maximum likelihood, maximum parsimony and distance methods. The LSU rDNA and the third codon position of *rbcL* were recoded R (A+G) and Y (T+C) because of substitution saturation detected among these positions. Two strategies for tree rooting and outgroup selection were explored, 1) one with a bolidomonad as the closest relative of the diatoms and, 2) another with bolidomonads plus more distantly related heterokontophyte outgroups. The topologies of pennates were nearly identical in all analyses. Pennates were clearly divided into three major subgroups, basal araphid, core araphid and raphid diatoms. The interclade relationship of core araphid diatoms, which was unresolved in previous SSU rDNA phylogenies, was resolved. We employed the Thorne/Kishino method of molecular dating, allowing for simultaneous constraints from the fossil record and varying rates of molecular evolution of different branches on the phylogenetic tree, to estimate the divergence time of pennates. Our estimation suggested that the pennates originated at least 156.9 Ma, which far predates its earliest fossil record at 75 Ma. Moreover the radiation of pennates into three major subgroups took place in a short period of geological time.

In summary, the undescribed diversity of araphid diatoms was shown to be considerably high. Molecular phylogenies confirmed that the araphid diatoms are paraphyletic, being divided into two groups, basal and core araphid diatoms. Basal araphid diatoms were exclusively found in the marine environment, whereas core araphid diatoms were heterogeneous in habitat, distributed from marine, brackish to limnic environments. Separation of these groups, including the emergence of raphid diatoms, took place in a short time, and they can be regarded as a rank of subclass. The taxonomic revision must be, however, only done after that the further analysis with larger dataset reveals the position of some problematic and key species.

3.3. Perspectives for future research

This study used four genetic markers for phylogenetic reconstruction of the diatoms. Although the resolution of phylogeny was, of course, dramatically increased, there were still some parts left unresolvable, e.g., the mediophycean clade/grade and the phylogenetic position of one araphid diatom, *Asteroplanus*. A simple strategy to overcome this problem is to increase the dataset, i.e., both genetic markers and species. This promises better resolution for overall topology if appropriate markers are selected. However, it is also possible that these *problematic* groups still remain unresolvable, because they often have a unique base composition and/or accelerated/decelerated substitution rate. Also, the largest difficulty may be derived from an explosive radiation in a short period, making it sometimes impossible to reconstruct the radiation pattern solely by sequence information. In fact, such difficulties can be seen in many lineages of life (for review, see Whitfield and Lockhart 2007).

Phylogenetic signals from totally different sources of information (e.g., fine-structure, karyotype or gene-architecture) may help to resolve problematic phylogenies. For example, a mobile repetitive molecule, such as the short interspersed repetitive element (SINE) is a powerful tool for phylogenetic reconstruction. SINEs are retroposons that are amplified via cDNA intermediates and are reintegrated into the host genome by retroposition (Rogers 1985; Weiner et al. 1986; Okada 1991a, b; Kazazian 2000). The integration of a SINE is irreversible, and the probability of independent insertions of a SINE at the same genomic position in different lineages is infinitely small. The polarity of a SINE insertion is fixed from its absence to its presence. These attributes imply that SINEs represent ideal, homoplasy-free markers for inferring phylogenetic relationships among organisms (Shedlock and Okada 2000; Okada et

al. 2004). Although SINEs themselves can only be applied for recent diversifications; it is worthwhile exploring similar markers for resolving deeper phylogenies of diatoms using whole genome information available.

In this study, four new genera were described (and several candidates are still being prepared for description) out of c. 400 strains isolated during 2 years, suggests the existence of a huge unexplored diversity among the araphid diatoms. Continuous effort should be made to reveal the entire picture of araphid diatoms. The observation of auxospore structure confirmed that it has evolutionary significance in diatoms. Further observation of the auxospore is, therefore, desired especially on the phylogenetically problematic and key species.

4. REFERENCES

- ALVERSON A.J. AND THERIOT E.C. 2005. Comments on recent progress toward reconstructing the diatom phylogeny. *Journal of Nanoscience and Nanotechnology* 5: 57–62.
- ALVERSON A.J., CANNONE J.J., GUTELL R.R. AND THERIOT E.C. 2006. The evolution of elongate shape in diatoms. *Journal of Phycology* 42: 655–668.
- AMATO A., ORSINI L., D'ALELIO D. AND MONTRESOR M. 2005. Life cycle, size reduction patterns, and ultrastructure of the pennate planktonic diatom *Pseudo-nitzschia delicatissima* (Bacillariophyta). *Journal of Phycology* 41: 542–556.
- ANDERSEN R.A. 2004. Biology and systematics of heterokont and haptophyte algae. *American Journal of Botany* 91: 1508–1522.
- CHEPURNOV V.A., MANN D.G., SABBE K. AND VYVERMAN W. 2004. Experimental studies on sexual reproduction in diatoms. *International Review of Cytology* 237: 91–154.
- COHN S.A., SPURCK T.P., PICKETT-HEAPS J.D. AND EDGAR L.A. 1989. Perizonium and initial valve formation in the diatom *Navicula cuspidata* (Bacillariophyceae). *Journal of Phycology* 25: 15–26.
- CRAWFORD R.M. 1974. The auxospore wall of the marine diatom *Melosira nummuloides* (Dillw.) C. Ag. and related species. *British Phycological Journal* 9: 9–20.
- EDLUND M.B. AND STOERMER E.F. 1997. Ecological, evolutionary, and systematic significance of diatom life histories. *Journal of Phycology* 33: 897–918.
- GUILLOU L., CHRETIENNOT-DINET M.-J., MEDLIN L.K., CLAUSTRE H., LOISEAUX-DE GOËR S. AND VAULOT D. 1999. *Bolidomonas*: a new genus with two species belonging to a new algal class, the Bolidophyceae class. nov. (Heterokonta). *Journal of Phycology* 35: 368–381.
- KACZMARSKA I., BATES S.S., EHRMAN J.M. AND LÉGER C. 2000. Fine structure of the gamete, auxospore and initial cell in the pennate diatom *Pseudo-nitzschia multiseriata* (Bacillariophyta). *Nova Hedwigia* 71: 337–357.
- KACZMARSKA I., EHRMAN J.M. AND BATES S.S. 2001. A review of auxospore structure, ontogeny and diatom phylogeny. In *Proceedings of the 16th International Diatom Symposium* (Ed. by A. Economou-Amilli), pp. 153–168. University of Athens, Greece.
- KAZAZIAN, H.H. JR. 2000. Genetics. L1 retrotransposons shape the mammalian genome. *Science* 289: 1152–1153.
- KIRCHNER O. 1973. Algen. In *Kryptogamen-Flora von Schlesien*. (ed. by F. Cohn), pp. 1–284. J. U. Kern's Verlag, Breslau.
- KOOISTRA W., DE STEFANO M., MANN D.G., SALMA N. AND MEDLIN L.K. 2003. Phylogenetic position of *Toxarium*, a pennate-like lineage within centric diatoms (Bacillariophyceae). *Journal of Phycology* 39: 185–197.
- MANN D.G. 1982. Structure, life history and systematics of *Rhoicosphenia* (Bacillariophyta). II. Auxospore formation and perizonium structure of *Rh. curvata*. *Journal of Phycology* 18: 264–274.
- MANN D.G. 1989. On auxospore formation in *Caloneis* and the nature of *Amphiraphia* (Bacillariophyta). *Plant Systematics and Evolution* 163: 43–52.
- MANN D.G. 1999. The species concept in diatoms. *Phycologia* 38: 437–495.
- MANN D.G. AND EVANS, K.M. 2007. Molecular genetics and the neglected art of diatomics. In: *Unravelling the algae – the past, present and future of algal molecular systematics* (Ed. by J. Brodie and J.M. Lewis), pp. 232–266. CRC Press, Boca Raton, Florida.

- MEDLIN L.K., ELWOOD, H.J., STICKEL, S., AND SOGIN, M.L. 1988. The characterization of enzymatically amplified eukaryotic 16S-like rRNA-coding regions. *Gene* 71: 491–499.
- MEDLIN L.K., ELWOOD H.J., STICKEL S., AND SOGIN M.L. 1991. Morphological and genetic variation within the diatom *Skeletonema costatum* (Bacillariophyta): evidence for a new species, *Skeletonema pseudocostatum*. *Journal of Phycology* 27: 514–524.
- MEDLIN L.K. AND KACZMARSKA I. 2004. Evolution of the diatoms: V. Morphological and cytological support for the major clades and a taxonomic revision. *Phycologia* 43: 245–270.
- NAGUMO T. 2003. Taxonomic studies of the subgenus *Amphora* Cleve of the genus *Amphora* (Bacillariophyceae) in Japan. *Bibliotheca Diatomologica* 49: 1–265.
- OHGAI M., TSUCHIDA H., SYAZUKI T., NAKASHIMA K., UEDA K. AND SAKUMA M. 1988. Effects of the environmental factors on the propagation of epiphytic diatom *Grammatophora marina* (Lyngb.) Kütz. *Nippon Suisan Gakkaishi* 54: 795–799. (In Japanese with English abstract.)
- OKADA N. 1991a. SINEs. *Current Opinion in Genetics & Development* 1: 498–504.
- OKADA N. 1991b. SINEs: short interspersed repeated elements of the eukaryotic genome. *Trends in Ecology & Evolution* 6: 358–361.
- OKADA N., SHEDLOCK A.M. AND NIKAIDO M. 2004. Retroposon mapping in molecular systematics. In *Mobile genetic elements* (eds. by W.J. Miller and P. Capy), pp. 189–226. Humana Press, N.J.
- PATRICK R. AND REIMER C.W. 1966. The diatoms of the United States. Vol 1. *Monographs, Academy of Natural Sciences of Philadelphia* 13: 1–688.
- POULÍČKOVÁ A. AND MANN D.G. 2006. Sexual reproduction in *Navicula cryptocephala* (Bacillariophyceae). *Journal of Phycology* 42: 872–886.
- POULÍČKOVÁ A., MAYAMA S., CHEPURNOV V.A. AND MANN D.G. 2007. Heterothallic auxosporulation, incunabula and perizonium in *Pinnularia* (Bacillariophyceae). *European Journal of Phycology* 42: 367–390
- ROGERS J.H. 1985. Origins of repeated DNA. *Nature* 317: 765–766.
- ROUND F.E., CRAWFORD R.M. AND MANN D.G. 1990. *The Diatoms. Biology and Morphology of the Genera*. Cambridge University Press, Cambridge, 747 pp.
- SCHMID A.-M.M. AND CRAWFORD R.M. 2001. *Ellerbeckia arenaria* (Bacillariophyceae): formation of auxospores and initial cells. *European Journal of Phycology* 36: 307–320.
- SHEDLOCK A.M. AND OKADA N. 2000. SINE insertions: powerful tools for molecular systematics. *Bioessays* 22: 148–160.
- SIMONSEN R. 1979. The diatom system: ideas on phylogeny. *Bacillaria* 2: 9–71.
- SORHANNUS U. 2004. Diatom phylogenetics inferred based on direct optimization nuclear-encoded SSU rRNA sequences. *Cladistics* 20: 487–497.
- SORHANNUS U. 2007. A nuclear-encoded small-subunit ribosomal RNA timescale for diatom evolution. *Marine Micropaleontology* 65: 1–12.
- STOSCH H.A. VON 1982. On auxospore envelopes in diatoms. *Bacillaria* 5: 127–156.
- TIFFANY M.A. 2005. Diatom auxospore scales and early stages in diatom frustule morphogenesis: their potential for use in nanotechnology. *Journal of Nanoscience and Nanotechnology* 5: 131–139.
- TOYODA K., IDEI M., NAGUMO T. AND TANAKA J. 2005. Fine-structure of the vegetative frustule, perizonium and initial valve of *Achnanthes yaquinensis* (Bacillariophyta). *European Journal of Phycology* 40: 269–279.

- TOYODA K., WILLIAMS D.M., TANAKA J. AND NAGUMO T. 2006. Morphological investigations of the frustule, perizonium and initial valves of the freshwater diatom *Achnanthes crenulata* (Bacillariophyceae). *Phycological Research* 54: 173-182.
- WEINER A.M., DEININGER P.L. AND EFSTRATIADIS A. 1986. Nonviral retroposons: genes, pseudogenes, and transposable elements generated by the reverse flow of genetic information. *Annual Review of Biochemistry* 55: 631–661.
- WILLIAMS D.M. AND KOCIOLECK P.J. 2007. Pursuit of a natural classification of diatoms: History, monophyly and the rejection of paraphyletic taxa. *European Journal of Phycology* 42: 313-319.
- WHITFIELD J.B. AND LOCKHART P.J. 2007. Deciphering ancient rapid radiations. *TRENDS in Ecology and Evolution* 22: 258-265.

5. SUMMARY

The diatoms are the most species-rich group of the eukaryotic algae, containing more than 10,000 described species. The classification of the diatom has long been based on the characters of the 'frustule', which is cell wall of the diatoms made by silica and highly sophisticated in shape. Historically the diatoms have been assumed to contain two major groups: the centrics and the pennates. The pennates were further subdivided into two groups by the presence or absence of a slit, called raphe, i.e., pennate possessing a raphe was 'raphid' diatoms, whereas pennates lacking a raphe were 'araphid' diatoms. However, recent molecular phylogenetic studies based on nuclear small subunit ribosomal RNA gene (SSU rDNA) had shown that although the pennates formed a monophyletic group, araphid diatoms were paraphyletic in the pennate lineage. The evolutionary significance of the auxospore, which is formed after the sexual reproduction of the diatoms, has recently been suggested. The current classification system of the diatoms was established based mainly on rDNA phylogenies but auxospore and cytological features were also taken into account. The entire group of pennates, including araphid and raphid diatoms, are now treated as one class. Therefore, the traditional morphology-based recognition of the pennates into two groups is no longer valid now.

The aim of this study was to obtain more complete picture of the phylogeny of 'araphid' diatoms, which was well-grouped in morphology but paraphyletic in SSU rDNA phylogenies. Samples were collected globally, and clonal cultures were established. Then detailed observation of the living cells and the frustule structures were undertaken based on the cultures. Probably because auxospore formation is rare in field specimens, there has not been any report of auxospore structures in araphid diatoms at the electron microscopic level. Given the report that the frequency of the auxospore formation can be increased when field specimens are inoculated into culture medium, this method was employed in this study to induce auxospore formation of araphid diatoms. As a result, the auxospores were successfully observed in four araphid diatom species. For phylogenetic reconstructions, LSU rDNA, *rbcL*, *psbA* were used as phylogenetic markers as well as SSU, which had routinely been used in the phylogenetic study of the diatoms.

Four new genera *Plagiostrata*, *Psammogramma*, *Psammoneis* and *Pseudostriatella*, were described based on detailed observations and phylogenetic analyses using culture strains. The paraphyly of araphid diatoms were recovered in four gene phylogeny, as well as SSU rDNA alone. The araphid diatoms were, in any case, divided into two groups 'basal' and 'core' araphid diatoms. These groups were further subdivided into several clades, which were not corresponded to the current framework of classifications, whereas these clades were well-supported by ecological/morphological features. The interclade relationship was resolved in four gene analyses that had been unresolvable in SSU rDNA alone in the past. The observation of the auxospores on four araphid diatoms, *Gephyria*, *Grammatophora*, *Pseudostriatella* and *Tabularia*, revealed that the transverse perizonial bands of *Pseudostriatella* were similar with the properizonium of bipolar centrics. On the other hand, the other three araphid diatom had a cigar-shaped perizonial band that can be seen in most of the raphid diatoms. The possession of centric-like feature of perizonium in *Pseudostriatella* was corresponded to its phylogenetic position in the basal araphid clade.

The paraphyly of araphid diatoms was strongly supported by the molecular phylogeny as well as the heterogeneity of their auxospore structures. Thus, araphid diatoms are, like the invertebrates and the cryptogams in animal and plant systematics, respectively, a dump for all pennates lacking a raphe. Most of the araphid clades were supported by ecological/morphological characters, although the current classification does not correspond to the clades. Therefore, more natural classification system should be established after further analyses with larger dataset.

6. ZUSAMMENFASSUNG

Die Diatomeen enthalten mehr als 10.000 beschriebene Arten und sind somit die artenreichste Gruppe der eukaryotischen Algen. Die Einordnung der Diatomeen stützte sich lange Zeit auf die Eigenschaften der aus Silikat bestehenden Zellwand (frustule), welche eine hohe Formenvielfalt zeigt. Seit den Anfängen der Diatomeenkunde wurde angenommen, dass Diatomeen sich aus zwei Gruppen zusammensetzen: den zentrischen und pennaten Formen. Die pennaten Diatomeen wurden in zwei weitere Gruppen unterteilt: je nachdem ob sie einen Spalt, genannt Raphe, auf ihrer Schale tragen oder nicht. Pennate mit Raphe werden als raphide und ohne als araphide Diatomeen bezeichnet. Jedoch haben neueste molekulare phylogenetische Untersuchungen, welche auf Analysen der kleinen Untereinheiten der ribosomalen RNA Gene (SSU rDNA) basierten, gezeigt, dass, obwohl die pennaten Diatomeen eine monophyletische Gruppe bilden, araphide Diatomeen sich paraphyletisch innerhalb der 'Pennaten Linie' verhalten. In letzter Zeit wurde die Fähigkeit zur Auxosporenbildung der Diatomeen nach der sexuellen Reproduktionsphase, ebenfalls als signifikantes Merkmal für die Evolution in Betracht gezogen. Das derzeitige Klassifizierungssystem für Diatomeen wurde hauptsächlich auf Basis der rDNA Phylogenie entwickelt, aber sowohl Auxosporen als auch andere zytologische Merkmale wurden mit einbezogen. Die gesamte Gruppe der pennaten Diatomeen, raphide und araphide eingeschlossen, werden nun als eine Klasse behandelt. Die traditionelle, auf der Morphologie basierende, Einordnung der pennaten Diatomeen in zwei Gruppen wird daher nicht weiter aufrecht erhalten.

Das Ziel dieser Arbeit war es, ein vollständigeres Bild zur Phylogenie der 'araphiden' Diatomeen, die der Morphologie nach einfach einzuordnen waren, dennoch paraphyletisch in der SSU rDNA erscheinen, aufzuzeigen. Proben wurden weltweit gesammelt und Klone in Kultur gehalten. Danach wurden detaillierte Beobachtungen an lebenden Zellen und Untersuchungen an der Schalenstruktur dieser Kulturen durchgeführt. Auxosporenbildung wurde bei Freilandformen selten beobachtet, daher konnten auch keine elektronenmikroskopischen Analysen von Auxosporen der araphiden Diatomeen erstellt werden. Basierend auf Berichten der Zunahme von Auxosporenbildung durch Überführung und Hälterung von Freilandproben in Kulturmedium, wurden in der vorliegenden Arbeit araphide Diatomeen in Kulturmedium überführt, um dies zu induzieren. In vier Arten der überführten araphiden Diatomeen konnte dies erfolgreich beobachtet werden.

Für die phylogenetischen Rekonstruktionen wurden die molekularen Marker für LSU rDNA, *rbcL*, *psbA* sowie SSU rDNA untersucht. Basierend auf detaillierten Beobachtungen und phylogenetischen Analysen wurden vier neue Gattungen in den gehälterten Kulturen beschrieben: *Plagiostriata*, *Psammogramma*, *Psammoneis* und *Pseudostriatella*. Die Paraphylie der araphiden Diatomeen konnte in 4-Gen-Phylogenien sowie in der SSU rDNA gezeigt werden. Die araphiden Diatomeen wurden in zwei Gruppen 'basal' und 'core' araphide Diatomeen eingeordnet. Diese wurden weiter unterteilt in verschiedene 'Clades', die nicht mit den üblichen Klassifizierungen übereinstimmen, obwohl diese neue Einteilung durch ökologische und morphologische Merkmale unterstützt werden. Die Beziehung innerhalb der 'Clades' wurde mit der 4-Gen-Analyse erschlossen, welche zuvor allein durch die SSU rDNA Analysen nicht detektierbar war. Die Beobachtungen der Auxosporen an den folgenden vier araphiden Diatomeen: *Gephyria*, *Grammatophora*, *Pseudostriatella* und *Tabularia* zeigten, dass das Querperizonalband von *Pseudostriatella* ähnlich dem Properizonium der bipolaren zentrischen Diatomeen ist. Andererseits zeigten die anderen drei araphiden Diatomeen ein Zigarren-ähnliches Perizonalband, dass in den meisten raphiden Diatomeen gefunden werden kann. Das Vorkommen des zentrischen Diatomeen ähnlichen Perizonium in *Pseudostriatella* stimmte mit seiner phylogenetischen Position im 'basal araphid clade' überein.

Die Paraphylie der araphiden Diatomeen wurde gut unterstützt durch die molekularen Phylogenien sowie durch die Heterogenität ihrer Auxosporenstruktur. Deswegen sind araphide Diatomeen wie die Invertebraten und Kryptogamen in der Tier- und Pflanzensystematik so etwas wie eine 'Müllhalde' für alle pennaten, die keine Raphe besitzen. Die meisten araphiden 'Clades' wurden unterstützt durch ihre ökologische und morphologische Charaktere, obwohl die jetzige Klassifizierung nicht mit diesen 'Clades' übereinstimmt. Deswegen sollte für die Diatomeen, nach weiteren Analysen mit einem größeren Datensatz, ein natürlicheres Klassifizierungssystem in der Zukunft etabliert werden.

7. SUMMARY (IN JAPANESE)

真核生物の中で珪藻は最大のグループであり、その種数は10万以上に達すると見積もられている。珪藻の細胞壁(被殻)は複雑な構造をもつため、珪藻は古くから主にその被殻の形態的特徴により分類が行われてきた。これまで珪藻はその形態から中心類と羽状類に二分され、さらに羽状類は縦溝と呼ばれる構造の有無により無縦溝珪藻と縦溝珪藻に分けられてきた。しかしこれまでの小サブユニット核リボソームRNA遺伝子(SSU rDNA)の塩基配列を用いた分子系統解析では羽状類は単系統を構成したものの、その系統の中で無縦溝類は側系統となった。珪藻は生活史中のごく限られた期間のみ増大胞子を形成するが、この構造の進化的意義が以前から指摘されてきた。近年rDNA遺伝子系統樹とこの増大胞子構造、さらに細胞学的特徴を考慮に入れた珪藻の新たな分類体系が提案され、そこで羽状類は一つの綱としてまとめられ、無縦溝珪藻と縦溝珪藻は分類学的地位を失った。

本研究の目的は、この形態的にはよくまとまっている一方SSU rDNA系統樹では側系統となる無縦溝珪藻の、より詳細な知見の収集と系統関係の解明である。まず無縦溝珪藻を中心とした珪藻類をサンプリングし培養株を設立し、それらを用い生細胞や被殻の詳細な観察を行った。天然試料中に増大胞子が含まれることは極めて稀であることから、これまで電子顕微鏡レベルでの増大胞子構造に関する報告は少なく、特に無縦溝珪藻においては皆無であった。そこで本研究では粗培養開始時に増大胞子形成の頻度が増すという報告を参照しこの方法を用いたところ、4種の無縦溝珪藻で増大胞子形成を誘発することに成功したため、これらについて電子顕微鏡を用い観察を行った。また系統解析には従来珪藻の分子系統学的研究に広く用いられてきたSSU rDNAに加えLSU rDNA, *rbcL*, *psbA*の遺伝子マーカーも加え、より詳細な系統関係の解明を目指した。

培養株に基づく詳細な形態学的、分子系統学的な検討を行った結果、*Plagiostriata*, *Psammogramma*, *Psammoneis*, *Pseudostriatella*の4属が新分類群として記載された。本研究で新たに得られた配列を加えSSU rDNA系統解析を行ったところ、これまでと同様無縦溝珪藻が側系統になり、さらに上記の4遺伝子を用いた系統解析でも同様の結果が得られた。何れの場合も無縦溝珪藻はbasalクレードとcoreクレードに分かれた。これらのクレードはさらに幾つかのサブクレードに細分されたが、これらのグルーピングは生態学的または形態学的形質によく支持された一方、従来の分類体系との不一致が多く見られた。これらのサブクレード間の系統関係はSSU rDNAでは十分な解像度が得られなかったが、4遺伝子系統解析により解明された。4種の無縦溝珪藻 *Gephyria media*, *Grammatophora marina*, *Pseudostriatella oceanica*, *Tabularia parva* について増大胞子を観察したところ、*Pseudostriatella*の増大胞子構造は中心類のMediophyceaeに見られるものに類似している一方、他の3種は縦溝珪藻と同様の形態であった。この増大胞子の形態的特徴は、4遺伝子系統解析において*Pseudostriatella*がbasalクレードに含まれるという結果とよく一致した。

分子系統解析および増大胞子形態は無縦溝珪藻の側系統性を強く支持した。つまり無縦溝珪藻を一つのグループとして捕らえてきた従来の分類体系は、かつて無脊椎動物や隠花植物がそうであったように、ある形質を欠くという点で定義されてきた人為分類と同様であったといえる。本研究は、無縦溝珪藻における分類体系の再構築の必要性を示唆した。

8. ACKNOWLEDGEMENT

I would like to express my deepest thanks to Linda Medlin for the possibility to carry out this work in her group, her constant guidance and encouragement during the work. I would like to thank Prof. Victor Smetacek, Prof. Ulrich Bathmann, Prof. Koen Sabbe, Prof. Thomas Hoffmeister and Richard Crawford for reviewing this dissertation. I am especially grateful to Prof. Jiro Tanaka and Prof. Tamotsu Nagumo for motivating me to start diatom research, which has made all the difference in my life.

Prof. David Mann and Wiebe Kooistra helped me considerably to complete some publications; I really learned a lot through the processes. Prof. Stephan Frickenhaus maintained Linux cluster, which made me possible to conduct huge amount of calculations comfortably. Thanks are also due to Prof. Andrzej Witkowski, Akira & Kikuko Harako, Akiyoshi Takahashi, for helping me to collect samples at the fields; and some samples were kindly provided by Tsuyoshi Watanabe, Beth Petkus, Satoko Matsumoto, Maki Taketa, Rafael Sousa, Tomoya Tadano, William Wardle, Shuji Ohtani and Zhongmin Sun. Thanks to my present and former colleagues in AWI, Andrea Reents, Annegret Müller, Bank Beszteri, Christine Gescher, Francisca Vermeulen, Helga Mehl, Friedel Hinz, Ines Jung, Katja Metfies, Katrin Bruder, Kerstin Töbe, Klaus Valentin, Maddalena Bayer, Monica Estanqueiro, Ramkumar Seenivasan, Sabine Strieben, Sara Beszteri, Sonja Dierks, Steffi Gäbler and Uwe John for the friendly atmosphere and advise throughout this work; and many Japanese diatomists, Prof. Tamotsu Nagumo, Prof. Masahiko Idei, Keigo Osada, Shigeki Mayama, Hidekazu Suzuki, Kensuke Toyoda and Tsuyoshi Watanabe for their continuous encouragement. Special thanks to family Beszteri (Bank, Sara, Marton and Jako) for supporting so many things in my German life; Helga Mehl for sharing our office for 3 years and teaching me German and German cultures; the paper meeting team (Steffi, Francisca and Lars) for sharing exciting topics from wide range of biology, expanding my scientific interest greatly. Last, but not least, this work could not have been achieved without the tolerance help and constant encouragement of my wife, Kyoko.

This work was financially supported by DAAD (Deutscher Akademischer Austausch Dienst/German Academic Exchange Service) A/05/00774, and conducted in Alfred Wegener Institute for polar and marine research.

9. Appendix

9.1. Publication XI:

Molecular evidence confirms sister relationship of *Ardissonaea*, *Climacospheia* and *Toxarium* within the bipolar centric diatoms (Bacillariophyta, Mediophyceae) and cladistic analyses confirms that extremely elongated shape has arisen twice in the diatoms

LINDA K. MEDLIN^{1*}, SHINYA SATO¹, WIEBE H.C.F. KOOISTRA² & DAVID G. MANN³

¹*Alfred-Wegener-Institute for Polar and Marine Research, Am Handelshafen 12, D-27570 Bremerhaven, Germany*

²*Stazione Zoologica A. Dohrn, Villa Comunale, 80121 Naples, Italy*

³*Royal Botanic Garden, Edinburgh EH3 5LR, Scotland, UK*

2008. *Journal of Phycology* (in press)

Abstract

With the use of a new kit from Qiagen to amplify total genome quantity, DNA was bulked up from two diatoms that are difficult to grow, viz., *Ardissonea* and *Climacosphenia*, and the nuclear SSU rRNA gene was successfully amplified. Results of Bayesian analyses showed that these diatoms are sister to *Toxarium* and belong to the bi- and multipolar centric diatoms. The results indicate that extremely elongate shape has arisen at least twice in diatoms, in the true pennates and in the bipolar centrics. The two lateral pattern centers of *Ardissonea* and *Climacosphenia* likely represent a modified annulus that subtends ribs internally as well as externally. Studies of sexual reproduction are needed to determine whether *Ardissonea*, *Climacosphenia*, and *Toxarium* achieve their elongate shape by similar means to each other and to true pennates, i.e., by controlling the expansion of the auxospores by sequential addition of silicified bands (to form a ‘properizonium’ or ‘perizonium’).

KEY WORDS: *Ardissonea*; Bayesian Inference; *Climacosphenia*; *Toxarium*; properizonium; perizonium

ABBREVIATIONS: LM, light microscopy

INTRODUCTION

Placement of *Ardissonea*, *Climacosphenia*, *Synedrosphenia* and *Toxarium* in a taxonomic treatment of the diatoms has been difficult. Given their valve structure (as this was interpreted at the time), extremely elongate shape (up to 15:1 or more, length to width ratio) and benthic lifestyle – living attached by mucilage masses secreted from one end of the cell – taxonomists originally had no qualms in considering that these taxa belong to the pennate diatoms (Schütt 1896, Karsten 1928). Indeed, *Ardissonea* and *Toxarium* species were included in the genus *Synedra* for most of the 20th century (Hustedt 1932, Hendeby 1964). Round et al. (1990) placed all four genera among the pennates, though they noticed that some traits encountered in most other rapheless pennates, viz. a central sternum and apical rimoportulae, were absent. On the other hand, all of them, apart from *Toxarium*, showed a valve organization with transverse striation: striae run across the whole width of the valve, perpendicular to the main axis, as is generally characteristic of pennate diatoms. In *Toxarium*, there is a wide axial area bearing an irregular scatter of pores; nevertheless, transverse striation typical of pennates was believed to be present, but restricted to a narrow marginal zone (e.g., Schütt 1896); the wide axial area was therefore interpreted as a ‘pseudoraphe’ (a term more or less equivalent to ‘sternum’).

Kooistra et al. (2003) examined the wall morphology, motility and phylogenetic relationships of *Toxarium undulatum* J. W. Bailey. Their molecular analyses indicated that, surprisingly, it belonged outside the pennates, among the bipolar centrics. More particularly, *Toxarium* was sister to *Lampriscus kittonii* A. W. F. Schmidt with 72% bootstrap support, putting it in one of the clades of bi- and multipolar centric diatoms. These generally have non-circular valves as a result of anisometric expansion of their auxospores (except in the Thalassiosirales, which have circular valves and whose auxospore formation is like that of the radial centrics, apparently through secondary loss of a properizonium) and correspond to the Mediophyceae of Medlin and Kaczmarska (2004). Kooistra et al. (2003) showed that the irregularly porous valve face of *T. undulatum* is not, and does not contain, a sternum and concluded that “If *Toxarium* and its putative close allies are excluded, the monophyletic ‘true pennate’ clade can be characterized by the possession of a single axial sternum subtending parallel ribs

and intervening rows of pores; in addition, there is either a raphe or apical labiate processes, or both (Round et al. 1990).” Kooistra et al. suggested that, if *T. undulatum* is a centric diatom, it should possess an annulus (the ring-like pattern center of centric diatoms) and identified its likely position as a break in the pore distribution near the valve face–mantle junction, which separates the largely irregular scatter of pores on the valve face from the orderly rows of pores on the mantle.

Alverson et al. (2006) challenged the validity of some of the findings in Kooistra et al. (2003). They pointed out improvements in alignment and phylogenetic analysis and noted that elongated shape is not unique to pennates but is also encountered in many bipolar centric diatoms. They also indicated that the position of *T. undulatum*, away from the pennates, could result from taxon sampling, although their results agreed with those in Kooistra et al. (2003) in recovering *T. undulatum* as sister to the multipolar centric *L. kittonii*. To help resolve the controversy between Kooistra et al. (2003) and Alverson et al. (2006), we have added nuclear SSU rDNA sequences of two taxa putatively close to *T. undulatum*, namely *Ardissonaea baculus* (Gregory) Grunow and *Climacosphenia moniligera* Ehrenberg to our data-set and inferred their phylogenetic relationships.

A point of contention between Kooistra et al. (2003) and Alverson et al. (2006) is what “elongated” means. Kooistra et al. claimed that the ‘elongate’ shape of *Toxarium* was a pennate-like characteristic, by implying that the elongate shape of some ‘bipolar centrals’ (excluding *Toxarium*) was, in some undefined manner, qualitatively different from the elongate shape of pennates. Alverson et al. made a different distinction between (a) ‘circular’ or ‘sub-circular’, (b) ‘elongate or biangular’, (c) ‘triangular’ and (d) ‘quadrangular’. On the basis of this scoring, the ‘elongate or biangular’ shape of *Toxarium* appears unremarkable, because this category is found in many bipolar centric diatoms. In our opinion, however, there is a marked and significant difference between the range of shapes exhibited by bipolar centric diatoms and the range of shapes exhibited by bipolar pennate diatoms and *Toxarium* and its putative relatives. So far as is known, this difference reflects changes in the ways in which auxospores control expansion (e.g., Medlin & Kaczmarek 2004) and produce the initial cells of the next generation.

Here, we use 18S rDNA data to establish the phylogenetic position of *Ardissonaea*, *Climacosphenia* and *Toxarium*, and we map some aspects of valve shape and structure, and some auxospore characteristics onto an 18S rDNA tree, to assess if states sometimes regarded as typical for pennates (e.g. a feather-like arrangement of the striae, formation of a perizonium) have been acquired only once.

MATERIAL AND METHODS

Cells of *Ardissonaea* and *Climacosphenia* are difficult to maintain in culture, and we were unable to grow *A. baculus* and *C. moniligera en masse* for large-scale DNA extraction. However, they grew and divided for a short period in enriched seawater media (e.g., f/2). DNA from these few cells was extracted using standard extraction procedures (Medlin et al. 1996). DNA concentrations were so low that no product of the desired gene could be obtained with standard PCR methods, so we used a genome amplification kit (REPLI-g, Qiagen, Hilden, Germany) to bulk up the entire genome content. Starting material ranged from 3.2 to 13.0 ng • μL^{-1} and was amplified to 330.4 and 93.0 ng • μL^{-1} for *A. baculus* and *C. moniligera*, respectively. From this bulked-up material, PCR products for the nuclear SSU rRNA gene were successfully amplified (Medlin et al. 1988) and sequenced according to Karsten et al. (2003). Obtained sequences of *A. baculus* and *C. moniligera* were aligned with those of 800+ other diatoms, including published and unpublished sequences. The taxa used for tree construction

were selected to include the closest relatives of *Toxarium* identified by Kooistra et al. (2003), together with representatives of other major lineages, ensuring that the range of morphologies in the diatoms were represented by at least one taxon from among the 800+ diatoms in a dataset maintained in the ARB program, which uses the SSU secondary structure model as a guide to alignment (<http://www.arb-home.de>). This resulted in a dataset of 54 taxa with 1821 positions; the taxon sampling differed from that in Kooistra et al. (2003) as an independent test of the association of the taxa within the Mediophyceae. This makes the fourth independent analysis of the position of *Toxarium* (Kooistra et al. 2003, Sorhannus 2004, Alverson et al. 2006, and here). In this data-set, the secondary structure determined how sequences are aligned, overruling primary sequence similarity. Because the secondary structure was used to guide the alignment, ambiguous positions were minimized, and alignment was aided in loop regions by the presence of many other sequences in the original dataset of 800+ sequences. Using the 50% position variability filter for all eukaryotes built into the ARB program, all positions in the molecule were selected for analysis.

We also generated an alignment based on sequence similarity using the same OTUs included in the ARB dataset. Sequences were at first aligned by Clustal (<http://www.ch.embnet.org/software/ClustalW-XXL.html> settings scoring matrix: Blosum, opening gap penalty: 10, end gap penalty 10, extending gap penalty 0.1, separation gap penalty 0.1) and then the most variable regions were further adjusted by eye. Because the latter procedure may introduce biases, two data-sets were analysed. One contained the complete sequences, as in the ARB-generated alignment (i.e., all positions in), whereas the other had highly variable regions (mostly peripheral regions of the SSU rRNA secondary structure) removed from the alignment, by reference to the variability map of *Saccharomyces cerevisiae* (Van de Peer et al. 1993). This was done to exclude the possibility of possible alignment bias, saturation of the phylogenetic signals and parallelisms, such as replication slippage (Morrison 2006), because the conservation of structure might be a result of functional constraints instead of evolutionary homology (Schultes et al. 1999). The first Clustal data-set contained 1897 positions and is a direct comparison to the ARB dataset in terms of number of bases selected for analysis and the second, with the most variable positions removed, contained 1482 positions. The full alignments and the nexus files are in the supplementary data. Phylogenies were obtained using Bayesian Inference (BI) with MrBayes version 3.1 (<http://mrbayes.csit.fsu.edu/>), run in parallel and performed as in Medlin and Kaczmarek (2004). We assumed that the analysis had been optimized if the independent runs converged on the same tree. State changes of ultrastructural characters of valve shape and auxospore development over the ARB tree were assessed in MacClade version 3.07 (Maddison and Maddison 1997). The ARB tree was chosen only as a matter of convenience. The position of *Toxarium*, *Climacosphenia* and *Ardissonea* is in the bipolar centrics in both trees.

The definition of any shape descriptor like ‘elongate’ (Kooistra et al. 2003) or ‘subcircular’ (Alverson et al. 2006) is arbitrary, because boundaries have to be set along a continuum. In addition, in elongate diatoms, the length:width ratio diminishes with ongoing mitotic divisions during the life cycle (Round et al. 1990). Nevertheless, in some diatoms, like *Toxarium* and *Climacosphenia*, the length:width ratio is always extreme. To explore the distribution of high length:width ratios among diatoms, we chose a ratio of 15:1 to separate very markedly (highly) elongate valves from less elongate, subcircular and circular valves. The longest recorded valves were used for this assessment, on the assumption that these will be closest to the initial cells. Initial cells are the first cells after sexual reproduction has restored the diatom to the largest cell size characteristic of the species (Round et al. 1990, Chepurnov et al. 2004) and thus should be free from any artefact induced as the cells divide and become smaller, thus changing their length-width ratio. Because initial cells are not known for most diatoms, our survey should be valid as long as there is no systematic bias in how well the lengths that have been recorded reflect the full size range. We added two additional categories: between 8:1 and

15:1, and less than 8:1 but not circular. Data on length:width ratios were obtained by consulting standard taxonomic references containing morphometric data for each species. Stria patterns and pattern centers were assessed by reference to Round et al. (1990).

RESULTS

The BI-tree inferred from 54 nuclear SSU rRNA gene sequences included in this study using the ARB secondary structure alignment resolved *T. undulatum* as sister to a clade with *A. baculus* and *C. moniligera*. These three in turn formed a clade sister to *Lampriscus*, all of these being within the bi- and multipolar mediophycean centric diatoms (Fig. 1a). This same sister relationship was recovered in the analyses by Kooistra et al. (2003), Sorhannus (2004) and Alverson et al. (2006). This result was also obtained from an analysis (results not shown) when *A. baculus* and *C. moniligera* were added to the entire ARB alignment of L. K. Medlin, which contains 800+ SSU sequences of diatom taxa. The BI-tree constructed from the full Clustal alignment also showed a sister relationship of *T. undulatum* to the *A. baculus*–*C. moniligera* clade; however these three taxa were sister to *Rhizosolenia* not *Lampriscus* (Fig. 1b). However, there was low support (68% PP) for this relationship and *R. pungens* was recovered on a long branch. In both the ARB tree and the Clustal tree with all positions included, all diatoms historically treated as pennates, with the exception of *Toxarium*, *Ardissonaea* and *Climacosphenia*, formed a well-supported clade (100%) and *Toxarium*, *Ardissonaea* and *Climacosphenia* are not placed anywhere near the pennate diatom in any of the four analyses now available (op cit). Within the ‘core pennates’, a clade containing *Asterioplanus*, *Asterionellopsis*, *Delphineis* and *Rhaphoneis* was resolved as sister to a clade containing both the other araphid pennates, including *Synedra*, and also the raphid pennates. The Coscinodiscophytina (radial centrics) and Mediophyceae (bi- and multipolar centrics) were monophyletic in the ARB tree but not in the Clustal tree. The reduced Clustal alignment (in supplementary data) produced more grades of clades, rather than the polytomies seen in several lineages in Fig. 1b.

We have coded four features of valve morphology in MacClade and mapped them over the ARB aligned tree. The first coded character is the ratio of the valve length to width (Fig. 2). The cladogram revealed that highly elongate valves, with aspect ratios > 15:1, occur in some genera of core pennates and in the clade comprising *Toxarium* and its allies. Surveys of the literature indicate that this result is not an artifact of taxon sampling within the bipolar centric diatoms. Among the pennates, some of the taxa that we sampled have a length to width ratio of less than 8:1, and there are also some other pennates with length to width ratios of greater than 15:1 that we did not include in this analysis. Length ratios between 8:1 and 15:1 do occur in the bipolar centrics, especially in the Cymatosiraceae.

The second character mapped over the tree was the organization of the pattern center on the valve face (Fig. 3a). All specimens in the core pennate clade possess a sternum or mid-rib from which striae are subtended perpendicularly. Most centric diatoms in the tree possess a circular annulus (a ring-like pattern center) or central region, from which striae extended outwards – and only outwards – in a radial fashion. In some species of *Odontella* and in *Attheya*, this pattern center is elongated, but still subtends a regular striation outwards and an irregular scatter of poroids inwardly. By contrast, in *A. baculus*, *C. moniligera*, and *T. undulatum*, the pattern center is apparently quite different. In *T. undulatum*, there is a break in the pore distribution near the valve face–mantle junction (Kooistra et al. 2003), which separates a largely irregular scatter of pores on the valve face from orderly but short rows of pores on the mantle. In *A. baculus* and *C. moniligera*, the valve face bears four sets of striae, organized around two longitudinal ribs placed near or at the margin on the valve face. One set of striae extends outwards from each rib, as in the striae subtended by the annulus in (other) centric diatoms, and

one set extends inwards. The two sets of inward-facing striae, which have no equivalent in any other centric diatoms, meet along the mid-line of the valve, forming a fault.

The third character mapped over the tree was closely related to the second and comprised the stria organization on the valve (see Fig. 3b). A radial organization of striae, as in the spokes of a wheel, was encountered in the valves of most centric diatoms, whereas in all members in the pennate clade, the striae were organized in a parallel fashion. However, parallel striation was also apparent in *Attheya*, in some species of *Odontella*, and in *A. baculus* and *C. moniligera*.

The fourth coded character was the type of auxospore (Fig. 3c). Auxospore formation has been studied in only a few diatoms and therefore most taxa in Fig. 3c have been coded as “unknown.” We treated our OTUs as representative of the genera to which they are currently assigned, so that if sexual reproduction had been studied in a different species of the same genus, we plotted that feature for our OTU. Nevertheless, all centric diatoms with circular or subcircular valves in which the auxospores have been studied have simple auxospore coverings with silica scales embedded in an organic matrix. Centric diatoms that have slightly elongate or multipolar valves possess properizonia, whereas in most pennates the auxospores have perizonial bands. Using this knowledge we also plotted a predicted type of auxospore across our tree (Fig. 3d).

DISCUSSION

We have demonstrated that molecular analysis is probably possible for any diatom, by applying genomic amplification methods to a few cells or even a single one. This will allow molecular phylogenetics to be extended to include taxa that are difficult to maintain in culture.

From the systematic perspective, results obtained in the present study confirm results in Kooistra et al. (2003) and Alverson et al. (2006) that *Toxarium* is not a pennate diatom, despite its highly elongate valve outline, its superficial resemblance (in LM) to many pennate diatoms, and its growth form – attachment of cells, singly or in clumps, to a solid substratum via a mucilage pad – which resembles that of many benthic araphid pennates, such as *Synedra* or *Tabularia*. The two trees we present differ significantly in where *Toxarium* is placed among the bi- and multipolar centrics, and in whether the bi- and multipolar centrics are a clade or a grade. There are also curious features in both trees, such as the sister relationships between *Aulacoseira* and *Attheya* and between *Rhizosolenia* and the *Toxarium* clade in the Clustal tree, and the position of *Attheya* at the base of the bi- and multipolar centrics in the ARB tree. Both of these go against previous trees and receive no support from other sources (e.g. morphology, growth form, reproduction). However, there is low support for most of these placements, which are likely the result of not using outgroups outside of the diatoms and poor sampling among the radial centrics in this analysis, as well as the alignment itself. These differences reflect different philosophies of alignment, in particular, the role of secondary structure in assessing homology. The effect of applying the ARB model of secondary structure is most dramatically seen in recovery of monophyly for the Coscinodiscophytina and Mediophyceae, which are paraphyletic in the Clustal trees. Alverson et al. (2006) used a different secondary structure model from that underlying the ARB alignment and this likely caused some of the differences in overall topology between their trees and that shown here (Fig. 1a); others reflect taxon sampling. However, the key issue is that the position of *Toxarium* outside the core pennates does not change, regardless of the type of alignment (Clustal vs. structure-guided) or the secondary structure model used. Placement of *Ardissonea* and *Climacosphenia* as sisters to *Toxarium* breaks down the longish branch leading to *Toxarium* in previous analyses, thereby reducing (though not eliminating) the possibility that the posi-

tion of this genus away from the pennates is erroneous because of long-branch attraction. The grouping of *Ardissonea* and *Climacosphenia* in the same clade as *Toxarium undulatum* was predicted by Kooistra et al. (2003), based on certain similarities in frustule ultrastructure, namely a distinctive girdle structure at the poles in *Toxarium* and *Ardissonea*, absence of apical pore fields, and absence of labiate processes. Moreover, the motility mechanism present in *Ardissonea* (Pickett-Heaps et al. 1991) and *Toxarium* (Kooistra et al. 2003) – involving secretion of mucilage from the girdle at the cell apices – appears to have a common origin.

Historically, the irregularly punctate axial area of *Toxarium* was interpreted as a ‘pseudoraphe’ and equivalent to the axial ‘sternum’ present in the pennates. Alverson et al. stated that (p. 655) “Interest in the classification of diatoms dates back to at least 1896 when diatoms with a round cell outline (centrics) were distinguished from those with a long and narrow cell outline (pennates) (Schütt 1896).” Schütt’s (1896, pp. 55, 56) distinction was in fact rather different, since he separated centrics from pennates primarily on the basis of pattern organization of the valve, not valve outline. Thus the ‘Centricae’ were ... “centrisch gebaut; Struktur regellos, concentrisch oder radiär, nicht gefiedert” [built in a centric fashion; structure irregular, concentric or radial, not like a feather], whereas the ‘Pennatae’ had valves that were “echt zygomorph, nicht centrisch gebaut. [truly bilaterally symmetrical, not built in a centric fashion]”. Karsten (1928) and Hustedt (1930, p. 216) also separated centric and pennate diatoms primarily on the basis of valve pattern. Schütt (1896) noted that pennates were generally “schiffchen- oder stabförmig” [boat-shaped or pole-shaped], whereas the only centrics achieving even a ‘schiffchen’ [boat-] shape were the Rutilarioideae. Nevertheless, the key issue with respect to the pennate–centric distinction was and remains the nature of the pattern center.

The present study confirms the finding in Kooistra et al. (2003) and Alverson et al. (2006) that *Toxarium* does not belong in a clade containing only those diatoms with a pennate organization. Instead, its close relatives in the gene trees are all centrally organized, even if the sister is erroneously *Rhizosolenia* in the Clustal tree. The pattern center of *Toxarium* is not obvious in mature valves and examination of some partly formed valves was not conclusive in Kooistra et al.’s (2003) study. Kooistra et al. (2003) suggested, however, that the break between the haphazardly distributed pores in the valve face and the transverse rows in the valve is homologous to an annulus, i.e., the ring- or disc-like pattern centers of centric diatoms, which often contain irregularly arranged pores (e.g. see illustrations of *Chrysanthemodiscus*, *Cerataulus*, *Eucampia*, *Hemidiscus* and *Triceratium* in Round et al. 1990).

Kooistra et al. (2003) noted that the highly elongate diatoms *Climacosphenia*, *Synedrosphenia* and *Ardissonea* have anomalous pattern centers, which correspond neither to the sternum of pennate diatoms, nor to the unifacial annulus of centric diatoms; this was also discussed by Mann (1984). *Climacosphenia*, *Synedrosphenia* and *Ardissonea* have strictly transapical striae, but these are subtended by two longitudinal rib-like elements, rather than one as in core pennate diatoms. The implication of Fig. 3a, b is that the two longitudinal rib-like elements are homologous to the annulus of centric diatoms and the sister to the *Toxarium*–*Ardissonea*–*Climacosphenia* clade in the ARB and Alverson et al. (2006) analyses, *Lampriscus*, has a simple circular annulus containing irregularly arranged poroids (Round et al. 1990 and unpublished images of F.E. Round archived with D.G.M.). It might be thought that the interpretation of the ribs as an annulus is far-fetched, but within the assemblage of centric lineages there are others in which the annulus deviates markedly from circular, e.g., in *Attheya* (Round et al. 1990, p. 341), and it appears that the ribs are continuous around the apices, at least in *Climacosphenia* (Round et al. 1990, pp. 32 and 443), as would be expected if the ribs are part of a single annulus.

However, the pattern centers of *Climacosphenia* and *Ardissonea* would differ from the annuli of most centric diatoms not only in their extreme elongation and size, but also by sub-

tending striae both internally and externally; they were therefore referred to as ‘bifacial’ annuli by Mann (1984). The fact that *Ardissonea* and *Climacosphenia* are resolved as nearest sisters suggests that the striae inside the annulus were acquired in the common ancestor of these two genera, after its separation from *Toxarium*. The last common ancestor of all three of them probably acquired the extremely elongated shape, following the separation from the lineage including *Lampriscus* because the latter is multipolar and has an almost circular valve outline. No molecular data are yet available for *Synedrosphenia*, but its frustule architecture (Round et al. 1990, pp. 444-445) is similar to that of *Ardissonea* and *Climacosphenia*, possessing a ‘bifacial annulus’ rather than a unifacial annulus or a single sternum, suggesting that *Synedrosphenia* is a close relative of these genera.

Removal of *Ardissonea*, *Climacosphenia*, *Toxarium*, and probably also *Synedrosphenia*, from the core or true pennates renders the description of the latter group more straightforward. According to Kooistra et al. (2003), the “‘true pennate’ clade can be characterized by the possession of a single axial sternum subtending parallel ribs and intervening rows of pores; in addition, there is either a raphe or apical labiate processes, or both” (see also Round et al. 1990). Radial organization of the striation pattern, with a circular annulus as the pattern center, must be the ancestral state in diatoms (Fig. 3b) and pennate-like organization, with sets of transverse striae, has evolved several times independently. For example, parallel striae are found in *Attheya* and *Papiliocellulus*, as well as in the *Ardissonea* clade and in pennates. This feature is related to the shape of the pattern center (see Fig. 3a) because in almost all diatom valves, the striae are orientated perpendicular to the pattern center. If that pattern center is a circle or disc, then the striae radiate. If the pattern center is a bar (a sternum), then the striae become parallel to one another, except at the tips of the bar.

Alverson et al. (2006) pointed out the ambiguity of the description “elongated”, as used by Kooistra et al. (2003) and we do, of course, agree that several genera of what we refer to as ‘bipolar’ centric diatoms are usually elongate. However, *Ardissonea*, *Climacosphenia* and *Toxarium* have cells that are far more elongate than in any diatom treated historically as being a centric; we have used an arbitrary threshold of 15:1 to demonstrate this, which separates *Ardissonea*, *Climacosphenia* and *Toxarium* from other centric diatoms but not from some pennates. For example, extreme length occurs in some species of *Nitzschia* and in *Thalassionema*, *Trichotoxon*, *Reimerothrix*, *Thalassiothrix* and *Synedra* (see Round et al. 1990, Hasle and Syvertsen 1996, Mann 1981, Prasad et al. 2001); as noted previously, it was in *Synedra* that *Toxarium* and *Ardissonea* were classified for many years (e.g. Hustedt 1932, Hendey 1964). Extreme elongation is not seen in bipolar centrics, except for *Toxarium* and its sisters, and such characteristics have clearly evolved several times in unrelated lineages. In terms of elongation, the nearest approach to *Toxarium* and its allies among bipolar centric diatoms occurs among the Cymatosirales (Hasle et al. 1983), but these are much smaller diatoms.

Shape in diatoms is generally created by anisometric expansion of the auxospores. Where the auxospores expand equally in all directions, the valve outline is a circle. Pennate diatoms, which are almost always elongate, generally achieve this through formation of special sets of stiffening bands called the perizonium (see Round et al. 1990), which has been suggested to be a synapomorphy for the group (Medlin and Kaczmarska 2004), alongside the sternum. Those centric diatoms that produce elongate or multipolar valves also possess stiffening elements in their auxospores, taking the form of a structure called the properizonium (von Stosch 1982), which again shepherds anisometric expansion of auxospores. Because *Toxarium* and its relatives belong among the lineages of polar and multipolar centric diatoms (Mediophyceae), one would expect that expansion of their auxospores would be accompanied by formation of a system of properizonial bands (Fig. 3c). However, to produce such a long shape, considerable modification is likely to have been necessary in auxospore development. How these taxa actually do it will remain unknown until sexual reproduction can be induced,

but it seems likely that all three genera probably control the expansion of their auxospores by using ring-shaped bands like those of true pennates (Fig. 3d). Yet, if so, these bands will only be analogous to the pennate perizonium.

Interestingly, the other main lineage of centric diatoms with fairly strongly elongate valves – the Cymatosirales – produce their shape via a quite different mechanism to that present in other bipolar diatoms. Von Stosch (in Hasle et al. 1983, p. 80) stated that the Cymatosirales have a unique method of producing elongate cells. Although the auxospores of Cymatosirales are “banded” (i.e. they possess properizonia), they are not elongate but *subglobular*, giving rise to strongly anisometric primary cells. Unfortunately, this was not illustrated (von Stosch indicated a manuscript ‘in preparation’, but this was never completed), but the only possible interpretation seems to be that the initial cells are produced after a strong bilateral contraction of the protoplast away from the ellipsoidal auxospore wall (cf. the smaller post-expansion change in shape during the formation of the initial cells in *Navicula cryptocephala* Kützinger: Poulíčková and Mann 2006). Such a mechanism can almost certainly be ruled out on physical grounds in *Toxarium*, *Climacosphenia* and *Ardissonaea*, because any ‘subglobular’ auxospores would have to be at least 500 µm in diameter to accommodate the initial cells.

In his analysis of the distinction between centric and pennate diatoms, Schütt (1896, p. 54) commented not only on pattern organization and shape, but also on cytological and reproductive differences, and these were clarified further by Karsten (1928) and von Stosch (1950); the latter showed that centric diatoms are oogamous (von Stosch 1950). Unfortunately, there are no reports of sexual reproduction in any of the three genera we examine here, nor in *Synedrosphenia*. Because allogamous sexual reproduction involves oogamy in all centric diatoms studied to date, we would expect *Ardissonaea*, *Toxarium* and their allies to produce eggs and sperm. However, *Ardissonaea* and *Toxarium* have actively motile vegetative cells, and so it is possible that they may exhibit gametangiogamy, as in the pennates. Given the difficulty of keeping *Climacosphenia* and *Ardissonaea* in culture, it may be most profitable to look for sexual stages in natural populations. We have kept clonal *Toxarium* cultures for several years but they have remained vegetative, and attempts to induce sexual reproduction by mixing cultures (in case of heterothally) have also failed thus far.

Our phylogenetic results support, without any doubt, the position of *Toxarium* and its allies outside the pennate diatoms and also supports our initial contention, which may have been initially poorly expressed, that their highly elongate shape has arisen independently from that in true pennates. This can clearly be seen in the character plots of Fig. 2. Alverson et al. (2006) suggested that taxon choice affected the recovery of *Toxarium* in the centric diatoms as reported by Kooistra et al. (2003). We agree fully with them that taxon choice and analysis methods can affect phylogenetic results, but the different approaches and sampling reported in the present paper do not move *Toxarium*, *Ardissonaea* and *Climacosphenia* from among the lineages of bipolar centrics. In all, four analyses have now placed *Toxarium* outside the pennate diatoms and a group comprising *Toxarium* and its allies with the pennates is never recovered (Kooistra et al. 2003, Sorhannus 2004, Alverson et al. 2006, this paper).

ACKNOWLEDGEMENT

Shinya Sato gratefully acknowledges the support of the DAAD for his stay at the laboratory of Linda K. Medlin. We express our thanks to two unknown reviewers for their constructive criticism and advice.

REFERENCES

- Alverson, A. J., Cannone, J. J., Gutell, R. R. & Theriot, E. C. 2006. The evolution of elongate shape in diatoms. *J. Phycol.* 42:655–68.
- Chepurnov, V. A., Mann, D. G., Sabbe, K. & Vyverman, W. 2004. Experimental studies on sexual reproduction in diatoms. *Int. Rev. Cytol.* 237: 91–154.
- Hasle, G. R. & Syvertsen, E. E. 1996. Marine diatoms. In Tomas, C. R. [Ed.] *Identifying marine diatoms and dinoflagellates*. Academic Press, San Diego, pp. 5–385.
- Hasle, G. R., von Stosch, H. A. & Syvertsen, E. E. 1983. Cymatosiraceae, a new diatom family. *Bacillaria* 6:9–156.
- Hendey, N. I. 1964. *An introductory account of the smaller algae of British coastal waters. Part V. Bacillariophyceae*. HMSO, London.
- Hustedt, F. 1930. Bacillariophyta (Diatomeae). In: *Die Süßwasser-Flora Mitteleuropas*, A. Pascher (Ed.), Heft 10, Gustav Fischer, Jena.
- Hustedt, F. 1932. Die Kieselalgen Deutschlands, Österreichs und der Schweiz. In *Dr L. Rabenhorsts Kryptogamenflora von Deutschland, Österreich und der Schweiz*, vol. 7 (2:2), Akademische Verlagsgesellschaft, Leipzig.
- Karsten, G. 1928. Bacillariophyta (Diatomaceae). In: *Die Natürlichen Pflanzenfamilien*, 2nd ed. (Ed. A. Engler & K. Prantl), vol. 2 Leipzig, W. Engelmann, pp. 105–203.
- Karsten, U., Schumann, R., Rothe, S., Jung, I. & Medlin, L. 2006. Temperature and light requirements for growth of two diatom species (Bacillariophyceae) isolated from an Arctic macroalga. *Polar Biol.* 29:1–11.
- Kooistra, W. H. C. F., De Stefano, M., Mann, D. G., Salma, N. & Medlin, L. K. 2003. Phylogenetic position of *Toxarium*, a pennate-like lineage within centric diatoms (Bacillariophyceae). *J. Phycol.* 39:185–97.
- Maddison, W. P. & Maddison D. R. 1997. *MacClade: analysis of phylogeny and character evolution*, version 3.07. Sinauer Associates, Inc.
- Mann, D. G. 1981. A new species of sigmoid *Nitzschia* (Bacillariophyta). *Israel J. Bot.* 30:1–10.
- Mann, D.G. 1984. An ontogenetic approach to diatom systematics. In: D.G. Mann [Ed.], *Proceedings of the 7th International Diatom Symposium*. O. Koeltz, Koenigstein, pp. 113–44.
- Medlin, L. K. & Kaczmarska, I. 2004. Evolution of the diatoms: V. Morphological and cytological support for the major clades and a taxonomic revision. *Phycologia* 43:245–70.
- Medlin, L. K., Elwood, H. J., Stickel, S. & Sogin, M. L. 1988. The characterization of enzymatically amplified eukaryotic 18S rRNA-coding regions. *Gene* 71:491–9.
- Medlin, L. K., Gersonde, R., Kooistra, W. H. C. F., & Wellbrock, U. 1996. Evolution of the diatoms (Bacillariophyta): II. Nuclear-encoded small-subunit rRNA sequences comparisons confirm a paraphyletic origin for the centric diatoms. *Mol. Biol. Evol.* 13:67–75.
- Morrison, D. A. 2006. Multiple sequence alignment for phylogenetic purposes. *Austr. Syst. Bot.* 19: 479–539.
- Pickett-Heaps, J. D., Hill, D. R. A. & Blazé, K. L. 1991. Active gliding motility in an araphid marine diatom, *Ardissonea* (formerly *Synedra*) *crystallina*. *J. Phycol.* 27:718–25.
- Pouličková, A. & Mann, D. G. 2006. Sexual reproduction in *Navicula cryptocephala* (Bacillariophyceae). *J. Phycol.* 42:872–86.

- Prasad, A. K. S. K., Nienow, J. A. & Riddle, K. A. 2001. Fine structure, taxonomy and systematics of *Reimerothrix* (Fragilariaceae: Bacillariophyta), a new genus of syndroid diatoms from Florida Bay, USA. *Phycologia* 40:35–46.
- Round, F. E., Crawford, R. M., & Mann, D.G. 1990. *The Diatoms. Biology and Morphology of the Genera*. Cambridge University Press, Cambridge, 747 pp.
- Schultes, E. A., Hraber, P. T. & LaBean, T. H. 1999. Estimating the contributions of selection and self-organization in RNA secondary structure. *J. Mol. Evol.* 49:76-83.
- Schütt, F. 1896. Bacillariales. In Engler, A. & Prantl, K. [Eds.] *Die natürlichen Pflanzenfamilien*. 1:31–153.
- Sorhannus, U. 2004. Diatom phylogenetics inferred based on direct optimization of nuclear-encoded SSU rRNA sequences. *Cladistics*, 20: 487-97.
- Stosch, H. A. von 1982. On auxospore envelopes in diatoms. *Bacillaria* 5:127–56.
- Van de Peer, Y., Neefs, J.-M., De Rijk, P. & De Wachter, R. 1993. Reconstructing evolution from eukaryotic small-ribosomal-subunit RNA sequences: calibration of the molecular clock. *J. Mol. Evol.* 37: 221-32.

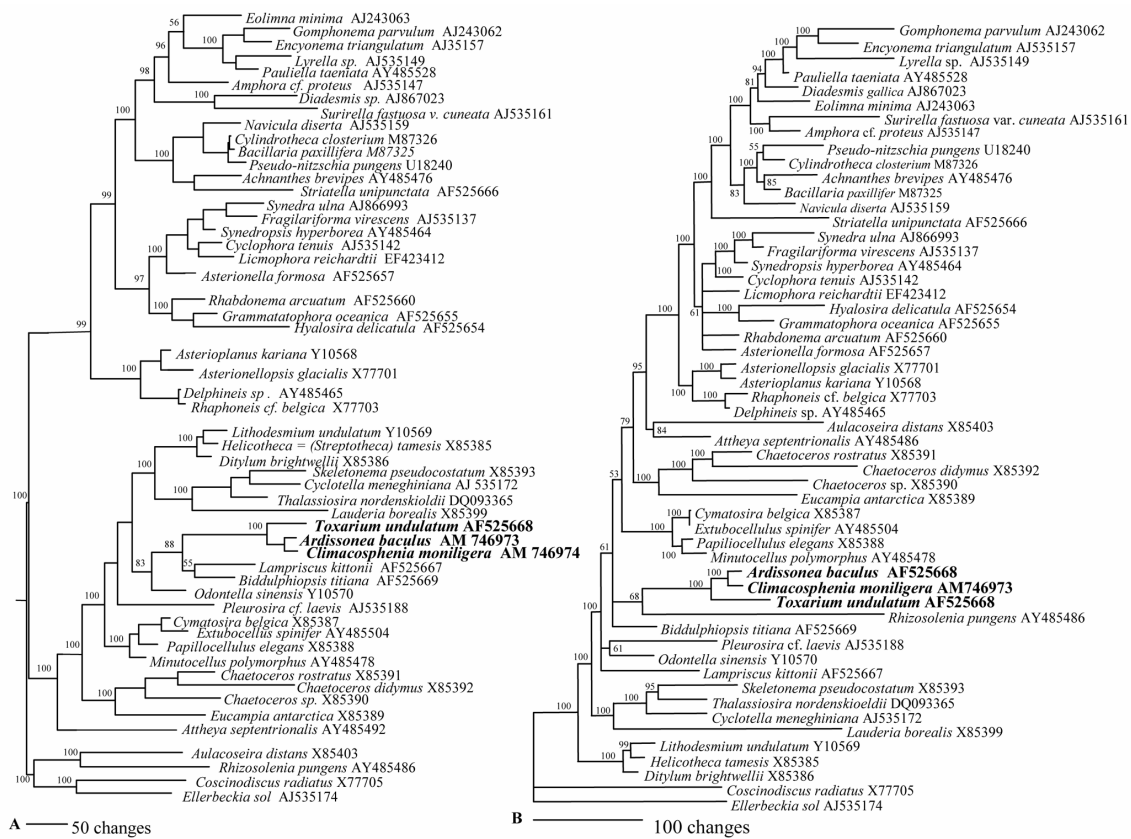


Fig. 1. Final fully resolved trees generated from 54 diatom nuclear SSU rRNA gene sequences by Bayesian inference using an unspecified GTR model with an undefined gamma distribution, during 1,000,000 generations, and saving every 1000th tree. Numbers on the nodes represent the posterior probabilities ($\times 100$, > 50) for consensus of the last 100 trees saved by the search. Two searches were run in parallel and the two runs converged on the same consensus tree. **A)** Tree obtained with ARB secondary structure alignment **B)** Tree obtained using Clustal alignment. For both trees, all bases were included in the alignment.

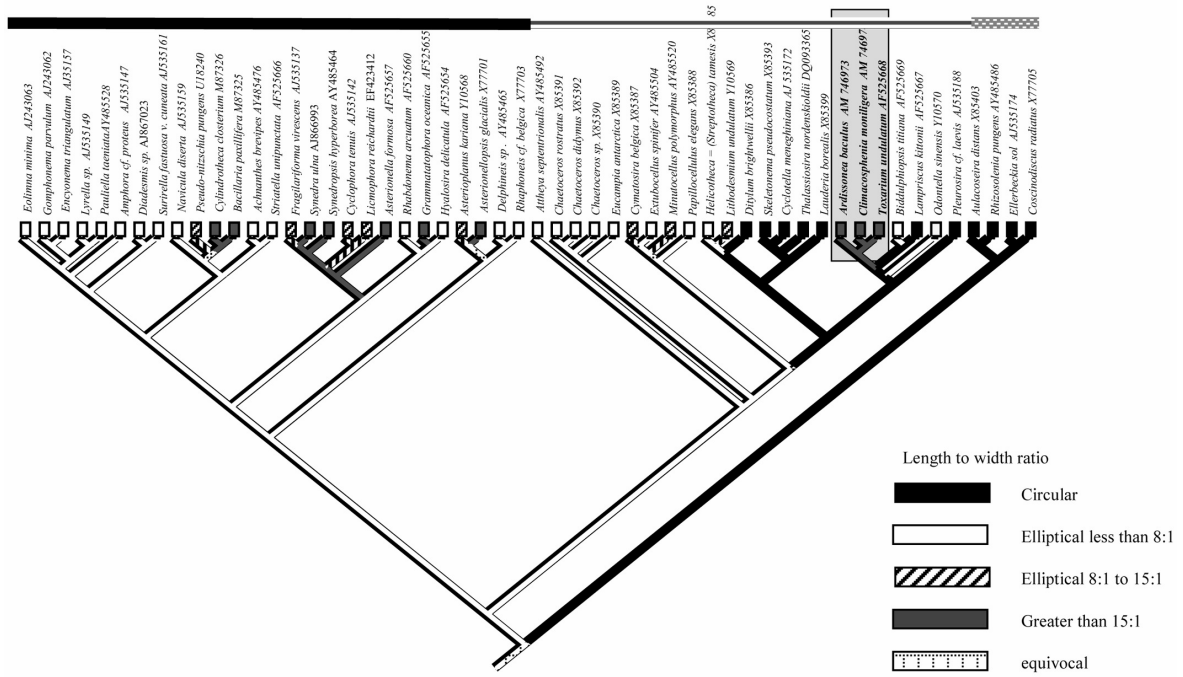


Fig. 2. Character plot of length : width ratio across the diatom data-set using the tree from the ARB alignment. Black bar marks pennate taxa. Light-grey horizontally striped bar marks mediophycean taxa. Dark- grey dotted bar marks coscinodiscophycean taxa. The light grey box marks the clade with *Toxarium*, *Ardissonaea* and *Climacosphenia*.

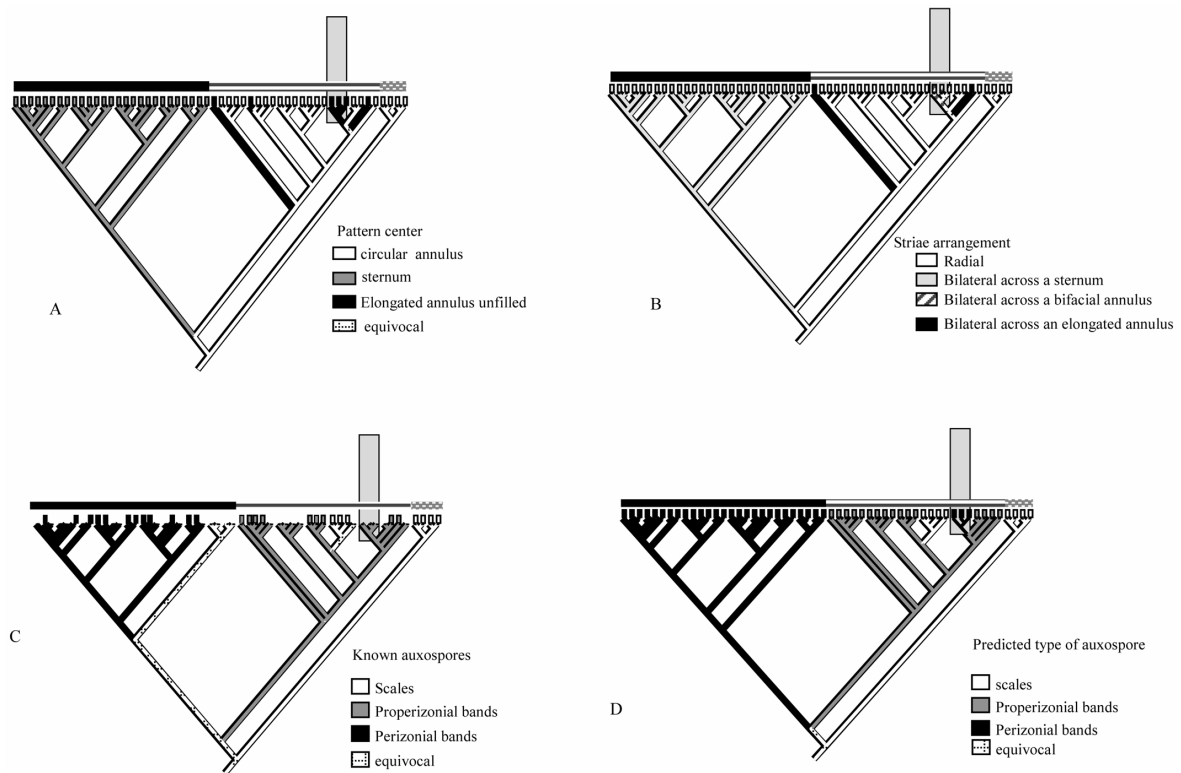


Fig. 3. Character plot of (a) pattern center, (b) stria arrangement, (c) known auxospore formation, and (d) predicted auxospore formation across the diatom data-set, using the tree from the ARB alignment. Bars from Fig. 1 mark the diatom classes; refer to Fig. 1 for species names. The light-grey box marks the clade with *Toxarium*, *Ardissonaea* and *Climacosphenia*.

9.2. Publication XII:

Molecular phylogeny and evolution of the diatoms

SHINYA SATO & LINDA K. MEDLIN

*Alfred-Wegener-Institute for Polar and Marine Research, Am Handelshafen 12, D-27570
Bremerhaven, Germany*

2006. *Aquabiology* 166: 477-483

Abstract

With the advent of the molecular biological methods, much attention has been directed recently towards understanding the phylogeny of diatoms. Here we review phylogenetic reconstruction of the diatoms with 18S rDNA sequences. In our analysis only one traditional group “raphid pennates” was recovered as a monophyletic lineage, whereas the “centric” and “araphid pennates” were not. Newly proposed hypothesis of diatom evolution is introduced based on molecular phylogeny and fossil records. Finally some problems of phylogenetic analyses and also further perspectives in this field are briefly reviewed.

KEYWORDS: diatom, evolution, phylogeny, systematics

1. はじめに

珪藻の分類体系はこれまで数多く提唱されてきたが、1979年のSimonsenによるもの¹⁾や1990年のRoundらによるもの²⁾が広く用いられてきた。これらは基本的に被殻(シリカから成る細胞壁)の形態に基づいているため直感的に理解しやすく、そのため現在でもこれに準じる研究者は多い。近年の分子生物学の発展により、珪藻研究の分野でも分子情報を用いて系統関係を推定する分子系統学が行われるようになった。2004年には初めて分子系統解析の結果を考慮した新たな分類体系が提唱され³⁾、これにより珪藻分類学は新たな段階に入ったといってもよいだろう。本稿では分子系統学が珪藻分類学にこれまで与えた影響と現状について述べる。また分子系統学的手法を実際のデータを用いて概説し、得られた結果から珪藻の進化について考察する。

なお本稿では中心類、羽状類、そして無縦溝類、縦溝類といった用語を使用する。これらのグループは現在の分類体系では採用されていない。しかし形態をイメージしやすく便利であるため、現在も頻繁に用いられている。ここでもこれらのグルーピングを用いることとする。ただし特に説明のない限り、これらは分類学的な階級は示さないものとする。

2. 分子系統学と分類

1990年代に入り珪藻研究にも分子系統学的手法が用いられるようになった。分子系統学ではDNAやタンパク質の配列を形質として扱うため、形質の解釈の違いといった問題はなく、客観的な比較が可能といえる。また形質が大量に得られるという利点もある。通常は形態形成とは独立した領域を分子マーカーとして系統解析に用いるため、形態観察とは全く異なるアプローチで系統推定を行うことになる。そのため両者の結果が一致すればその系統関係は強く支持されたといえる。逆に得られた分子系統樹が形態と対応しない場合、結果の解釈には慎重な考察が要求される。

実際、1993年に初めて公表された珪藻の分子系統学的研究⁴⁾の結果は、形態に基づき構築された体系とは一致しなかった。核ゲノム中に存在する18S rDNA (18S リボソームDNA; Sは沈降係数を表す)を分子マーカーとして用いて構築されたこの系統樹では、中心類、無縦溝類ともに側系統となり、単系統を形成するのは縦溝類のみであった。この結果は、これまで形態に基づき構築されてきた高次の分類体系が系統を反映していない可能性を示唆していた。その後同様の結果が核ゲノムの28SrDNAの部分配列による系統解析⁵⁾、ミトコ

ンドリアゲノムのCoxI遺伝子⁶⁾、葉緑体ゲノムのrbcL, tufA, psaA⁷⁾等の系統解析により蓄積されるにつれ、高次分類を見直す必要性が認識されるようになった。これらの結果を受け2004年に提唱された新たな分類体系は、18S rDNAの大規模な系統解析に加え、被殻形態と増大胞子形態、細胞小器官配列様式といった特徴も加味されたものであった。2005年に国際原生生物学会により公表された原生生物の新体系⁸⁾も、この体系を採用しており今後これが広く用いられることと思われる。ただし、現段階で整理されたのはひとまず綱のランクまでに関してのみである。目より低次のランクでは1990年に提唱された体系に従っているが、この体系は形態観察に基づき構築されたもので、必ずしも系統学的ではない。そのため分子系統では多系統となる分類群も少なくないのが現状である。分子系統学的研究の結果を受けて現在の体系を即刻改訂する必要はないが、少なくともこれらのグループについての分類学的再検討を行うことは今後の珪藻分類学の課題である。

3. 分子系統樹の作成

ここでは実際に珪藻から塩基配列を決定し、分子系統樹を作成するまでの流れを概説する(図1)。

まずは採集したサンプルから目的の1細胞をキャピラリーピペットで単離し、培養液に移し、細胞が十分な数に増えるのを待つ。珪藻は単細胞生物であるため、通常のPCRに十分な量のDNAを得るためにまず単離培養により多数の細胞を得る必要がある。最適な水温、光環境、培養液を用いれば大抵の場合数週間程度で目的数に達する(図2)。ここからDNAを抽出し、目的の領域をPCR法により増幅し、シーケンサーによりこの増幅されたDNA断片の塩基配列を決定する。今回解析に用いる18S rDNAは多くの生物群で配列が決定されており、webデータベースに登録されている。ここから配列を入手し、今回決定した配列と合わせてアラインメント(各配列の相同領域が対応するよう整列する作業)を行う。配列から樹形を推定する方法は数多くあるが、現在広く用いられているものに近隣結合法、最節約法、最尤法、ベイズ法等がある。今回、複雑な置換モデルに基づき解析を行うことが可能なベイズ法⁹⁾を用い解析を行った。通常は得られた系統樹に対しブーツストラップ法等による統計学的評価を行うが、ベイズ法では系統樹と共にベイズ事後確率として統計学的信頼度が得られるため計算時間が比較的短くて済むという利点もある。

4. 系統樹からわかること

得られた系統樹を図3に示す。これまでの分子系統学的研究で報告された結果と同様、従来用いられていた体系では縦溝類のみが単系統となっている。無縦溝類は2つの単系統群から成り、目のランクではその多くが多系統となっていることが分かる。実はこの無縦溝類は、それ自体を特徴付ける独自の形質をもたない。羽状類珪藻のうち縦溝類でない珪藻が、すべてこのグループにまとめられているのである。このような経過は動物における無脊椎動物や植物における隠花植物と似ており、今後無縦溝類に対する分類学的再検討と整理がなされるだろう。

珪藻の中には浮遊生活を営むものが多く知られており、これらは系統樹上にモザイク状に分布している(図3 ●)。これは付着生活から浮遊生活への移行、もしくはその逆が進化の過程で何度も起こっていることを物語っている。また系統樹から、浮遊性珪藻は中心類に多いことが見て取れる。この傾向は中心類と羽状類の有性生殖様式の違いに関係していると考えられる。一般的に中心類の有性生殖では1つの卵と多数の精子(分類群ごとに異なる)

るが、4-32個程度)による卵生殖であり、羽状類では1-2個のアメーバ状配偶子による同形配偶である¹⁰⁾。浮遊した状態で精子を卵に到達させるためには多数の精子を放出したほうが受精確率は上がる。一方、接合し配偶子を交換する羽状類の場合は多数の精子を形成する必要はない。ただ同形配偶の無縦溝類でも多数の浮遊性種が知られているため、生活型の進化を有性生殖様式のみでは説明できないだろう。同様に海産種と淡水産種も系統樹上に散在しており(図3 ■), 生育域の移動も複数回あったことが示唆される。これら生活型や生育域の変化といった過去に起こったイベントは、観察からはなかなか見つけにくい。同じ環境に生育し同じ適応帯に入っている生物は、しばしば収斂進化により形態的には類似するためである。このような場合、環境に対し中立な分子マーカーを用いる限り、分子系統学的研究は過去を復元する際の強力なツールとなる。

縦溝珪藻の単系統性は高い統計学的信頼度で支持されており、またこの結果はこれまで発表されたほぼ全ての分子系統解析でも同様である(今回の解析も含め、稀にストリアテラ目珪藻 *Striatella* が縦溝珪藻クレードの根元付近で分岐するが、これはこの種における進化速度が極端に早いための解析誤差であると思われる)。このことは珪藻の進化の過程で縦溝の獲得がたった一回だけ起こったイベントであることを示している。短い縦溝に加え唇状突起(一般的に中心類と無縦溝類はもつが縦溝類はもたない構造)をもつことから縦溝類の祖先的なグループであると考えられてきた²⁾イチモンジケイソウ *Eunotia* は、分子系統樹上で縦溝珪藻クレードの根元付近で分岐している。イチモンジケイソウの系統学的位置については諸説あり未だ結論が得られていないが、分子系統解析の結果はこの珪藻の縦溝が祖先的な形質であるとする説を支持している。

縦溝類は水分のある場所なら地球上まさしくいたるところに出現する。強酸性、強アルカリ性の温泉に生育しているかと思えば、低温の極海で一次生産者として生態的に重要な役割を果たしているものもある。樹木の表面や土壌など、水分がわずかしかない場所にも生育している。さらに鯨の体表にのみ生育するという種類もある。また海岸を漂っているビニールなどを顕微鏡で調べてみても大抵の場合このグループが着生している。ビルの屋上などに水を張って放置しておく風に乗って飛ばされてやってきた縦溝珪藻が増殖して、水がいつの間にか茶色く色づいていたりする。縦溝は細胞の移動だけでなく浸透圧調節にも一役買っているという説もあり¹¹⁾、このことは縦溝類がいたるところに生育できる理由の一つであろう。いずれにせよこの一度きりの縦溝獲得イベントが縦溝類の大躍進の一端を担っていることは間違いないだろう。

5. 珪藻の姉妹群

今回の解析ではボリド藻という海産ピコプランクトンを外群とした。この小さな鞭毛藻は、これまでのいずれの分子系統解析でも珪藻の姉妹群となっている。しかしながら現在のところ、この藻類から珪藻との関わりを示唆するようなシリカの構造といった直接的な証拠は見つかっていない。また小さな細胞内に細胞小器官がぎっしりと詰め込まれているため、細胞小器官配列を珪藻と比較するのも不可能である。パルマ藻はシリカから成るスケールを持つため珪藻との系統学的関連が取り沙汰されているが、これまで培養が成功していないため塩基配列は得られていない。なお、環境クローン配列(環境水から直接DNAを抽出して得られた塩基配列で、未知の系統に属する生物の存在を示唆する)を用いた系統解析からは、ボリド藻よりも珪藻に近縁な生物は今のところ発見されていない¹²⁾。しかしここ10年で多くのピコプランクトン群が発見されていることを顧みると、未発見の珪藻の真の姉妹群が未だ海洋に潜んでいる可能性は十分に考えられる。

6. 珪藻の誕生

珪藻はストラメノパイルという大グループに含まれることは形態学的、分子系統学的研究から明らかである¹³⁾が、珪藻の他にもシリカを利用する生物群を含んでおり、この能力は珪藻自身により独自に獲得されたとは考えにくい。しかし姉妹群のボリド藻は細胞壁にシリカ構造を持たないことから、珪藻がシリカの被殻形成を始めたことは確かであろう。それでは珪藻はいつ、どのようにしてシリカの被殻を獲得したのだろうか。分子系統学的手法の発達により、このような問題に対しても新たなアプローチが可能となった。分子時計(進化速度の一定性)を仮定し化石の出現記録で年代補正をした研究では、珪藻は少なくとも2億3800~2億6600万年前には存在していなかっただろうと結論付けられた¹⁴⁾。信頼できる最古の珪藻化石の年代は約1億9000万年前¹⁵⁾とされているため、珪藻はこの期間(2億6600万年前~1億9000万年前)に出現したのはほぼ間違いない。2億5000万年前のペルム紀末には地球史上最大の絶滅事件が起きており、珪藻の出現もこのイベントと関連しているとする説もある¹⁶⁾。

2004年に開催された国際珪藻学会会議で、1億7500万年前の陸水域からの珪藻化石発見が報告された¹⁷⁾。外群のボリド藻も含め珪藻の分子系統樹において初期に分岐するものの多くが海産であるため、この年代の珪藻がかつての陸水域で発見されたことは参加者に大きな驚きをもたらした。この発見を受け、珪藻のシリカ被殻獲得についての以下の仮説が新たに提唱された¹⁵⁾。

初期の珪藻はボリド藻(前述)のように鞭毛を持ち、シリカの細胞壁をもたない海産浮遊性細胞であった。当時の海水面は非常に高く氾濫が頻発しており、この細胞はしばしば陸地へと流された。彼らの一部は陸地にできた池に取り残され、やがて池の乾燥とともに死ぬ、といったことが繰り返された。あるときシリカを細胞内に取り入れ、代謝に利用するものが現れた。哺乳類細胞株においてシリカは老化を防ぐ、有害金属の影響を軽減する、菌類からの攻撃を防ぐ、休眠状態を長く存続させる、といった働きがあることが知られている¹⁸⁾。シリカが珪藻に対しても同様の効果をもたらすと仮定すると、このシリカを取り込んだ細胞は他の細胞に比べ生存に有利であったに違いない。シリカは土壤中に豊富に存在するため珪藻にとっても利用しやすく、やがて過剰摂取されたシリカは液胞内に蓄えられた。液胞内の酸性の環境下ではシリカは重合体化し、もはや細胞の老化防止等の反応に利用されなくなった。細胞にとって有用でなくなったシリカ重合体はやがて細胞外へと押しやられた。この状態はおそらくパルマ藻や、スケールに覆われた増大胞子(auxospore)のような形態だったのではないだろうか(図4)。細胞がシリカで覆われていることは物理的にも、また乾燥に対しても有利であったに違いない。やがて洪水で再び海へと流された細胞はもはやその重さのために底性生活を強いられた。18S rDNA系統樹で最も初期に分岐するのは底性珪藻として知られるパラリア目であり、この仲間は重度にシリカ沈着した細胞壁を持つことからこの説は支持される。やがて細胞を覆っているスケール状シリカのうち2枚が肥大し上下の殻となり、残りは帯片へと形を変えていった(図4)。珪藻の殻の形成様式と増大胞子表面に見られるスケールの形成様式に非常に高い類似性がみられることから²⁾、殻はスケール起源であるとする説は受け入れられている。18S rDNA系統樹のごく初期に分岐する中心類ツツガタケイソウ目やコレスロン目では、帯片は通常見られるような帯状ではなくスケール状であることも興味深い。

この仮説はシリカが珪藻の代謝においてもプラスに働くという前提¹⁸⁾に基づいているが、これに対しては反論もあり現在論争となっている¹⁸⁻²¹⁾。この他にも、珪藻がなぜシリカの細胞壁をもつのか?という問いに対して数多くの説が提唱されている²²⁾。

上記の研究では年代推定の際に分子時計を仮定しているため、進化速度の極端に異なる分類群は解析から除かれている。しかし実際は進化速度が分類群ごとに異なるのは一般的であり、多くの分類群や遺伝子で分子時計が厳密には成立しないことが報告されている²³⁾。近年ベイズ法を用いる分岐年代推定法²⁴⁾が開発され、進化速度の一定性を仮定せずに解析を行えるようになった。また石油中に含まれるアルケンの一種が、特定の珪藻によってのみ合成される"分子化石"であることが解明され、この珪藻の出現年代が高い精度で決定された²⁵⁾。今後ベイズ法による分岐年代推定と分子化石による年代補正により、より詳細な珪藻進化の道筋が明らかにされるだろう。

7. 分子系統解析における注意点

分子系統学的手法はこれまで述べたように、分類学のみならず進化の全体像を把握するうえでも、新しい視点からのアプローチを可能にした。しかしこの分野は未だ発展途上でもあるため、解析を行う際、認識しておかなければならない点もある。今回は18SrDNA配列により系統樹を構築したがこれはあくまでも遺伝子の系統樹であり、それぞれの種の系統樹と厳密に一致するとは限らない。現在ではより確実な種の系統樹を導くためには、複数の分子マーカーを用いるほうがよいとされている。またDNAやアミノ酸配列以外にも、挿入配列の有無、遺伝子の配列や遺伝コードの変化などの情報も系統推定に有用であることが確かめられている。解析に用いる分類群の種類や数、そして外群選択は樹形に影響を与えることが知られている。塩基置換モデルが実際のデータを正しく反映していなかった場合は、もちろん誤った結果を導く可能性がある。さらに、データセットによっては異なる系統樹構築法により全く異なる結果が得られる場合もある。このように現段階では確立された方法論が無い以上できる限り多くの方法を試し、さらに形態学的、生態学的情報を元に総合的に判断を下すのが最善の選択だろう。

8. おわりに

最後に珪藻の分子系統学的研究について、今回触れなかった部分について簡単に述べる。

本稿では主に珪藻全体を扱った分子系統学的研究を紹介したが、用いる分子マーカーによっては種分化といった短いタイムスケールの進化も扱うことができる。進化速度の速い領域を分子マーカーとしたところ、セラフォラ属珪藻の一種*Sellaphora pupula*において幾つかの明瞭なグループが認識された。これらは生殖的にも互いに隔離されている隠蔽種群(形態での区別が困難な生物学的種の集まり)であることが判明した²⁶⁾。さらに形態計測により僅かながら形態的差異が観察され、これらの結果を踏まえ5つの種が記載された²⁷⁾。珪藻は精巧なつくりの被殻が人目を引くため、古くから形態学的研究に重点が置かれてきた。そのため、一般的に珪藻では種といえば形態種を指す。このセラフォラにおける一連の研究は今後の珪藻分類学のみならず、珪藻における種概念を考える上での重要なステップである。その後これまでに幾つかの隠蔽種群が報告されている。

全ゲノム解読は生き物の基本的な構造を知る上での莫大な量の情報を提供し、またこれは進化の道筋を解明する際の重要な手がかりとなる。珪藻では2002年に中心類タラシオシラ *Thalassiosira pseudonana* の全ゲノム解読が終了した²⁸⁾。これにより、尿素サイクルの発見や脂肪の代謝方法の解明など、生物としての珪藻を理解するうえでの大躍進を遂げた。さらに縦溝類フェオダクチルム *Phaeodactylum tricornutum* の全ゲノム解読も終了しており、これをタラシオシラゲノムと比較することでさらに新たな知見が得られるだろう。現在、極域に

生育する縦溝類フラジラリオプシス *Fragilariopsis cylindrus* と、ドウモイ酸と呼ばれる毒素を産生する縦溝類ニセササノハケイソウ *Pseudo-nitzschia multiseries* の全ゲノム解読プロジェクトがそれぞれ進行中であり、これらの成果にも注目したい。

引用文献

- 1) Simonsen, R.: The diatom system: ideas on phylogeny, *Bacillaria*, **2**: 9-72, 1979.
- 2) Round, F. E., R. M. Crawford and D. G. Mann: *The diatoms: Biology and Morphology of the genera*, Cambridge University Press, Cambridge, 1990. pp. 1-747.
- 3) Medlin, L. K. and I. Kaczmarek: Evolution of the diatoms: V. Morphological and cytological support for the major clades and a taxonomic revision, *Phycologia*, **43**: 245-270, 2004.
- 4) Medlin, L. K., D. M. Williams and P. A. Sims: The evolution of the Diatoms (Bacillariophyta). I. Origin of the group and assessment of the monophyly of its major divisions, *European Journal of Phycology*, **28**: 261-275, 1993.
- 5) Sörhannus, U., F. Gasse, R. Perasso and A. Baroin-Tourancheau: A preliminary phylogeny of diatoms based on 28S ribosomal RNA sequence data, *Phycologia*, **34**: 65-73, 1995.
- 6) Ehara M., Y. Inagaki, K. I. Watanabe and T. Ohama: Phylogenetic analysis of diatom *coxI* genes and implications of a fluctuating GC content on mitochondrial genetic code evolution, *Current Genetics*, **37**: 29-33, 2000.
- 7) Medlin, L. K., W. H. C. F. Kooistra and A.-M. M. Schmid: A review of the evolution of the diatoms - a total approach using molecules, morphology and geology, In: Witkowski, A. and J. Sieminska (Eds.), *The Origin and Early Evolution of the Diatoms: Fossil, Molecular and Biogeographical Approaches*, W. Szafer Institute of Botany, Polish Academy of Sciences, Cracow, pp. 13-35, 2000.
- 8) Adl, S. M., A. G. Simpson, M. A. Farmer, R. A. Andersen, O. R. Anderson, J. R. Barta, S. S. Bowser, G. Brugerolle, R. A. Fensome, S. Fredericq, T. Y. James, S. Karpov, P. Kugrens, J. Krug, C. E. Lane, L. A. Lewis, J. Lodge, D. H. Lynn, D. G. Mann, R. M. McCourt, L. Mendoza, O. Moestrup, S. E. Mozley-Standridge, T. A. Nerad, C. A. Shearer, A. V. Smirnov, F. W. Spiegel and M. F. Taylor: The new higher level classification of eukaryotes with emphasis on the taxonomy of protists, *The Journal of Eukaryotic Microbiology*, **52**: 399-451, 2005.
- 9) Huelsenbeck, J. P., F. Ronquist, R. Nielsen and J. P. Bollback: Evolution - Bayesian inference of phylogeny and its impact on evolutionary biology, *Science*, **294**: 2310-2314, 2001.
- 10) Chepurinov V. A., D. G. Mann, K. Sabbe and W. Vyverman: Experimental studies on sexual reproduction in diatoms, *International Review of Cytology*, **237**: 91-154, 2004.
- 11) Mann, D. G.: Crossing the Rubicon: the effectiveness of the marine/freshwater interface as a barrier to the migration of diatom germplasm, In: Mayama, S. and M. Idei and I. Koizumi (Eds), *Proceedings of the 14th International Diatom Symposium*, Koeltz Scientific Books, Koenigstein, pp. 1-21, 1999.
- 12) Moreira, D. and P. López-García: The molecular ecology of microbial eukaryotes unveils a hidden world, *TRENDS in Microbiology*, **10**: 31-38, 2002.
- 13) Bhattacharya, D., H. S. Yoon and J. D. Hackett: Photosynthetic eukaryotes unite: endosymbiosis connects the dots. *BioEssays*, **26**: 50-60, 2004

- 14) Kooistra, W. H. C. F. and L. K. Medlin: Evolution of the diatoms (Bacillariophyta). IV. A reconstruction of their age from small subunit rRNA coding regions and the fossil record, *Molecular Phylogenetics and Evolution*, 6: 391-407, 1996.
- 15) Sims, P. A., D. G. Mann and L. K. Medlin: Evolution of the diatoms: insights from fossil, biological and molecular data, *Phycologia*, 45: 361-402, 2006.
- 16) Medlin, L. K., W. H. C. F. Kooistra, R. Gersonde, P. A. Sims and U. Wellbrock: Is the origin of the diatoms related to the end-Permian mass extinction?, *Nova Hedwigia*, 65: 1-11, 1997.
- 17) Harwood, D. M., K. H. Chang and V. A. Nikolaev: Late Jurassic to earliest Cretaceous diatoms from Jasong Synthem, Southern Korea: Evidence for a terrestrial origin, In: Witkowski, A., T. Radziejewska, B. Wawrzyniak-Wydrowska, G. Daniszewska-Kowalczyk and M. Bak (Eds), *Abstracts, 18th International Diatom Symposium*, Miedzysdroje, Poland, p. 81, 2004.
- 18) Medlin, L. K.: Why silica or better yet why not silica? Speculations as to why the diatoms utilise silica as their cell wall material, *Diatom Research*, 17: 453-459, 2002.
- 19) Schmid, A.-M. M.: The evolution of the silicified diatom cell wall - revisited, *Diatom Research*, 18: 191-195, 2003.
- 20) Medlin, L. K.: Comment in reply to Schmid (2003) "The evolution of the silicified diatom cell wall - revisited", *Diatom Research*, 19: 345-351, 2004.
- 21) Schmid, A.-M. M.: The wall and membrane systems in diatoms: comment in reply to Medlin (2004), *Diatom Research*, 20: 211-216, 2005.
- 22) Raven, J. A. and A. M. Watte: The evolution of silicification in diatom: inescapable sinking and sinking as escape? *New Phytologist*, 162: 45-61, 2004.
- 23) Ayala, F. J.: Neutralism and selectionism: the molecular clock, *Gene*, 261: 27-33, 2000.
- 24) Thorne, J. L., H. Kishino and I. S. Painter: Estimating the rate of evolution of the rate of molecular evolution, *Molecular Biology and Evolution*, 15: 1647-1657, 1998.
- 25) Damste J. S. S., G. Muyzer, B. Abbas, S. W. Rampen, G. Masse, W. G. Allard, S. T. Belt, J.-M. Robert, S. J. Rowland, J. M. Moldowan, S. M. Barbanti, F. J. Fago, P. Denisovich, J. Dahl, L. A. F. Trindade and S. Schouten: The rise of the rhizosolenid diatoms, *Science*, 304: 584-587, 2004.
- 26) Behnke, A., T. Friedl, V. A. Chepurnov, and D. G. Mann: Reproductive compatibility and rDNA sequence analyses in the *Sellaphora pupula* species complex (Bacillariophyta), *Journal of Phycology*, 40: 193-208, 2004.
- 27) Mann, D. G., S. M. McDonald, M. M. Bayer, S. J. M. Droop, V. A. Chepurnov, R. E. Loke, A. Ciobanu and J. M. H. Du Buf: The *Sellaphora pupula* species complex (Bacillariophyceae): morphometric analysis, ultrastructure and mating data provide evidence for five new species, *Phycologia*, 43: 459-482, 2004.
- 28) Armbrust, E. V., J. A. Berges, C. Bowler, B. R. Green, D. Martinez, N. H. Putnam, S. Zhou, A. E. Allen, K. E. Apt, M. Bechner, M. A. Brzezinski, B. K. Chaal, A. Chiovitti, A. K. Davis, M. S. Demarest, J. C. Detter, T. Glavina, D. Goodstein, M. Z. Hadi, U. Hellsten, M. Hildebrand, B. D. Jenkins, J. Jurka, V. V. Kapitonov, N. Kroger, W. W. Lau, T.W. Lane, F. W. Larimer, J. C. Lippmeier, S. Lucas, M. Medina, A. Montsant, M. Obornik, M. S. Parker, B. Palenik, G. J. Pazour, P. M. Richardson, T. A. Rynearson, M. A. Saito, D. C. Schwartz, K. Thamatrakoln, K. Valentin, A. Vardi, F. P. Wilkerson and D. S. Rokhsar: The genome of the diatom *Thalassiosira pseudonana*: ecology, evolution, and metabolism, *Science*, 306: 79-86, 2003.

-
- 29) Mann, D. G. and H. J. Marchant: The origin of the diatom and its life cycle, In: Green, J. C., B. S. C. Leadbeater and W. L. Diver (Eds.), *The chromophyte algae: problems and perspectives*, Clarendon Press, Oxford, pp. 307-323, 1989.

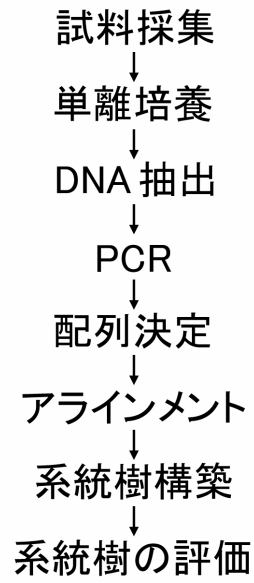


図 1. 分子系統樹作成までの流れ



図 2. 恒温室内の珪藻培養の様子

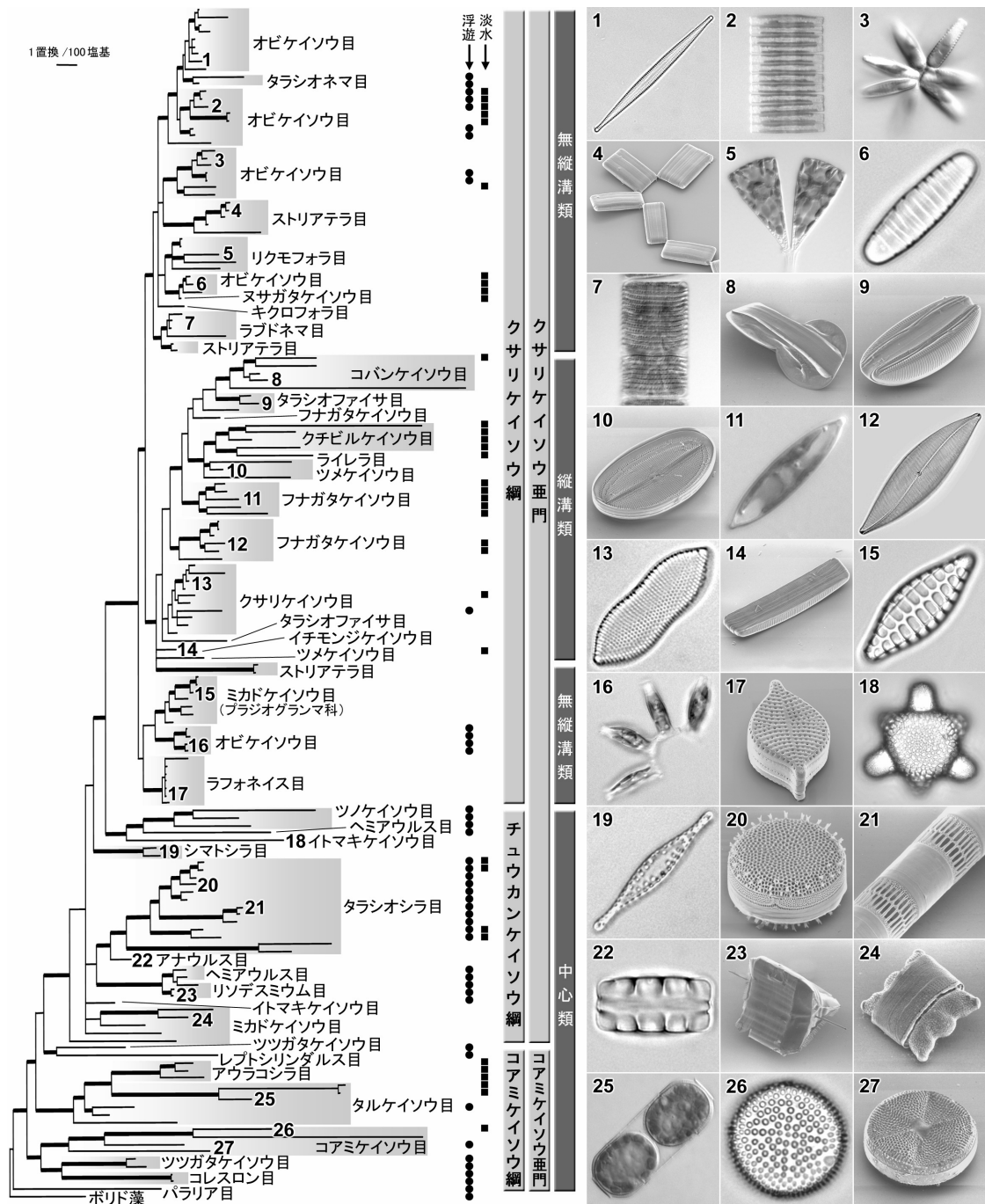


図3. 珪藻の18S rDNA 系統樹(ベイズ法)

太い枝は高い統計学的信頼度により支持された部分(ベイズ事後確率 0.9-1)。プランクトン珪藻 = ●, 淡水産珪藻 = ■。新しい体系³⁾が薄灰色(左2列), 従来の体系²⁾が濃灰色(右列)の枠内に表示。生細胞の光学顕微鏡写真(2, 3, 5, 7, 11, 16, 25), 洗浄済被殻の光学顕微鏡写真(1, 6, 13, 15, 18-19, 22, 26), 走査型電子顕微鏡写真(4, 8-10, 14, 17, 20-21, 23-24, 27)。

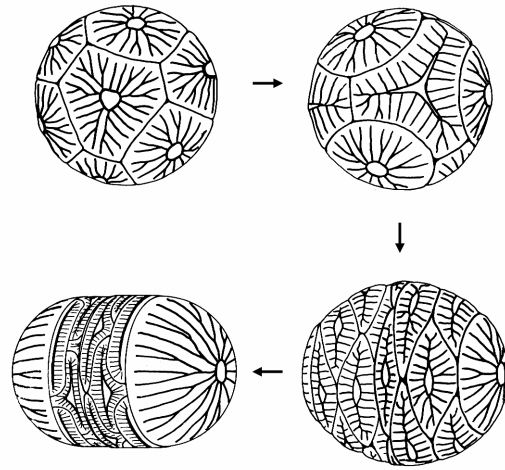


図 4. スケールから殻, 帯片への分化²⁹⁾

9.3. Curriculum vitae:

Shinya Sato

Born: 18 July 1978

Family status: Married

Nationality: Japan

Address: Am Handelshafen 12, D-27570 Bremerhaven, Germany

Telephone: +49/471 4831-1556

E-mail: shinya.sato@awi.de

auxospore@yahoo.co.jp

Current position

Since 06/2008 Alfred Wegener Institute for Polar and Marine Research, Germany
Wissenschaftlicher Mitarbeiter (research associate)

Education

06/2005 - 05/2008 Alfred-Wegener-Institut for Polar and Marine Research, Germany, as PhD candidate

04/2004 - 05/2005 Alfred-Wegener-Institut for Polar and Marine Research, Germany, as guest researcher

04/2002 - 03/2004 Specialized fields of Aquatic Biology at Phycological Laboratory, Course of Aquatic Biosciences, Graduate School of Tokyo University of Fisheries, Japan

04/1998 - 03/2002 Department of Aquatic Biosciences, Tokyo University of Fisheries, Japan

Degree

PhD 07/2008: *Natural Science (obtained first class honour - summa cum laude)*
Advisor: Dr. Linda K. Medlin
University of Bremen, Germany
Dissertation: <http://elib.suub.uni-bremen.de/diss/docs/00011057.pdf>

MS 03/2004: *Fisheries Science*
Advisors: Prof. Tamotsu Nagumo and Prof. Jiro Tanaka
Graduate School of Tokyo University of Fisheries, Japan

BSc 03/2002: *Fisheries Science*
Advisors: Prof. Tamotsu Nagumo and Prof. Jiro Tanaka
Tokyo University of Fisheries, Japan

Publications

[peer reviewed]

- 10) **Sato S, Kooistra WHCF, Watanabe T, Matsumoto S, Medlin LK** (2008) Phylogenetics and morphometrics reveal pseudocryptic diversity in a new araphid diatom genus *Psammoneis* (Plagiogrammaceae, Bacillariophyta) gen. nov.. *Phycologia* (in press)
- 9) **Sato S, Mann DG, Nagumo T, Tanaka J, Tadano T, Medlin LK** (2008) Auxospore fine structure and variation in modes of cell size changes in *Grammatophora marina* (Bacillariophyta). *Phycologia* 47: 12-27.
- 8) **Medlin LK, Sato S, Mann DG, Kooistra WHCF** (2008) Molecular evidence confirms sister relationship of *Ardissonea*, *Climacosphenia* and *Toxarium* within the bipolar centric diatoms. *Journal of Phycology* (in press)
- 7) **Sato S, Kuriyama K, Tadano T, Medlin KL** (2008) Auxospore fine structure in a marine araphid diatom *Tabularia parva* (Bacillariophyta). *Diatom Research* (in press)
- 6) **Sato S, Matsumoto S, Medlin LK** (2008) Fine structure and 18S rDNA phylogeny of a marine araphid pennate diatom *Plagiostriata goreensis* gen. et sp. nov. (Bacillariophyta). *Phycological Research* (in press)
- 5) **Sato S, Watanabe T, Crawford RM, Kooistra WHCF, Medlin LK** (2008) Morphology of four plagiogrammacean diatoms; *Dimeregramma minor* var. *nana*, *Neofragilaria nicobarica*, *Plagiogramma atomus* and *Psammogramma vigoensis* gen. et sp. nov., and their phylogenetic relationship inferred from partial 28S rDNA. *Phycological Research* (in press)
- 4) **Sato S, Mann DG, Matsumoto S, Medlin LK** (2008) *Pseudostriatella pacifica* gen. et sp. nov. (Bacillariophyta); a new araphid diatom genus and its fine-structure, auxospore and phylogeny. *Phycologia* 47: 371-391.
- 3) **Sato S, Medlin LK** (2006) Note: Motility of non-araphid diatoms. *Diatom Research* 21: 473-477.
- 2) **Sato S, Nagumo T, Tanaka J** (2004) Morphology and taxonomy of marine attached diatoms in genus *Grammatophora* Ehrenberg (Bacillariophyceae) in Japan. *The Japanese Journal of Phycology* 52: 183-187.
- 1) **Sato S, Nagumo T, Tanaka J** (2004) Auxospore formation and initial cell in the marine araphid diatom *Gephyria media* (Bacillariophyceae). *Journal of Phycology* 40: 684-691.

[submitted manuscripts]

- 2) **Bruder K, Sato S, Medlin LK** (submitted) Morphological and Molecular Investigations of Naviculoid Diatoms. IV. *Pinnularia* vs. *Caloneis*. *Diatom*
- 1) **Sato S, Kooistra WHCF, Mayama S, Medlin LK** (submitted) Phylogeny and divergence time estimation of 'araphid' diatoms. *Molecular phylogenetics and evolution*

[non peer reviewed]

- 3) **Sato S, Medlin LK** (2006) Molecular phylogeny and evolution of the diatoms. *Aquabiology* 166: 477-483 (in Japanese with English abstract).
- 2) **Sato S** (2004) Meeting report of the 18th International Diatom Symposium at Poland. *Diatom* 20: 242 (in Japanese).
- 1) **Sato S** (2002) Meeting report of the 17th International Diatom Symposium at Canada. *Diatom* 18: 96 (in Japanese).

Presentations

[International meetings]

- 7) **Sato S, Medlin LK** (2007) *Pseudostriatella pacifica* gen. et sp. nov., A new taxon of marine araphid diatoms: Morphology, ecology and phylogeny. 4th European Phycological Congress. Oviedo, SPAIN.
- 6) **Watanabe T, Sato S, Susuki H, Nagumo T, Tanaka J** (2007) Three morphological variations among the genus *Rhaphoneis*. 4th European Phycological Congress. Oviedo, SPAIN.
- 5) **Sato S, Beszteri B, Tanaka J, Medlin LK** (2007) Phylogeny of the araphid diatoms: Diversification in the age of macroalgae and seagrasses. 19th International Seaweed Symposium. Kobe, JAPAN.
- 4) **Sato S, Medlin LK** (2006) Phylogeny of araphid diatoms. 19th International diatom symposium. Irkutsk, RUSSIA.
- 3) **Sato S, Medlin KL, Nagumo T, Tanaka J** (2004) Are the scales on the auxospore any longer the patent for centric diatoms? 18th International diatom symposium. Miedzyzdroje, POLAND.
- 2) **Sato S, Nagumo T, Tanaka J** (2002) Morphology and taxonomy of marine attached diatom genus *Grammatophora* Ehrenberg (Bacillariophyceae) in Japan. 3rd Asian Pacific Phycological Forum Algae2002. Tsukuba, JAPAN.
- 1) **Sato S, Nagumo T, Tanaka J** (2002) Morphology of marine attached diatom genus *Grammatophora* Ehrenberg in Japan. 17th International Diatom Symposium. Ottawa, CANADA.

[Regional meetings]

- 8) **Sato S, Medlin LK** (2007) Phylogeny and evolution of araphid diatoms. 31st meeting of the Japanese Society of Phycology.
- 7) **Watanabe T, Sato S, Nagumo T, Tanaka J** (2007) Diatom flora of Uchibanare Island, Iriomote, Okinawa. 31st meeting of the Japanese Society of Phycology.
- 6) **Sato S, Nagumo T, Tanaka J, Medlin KL** (2005) Life cycle of pennate diatom genus *Grammatophora*. 26th meeting of the Japanese Society of Diatomology.
- 5) **Sato S, Nagumo T, Tanaka J** (2003) The evolution of the marine attached diatom *Grammatophora*. 23rd Workshop of the Japanese Society of Diatomology.
- 4) **Sato S, Nagumo T, Tanaka J** (2003) Taxonomical discussion of the marine attached diatom *Grammatophora japonica*. 24th meeting of the Japanese Society of Diatomology.
- 3) **Sato S, Nagumo T, Tanaka J** (2003) Auxospore formation of the marine attached diatom *Gephyria media* Arnott. 27th Conference of the Japanese Society of Phycology.
- 2) **Sato S, Nagumo T, Tanaka J** (2002) Fine structure of the marine attached diatom *Grammatophora angulosa* Ehrenberg. 22nd Workshop of the Japanese Society of Diatomology.
- 1) **Sato S, Nagumo T, Tanaka J** (2002) Morphology of marine attached diatom *Grammatophora* sp. and its colony formation. 23rd meeting of the Japanese Society of Diatomology.

Awards

- 2002 Best student poster award in 17th International Diatom Symposium
- 2004 Best student poster award in 18th International Diatom Symposium
- 2005-2008 DAAD scholarship for doctoral research in Germany

Society Memberships

- British Phycological Society
- International Society of Diatom Research
- Japanese Society of Diatomology
- Japanese Society of Phycology

